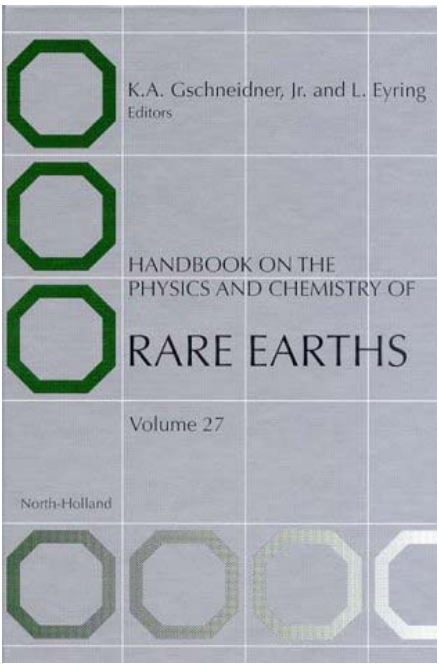

Handbook on the Physics and Chemistry of Rare Earths, volume 27

Elsevier, 1999

Edited by: Karl A. Gschneidner, Jr. and LeRoy Eyring
ISBN: 978-0-444-50342-8

Handbook on the Physics and Chemistry of Rare Earths
Vol. 27
edited by K.A. Gschneidner, Jr. and L. Eyring

PREFACE

Karl A. GSCHNEIDNER, Jr., and LeRoy EYRING

These elements perplex us in our rearches [sic], *baffle us in our speculations, and haunt us in our very dreams. They stretch like an unknown sea before us – mocking, mystifying, and murmuring strange revelations and possibilities.*

Sir William Crookes (February 16, 1887)

This volume of the *Handbook* is the last volume to be published with a 19xx imprint and contains three chapters which deal with rare earth alloys and intermetallic compounds.

Chapter 173 is by P.S. Salamakha, O.L. Sologub and O.I. Bodak and deals with ternary rare-earth–germanium alloys – their phase diagrams and the crystal structures of the intermediate phases. The largest number of intermetallic phases are found in the Group-VIII metals, i.e. iron, cobalt and nickel and their congeners ruthenium, rhodium and palladium. Although there is a paucity of data for the congeners in the third row of transition metals, the little information available indicates that osmium, iridium and platinum will also form as many intermetallic compounds. Of the group-VIII metals the first member of each row (iron, ruthenium and osmium) forms only about half (10) the number of compounds as the other two members, cobalt and nickel and their congeners.

Another interesting observation is that the ternary alloy systems of the rare earths and germanium with the s and p elements have hardly been investigated. And of those that have been studied, only a few intermediate phases have been observed in the ternary systems. The chapter ends with a discussion of the general trends and unusual features observed in the various sets of ternary phase diagrams.

In a companion chapter (174) P.S. Salamakha describes in detail the various structure types that have been adopted by the rare-earth–germanium ternary intermetallic compounds. The correlations, crystal chemistry and interrelationships of the 135 structure types are discussed. Two distinct behaviors are found depending on the nature of the outer bonding electrons: the p elements behave differently from the s and d elements, which behave similarly. When the third component is a p element the compounds maintain the same R to Ge ratio as found in the binary R_xGe_y phases, e.g. RGe_2 and R_3Ge_5, where R is a rare earth metal. As one might expect many of the compounds have variable composition at a constant R content. For the s and d metals the compounds tend to fall on lines

connecting the three elements with binary phases of simple compositions, such as the R–MGe, M–RGe_2, Ge–RM lines, where M is an element other than R or Ge. The line connecting the RM_2–RGe_2 binary phases also has several phases lying on it, including RMGe. The equiatomic composition RMGe has 20 known structure types.

Quaternary compounds and superstructures are also reviewed by Salamakha.

The last chapter (175) deals with scandium alloys and intermetallic compounds – binary, ternary and higher order systems. In their review B.Ya. Kotur and E. Gratz summarize the various phase diagrams of scandium systems and present the crystal structure properties of the various intermediate phases. The general trends observed in the phase relationships and crystal chemistry of these materials are discussed, and may be useful in finding new scandium phases. In the last section of their chapter Kotur and Gratz present physical property data on scandium intermetallic phases. The results are divided into three groups – compounds which have (1) a magnetic ground state, (2) a superconducting ground state and (3) those with neither a magnetic or a superconducting ground state.

CONTENTS

CONTENTS OF VOLUMES 1–26

VOLUME 4: Non-metallic compounds – II

1979, 1st repr. 1984; ISBN 0-444-85216-6

VOLUME 5

1982, 1st repr. 1984; ISBN 0-444-86375-3

VOLUME 6

1984; ISBN 0-444-86592-6

VOLUME 7

1984; ISBN 0-444-86851-8

VOLUME 8
1986; ISBN 0-444-86971-9

VOLUME 9
1987; ISBN 0-444-87045-8

VOLUME 10: High energy spectroscopy
1988; ISBN 0-444-87063-6

VOLUME 11: Two-hundred-year impact of rare earths on science
1988; ISBN 0-444-87080-6

VOLUME 12

1989; ISBN 0-444-87105-5

VOLUME 13

1990; ISBN 0-444-88547-1

VOLUME 14

1991; ISBN 0-444-88743-1

VOLUME 15

1991; ISBN 0-444-88966-3

MASTER INDEX, Vols. 1–15
1993; ISBN 0-444-89965-0

VOLUME 16
1993; ISBN 0-444-89782-8

VOLUME 17: Lanthanides/Actinides: Physics – I
1993; ISBN 0-444-81502-3

VOLUME 18: Lanthanides/Actinides: Chemistry
1994; ISBN 0-444-81724-7

VOLUME 19: Lanthanides/Actinides: Physics – II

1994; ISBN 0-444-82015-9

VOLUME 20

1995; ISBN 0-444-82014-0

VOLUME 21

1995; ISBN 0-444-82178-3

VOLUME 22

1996; ISBN 0-444-82288-7

VOLUME 23

1996; ISBN 0-444-82507-X

VOLUME 24

1997; ISBN 0-444-82607-6

VOLUME 25

1998; ISBN 0-444-82871-0

VOLUME 26

1999; ISBN 0-444-50815-1

Handbook on the Physics and Chemistry of Rare Earths
Vol. 27
edited by K.A. Gschneidner, Jr. and L. Eyring

Chapter 173

TERNARY RARE-EARTH–GERMANIUM SYSTEMS

P.S. SALAMAKHA[1], O.L. SOLOGUB[1] AND O.I. BODAK[2]
[2] Department of Inorganic Chemistry, L'viv State University, Kyryla and Mefodiya 6, 290005 L'viv, Ukraine
[1] Departamento de Química, Instituto Tecnológico e Nuclear, P-2686-953 Sacavém, Portugal

Contents

Symbols and abbreviations

a, b, c	Unit cell dimensions (in nm)
at.%	Composition in atomic percent
h	Hours
M	s-, p-, d-, f-element
O	Orthorhombic structure
R, R′	Rare-earth metal, Y, Sc, and the lanthanides
r_R	Atomic radius of the R component
T	Tetragonal structure
x	indicates variable component contents, when it is used as index in compound compositional formula. The expression $N-x$ (where N is a number) means N minus x, with the x value given in the text
X_R	Electronegativity of the R component
α, β, γ	unit cell angles (in degrees)
~	Precedes the composition formula of a compound to indicate that the composition is given approximately

1. Introduction

The aim of this chapter is to systematize the current knowledge concerning phase diagrams and crystal structures of ternary metal germanides with the R elements (R ≡ Sc, Y, and the lanthanides). The isothermal sections for the ternary R–s, p, d, f element–Ge systems have been extensively studied in recent years by the researchers at the Inorganic Chemistry Department at L'viv University. The crystal structure of ternary compounds has been investigated by various groups of authors. The present status of information on phase diagrams and formation of rare-earth metal germanides is summarized in tables 1, 2 and 3.

This review consists of six sections. Sections 2–5 review the literature published on the systems, i.e., isothermal sections and crystallographic characteristics of ternary compounds, and outline the experimental methods that have been utilized. All lattice parameter values in this chapter are reported in nm units. The literature was searched back to the year 1966.

The phase diagrams of R–M–Ge systems presented in the following sections are listed in the order of Mendeleyevs Table, and divided into four major groups:

(a) R–s element–Ge systems. In this group, lithium-containing ternary systems are the most studied (see table 1).

(b) R–p element–Ge systems. As one can see from table 1, information on these systems is still scarce. Phase diagrams have been investigated for only a few ternary R–M–Ge combinations.

(c) R–d element–Ge systems. Phase diagrams have been established for a large number of possible combinations, and crystal structures have been determined for a majority of compounds observed (table 2).

Table 1
Formation of ternary compounds and phase equilibria within ternary R–s,p element–Ge systems[a]

	Li	Na	K	Rb	Cs	Be	Mg	Ca	Sr	Ba	B	Al	Ga	In	Tl	C	Si	Sn	Pb	P	As	Sb	Bi
Sc	1											1											
Y	3										0■	3▲	5	1		1	2■						
La	3										0■	5▲		1			0■						
Ce	6■										0■	5▲	4	1		1	0■						
Pr	6■											4		1		1	0■						
Nd	5■										0	5	5	1		1	0						
Sm	4■											4		1		1	0						
Eu	1						2					2											
Gd	3■										0	5▲	6	1		1	0■						
Tb	3										0	3		1		1	0						
Dy	3										0	3		1		1	0						
Ho	7■											3		1		1	0						
Er	4▲											3				1							
Tm	4■											2	8			1							
Yb	4▲						1					3		1									
Lu	4■											2				1							

[a] The number in a table cell corresponds to the number of ternary germanide compounds observed; a solid square indicates that a complete isothermal section has been established; a solid triangle indicates that a partial isothermal section has been established.

Table 2
Formation of ternary compounds and phase equilibria within ternary R–d element–Ge systems[a]

	Ti	V	Cr	Mn	Fe	Co	Ni	Cu	Zn	Zr	Nb	Mo	Tc	Ru	Rh	Pd	Ag	Cd	Hf	Ta	W	Re	Os	Ir	Pt	Au	Hg
Sc		3■	4■	6■	8■	8■	10■	2■			1■	1■		3	3	1	1		0■	1■	0■	3■	3	2	1	1	
Y			1■	2	5	8	10■	4			1	1■		3	10	3	2						2	7	5	1	
La				2	3	5	9	4	1					5	6	5	4■						1	6	3	1	
Ce				4■	7■	11■	20■	8■	9■					7■	20■	16■	8■						1	5	12■	2	
Pr				2	9■	13■	11■	6	1					5	7	3	6						1	6	4	2	
Nd		0■	2■	4■	10■	16■	11■	7■	1	0■	0■	0■		7▲	10	6	5■		0■	0■	0■	0■	3▲	8	5	5▲	
Sm				4	10■	20■	12■	5	1					7■	15■	10■	3						1	6	21■	2	
Eu				1	0■	4■	6■	4■	1					1	2	2	4■						1	2	2	1	
Gd				9■	4	10	8	5			1			4	8	5	4					1	1	7	4	2	
Tb			1	4■	6■	10■	10■	5■			1	1		3	7	4	2						2	8	4	1	
Dy			1	3	6	9	10■	5			1	1		3	7	4	1						2	7	4	1	
Ho			1	3	6■	11■	10■	5			1	1		7■	14▲	10■	1■					1	3■	13▲	10▲	1	
Er			1	2	10■	17■	14■	6			1	1		3	9	3	1						4	6	2	1	
Tm				2	10■	15■	12■	5			1	1		3	7	3	1						4	5	3	1	
Yb				4■	5■	8■	12■	4■			1			2	4	10■	1						2	3	3■	1	
Lu				3	6	7	8	4			1	1		4	6	2	2■					1	3	3		1	

[a] The number in a table cell corresponds to the number of ternary germanide compounds observed; a solid square indicates that a complete isothermal section has been established; a solid triangle indicates that a partial isothermal section has been established.

Table 3
Formation of ternary compounds and phase equilibria within ternary R–R′–Ge systems[a]

Sc																
Y	3■															
La	2															
Ce	4■	2■	0■													
Pr	2															
Nd	3■															
Sm	3															
Eu	1															
Gd	0		0	0■												
Tb	0															
Dy	3■			1												
Ho				1							1					
Er				1												
Tm				1									1			
Yb																
Lu				2■			3									
	Sc	Y	La	Ce	Pr	Nd	Sm	Eu	Gd	Tb	Dy	Ho	Er	Tm	Yb	Lu

[a] The number in a table cell corresponds to the number of ternary germanide compounds observed; a solid square indicates that a complete isothermal section has been established.

(d) R–f element–Ge systems. Isothermal sections were constructed for a small number of ternary R–R′–Ge systems (table 3).

The general features and tendencies in the R–s, p, d, f element–Ge systems are discussed in sect. 6.

A detailed description of the structure types and crystal chemistry of ternary germanides will found in the next chapter (174) of this volume; the physical properties of ternary germanides are not included in the present review.

2. Rare-earth–s element–germanium systems

2.1. *R–Li–Ge systems*

2.1.1. *Sc–Li–Ge*

The only piece of information available on the interaction of components in the Sc–Li–Ge system is due to the work of Grund (1985) who identified and characterized by X-ray powder diffraction the compound ScLiGe (MgAgAs type, $a = 0.6407$). Sample was obtained by heating the mixture of elements in the ratio 1:2:1 in a Ta crucible which was placed into an argon filled quartz ampoule. The heating schedule was 2 to 4 h at 770 K followed by 9 to 12 h at 1070 K. The resulting alloy was not single phase ScLiGe, the other phases were not identified.

2.1.2. *Y–Li–Ge*

No ternary phase diagram exists for the Y–Li–Ge system; however the formation of three ternary compounds has been reported by Czybulka et al. (1979), Pavlyuk et al. (1990) and Pavlyuk (1993).

YLiGe was found to adopt a ZrNiAl type with lattice parameters $a = 0.7065$, $c = 0.4233$ (Czybulka et al. 1979). The measured and X-ray-derived densities were 4.56 g cm^{-3} and 4.58 g cm^{-3}, respectively. The alloy was prepared by heating the elements in the stoichiometric ratio 1:2:1 in a Ta crucible under dry Ar to a temperature above 1000 K. The sample was annealed under unspecified conditions until only YLiGe and excess Li were detected by X-ray analysis. The stoichiometry was confirmed by chemical analysis (33.3 at.% Y, 32.0 at.% Li and 34.7 at.% Ge). The purity of the starting components is unstated.

Y_4LiGe_4 was found to adopt the Tm_4LiGe_4 type ($a = 0.7144$, $b = 1.4799$, $c = 0.7757$; X-ray powder diffraction) by Pavlyuk et al. (1990). Samples were arc melted from the elements (Y 99.90 at.%, Li 98.2 at.%, Ge 99.999 at.%) under purified Ar at a pressure of 1.01×10^5 Pa and annealed at 470 K for 240 h in a Ta container which was placed in a vacuum sealed quartz ampoule. Finally the alloy was quenched in ice-cold water.

$Y_3Li_2Ge_3$ crystallizes with $Hf_3Ni_2Si_3$-type structure, $a = 0.4102$, $b = 1.0690$, $c = 1.4212$ (Pavlyuk 1993; X-ray powder diffraction). The sample preparation procedure was the same as for Y_4LiGe_4.

2.1.3. *La–Li–Ge*

No phase diagram exists at present for the ternary La–Li–Ge system; however a series of ternary compounds have been prepared and characterized by Pavlyuk et al. (1986, 1989a).

$LaLiGe_2$ was found to crystallize with a $CaLiSi_2$ type, $a = 0.7922$, $b = 0.4032$, $c = 1.0946$ (Pavlyuk et al. 1986; X-ray powder diffraction). Samples were arc melted from the elements (La 99.96 at.%, Li 98.2 at.%, Ge 99.999 at.%) under purified Ar at a pressure of 1.01×10^5 Pa and annealed at 470 K for 240 h in Ta containers.

Pavlyuk et al. (1989a) investigated the crystal structure for $La_2Li_2Ge_3$ ($La_2Li_2Ge_3$ type, $a = 0.4487$, $b = 1.8936$, $c = 0.7036$; X-ray powder diffraction) and for $LaLi_2Ge$ ($AlCr_2C$ type, $a = 0.4556$, $c = 0.7759$; X-ray powder diffraction) compounds. The alloys were prepared in the same manner as $LaLiGe_2$.

2.1.4. *Ce–Li–Ge*

An isothermal section of the Ce–Li–Ge system at 470 K was reported by Pavlyuk et al. (1989a) from an X-ray powder analysis of 154 alloys (fig. 1). The samples were obtained by arc melting the elements in purified argon under a pressure of 1.01×10^5 Pa and annealing at 470 K for 500 h in a Ta container. Finally the alloys were water quenched. Purity of the starting components was Ce 99.56%, Li 98.2% and Ge 99.999%. Six ternary compounds were found to exist. The immiscibility gap which exists in the Ce–Li binary system, extends in the ternary system to 17 at.% Ge.

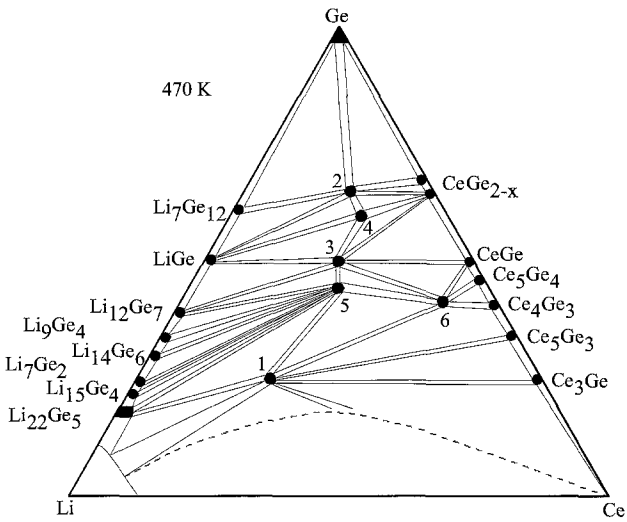

Fig. 1. Ce–Li–Ge, isothermal section at 470 K. The dashed line indicates the liquid immiscibility gap region.

Information on the ternary phases in the Ce–Li–Ge system is due to the work of two independent groups of authors.

Schuster and Czybulka (1974) investigated the crystal structure of the $CeLi_2Ge$ (1)[1] compound by means of X-ray powder and single-crystal analyses from samples which were obtained by melting of elements at 1270 K followed by long-term annealing at 1070 K and rapid quenching. The results of chemical analysis were Ce 24.6 at.%, Li 47.6 at.%, and Ge 27.8 at.%. This phase was found to adopt an orthorhombic structure with lattice parameters $a = 1.8738$, $b = 0.6926$, $c = 0.4519$. The measured density was 5.143, in agreement with the X-ray density. At variance with these data, Pavlyuk et al. (1989a) announced the $AlCr_2C$ type for the $CeLi_2Ge$ alloy which was arc melted and annealed at 470 K ($a = 0.4537$, $c = 0.7569$; X-ray powder diffraction).

Czybulka and Schuster (1979) prepared the compound $Ce_5Li_3Ge_4$ by melting components, of unspecified purity, in the atomic ratio 1:2:1 and subsequently annealing for 24 h at 1150 K. The product contained the ternary compound together with a small amount of $Li_{22}Ge_5$ and some unreacted Li. The excess of Li was extracted chemically. Chemical analysis gave Ce 42.7 at.%, Li 25.5 at.%, and Ge 31.8 at.%. The lattice parameters were $a = 0.4476$, $b = 1.8846$, $c = 0.6947$ with a measured density of 5.582 g cm^{-3} and an X-ray density (based on space group Cm2m) of 5.734 g cm^{-3}. Pavlyuk et al. (1988b) observed a ternary phase with almost identical lattice parameters ($a = 0.44795$, $b = 1.8846$, $c = 0.69570$) and with the composition $Ce_2Li_2Ge_3$ (5) (X-ray single-crystal diffraction).

The remaining four ternary compounds were prepared in the same manner as described by Pavlyuk et al. (1989a): Ce_2LiGe_6 (2), Pr_2LiGe_6 type, $a = 0.4140$, $b = 2.1054$, $c = 0.4363$ (Pavlyuk et al. 1988b); $CeLiGe_2$ (3), $CaLiSi_2$ type, $a = 0.7185$, $b = 0.3965$, $c = 1.0748$

[1] Numbers in parentheses refer to corresponding locations in figures and tables.

(Pavlyuk et al. 1986); Ce_2LiGe_5 (4), Ce_2MnGe_5 type, $a=0.4360$, $b=0.4197$, $c=2.0711$ (Pavlyuk et al. 1989a); $Ce_{26}Li_5Ge_{22+x}$ (6) $x=0.37$, own structure type, $a=1.5402$, $c=1.0900$ (Pavlyuk et al. 1987b).

2.1.5. *Pr–Li–Ge*

The isothermal section for the Pr–Li–Ge system at 470 K was established by Pavlyuk (1993) and Bodak et al. (1995) (fig. 2). For sample preparation, see Ce–Li–Ge. One ternary compound, PrLiGe, was confirmed, and five ternary phases were observed for the first time. No homogeneous ranges were encountered for the ternary compounds. The liquid immiscibility region, existing in the Pr–Li binary system, extends to 17 at.% Ge in the ternary system.

Grund et al. (1986) reported the crystal structure of the PrLiGe (6) compound: ZrNiAl type, $a=0.7048$, $c=4242$. The sample was prepared by heating the elements (99.99 mass% Pr, 99.7 mass% Li, 99.999 mass% Ge) in the ratio 1:2:1 in a Ta crucible which was placed in an Ar-filled quartz ampoule. The heating schedule was 5–12 h at 850 K followed by 12–15 h at 1170 K. Excess Li was extracted from the product chemically. Chemical analysis confirmed the stoichiometry to be 33.2 at.% Pr, 34.5 at.% Li, and 32.3 at.% Ge.

Five other ternary compounds were observed and characterized by the Ukrainian group at L'viv University: Pr_2LiGe_6 (1) belongs to a new structure type, $a=0.41268$, $b=2.10520$, $c=0.43455$ (Pavlyuk et al. 1988a); $PrLi_2Ge$ (2) adopts $AlCr_2C$ with $a=0.4499$, $c=0.7543$ (Pavlyuk et al. 1989a); $PrLiGe_2$ (3) is of the $CaLiSi_2$ type, $a=0.7813$, $b=0.3948$, $c=1.0695$ (Pavlyuk et al. 1986); Pr_2LiGe_5 (4) crystallizes with the Ce_2MnGe_5 type, $a=0.4299$, $b=0.4157$, $c=2.0597$ (Pavlyuk et al. 1989a); $Pr_2Li_2Ge_3$ (5) belongs to the

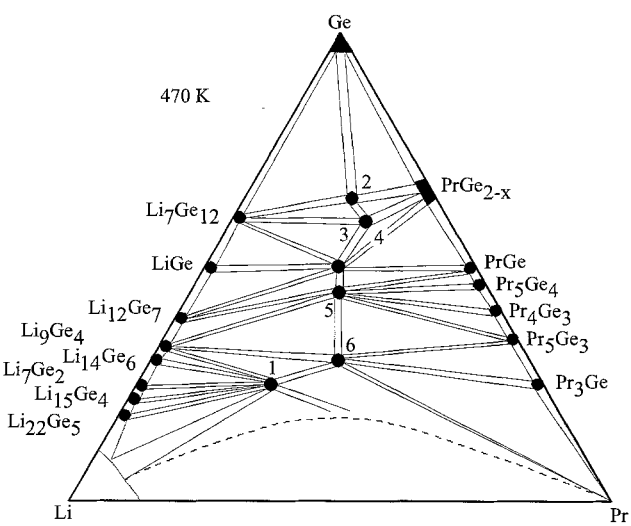

Fig. 2. Pr–Li–Ge, isothermal section at 470 K. The dashed line indicates the liquid immiscibility gap region.

$Ce_2Li_2Ge_3$ type, $a=0.4422$, $b=1.8653$, $c=0.6908$ (Pavlyuk et al. 1989a). The alloys for investigations were prepared in the same manner as used for the investigation of the Pr–Li–Ge isothermal section.

2.1.6. *Nd–Li–Ge*

Pavlyuk and Bodak (1992a) were the first to investigate the phase equilibria within the Nd–Li–Ge system at 470 K over the whole concentration region by X-ray powder diffraction from the samples which were prepared in the manner indicated in the present review in the Ce–Li–Ge section. Phase relations are characterized by the existence of five ternary compounds (fig. 3). The liquid immiscibility field, originating from the Nd–Li binary system, extends to 17 at.% Ge at higher temperatures in the ternary system.

NdLiGe (5) was found to crystallize with the ZrNiAl type with lattice parameters as $a=0.7267$, $c=0.4351$ by Czybulka et al. (1990) (X-ray diffraction). Results of chemical analysis confirmed the stoichiometry (33.3 at.% Nd, 34.1 at.% Li and 32.6 at.% Ge). The alloy was obtained by heating the elements in the ratio 1:2.5:1 in a Ta crucible under dry Ar for 12 h at 770 K followed by slow heating to 1100 K and holding at 1100 for 48 h.

The crystal structure of the $NdLiGe_2$ (2) compound was investigated by Pavlyuk et al. (1986). It was found to adopt the $CaLiSi_2$ type with lattice parameters as $a=0.7728$, $b=0.3915$, $c=1.0564$. For experimental details, see Nd–Li–Ge.

Pavlyuk et al. (1989a) prepared and characterized the compounds $NdLi_2Ge$ (1), $AlCr_2C$ type, $a=0.4445$, $b=0.7455$; Nd_2LiGe_5 (3), Ce_2MnGe_5 type, $a=0.4297$, $b=0.4152$, $c=2.0378$; $Nd_2Li_2Ge_3$ (4), $Ce_2Li_2Ge_3$ type, $a=0.4414$, $b=1.8621$, $c=0.6892$. For sample preparation, see Nd–Li–Ge.

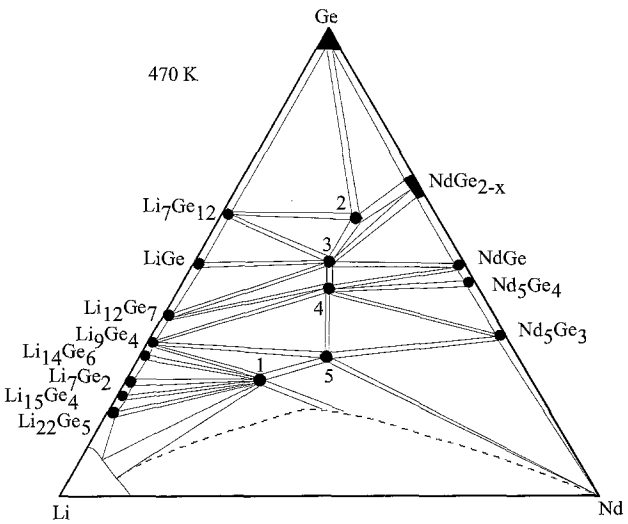

Fig. 3. Nde–Li–Ge, isothermal section at 470 K. The dashed line indicates the liquid immiscibility gap region.

2.1.7. *Sm–Li–Ge*

The phase-field distribution in the ternary Sm–Li–Ge system at 470 K is characterized by existence of four ternary compounds (fig. 4) (Pavlyuk 1993, Bodak et al. 1995). No homogeneous ranges were encountered for the ternary compounds. The immiscibility gap which exists in the Sm–Li binary system, extends in the ternary system to 17 at.% Ge. The alloys were synthesized by arc melting in a purified Ar atmosphere under a pressure of 1.01×10^5 Pa using 99.89 mass% Sm, 98.2 mass% Li and 99.999 mass% Ge. The resulting buttons were annealed at 470 K for 500 h in a Ta container. Finally the alloys were water quenched.

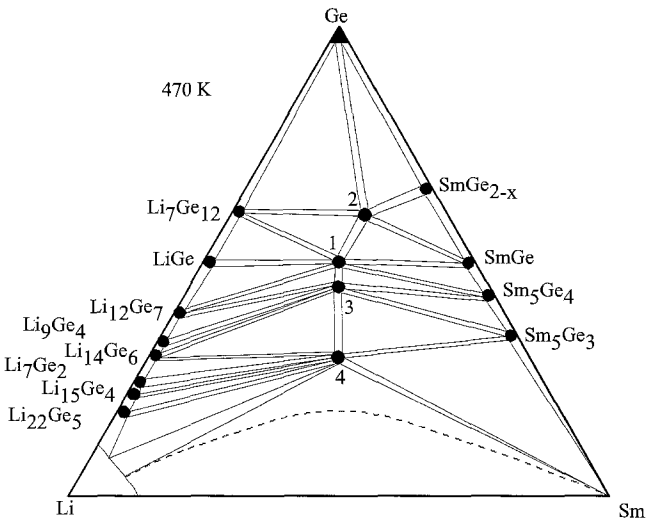

Fig. 4. Sm–Li–Ge, isothermal section at 470 K. The dashed line indicates the liquid immiscibility gap region.

SmLiGe (4) was found to crystallize with the ZrNiAl type with a lattice parameters $a = 0.7192$, $c = 0.4308$ by Czybulka et al. (1990) (X-ray diffraction). Chemical analysis gave 33.5 at.% Sm, 32.3 at.% Li and 34.2 at.% Ge, confirming the stoichiometry. The alloy was obtained by heating the elements in the ratio 1:2.5:1 in a Ta crucible under dry Ar for 12 h at 770 K followed by slow heating to 1100 K and holding at 1100 K for 48 h. Pavlyuk (1989) confirmed the crystal structure and determined the lattice parameters as $a = 0.7193$, $c = 0.4316$.

$SmLiGe_2$ (1) was observed to adopt the $CaLiSi_2$ type, $a = 0.7741$, $b = 0.3973$, $c = 1.0488$ (Pavlyuk et al. 1986; X-ray diffraction). For experimental details, see Sm–Li–Ge.

Pavlyuk et al. (1989a) prepared and characterized the following compounds: Sm_2LiGe_5 (2), Ce_2MnGe_5 type, $a = 0.4238$, $b = 0.4123$, $c = 2.0287$; $Sm_2Li_2Ge_3$ (3), $Ce_2Li_2Ge_3$ type, $a = 0.4394$, $b = 1.8537$, $c = 0.6860$. For sample preparation, see Sm–Li–Ge.

2.1.8. *Eu–Li–Ge*

The only information available on the interaction of the components in the Eu–Li–Ge system is the formation of the $EuLiGe_2$ compound which was observed by Pavlyuk et al. (1986). It was reported to adopt the $CaLiSi_2$ type, $a = 0.8174$, $b = 0.3977$, $c = 1.0988$ from X-ray powder diffraction analysis. For sample preparation, see Ce–Li–Ge.

2.1.9. *Gd–Li–Ge*

Figure 5 represents the isothermal section of the Gd–Li–Ge system at 470 K after Pavlyuk (1989). For sample preparation, see Ce–Li–Ge. Phase relations are characterized by the existence of three ternary compounds. The liquid immiscibility gap which exists in the Gd–Li system, extends to 22 at.% Ge in the ternary system.

Czybulka et al. (1979) reported the crystallographic characteristics for the GdLiGe compound (ZrNiAl type, $a = 0.7135$, $c = 0.4285$). The measured and X-ray densities were 6.17 g cm^{-3} and 6.23 g cm^{-3}, respectively. The alloy was prepared by heating the elements in the stoichiometric ratio 1:2:1 in a Ta crucible under dry Ar to a temperature above 1000 K. The sample was annealed under unspecified conditions until only GdLiGe and excess Li were detected by X-ray analysis. The stoichiometry was confirmed by chemical analysis (34.0 at.% Gd, 33.2 at.% Li and 32.8 at.% Ge).

$GdLiGe_2$ and Gd_4LiGe_4 were found to adopt the $CaLiSi_2$ type ($a = 0.7784$, $b = 0.3867$, $c = 1.0416$; X-ray powder diffraction) by Pavlyuk (1989) and the Tm_4LiGe_4 type ($a = 0.7159$, $b = 1.4749$, $c = 0.7713$; X-ray powder diffraction) by Pavlyuk et al. (1990), respectively. For sample preparation, see Gd–Li–Ge.

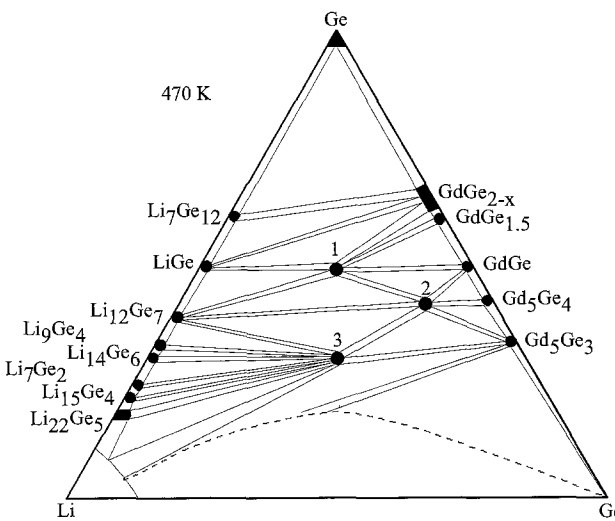

Fig. 5. Gd–Li–Ge, isothermal section at 470 K. The dashed line indicates the liquid immiscibility gap region.

2.1.10. *Tb–Li–Ge*

Information on the interaction of terbium with lithium and germanium is due to the work of two groups of authors: Grund et al. (1986) and Pavlyuk (1993).

Grund et al. (1986) investigated the crystal structure of TbLiGe. The structure type was established as ZrNiAl with lattice parameters $a = 0.7083$, $c = 0.4257$ from X-ray powder diffraction analysis. The measured density was 6.44 g cm^{-3} and the X-ray density 6.42 g cm^{-3}. The sample was prepared by heating the elements (99.99 mass% Tb, 99.7 mass% Li, 99.999 mass% Ge) in the ratio 1:2:1 in a Ta crucible which was placed in an Ar-filled quartz ampoule. The heating schedule was 5–12 h at 850 K followed by 12–15 h at 1170 K. Excess Li was extracted from the product chemically. Chemical analysis confirmed the stoichiometry to be 32.5 at.% Tb, 34.1 at.% Li and 33.4 at.% Ge.

Two more compounds were observed and characterized by Pavlyuk (1993): Tb_4LiGe_4 with the Tm_4LiGe_4 type, $a = 0.7079$, $b = 1.4682$, $c = 0.7699$ (X-ray powder diffraction) and $Tb_3Li_2Ge_3$ with the $Hf_3Ni_2Si_3$ type, $a = 0.4107$, $b = 1.0740$, $c = 1.4198$ (X-ray powder diffraction). For experimental details, see Ce–Li–Ge.

2.1.11. *Dy–Li–Ge*

Little information exists on the Dy–Li–Ge system, however three ternary compounds were found and characterized.

Grund et al. (1986) reported the crystal structure of the DyLiGe compound: ZrNiAl type, $a = 0.7048$, $c = 0.4242$. The measured density was 6.46 g cm^{-3} and the X-ray density 6.61 g cm^{-3}. Results of chemical analysis confirmed the stoichiometry to be 33.2 at.% Dy, 34.5 at.% Li and 32.3 at.% Ge. For sample preparation, see Tb–Li–Ge.

Two more compounds were observed and characterized by Pavlyuk (1993): Dy_4LiGe_4 with the Tm_4LiGe_4 type, $a = 0.7064$, $b = 1.4654$, $c = 0.7681$ (X-ray powder diffraction) and $Dy_3Li_2Ge_3$ with the $Hf_3Ni_2Si_3$ type, $a = 0.4097$, $b = 1.0602$, $c = 1.4121$ (X-ray powder diffraction). For experimental details, see Ce–Li–Ge.

2.1.12. *Ho–Li–Ge*

Phase relations have been established for the ternary Ho–Li–Ge system at 470 K by Pavlyuk (1993) (fig. 6); seven ternary compounds have been observed and characterized. The immiscibility gap which exists in the Ho–Li binary system, extends in the ternary system to 17 at.% Ge. For experimental details, see Ce–Li–Ge.

From the preliminary investigation of the interaction of holmium with lithium and germanium, HoLiGe was found to crystallize with ZrNiAl type with lattice parameters $a = 0.7036$, $c = 0.4241$ by Czybulka et al. (1990) (X-ray diffraction). Chemical analysis gave 33.4 at.% Ho, 34.2 at.% Li and 32.4 at.% Ge. The alloy was obtained by heating the elements in the ratio 1:2.5:1 in a Ta crucible under dry Ar for 12 h at 770 K followed by slow heating to 1100 K and holding at 1100 K for 48 h.

Investigating the phase equilibria in the ternary Ho–Li–Ge system, Pavlyuk (1993) observed and characterized three ternary compounds: Ho_4LiGe_4 was found to adopt a Tm_4LiGe_4 type, $a = 0.7039$, $b = 1.4649$, $c = 0.7674$ (X-ray powder diffraction); $Ho_3Li_2Ge_3$

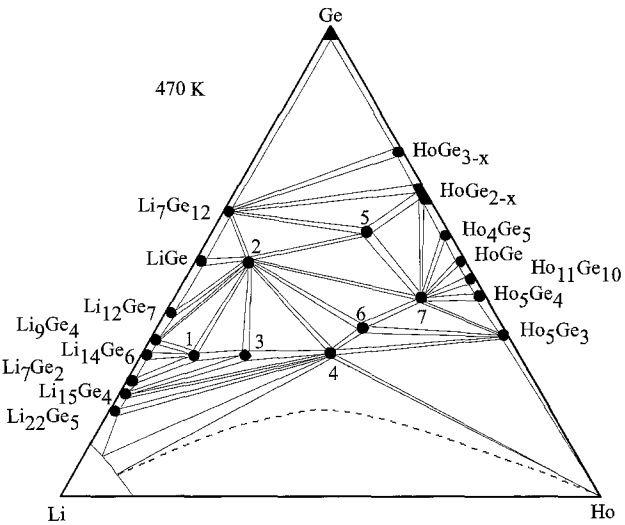

Fig. 6. Ho–Li–Ge, isothermal section at 470 K. The dashed line indicates the liquid immiscibility gap region.

was reported to crystallize with the $Hf_3Ni_2Si_3$ type, $a=0.4003$, $b=1.0509$, $c=1.4097$ (X-ray powder diffraction); $TmLi_{1-x}Ge_2$ type was announced for the $HoLi_{1-x}Ge_2$ compound, $a=0.4017$, $b=0.8126$, $c=0.3881$, $\gamma=104.24°$. Three more ternary compounds with an unknown structure were observed by Pavlyuk (1993), $HoLi_6Ge_3$, $HoLi_4Ge_5$ and $Ho_2Li_5Ge_3$. For experimental details, see Ce–Li–Ge.

2.1.13. *Er–Li–Ge*

A partial isothermal section for the Er–Li–Ge system was constructed by Pavlyuk (1993); four ternary compounds were found to exist (fig. 7). For sample preparation, see Ce–Li–Ge.

ErLiGe (2) was found to crystallize with a ZrNiAl type with lattice parameters $a=0.7005$, $c=0.4214$ (Pavlyuk 1989; Pavlyuk et al. 1991a) from X-ray powder diffraction of arc melted in a purified Ar atmosphere under a pressure of 1.01×10^5 Pa samples which were annealed in Ta containers at 470 K for 240 h. Purity of the starting components was 99.82 mass% Er, 98.2 mass% Li and 99.999 mass% Ge. Czybulka et al. (1990) confirmed the crystal structure for the compound of equiatomic composition, ZrNiAl type, $a=0.6985$, $c=0.4219$ (X-ray single-crystal data). Chemical analysis gave 33.6 at.% Er, 32.4 at.% Li and 34.0 at.% Ge. For sample preparation, see Ho–Li–Ge.

Pavlyuk et al. (1990) reported on the crystal structure investigation for the Er_4LiGe_4 (4) compound, Tm_4LiGe_4 type, $a=0.7031$, $b=1.4555$, $c=0.7664$ (X-ray powder diffraction). For sample preparation, see Er–Li–Ge system after Pavlyuk (1989) and Pavlyuk et al. (1991a).

Two more ternary compounds were observed and characterized by Pavlyuk (1993): $Er_3Li_2Ge_3$ (3) was reported to crystallize with the $Hf_3Ni_2Si_3$ type, $a=0.4001$, $b=$

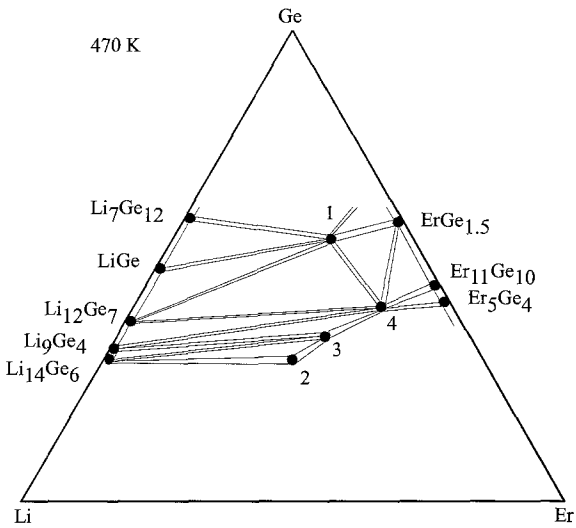

Fig. 7. Er–Li–Ge, partial isothermal section at 470 K (30–70 at.% Ge).

1.0498, $c = 1.4091$ (X-ray powder diffraction); $TmLi_{1-x}Ge_2$ type was announced for the $ErLi_{1-x}Ge_2$ (1) compound, $a = 0.4007$, $b = 0.8101$, $c = 0.3876$, $\gamma = 104.24°$. For experimental details, see Er–Li–Ge after Pavlyuk (1989) and Pavlyuk et al. (1991a).

2.1.14. *Tm–Li–Ge*

The phase diagram for the Tm–Li–Ge system was constructed by Pavlyuk (1989) (fig. 8). Phase relations are characterized by existence of four ternary compounds. No

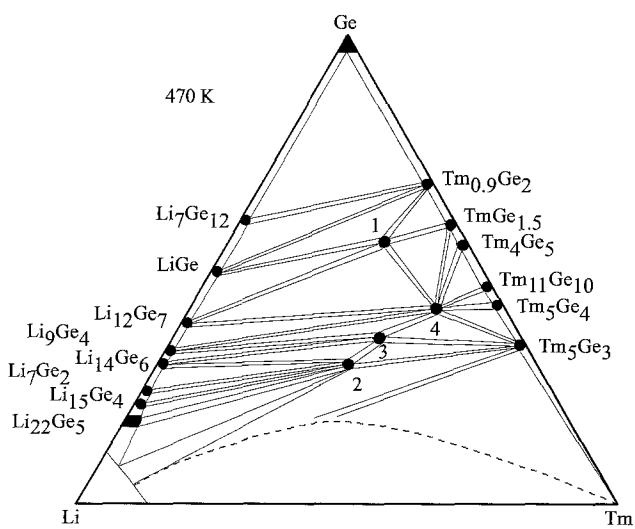

Fig. 8. Tm–Li–Ge, isothermal section at 470 K. The dashed line indicates the liquid immiscibility gap region.

homogeneity regions were observed for the ternary phases. The liquid immiscibility gap which originates from the Tm–Li binary system, stretches to 23 at.% Ge in the ternary system. For sample preparation, see Ce–Li–Ge system.

The crystal structure for four ternary compounds was established by the Ukrainian group at L'viv University: $TmLi_{1-x}Ge_2$ (1) crystallizes with its own structure type, $a=0.4008$, $b=0.8123$, $c=0.3875$, $\gamma=104.24°$ (Pavlyuk et al. 1991b; X-ray single-crystal data); TmLiGe (2) belongs to the ZrNiAl type, $a=0.6917$, $c=0.4813$ (Pavlyuk et al. 1991a; X-ray powder diffraction); $Tm_3Li_2Ge_3$ (3) adopts the $Hf_3Ni_2Si_3$ type, $a=0.3990$, $b=1.0506$, $c=1.4090$ (Pavlyuk and Bodak 1992b); Tm_4LiGe_4 (4) represents a new type of structure, $a=0.7013$, $b=1.4429$, $c=0.7524$ (Pavlyuk et al. 1990; X-ray single-crystal diffraction data). For experimental details, see Ce–Li–Ge.

2.1.15. *Yb–Li–Ge*

The phase-field distribution in the ternary Yb–Li–Ge system at 470 K is characterized by existence of four ternary compounds (fig. 9) (Pavlyuk 1993 and Bodak et al. 1995). No homogeneous ranges were encountered for the ternary compounds. The immiscibility gap which exists in the Yb–Li binary system, extends in the ternary system to 17 at.% Ge. The alloys were synthesized by arc melting in a purified Ar atmosphere under a pressure of 1.01×10^5 Pa. The resulting buttons were annealed at 470 K for 500 h in a Ta container which were placed in the evacuated vacuum sealed quartz tube. Finally the alloys were quenched in ice cold water. The purity of the starting materials was Yb 99.82 mass%, Li 98.2 mass% and Ge 99.999 mass%.

Grund et al. (1986) reported the crystal structure of the YbLiGe (1) compound: ZrNiAl type, $a=0.6939$, $c=4183$. The measured density was 7.18 g cm^{-3} and the X-ray density 7.21 g cm^{-3}. Results of chemical analysis confirmed the stoichiometry and gave

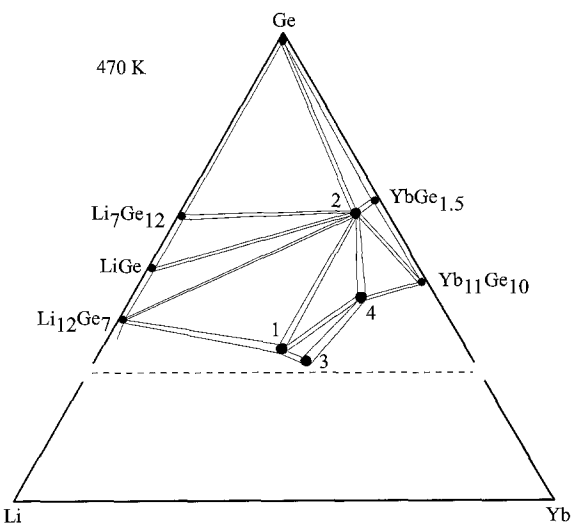

Fig. 9. Yb–Li–Ge, partial isothermal section at 470 K (30–70 at.% Ge).

33.6 at.% Yb, 33.2 at.% Li and 33.2 at.% Ge. For sample preparation, see Tb–Li–Ge. The crystal structure was confirmed by Pavlyuk (1993) and Bodak et al. (1995): $a = 0.6944$, $c = 0.4190$.

The results of X-ray single-crystal investigation for three other compounds are the following: Yb_8LiGe_{13} (2) belongs to a new structure type, $a = 1.1317$, $b = 1.5577$, $c = 1.0817$, $\gamma = 106.24°$ (Pavlyuk et al. 1987a); $Yb_5Li_4Ge_4$ (3) crystallizes with the $Nb_5Cu_4Si_4$ type, $a = 1.1210$, $c = 0.43698$ (Pavlyuk et al. 1989b); Yb_4LiGe_4 (4) adopts the Tm_4LiGe_4 type, $a = 0.701$, $b = 1.441$, $c = 0.753$ (Pavlyuk et al. 1990). The samples were prepared in the same manner as the alloys for the investigations of the Yb–Li–Ge phase diagram.

2.1.16. *Lu–Li–Ge*

The phase diagram for the Lu–Li–Ge system was constructed by Pavlyuk (1993) (fig. 10). The phase relations are characterized by existence of four ternary compounds. No homogeneity regions were observed for the ternary phases. The liquid immiscibility gap which originates from the Lu–Li binary system, stretches to 23 at.% Ge in the ternary system. For sample preparation, see Ce–Li–Ge.

The crystal structure for four ternary compounds was established by the Ukrainian group at L'viv University: $LuLi_{1-x}Ge_2$ (1) crystallizes with the $TmLi_{1-x}Ge_2$ structure type, $a = 0.3988$, $b = 0.8019$, $c = 0.3867$, $\gamma = 104.2°$ (Pavlyuk et al. 1991b; X-ray powder diffraction); LuLiGe (2) belongs to the ZrNiAl type, $a = 0.6933$, $c = 0.4200$ (Pavlyuk et al. 1991a; X-ray powder diffraction); $Lu_3Li_2Ge_3$ (3) adopts the $Hf_3Ni_2Si_3$ type, $a = 0.3959$, $b = 1.0475$, $c = 1.4051$ (Pavlyuk and Bodak 1992b); Lu_4LiGe_4 (4) has the Tm_4LiGe_4 type of structure, $a = 0.7000$, $b = 1.4322$, $c = 0.7524$ (Pavlyuk et al. 1990; X-ray powder diffraction data). For experimental details, see Ce–Li–Ge.

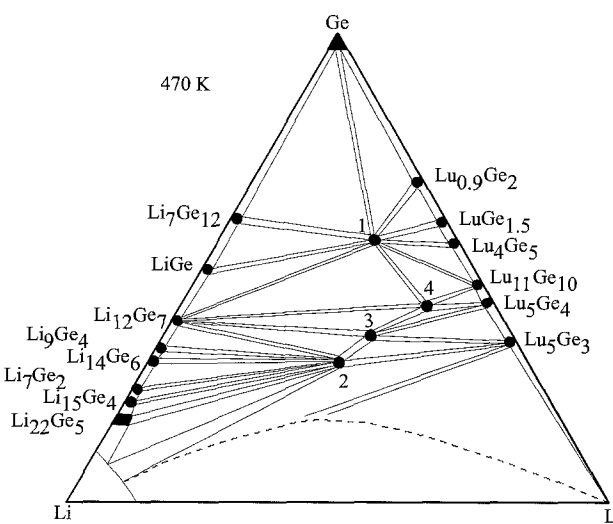

Fig. 10. Lu–Li–Ge, isothermal section at 470 K. The dashed line indicates the liquid immiscibility gap region.

2.2. *R–Mg–Ge systems*

2.2.1. *Eu–Mg–Ge*

The information on the interaction of the components in the Eu–Mg–Ge system is due to Zmii et al. (1973) and Merlo et al. (1993).

Zmii et al. (1973) investigated the crystal structures of $EuMg_3Ge_3$ compound (own structure type, $a=0.4485$, $b=3.060$, $c=0.4485$; X-ray single-crystal diffraction).

Merlo et al. (1993) synthesized EuMgGe compound and established its crystal structure as the TiNiSi type, $a=0.7756$, $b=0.4580$, $c=0.8444$ from X-ray powder diffraction. The alloy was obtained from metals with a purity of 99% for europium, and 99.999% for magnesium and germanium. The proper amounts of constituent elements were placed in sealed tantalum crucibles, which were arc welded under argon, melted in an induction furnace and annealed for 1 month at 870 K.

2.2.2. *Yb–Mg–Ge*

Merlo et al. (1993) investigated the crystal structure of YbMgGe compound by the X-ray single-crystal method. It was found to adopt the TiNiSi type, $a=0.7474$, $b=0.4436$, $c=0.8343$. The sample was synthesized in the same manner as EuMgGe.

3. Rare-earth–p element–germanium systems

3.1. *R–B–Ge systems*

3.1.1. *Y–B–Ge*

The isothermal section of the Y–B–Ge system at 1070 K (fig. 11) was investigated by Marko et al. (1978) using X-ray powder analysis of samples prepared by arc melting solid pieces of yttrium and germanium with compacted powder of boron. The melted buttons were then annealed in evacuated quartz tubes at 1070 K. No ternary compounds were observed.

3.1.2. *La–B–Ge*

An early investigation of the La–B–Ge system reported on the existence of solid solution of boron in the binary La_5Ge_3 compound which was observed by X-ray methods (Mayer and Felner 1974). Samples were obtained by heating of mixture of starting components up to 1870 K in the He atmosphere in tantalum crucibles. The phase relations in the complete isothermal section at 970 K have been determined by Marko et al. (1978). For sample preparation, see Y–B–Ge. Phase relations are characterized by the absence of ternary compounds (fig. 12). No solubility of boron in the La_5Ge_3 compound has been observed.

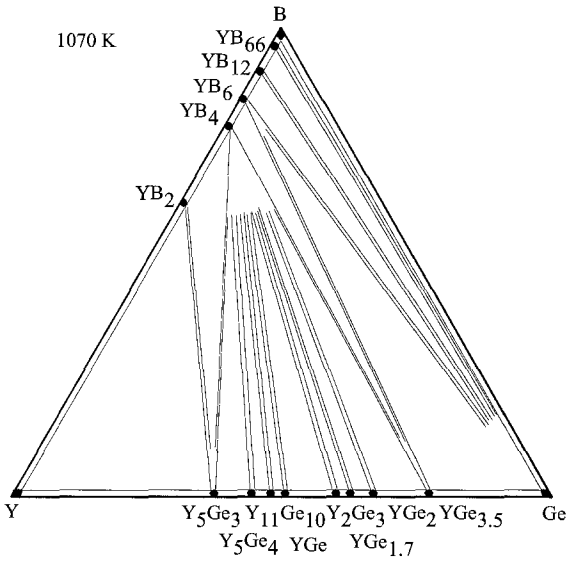

Fig. 11. Y–B–Ge, isothermal section at 1070 K.

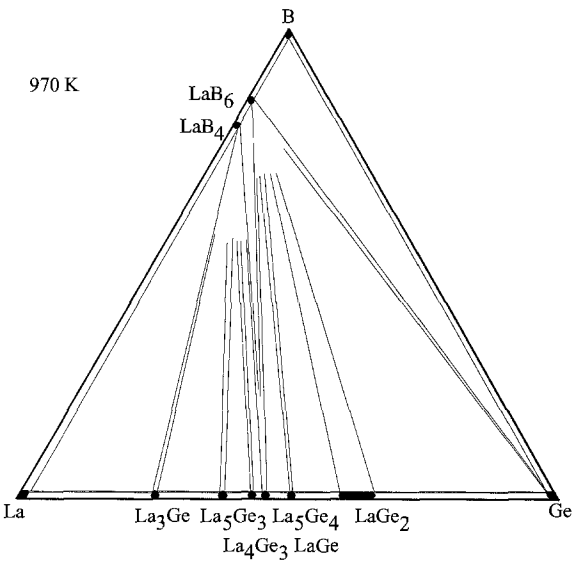

Fig. 12. La–B–Ge, isothermal section at 970 K.

3.1.3. *Ce–B–Ge*

Phase relations in the isothermal section at 870 K have been determined by Marko and Kuz'ma (1979) from X-ray powder diffraction analysis (fig. 13). For sample preparation, see Y–B–Ge. No ternary compounds have been found. Mutual solid solubilities of the binary compounds were found to be negligible.

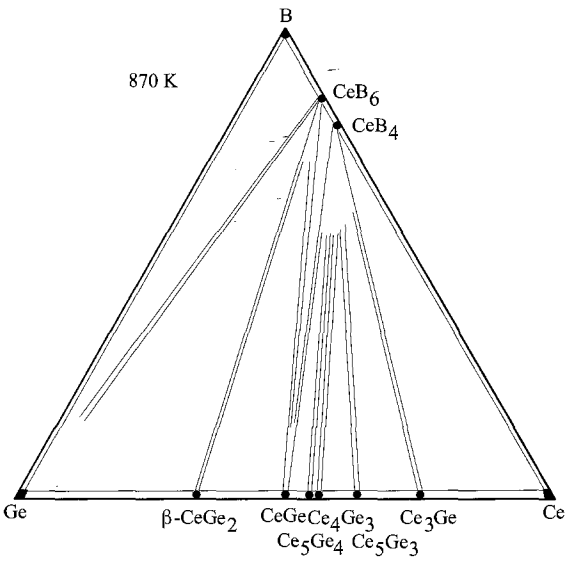

Fig. 13. Ce–B–Ge, isothermal section at 870 K.

3.1.4. *Nd–B–Ge*

No phase diagram exists for the Nd–B–Ge system, however the solubility of boron in the Nd_5Ge_3 compound has been studied by means of X-ray diffraction (Mayer and Felner 1974). The limits of solid solution have not been reported. Samples were obtained by heating of mixture of starting components up to 1870 K in the He atmosphere in Ta crucibles.

3.1.5. *Gd–B–Ge*

The only information on the Gd–B–Ge system is due to Mayer and Felner (1974) who investigated the solubility of boron in the Gd_5Ge_3 compound by means of X-ray diffraction. The limits of solid solution have not been indicated. For sample preparation, see La–B–Ge.

3.1.6. *Tb–B–Ge*

No ternary phase diagram exists for the Tb–B–Ge system; however the formation of a solid solution originating at the binary Tb_5Ge_3 compound has been observed (Mayer and Felner 1974). The maximum concentration of boron in Tb_5Ge_3 has not been shown. For experimental details, see La–B–Ge.

3.1.7. *Dy–B–Ge*

Solubility of boron in the Dy_5Ge_3 compound has been studied by X-ray methods (Mayer and Felner 1974). For experimental details, see La–B–Ge.

3.2. *R–Al–Ge systems*

3.2.1. *Sc–Al–Ge*

No phase diagram exists for the Sc–Al–Ge system, however the formation of $Sc_{11}Al_2Ge_8$ compound has been reported by Zhao et al. (1991). It was found to crystallize with a new ordered variant of the $Ho_{11}Ge_{10}$ type with Al atoms substituting for Ge atoms on one crystallographic site. The lattice parameters are $a = 1.0419$, $c = 1.4974$. A single crystal was isolated from a sample which was arc melted in an argon atmosphere. Purity of starting components was 99.99 mass% for Sc, Al and Ge.

The same group of authors observed and characterized the ScAlGe compound, YAlGe type, $a = 0.3934$, $b = 0.9928$, $c = 0.5519$ (Zhao and Parthé 1990; X-ray powder diffraction).

3.2.2. *Y–Al–Ge*

Figure 14 represents the partial isothermal section of the Y–Al–Ge system at 770 K after Muravyeva et al. (1971). Three ternary compounds were found to exist from X-ray phase analysis of alloys prepared by arc melting the proper amounts of pure components in an argon atmosphere. The resulting buttons were annealed for two weeks at 770 K and finally quenched in ice-cold water. Purity of starting components was greater than 99.9 mass%.

Muravyeva et al. (1971) reported on the crystal structure investigation for the $YAl_{1.7-2.2}Ge_{2.3-1.8}$ (1) ($CaAl_2Si_2$type, $a = 0.4196$–0.4196, $b = 0.6702$–0.6775; X-ray powder diffraction).

The $YAl_{0.9-1.3}Ge_{1.1-0.7}$ compound (3) was claimed by Yanson (1975) to adopt the DyAlGe type ($Cmc2_1$ space group) at the equiatomic composition with lattice parameters $a = 0.4200$, $b = 1.062$, $c = 0.5908$ (X-ray powder diffraction data). At variance with these data, Zhao and Parthé (1990) announced the YAlGe type with Cmcm space

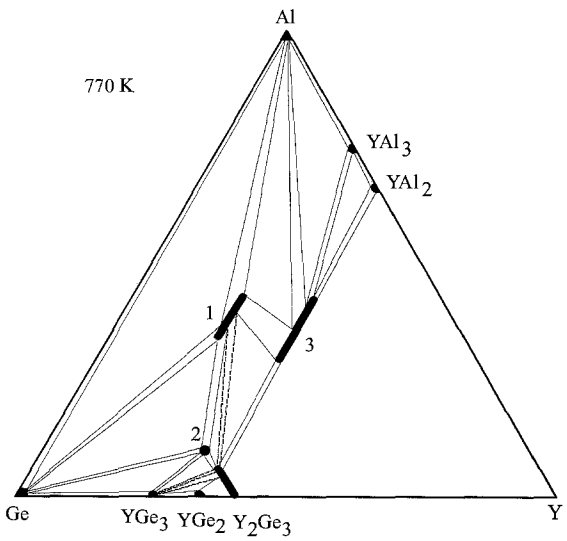

Fig. 14. Y–Al–Ge, partial isothermal section at 770 K (0–33 at.% Y).

group and lattice parameters $a = 0.40504$, $b = 1.04440$, $c = 0.57646$ (X-ray single-crystal diffraction).

Y_3AlGe_6 (2) has a hexagonal lattice with unknown unit cell dimensions (Yanson 1975).

3.2.3. *La–Al–Ge*

Phase equilibria in the partial isothermal section (0–33 at.% La) at 770 K have been derived by Muravyeva and Zarechnyuk (1970) by means of X-ray powder diffraction of alloys, as shown in fig. 15. For sample preparation, see Y–Al–Ge. Five ternary compounds were found to exist. $LaGe_2$ dissolves 13 at.% Al.

The formation of two ternary compounds was reported in the early investigations performed by Raman and Steinfink (1967): $LaAl_{1.5-1.8}Ge_{0.5-0.2}$ (5) with AlB_2 type, $a =$ 0.435–0.440, $c = 0.442$–0.440 and LaAlGe (4), α-$ThSi_2$ type, $a = 0.4307$, $c = 1.472$. The structure of the latter phase has been confirmed by Zhao and Parthé (1990), $a = 0.4341$, $c = 1.4784$ (X-ray powder diffraction). The alloy was prepared by arc melting under an argon atmosphere followed by annealing at 873 K for 100 h.

Muravyeva et al. (1971) observed the $CaAl_2Si_2$ type for the $LaAl_2Ge_2$ compound (2) ($a = 0.428$, $c = 0.700$; X-ray powder diffraction).

Two more ternary compounds which had been indicated as ~$LaAlGe_3$ (1) and ~$LaAl_{0.8-1}Ge_{2.2-2}$ (3) by Muravyeva and Zarechnyuk (1970) in the course of investigation of the isothermal section, have been characterized by the researchers from Geneva University. $La_2Al_{1+x}Ge_{6-x}$ ($x = 0.60$) is a new structure type which is a vacancy variant of the orthorhombic $SmNiGe_3$ structure, $a = 0.8373$, $b = 0.8833$, $c = 1.0887$, $\beta = 101.34°$ (Zhao and Parthé 1991a; X-ray single-crystal diffraction data). $La_2Al_3Ge_4$ was announced to crystallize with the $Ba_2Cd_3Bi_4$ type, $a = 0.6146$, $b = 1.5194$, $c = 0.8037$ (X-ray single-

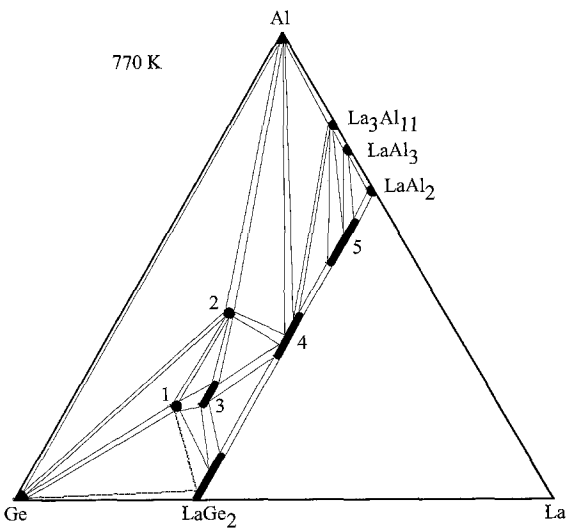

Fig. 15. La–Al–Ge, partial isothermal section at 770 K (0–33 at.% La).

crystal diffraction, Zhao and Parthé 1991b). Single crystals were isolated from samples obtained by arc melting the proper amounts of pure components in an argon atmosphere (La, Al and Ge: 99.99 mass%). The weight losses were 0.4% and 0.5% for $La_2Al_{1+x}Ge_{6-x}$ ($x = 0.60$) and $La_2Al_3Ge_4$, respectively. The alloys were annealed at 770 K for two months in an Ar-filled silica tube.

3.2.4. *Ce–Al–Ge*

The isothermal section of the Ce–Al–Ge system at 770 K (0–33 at.% Ce) was reported by Muravyeva and Zarechnyuk (1970) from an X-ray powder analysis of alloys prepared by arc melting the elements in purified argon and annealing at 770 K for two weeks. Finally the alloys were quenched in water. The purity of the starting components was greater than 99.9 mass%. Five ternary compounds were found to exist (fig. 16). For all of them except $CeAl_2Ge_2$, the formation of homogeneity regions was observed.

Information on the ternary phases in the Ce–Al–Ge system is due to the work of three independent groups of authors.

The formation of one ternary compound was reported in an early investigation performed by Raman and Steinfink (1967): $CeAl_{0.5-0.6}Ge_{0.5-0.4}$ (5) with the AlB_2 type, $a = 0.433–0.436$, $c = 0.432–0.429$.

Muravyeva and Zarechnyuk (1970) observed the $CaAl_2Si_2$ type for the $CeAl_2Ge_2$ compound (2) ($a = 0.427$, $c = 0.695$; X-ray powder diffraction). For sample preparation, see above.

Three more ternary compounds which had earlier been indicated as $\sim CeAl_{0.5-0.8}Ge_{3.5-3.2}$ (1), $\sim CeAl_{0.8-1}Ge_{2.2-2}$ (3) and $CeAl_{0.7-1.2}Ge_{1.3-0.8}$ (4) by Muravyeva and Zarechnyuk (1970) during the investigation of the isothermal section, have been characterized by the group of authors from Geneva University. $Ce_2Al_{1+x}Ge_{6-x}$ (1) was found to adopt the

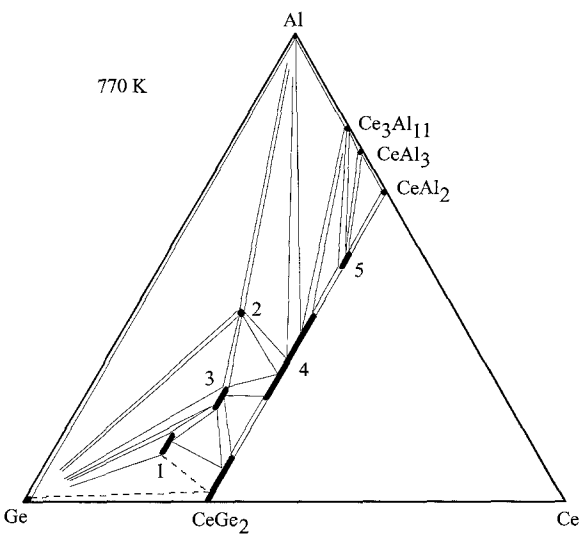

Fig. 16. Ce–Al–Ge, partial isothermal section at 770 K (0–33 at.% Ce).

$La_2Al_{1+x}Ge_{6-x}$-type structure, $a = 0.8292$, $b = 0.8691$, $c = 1.0739$, $\beta = 101.15°$ (Zhao and Parthé 1991a; X-ray powder diffraction data). $Ce_2Al_3Ge_4$ (3) was announced to crystallize with the $Ba_2Cd_3Bi_4$ type, $a = 0.60935$, $b = 1.5061$, $c = 0.7974$ (X-ray powder diffraction; Zhao and Parthé 1991b). α-$ThSi_2$-type structure was observed for the CeAlGe (4) compound, $a = 0.42889$, $c = 1.4721$ (X-ray powder diffraction, Zhao and Parthé 1990). Samples were obtained by arc melting the proper amounts of pure components in an argon atmosphere (Ce, Al and Ge: 99.99 mass%). The alloys were annealed at 770 K for two months in an Ar-filled silica tube.

3.2.5. *Pr–Al–Ge*

No phase diagram is available for the ternary Pr–Al–Ge system, however information on the formation and crystal structure of four compounds exists due to the work of the Ukrainian scientific group from L'viv University as well as of the group of authors from Geneva University.

PrAlGe belongs to the α-$ThSi_2$ type, $a = 0.4273$, $c = 1.463$ (Ryabokon' 1974; X-ray powder diffraction). Zhao and Parthé (1990) confirmed the structure for the equiatomic compound, $a = 0.42642$, $b = 1.4685$ (X-ray powder diffraction). Samples were obtained by arc melting the proper amounts of pure components in an argon atmosphere (Pr, Al and Ge: 99.99 mass%). The alloy was annealed at 870 K for 100 h in a silica tube.

Zarechnyuk et al. (1970) observed the $CaAl_2Si_2$ type for the $PrAl_2Ge_2$ compound ($a = 0.4264$, $c = 0.6896$; X-ray powder diffraction). The alloy was prepared by arc melting the elements in purified argon and annealing at 770 K for two weeks. Finally the sample was quenched in water. The purity of the starting components was greater than 99.9 mass%.

Two more ternary compounds have been observed and characterized by Zhao and Parthé (1991a,b). $Pr_2Al_{1+x}Ge_{6-x}$ was found to adopt the $La_2Al_{1+x}Ge_{6-x}$ type structure, $a = 0.8244$, $b = 0.8630$, $c = 1.0711$, $\beta = 101.09°$ (Zhao and Parthé 1991a; X-ray powder diffraction data). $Pr_2Al_3Ge_4$ (3) was announced to crystallize with the $Ba_2Cd_3Bi_4$ type, $a = 0.6056$, $b = 1.5000$, $c = 0.7920$ (X-ray powder diffraction, Zhao and Parthé 1991b). In both cases samples were obtained by arc melting the proper amounts of pure components in an argon atmosphere (Pr, Al and Ge: 99.99 mass%). The alloys were annealed at 770 K for two months in an Ar-filled silica tubes.

3.2.6. *Nd–Al–Ge*

No phase diagram is available yet for the ternary Nd–Al–Ge system, however information on the existence and crystal structure of five compounds exists due to the work of different scientific groups.

The formation of the $NdAl_{1.0-1.25}Ge_{1.0-0.75}$ compounds was reported in an early investigation performed by Raman and Steinfink (1967): AlB_2 type, $a = 0.4298$–0.4308, $c = 0.4210$–0.4204.

NdAlGe belongs to the α-$ThSi_2$ type, $a = 0.4272$, $c = 1.466$ (Ryabokon' 1974; X-ray powder diffraction). Zhao and Parthé (1990) confirmed the structure for the equiatomic compound, $a = 0.4233$, $b = 1.4638$ (X-ray powder diffraction). Samples were obtained by

arc melting the proper amounts of pure components in an argon atmosphere (Nd, Al and Ge: 99.99 mass%). The alloy was annealed at 870 K for 100 h in a silica tube.

Zarechnyuk et al. (1970) observed the $CaAl_2Si_2$ type for the $NdAl_2Ge_2$ compound (a = 0.4265, c = 0.6827; X-ray powder diffraction). The alloy was prepared by arc melting the elements in purified argon and annealing at 770 K for two weeks. Finally the sample was quenched in water. The purity of the starting components was greater than 99.9 mass%.

$Nd_2Al_{1+x}Ge_{6-x}$ was found to adopt the $La_2Al_{1+x}Ge_{6-x}$-type structure, a = 0.8220, b = 0.8623, c = 1.0671, β = 101.05° (Zhao and Parthé 1991a; X-ray powder diffraction data). Samples were obtained by arc melting the proper amounts of pure components in an argon atmosphere (Nd, Al and Ge: 99.99 mass%). The alloys were annealed at 770 K for two months in an Ar-filled silica tube.

$Nd_2Al_3Ge_4$ was announced to crystallize with the $Ba_2Cd_3Bi_4$ type, a = 0.6042, b = 1.4965, c 0.7897 (X-ray powder diffraction, Zhao and Parthé 1991b). The sample was obtained in the same manner as indicated for the $Nd_2Al_{1+x}Ge_{6-x}$ compound.

3.2.7. *Sm–Al–Ge*

No phase diagram has been derived yet for the ternary Sm–Al–Ge system, however information on the formation and crystal structure of four compounds exists due to the work of scientific groups from L'viv University and Geneva University.

SmAlGe belongs to the α-$ThSi_2$ type, a = 0.4188, c = 1.452 (Ryabokon' 1974; X-ray powder diffraction). Zhao and Parthé (1990) confirmed the structure for the equiatomic compound, a = 0.41957, b = 1.4588 (X-ray powder diffraction). Samples were obtained by arc melting the proper amounts of pure components in an argon atmosphere (Sm, Al and Ge: 99.99 mass%). The alloy was annealed at 870 K for 100 h in a silica tube.

Zarechnyuk et al. (1970) observed the $CaAl_2Si_2$ type for the $PrAl_2Ge_2$ compound (a = 0.4233, c = 0.6805; X-ray powder diffraction). The alloy was prepared by arc melting the elements in purified argon and annealing at 770 K for two weeks. Finally the sample was quenched in water. The purity of the starting components was greater than 99.9 mass%.

Two more ternary compounds have been observed and investigated by the group of authors from Geneva University. $Sm_2Al_{1+x}Ge_{6-x}$ was found to adopt the $La_2Al_{1+x}Ge_{6-x}$-type structure, a = 0.8105, b = 0.8458, c = 1.0613, β = 101.00° (Zhao and Parthé 1991a; X-ray powder diffraction data). $Sm_2Al_3Ge_4$ was announced to crystallize with the $Ba_2Cd_3Bi_4$ type, a = 0.6007, b = 1.4921, c = 0.7820 (X-ray powder diffraction, Zhao and Parthé 1991b). Samples were obtained by arc melting the proper amounts of pure components in an argon atmosphere (Sm, Al and Ge: 99.99 mass%). The alloys were annealed at 770 K for two months in an Ar-filled silica tube.

3.2.8. *Eu–Al–Ge*

Little information exists on the interaction of components in the ternary Eu–Al–Ge system. Two ternary compounds were observed and characterized.

Zarechnyuk et al. (1970) observed the $CaAl_2Si_2$ type for the $EuAl_2Ge_2$ compound (a = 0.422, c = 0.731; X-ray powder diffraction). The alloy was prepared by arc melting the

elements in purified argon and annealing at 770 K for two weeks. Finally the sample was quenched in water. The purity of the starting components was greater than 99.9 mass%.

The α-$ThSi_2$ type was indicated for the EuAlGe compound, $a = 0.42000$, $c = 1.4604$ (X-ray powder diffraction, Zhao and Parthé 1990). Samples were obtained by arc melting the proper amounts of pure components in an argon atmosphere (Eu, Al and Ge: 99.99 mass%). The alloy was annealed at 870 K for two months in a silica tube.

3.2.9. *Gd–Al–Ge*

Figure 17 represents the partial isothermal section of the Gd–Al–Ge system at 770 K after Zarechnyuk et al. (1981) from X-ray powder phase analysis of samples which were arc melted and annealed in evacuated quartz tubes for two weeks. Three ternary compounds were found to exist.

Zarechnyuk et al. (1970) observed the $CaAl_2Si_2$ type for the $GdAl_2Ge_2$ (1) compound ($a = 0.4248$, $c = 0.6714$; X-ray powder diffraction). The alloy was prepared by arc melting the elements in purified argon and annealing at 770 K for two weeks. Finally the sample was quenched in water. The purity of the starting components was greater than 99.9 mass%.

GdAlGe (3) was found to crystallize with the α-$ThSi_2$ type, $a = 0.4152$, $c = 1.4421$ (Ryabokon' 1974; X-ray powder diffraction). The sample was arc melted and annealed at 770 K. Contrary to these data, Zhao and Parthé (1990) found two types of structure for the equiatomic composition: a compound with the α-$ThSi_2$ type was found to exist above 1300 K ($a = 0.41521$, $c = 1.4415$; X-ray powder diffraction), and YAlGe-type was realized below 1300 K ($a = 0.4063$, $b = 1.0513$, $c = 0.5801$). The phase transition temperature was determined from thermal differential analysis. Samples were obtained by arc melting

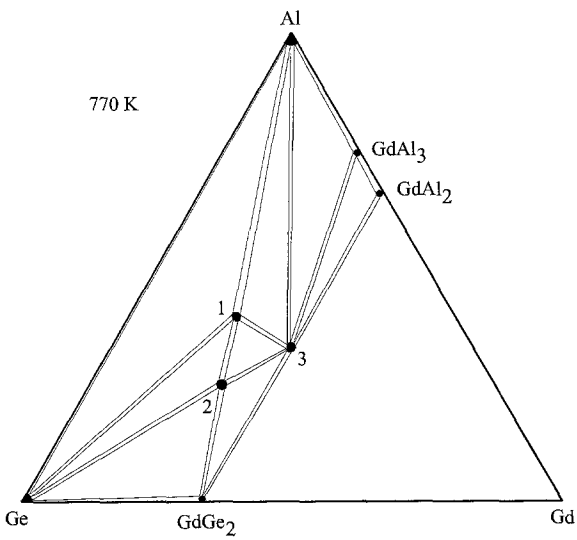

Fig. 17. Gd–Al–Ge, partial isothermal section at 770 K (0–33 at.% Gd).

the proper amounts of pure components in an argon atmosphere (Gd, Al and Ge: 99.99 mass%).

At variance with the phase diagram proposed by Zarechnyuk et al. (1981), two more compounds have been characterized by the scientific group from Geneva University. $Gd_2Al_{1+x}Ge_{6-x}$ was found to adopt the $La_2Al_{1+x}Ge_{6-x}$-type structure, $a=0.8041$, $b=0.8351$, $c=1.0546$, $\beta=100.81°$ (Zhao and Parthé 1991a; X-ray powder diffraction data). $Gd_2Al_3Ge_4$ was announced to crystallize with the $Ba_2Cd_3Bi_4$ type, $a=0.5948$, $b=1.4875$, $c=0.7762$ (X-ray powder diffraction, Zhao and Parthé 1991b). Samples were obtained by arc melting the proper amounts of pure components in an argon atmosphere (Gd, Al and Ge: 99.99 mass%). The alloys were annealed at 770 K for two months in an Ar-filled silica tube. These two phases are not shown in the 770 K isothermal section, fig. 17.

3.2.10. *Tb–Al–Ge*

No phase diagram has been derived yet for the ternary Tb–Al–Ge system, however information on the investigation of the crystal structure of three compounds exists due to the work of different scientific groups.

The TbAlGe compound was claimed by Yanson (1975) to adopt the DyAlGe type ($Cmc2_1$ space group) with lattice parameters as $a=0.4121$, $b=1.052$, $c=0.5831$ from X-ray powder diffraction of alloy which was obtained by arc melting and homogenized at 770 K. At variance with these data, Zhao and Parthé (1990) announced that this phase had the YAlGe type structure with Cmcm space group and lattice parameters $a=0.4044$, $b=1.0434$, $c=0.5767$ (X-ray powder diffraction). The sample was obtained by arc melting the proper amounts of pure components in an argon atmosphere (Tb, Al and Ge: 99.99 mass%). The alloy was annealed at 870 K for 100 h in a silica tube.

Zarechnyuk et al. (1970) observed the $CaAl_2Si_2$ type for the $TbAl_2Ge_2$ compound ($a=0.424$, $c=0.663$; X-ray powder diffraction). The alloy was prepared by arc melting the elements in purified argon and annealing at 770 K for two weeks. Finally the sample was quenched in water. The purity of the starting components was greater than 99.9 mass%.

$Tb_2Al_3Ge_4$ was announced to crystallize with the $Ba_2Cd_3Bi_4$ type, $a=0.5914$, $b=1.4834$, c 0.7720 (X-ray powder diffraction, Zhao and Parthé 1991b). The sample was obtained by arc melting the proper amounts of pure components in an argon atmosphere (Ce, Al and Ge: 99.99 mass%). The resulting alloy was annealed at 770 K for two months in an Ar-filled silica tube.

3.2.11. *Dy–Al–Ge*

Formation and crystal structure of three compounds have been reported in the Dy–Al–Ge system.

DyAlGe was claimed by Yanson (1975) to crystallize with a new structure type ($Cmc2_1$ space group) with lattice parameters $a=0.4091$, $b=1.046$, $c=0.5903$ (X-ray powder diffraction data) from the alloy which was synthesized by arc melting and annealed at 770 K. At variance with these data, Zhao and Parthé (1990) announced the YAlGe type for DyAlGe with Cmcm space group and lattice parameters $a=0.4035$, $b=1.0396$, $c=0.5752$

(X-ray powder diffraction). Samples were obtained by arc melting the proper amounts of pure components in an argon atmosphere (Dy, Al and Ge: 99.99 mass%). The alloy was annealed at 870 K for 100 h in a silica tube.

Zarechnyuk et al. (1970) observed the $CaAl_2Si_2$ type for the $DyAl_2Ge_2$ compound (a = 0.421, c = 0.667; X-ray powder diffraction). The alloy was prepared by arc melting the elements in purified argon and annealing at 770 K for two weeks. Finally the sample was quenched in water. The purity of the starting components was greater than 99.9 mass%.

$Dy_2Al_3Ge_4$ was reported to crystallize with the $Ba_2Cd_3Bi_4$ type, a = 0.5881, b = 1.4800, c = 0.7690 (X-ray powder diffraction, Zhao and Parthé 1991b). Samples were obtained by arc melting the proper amounts of pure components in an argon atmosphere (Dy, Al and Ge: 99.99 mass%). The resulting alloy was annealed at 770 K for two months in an Ar-filled silica tube.

3.2.12. *Ho–Al–Ge*

No phase diagram has been constructed for the ternary Ho–Al–Ge system, however data on the formation and crystal structure of three compounds exist due to the independent investigations of research groups from L'viv University and Geneva University.

The HoAlGe compound was claimed by Yanson (1975) to adopt a DyAlGe type ($Cmc2_1$ space group) with lattice parameters a = 0.4123, b = 1.040, c = 0.5827 (X-ray powder diffraction data). For sample preparation, see Dy–Al–Ge. At variance with these data, Zhao and Parthé (1990) found the YAlGe type structure with Cmcm space group and lattice parameters a = 0.4031, b = 1.0357, c = 0.5729 for this alloy (X-ray powder diffraction). Samples were obtained by arc melting the proper amounts of pure components in an argon atmosphere (Ho, Al and Ge: 99.99 mass%). The alloy was annealed at 870 K for 100 h in a silica tube.

Zarechnyuk et al. (1970) observed the $CaAl_2Si_2$ type for the $HoAl_2Ge_2$ compound (a = 0.4196, c = 0.6668; X-ray powder diffraction). The alloy was prepared by arc melting the elements in purified argon and annealing at 770 K for two weeks. Finally the sample was quenched in water. The purity of the starting components was greater than 99.9 mass%.

$Ho_2Al_3Ge_4$ was announced to crystallize with the $Ba_2Cd_3Bi_4$ type, a = 0.5865, b = 1.4765, c 0.7657 (X-ray powder diffraction; Zhao and Parthé 1991b). The sample was obtained by arc melting the proper amounts of pure components in an argon atmosphere (Ho, Al and Ge: 99.99 mass%). The resulting alloy was annealed at 770 K for two months in an Ar-filled silica tube.

3.2.13. *Er–Al–Ge*

Formation and crystal structure of three compounds have been reported in the Er–Al–Ge system.

The ErAlGe compound was claimed by Yanson (1975) to adopt a DyAlGe type ($Cmc2_1$ space group) with lattice parameters a = 0.4101, b = 1.034, c = 0.5840 (X-ray powder diffraction data). The alloy was synthesized in the same manner as DyAlGe. At variance with these data, Zhao and Parthé (1990) found that this phase had the YAlGe type

structure with Cmcm space group and lattice parameters $a = 0.4010$, $b = 1.0314$, $c = 0.5704$ (X-ray powder diffraction). Samples were obtained by arc melting the proper amounts of the pure components in an argon atmosphere (Er, Al and Ge: 99.99 mass%). The alloy was annealed at 870 K for 100 h in a silica tube.

Zarechnyuk et al. (1970) observed the $CaAl_2Si_2$ type for the $ErAl_2Ge_2$ compound ($a =$ 0.4184, $c = 0.6662$; X-ray powder diffraction). The alloy was prepared by arc melting the elements in purified argon and annealing at 770 K for two weeks. Finally the sample was quenched in water. The purity of the starting components was greater than 99.9 mass%.

$Er_2Al_3Ge_4$ was announced to crystallize with a $Ba_2Cd_3Bi_4$ type, $a = 0.5838$, $b = 1.4747$, $c = 0.7637$ (X-ray powder diffraction; Zhao and Parthé 1991b). Samples were obtained by arc melting the appropriate amounts of the pure components in an argon atmosphere (Er, Al and Ge: 99.99 mass%). The resulting alloy was annealed at 770 K for two months in an Ar-filled silica tube.

3.2.14. *Tm–Al–Ge*

Little information exists on the ternary Tm–Al–Ge system; however two ternary compounds were observed and characterized.

Contrary to the data presented by Yanson (1975) for the TmAlGe compound (DyAlGe type, $a = 0.402$, $b = 1.033$, $c = 0.5865$; X-ray powder diffraction), Zhao and Parthé (1990) indicated the YAlGe type for the compound of equiatomic composition (Cmcm space group, $a = 0.4010$, $b = 1.0314$, $c = 0.5704$; X-ray powder diffraction). Samples were obtained by arc melting the proper amounts of the pure components in an argon atmosphere (Tm, Al and Ge: 99.99 mass%). The alloy was annealed at 870 K for 100 h in a silica tube.

Zarechnyuk et al. (1970) observed the $CaAl_2Si_2$ type for the $TmAl_2Ge_2$ compound ($a =$ 0.4184, $c = 0.6662$; X-ray powder diffraction). The alloy was prepared by arc melting the elements in purified argon and annealing at 770 K for two weeks, and finally quenched in water. The purity of the starting components was greater than 99.9 mass%.

3.2.15. *Yb–Al–Ge*

Formation and crystal structure of three compounds have been reported in the Yb–Al–Ge system.

The YbAlGe compound was claimed by Yanson (1975) to adopt a DyAlGe type ($Cmc2_1$ space group) with lattice parameters $a = 0.4307$, $b = 1.057$, $c = 0.5935$. For experimental details, see Dy–Al–Ge.

Zarechnyuk et al. (1970) observed the $CaAl_2Si_2$ type for the $YbAl_2Ge_2$ compound ($a =$ 0.4118, $c = 0.705$; X-ray powder diffraction). The alloy was prepared by arc melting the elements in purified argon and annealing at 770 K for two weeks. Finally the sample was quenched in water. The purity of the starting components was greater than 99.9 mass%.

$Yb_7Al_5Ge_8$ was reported by Zhao and Parthé (1991c) to crystallize with a new structure type, $a = 1.5958$, $b = 0.42871$, $c = 1.2611$, $\beta = 95.78°$ (X-ray single-crystal data). A single crystal was obtained from the as-cast sample which was prepared by reaction of the pure

metals in a high-frequency furnace under an argon atmosphere (Yb 99.9, Al 99.99 and Ge 99.99 mass%). The reaction was observed at a temperature of about 773 K and the sample was left in the furnace at 1000 K for half an hour.

3.2.16. *Lu–Al–Ge*

Little information exists on the ternary Lu–Al–Ge system; however two ternary compounds were observed and characterized.

Zhao and Parthé (1990) indicated the YAlGe type structure for the LuAlGe compound (Cmcm space group, $a = 0.3999$, $b = 1.0227$, $c = 0.5659$; X-ray powder diffraction). Samples were obtained by arc melting the proper amounts of the pure components in an argon atmosphere (Lu, Al and Ge: 99.99 mass%). The alloy was annealed at 870 K for 100 h in a silica tube.

Zarechnyuk et al. (1970) observed the $CaAl_2Si_2$ type for the $LuAl_2Ge_2$ compound ($a = 0.417$, $c = 0.663$; X-ray powder diffraction). The alloy was prepared by arc melting the elements in purified argon and annealing at 770 K for two weeks. Finally the sample was quenched in water. The purity of the starting components was greater than 99.9 mass%.

3.3. *R–Ga–Ge systems*

3.3.1. *Y–Ga–Ge*

Investigations in the ternary system Y–Ga–Ge are due to Belyavina et al. (1996). Five ternary compounds were found to exist from X-ray powder phase analysis: $Y_{1.13}Ga_{0.5-1.0}Ge_{3.37-2.87}$ ($SmNiGe_3$-type structure, $a = 0.3984$, $b = 2.0703$, $c = 0.4120$); $Y_2Ga_{2.70-3.60}Ge_{4.30-3.40}$ (La_2AlGe_6 type, $a = 0.7969$, $b = 1.0550$, $c = 2.0763$, $\gamma = 100.97°$); $Y_{2.25}Ga_{0.67}Ge_{6.08}$ (Pr_2LiGe_6 type, $a = 0.3956$, $b = 2.0763$, $c = 0.4100$); $Y_3Ga_{1.4-3.0}Ge_{3.6-2.0}$ (α-$GdSi_2$ type); $Y_3Ga_{3.4}Ge_{1.6}$ (α-$ThSi_2$ type). Samples were prepared by arc melting high purity components and annealed at 670 K.

3.3.2. *Ce–Ga–Ge*

While no phase diagram is available for the Ce–Ga–Ge system, X-ray phase analysis of 180 ternary alloys indicated the formation of four ternary compounds in the Ce–Ga–Ge system (Gryniv et al. 1989). Alloys were synthesized by arc melting metal ingots in an argon atmosphere followed by annealing at 870 K.

$Ce_2Ga_{1.6}Ge_{5.4}$ was observed to crystallize with a new structure type, $a = 0.8664$, $b = 0.8307$, $c = 2.1550$ (Gryniv et al. 1989). $Ce_4Ga_4Ge_7$ belongs to the $La_4Ga_4Ge_7$ type with lattice parameters $a = 0.8414$, $b = 0.8620$, c 3.109 (Gryniv et al. 1989). CeGaGe is reported to form the α-$ThSi_2$ type, $a = 0.4292$, $c = 1.4518$. Ce_5Ga_2Ge was found to adopt the Cr_5B_3 structure type, $a = 0.8019$, $c = 1.3850$ (Gryniv et al. 1989).

3.3.3. *Nd–Ga–Ge*

Five ternary compounds were observed and characterized for the Nd–Ga–Ge system from X-ray powder diffraction of alloys which were arc melted and annealed at 870 K (Opainych et al. 1992). Crystallographic data for these compounds are as follows:

$Nd_2(Ga_xGe_{1-x})_7$, $Ce_2(Ga,Ge)_7$ type, $a=0.8511$–0.8552, $b=0.8151$–0.863, $c=2.1210$–2.1379; $Nd_4(Ga_xGe_{1-x})_{11}$, $x=0.33$–0.43, $La_4(Ga,Ge)_{11}$ type, $a=0.8213$–0.8314, $b=0.8311$–0.8463, $c=0.3591$–0.3600; $NdGa_{1+x}Ge_{1-x}$, $x=0$–0.2, α-$ThSi_2$ type, $a=0.4240$–0.4238, $c=1.4511$–1.4510; $Nd(Ga_xGe_{1-x})_2$, $x=0.75$–0.85, AlB_2 type, $a=0.4247$–0.4231, $c=0.4245$–0.4229; $Nd_5(Ga_{0.53}Ge_{0.47})_3$, Cr_5B_3 type, $a=0.7939$, $c=1.3908$.

3.3.4. *Gd–Ga–Ge*

Golovata et al. (1996) reported results of the X-ray powder phase analysis of alloys of Gd–Ga–Ge system at 1070 K and 670 K. Six ternary compounds were found to exist. They are $GdGa_{0.32-0.55}Ge_{3.00-2.77}$, $Gd_2Ga_{2.34-3.58}Ge_{4.66-3.42}$, $GdGa_{3.00-3.09}Ge_{0.50-0.41}$, $GdGa_{0.29-0.36}Ge_{1.93-1.86}$, $GdGa_{1.21-1.36}Ge_{0.82-0.67}$, and $GdGa_{0.03-0.13}Ge_{0.88-0.78}$. The crystal structure and lattice parameters were determined for two compounds by X-ray powder diffraction: $GdGa_{0.32-0.55}Ge_{3.00-2.77}$ ($SmNiGe_3$ type, $a=0.4005$, $b=2.0826$, $c=0.4161$ for $GdGa_{0.32}Ge_{3.00}$) and $Gd_2Ga_{2.34-3.58}Ge_{4.66-3.42}$ (La_2AlGe_6 type, $a=0.8182$, $b=1.0812$, $c=0.8420$, $\gamma=100.85°$ for $GdGa_{3.15}Ge_{3.85}$).

3.3.5. *Tm–Ga–Ge*

The formation of eight ternary compounds is reported for the Tm–Ga–Ge system (Gryniv and Myakush 1989) from arc-melted samples annealed at 870 K. They are: $Tm_2Ga_{0.5}Ge_{4.5}$ (new structure type, $a=0.3915$, $b=0.4048$, $c=1.8209$; X-ray powder diffraction), $TmGa_{1.94}Ge_{0.06}$ (AlB_2 type, $a=0.4171$, $c=0.3995$; X-ray powder diffraction), $Tm_3(Ga_{0.5}Ge_{0.5})_5$ (new structure type, $a=0.7748$, $c=1.0836$; X-ray single-crystal method), $Tm_{10}Ga_6Ge_9$ (unknown structure type), $Tm_{11}Ga_2Ge_{12}$ (unknown type), $Tm_3Ga_{3.2-2.4}Ge_{0.4-1.2}$ (unknown type), $Tm_5Ga_3Ge_2$ (unknown type), $Tm_4Ga_7Ge_9$ (unknown type).

3.4. *R–In–Ge systems*

No phase diagrams exist for the R–In–Ge system, however a series of ternary compounds, La_2InGe_2, have been observed and characterized by Zaremba et al. (1997) (see table 4).

Table 4
Lattice parameters for the R_2InGe_2 compounds, Mo_2FeB_2-type[a]

Compound	Lattice parameters (nm)		Compound	Lattice parameters (nm)	
	a	*c*		*a*	*c*
Y_2InGe_2	0.7339	0.4242	Gd_2InGe_2	0.7378	0.4248
La_2InGe_2	0.7664	0.4450	Tb_2InGe_2	0.7337	0.4215
Ce_2InGe_2	0.7577	0.4391	Dy_2InGe_2	0.7322	0.4187
Pr_2InGe_2	0.7546	0.4374	Ho_2InGe_2	0.7303	0.4167
Nd_2InGe_2	0.7496	0.4342	Yb_2InGe_2	0.7205	0.4294
Sm_2InGe_2	0.7445	0.4289			

[a] Source: Zaremba et al. (1997).

Alloys were synthesized by arc melting pure metals (99.9 mass% R; 99.99 mass% In and Ge) followed by annealing for 700 h at 870 K in evacuated quartz tubes. Crystal structure was investigated by the single-crystal method for the La_2InGe_2 compound, for other phases the X-ray powder method was employed.

3.5. *R–C–Ge systems*

The only information on the interaction of the components in the ternary R–C–Ge systems is due to Mayer and Shidlowsky (1969), who investigated the crystal structure of R_5CGe_3 compounds. They were found to form a partly filled Mn_5Si_3 type. Crystallographic characteristics of the isotypic R_5CGe_3 series are listed in table 5. The samples were synthesized by melting of the pure components in an induction furnace at 1773–1873 K.

Table 5
Lattice parameters for the R_5CGe_3 compounds, Mn_5Si_3-type[a]

Compound	Lattice parameters (nm)		Compound	Lattice parameters (nm)	
	a	*c*		*a*	*c*
Y_5CGe_3	0.845	0.645	Tb_5CGe_3	0.849	0.641
Ce_5CGe_3	0.884	0.672	Dy_5CGe_3	0.845	0.642
Pr_5CGe_3	0.879	0.671	Ho_5CGe_3	0.837	0.638
Nd_5CGe_3	0.874	0.668	Er_5CGe_3	0.834	0.637
Sm_5CGe_3	0.864	0.659	Tm_5CGe_3	0.830	0.632
Gd_5CGe_3	0.857	0.652	Lu_5CGe_3	0.823	0.626

[a] Source: Mayer and Shidlowsky (1969).

3.6. *R–Si–Ge systems*

3.6.1. *Y–Si–Ge*

The isothermal section of the Y–Si–Ge phase diagram at 870 K was constructed by Muratova (1976) using X-ray powder diffraction data of arc-melted alloys annealed for 400 h. The purity of the starting components was greater than 99.90 mass%. The phase relations are characterized by the existence of two ternary compounds and by the formation of three continuous solid solutions between isostructural binary compounds: $Y_5(Si,Ge)_3$, Y(Si,Ge) and $Y_2(Si,Ge)_3$ (fig. 18). Three extended ranges of solid solutions were found to exist within the Y–Si–Ge system at 870 K, originating at Y_5Ge_4, $Y_{11}Ge_{10}$ and YGe_2, which dissolve 20, 15 and 37 at.% Si, respectively.

$YSi_{1.4}Ge_{0.6}$ (1) was reported to crystallize with the α-$GdSi_2$ type, $a = 0.4044$, $b = 0.3988$, $c = 1.348$ (Muratova 1976; X-ray powder diffraction). For the experimental procedure, see above.

$YSi_{1.8}Ge_{0.2}$ (2) belongs to the α-$ThSi_2$ type, $a = 0.4002$, $c = 1.336$ (Muratova 1976; X-ray powder diffraction). The samples were synthesized in the same manner as that applied for the investigation of the Y–Si–Ge isothermal section.

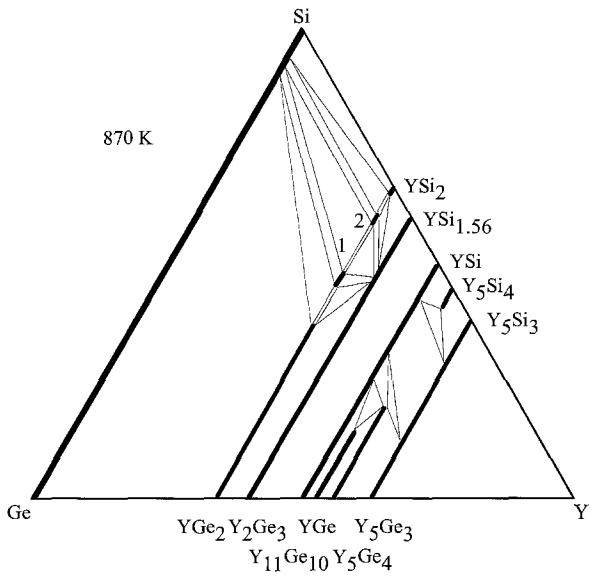

Fig. 18. Y–Si–Ge, isothermal section at 870 K.

3.6.2. *La–Si–Ge*

The phase equilibria in the La–Si–Ge system at 870 K (fig. 19) were investigated by Muratova et al. (1974) and Bodak and Muratova (1981) by means of X-ray phase analysis of alloys which were arc melted and subsequently annealed in evacuated silica tubes for 400 h and finally quenched in water. Starting materials were La 99.79 mass%,

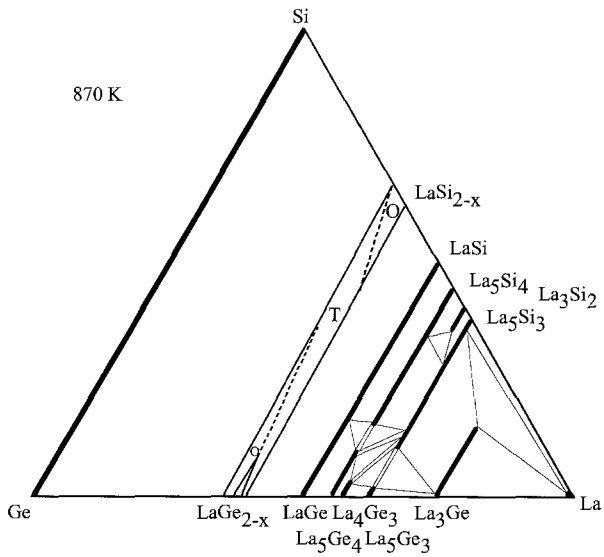

Fig. 19. La–Si–Ge, isothermal section at 870 K.

Si 99.9 mass% and Ge 99.99 mass%. Phase relations are characterized by the formation of continuous solid solution originating at the isotypic binary compounds LaSi and LaGe. A complete solid solution with successive changing of the tetragonal α-$ThSi_2$ (T) and orthorhombic α-$GdSi_2$ (O) structure types was also observed between $LaSi_{2-x}$ and $LaGe_{2-x}$. No ternary compounds were found. La_3Ge and La_5Ge_4 dissolve 15 and 10 at.% Si. Solubilities of Ge in La_5Si_3 and La_5Si_4 were reported to be approximately 27.5 and 29.5 at.%, respectively.

3.6.3. *Ce–Si–Ge*

Investigations in the ternary system Ce–Si–Ge were performed by two different research groups, i.e. Haschke et al. (1966) and Bodak and Muratova (1979).

Phase relations in an isothermal section at 1070 K were determined by Haschke et al. (1966) by means of X-ray powder diffraction methods (fig. 20). Samples were synthesized by heating compacted mixtures of 99.9 mass% purity for a few minutes in an induction furnace slightly above the melting point. The formation of two complete solid solutions was reported: Ce(Si,Ge) and $Ce(Si,Ge)_{2-x}$. No ternary compounds were observed.

A partial isothermal section at 870 K within 0–50 at.% Ce is presented in fig. 21 from X-ray powder analysis of 92 alloys which were arc melted from ingots of pure metals and annealed in evacuated quartz tubes for 400 h (Bodak and Muratova 1979). The purity of the metals was greater than 99.9 mass%. A continuous solid solution with successive changing of the α-$ThSi_2$ (T) and α-$GdSi_2$ (O) structure types was observed between $CeSi_{2-x}$ and $CeGe_{2-x}$. No ternary compounds were found.

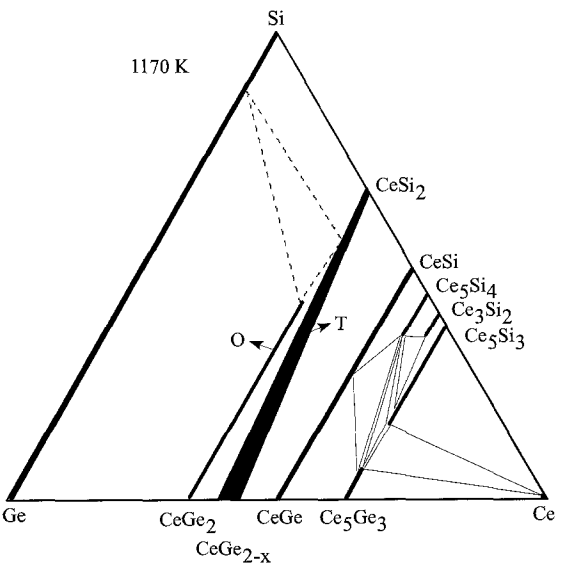

Fig. 20. Ce–Si–Ge, isothermal section at 1170 K.

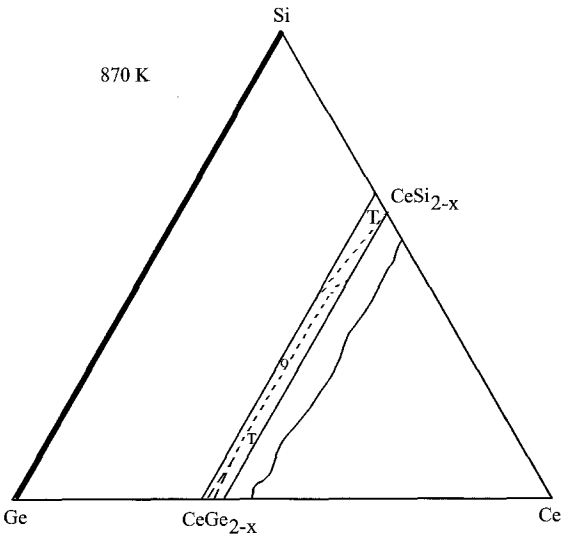

Fig. 21. Ce–Si–Ge, partial isothermal section at 870 K (0–40 at.% Ce).

3.6.4. *Pr–Si–Ge*

The phase relations in the Pr–Si–Ge ternary system at 873 K were investigated by Muratova and Bodak (1974) using X-ray powder analysis (fig. 22). Samples were obtained by arc melting, and homogenized at 873 K for 500 h. No ternary compounds were found, but a continuous solid solution $Pr(Si,Ge)_{2-x}$ was observed. The solubilities of germanium

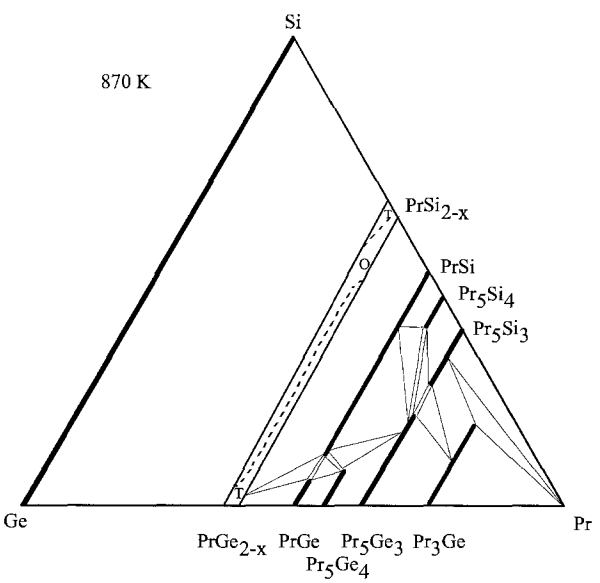

Fig. 22. Pr–Si–Ge, isothermal section at 870 K.

in Pr_5Si_3, Pr_5Si_4 and PrSi were determined as 12.5, 7 and 40 at.%, respectively, whereas Pr_3Ge and Pr_5Ge_3 dissolve 18 and 20 at.% Si, respectively.

Muratova (1974) reported on the X-ray powder investigation of the crystal structure of alloys within the homogeneity field $Pr(Si,Ge)_{2-x}$. The Ge-rich region of solid solution was found to crystallize with a tetragonal α-$ThSi_2$ type (T). With increasing Ge/Si exchange, a continuous transition into the orthorhombic α-$GdSi_2$ (O) was observed; no two-phase field was established.

3.6.5. *Gd–Si–Ge*

The phase equilibria in the Gd–Si–Ge system at 870 K (fig. 23) were investigated by Muratova et al. (1975) by means of X-ray phase analysis of alloys which were arc melted and subsequently annealed in evacuated silica tubes for 400 h and finally quenched in water. The purity of the starting materials was greater than 99.9 mass%. No ternary compounds were observed. Phase relations are characterized by the existence of three continuous solid solutions: $Gd(Si,Ge)_{2-x}$, $Gd_5(Si,Ge)_3$ and $Gd_2(Si,Ge)_3$. The crystal structure of $Gd(Si,Ge)_{2-x}$ solid solution was said to change with increasing Si content from α-$GdSi_2$ (O) type through α-$ThSi_2$ type (T) to α-$GdSi_2$ (O) type (Muratova 1974; X-ray powder diffraction). Binary compounds GdGe, GdSi and Gd_5Ge_4 dissolve 33, 10 and 8 at.% of third component respectively (Muratova et al. 1975).

During a study of the magnetic properties of alloys heat treated at 1870 K for 5 hours in the pseudobinary system $Gd_5(Si_xGe_{1-x})_4$, Holtzberg et al. (1967) report extended solubility of Si in Gd_5Ge_4 ($0.0 \leqslant x \leqslant 0.3$) and Ge in Gd_5Si_4 ($0.5 \leqslant x \leqslant 1.0$). They also

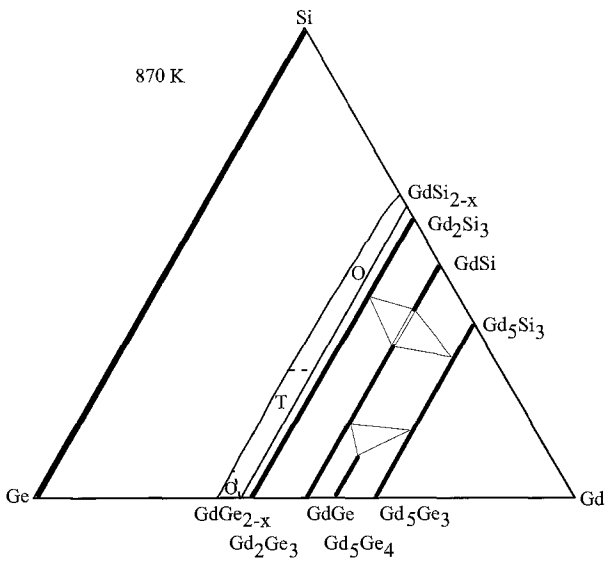

Fig. 23. Gd–Si–Ge, isothermal section at 870 K.

acknowledge the existence of the ternary intermediate phase with unidentified crystal structure extending between $0.3 < x < 0.5$. These seemingly contradicting experimental results regarding the phase relations in the Gd_5Ge_4–Gd_5Si_4 pseudobinary system suggest that the Gd_5Si_4-based solid solution and the ternary phase are probably high-temperature phases, which decompose during the heat treatment between 870 K and 1870 K, and that the solid solubility of Si in Gd_5Ge_4 is strongly temperature dependent.

Pecharsky and Gschneidner (1997) investigated 12 as-cast alloys from the pseudobinary system $Gd_5(Si_xGe_{1-x})_4$ by X-ray single-crystal and powder diffraction. The Gd_5Si_4-based solid solution where Ge statistically substitutes for Si maintains the Sm_5Ge_4-type orthorhombic crystal structure of the binary Gd_5Si_4 compound and extends from $0.5 < x \leqslant 1$. The Gd_5Ge_4-based solid solution where Si statistically substitutes for Ge also maintains the Sm_5Ge_4-type orthorhombic crystal structure of the binary Gd_5Si_4 compound and extends from $0 < x \leqslant 0.2$. The crystal structure of the ternary phase, which exists for $0.24 \leqslant x \leqslant 0.5$, has been determined for the first time, and it was shown to be a monoclinically distorted derivative of orthorhombic Sm_5Ge_4-type ($P112_1/a$ space group, $a = 0.75808$, $b = 1.4802$, $c = 0.77799$, $\gamma = 93.190$) for $Gd_5Si_2Ge_2$.

4. R–d element–germanium systems

4.1. *Sc–d element–Ge systems*

4.1.1. *Sc–V–Ge*

The phase equilibria in the Sc–V–Ge system were investigated by Kotur (1987) by means of X-ray analysis of alloys which were arc melted and subsequently annealed in evacuated silica tubes for 350–650 h at 1070 K and finally quenched in water (fig. 24). Starting

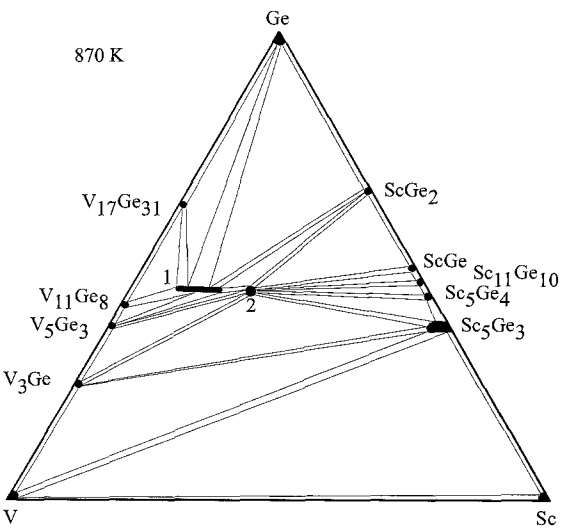

Fig. 24. Sc–V–Ge, isothermal section at 870 K.

materials were Sc 99.92 mass%, V 99.9 mass% and Ge 99.99 mass%.

Two ternary compounds were observed at 1070 K: $Sc_{1-1.8}V_{5-4.2}Ge_5$ (1) with the V_6Si_5-type structure ($a=0.7872$–0.7850, $c=0.5091$–0.5157) and $Sc_2V_3Ge_4$ (2) with the $Ce_2Sc_3Si_4$-type structure ($a=0.6614$, $b=1.2774$, $c=0.6776$) (Kotur et al. 1986).

Kotur et al. (1983) reported on the preliminary X-ray single-crystal investigation of a $Sc_xV_{5-x}Ge_3$ sample which was isotypic to Sc_5Ge_3 ($a=0.743$, $c=0.502$). The single crystal was obtained from a cast alloy. This phase is not shown in the 870 K isothermal section, fig. 24.

4.1.2. *Sc–Cr–Ge*

The isothermal section of the Sc–Cr–Ge phase diagram at 1070 K was constructed by Kotur et al. (1988b). The phase relations are characterized by the formation of four ternary compounds and by the existence of a solid solution range of Cr in Sc_5Ge_3 (7.5 at.%) (fig. 25). For details of sample preparation, see Sc–V–Ge.

Venturini et al. (1985a) investigated the crystal structure of the $ScCrGe_2$ (3) compound ($TiMnSi_2$-type structure: $a=0.937$, $b=1.009$, $c=0.813$). The sample was arc melted and annealed at 1073 K in an evacuated quartz capsule. The purity of the starting materials was 99.9 mass%.

Kotur et al. (1988a) confirmed the existence of this compound with similar lattice parameters ($a=0.9355$, $b=1.0148$, $c=0.8141$) and investigated the crystal structure of the other three compounds: $ScCr_6Ge_6$ (1) with the $HfFe_6Ge_6$-type ($a=0.5102$, $c=0.8229$), $Sc_2Cr_4Ge_5$ (2) with the $Nb_2Cr_4Si_5$-type ($a=0.7821$, $b=1.6662$, $c=0.5146$) and $Sc_7Cr_{4+x}Ge_{10-x}$ ($x=1.3$) (4) with the $Sc_7Cr_{4+x}Si_{10-x}$ type ($a=1.0150$, $c=1.4352$).

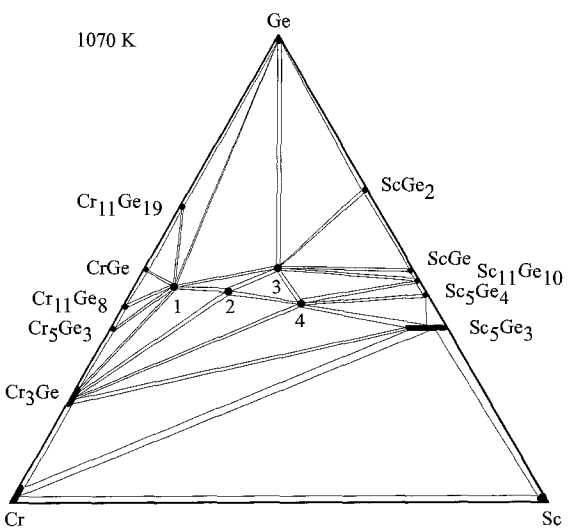

Fig. 25. Sc–Cr–Ge, isothermal section at 1070 K.

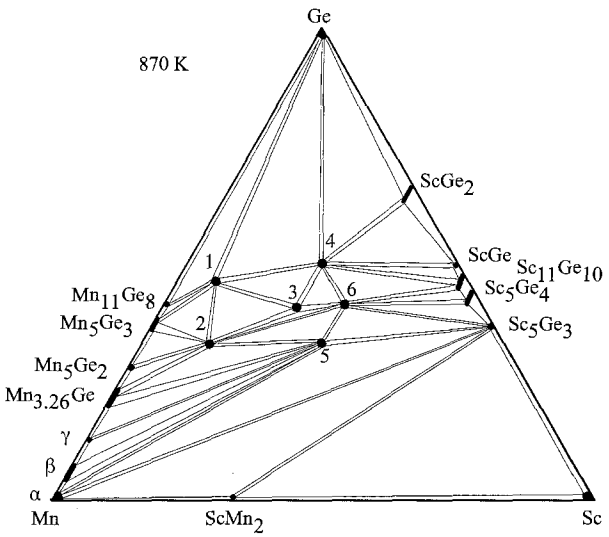

Fig. 26. Sc–Mn–Ge, isothermal section at 870 K.

4.1.3. *Sc–Mn–Ge*

The ternary phase diagram of the Sc–Mn–Ge system at 870 K was studied by means of X-ray powder diffraction by Andrusyak and Kotur (1991) (fig. 26). For sample preparation, see Sc–V–Ge. Six ternary manganese germanides of scandium were found and investigated (Andrusyak 1988).

Crystallographic data for the ternary compounds which were observed in the course of phase-equilibrium studies in the Sc–Mn–Ge system at 870 K are listed in table 6.

Venturini et al. (1992) investigated the crystal structure for the $ScMn_6Ge_6$ compound at 1073 K and confirmed the same structure type with similar lattice parameters. The alloy was synthesized by a powder metallurgical reaction in an evacuated silica tube at 1073 K for 14 days.

Table 6
Crystallographic data for the ternary Sc–Mn–Ge compounds at 870 K

No.	Compound	Structure	Lattice parameters (nm)			Reference
			a	*b*	*c*	
1	$ScMn_6Ge_6$	$HfFe_6Ge_6$	0.5176		0.8099	Andrusyak (1986)
			0.5177		0.8084	Venturini et al. (1992)
2	$ScMn_6Ge_4$	$ZrFe_6Ge_4$	0.5066		2.0013	Kotur (1995)
3	$Sc_3Mn_7Ge_8$	unknown				Andrusyak and Kotur (1991)
4	$ScMnGe_2$	$ZrCrSi_2$	1.0191	0.9342	0.8083	Andrusyak and Kotur (1991)
5	ScMnGe	ZrNiAl	0.6677		0.3946	Kotur and Andrusyak (1984a)
6	$Sc_7Mn_{4+x}Ge_{10-x}$ ($x = 1.3$)	$Sc_7Cr_{4+x}Si_{10-x}$	0.9995		1.4168	Kotur et al. (1988a)

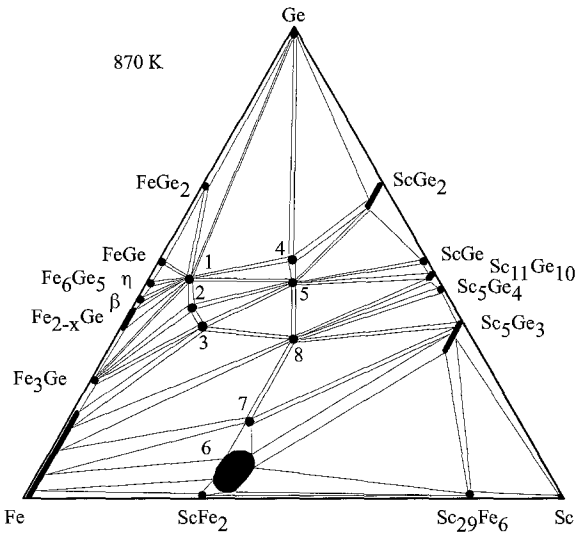

Fig. 27. Sc–Fe–Ge, isothermal section at 870 K.

4.1.4. *Sc–Fe–Ge*

The phase-field distribution in the Sc–Fe–Ge system at 870 K is characterized by the formation of eight ternary compounds and by the existence of substitutional exchange of Ge/Fe in the solid solutions $Sc_5(Fe_xGe_{1-x})_3$ for $0 < x < 0.15$ and $Sc(Fe_xGe_{1-x})_2$ for $0 < x < 0.1$ after Andrusyak and Kotur (1991) (fig. 27). For details of sample preparation, see Sc–V–Ge. The starting materials were Sc 99.92 mass%, Fe 99.95 mass%, and Ge 99.99 mass%.

Table 7
Crystallographic data for the ternary Sc–Fe–Ge compounds

No.	Compound	Structure	Lattice parameters (nm)			Reference
			a	*b*	*c*	
1	$ScFe_6Ge_6$	$HfFe_6Ge_6$	0.5069		0.8077	Olenych et al. (1981)
			0.5062		0.8056	Andrusyak (1986)
			0.5087		0.8079	Venturini et al. (1992)
2	$ScFe_6Ge_5$	own	0.5063		0.4411	Kotur (1995)
3	$ScFe_6Ge_4$	$ZrFe_6Ge_4$	0.5066		2.0013	Kotur (1995)
4	$ScFeGe_2$	$TiMnSi_2$	0.922	1.009	0.800	Venturini et al. (1985a)
			0.9227	1.0098	0.8263	Andrusyak and Kotur (1991)
5	$Sc_4Fe_4Ge_{6.6}$	$Zr_4Co_4Ge_7$	1.3296		0.5235	Andrusyak and Kotur (1989)
6	$Sc_{1-1.17}Fe_{1.94-1.70}Ge_{0.06-0.30}$	$MgCu_2$	0.7060[a]			Kotur (1995)
7	Sc_2Fe_3Ge	$MgZn_2$	0.5006		0.8147	Andrusyak and Kotur (1991)
8	ScFeGe	ZrNiAl	0.6547		0.3895	Kotur and Andrusyak (1984a)

[a] For $ScFe_{1.79}Ge_{0.21}$.

The $ScFe_6Ge_6$ compound with the $HfFe_6Ge_6$-type was observed by Olenych et al. (1981). Samples were obtained by arc melting and annealing for 300 h at 1070 K. Andrusyak (1986) and Venturini et al. (1992) confirmed the formation and crystal structure of this compound at 870 K and 1173 K respectively.

The existence and structural characteristics of the $ScFeGe_2$ compound at 1073 K was reported by Venturini et al. (1985a) (X-ray powder diffraction method) and was confirmed by Andrusyak and Kotur (1991) at 870 K.

The formation and crystal structure of six other ternary compounds were reported by Kotur and Andrusyak (1984a), Andrusyak and Kotur (1989, 1991).

Crystallographic data on the ternary Sc–Fe–Ge compounds are listed in table 7.

4.1.5. *Sc–Co–Ge*

A systematic study of the Sc–Co–Ge system at 870 K was performed by Kotur and Andrusyak (1991). For sample preparation, see Sc–V–Ge. The starting materials were Sc 99.92 mass%, Co 99.92 mass% and Ge 99.99 mass%. Seven ternary compounds were found to exist (see fig. 28). The limits of solid solutions origining at $ScCo_2$, $ScGe_2$, $Sc_{11}Ge_{10}$, Sc_5Ge_4 and Sc_5Ge_3 were established as 11.5 at.% Ge and 6 at.%, 4 at.%, 4 at.%, 3 at.% Co, respectively, by means of X-ray powder diffraction. The lattice parameter of $ScCo_{2-1.65}Ge_{0-0.35}$ varies linearly within $a = 0.6902$–0.6984. Simarily for $ScGe_2$ the solid-solution range of Co is given by $ScCo_{0-0.18}Ge_{2-1.82}$ (Kotur 1995).

The crystallographic characteristics for the ternary Sc–Co–Ge compounds are presented in table 8.

A single crystal of the $Sc_3Co_2Ge_3$ compound, which is not shown in fig. 28, was obtained from an arc-melted and slowly cooled sample: $Hf_3Ni_2Si_3$ type, $a = 0.4078$, $b = 0.9930$, $c = 1.3243$ (Kotur and Andrusyak 1991).

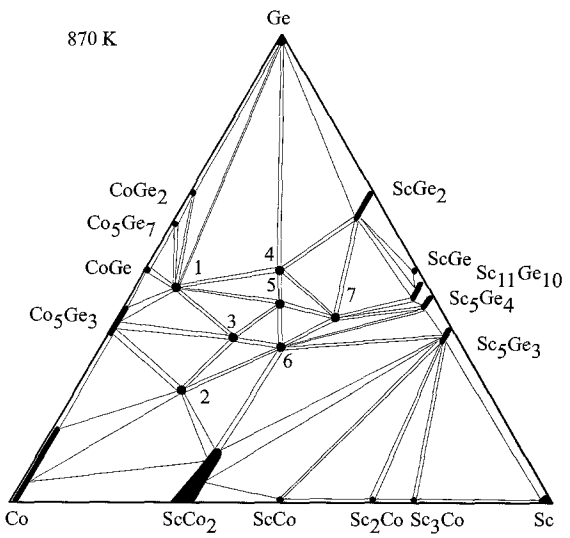

Fig. 28. Sc–Co–Ge, isothermal section at 870 K.

Table 8
Crystallographic data for the ternary Sc–Co–Ge compounds

No.	Compound	Structure	Lattice parameters (nm)			Reference
			a	*b*	*c*	
1	$ScCo_6Ge_6$	$HfFe_6Ge_6$	0.5056		0.7799	Buchholz and Schuster (1981)
			0.5064		0.7778	Kotur and Andrusyak (1991)
2	$Sc_4Co_{11}Ge_5$	unknown				Kotur and Andrusyak (1991)
3	$Sc_4Co_7Ge_6$	$U_4Re_7Si_6$	0.7850			Kotur and Andrusyak (1991)
4	$ScCoGe_2$	$TiMnSi_2$	0.919	1.009	0.796	Venturini et al. (1985a)
			0.9186	1.0102	0.7958	Kotur (1995)
5	$Sc_4Co_4Ge_7$	$Zr_4Co_4Ge_7$	1.3215		0.5229	Andrusyak and Kotur (1989)
6	ScCoGe	TiNiSi	0.6495	0.4000	0.7072	Kotur and Andrusyak (1984a)
7	Sc_2CoGe_2	Sc_2CoSi_2	0.9595	0.9828	0.3914	Kotur and Andrusyak (1991)
				$\gamma = 123.2°$		

4.1.6. *Sc–Ni–Ge*

In the course of phase-equilibrium studies in the Sc–Ni–Ge system at 870 K, Kotur and Andrusyak (1991) observed eight ternary nickel germanides of scandium (see fig. 29). For details of sample preparation, see Sc–V–Ge. The binary germanides of scandium dissolve 2–8 at.% Ni; the solubility of Ge in $ScNi_2$ is 3.5 at.% (Kotur 1995).

Crystallographic data for the ternary Sc–Ni–Ge compounds observed at 870 K are listed in table 9.

Andrusyak (1988) studied the crystal structure of the $Sc_9Ni_5Ge_8$ compound by the

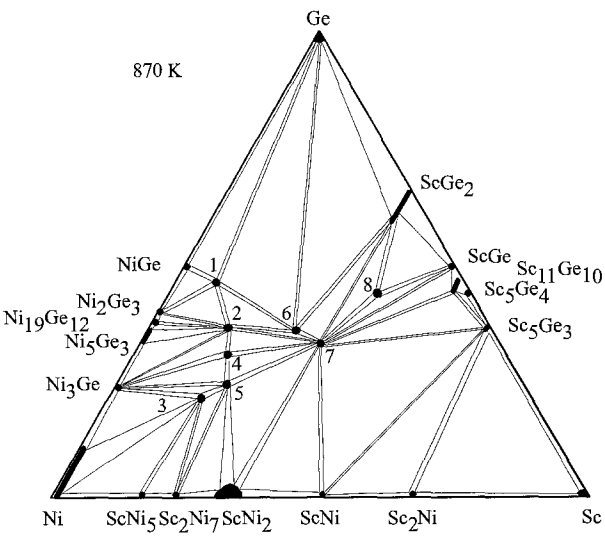

Fig. 29. Sc–Ni–Ge, isothermal section at 870 K.

Table 9
Crystallographic data for the ternary Sc–Ni–Ge compounds

No.	Compound	Structure	Lattice parameters (nm)			Reference
			a	*b*	*c*	
1	$ScNi_6Ge_6$	$ScNi_6Ge_6$	1.0152		0.7813	Buchholz and Schuster (1981)
			1.0158		0.7816	Andrusyak (1986)
2	$Sc_3Ni_{11}Ge_4$	$Sc_3Ni_{11}Si_4$	0.8130		0.8505	Kotur and Andrusyak (1991)
3	$Sc_{12.3}Ni_{40.7}Ge_{31}$	own	1.7865		0.8220	Bodak et al. (1990)
4	$Sc_6Ni_{18}Ge_{11}$	$Sc_6Ni_{18}Si_{11}$	1.8322	1.2461	0.8191	Andrusyak and Kotur (1987)
5	$Sc_6Ni_{16}Ge_7$	$Mg_6Cu_{16}Si_7$	1.1654			Gladyshevsky et al. (1962)
6	$Sc_3Ni_4Ge_4$	$Gd_6Cu_8Ge_8$	1.2910	0.6598	0.3908	Kotur and Sikirica (1982)
7	ScNiGe	TiNiSi	0.6454	0.4071	0.7068	Kotur and Andrusyak (1984a)
8	$Sc_{13}Ni_6Ge_{15}$	unknown				Kotur (1995)

X-ray single-crystal method (own type of structure, $a=2.0426$, $b=0.9129$, $c=0.39822$). The single crystal was obtained from an as-cast sample.

Andrusyak and Kotur (1989) reported on X-ray single-crystal investigation of the $Sc_4Ni_4Ge_{7-x}$ ($x=0.8$) compound which existed in arc melted alloys and decomposed at 870 K ($Zr_4Co_4Ge_7$ type, $a=1.3276$, $c=0.5225$.

Neither of these two phases are shown in the 870 K isothermal section, fig. 29.

4.1.7. *Sc–Cu–Ge*

Kotur and Andrusyak (1984b) studied phase equilibria in the Sc–Cu–Ge system (fig. 30)

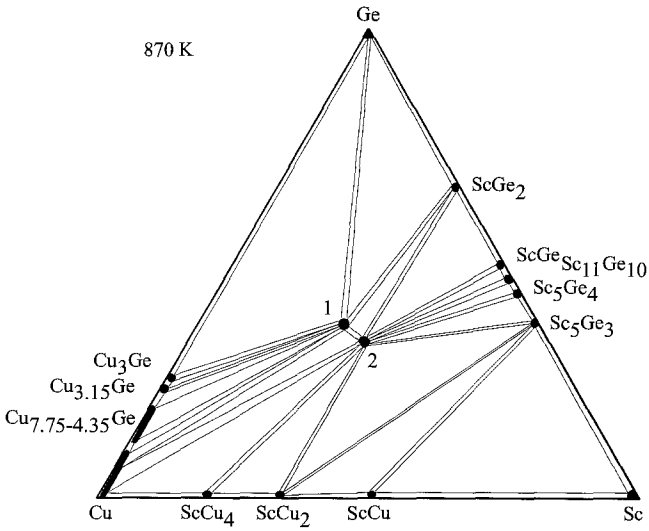

Fig. 30. Sc–Cu–Ge, isothermal section at 870 K.

and reported the existence of two compounds at 870 K. For sample preparation, see Sc–V–Ge.

The crystal structure for the $Sc_3Cu_4Ge_4$ compound (1) was studied by Thirion et al. (1983) ($Gd_6Cu_8Ge_8$ type, $a=1.330$, $b=0.6516$, $c=0.3996$) and was confirmed by Kotur and Andrusyak (1984b) ($a=1.332$, $b=0.6523$, $c=0.4004$).

The crystallographic characteristics for the ScCuGe compound (2) (ZrNiAl type, $a=0.6515$, $c=0.3972$) reported by Kotur and Andrusyak (1984b) are in good agreement with those announced earlier by Dwight et al. (1973).

4.1.8. *Sc–Nb–Ge*

The isothermal section of the Sc–Nb–Ge phase diagram at 1070 K was investigated by Kotur (1986) (fig. 31). The phase relations are characterized by the formation of one

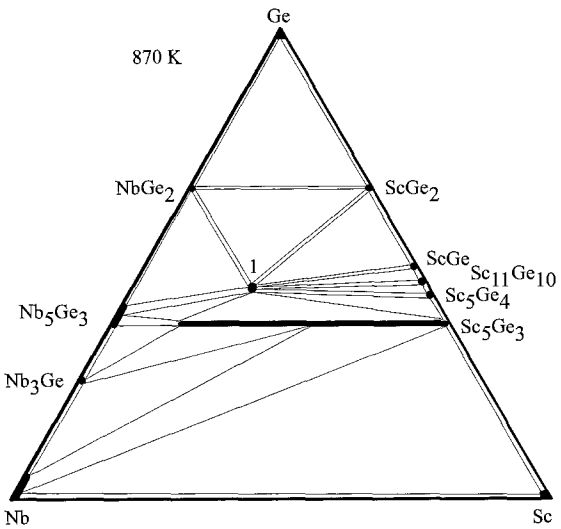

Fig. 31. Sc–Nb–Ge, isothermal section at 870 K.

ternary $Sc_2Nb_3Ge_4$ compound and by the existence of a rather extended substitutional exchange of Sc/Nb in the $(Sc_{1-x}Nb_x)_5Ge_3$ solid solution for $0<x<0.8$ with the following unit cell dimensions for the Nb-rich end boundary sample: $a=0.7752$, $c=0.5362$. For sample preparation, see Sc–V–Ge. The starting components were Sc 99.92 mass%, Nb 99.9 mass%, Ge 99.99 mass%.

$Sc_2Nb_3Ge_4$ belongs to the $Ce_2Sc_3Ge_4$-type with lattice parameters $a=0.6860$, $b=1.339$, $c=0.7160$ (Kotur 1986, X-ray powder diffraction).

4.1.9. *Sc–Mo–Ge*

The phase diagram for Sc–Mo–Ge was reported by Kotur and Bodak (1988) (fig. 32). For the details of synthesis, see Sc–V–Ge.

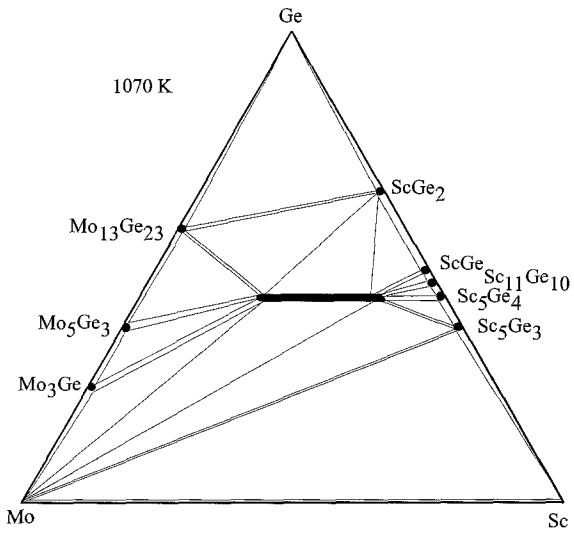

Fig. 32. Sc–Mo–Ge, isothermal section at 1070 K.

Only one ternary compound was found to exist at 1070 K, $Sc_{2-4}Mo_{3-1}Ge_4$ with Sm_5Ge_4 structure type, $a = 0.6691$–0.6813, $b = 1.2872$–1.3285, $c = 0.6905$–0.7027 (X-ray powder diffraction method).

4.1.10. *Sc–Ru–Ge*

No ternary phase diagram has been established for the Sc–Ru–Ge system, but three ternary compounds have been characterized by various authors.

ScRuGe crystallizes with the ZrNiAl-type of structure, $a = 0.6962$, $c = 0.3468$ (Hovestreydt et al. 1982; X-ray powder diffraction). The sample was arc melted under an argon atmosphere and annealed at 1270 K for 1–2 weeks in an evacuated silica tube.

According to X-ray powder diffraction data reported by Venturini et al. (1985a), the compound $ScRuGe_2$ is isostructural with $TiMnSi_2$ ($a = 0.928$, $b = 1.032$, $c = 0.812$). For sample preparation, see Sc–Cr–Ge.

Engel et al. (1984) reported the crystal structure of the $Sc_4Ru_7Ge_6$ compound crystallizing with the $U_4Re_7Si_6$-type of structure ($a = 0.8129$, X-ray powder diffraction data). The sample was prepared by arc melting a cold-pressed mixture of proper amounts of binary $ScGe_2$ alloy and ruthenium. The ternary alloy was finally annealed at 1270 K for 5 weeks. The starting materials were Sc 99.95 mass%, Ge 99.999 mass%, Ru 99.9 mass%.

4.1.11. *Sc–Rh–Ge*

No ternary phase diagram is available for the Sc–Rh–Ge system. However, four ternary phases have been identified.

Hovestreydt et al. (1982) reported two types of structures for the ScRhGe compound: TiNiSi type, $a=0.6497$, $b=0.4112$, $c=0.7385$ and ZrNiAl type, $a=0.6672$, $c=0.3794$. For sample preparation, see Sc–Ru–Ge.

$Sc_4Rh_7Ge_6$ was found to be isostructural with the $U_4Re_7Si_6$-type ($a=0.81255$) by Engel et al. (1984). The crystal structure was determined on a single crystal and was refined to an R value of 0.056 for 99 independent reflections. For details concerning the sample preparation, see Sc–Ru–Ge.

$ScRhGe_2$ was observed to adopt the $TiMnSi_2$-type structure ($a=0.9302$, $b=1.0359$, $c=0.8146$) by Parthé and Chabot (1984).

Venturini et al. (1986a) investigated the crystal structure of the $Sc_4Rh_6Ge_{19}$ compound. It was found to crystallize with its own structure type, $a=1.2605$. Samples were obtained by heating a mixture of starting components (Sc, Rh, Ge: 99.999 mass%) in an evacuated quartz tube at 1173 K.

4.1.12. *Sc–Pd–Ge*

Only one compound was reported for the Sc–Pd–Ge system: ScPdGe, ZrNiAl-type of structure, $a=0.6715$, $c=0.3925$ (Hovestreydt et al. 1982, X-ray powder diffraction). For sample preparation, see Sc–Ru–Ge.

4.1.13. *Sc–Ag–Ge*

The isothermal section at 870 K was constructed by Kotur and Boichuk (1988) (fig. 33). For experimental details, see Sc–V–Ge. The starting materials were Sc 99.92 mass%, Ag 99.99 mass%, Ge 99.999 mass%.

Only one compound was found for the Sc–Ag–Ge combination by Kotur and Boichuk (1988): ScAgGe with the ZrNiAl type, $a=0.6882$, $c=0.4026$.

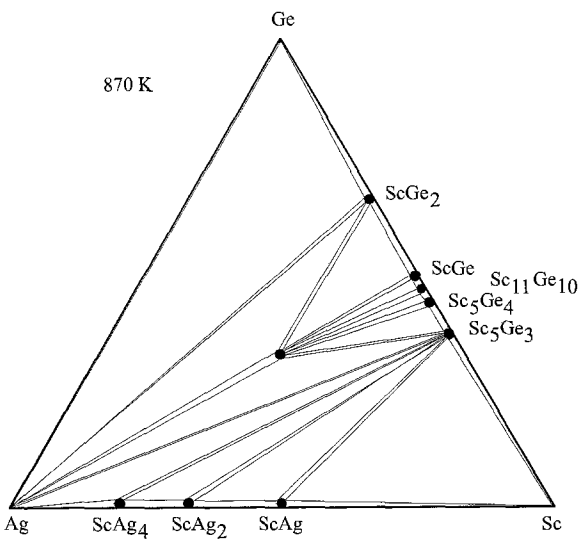

Fig. 33. Sc–Ag–Ge, isothermal section at 870 K.

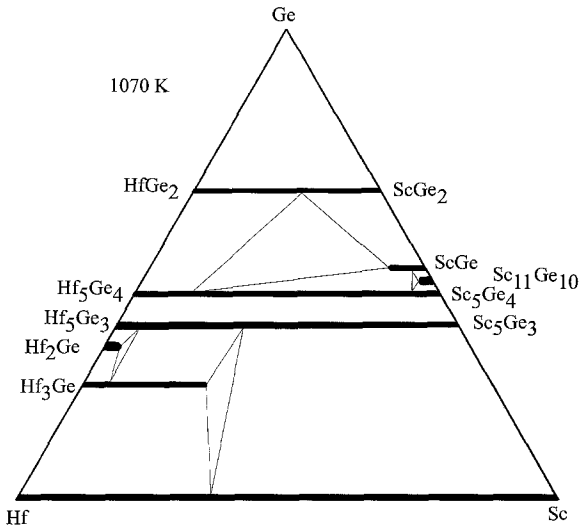

Fig. 34. Sc–Hf–Ge, isothermal section at 1070 K.

4.1.14. *Sc–Hf–Ge*

The isothermal section of the Sc–Hf–Ge phase diagram at 1070 K was reported by Kotur (1991) (fig. 34). No ternary compounds were observed. Continuous solid solutions between isotypic pairs of binary germanides $ScGe_2$–$HfGe_2$, Sc_5Ge_4–Hf_5Ge_4 and Sc_5Ge_3–Hf_5Ge_3 were observed. Also ~25 at.% Sc substitutes for Hf in Hf_3Ge.

4.1.15. *Sc–Ta–Ge*

The phase-field distribution in the Sc–Ta–Ge system at 1070 K (fig. 35) is characterized

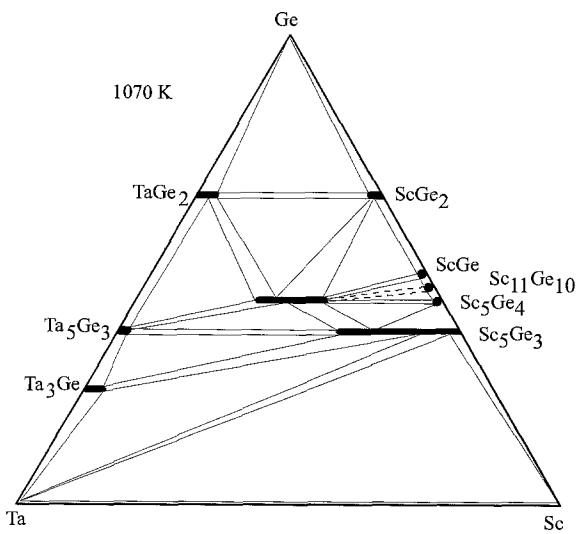

Fig. 35. Sc–Ta–Ge, isothermal section at 1070 K.

by the formation of a ternary $Sc_{2-3}Ta_{3-2}Ge_4$ compound with a large homogeneity region and by the existence of the $Sc_{5-3.25}Ta_{0-1.75}Ge_3$ solid solution originating at Sc_5Ge_3, after Kotur and Bodak (1990). For sample preparation, see Sc–V–Ge. Starting materials were Sc 99.92 mass%, Ta 99.99 mass%, Ge 99.99 mass%.

$Sc_{2-3}Ta_{3-2}Ge_4$ was found to crystallize with a Sm_5Ge_4 type, $a = 0.6823$–0.6855, $b = 1.3177$–1.3230, $c = 0.6977$–0.6993, from X-ray powder diffraction of an arc melted alloy annealed at 1070 K (Kotur and Bodak 1990).

4.1.16. *Sc–W–Ge*

No ternary compounds were observed by Kotur et al. (1989) in the ternary Sc–W–Ge system at 1070 K (fig. 36). The binary Sc_5Ge_3 compound dissolves 3 at.% W. For sample preparation, see Sc–V–Ge.

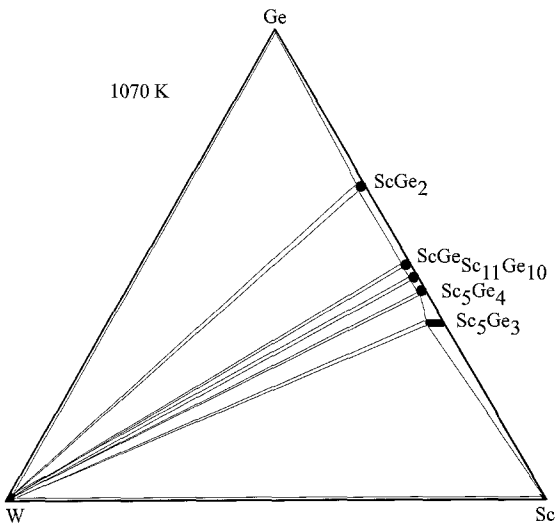

Fig. 36. Sc–W–Ge, isothermal section at 1070 K.

4.1.17. *Sc–Re–Ge*

Figure 37 represents the isothermal section of the Sc–Re–Ge system at 1070 K after Kotur (1995). For sample preparation, see Sc–V–Ge. The mutual solid solubility of components in binary compounds is negligible.

In the course of phase studying the equilibria in the Sc–Re–Ge system at 1070 K, the formation of the $ScReGe_2$ compound (1) with $TiMnSi_2$-type structure has been confirmed and the existence of two compounds [$Sc_3Re_2Ge_3$ (2) and $Sc_9Re_3Ge_8$ (3)] with unknown structures has been observed by Kotur 1995.

The lattice parameters for $ScReGe_2$ are as follows $a = 0.939$, $b = 1.017$, $c = 0.832$ after Venturini et al. (1985a) (powder diffraction data; for sample preparation, see Sc–Cr–Ge) and $a = 0.9385$, $b = 1.0173$, $c = 0.8323$ after Kotur (1995).

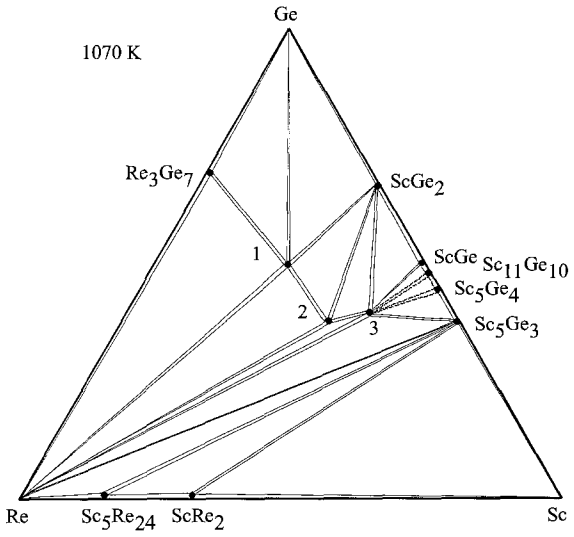

Fig. 37. Sc–Re–Ge, isothermal section at 1070 K.

4.1.18. *Sc–Os–Ge*

No phase diagram is established for the Sc–Os–Ge system.

ScOsGe was observed to adopt the ZrNiAl-type structure with lattice parameters $a = 0.6928$, $c = 0.3407$ (Hovestreydt et al. 1982; X-ray powder diffraction analysis). For sample preparation, see Sc–Ru–Ge.

$ScOsGe_2$ crystallizes with the $TiMnSi_2$-type structure, $a = 0.929$, $b = 1.033$, $c = 0.817$ (Venturini et al. 1985a; powder X-ray diffraction data). For the experimental details, see Sc–Cr–Ge.

Engel et al. (1984), from X-ray powder diffraction data, characterized the compound $Sc_4Os_7Ge_6$ to be isostructural with $U_4Re_7Si_6$, $a = 0.8146$. The sample was synthesized in the same manner as $Sc_4Ru_7Ge_6$.

4.1.19. *Sc–Ir–Ge*

No ternary phase diagram is available for the Sc–Ir–Ge system; however, the formation of two ternary scandium iridium germanides has been reported so far.

From X-ray powder analysis Hovestreydt et al. (1982) reported ScIrGe to crystallize with the TiNiSi-type structure. The crystallographic data were: $a = 0.6446$, $b = 0.4107$, $c = 0.7482$. For sample preparation, see Sc–Ru–Ge.

$Sc_4Ir_7Ge_6$ is isotypic with the crystal structure of $U_4Re_7Si_6$, $a = 0.8146$ (Engel et al. 1984; X-ray powder diffraction). The details of sample preparation are the same as for $Sc_4Ru_7Ge_6$.

4.1.20. *Sc–Pt–Ge*

No phase diagram has been established for the Sc–Pt–Ge system. Only one study on the interaction of scandium with platinum and germanium has been reported. According

to Hovestreydt et al. (1982), ScPtGe was found to be isostructural with the TiNiSi-type structure, $a=0.6585$, $b=0.4215$, $c=0.7141$ (X-ray powder diffraction). For sample preparation, see Sc–Ru–Ge.

4.1.21. *Sc–Au–Ge*

Little information exists on the Sc–Au–Ge system; only one ternary germanide has been characterized.

The crystal structure of the ScAuGe compound has been investigated by Pöttgen et al. (1996a) by the X-ray single-crystal method. It was found to crystallize with a LiGaGe type, $a=0.43082$, $c=0.68458$. The alloy has been prepared by melting a mixture of the elements in an arc furnace and subsequently annealing at 1070 K.

4.2. *Y–d element–Ge systems*

4.2.1. *Y–Cr–Ge*

The phase equilibria in the Y–Cr–Ge system were investigated by Bodak and Gladyshevsky (1985) by means of X-ray analysis of alloys which were arc melted and subsequently annealed in evacuated silica tubes at 870 K and finally quenched in water. The isothermal section of the Y–Cr–Ge system at 870 K is presented in fig. 38.

Brabers et al. (1994) reported the existence of a compound YCr_6Ge_6 with the $HfFe_6Ge_6$ type ($a=0.5167$, $c=0.8273$; X-ray powder diffraction). The sample was prepared by arc melting and subsequent annealing at 1073 K for three weeks in a sealed tube. This phase is not shown in the 870 K isothermal section of the Y–Cr–Ge system (fig. 38).

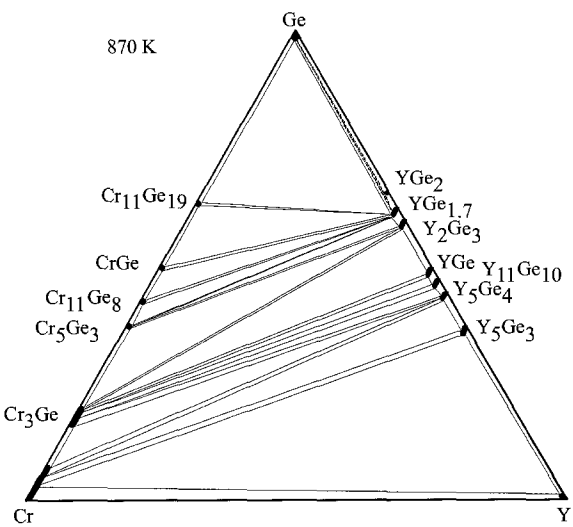

Fig. 38. Y–Cr–Ge, isothermal section at 870 K.

4.2.2. *Y–Mn–Ge*

No ternary phase diagram is available for the Y–Mn–Ge system. Two ternary compounds have been reported for yttrium–manganese–germanium combinations.

YMn_6Ge_6 was found to crystallize in the $HfFe_6Ge_6$-type structure by Venturini et al. (1992), $a = 0.5233$, $c = 0.8153$ (X-ray powder diffraction data). The alloy was synthesized by powder metallurgical reaction in evacuated silica tube at 1073 K for 14 days.

Rossi et al. (1978b) reported on investigation of the crystal structure of the YMn_2Ge_2 compound ($CeGa_2Al_2$ type, $a = 0.3995$, $c = 1.0886$; X-ray powder method). The alloy was obtained by melting under argon in an induction furnace and was annealed at 770 K for one week. The metals used were of purity greater than 99.9 mass% for Y, and greater than 99.99 mass% for Mn and Ge.

4.2.3. *Y–Fe–Ge*

No phase diagram has been constructed for the Y–Fe–Ge system; five ternary compounds have been found and characterized by various authors.

YFe_6Ge_6 was reported to be isotypic with the crystal structure of YCo_6Ge_6 with lattice parameters $a = 0.5110$, $c = 0.4049$ (Mruz et al. 1984). The sample was prepared by arc melting proper amounts of starting components followed by annealing at 870 K for two weeks. At variance with the data of Mruz et al. (1984), YFe_6Ge_6 was found to crystallize with the $TbFe_6Sn_6$ type, $a = 0.8116$, $b = 1.7672$, $c = 0.5120$, by Venturini et al. (1992) from X-ray powder diffraction data. The alloy was obtained by powder metallurgical reaction in an evacuated silica tube at 1173 K for two weeks.

Pecharsky et al. (1989) reported $YFe_{0.33}Ge_2$ to crystallize with the $CeNiSi_2$-type ($a = 0.4118$, $b = 1.5903$, $c = 0.4002$; X-ray powder analysis). The alloy was arc melted and annealed at 870 K. The purity of the starting materials was greater than 99.9 mass%.

YFe_4Ge_2 is isotypic with the crystal structure of $ZrFe_4Si_2$ with lattice parameters $a = 0.7314$, $c = 0.3864$, after Fedyna (1988). The alloy was prepared by arc melting the proper amounts of starting components followed by annealing at 870 K for 400 hours.

Oleksyn (1990) investigated the crystal structure of the $Y_{117}Fe_{52}Ge_{112}$ compound by the X-ray powder method ($Tb_{117}Fe_{52}Ge_{112}$ type, $a = 2.8409$). The alloy was synthesized by arc melting followed by annealing at 1070 K for 350 h. The starting materials were Y 99.83 mass%, Fe 99.9 mass%, Ge 99.99 mass%.

According to X-ray single-crystal data, YFe_2Ge_2 was found to be isostructural with the $CeGa_2Al_2$ type, with lattice parameters $a = 0.3961$, $c = 1.0421$ (Venturini and Malaman 1996). Samples were prepared from stoichiometric amounts of pure elements. After a first reaction in a silica tube under argon, the mixture was melted in an induction furnace.

4.2.4. *Y–Co–Ge*

The phase diagram of the Y–Co–Ge system has not been established; eight ternary compounds have been identified for yttrium–cobalt–germanium combinations.

Méot-Meyer et al. (1985a) reported the crystal structure of the $YCo_{1-x}Ge_2$, $x = 0.55$ ($CeNiSi_2$ type, $a = 0.4106$, $b = 1.612$, $c = 0.4026$). Samples were prepared by powder

metallurgical reaction and annealed in evacuated silica tube at 1173 K. Pecharsky et al. (1989) investigated the formation and crystal structure of the $YCo_{1-x}Ge_2$ compound by X-ray powder analysis of arc melted alloys annealed at 870 K. The $CeNiSi_2$-type structure was confirmed and in addition, the existence of an extended homogeneity region was observed: $0.2 < x < 0.9$, $a = 0.4067$–0.4115, $b = 1.5840$–1.6080, $c = 0.3946$–0.4019.

The crystal structure of $Y_3Co_4Ge_{13}$ ($Yb_3Rh_4Sn_{13}$ type, $a = 0.8757$; X-ray powder diffraction) was investigated by Venturini et al. (1985b) from a sample which was prepared by heating a compacted mixture of starting materials (Y in pieces, 99.9 mass%; Co and powder Ge, 99.99 mass%) in an evacuated quartz tube at 1073 K.

Bruskov et al. (1986) reported on the single-crystal investigation of $Y_3Co_4Ge_{13}$ (own structure type, $a = 0.8769$). The single crystal was obtained from arc melted and annealed at 870 K alloy.

McCall et al. (1973a) mentioned the existence of the YCo_2Ge_2 compound with the $CeGa_2Al_2$-type. Venturini and Malaman (1996) confirmed the crystal structure for the YCo_2Ge_2 compound and established the lattice parameters ($a = 0.39698$, $c = 1.0025$; X-ray single-crystal data). The sample was prepared in the same manner as YFe_2Ge_2.

From an X-ray powder analysis of alloy annealed at 1173 K, $Y_2Co_3Ge_5$ was reported to adopt the $Lu_2Co_3Si_5$ type structure, $a = 0.9642$, $b = 1.180$, $c = 0.5707$, $\beta = 91.9°$ (Venturini et al. 1986b).

The crystal structure of the YCo_6Ge_6 compound was reported by Buchholz and Schuster (1981) (own structure type, $a = 0.5074$, $c = 0.39908$). Samples were melted under an argon atmosphere in a corundum crucible at 1073–1273 K.

Gorelenko et al. (1984) reported the crystal structure of YCoGe (TiNiSi type, $a = 0.6880$, $b = 0.4212$, $c = 0.7258$; X-ray powder analysis). The alloy was obtained by arc melting and annealing in an evacuated quartz tube at 870 K for 350 hours.

$Y_3Co_2Ge_4$ crystallizes with the $Tb_3Co_2Ge_4$ type structure, $a = 1.0608$, $b = 0.8050$, $c = 0.4181$, $\gamma = 107.80°$. Samples were prepared by arc melting and annealing at 873 K for 1450 h. The starting materials were: Y (>99.9 mass%), Co (99.99 mass%), Ge (99.999 mass%) (Mruz et al. 1989).

Y_2CoGe_6 is isotypic with Ce_2CuGe_6, $a = 0.3940$, $b = 0.3993$, $c = 2.1426$ (Oleksyn et al. 1991; X-ray powder diffraction data). The sample was melted in an arc furnace and annealed at 1070 K in an evacuated quartz capsule for 400 h. The purity of the starting materials was greater than 99.9 mass%.

4.2.5. *Y–Ni–Ge*

Figure 39 represents the isothermal sections of Y–Ni–Ge phase diagram at 1070 K (0–33 at.% Y) and at 670 K (33–100 at.% Y) which were studied by Koterlyn et al. (1988). The isothermal sections were constructed by means of X-ray powder analysis of alloys, which were arc melted and subsequently annealed in evacuated silica tubes for 400 h and finally quenched in water. Starting materials were Y 99.99 mass%, Ni 99.98 mass% and Ge 99.99 mass%.

The ternary phase diagram is characterized by the existence of ten ternary compounds and by the formation of a substitutional exchange of Ge/Ni in the solid solutions

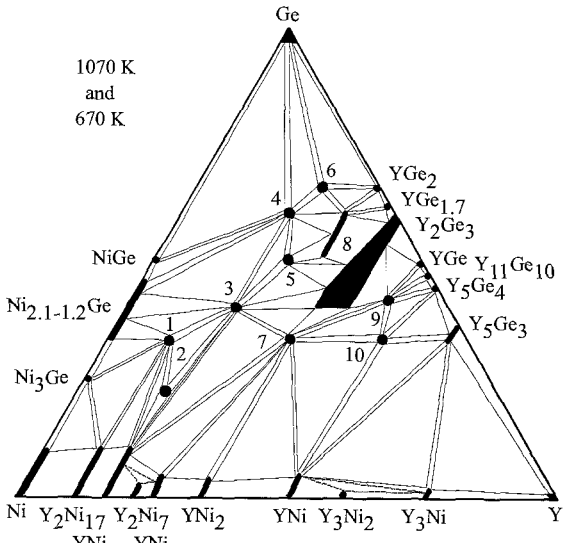

Fig. 39. Y–Ni–Ge, isothermal section at 1070 K (0–33 at.% Y) and at 670 K (33–100 at.% Y).

$Y_2(Ni_{1-x}Ge_x)_{17}$ and $Y(Ni_{1-x}Ge_x)_5$ for $0 < x < 0.12$. This behavior corresponds to the solid solution range of Ge in nickel. Nonstoichiometry and a homogeneity range were observed for $YNi_{1-x}Ge_2$ ($0.4 < x < 0.7$) (8). The binary compound Y_2Ge_3 dissolves 20 at.% Ni.

YNi_5Ge_3 (1) was reported to crystallize with an YNi_5Si_3type, $a = 1.9108$, $b = 0.3864$, $c = 0.6773$ by Fedyna (1988). The alloy, arc melted and annealed at 870 K, was investigated by X-ray powder diffraction analysis. Starting materials were Y 99.83 mass%, Ni 99.99 mass%, Ge 99.99 mass%.

$Y_3Ni_{11}Ge_4$ (2) belongs to the $Sc_3Ni_{11}Si_4$ type, $a = 0.8319$, $c = 0.8821$ after Fedyna (1988). For sample preparation, see the previous paragraph.

The YNi_2Ge_2 (3) compound was found to adopt the $CeGa_2Al_2$-type structure, $a = 0.4043$, $c = 0.9763$ (Rieger and Parthé 1969b). Venturini and Malaman (1996) confirmed the crystal structure for the YNi_2Ge_2 compound and established the lattice parameters $a = 0.39698$, $c = 1.0025$ from X-ray single crystal diffraction. The sample was prepared in the same manner as YFe_2Ge_2, see Y–Fe–Ge.

$YNiGe_3$ (4) with the $ScNiSi_3$-type of structure ($a = 2.1657$, $b = 0.4102$, $c = 0.4092$, X-ray powder diffraction analysis) was reported by Bodak et al. (1985). For the details of sample preparation and purity of starting materials, see YNi_5Ge_3.

Y_2NiGe_6 (6) has been found by Oleksyn (1990) from X-ray powder diffraction to be isostructural with Ce_2CuGe_6-type structure ($a = 0.3956$, $b = 2.1265$, $c = 0.4007$). The sample was prepared by arc melting ingots of the constituting elements and annealing at 1070 K for 700 h. For the purity of starting materials, see YNi_5Ge_3, above.

Pecharsky et al. (1989) investigated the formation and crystal structure of the

$YNi_{1-x}Ge_2$ (8) compound by X-ray powder analysis of arc melted alloys annealed at 870 K ($CeNiSi_2$ type, $a = 0.4090$–0.4101, $b = 1.607$–1.629, $c = 0.3969$–0.4012). For sample preparation, see $YFe_{1-x}Ge_2$ under Y–Fe–Ge.

Gorelenko et al. (1984) reported the crystal structure of YNiGe (8) (TiNiSi type, $a = 0.6970$, $b = 0.4212$, $c = 0.7258$; X-ray powder analysis). The alloy was obtained by arc melting and annealing in an evacuated quartz tube at 870 K for 350 hours.

Bodak et al. (1982) reported on the crystal structure of Y_3NiGe_2 (10) from X-ray powder diffraction (La_3NiGe_2 type, $a = 1.1304$, $b = 0.4215$, $c = 1.1299$). The proper amounts of starting components were arc melted and annealed at 870 K.

The crystal structure of two ternary compounds $YNiGe_2$ (5) and $Y_{4.75}NiGe_{4.25}$ (9) has not been determined (Koterlyn et al. 1988).

4.2.6. *Y–Cu–Ge*

No isothermal section is available for the Y–Cu–Ge system; four ternary compounds have been found and analyzed by different groups of authors.

Rieger and Parthé (1969a) investigated the occurrence of the AlB_2-type structure by means of X-ray powder diffraction of arc melted alloys. The data presented were $YCu_{1-0.67}Ge_{1-1.33}$ with $a = 0.404$–0.4217, $c = 0.405$–0.3696. In variance with the data by Rieger and Parthé (1969a), Iandelli (1993) observed YCuGe with the $CaIn_2$-type ($a = 0.4228$, $c = 0.7325$, X-ray powder analysis). The alloy was prepared from filings or powders of metals (yttrium 99.7 mass%, copper and germanium 99.99 mass%), which were mixed and sealed in tantalum crucible under argon, melted by induction heating and annealed for 10 days at 1023 K.

$Y_6Cu_8Ge_8$ crystallizes with the $Gd_6Cu_8Ge_8$-type structure and the lattice parameters are $a = 1.392$, $b = 0.665$, $c = 0.419$ (Hanel and Nowotny 1970).

Konyk et al. (1988) investigated the crystal structure of Y_2CuGe_6 alloy prepared by arc melting under argon and annealed at 870 K in evacuated quartz tube for 720 h. From X-ray powder analysis a Ce_2CuGe_6-type was claimed, $a = 0.3993$, $b = 0.4108$, $c = 2.0980$.

Rieger and Parthé (1969b) prepared YCu_2Ge_2 with a $CeGa_2Al_2$-type of structure, $a = 0.4035$, $c = 1.0303$.

4.2.7. *Y–Nb–Ge*

The phase diagram of the Y–Nb–Ge system has not been established. The existence of a compound $Y_2Nb_3Ge_4$ with the $Ce_2Sc_3Si_4$-type ($a = 0.6964$, $b = 1.3572$, $c = 0.7182$) was reported by Le Bihan et al. (1996a) from X-ray powder diffraction data of arc melted alloy. The starting materials were: Y and Nb 99.99 mass%, Ge 99.999 mass%.

4.2.8. *Y–Mo–Ge*

No ternary compounds or solid solutions were found in the Y–Mo–Ge system at 870 K by Bodak and Gladyshevsky (1985) from X-ray powder diffraction of arc melted samples which were annealed at 870 K for three weeks (see fig. 40).

The existence of a compound $Y_2Mo_3Ge_4$ with the $Ce_2Sc_3Si_4$ type ($a = 0.6912$, $b = 1.3134$, $c = 0.7067$) was reported by Le Bihan et al. (1996b) from X-ray powder diffraction of arc melted alloy. For the purity of the starting materials, see Y–Nb–Ge.

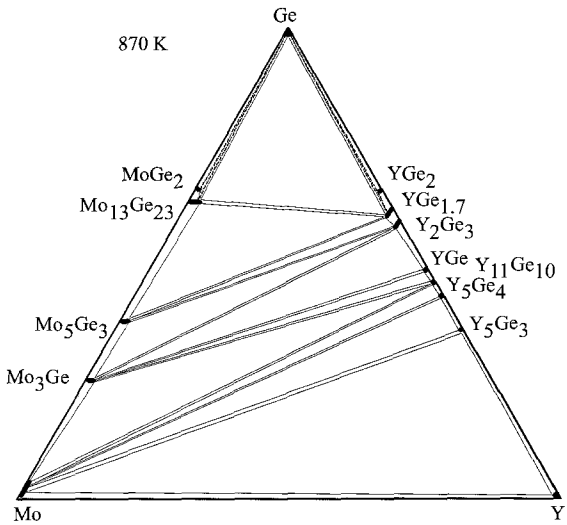

Fig. 40. Y–Mo–Ge, isothermal section at 870 K.

4.2.9. *Y–Ru(Rh, Pd)–Ge*

The ternary Y–Ru(Rh, Pd)–Ge systems have been studied only with respect to the formation of compounds with specific composition and structure. Their crystallographic characteristics are listed in table 10.

Table 10
Crystallographic data for the ternary Y–Ru(Rh, Pd)–Ge compounds

Compound	Structure	Lattice parameters (nm)			Reference
		a	*b*	*c*	
YRu_2Ge_2	$CeGa_2Al_2$	0.4225		0.9837	Francois et al. (1985)
$Y_2Ru_3Ge_5$	$U_2Co_3Si_5$	0.9808	1.243	0.5735	Venturini et al. (1986b)
$Y_3Ru_4Ge_{13}$	$Yb_3Rh_4Sn_{13}$	0.8962			Segre et al. (1981a)
YRh_2Ge_2	$CeGa_2Al_2$	0.4103		1.0207	Francois et al. (1985)
$Y_2Rh_3Ge_5$	$Lu_2Co_3Si_5$	0.9963	1.2045 $\beta = 91.9°$	0.5820	Venturini et al. (1986b)
$Y_5Rh_4Ge_{10}$	$Sc_5Co_4Si_{10}$	1.2944		0.4270	Venturini et al. (1984)
Y_2Rh_3Ge	own	0.5552		1.182	Cenzual et al. (1987)
$Y_3Rh_2Ge_2$	$La_3Ni_2Ga_2$	0.5563	0.7814	1.182	Gladyshevsky et al. (1991a)
$Y_3Rh_4Ge_{13}$	$Yb_3Rh_4Sn_{13}$	0.8923			Venturini et al. (1985b)
$Y_4Rh_{13}Ge_9$	$Ho_4Ir_{13}Ge_9$				Verniere et al. (1995)
YRhGe	TiNiSi	0.6899	0.4276	0.7550	Hovestreydt et al. (1982)
YPd_2Ge	YPd_2Si	0.7352	0.7036	0.5562	Jorda et al. (1983)
Y_2PdGe_6	Ce_2CuGe_6	0.4079	0.4016	2.1525	Sologub et al. (1995a)
YPdGe	KHg_2	0.4365	0.6952	0.7549	Hovestreydt et al. (1982)

4.2.10. *Y–Ag–Ge*

No phase diagram is available for the Y–Ag–Ge system. Protsyk (1994) reported the existence of the $YAg_{0.33}Ge_{1.67}$ compound with α-$ThSi_2$ type (a 0.4070, c = 1.3710; X-ray powder diffraction data). Samples were arc melted and annealed at 870 K for 400 hours.

Gibson et al. (1996) investigated the crystal structure of the YAgGe compound (ZrNiAl type, a = 0.71180, c = 0.41968). The sample was prepared from the elements by arc melting and annealing at 970 K for ten days.

4.2.11. *Y–Os(Ir, Pt)–Ge*

The ternary Y–Os(Ir, Pt)–Ge systems have been studied only with respect to the formation of compounds with specific composition and structure. Their crystallographic data are presented in table 11.

Table 11
Crystallographic data for the ternary Y–Os(Ir, Pt)–Ge compounds

Compound	Structure	Lattice parameters (nm)			Reference
		a	b	c	
$Y_5Os_4Ge_{10}$	$Sc_5Co_4Si_{10}$	1.3006		0.4229	Braun et al. (1980)
$Y_3Os_4Ge_{13}$	$Yb_3Rh_4Sn_{13}$	0.8985			Segre et al. (1981a)
$YIrGe_2$	own	0.4264	1.5976	0.8813	Francois et al. (1987)
$Y_2Ir_3Ge_5$	$U_2Co_3Si_5$	1.0133	1.172	0.5955	Venturini et al. (1986b)
$Y_4Ir_7Ge_6$	$U_4Re_7Si_6$	0.8324			Francois et al. (1985)
$Y_5Ir_4Ge_{10}$	$Sc_5Co_4Si_{10}$	1.2927		0.4308	Braun et al. (1980)
$Y_3Ir_4Ge_{13}$	$Yb_3Rh_4Sn_{13}$	0.8948			Venturini et al. (1985a)
$Y_4Ir_{13}Ge_9$	$Ho_4Ir_{13}Ge_9$				Verniere et al. (1995)
YIrGe	TiNiSi	0.6843	0.4265	0.7619	Hovestreydt et al. (1982)
$YPtGe_2$	$YIrGe_2$	0.4307	1.5976	0.8813	Francois et al. (1987)
$Y_3Pt_4Ge_6$	own	0.8692	0.4306 β = 99.45°	1.3161	Venturini and Malaman (1990)
YPt_2Ge_2	$LaPt_2Ge_2$	0.4314	0.4358 β = 91.08°	0.9659	Venturini et al. (1989a)
YPtGe	TiNiSi	0.6986	0.4338	0.7557	Hovestreydt et al. (1982)
Y_2PtGe_6	Ce_2CuGe_6	0.4057	0.4012	2.1677	Sologub et al. (1995a)

4.2.12. *Y–Au–Ge*

No ternary phase diagram is available for the Y–Au–Ge system, however, a ternary compound of yttrium with gold and germanium with the 1:1:1 stoichiometric ratio has been identified and studied by means of X-ray and metallographic analyses by Rossi et al. (1992). It was found to adopt the LiGaGe type with lattice parameters a = 0.4408, c = 0.7307. The sample was prepared by melting the metals (purity around 99.9 mass% for

yttrium and 99.99 mass% for gold and germanium) in an induction furnace and annealing at 1070 K for one week.

4.3. *La–d element–Ge systems*

4.3.1. *La–Mn–Ge*

No phase diagram is available for the system La–Mn–Ge, however, two ternary compounds have been observed and characterized.

The $LaMn_2Ge_2$ compound has been prepared and studied by Rossi et al. (1978b). It was found to be of $CeGa_2Al_2$ type with lattice parameters $a = 0.4108$, $c = 1.0685$. The alloy was obtain by melting under argon atmosphere in an induction furnace. The sample was then annealed at 500°C for one week. The lanthanum used was of a purity greater than 99.9 mass%, for manganese and germanium the purity was greater than 99.99 mass%.

The LaMnGe compound with PbFCl-type was observed by Welter et al. (1995); $a = 0.4254$, $c = 0.7425$. The compound was prepared from commercially available high purity elements. Compacted pellet of stoichiometric mixture was sealed under argon (100 mmHg) in silica tube which was heated at 1273 K as a preliminary homogenization treatment and then melted in an induction furnace. The resulting ingot was annealed for 2 weeks at 1173 K.

4.3.2. *La–Fe–Ge*

No phase diagram is available at present for the La–Fe–Ge system; the formation of three ternary germanides has been reported by various authors.

The $LaFe_{0.67}Ge_{1.33}$ compound was found to adopt the AlB_2-type structure ($a = 0.4223$, $c = 0.4316$; X-ray powder diffraction) (Felner and Schieber 1973). The sample was prepared by melting elements together (lanthanum 99.9 mass%, Ge 99.99 mass%, Fe 99.95 mass%). The metals were mixed and heated in an alumina crucible in an induction furnace under the protective atmosphere of argon. The sample was homogenized by annealing at 1870 K for about 30 min.

The $LaFe_2Ge_2$ compound was initially investigated by Rossi et al. (1978a) ($CeGa_2Al_2$ type, $a = 0.4110$, $c = 1.0581$) by means of X-ray diffraction. Bara et al. (1990) confirmed the crystal structure of the $LaFe_2Ge_2$ compound ($a = 0.4128$, $c = 1.0602$; X-ray powder diffraction) from an arc melted sample, annealed for 1 week at 1073 K. The purity of the starting elements was La, 4N; Fe, 3N; Ge, 5N.

Francois et al. (1990) investigated the occurrence of the $CeNiSi_2$ type for lanthanum–iron–germanium combinations from the alloys annealed at 1173 K ($LaFe_{0.60-0.69}Ge_2$; $a = 0.4347$–0.4359, $b = 1.683$–1.679, $c = 0.4210$–0.4225).

4.3.3. *La–Co–Ge*

The equilibrium phase diagram for the La–Co–Ge system has not been reported. Lanthanum–cobalt–germanium combinations have been investigated only with respect to

the formation and crystal structure of compounds with various stoichiometries. To date five compounds have been identified.

Méot-Meyer et al. (1985a) reported the crystal structure of $LaCo_{0.96}Ge_2$ ($CeNiSi_2$ type, $a=0.4309$, $b=1.688$, $c=0.4238$). The sample was prepared by powder metallurgical reaction and annealed in evacuated silica tube at 1173 K. Pecharsky et al. (1989) investigated the formation and crystal structure of the $LaCo_{1-x}Ge_2$ compound by X-ray powder analysis of arc melted alloy annealed at 870 K. The $CeNiSi_2$-type structure was confirmed for the sample of stoichiometric composition ($a=0.4335$, $b=1.6945$, $c=0.4279$).

McCall et al. (1973b) investigated the crystal structure of the $LaCo_2Ge_2$ compound ($BaAl_4$ type, $a=0.4123$, $c=1.0277$; X-ray powder diffraction). The sample was melted in an induction furnace. Starting components were Co, Ge (5N) and La (3N).

The crystal structure of $LaCoGe_3$ ($BaNiSn_3$ type, $a=0.4350$, $c=0.9865$; X-ray powder diffraction) was investigated by Venturini et al. (1985b) from a sample which was prepared by heating a compacted mixture of starting materials (La in pieces, 99.9 mass%; Co and powder Ge, 99.99 mass%) in an evacuated quartz tube at 1073 K. Later the crystal structure of $LaCoGe_3$ compound was confirmed by Pecharsky et al. (1993) by means of metallography and room-temperature X-ray powder diffractometry. The crystal structure has been established and lattice parameters have been measured ($BaNiSn_3$ type, $a=0.43497$, $c=0.98679$). The alloy was prepared by arc melting pieces of the metals under an argon atmosphere and then heat treating it at 1173 K for 7 days in a helium-filled quartz tube. The starting metals were La 99.79 mass%, Co and Ge >99.999 mass%.

The LaCoGe compound with PbFCl-type structure was observed by Welter et al. (1993a); $a=0.4194$, $c=0.7028$. The compound was prepared from commercially available high-purity elements. A compacted pellet of stoichiometric mixture was sealed under argon (100 mmHg) in a silica tube which was heated at 1173 K as a preliminary homogenization treatment and then melted in an induction furnace. The resulting ingot was annealed for 2 weeks at 1173 K.

The crystal structure of the $La_6Co_{13}Ge$ compound was reported by Weitzer et al. (1990) ($Nd_6Fe_{13}Si$ type, $a=0.80620$, $c=2.29224$). The sample was melted under argon and annealed at 1073 K for 5 days. Starting materials were commercially available high-purity elements.

4.3.4. *La–Ni–Ge*

No phase diagram is available for the La–Ni–Ge system, but nine ternary phases have been identified.

Bodak et al. (1982) investigated the crystal structure of the La_3NiGe_2 compound (own structure type, $a=1.2041$, $b=0.4358$, $c=1.1871$) by the single-crystal diffraction method. For sample preparation and purity of starting elements, see Y–Ni–Ge.

The $LaNi_2Ge_2$ compound was found to adopt the $CeGa_2Al_2$-type structure, $a=0.4187$, $c=0.9918$ (Rieger and Parthé 1969b).

Pecharsky et al. (1989) reported the crystal structure of the $LaNiGe_2$ ($CeNiSi_2$ type, $a = 0.4314$, $b = 1.688$, $c = 0.4235$) from X-ray powder analysis of arc melted alloy annealed at 870 K. The stoichiometric composition and crystal structure type were confirmed by Francois et al. (1990). For sample preparation, see La–Fe–Ge.

Gladyshevsky and Bodak (1965) determined the AlB_2-type structure for the compound $LaNi_{0.67-0.5}Ge_{1.33-1.5}$, $a = 0.4202$–0.4193, $c = 0.4306$–0.4336 (X-ray powder diffraction).

Bruskov (1984) investigated the crystal structure for the compounds $La_3Ni_4Ge_4$ ($U_3Ni_4Si_4$-type structure, $a = 0.4223$, $b = 0.4230$, $c = 2.4156$; X-ray single-crystal method); $La_{11}Ni_4Ge_6$ (own structure type, $a = 1.8637$, $b = 0.4384$, $c = 1.4191$, $\beta = 106{,}13°$; X-ray single-crystal method); La_8NiGe_5 (own structure type, $a = 1.5586$, $b = 1.8384$, $c = 1.1351$; X-ray single-crystal method); $La(Ni_{0.82}Ge_{0.18})_{13}$ ($NaZn_{13}$ type, $a = 1.1371$); and La_2NiGe (own structure type, $a = 0.7947$, $c = 1.4262$; X-ray single-crystal method). For sample preparation, see Y–Ni–Ge.

4.3.5. *La–Cu–Ge*

No phase diagram is available for the system La–Cu–Ge, however the crystallographic characteristics for a series of ternary compounds are presented in the literature.

Rieger and Parthé (1969a) investigated the occurrence of the AlB_2-type structure by means of X-ray powder diffraction of arc melted alloys. The data presented were $LaCu_{1-0.67}Ge_{1-1.33}$ with $a = 0.4323$–0.4223, $c = 0.4050$–0.4322. Iandelli (1993) confirmed AlB_2-type ($a = 0.4335$, $c = 0.4040$, X-ray powder analysis) from the LaCuGe alloy which was prepared from filings or powders of the metals (La 99.7 mass%, Co and Ge 99.99 mass%), sealed in a tantalum crucible under argon followed by melting in an induction furnace; afterwards the sample was annealed for 10 days at 1023 K.

Konyk et al. (1988) reported on the crystal structure of La_2CuGe_6 alloy prepared by arc melting under argon and annealed at 870 K in an evacuated quartz tube for 720 h. From X-ray powder analysis a Ce_2CuGe_6-type was claimed, $a = 0.4100$, $b = 0.4258$, $c = 2.1838$.

Rieger and Parthé (1969b) prepared $LaCu_2Ge_2$ with the $CeGa_2Al_2$-type of structure, $a = 0.4265$, $c = 1.0170$.

Francois et al. (1990) reported the crystal structure of the $LaCu_{0.82-0.92}Ge_2$ ($CeNiSi_2$ type, $a = 0.4335$–4333, $b = 1.740$–1740, $c = 0.4175$–0.4193). For sample preparation, see La–Fe–Ge.

4.3.6. *La–Zn–Ge*

No isothermal section is available for the ternary La–Zn–Ge system, however one ternary compound was observed and characterized by Rossi and Ferro (1996). $LaZn_{1.5}Ge_{0.5}$ was found to crystallize with an AlB_2 type, $a = 0.4471$, $c = 0.4032$ from X-ray powder diffraction of melted in an induction furnace alloy which was afterwards annealed at 1070 K for one week. An electronic micrographic examination as well as microprobe analysis were carried out. The metals employed in the synthesis of sample had a nominal purity of 99.9 mass% for La, and 99.999 mass% for other metals.

4.3.7. *La–Ru–Ge*

The phase diagram for the La–Ru–Ge system is not yet available, however several groups of authors investigated lanthanum–ruthenium–germanium combinations with respect to the formation and crystal structure of compounds.

Venturini et al. (1985b) reported on the X-ray powder diffraction study of the $LaRuGe_3$ compound from the sample which was prepared by heating a mixture of the starting components (La 3N, Ru 4N, Ge 4N) in evacuated quartz tube at 1073 K. The crystal structure was found to adopt the $BaNiSn_3$ type, $a = 0.4414$, $c = 1.0123$.

Venturini and Malaman (1996) reported on the single crystal refinement of the $CeGa_2Al_2$-type structure of the $LaRu_2Ge_2$ composition, $a = 0.42866$, $c = 1.0121$. Samples were prepared from stoichiometric amounts of pure elements. After a first reaction in a silica tube under argon, the mixture was melted in an induction furnace.

$La_2Ru_3Ge_5$ was found to crystallize with $U_2Co_3Si_5$-type ($a = 1.00108$, $b = 1.2496$, $c = 0.59256$, X-ray single-crystal diffraction method) by Venturini et al. (1989b).

The crystal structure of the LaRuGe compound was investigated by Welter et al. (1993b). It was found to adopt the PbFCl-type structure, $a = 0.4294$, $c = 0.7019$ (X-ray powder diffraction). The compound was prepared from commercially available high purity elements. A compact of a stoichiometric mixture was heated in sealed under argon silica tube at 1173 K for preliminary homogenization and then melted in an induction furnace.

$La_3Ru_2Ge_2$ compound was found to crystallize with $La_3Ni_2Ga_2$-type ($a = 0.5787$, $b = 0.7946$, $c = 1.3729$, X-ray powder diffraction) from the arc melted and annealed at 870 K sample (Bodak et al. 1989a).

4.3.8. *La–Rh–Ge*

Venturini et al. (1985b) reported on the X-ray powder diffraction study of the $LaRhGe_3$ compound from the sample which was prepared by heating the mixture of starting components (La 3N, Rh 4N, Ge 4N) in evacuated quartz tube at 1073 K. The crystal structure was found to adopt the $BaNiSn_3$ type, $a = 0.4419$, $c = 1.0046$.

Venturini and Malaman (1996) reported on the single crystal refinement of the $CeGa_2Al_2$-type structure germanide of the $LaRh_2Ge_2$ composition, $a = 0.4174$, $c = 1.0519$. Samples were prepared from stoichiometric amounts of pure elements. After a first reaction in a silica tube under argon, the mixture was melted in an induction furnace.

$La_2Rh_3Ge_5$ was found to crystallize with $U_2Co_3Si_5$-type structure ($a = 1.0135$, $b = 1.2177$, $c = 0.60410$, X-ray single-crystal diffraction method) by Venturini et al. (1989a).

Gladyshevsky et al. (1991a) reported on the crystal structure for the $La_3Rh_2Ge_2$ compound ($La_3Ni_2Ge_2$ type, $a = 0.5766$, $b = 0.8195$, $c = 1.3609$; X-ray powder diffraction). The alloy was prepared by arc melting and annealing at 1070 K.

Francois et al. (1990) reported the crystal structure of $LaRhGe_2$ ($CeNiSi_2$ type, $a = 0.4375$, $b = 1.715$, $c = 0.4367$). For sample preparation, see $LaFeGe_2$ under La–Fe–Ge.

$La_3Rh_4Ge_4$ crystallizes with $U_3Ni_4Si_4$ type, $a = 0.4174$, $b = 0.4241$, $c = 2.5234$ (Parthé and Chabot 1984).

4.3.9. *La–Pd–Ge*

Phase relations have not been established for the La–Pd–Ge system; formation and crystal structure for five ternary compounds have been reported so far.

Venturini and Malaman (1996) reported on the single crystal refinement of the $CeGa_2Al_2$-type structure germanide of the $LaPd_2Ge_2$ composition, $a = 0.43669$, $c = 1.0027$. For the details of synthesis, see $LaRu_2Ge_2$ under La–Ru–Ge.

Francois et al. (1990) reported the crystal structure of the $LaPdGe_2$ ($CeNiSi_2$ type, $a = 0.4379$, $b = 1.737$, $c = 0.4382$). For sample preparation, see $LaFeGe_2$ under La–Ru–Ge.

According to an X-ray powder diffraction analysis Hovestreydt et al. (1982) reported the compound LaPdGe adopted the KHg_2-type structure, $a = 0.4518$, $b = 0.7409$, $c = 0.7740$. An alloy was arc melted under argon and annealed at 1270 K for 1–2 weeks. Starting materials were La (3N), Pd (4N) and Ge (5N).

The crystal structure of the compound $LaPd_2Ge$ was found to be of the YPd_2Si type ($a = 0.7711$, $b = 0.6972$, $c = 0.5828$; X-ray powder diffraction) by Jorda et al. (1983). The sample was obtained by induction heating of pressed powder compacts in a levitation coil under an argon atmosphere pressure of 4 atm. After the rapid reaction in the liquid state the molten sample was dropped into a boron nitride crucible. Then alloy was annealed in evacuated quartz tube for 10 days at 1173 K. Starting materials were Pd 99.99 mass%, Ge, specpure quality, La 99.9 mass%.

Sologub et al. (1995a) reported on the X-ray powder analysis of the La_2PdGe_6 compound which was found to crystallize with the Ce_2CuGe_6 type structure, $a = 0.4211$, $b = 0.4110$, $c = 2.2265$. The sample was synthesized by argon arc melting followed by a heat treatment at 870 K for 150 hours. Starting materials used were obtained from Johnson & Matthey, UK (99.9 mass%).

4.3.10. *La–Ag–Ge*

A systematic study of the La–Ag–Ge system at 770 K was performed by Protsyk (1994). The samples were prepared by arc melting under argon and annealed in evacuated quartz ampoules at 770 K for 500 hours. Starting materials were La 99.98 mass%, Ag 99.9 mass% and Ge 99.99 mass%. Phase relations are characterized by the formation of four ternary compounds (see fig. 41).

Sologub et al. (1995a) reported on the X-ray powder analysis of the La_2AgGe_6 (2) compound which was found to crystallize with the Ce_2CuGe_6-type structure, $a = 0.43409$, $b = 0.41598$, $c = 2.1901$. For the experimental details, see La_2PdGe_6 under La–Pd–Ge.

LaAgGe (3) with the LiGaGe-type of structure ($a = 0.45587$, $c = 0.78969$; X-ray powder diffraction data) was observed by Pecharsky et al. (1991) from arc melted alloy heat-treated at 1023 K in a helium-filled sealed quartz tube for one week. The lanthanum was 99.79 mass% pure; the silver was 99.99 mass% pure and the germanium was 99.999 mass% pure.

The existence of $LaAg_2Ge_2$ (1) ($CeGa_2Al_2$-type structure, $a = 0.4358$, $c = 1.0982$) and $LaAg_{0.8}Ge_{1.2}$ (4) (AlB_2 type, $a = 0.4366$, $c = 0.4280$) was reported by Protsyk (1994) from X-ray powder diffraction of alloy annealed at 773 K.

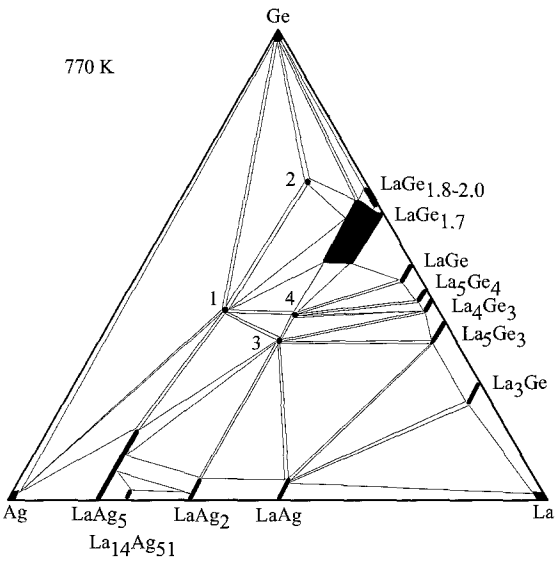

Fig. 41. La–Ag–Ge, isothermal section at 770 K.

4.3.11. *La–Os–Ge*

Little information exists on the interaction of lanthanum and osmium with germanium. One ternary compound was observed and characterized within the La–Os–Ge system. The crystal structure of the $LaOsGe_3$ compound ($BaNiSn_3$ type, $a = 0.4441$, $c = 1.0124$; X-ray powder diffraction) was investigated by Venturini et al. (1985b) from the sample which was prepared by heating a compacted mixture of the starting materials (La in pieces, 99.9 mass%; Os and powder Ge, 99.99 mass%) in an evacuated quartz tube at 1073 K.

4.3.12. *La–Ir–Ge*

No ternary phase diagram has been established for the La–Ir–Ge system, however five ternary compounds have been characterized.

Venturini et al. (1985b) reported on the X-ray powder diffraction study of the $LaIrGe_3$ compound from a sample prepared by heating a mixture of starting components (La 3N, Ir 4N, Ge 4N) in an evacuated quartz tube at 1073 K. The crystal structure was found to be $BaNiSn_3$ type, $a = 0.4428$, $c = 1.0042$.

$La_2Ir_3Ge_5$ was found to crystallize with $U_2Co_3Si_5$-type structure ($a = 1.0218$, $b = 1.2028$, $c = 0.6091$, X-ray single-crystal diffraction method) by Venturini et al. (1989b).

Francois et al. (1990) reported the crystal structure of $LaIrGe_2$ ($CeNiSi_2$ type, $a = 0.4389$, $b = 1.716$, $c = 0.4389$). For sample preparation, see $LaFeGe_2$ under La–Fe–Ge.

According to X-ray powder diffraction analysis reported by Hovestreydt et al. (1982) the compound LaIrGe adopted the LaPtSi-type structure, $a = 0.43166$, $c = 1.4430$. The alloy was arc melted under argon and annealed at 1270 K for 1–2 weeks. Starting materials were La (3N), Ir (4N) and Ge (5N).

$LaIr_2Ge_2$ is isotypic with the crystal structure of $CaBe_2Ge_2$ with lattice parameters $a = 0.4273$, $c = 1.0134$ (Francois et al. 1985).

Verniere et al. (1995) observed the existence of the $La_4Ir_{13}Ge_9$ compound with $Ho_4Ir_{13}Ge_9$-type structure from an arc melted sample annealed at 1170 K for 8 days. No lattice parameters were given. The purity of the starting elements was 3N for the lanthanum, 4N for the iridium and 6N for the germanium.

4.3.13. *La–Pt–Ge*

Francois et al. (1990) reported the crystal structure of $LaPtGe_2$ ($CeNiSi_2$ type, $a = 0.4404$, $b = 1.720$, $c = 0.4404$). For sample preparation, see La–Fe–Ge.

According to X-ray powder diffraction analysis reported by Hovestreydt et al. (1982) the compound LaPtGe adopted the LaPtSi-type structure, $a = 0.4266$, $c = 0.14970$. The alloy was arc melted under argon and annealed at 1270 K for 1–2 weeks. Starting materials were La (3N), Pt (4N) and Ge (5N).

The existence of the $LaPt_2Ge_2$ compound ($CeGa_2Al_2$ type, $a = 0.4412$, $c = 0.9923$) was reported by Rossi et al. (1979) from X-ray powder diffraction of the induction melted sample which was annealed at 773 K for 1 week. Starting components were La (3N), Pt (4N) and Ge (4N). Venturini et al. (1989a) investigated the crystal structure of $LaPt_2Ge_2$ from an arc melted sample annealed at 1273 K for 5 days. The crystal structure was found to belong to a new structure type, $a = 0.4301$, $b = 0.4346$, $c = 0.9682$, $\beta = 91.26°$. Starting materials were La (3N), Pt (4N) and Ge (4N).

4.3.14. *La–Au–Ge*

No ternary phase diagram exists for the La–Au–Ge system, however, a ternary compound of lanthanum with gold and germanium of the 1:1:1 stoichiometric ratio has been identified and studied by means of X-ray and metallographic analyses by Rossi et al. (1992). The LaAuGe compound was found to adopt the LiGaGe-type structure with lattice parameters $a = 0.4463$, $c = 0.8169$. The sample was prepared by melting the metals (around 99.9 mass% for lanthanum and 99.99 mass% for gold and germanium) in an induction furnace and annealing at 1070 K for one week.

4.4. *Ce–d element–Ge systems*

4.4.1. *Ce–Mn–Ge*

The phase equilibria in the Ce–Mn–Ge system (fig. 42) have been investigated by Konyk (1989) by means of X-ray analysis of 104 alloys which were arc melted and subsequently annealed in evacuated silica tubes for 400–720 h at 670 K and finally quenched in water. Starting materials were Ce 99.85 mass%, Mn 99.91 mass% and Ge 99.99 mass%. The existence of one ternary compound was confirmed [$CeMn_2Ge_2$ (1)] and the formation of three new ternary cerium manganese germanides was observed [Ce_2MnGe_6 (2), Ce_2MnGe_5 (3) and CeMnGe (4)].

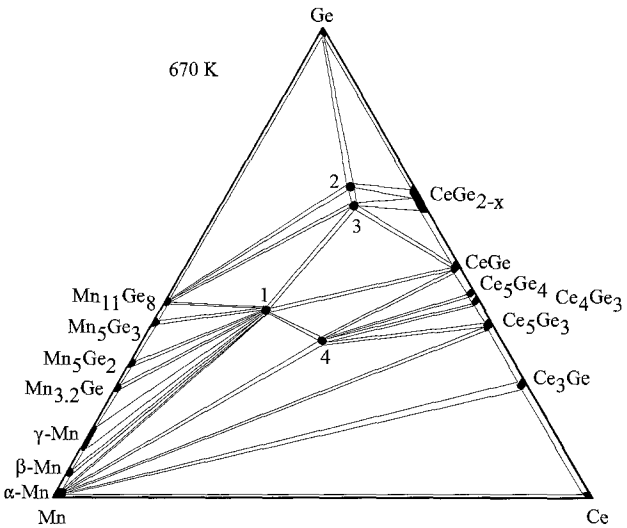

Fig. 42. Ce–Mn–Ge, isothermal section at 670 K.

The formation of the $CeMn_2Ge_2$ compound ($CeGa_2Al_2$ type, $a=0.4144$, $c=1.0970$; for sample preparation, see $LaMn_2Ge_2$) was reported in an early investigation of the ternary rare-earth germanides with the stoichiometric ratio 1:2:2 by Rossi et al. (1978b). Crystallographic characteristics after Konyk (1989) are as follows: $CeGa_2Al_2$ type, $a=0.4135$, $c=1.0928$.

The Ce_2MnGe_6 compound crystallizes with the Ce_2CuGe_6-type of structure with lattice parameters $a=0.4103$, $b=0.4342$, $c=2.188$ (Konyk 1989).

Ce_2MnGe_5 was reported by Konyk (1989) to crystallize with a new structure type, $a=0.4308$, $b=0.4170$, $c=2.1134$ (X-ray powder diffraction data).

CeMnGe was found to be isostructural with the PbFCl type, $a=0.4235$, $c=0.7393$ (Konyk 1989). The crystal structure of CeMnGe was recently confirmed by Welter et al. (1995) (PbFCl type, $a=0.4235$, $c=0.7386$; powder X-ray diffraction). For details of the experimental procedure, see LaMnGe.

4.4.2. *Ce–Fe–Ge*

The isothermal sections for the Ce–Fe–Ge phase diagram at 870 K were reported by Salamakha et al. (1996a) from a combined X-ray and micrography examination of 139 alloys. For details of sample preparation, see Ce–Mn–Ge. The microstructure of the alloys was revealed by etching in dilute solutions of HCl and HF. Starting materials were Ce 99.85 mass%, Fe 99.90 mass%, Ge 99.99 mass%.

The phase relations are characterized by the formation of seven ternary compounds (fig. 43); the crystal structure has been determined for three of these. Mutual solid solubilities of the binary compounds have been found to be insignificantly small. Crystallographic characteristics for these ternary compounds are summarized in table 12.

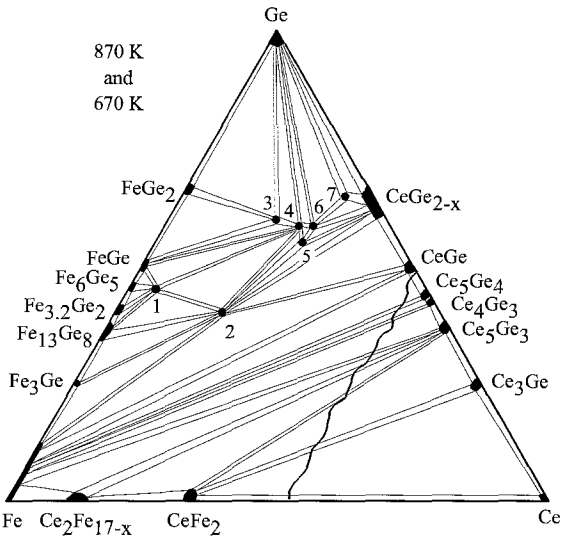

Fig. 43. Ce–Fe–Ge, isothermal sections at 870 K (0–50 at.% Ce) and at 670 (50–100 at.% Ce).

Table 12
Crystallographic data for the ternary Ce–Fe–Ge compounds at 870 K

No.	Compound	Structure	Lattice parameters (nm)			Reference
			a	*b*	*c*	
1	~$CeFe_{10}Ge_9$	unknown				Salamakha et al. (1996b)
2	$CeFe_2Ge_2$	$CeGa_2Al_2$	0.4070		1.0483	Rossi et al. (1978a)
			0.4069		1.04495	Bara et al. (1990)
3	$CeFeGe_3$	$BaNiSn_3$	0.4339		0.9974	Salamakha et al. (1996b)
4	~$Ce_3Fe_2Ge_7$	unknown				Salamakha et al. (1996b)
5	$CeFe_{0.64}Ge_2$	$CeNiSi_2$	0.4278	1.6608	0.4150	Pecharsky et al. (1989)
6	~Ce_2FeGe_4	unknown				Salamakha et al. (1996b)
7	~Ce_6FeGe_{13}	unknown				Salamakha et al. (1996b)

4.4.3. *Ce–Co–Ge*

Phase equilibria in the Ce–Co–Ge system have been determined by Konyk (1989) by means of powder X-ray and micrographic analyses of 160 ternary alloys at 870 K (0–50 at.% Ce) and at 670 K (50–100 at.% Ce) (fig. 44). The phase relations are characterized by the formation of eleven ternary compounds and by the existence of two substitutional solid solution ranges: Ge in $CeCo_5$ (12 at.%) and Ge in Ce_2Co_{17} (10 at.%). For sample preparation, see Ce–Mn–Ge. The purity of the starting materials was Ce 99.85 mass%, Co 99.90 mass%, Ge 99.99 mass%.

Crystallographic data for the ternary compounds are summarized in table 13.

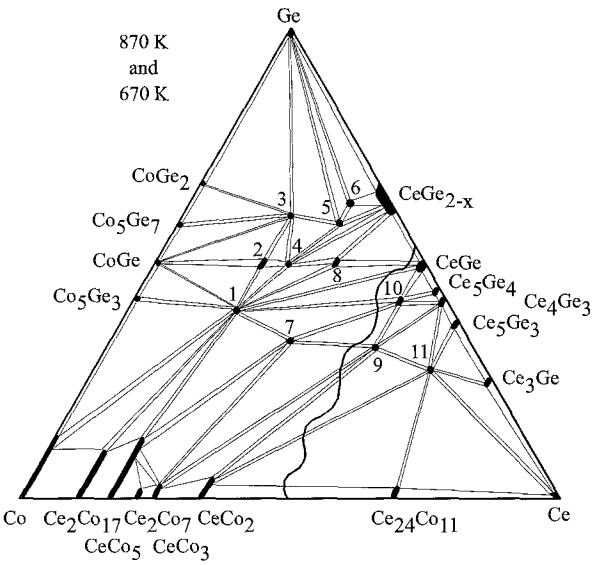

Fig. 44. Ce–Co–Ge, isothermal sections at 870 K (0–50 at.% Ce) and at 670 (50–100 at.% Ce).

Table 13
Crystallographic data for the ternary Ce–Co–Ge compounds

No.	Compound	Structure	Lattice parameters (nm)			Reference
			a	*b*	*c*	
1	$CeCo_2Ge_2$	$CeGa_2Al_2$	0.4071		1.0170	McCall et al. (1973b)
2	$Ce_2Co_3Ge_5$	$Lu_2Co_3Si_5$	1.1376	0.5847	1.1796	Konyk (1989)
					$\gamma = 120.77°$	
		$U_2Co_3Si_5$	0.9814	1.184	0.5862	Venturini et al. (1986b)
3	$CeCoGe_3$	$BaNiSn_3$	0.4329		0.9850	Konyk (1989)
			0.4319		0.98298	Pecharsky et al. (1993)
			0.4317		0.9833	Venturini et al. (1985b)
4	$CeCoGe_2$	$CeNiSi_2$	0.4253	1.6773	0.4213	Pecharsky et al. (1989)
			0.4245	1.674	0.4197	Méot-Meyer et al. (1985a)
5	$\sim Ce_3CoGe_6$	unknown				Konyk (1989)
6	$\sim Ce_{15}Co_4Ge_{31}$	unknown				Konyk (1989)
7	CeCoGe	PbFCl	0.4198		0.6887	Konyk (1989)
			0.4170		0.6865	Welter et al. (1993a)
8	$CeCo_{0.5}Ge_{1.5}$	AlB_2	0.4177		0.4233	Konyk (1989)
			0.4182		0.4151	Gladyshevsky and Bodak (1965)
9	Ce_3CoGe_2	La_3NiGe_2	1.1951	0.4302	1.1477	Konyk (1989)
10	$\sim Ce_5CoGe_4$	unknown				Konyk (1989)
11	$\sim Ce_5CoGe_2$	unknown				Konyk (1989)

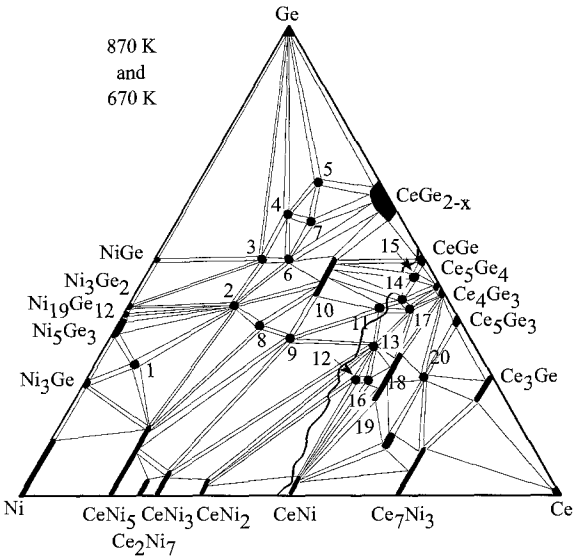

Fig. 45. Ce–Ni–Ge, isothermal sections at 870 K (0–50 at.% Ce) and at 670 (50–100 at.% Ce).

4.4.4. *Ce–Ni–Ge*

Information about the phase equilibria in the Ce–Ni–Ge system is due to the work of Salamakha et al. (1996b) who employed X-ray phase analysis of 227 alloys which were arc melted and annealed at 870 K (0–50 at.% Ce) and 670 K (50–100 at.% Ce) in evacuated quartz tubes for two weeks (fig. 45). Twenty ternary compounds were found and characterized. A large homogeneity range was observed for the $CeNi_5$ compound by the same authors; the maximum concentration of Ge in $Ce(Ni,Ge)_5$ solid solution was indicated as 15 at.%.

Crystallographic information on the ternary compounds is summarized in table 14 (overleaf).

One more compound was observed by Belsky et al. (1987) in arc melted alloys, Ce_5NiGe_2. A new structure type was reported with lattice parameters $a = 1.1760$, $c = 0.6429$.

4.4.5. *Ce–Cu–Ge*

Salamakha et al. (1996c) were the first to derive the phase equilibria in an isothermal section at 870 K, employing room-temperature X-ray powder diffraction analysis. Alloys were synthesized by arc melting proper amounts of the constituent elements (Ce 99.85 mass%, Cu 99.99 mass%, Ge 99.99 mass%) under high purity argon on a water cooled copper hearth. Finally alloys were annealed at 870 K in evacuated quartz tubes for two weeks and quenched in water. Phase-field distributions are characterized by existence of eight ternary compounds and one solid solution originating at $CeGe_{2-x}$. The solid-solution limit was established as 10 at.% Cu. The isothermal section of the Ce–Cu–Ge system at 870 K is presented in fig. 46.

Table 14
Crystallographic data for the ternary Ce–Ni–Ge compounds

No.	Compound	Structure	Lattice parameters (nm)			Reference
			a	*b*	*c*	
1	$CeNi_{8.5}Ge_{4.5}$	$CeNi_{8.5}Si_{4.5}$	0.79702		1.17516	Salamakha et al. (1996c)
2	$CeNi_2Ge_2$	$CeGa_2Al_2$	0.4150		0.9854	Bodak et al. (1966)
3	$Ce_2Ni_3Ge_5$	$U_2Co_3Si_5$	0.9790	1.1842	0.5928	Salamakha et al. (1996c)
4	$CeNiGe_3$	$SmNiGe_3$	0.4140	2.1824	0.4174	Salamakha et al. (1996c)
5	Ce_2NiGe_6	Ce_2CuGe_6	0.40695	0.41668	2.1705	Salamakha et al. (1996c)
6	$CeNiGe_2$	$CeNiSi_2$	0.4260	1.6793	0.4215	Salamakha et al. (1996c)
			0.4244	1.6647	0.4199	Bodak et al. (1966)
7	$Ce_3Ni_2Ge_7$	$U_3Fe_2Si_7$	0.4243	2.5758	0.4289	Konyk (1988)
8	$Ce_3Ni_4Ge_4$	$U_3Ni_4Si_4$	0.41162	0.41829	2.3962	Salamakha et al. (1996c)
9	CeNiGe	TiNiSi	0.72418	0.43078	0.72408	Salamakha et al. (1996c)
10	$Ce(Ni,Ge)_2$	AlB_2	0.41618–0.41734		0.42665–0.41926	Salamakha et al. (1996c)
11	$\sim Ce_{4.7}Ni_{1.3}Ge_{4.0}$	unknown				Salamakha et al. (1996c)
12	$\sim Ce_2NiGe$	unknown				Salamakha et al. (1996c)
13	Ce_3NiGe_2	La_3NiGe_2	1.1924	0.4311	1.1624	Bodak et al. (1982)
14	$\sim Ce_{5.0}Ni_{0.8}Ge_{4.2}$	unknown				Salamakha et al. (1996c)
15	$\sim Ce_{5.0}Ni_{0.4}Ge_{4.6}$	unknown				Salamakha et al. (1996c)
16	$Ce_{11}Ni_4Ge_6$	$La_{11}Ni_4Ge_6$	1.8236	0.4321	1.3939	Salamakha et al. (1996c)
				$\gamma = 106.7°$		
17	$\sim Ce_{5.2}Ni_{0.8}Ge_{4.0}$	unknown				Salamakha et al. (1996c)
18	$\sim Ce_{11}Ni_4Ge_5$	unknown				Salamakha et al. (1996c)
19	$\sim Ce_5Ni_2Ge$	unknown				Salamakha et al. (1996c)
20	$\sim Ce_5NiGe_2$	unknown				Salamakha et al. (1996c)

Rieger and Parthé (1969a) investigated the occurrence of the AlB_2-type structure by means of X-ray powder diffraction of arc melted alloys. The data presented were $CeCu_{1-0.67}Ge_{1-1.33}$ with $a = 0.4296$–0.4197, $c = 0.3988$–0.4215. Salamakha et al. (1996c) reported on the existence of two compounds with AlB_2-type within the Ce–Cu–Ge system at 870 K: CeCuGe (5) ($a = 0.4316$, $c = 0.3967$) and $CeCu_{0.6-0.8}Ge_{1.4-1.2}$ (6) ($a =$ 0.4214–0.4188, $c = 0.4206$–0.4264). Iandelli (1993) confirmed AlB_2-type ($a = 0.4308$ $c =$ 0.3966, X-ray powder analysis) from an alloy of the stoichiometric composition which was prepared from a mixture of filings or powders of the metals (cerium 99.7 mass%, copper and germanium 99.99 mass%) which were sealed in tantalum crucibles under argon followed by melting in an induction furnace; afterwards the sample was annealed for 10 days at 1023 K.

Konyk et al. (1988) reported on the crystal structure of Ce_2CuGe_6 (2) alloy prepared by arc melting under argon and annealed at 870 K in an evacuated quartz tube for 720 h. From X-ray powder diffraction analysis a new structure type was suggested, $a = 0.40756$, $b =$

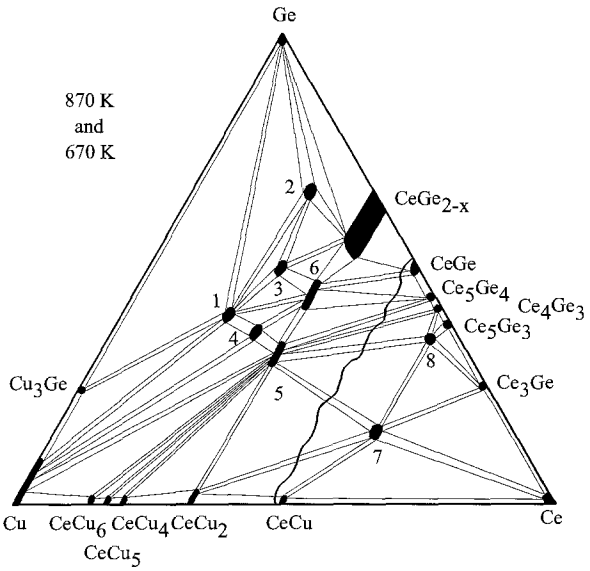

Fig. 46. Ce–Cu–Ge, isothermal sections at 870 K (0–50 at.% Ce) and at 670 (50–100 at.% Ce).

0.42152, $c = 2.15408$. The crystal structure was confirmed later by Sologub et al. (1995a), $a = 0.42116$, 0.40725, $c = 2.1584$ (X-ray powder analysis).

Rieger and Parthé (1969b) prepared $CeCu_2Ge_2$ (1) with the $CeGa_2Al_2$-type structure, $a = 0.4172$, $c = 1.0212$.

Francois et al. (1990) reported the crystal structure of $CeCu_{0.86}Ge_2$ (4) ($CeNiSi_2$ type, $a = 0.4276$, $b = 1.729$, $c = 0.4145$). For sample preparation, see $LaFeGe_2$.

The $Ce_2Cu_3Ge_3$ compound (3) was found to crystallize with a new structure type, $a = 0.41680$, $c = 1.7409$, $c = 0.42108$, X-ray powder data (Konyk 1988). For sample preparation, see Ce–Cu–Ge.

Salamakha et al. (1996c) reported the existence of two cerium copper germanides of unknown structure, $Ce_{0.60}Cu_{0.25}Ge_{0.15}$ (7) and $Ce_{0.60}Cu_{0.05}Ge_{0.35}$ (8), from X-ray powder diffraction of the alloys which were prepared in the same manner as discussed above.

4.4.6. *Ce–Zn–Ge*

The isothermal section of the equilibrium phase diagram of the Ce–Zn–Ge system at 470 K has been investigated by Opainych (1996) by X-ray powder diffraction analysis. Samples were prepared by argon arc melting from ingots of the high-purity elements (Ce 99.97 mass%, Zn 99.98 mass%, Ge 99.99 mass%) under a pressure of 1.1 atm. Weight losses due to vaporization while melting were compensated beforehand by extra amounts of Zn (about 0.5 mass%). The arc melted buttons were annealed at 470 K for 1500 hours in evacuated quartz tubes and finally quenched by submerging the capsules into cold water.

The phase relations after Opainych (1996) are characterized by the formation of eight ternary compounds (fig. 47). The solid solubility of the third component in the Ce–Zn and Ce–Ge binary compounds has been found to be negligible.

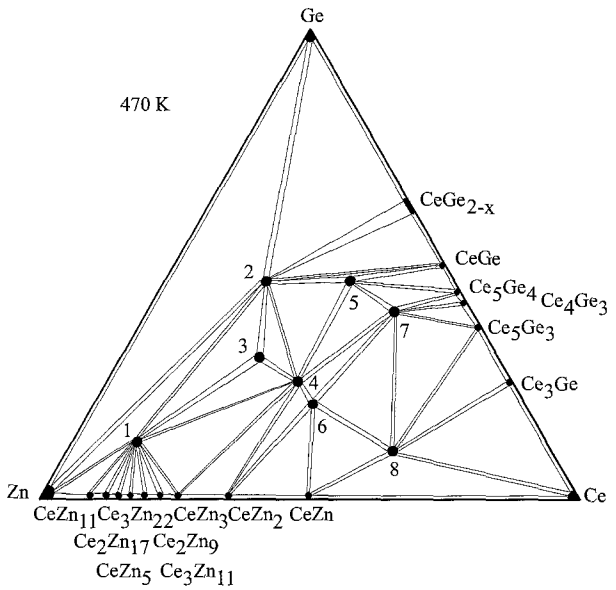

Fig. 47. Ce–Zn–Ge, isothermal section at 470 K.

The $Ce_4Zn_8Ge_{11-x}$ (2) compound was found to crystallize in an own structure type with lattice parameters $a = 0.59468$, $c = 2.4740$ (Opainych 1996; X-ray single-crystal analysis). For sample preparation, see above.

Opainych (1996) reported on the investigation of $Ce_2Zn_{15}Ge_2$ ($Ce_2Al_2Co_{15}$ type, $a = 0.9021$, $c = 1.3787$) (1), $CeZn_{1.8}Ge_{1.2}$ ($AuCu_3$ type, $a = 0.5420$) (3) and $Ce(Zn,Ge)_2$ (α-$ThSi_2$ type, $a = 0.4231$, $c = 1.4219$) (5) from X-ray powder analysis of arc melted alloys annealed at 470 K.

The existence of four ternary phases with unknown structure has been observed by Opainych (1996) in the course of investigating the isothermal section of the Ce–Zn–Ge system at 470 K. They exist at the following compositions: ~$Ce_7Zn_8Ge_5$ (4), ~Ce_2Zn_2Ge (6), ~$Ce_9Zn_3Ge_8$ (7) and ~Ce_6Zn_3Ge (8).

One more ternary compound which was not observed in the course of phase-equilibrium studies, was characterized by Rossi and Ferro (1996). $CeZn_{1.5}Ge_{0.5}$ was found to be isotypic with an AlB_2 type, $a = 0.4447$, $c = 0.3924$ from X-ray powder diffraction of an induction melted alloy which was afterwards annealed at 1070 K for one week. An electronic micrographic examination as well as microprobe microanalysis were carried out. The metals employed in the synthesis of samples had a nominal purity of 99.9 mass% for cerium, and 99.999 mass% for other metals.

4.4.7. *Ce–Ru–Ge*

The phase equilibria in the Ce–Ru–Ge system have been investigated by Shapiev (1993) by means of X-ray and metallographic analyses of 125 ternary alloys, which were arc

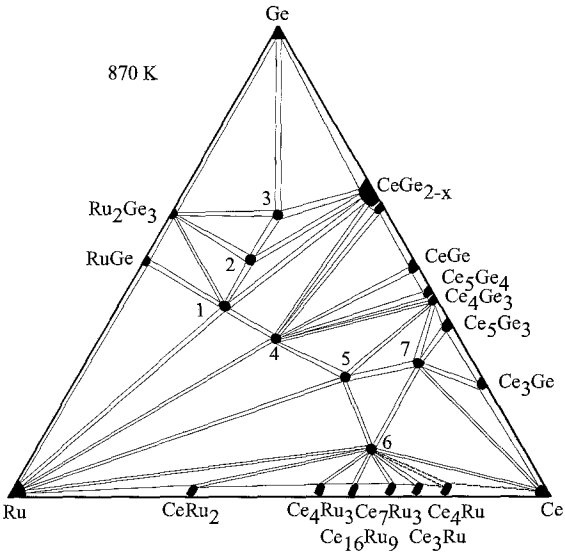

Fig. 48. Ce–Ru–Ge, isothermal section at 870 K.

melted and subsequently annealed in evacuated silica tubes at 870 K for 1000 hours and finally quenched in water. Starting materials were Ce 99.0 mass%, Ru 99.99 mass%, Ge 99.99 mass%. According to phase diagram, seven ternary compounds exist within the Ce–Ru–Ge system at 870 K (fig. 48). The mutual solid solubilities of binary compounds were found to be small, i.e. approximately 1–2 at.% of third component.

Early investigations of the $CeRu_2Ge_2$ (1) compound determined it to have the $CeGa_2Al_2$-type structure: $a = 0.4263$, $c = 1.008$ after Felner and Nowik (1985) from X-ray powder analysis of induction melted alloy and $a = 0.4270$, $c = 1.0088$ (Francois et al. 1985) from X-ray powder analysis of alloy obtained by powder metallurgical reaction at 1273 K. Starting components were Ce (3N), Ru (4N) and Ge (4N). The crystal structure type was confirmed by Shapiev (1993) with lattice parameters $a = 0.42717$, $c = 1.0054$ from arc melted alloy annealed at 870 K.

Venturini et al. (1986b) and Shapiev (1993) reported the structure for the $Ce_2Ru_3Ge_5$ compound (2) crystallizing with the $U_2Co_3Si_5$-type structure. Lattice parameters were reported to be $a = 0.99197$, $b = 1.238$, $c = 0.5887$ (Venturini et al. 1986b; X-ray powder diffraction; for sample preparation, see $La_2Ru_3Ge_5$) and $a = 1.003$, $b = 1.204$, $c = 0.5895$ (Shapiev 1993).

The crystal structure of the CeRuGe compound (4) was investigated by Welter et al. (1993b). It was found to adopt the PbFCl type, $a = 0.4275$, $c = 0.6871$ (X-ray powder diffraction). The compound was prepared from commercially available high-purity elements. A compacted stoichiometric mixture pellet was heated to 1173 K under argon in a sealed silica tube for preliminary homogenization and then melted in an induction furnace. Shapiev (1993) reported the same crystal structure with slightly different lattice parameters: $a = 0.4195$, $c = 0.6916$.

$Pr_3Rh_4Sn_{13}$-type structure was announced for the $Ce_3Ru_4Ge_{13}$ compound ($a = 0.9045$) by Segre et al. (1981a) from X-ray powder analysis of an arc melted sample annealed at 1523 K for 1 day and at 1273 K for 7 days. Starting materials were Ce (3N), Ru (3N), Ge (6N). Ghosh et al. (1995) reported on combined X-ray and neutron diffraction studies of the $Ce_{4-x}Ru_4Ge_{12+x}$ alloys ($a = 0.90661$ for $x = 0$ and $a = 0.90494$ for $x = 1$). The samples were arc melted and annealed at 1170 K for two weeks. At variance with these data, Shapiev observed $CeRuGe_3$ (3) with the $ScNiSi_3$ type, lattice parameters $a = 2.185$, $b = 0.4234$, $c = 0.4285$, from X-ray powder analysis of arc melted alloy annealed at 870 K.

Gladyshevsky et al. (1992) reported on the existence of the Ce_5RuGe_2 (7) compound with a S_5HfY_2-anti-type structure, $a = 1.2255$, $b = 0.8898$, $c = 0.8008$ (X-ray single-crystal data). The single crystal was obtained from an alloy which was arc melted and annealed at 870 K.

Two compounds of unknown structure [~Ce_2RuGe (5) and ~Ce_5Ru_2Ge (6)] were observed by Shapiev (1993) from arc melted samples annealed at 870 K.

$Ce_3Ru_2Ge_2$ was found to crystallize with $La_3Ni_2Ga_2$-type ($a = 0.5751$, $b = 0.7934$, $c = 1.3657$, X-ray powder diffraction) from an arc melted and sample annealed at 870 K (Bodak et al. 1989b). This phase is not shown in the Ce–Ru–Ge phase diagram of fig. 48.

4.4.8. *Ce–Rh–Ge*

The phase equilibria in the Ce–Rh–Ge system have been investigated by Shapiev (1993) by means of X-ray and metallographic analyses of 219 ternary alloys, which were arc melted and subsequently annealed in evacuated silica tubes for 1000 hours at 870 K and finally quenched in water. Starting materials were Ce 99.0 mass%, Rh 99.99 mass%, Ge 99.99 mass%. According to the phase diagram, twenty ternary compounds exist within the Ce–Rh–Ge system at 870 K (fig. 49). The limits of solid solutions originating at binary Ce–Rh and Rh–Ge compounds are not indicated by Shapiev (1993).

Venturini et al. (1985b) reported on an X-ray powder diffraction study of the $CeRhGe_3$ compound (9) from a sample which was prepared by heating a mixture of starting components (Ce 3N, Rh 4N, Ge 4N) in an evacuated quartz tube at 1073 K. The crystal structure was found to adopt the $BaNiSn_3$-type ($a = 0.4394$, $c = 1.0026$). Shapiev (1993) confirmed the crystal structure and reported the lattice parameters $a = 0.4394$, $c = 1.0019$.

Early investigations on the $CeRh_2Ge_2$ compound (7) determined the $CeGa_2Al_2$-type: $a = 0.4161$, $c = 1.045$ (Felner and Nowik (1985)) and $a = 0.4160$, $c = 1.0438$ (Francois et al. 1985). For sample preparation, see $CeRu_2Ge_2$. The crystal structure type was confirmed by Shapiev (1993): $a = 0.4154$, $c = 1.0472$ from X-ray powder diffraction of an alloy which was arc melted and annealed at 870 K.

$Ce_2Rh_3Ge_5$ (8) was found to crystallize with $U_2Co_3Si_5$-type ($a = 1.0097$, $b = 1.209$, $c = 0.5987$) by Venturini et al. (1986b) from X-ray powder analysis. Lattice parameters after Shapiev are $a = 0.9856$, $b = 1.2049$, $c = 0.5851$.

Hovestreydt et al. (1982) reported the crystal structure of the CeRhGe compound (15) (TiNiSi type, $a = 0.7424$, $b = 0.4468$, $c = 0.7120$; X-ray powder data) from an arc melted sample annealed at 1270 K for 1–2 weeks. Starting components were Ce (3N), Rh (4N)

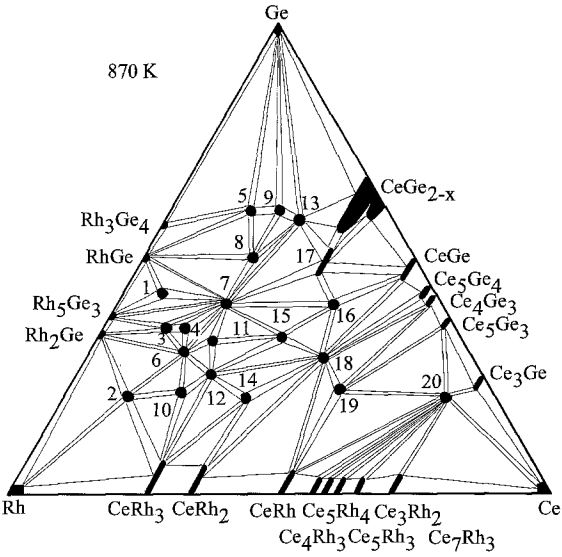

Fig. 49. Ce–Rh–Ge, isothermal section at 870 K.

and Ge (5N). Shapiev (1993) confirmed the TiNiSi-type for the sample annealed at 870 K ($a=0.7199$, $b=0.4352$, $c=0.7378$; X-ray powder diffraction).

Gladyshevsky et al. (1991a) reported on the crystal structure of the $Ce_3Rh_2Ge_2$ (18) compound ($La_3Ni_2Ge_2$ type, $a=0.57001$, $b=0.8099$, $c=1.3461$; X-ray single-crystal method). For the details of sample preparation, see $La_3Rh_2Ge_2$.

$CeRh_{1-x}Ge_{2+x}$ (13) with a new structure type was investigated by Shapiev et al. (1991): $a=0.4322$, $b=0.4329$, $c=1.7107$ by a single-crystal method. For the experimental procedure, see Ce–Rh–Ge.

Verniere et al. (1995) mentioned the existence of $Ce_4Rh_{13}Ge_9$ (4) with $Ho_4Ir_{13}Ge_9$-type. No lattice parameters were given. For experimental details and purity of starting metals see La–Ir–Ge. Salamakha and Sologub (1997) investigated the crystal structure and established the lattice parameters $a=0.4055$, $b=1.1372$, $c=1.9804$ (X-ray powder data; arc melted sample annealed at 870 K).

Investigating the phase diagram, Shapiev (1993) established the crystal structure for $Ce_3Rh_4Ge_{13}$ (5) ($Y_3Co_4Ge_{13}$ type, $a=0.908$), for $CeRh_{1.4}Ge_{0.6}$ (14) ($MgZn_2$ type, $a=0.5310$, $c=0.8950$) and for $CeRh_{0.5}Ge_{1.5}$ (16) (AlB_2 type, $a=0.4220$, $a=0.4208$), and observed ten compounds with unknown structures: $CeRh_7Ge_6$ (1), $CeRh_6Ge_2$ (2), $CeRh_5Ge_3$ (3), $Ce_3Rh_9Ge_5$ (6), $Ce_2Rh_5Ge_2$ (10), $Ce_2Rh_4Ge_3$ (11), $CeRh_2Ge$ (12), Ce_2RhGe_2 (17), Ce_2RhGe (19), Ce_7RhGe_2 (20).

4.4.9. *Ce–Pd–Ge*

A systematic study of the Ce–Pd–Ge system at 870 K was performed by Gribanov (1994) over the whole concentration region by means of X-ray powder and single-crystal analyses as well as using metallography and microprobe analyses. The samples were prepared

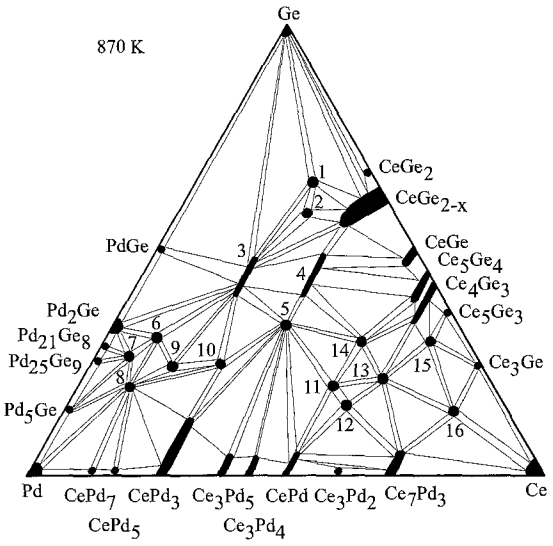

Fig. 50. Ce–Pd–Ge, isothermal section at 870 K.

by arc melting under argon the proper amount of starting elements, and annealed in evacuated quartz ampoules at 870 K for 720 hours. Starting materials were 99.8 mass% pure or better.

The phase-field distribution in the isothermal section at 870 K is characterized by existence of sixteen ternary compounds (fig. 50). Maximum solubility of germanium in the binary compounds of Ce–Pd and Ce–Ge systems is 12 at.% Ge for $CePd_3$. $CeGe_{2-x}$ dissolves 11 at.% Pd. Solubility of cerium in the palladium germanides was found to be negligible. As reported by Gribanov (1994), homogeneity fields were observed for the compounds $CePd_2Ge_2$ (3) and $Ce(Pd,Ge)_2$ (4).

The crystal structure of the compounds $Ce_3Pd_{20}Ge_6$ (8) (own structure type, $a=$ 1.24453, Gribanov et al. 1994) and $Ce_7Pd_4Ge_2$ (12) (own structure type, $a=0.9315$, $b=$ 1.2277, $c=1.2698$, $\beta=114.31°$, Gribanov et al. 1993b) was investigated by the X-ray single-crystal analysis of specimens obtained from alloys annealed at 870 K.

The existence of the $CePd_2Ge_2$ (3) compound ($CeGa_2Al_2$ type, $a=0.4369$, $c=1.0055$) was reported by Rossi et al. (1979). For details of sample preparation see $LaMn_2Ge_2$ under La–Mn–Ge. The existence of the 1:2:2 compound was confirmed by Gribanov (1994) ($CeGa_2Al_2$ type, $a=0.4359$, $b=1.001$; X-ray powder diffraction) while investigating the Ce–Pd–Ge phase diagram at 870 K.

According to an X-ray powder diffraction analysis reported by Hovestreydt et al. (1982) the compound CePdGe (5) adopts the KHg_2-type structure. For sample preparation, see La–Pd–Ge. Starting materials were Ce (3N), Pd (4N) and Ge (5N). The existence of the CePdGe compound was later confirmed by Gribanov (1994) (KHg_2 type, $a=0.4480$, $b=$ 0.7288, $c=0.7672$; X-ray powder data).

The crystal structure of the compound $CePd_2Ge$ (10) was found to be of the YPd_2Si type ($a=0.7668$, $b=0.6972$, $c=0.5757$; X-ray powder diffraction) by Jorda et al. (1983).

For the experimental procedure, see $LaPd_2Ge$ under La–Pd–Ge. Starting materials were Pd 99.99 mass%, Ge specpure quality; Ce 99.9 mass%. Gribanov (1994) confirmed the structure type and determined the lattice parameters $a = 0.6980$, $b = 0.7702$, $c = 0.5789$ from X-ray powder analysis.

Sologub et al. (1995a) reported on the X-ray powder analysis of the Ce_2PdGe_6 (1) compound which was found to crystallize with the Ce_2CuGe_6 type, $a = 0.41784$, $b = 0.40900$, $c = 2.2043$. For the experimental procedure, see La_2PdGe_6 under La–Pd–Ge. The starting materials used were obtained from Johnson & Matthey, UK (99.9 mass%).

$Ce(Pd,Ge)_2$ (4) was found to crystallize with the AlB_2 type, $a = 0.42946$, $c = 0.41732$ (Gribanov 1994; X-ray powder diffraction data).

The formation of nine more ternary phases with unknown structure has been observed by Gribanov et al. (1994) while investigating the isothermal section of the Ce–Pd–Ge system at 870 K: ~$Ce_{0.05}Pd_{0.68}Ge_{0.27}$ (7), ~$Ce_{0.10}Pd_{0.60}Ge_{0.30}$ (6), ~$Ce_{0.16}Pd_{0.60}Ge_{0.24}$ (9), ~$Ce_{0.25}Pd_{0.17}Ge_{0.58}$ (2), ~$Ce_{0.50}Pd_{0.30}Ge_{0.20}$ (11), ~$Ce_{0.50}Pd_{0.20}Ge_{0.30}$ (14), ~$Ce_{0.58}Pd_{0.20}Ge_{0.22}$ (13), ~$Ce_{0.62}Pd_{0.08}Ge_{0.30}$ (15) and ~$Ce_{0.75}Pd_{0.10}Ge_{0.15}$ (16).

4.4.10. *Ce–Ag–Ge*

The phase equilibria in the Ce–Ag–Ge system were investigated by Protsyk (1994) by means of X-ray analysis of 80 alloys which were arc melted and subsequently annealed in evacuated silica tubes for 500 h at 770 K and finally quenched in water. Starting materials were Ce 99.85 mass%, Ag 99.9 mass% and Ge 99.99 mass%. The formation of ten new ternary silver germanides of cerium was observed (fig. 51). The $CeAg_5$ compound was found to dissolve 10 at.% Ge. Crystal structure was established for four germanides; six ternary compounds were reported to be of unknown structure type. Crystallographic characteristics of ternary cerium silver germanides are listed in table 15.

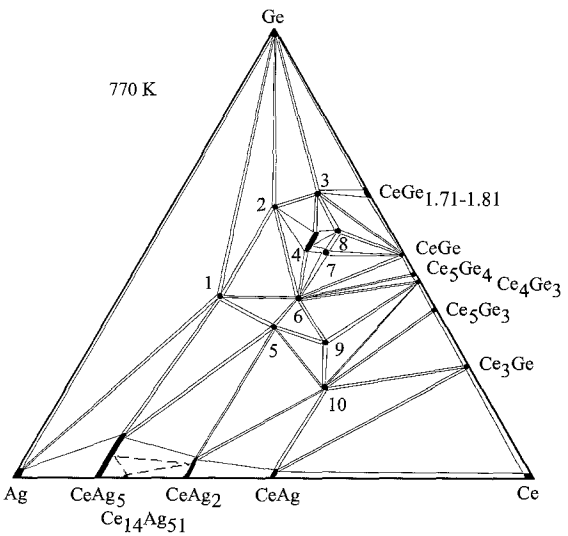

Fig. 51. Ce–Ag–Ge, isothermal section at 770 K.

Table 15
Crystallographic data for the ternary Ce–Ag–Ge compounds

No.	Compound	Structure	Lattice parameters (nm)			Reference
			a	*b*	*c*	
1	$CeAg_2Ge_2$	$CeGa_2Al_2$	0.4296		1.0955	Protsyk (1994)
3	Ce_2AgGe_6	Ce_2CuGe_6	0.43089	0.4144	2.1674	Sologub et al. (1995a)
5	CeAgGe	LiGaGe	0.45442		0.77108	Pecharsky et al. (1991)
6	$CeAg_{0.8}Ge_{1.2}$	AlB_2	0.4375		0.4129	Protsyk (1994)
8	$CeAg_{0.33}Ge_{1.67}$	α-$ThSi_2$	0.4239		1.4697	Protsyk (1994)

4.4.11. *Ce–Os–Ge*

The only information on the interaction of components in the Ce–Os–Ge system is from Segre et al. (1981a) who announced a $Pr_3Rh_4Sn_{13}$-type for the $Ce_3Os_4Ge_{13}$ compound ($a=0.9075$) from X-ray powder analysis of an arc melted sample annealed at 1523 K for 1 day and at 1273 K for 7 days. Starting materials were Ce (3N), Os (3N), Ge (6N).

4.4.12. *Ce–Ir–Ge*

No ternary phase diagram has been established for the Ce–Ir–Ge system, however five ternary compounds have been observed and characterized by various groups of authors.

$Ce_2Ir_3Ge_5$ was found to crystallize with $U_2Co_3Si_5$-type ($a=1.0189$, $b=1.197$, $c=0.6060$; X-ray powder diffraction method) by Venturini et al. (1985b).

Venturini et al. (1985b) reported on the X-ray powder diffraction study of the $Ce_3Ir_4Ge_{13}$ compound from a sample which was prepared by heating a mixture of starting components (Ce 3N, Ir 4N, Ge 4N) in an evacuated quartz tube at 1073 K. The crystal structure was found to adopt the $Yb_3Rh_4Sn_{13}$ type, $a=0.9061$.

$CeIr_2Ge_2$ is isotypic with the crystal structure of $CaBe_2Ge_2$ with lattice parameters $a=0.4246$, $c=1.0098$ (Francois et al. 1985).

Verniere et al. (1995) observed the existence of the $Ce_4Ir_{13}Ge_9$ compound with a $Ho_4Ir_{13}Ge_9$ type from X-ray powder analysis and metallographic examination. No lattice parameters are available. For the experimental procedure, see $La_4Ir_{13}Ge_9$.

Hovestreydt et al. (1982) reported the compound CeIrGe to adopt the TiNiSi type, $a=0.7071$, $b=0.4375$, $c=0.7574$, from X-ray powder diffraction. For sample preparation, see La–Pd–Ge.

4.4.13. *Ce–Pt–Ge*

A systematic study of the Ce–Pt–Ge system at 870 K was performed by Gribanov et al. (1996) over the whole concentration region by means of X-ray powder and single-crystal analyses as well as using metallography and microprobe analyses. The samples were prepared by arc melting under argon and annealed in evacuated quartz ampoules at 870 K for 720 hours. Starting materials were 99.8 mass% pure or better. In the metallographic studies, Pt-rich samples (>50 at.% Pt) were etched in an HNO_3+HCl (1:1) solution.

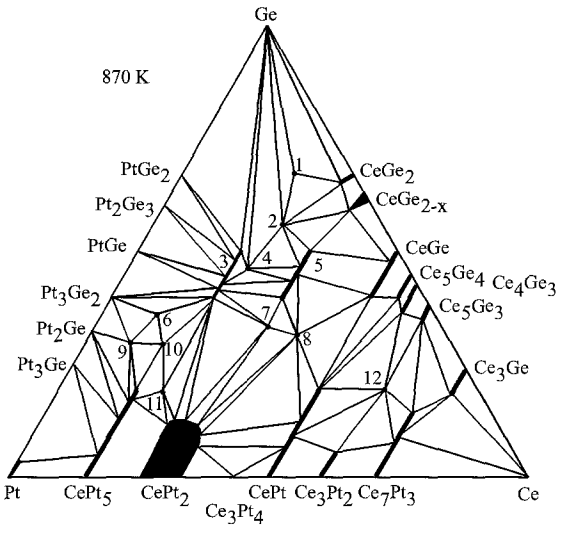

Fig. 52. Ce–Pt–Ge, isothermal section at 870 K.

A mixture of $HNO_3 + H_2O$ (2:1) was used for etching alloys with <50 at.% Ce. Ce-rich samples (>50 at.% Ce) were etched by highly diluted HNO_3.

Phase relations are characterized by the existence of twelve ternary compounds and by the formation of extended solid solutions originating at Ce–Pt and Ce–Ge binary compounds (see fig. 52). $CePt_5$ and CePt dissolve up to 20 at.% Ge. The maximum concentration of Ge in $Ce_7(Pt,Ge)_3$ was observed as 15 at.%. A large homogeneity range of not less than 24–33 at.% Ce was determined for the $CePt_2$ compound; the limits of extension of $CePt_2$ into the ternary system were not indicated by the author. The binary phases of the Pt–Ge system and the remaining binary phases in the other two systems dissolve less than 5 at.% of third component.

The crystal structures of the compounds $Ce_3Pt_4Ge_6$ (4) (own structure type, $a = 0.4419$, $b = 0.4422$, $c = 2.6222$; Gribanov et al. 1992a), $Ce_2Pt_7Ge_4$ (10) (own structure type, $a = 1.9866$, $b = 0.4089$, $c = 1.1439$; Gribanov et al. 1992b) and $Ce_3Pt_{23}Ge_{11}$ (9) (own structure type, $a = 1.71833$; Gribanov et al. 1993a) were investigated by X-ray single-crystal analysis of specimens obtained from alloys annealed at 870 K. $Ce(Pt,Ge)_2$ (5) was found to crystallize with the AlB_2 type, $a = 0.4272$, $c = 0.4204$ (Gribanov et al. 1996; X-ray powder analysis).

According to an X-ray powder diffraction analysis reported by Hovestreydt et al. (1982) the compound CePtGe (7) adopted the KHg_2-type of structure, $a = 0.4450$, $b = 0.7347$, $c = 0.7615$. For sample preparation, see La–Pd–Ge. The crystal structure was confirmed later by Rogl et al. (1989), $a = 0.44515$, $b = 0.73439$, $c = 0.76161$ (X-ray powder diffraction), and by Gribanov et al. (1996), $a = 0.4445$, $b = 0.7239$, $c = 0.7609$ (X-ray powder diffraction).

The existence of the $CePt_2Ge_2$ (3) compound ($CeGa_2Al_2$ type, $a = 0.440$, $c = 0.987$) was reported by Rossi et al. (1979). For sample preparation see $LaMn_2Ge_2$ under La–Mn–Ge.

Dommann et al. (1985) observed the $CaBe_2Ge_2$-type for the $CePt_2Ge_2$ compound with lattice parameters $a=0.4397$, $c=0.9802$ (X-ray single-crystal data) from an arc melted sample. Starting materials were Ce (3N), Ge (4N), Pt (3N). $CaBe_2Ge_2$-type was confirmed by Gribanov et al. (1996) for $CePt_2Ge_2$; $a=0.44033$, $c=0.9808$ from an alloy annealed at 870 K (X-ray powder diffraction) and was shown to exist over a wide composition range, see fig. 52. Venturini et al. (1989a) investigated the crystal structure of $CePt_2Ge_2$ from an arc melted sample annealed at 1273 K for 5 days. The crystal structure was found to belong to the $LaPt_2Ge_2$ type, $a=0.4389$, $b=0.4402$, $c=0.9818$, $\beta=90.83°$. Starting materials were Ce (3N), Pt (4N) and Ge (4N).

Sologub et al. (1995a) reported on the X-ray powder analysis of the Ce_2PtGe_6 (1) compound which was found to crystallize with the Ce_2CuGe_6 type, $a=0.41503$, $b=0.40858$, $c=2.2183$. For sample preparation, see La_2PdGe_6 under La–Pd–Ge. Gribanov et al. (1996) confirmed the structure type and obtained the lattice parameters $a=0.4142$, $b=0.4082$, $c=2.209$ (X-ray powder diffraction).

Francois et al. (1987) reported the crystal structure of the $CePtGe_2$ ($YIrGe_2$ type, $a=0.4428$, $b=1.648$, $c=0.8795$; X-ray powder data). The sample was prepared by heating the mixture of powders of starting components [Ce (3N), Ir (3N) and Ge (3N)] in an evacuated silica tube at 1173 K. The existence of the $CePtGe_2$ compound was not confirmed by Gribanov et al. (1996) at 870 K.

The formation of five more ternary phases with unknown structure has been observed by Gribanov et al. (1996) while investigating the isothermal section of the Ce–Pt–Ge system at 870 K. They exist at the compositions ~$Ce_{11}Pt_{53}Ge_{36}$ (6), ~$Ce_{20}Pt_{60}Ge_{20}$ (11), ~$Ce_{25}Pt_{20}Ge_{55}$ (2), ~$Ce_{40}Pt_{28}Ge_{32}$ (8), ~$Ce_{62}Pt_{18}Ge_{20}$ (12).

4.4.14. *Ce–Au–Ge*

Little information exists about the Ce–Au–Ge system; three ternary germanides were characterized.

A ternary compound of cerium with gold and germanium of the stoichiometric ratio 1:1:1 was identified and studied by means of X-ray and metallographic analyses by Rossi et al. (1992). The CeAuGe compound was found to have the LiGaGe-type structure with lattice parameters $a=0.4464$, $c=0.7910$. The sample was prepared by melting the metals (~99.9 mass% for cerium and 99.99 mass% for gold and germanium) in an induction furnace and annealing at 1070 K for one week. The crystal structure of the CeAuGe compound has been confirmed by Pöttgen et al. (1996a) from an alloy which was prepared by melting a mixture of the elements in an arc furnace and subsequently annealing at 1070 K ($a=0.44603$, $c=0.79360$; X-ray powder data).

Ce_2AuGe_6 was reported to crystallize with a Ce_2CuGe_6 type, $a=0.42587$, $b=0.41263$, $c=2.1852$ (Sologub et al. 1995a; X-ray powder data). For sample preparation, see La_2PdGe_6 under La–Pd–Ge.

The structure of $CeAu_{0.75}Ge_{1.25}$ was derived by Jones et al. (1997) from single-crystal X-ray data: AlB_2 structure type, $a=0.4335$, $c=0.4226$. The sample was prepared from the elemental components by arc melting and subsequent annealing at 1170 K.

4.5. *Pr–d element–Ge systems*

4.5.1. *Pr–Mn–Ge*

No phase diagram exists for the system Pr–Mn–Ge, however, a series of ternary compounds have been observed and characterized.

The $PrMn_2Ge_2$ compound have been prepared and studied by Rossi et al. (1978b). It was found to be of $CeGa_2Al_2$ type with following lattice parameters $a = 0.4117$, $c = 1.0902$. The alloy was obtain by melting under argon in an induction furnace. The samples were then annealed at 770 K for one week. Praseodymium used was of purity greater than 99.9 mass%, for manganese and germanium the purity was greater than 99.99 mass%.

A PrMnGe compound with PbFCl-type structure was observed by Welter et al. (1995); $a = 0.4182$, $c = 0.7308$. The compound was prepared from commercially available high purity elements. A compacted pellet of stoichiometric mixture was sealed under argon (100 mmHg) in a silica tube, heated at 1273 K as a preliminary homogenization treatment and then melted in an induction furnace. The resulting ingot was annealed for 2 weeks at 1173 K.

4.5.2. *Pr–Fe–Ge*

Phase equilibria for the complete isothermal section at 870 K have been determined by Fedyna (1988) using X-ray powder diffraction and microstructural analyses of 209 ternary alloys synthesized by arc melting ingots of Pr (99.75 mass%), Fe (99.90 mass%) and Ge (99.99 mass%). The alloys were annealed in evacuated quartz tubes for 500–900 hours at 870 K. The total number of compounds observed was nine. The mutual solid solubilities of the binary compounds were reported to be negligible. Phase equilibria in the isothermal section at 870 K are presented in fig. 53.

$PrFe_6Ge_6$ (1) was observed and studied by Mruz et al. (1984). It was found to crystallize with YCo_6Ge_6 type, lattice parameters $a = 0.5091$, $c = 0.4036$, by X-ray powder diffraction

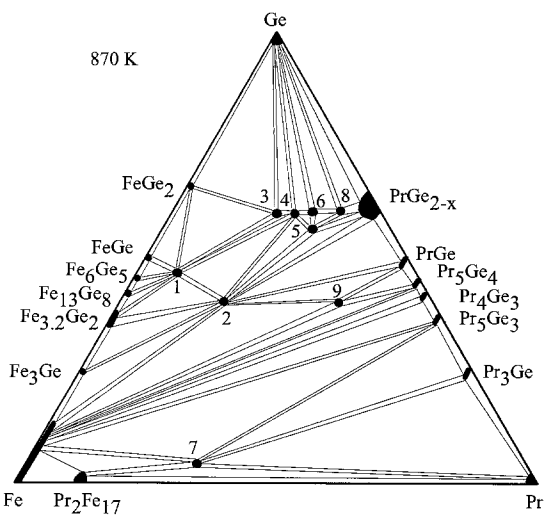

Fig. 53. Pr–Fe–Ge, isothermal section at 870 K.

of arc melted alloy annealed at 870 K. The existence of the $PrFe_6Ge_6$ compound was confirmed by Fedyna (1988) while constructing the isothermal section.

The formation and crystal structure of the $PrFe_2Ge_2$ (2) compound was reported in an early investigation of praseodymium–iron–germanium combinations by Rossi et al. (1978a,b): $CeGa_2Al_2$ type, $a = 0.4055$, $c = 1.0540$ was later confirmed by Bara et al. (1990), $a = 0.4060$, $c = 1.0508$. For sample preparation, see $LaMn_2Ge_2$ under La–Mn–Ge, and $LaFe_2Ge_2$ under La–Fe–Ge, respectively.

The crystal structures of four more compounds within Pr–Fe–Ge system at 870 K were determined by Fedyna (1988): $PrFeGe_3$ (3) with $BaNiSn_3$ type, $a = 0.4312$, $c = 0.9932$; $PrFe_{1-x}Ge_2$, $x = 0.45$ (5) with $CeNiSi_2$ type, $a = 0.4253$, $b = 1.6478$, $c = 0.4130$; $Pr_4Fe_{1-x}Ge_7$, $x = 0.15$ (8) with Sm_4CoGe_7 type, $a = 0.42166$, $b = 3.0520$, $c = 0.41278$; $Pr_{117}Fe_{52}Ge_{112}$ (9) with $Tb_{117}Fe_{52}Ge_{112}$ type, $a = 2.9428$.

$Pr_6Fe_{13}Ge$ (7) was found to adopt the $Nd_6Fe_{13}Si$ type by Weitzer et al. (1990), $a = 0.80986$, $c = 2.30836$. For sample preparation, see $La_6Co_{13}Ge$ under La–Co–Ge.

The crystal structures of two germanides ~$Pr_{2.3}Fe_{1.7}Ge_6$ (4) and ~$Pr_{2.7}Fe_{1.3}Ge_6$ (6) have not been solved yet.

4.5.3. *Pr–Co–Ge*

Isothermal sections of the Pr–Co–Ge system at 1070 K (0–33 at.% Pr) and 670 K (33–100 at.% Pr) were derived by Fedyna (1988) employing X-ray phase and partly microstructural analyses of 287 alloys prepared by arc melting solid pieces of Pr (99.75 mass%), Co (99.90 mass%) and Ge (99.99 mass%). The melted buttons were then annealed in evacuated silica tubes for 500–900 hours. Thirteen ternary compounds were found to exist. The solubilities of cobalt in $PrGe_{2-x}$ and Pr_5Ge_3 binaries were established as 11 at.% and 8 at.%, respectively, from the variation of lattice parameters. Figure 54 represents the

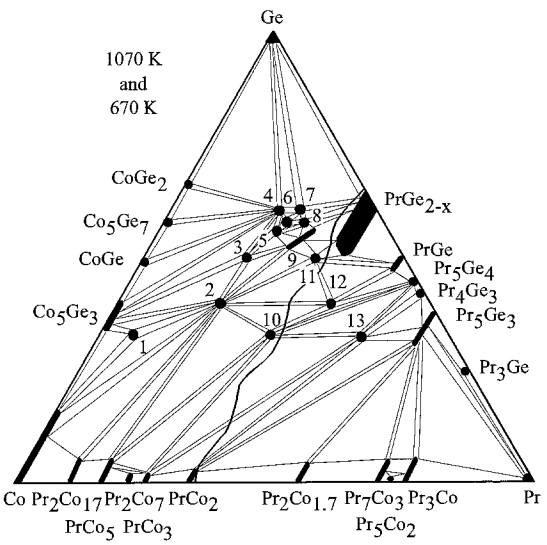

Fig. 54. Pr–Co–Ge, isothermal sections at 1070 K (0–33 at.% Pr) and at 670 (33–100 at.% Pr).

Table 16
Crystallographic data for the ternary Pr–Co–Ge compounds

No.	Compound	Structure	Lattice parameters (nm)			Reference
			a	*b*	*c*	
1	$Pr_{1-x}(Co,Ge)_{13}$, $x=0.31$	$CeNi_{8.5}Si_{4.5}$	0.7932		1.1817	Fedyna (1988)
2	$PrCo_2Ge_2$	$CeGa_2Al_2$	0.4048		1.0178	Fedyna (1988)
3	$Pr_2Co_3Ge_5$	$U_2Co_3Si_5$	0.9783	1.1896	0.5831	Fedyna (1988)
4	$PrCo_{1-x}Ge_3$, $x=0.136$	$BaNiSn_3$	0.43107		0.98332	Fedyna (1988)
5	$\sim Pr_{2.3}Co_{2.1}Ge_{5.6}$	unknown				Fedyna (1988)
6	$\sim Pr_{2.3}Co_{1.8}Ge_{5.8}$	unknown				Fedyna (1988)
7	$\sim Pr_{2.5}Co_{1.5}Ge_{6.0}$	unknown				Fedyna (1988)
8	$\sim Pr_{2.7}Co_{1.5}Ge_{5.8}$	unknown				Fedyna (1988)
9	$PrCo_{1-x}Ge_2$, $x=0.10$–0.52	$CeNiSi_2$	0.4249–0.4262	1.6650–1.6770	0.4136–0.4230	Fedyna (1988)
10	PrCoGe	PbFCl	0.4181		0.6842	Fedyna (1988)
11	$PrCo_{0.5}Ge_{1.5}$	AlB_2	0.4163		0.4193	Fedyna (1988)
12	$Pr_{117}Co_{52}Ge_{112}$	$Tb_{117}Fe_{52}Ge_{112}$	2.9318			Fedyna (1988)
13	Pr_3CoGe_2	La_3NiGe_2	1.1840	0.4272	1.1519	Fedyna (1988)

isothermal sections of the Pr–Co–Ge system at 1070 K and 670 K.

Crystallographic information on the Pr–Co–Ge ternary compounds is summarized in table 16.

The crystal structure of $PrCoGe_3$ ($BaNiSn_3$ type, $a=0.4307$, $c=0.9803$; X-ray powder diffraction) was investigated by Venturini et al. (1985b) from a sample prepared by heating a compacted mixture of starting materials (Pr in pieces, 99.9 mass%; Co and Ge in powder, 99.99 mass%) in an evacuated quartz tube at 1073 K. Later the same structure type was indicated by Fedyna (1988) for a sample with composition $PrCo_{1-x}Ge_3$, $x=0.136$ (see table 16; X-ray powder diffraction data; for the experimental procedure, see above).

4.5.4. *Pr–Ni–Ge*

The isothermal sections of the Pr–Ni–Ge phase diagram at 870 K (0–50 at.% Pr) and at 670 K (50–100 at.% Pr) was constructed by Fedyna (1988) from X-ray powder and microstructural analyses of 255 alloys. A detailed description of the experimental procedure is given under Pr–Fe–Ge. Starting materials were Pr (99.75 mass%), Ni (99.99 mass%) and Ge (99.99 mass%).

The phase relations are characterized by the existence of eleven ternary compounds and by the formation of an extended homogeneity region for the $Pr(Ni,Ge)_{2-x}$ (9) compound as well as two solid solutions originating at $PrNi_5$ (20 at.% Ge) and $PrGe_{2-x}$ (9 at.% Ni). The isothermal section of the Pr–Ni–Ge system after Fedyna (1988) is presented in fig. 55.

Bodak et al. (1982) investigated the crystal structure of the Pr_3NiGe_2 compound (10) (Pr_3NiGe_2 structure type, $a=1.1810$, $b=0.4293$, $c=1.1611$) by the X-ray powder

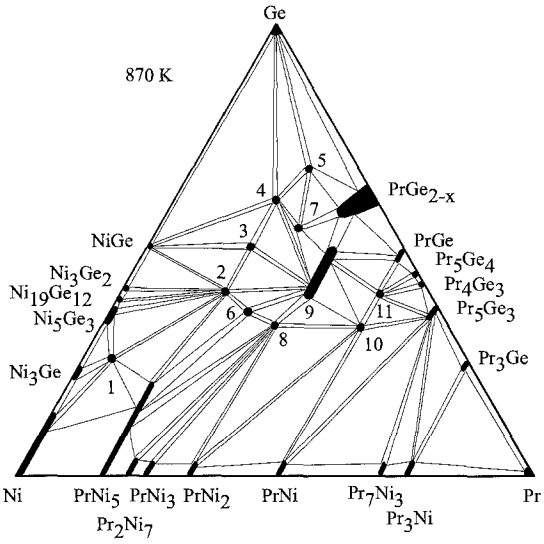

Fig. 55. Pr–Ni–Ge, isothermal section at 870 K.

diffraction method. For sample preparation and purity of starting elements, see Y_3NiGe_2 under Y–Ni–Ge.

Early investigations of the interaction of germanium with praseodymium and nickel has shown the existence of $PrNi_{0.6}Ge_{1.4}$ with AlB_2 type, $a = 0.4161$, $c = 0.4207$ (Gladyshevsky and Bodak 1965, Rieger and Parthé 1969a; X-ray powder diffraction). Fedyna (1988) confirmed the AlB_2-type for this composition and observed the formation of a large homogeneity field with the formula $Pr(Ni_{0.42-0.28}Ge_{0.58-0.72})_{2-x}$, $x = 0.14$ (9) and lattice parameters $a = 0.4158$–0.4150, $c = 0.4134$–0.4220.

$PrNi_2Ge_2$ (2) is isotypic with $CeGa_2Ge_2$; $a = 0.4136$, $c = 0.9844$ (Rieger and Parthé 1969b; X-ray powder diffraction).

The crystal structures of seven other compounds have been studied by Fedyna (1988). $Pr_{1-x}(Ni,Ge)_{13}$, $x = 0.24$ (1) belongs to the $CeNi_{8.5}Si_{4.5}$-type; $Pr_2Ni_3Ge_5$ (3) crystallizes with the $U_2Co_3Si_5$-type structure, $a = 0.9812$, $b = 1.1832$, $c = 0.5912$ (powder X-ray diffraction data); $PrNiGe_3$ (4) is isostructural with the $ScNiSi_3$ type, $a = 2.1779$, $b = 0.41052$, c 0.41440; Pr_2NiGe_6 (5) was reported to crystallize with the Ce_2CuGe_6 type, $a = 0.40343$, $b = 0.41124$, $c = 2.1722$; $Pr_3Ni_4Ge_4$–(6) was claimed to adopt the $U_3Ni_4Ge_4$-type structure, $a = 0.4098$, $b = 0.4182$, $c = 2.4013$; $PrNi_{1-x}Ge_2$, x=0.33 (7) is isotypic with $CeNiSi_2$, $a = 0.4210$, $b = 1.668$, $c = 0.4160$; PrNiGe (8) was found to be of TiNiSi type, $a = 0.72757$, $b = 0.43429$, $c = 0.72981$.

Investigating the isothermal section, Fedyna (1988) observed the ~$Pr_{0.5}Ni_{0.1}Ge_{0.4}$ (11) compound with unknown crystal.

4.5.5. *Pr–Cu–Ge*

Praseodymium–copper–germanium combinations were investigated by various groups of authors, however no isothermal section was constructed for the Pr–Cu–Ge system so far.

Rieger and Parthé (1969a) investigated the occurrence of the AlB_2-type structure by means of X-ray powder diffraction of arc melted alloys. The data presented were $PrCu_{1-0.67}Ge_{1-1.33}$ with $a = 0.4374$–0.4183, $c = 0.3971$–0.4197. Iandelli (1993) confirmed the AlB_2-type ($a = 0.4288$, $c = 0.3942$; X-ray powder analysis) from the PrCuGe alloy which was prepared from mixed filings or powders of metals (praseodymium 99.7 mass%, copper and germanium 99.99 mass%) and sealed in tantalum crucibles under argon followed by melting in an induction furnace. Afterwards the sample was annealed for 10 days at 1023 K.

Sologub et al. (1995a) investigated the crystal structure of Pr_2CuGe_6 alloy which was prepared by arc melting under argon and annealed at 1070 K in an evacuated quartz tube for 150 h. From X-ray powder analysis the compound was determined to have the Ce_2CuGe_6-type structure, $a = 0.41950$, $b = 0.40585$, $c = 2.1485$.

$Pr_2Cu_3Ge_3$ was found to crystallize with the $Ce_2Cu_3Ge_3$ structure type, $a = 0.4141$, $c = 1.7371$, $c = 0.4183$, X-ray powder data (Konyk 1988). For sample preparation, see Ce–Cu–Ge.

Rieger and Parthé (1969b) synthesized $PrCu_2Ge_2$ with the $CeGa_2Al_2$-type structure, $a = 0.4154$, $c = 1.0206$.

The existence of a compound $Pr_6Cu_8Ge_8$ with the $Gd_6Cu_8Ge_8$ structure ($a = 1.421$, $b = 0.6687$, $c = 0.4293$) was reported by Fedyna et al. (1995) from X-ray powder diffraction data of arc melted alloy annealed at 870 K.

Francois et al. (1990) reported the crystal structure of the $PrCu_{0.76}Ge_2$ compound ($CeNiSi_2$ type, $a = 0.4247$, $b = 1.724$, $c = 0.4109$). For sample preparation, see $LaFeGe_2$ under La–Fe–Ge.

4.5.6. *Pr–Zn–Ge*

No isothermal section is available for the ternary Pr–Zn–Ge system, however one ternary compound was observed and characterized by Rossi and Ferro (1996). $PrZn_{1.5}Ge_{0.5}$ was found to crystallize with AlB_2 type, $a = 0.4440$, $c = 0.3883$, from X-ray powder diffraction of an alloy melted in an induction furnace and then annealed at 1070 K for one week. An electronic micrographic examination as well as microprobe microanalysis were carried out. The metals employed in sample synthesis had a nominal purity of 99.9 mass% for praseodymium, and 99.999 mass% for the other metals.

4.5.7. *Pr–Ru–Ge*

The phase diagram for the Pr–Ru–Ge system is not available yet, however several groups of authors investigated praseodymium–ruthenium–germanium combinations with respect to the formation and crystal structure of the compounds.

Early investigations of the $PrRu_2Ge_2$ compound determined the $CeGa_2Al_2$-type: $a = 0.4263$, $c = 1.0022$ (Francois et al. 1985) from X-ray powder analysis of alloy obtained by powder metallurgical reaction at 1273 K. Starting components were Pr (3N), Ru (4N) and Ge (4N).

Venturini et al. (1986b) reported that the $Pr_2Ru_3Ge_5$ compound has the $U_2Co_3Si_5$-type structure. The lattice parameters were reported as $a = 0.9933$, $b = 1.247$, $c = 0.5846$ from X-ray powder diffraction.

$Pr_3Rh_4Sn_{13}$-type was announced for the $Pr_3Ru_4Ge_{13}$ compound ($a=0.907$) by Segre et al. (1981a) from X-ray powder analysis of an arc melted sample annealed at 1523 K for 1 day and at 1273 K for 7 days. Starting materials were Pr (3N), Ru (3N), Ge (6N).

The crystal structure of the PrRuGe compound was investigated by Welter et al. (1993b). It was found to adopt the PbFCl type, $a=4268$, $c=0.6842$ (X-ray powder diffraction). The compound was prepared from commercially available high-purity elements. A compacted stoichiometric mixture in a silica tube sealed under argon was heated to 1173 K for preliminary homogenization and then melted in an induction furnace.

$Pr_3Ru_2Ge_2$ was found to crystallize with the $La_3Ni_2Ga_2$ type ($a=0.5699$, $b=0.7909$, $c=1.3593$, X-ray powder diffraction) from an arc melted sample annealed at 870 K (Bodak et al. 1989a).

4.5.8. *Pr–Rh–Ge*

Phase equilibria in the system Pr–Rh–Ge have not been established yet, but at least six different ternary phases have been verified.

$Pr_2Rh_3Ge_5$ was found to crystallize with $U_2Co_3Si_5$-type structure ($a=1.0073$, $b=1.209$, c 0.5969) by Venturini et al. (1986b) from X-ray powder analysis.

Early investigations of the $PrRh_2Ge_2$ compound determined it to have the $CeGa_2Al_2$-type structure: $a=0.4147$, $c=1.0436$ (Francois et al. 1985). For sample preparation, see $CeRu_2Ge_2$ under Ce–Ru–Ge.

Venturini et al. (1985b) reported an X-ray powder diffraction study of the $PrRhGe_3$ compound from a sample prepared by heating of a mixture of the starting components (Pr 3N, Rh 4N, Ge 4N) in an evacuated quartz tube at 1073 K. The crystal structure was found to adopt the $BaNiSn_3$ type, $a=0.4383$, $c=1.0011$.

Hovestreydt et al. (1982) reported the crystal structure of the PrRhGe compound (TiNiSi type, $a=0.7376$, $b=0.4476$, $c=0.7124$; X-ray powder data) from an arc melted sample annealed at 1270 K for 1–2 weeks. Starting components were Pr (3N), Rh (4N) and Ge (5N).

Gladyshevsky et al. (1991a) reported on the crystal structure of $Pr_3Rh_2Ge_2$ ($La_3Ni_2Ge_2$ type, $a=0.5674$, $b=0.8059$, $c=1.3445$; X-ray powder diffraction). For the details of sample preparation, see $La_3Rh_2Ge_2$ under La–Rh–Ge

Pr_2Rh_3Ge crystallizes with the Y_2Rh_3Ge-type of structure with lattice parameters $a=0.5626$, $c=1.193$ (Cenzual et al. 1987).

Verniere et al. (1995) mentioned the existence of $Pr_4Rh_{13}Ge_9$ compound with $Ho_4Ir_{13}Ge_9$-type; no lattice parameters were given. For the experimental details, see $La_4Rh_{13}Ge_9$ under La–Rh–Ge.

4.5.9. *Pr–Pd–Ge*

Phase relations have not been yet established for the Pr–Pd–Ge system; only three ternary compounds have been observed.

Sologub et al. (1995a) reported on the X-ray powder analysis of the Pr_2PdGe_6, compound which was found to crystallize with the Ce_2CuGe_6 type structure, $a=0.4152$, $b=0.4073$, $c=2.197$. Samples were synthesized by argon arc melting followed by a heat

treatment at 870 K for 150 hours. Starting materials used were obtained from Johnson & Matthey, UK (99.9 mass%).

According to an X-ray powder diffraction analysis reported by Hovestreydt et al. (1982), the compound PrPdGe adopts the KHg_2-type structure, $a = 0.4472$, $b = 0.7256$, $c = 0.7654$. The alloy was arc melted under argon and annealed at 1270 K for 1–2 weeks. The starting materials were Pr (3N), Pd (4N) and Ge (5N).

The crystal structure of the compound $PrPd_2Ge$ was found to be of the YPd_2Si type ($a = 0.7617$, $b = 0.6993$, $c = 0.5735$; X-ray powder diffraction) by Jorda et al. (1983). The sample was obtained by induction melting under an argon atmosphere and annealing in evacuated quartz tube for 10 days at 1173 K. The starting materials were palladium (4N), germanium (4N), praseodymium (3N).

4.5.10. *Pr–Ag–Ge*

Information on interaction of praseodymium with silver and germanium is due to the work of several groups of authors; six ternary compounds have been observed and analyzed. Crystallographic characteristics of the ternary Pr–Ag–Ge phases are listed in table 17.

Table 17
Crystallographic data for the ternary Pr–Ag–Ge compounds

Compound	Structure	Lattice parameters (nm)			Reference
		a	*b*	*c*	
Pr_2AgGe_6	Ce_2CuGe_6	0.42887	0.41295	2.1610	Sologub et al. (1995a)
		0.42856	0.41263	2.15869	Savysyuk and Gladyshevsky (1995)
$PrAg_{0.8}Ge_{1.2}$	AlB_2	0.4356		0.4130	Protsyk (1994)
		0.43793		0.40903	Savysyuk and Gladyshevsky (1995)
$PrAg_2Ge_2$	$CeGa_2Al_2$	0.42801		1.09977	Savysyuk and Gladyshevsky (1995)
$Pr_3Ag_4Ge_4$	$Gd_3Cu_4Ge_4$	0.4342	0.71126	1.47306	Savysyuk and Gladyshevsky (1995)
$PrAg_{1.4}Ge_{0.6}$	Fe_2P	0.72989		0.43340	Savysyuk and Gladyshevsky (1995)
PrAgGe	LiGaGe	0.45276		0.76357	Savysyuk and Gladyshevsky (1995)

Savysyuk and Gladyshevsky (1995) employed X-ray powder diffraction analysis of arc melted samples, which were homogenized by annealing at 773 K and 1073 K for 1000 hours. For detailed experimental procedure for Pr_2AgGe_6 (Sologub et al. 1995a) and $PrAg_{0.8}Ge_{1.2}$ (Protsyk 1994), see La_2AgGe_6 (under La–Ag–Ge) and Ce–Ag–Ge, respectively.

4.5.11. *Pr–Os–Ge*

No phase diagram exists at present for the system Pr–Os–Ge, however, one ternary germanide has been observed and characterized by Segre et al. (1981a). $Pr_3Os_4Ge_{13}$ was found to crystallize with the $Pr_3Rh_4Sn_{13}$-type structure, $a = 0.9098$. For sample preparation, see $Ce_3Ru_4Ge_{13}$ under Ce–Ru–Ge.

4.5.12. *Pr–Ir–Ge*

Phase relations have not yet been established for the Pr–Ir–Ge system; information concerning the formation of six compounds and their crystal structure is due to the work of different groups of authors.

Francois et al. (1987) reported the crystal structure of the $PrIrGe_2$ ($YIrGe_2$ type, $a=0.4393$, $b=1.617$, $c=0.8908$). The sample was prepared by heating the mixture of powders of starting components (Pr 3N, Ir 3N and Ge 3N) in evacuated silica tube at 1173 K.

According to an X-ray powder diffraction analysis reported by Hovestreydt et al. (1982), the compound PrIrGe adopts the TiNiSi-type structure, $a=0.7357$, $b=0.4440$, $c=0.71197$. For the experimental procedure, see La–Ir–Ge.

$PrIr_2Ge_2$ is isotypic with the crystal structure of $CaBe_2Ge_2$ with lattice parameters $a=0.4235$, $c=1.0057$ (Francois et al. 1985).

$Pr_2Ir_3Ge_5$ was found to crystallize with the $U_2Co_3Si_5$ type (a=1.0185, $b=1.190$, $c=0.6045$) by Venturini et al. (1986b) from X-ray powder analysis.

Verniere et al. (1995) observed the existence $Pr_4Ir_{13}Ge_9$ compound with $Ho_4Ir_{13}Ge_9$-type. Lattice parameters have not been established. For the experimental procedure, see $La_4Ir_{13}Ge_9$ under La–Ir–Ge.

Venturini et al. (1985b) reported on the X-ray powder diffraction study of the $Pr_3Ir_4Ge_{13}$ compound from a sample which was prepared by heating a mixture of starting components (Pr 3N, Ir 4N, Ge 4N) in an evacuated quartz tube at 1073 K. The crystal structure was found to adopt the $Yb_3Rh_4Sn_{13}$-type structure, $a=0.9053$.

4.5.13. *Pr–Pt–Ge*

Francois et al. (1987) reported the crystal structure of the $PrPtGe_2$ ($YIrGe_2$ type, $a=0.4416$, $b=1.644$, $c=0.8793$). For sample preparation, see $PrIrGe_2$ under Pr–Ir–Ge.

Venturini et al. (1989a) investigated the crystal structure of $PrPt_2Ge_2$ from an arc melted sample annealed at 1273 K for 5 days. The crystal structure was found to belong to the $LaPt_2Ge_2$ type, $a=0.4374$, $b=0.4396$, $c=0.9779$, $\beta=91.94^\circ$. The starting materials were Pr (3N), Pt (4N) and Ge (4N).

According to an X-ray powder diffraction analysis reported by Hovestreydt et al. (1982), the compound PrPtGe adopts the KHg_2-type of structure, $a=0.4438$, $b=0.7292$, $c=0.7616$. For the experimental procedure, see La–Ir–Ge.

Sologub et al. (1995a) reported on the X-ray powder analysis of the Pr_2PtGe_6 compound which was found to crystallize with the Ce_2CuGe_6 type structure, $a=0.4134$, $b=0.4070$, $c=2.2084$. For sample preparation, see La_2PdGe_6 under La–Pd–Ge.

4.5.14. *Pr–Au–Ge*

No ternary phase diagram exists for the Pr–Au–Ge system, however, a ternary compound of praseodymium with gold and germanium in the stoichiometric ratio 1:1:1 has been identified and studied by means of X-ray powder diffractometry and metallography by Rossi et al. (1992). The PrAuGe compound was found to adopt the LiGaGe type

with lattice parameters $a = 0.4457$, $c = 0.7803$. The sample was prepared by melting the metals (99.9 mass% for praseodymium and 99.99 mass% for gold and germanium) in an induction furnace and annealing at 1070 K for one week.

Sologub et al. (1995a) reported on the X-ray powder analysis of the Pr_2AuGe_6 compound which was found to crystallize with the Ce_2CuGe_6 type, $a = 0.4241$, $b = 0.4113$, $c = 2.1172$. For sample preparation, see La_2PdGe_6 under La–Pd–Ge.

4.6. *Nd–d element–Ge systems*

4.6.1. *Nd–V–Ge*

The phase equilibria in the Nd–V–Ge system have been investigated by Salamakha et al. (1994) by means of X-ray analysis of 40 ternary alloys. No ternary compounds were observed. The isothermal section of the phase diagram at 870 K is shown in fig. 56.

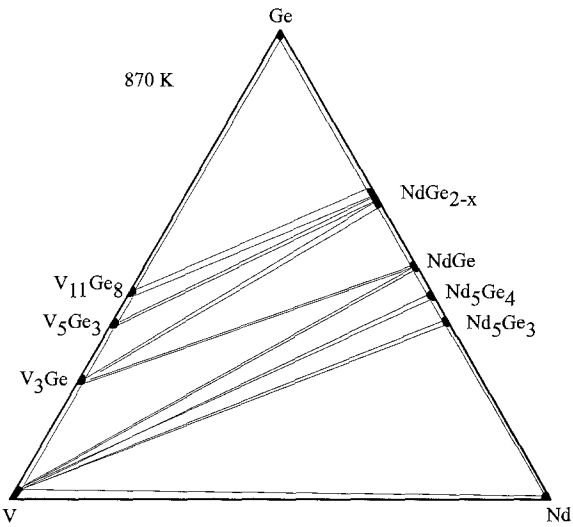

Fig. 56. Nd–V–Ge, isothermal section at 870 K.

The ternary samples used to derive the phase relations in the ternary section at 870 K, each with a total weight of 2 g, were synthesized by arc melting proper amounts of the constituent elements under high-purity argon on a water-cooled copper hearth. The starting materials were used in the form of ingots of high-purity elements: neodymium (99.85 mass%), vanadium (99.99 mass%), germanium (99.99 mass%). The weight losses were generally less than 1%. The alloys were annealed at 870 K in evacuated quartz tubes for 2 weeks and quenched in ice cold water.

4.6.2. *Nd–Cr–Ge*

The isothermal section of the Nd–Cr–Ge phase diagram at 870 K was constructed by Salamakha et al. (1994). The phase relations are characterized by the formation of two

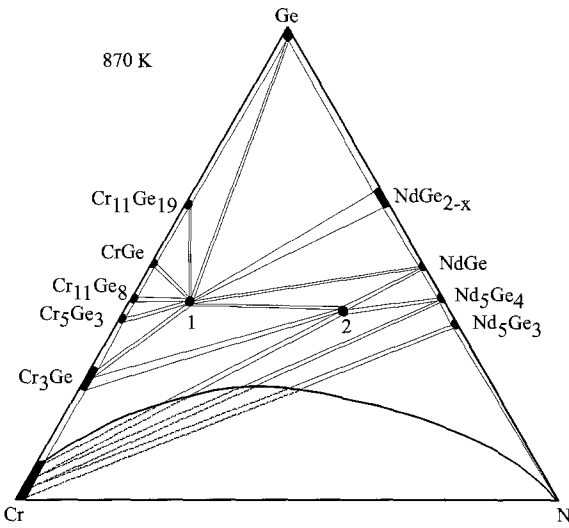

Fig. 57. Nd–Cr–Ge, isothermal section at 870 K. The curved line indicates the liquid immiscibility gap region.

ternary compounds, $Nd_2Cr_9Ge_8$ (1) and $Nd_{117}Cr_{52}Ge_{112}$ (2), and by a region of liquid immiscibility that stretches up to 20 at.% Ge (fig. 57). For details of sample preparation, see Nd–V–Ge. The purity of the starting materials was Nd 99.85 mass%, Cr 99.93 mass%, Ge mass 99.99%.

$Nd_2Cr_9Ge_8$ (own structure type, $a=0.9388$, $b=0.4046$, $c=0.8045$) was observed by Bodak et al. (1989a) from X-ray single-crystal analysis. For sample preparation, see Nd–V–Ge.

Salamakha et al. (1994) observed the $Nd_{117}Cr_{52}Ge_{112}$ compound in the course of investigating the Nd–Cr–Ge isothermal section. It was found to crystallize with the $Tb_{117}Fe_{52}Ge_{112}$-type structure, $a=2.9439$ from X-ray powder analysis.

4.6.3. *Nd–Mn–Ge*

The phase-field distribution in the Nd–Mn–Ge system at 870 K is characterized by the formation of three ternary compounds: $NdMn_6Ge_6$ (1), $NdMn_2Ge_2$ (2) and $NdMn_xGe_2$ (3) after Salamakha et al. (1994) (fig. 58). The samples were prepared by argon arc melting. Weight losses due to vaporization while melting were compensated beforehand by extra amounts of manganese (about 0.5 mass%). The arc melted buttons were annealed at 870 K for 2 weeks in vacuum-sealed quartz capsules and finally quenched by submerging the ampoules into cold water. The starting materials were Nd 99.85 mass%, Mn 99.98 mass%, Ge 99.99 mass%.

$NdMn_6Ge_6$(1) has been found by Salamakha et al. (1994) from X-ray powder diffraction to be isostructural with the YCo_6Ge_6 type, $a=0.5249$, $c=0.4098$. For the experimental procedure, see above.

$NdMn_2Ge_2$ (2) was reported to crystallize with the $CeGa_2Al_2$-type structure, $a=0.4105$, $c=1.0216$ (Salamakha et al. 1994; X-ray powder diffraction).

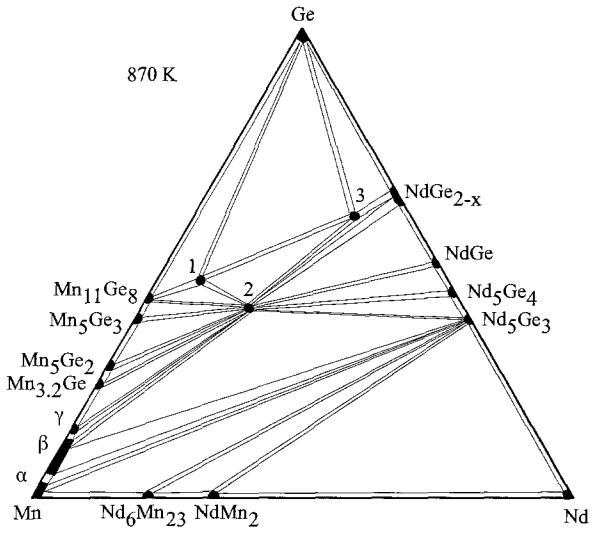

Fig. 58. Nd–Mn–Ge, isothermal section at 870 K.

The crystallographic characteristics for $NdMn_xGe_2$ (3) were reported by Salamakha et al. 1994 from X-ray powder analysis ($CeNiSi_2$ type, $a = 0.4232$, $b = 1.653$, $c = 0.4092$).

A compound of equiatomic composition with the PbFCl type was observed by Welter et al. (1995) at 1070 K with lattice parameters $a = 0.4134$, $c = 0.7375$. For sample preparation, see Pr–Mn–Ge. Apparently the NdMnGe phase does not exist at 870 K (fig. 58).

4.6.4. *Nd–Fe–Ge*

Figure 59 represents the isothermal section of the Nd–Fe–Ge system at 870 K as derived

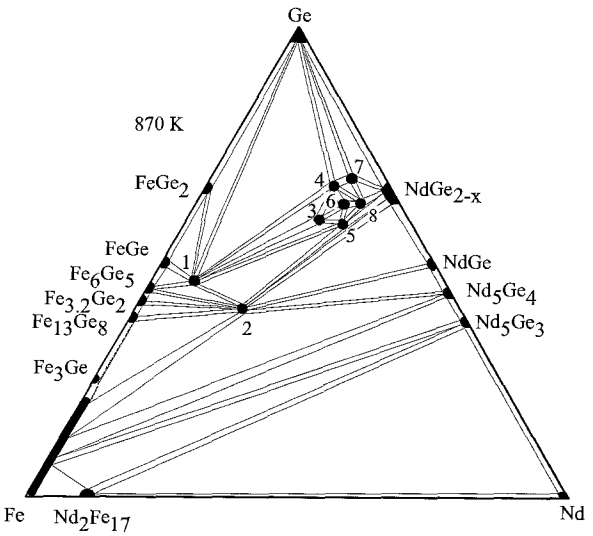

Fig. 59. Nd–Fe–Ge, isothermal section at 870 K.

Table 18
Crystallographic data for the ternary Nd–Fe–Ge compounds at 870 K

No.	Compound	Structure	Lattice parameters (nm)			Reference
			a	*b*	*c*	
1	$NdFe_6Ge_6$	YCo_6Ge_6	0.5142		0.4049	Salamakha et al. (1996b)
2	$NdFe_2Ge_2$	$CeGa_2Al_2$	0.4038		1.0510	Salamakha et al. (1996b)
3	~$Nd_5Fe_3Ge_{12}$	unknown				Salamakha et al. (1996b)
4	~$Nd_5Fe_2Ge_{13}$	unknown				Salamakha et al. (1996b)
5	$NdFe_{0.37}Ge_2$	$CeNiSi_2$	0.4214	1.6450	0.4084	Salamakha et al. (1996b)
6	~Nd_3FeGe_7	unknown				Salamakha et al. (1996b)
7	~Nd_4FeGe_{10}	orthorhomb	0.422	0.403	2.828	Salamakha et al. (1996b)
8	$Nd_4Fe_{0.64}Ge_7$	$Sm_4Co_{1-x}Ge_7$	0.4198	0.4095	3.037	Salamakha et al. (1996b)

from X-ray phase analysis of 150 samples by Salamakha et al. (1996b). The phase-field distribution is characterized by the presence of eight ternary compounds. The binary compound Fe_3Ge does not appear in the Nd–Fe–Ge ternary. None of the binary phases shows an appreciable range of mutual solid solubility. For the experimental details, see Nd–V–Ge. The starting materials were Nd 99.85 mass%, Fe 99.98 mass%, Ge 99.99 mass%.

Crystallographic data of the ternary phases, observed by Salamakha et al. (1996b) investigating the isothermal section of the Nd–Fe–Ge system, are listed in table 18.

Two more ternary compounds are known from early investigations of ternary neodymium–iron–germanium combinations performed by Felner and Schieber (1973) and Weitzer et al. (1990) which have not been observed in the course of studying the Nd–Fe–Ge isothermal section at 870 K. The $NdFe_{0.67}Ge_{1.33}$ compound was found to adopt the AlB_2 type ($a=0.4174$, $c=0.4163$; X-ray powder diffraction) (Felner and Schieber 1973). The samples were prepared by melting elements together (Nd 99.9 mass%, Ge 99.99 mass%, Fe 99.95 mass%). The metals were mixed and heated in an alumina crucible in an induction furnace at about 1870 K under a protective argon atmosphere. The samples were homogenized by annealing them in the induction furnace at the melting temperature for about 30 min. The crystal structure of the $Nd_6Fe_{13}Ge$ compound was reported by Weitzer et al. (1990) ($Nd_6Fe_{13}Si$ type, $a=0.8043$, $c=2.3204$). The sample was melted under argon and annealed at 1073 K for 5 days. The starting materials were commercially available high-purity elements.

4.6.5. *Nd–Co–Ge*

The isothermal section of the Nd–Co–Ge system at 870 K is shown in fig. 60. The phase-field distribution is characterized by the presence of sixteen ternary compounds as reported by Salamakha (1997). Mutual solid solubilities of the binary compounds are insignificantly small. For sample preparation, see Nd–V–Ge. The starting materials were Nd 99.85 mass%, Co 99.99 mass%, Ge 99.99 mass% pure.

Crystallographic data of the ternary Nd–Co–Ge compounds are listed in table 19.

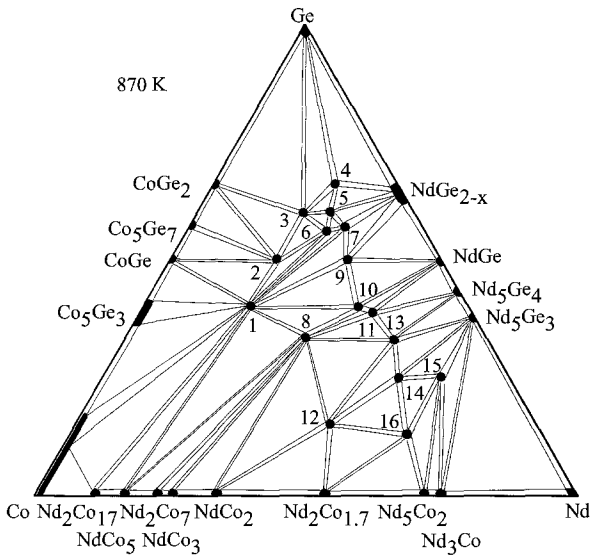

Fig. 60. Nd–Co–Ge, isothermal section at 870 K.

Table 19
Crystallographic data for the ternary Nd–Co–Ge compounds

No.	Compound	Structure	Lattice parameters (nm)			Reference
			a	*b*	*c*	
1	$NdCo_2Ge_2$	$CeGa_2Al_2$	0.4042		1.0183	Salamakha (1997)
2	$Nd_2Co_3Ge_5$	$U_2Co_3Si_5$	0.9710	1.203	0.5707	Salamakha (1997)
3	$NdCoGe_3$	$BaNiSn_3$	0.4296		0.9811	Salamakha (1997)
			0.4297		0.9812	Venturini et al. (1985b)
4	$\sim Nd_5Co_2Ge_{13}$	unknown				Salamakha (1997)
5	$\sim Nd_5Co_3Ge_{12}$	unknown				Salamakha (1997)
6	$\sim Nd_3Co_2Ge_7$	unknown				Salamakha (1997)
7	$NdCo_{0.55}Ge_2$	$CeNiSi_2$	0.4212	1.6509	0.4087	Pecharsky et al. (1989)
			0.4210	1.670	0.4152	Méot-Meyer et al. (1985a)
8	NdCoGe	PbFCl	0.4149		0.6786	Salamakha (1997)
			0.4140		0.6785	Welter et al. (1993a)
9	$NdCo_{0.5}Ge_{1.5}$	AlB_2	0.4144		0.4151	Salamakha (1986)
10	Nd_2CoGe_2	Sc_2CoSi_2	1.0882	0.4301	1.0438	Bodak et al. (1986)
				$\beta = 118.60°$		
11	$Nd_{117}Co_{52}Ge_{112}$	$Tb_{117}Fe_{52}Ge_{112}$	2.9162			Salamakha (1997)
12	$Nd_6Co_5Ge_{2.2}$	own	0.9272		0.4188	Salamakha et al. (1986)
13	Nd_3CoGe_2	La_3NiGe_2	1.207	0.403	1.157	Salamakha (1997)
14	$\sim Nd_{11}Co_4Ge_5$	unknown				Salamakha (1997)
15	$\sim Nd_5CoGe_2$	unknown				Salamakha (1997)
16	$\sim Nd_5Co_2Ge$	unknown				Salamakha (1997)

Venturini et al. (1986b), from X-ray powder diffraction analysis of a sample synthesized by powder metallurgical reaction at 1173 K, characterized the compound $Nd_2Co_3Ge_5$ to be isostructural with the $Lu_2Co_3Si_5$-type ($a=1.115$, $b=1.193$, $c=0.5812$, $\gamma=118.45°$). These data suggest that $Nd_2Co_3Ge_5$ has two polymorphic phases (compound 2, table 19).

4.6.6. *Nd–Ni–Ge*

Figure 61 shows the isothermal section of the Nd–Ni–Ge system at 870 K as derived from X-ray phase analysis of 180 arc melted samples which were annealed and subsequently quenched in water (Salamakha et al. 1996c). Starting materials were Nd 99.85 mass%, Ni 99.99 mass%, Ge 99.99 mass%. The phase-field distribution is characterized by the presence of nine ternary compounds. The binary compounds Nd_2Ni_{17} and $NdNi_5$ dissolve approximately 15 at.% Ge.

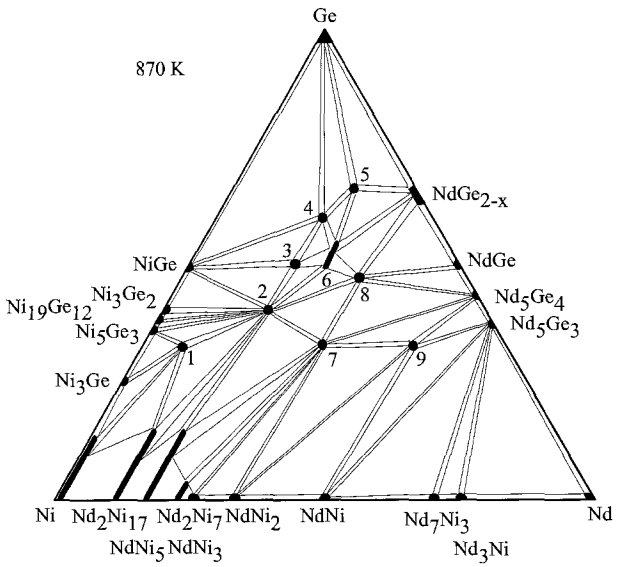

Fig. 61. Nd–Ni–Ge, isothermal section at 870 K.

Crystallographic data for the ternary phases of the Nd–Ni–Ge system are listed in table 20.

Additionally two ternary compounds of an unknown structure type, ~Nd_5NiGe_2 and ~Nd_5Ni_2Ge, have been observed by Salamakha et al. (1996c) in "as-cast" samples (X-ray powder analysis).

4.6.7. *Nd–Cu–Ge*

Information about the phase equilibria in the Nd–Cu–Ge system (fig. 62) is due to the work of Salamakha (1988) who employed X-ray phase analysis of argon arc melted ternary alloys; the samples were annealed in vacuum-sealed quartz ampoules at 870 K for

Table 20
Crystallographic data for the ternary Nd–Ni–Ge compounds

No.	Compound	Structure	Lattice parameters (nm)			Reference
			a	*b*	*c*	
1	$NdNi_{8.5}Ge_{4.5}$	$CeNi_{8.5}Si_{4.5}$	0.7942		1.1732	Salamakha et al. (1996c)
2	$NdNi_2Ge_2$	$CeGa_2Al_2$	0.4115		0.9842	Rieger and Parthé (1969a,b)
3	$Nd_2Ni_3Ge_5$	unknown				Salamakha et al. (1996c)
4	$NdNiGe_3$	$SmNiGe_3$	2.1733	0.4123	0.4124	Bodak et al. (1985)
5	Nd_2NiGe_6	Ce_2CuGe_6	0.4031	0.4110	2.1718	Salamakha et al. (1996c)
6	$NdNi_{1-0.8}Ge_{2-2.2}$	$CeNiSi_2$	0.4199–0.4202	1.6765–1.6742	0.4174–0.4154	Pecharsky et al. (1989)
7	NdNiGe	TiNiSi	0.7232	0.4253	0.7307	Salamakha et al. (1996c)
8	$NdNi_{0.6}Ge_{1.4}$	AlB_2	0.4157		0.4145	Salamakha (1986)
9	Nd_3NiGe_2	La_3NiGe_2	1.1764	0.4279	1.1159	Bodak et al. (1982)

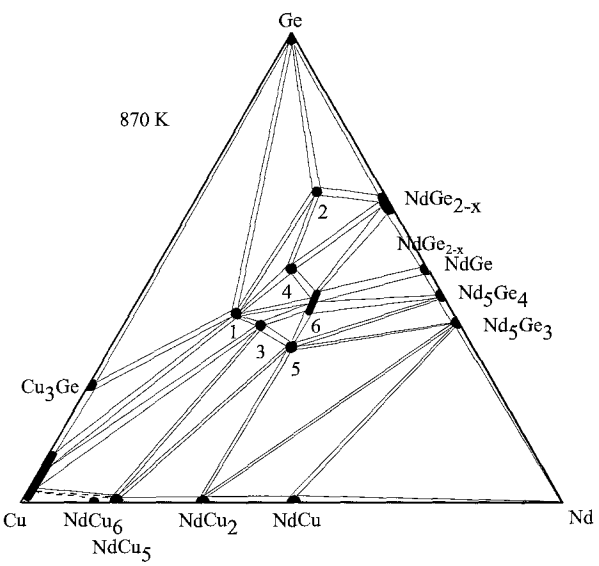

Fig. 62. Nd–Cu–Ge, isothermal section at 870 K.

300 hours. The formation of six ternary phases has been reported. Mutual solid solubilities of the binaries were reported to be negligible.

The crystallographic characteristics of the ternary compounds of the Nd–Cu–Ge system at 870 K are listed in table 21.

One more compound has been observed and investigated by Salamakha et al. (1996d) from an as-cast sample: $Nd_6Cu_8Ge_8$ ($Gd_6Cu_8Ge_8$ type, $a=0.4302$, $b=0.6711$, $c=1.4249$; X-ray single-crystal method).

Table 21
Crystallographic data for the ternary Nd–Cu–Ge compounds

No.	Compound	Structure	Lattice parameters (nm)			Reference
			a	*b*	*c*	
1	$NdCu_2Ge_2$	$CeGa_2Al_2$	0.4129		1.0216	Rieger and Parthé (1969a,b)
2	Nd_2CuGe_6	Ce_2CuGe_6	0.4059	0.4172	2.1359	Konyk et al. (1988)
3	$Nd_2Cu_3Ge_3$	$Ce_2Cu_3Ge_3$				Salamakha (1988)
4	$NdCuGe_2$	$CeNiSi_2$	0.4215	1.714	0.4077	Salamakha (1988)
5	NdCuGe	AlB_2	0.4272		0.3881	Salamakha (1986)
6	$NdCu_{0.71-0.56}Ge_{1.29-1.44}$	AlB_2	0.4172–0.4151		0.4160–0.4188	Salamakha (1986, 1988)

4.6.8. *Nd–Zn–Ge*

No isothermal section is available for the ternary Nd–Zn–Ge system, however one ternary compound was observed and characterized by Rossi and Ferro (1996). $NdZn_{1.5}Ge_{0.5}$ was found to crystallize with the AlB_2 type, $a = 0.4432$, $c = 0.3820$, from X-ray powder diffraction of an induction-melted alloy which was annealed at 1070 K for one week. Electronic micrographic examination as well as microprobe microanalysis was carried out. The metals employed in sample synthesis had a nominal purity of 99.9 mass% for neodymium, and 99.999 mass% for the other metals.

4.6.9. *Nd–Zr–Ge*

Salamakha and Starodub (1991) were the first to investigate the phase relations within the isothermal section at 870 K over the whole concentration region by X-ray powder analysis (fig. 63). No ternary compounds were observed. For sample preparation, see Nd–V–Ge.

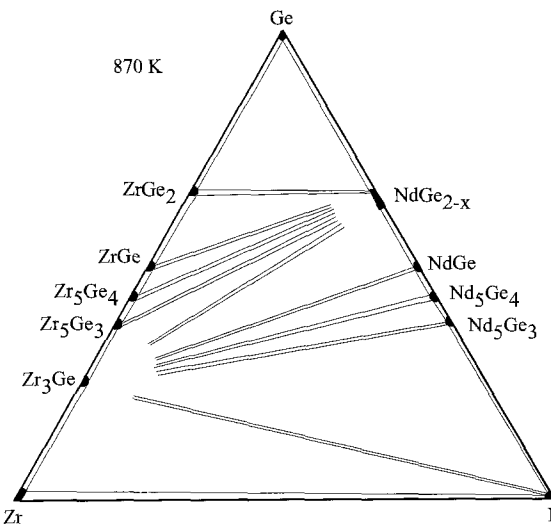

Fig. 63. Nd–Zr–Ge, isothermal section at 870 K.

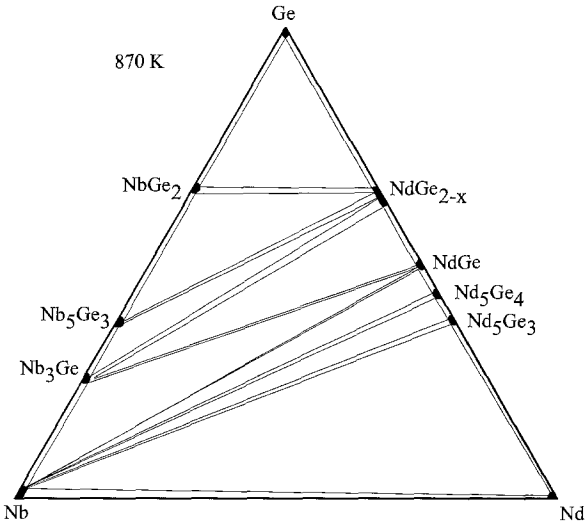

Fig. 64. Nd–Nb–Ge, isothermal section at 870 K.

4.6.10. *Nd–Nb–Ge*

The phase relations in the ternary system Nd–Nb–Ge at 870 K are presented in fig. 64 after Salamakha (1997). As determined from X-ray powder diffraction analysis of samples annealed at 870 K, phase equilibria revealed the absence of ternary compounds. For sample preparation, see Nd–V–Ge.

4.6.11. *Nd–Mo–Ge*

Salamakha (1997) reported the Nd–Mo–Ge phase diagram shown in fig. 65. No ternary compounds or solid solutions have been observed at 870 K. For sample preparation, see Nd–V–Ge.

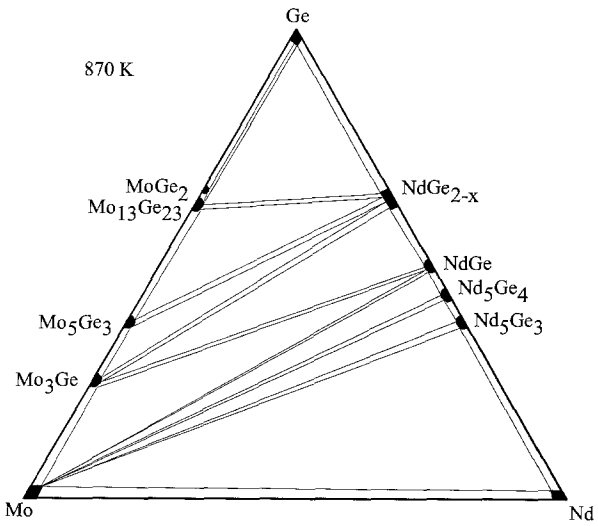

Fig. 65. Nd–Mo–Ge, isothermal section at 870 K.

4.6.12. *Nd–Ru–Ge*

Phase equilibria in the Nd–Ru–Ge system have been derived by Salamakha et al. (1996e) by means of powder X-ray analysis of samples prepared by direct arc melting of high-purity components (Nd 99.85 mass%, Ru 99.9 mass%, Ge 99.99 mass%), annealed at 870 K for two weeks in evacuated quartz ampoules and quenched in cold water. The isothermal section is shown in fig. 66. The phase relations are characterized by the existence of seven ternary neodymium–ruthenium germanides. Mutual solid solubilities of the binary compounds were observed to be negligible.

Crystallographic data of ternary Nd–Ru–Ge compounds are listed in table 22.

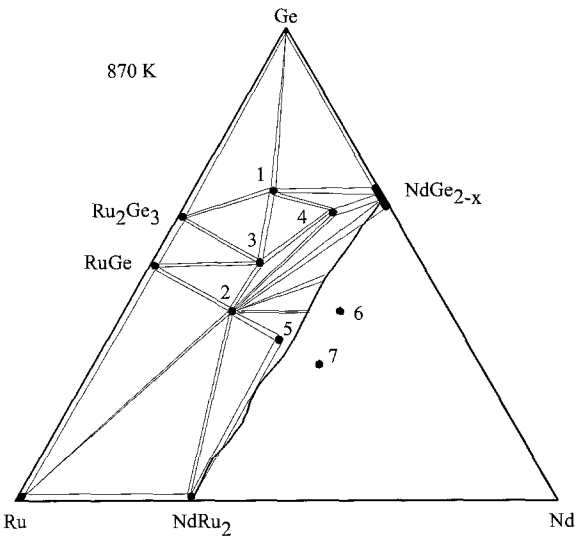

Fig. 66. Nd–Ru–Ge, partial isothermal section at 870 K (0–33 at.% Nd).

Table 22
Crystallographic data for the ternary Nd-Ru-Ge compounds

No.	Compound	Structure	Lattice parameters (nm)			Reference
			a	*b*	*c*	
1	$Nd_3Ru_4Ge_{13}$	$Y_3Co_4Ge_{13}$	0.9055			Salamakha et al. (1989a)
		$Yb_3Rh_4Sn_{13}$	0.9055			Segre et al. (1981b)
2	$NdRu_2Ge_2$	$CeGa_2Al_2$	0.4250		0.9953	Salamakha et al. (1996e)
			0.4257		0.9986	Salamakha et al. (1989a)
3	$Nd_2Ru_3Ge_5$	$U_2Co_3Si_5$	0.9897	1.243	0.5819	Salamakha et al. (1996e)
4	~Nd_3RuGe_6	orthorhombic				Salamakha et al. (1996e)
5	NdRuGe	PbFCl	0.4267		0.6791	Salamakha et al. (1996e)
6	~Nd_2RuGe_2	monoclinic				Salamakha et al. (1996e)
7	$Nd_3Ru_2Ge_2$	$La_3Ni_2Ga_2$	0.5658	0.7863	1.3581	Bodak et al. (1989a)

Table 23
Crystallographic characteristics of the ternary Nd–Rh(Pd)–Ge compounds

Compound	Structure	Lattice parameters (nm)			Reference
		a	*b*	*c*	
$NdRh_2Ge_2$	$CeGa_2Al_2$	0.4143		1.0408	Francois et al. (1985)
$Nd_2Rh_3Ge_5$	$U_2Co_3Si_5$	1.0041	1.2083	0.5931	Venturini et al. (1986b)
$Nd_3Rh_4Ge_{13}$	$Yb_3Rh_4Sn_{13}$	0.9018			Venturini et al. (1985b)
NdRhGe	TiNiSi	0.7229	0.4443	0.7322	Hovestreydt et al. (1982)
$NdRh_{0.5}Ge_{1.5}$	AlB_2	0.4237		0.4087	Salamakha et al. (1989a)
$Nd_4Rh_4Ge_3$	own	2.1021	0.7941	0.5652	Salamakha (1989)
			$\gamma = 110.08°$		
$Nd_3Rh_2Ge_2$	$La_3Ni_2Ga_2$	0.5654	0.8017	1.3411	Gladyshevsky et al. (1991a)
$NdRh_xGe_2$	$CeNiSi_2$	0.4282	1.693	0.4261	Francois et al. (1990)
Nd_2RhGe_2	Sc_2CoSi_2				Salamakha (1989)
$Nd_4Rh_{13}Ge_9$	$Ho_4Ir_{13}Ge_9$				Verniere et al. (1995)
$NdPd_2Ge_2$	$CeGa_2Al_2$	0.4300		0.9865	Rossi et al. (1979)
Nd_2PdGe_6	Ce_2CuGe_6	0.4139	0.4060	2.187	Sologub et al. (1995a)
NdPdGe	KHg_2	0.4452	0.7205	0.7639	Hovestreydt et al. (1982)
$NdPd_2Ge$	YPd_2Si	0.7598	0.6992	0.5749	Jorda et al. (1983)
$NdPd_xGe_2$	$CeNiSi_2$	0.4261	1.724	0.4218	Francois et al. (1990)
$NdPd_{0.6}Ge_{1.4}$	AlB_2	0.4238		0.4170	Salamakha et al. (1989a)

4.6.13. *Nd–Rh(Pd)–Ge*

No ternary phase diagrams have been established for the Nd–Rh–Ge system and the Nd–Pd–Ge system, but the crystal structures of ternary compounds have been characterized by several groups of authors. Crystallographic data for the ternary neodymium–rhodium germanides and neodymium–palladium germanides are compiled in table 23.

4.6.14. *Nd–Ag–Ge*

Phase equilibria have been established in the ternary Nd–Ag–Ge system over the whole concentration region for the isothermal sections at 870 K and 1070 K by Salamakha et al. (1996f) and Zaplatynsky et al. (1996) (figs. 67a,b). The existence of four and five ternary compounds respectively have been observed. Samples were melted from pieces of high purity components (Nd 99.85 mass%, Ag 99.99 mass%, Ge 99.99 mass%) under argon atmosphere in an arc furnace with water-cooled copper hearth. The ingots were subsequently annealed at 870 K (1070 K) and quenched in cold water. The isothermal sections were constructed using X-ray powder diffraction film data obtained by the Debye–Scherrer technique with non-filtered CrK radiation.

Crystallographic characteristics of the ternary phases which exist within the Nd–Ag–Ge system at 870 K and 1070 K are listed in table 24.

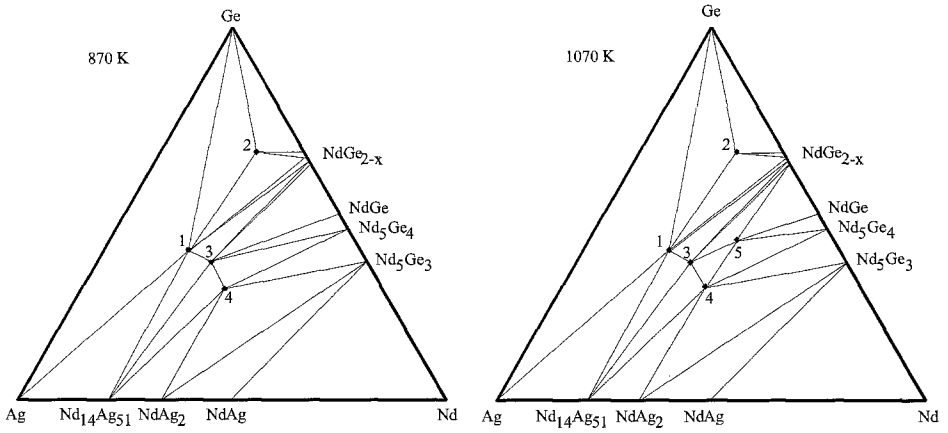

Fig. 67. Nd–Ag–Ge, isothermal sections at 870 K (a) and 1070 K (b).

Table 24
Crystallographic data for the ternary Nd–Ag–Ge compounds

No.	Compound	Structure	Lattice parameters (nm)			Reference
			a	*b*	*c*	
1	$NdAg_2Ge_2$	$CeGa_2Al_2$	0.4244		1.0978	Salamakha et al. (1996f)
2	Nd_2AgGe_6	Ce_2CuGe_6	0.4271	0.4117	2.1517	Salamakha et al. (1996f)
3	$Nd_6Ag_8Ge_8$	$Gd_6Cu_8Ge_8$	1.4636	0.7082	0.4407	Salamakha et al. (1996d)
4	$NdAg_{1.1}Ge_{0.9}$	Fe_2P	0.7339		0.4329	Salamakha et al. (1996f)
5	$NdAg_{0.7}Ge_{1.3}$	AlB_2	0.4335		0.4072	Zaplatynsky et al. (1996)

4.6.15. *Nd–Hf–Ge*

Salamakha and Starodub (1991) reported the phase diagram shown in fig. 68. No ternary compounds or solid solutions have been observed at 870 K. For sample preparation, see Nd–V–Ge.

4.6.16. *Nd–Ta–Ge*

The results of X-ray investigations of the isothermal section of the Nd–Ta–Ge systems at 870 K are shown in fig. 69 after Salamakha (1997). No ternary compounds were observed. For sample preparation, see Nd–V–Ge.

4.6.17. *Nd–W–Ge*

Salamakha (1997) derived the Nd–W–Ge phase diagram shown in fig. 70. No solid solibility or ternary compounds have been found at 870 K. For sample preparation, see Nd–V–Ge.

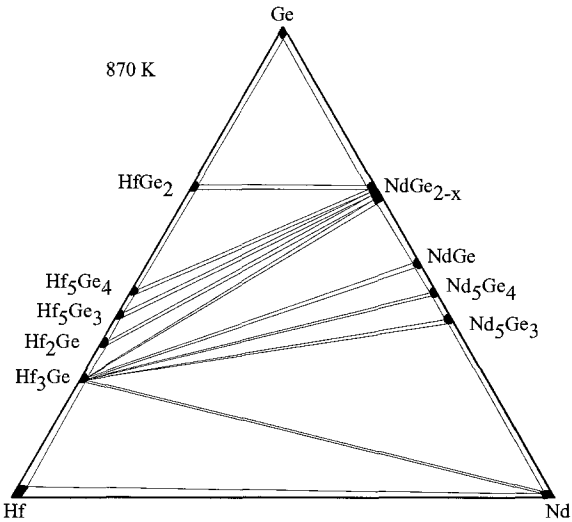

Fig. 68. Nd–Hf–Ge, isothermal section at 870 K.

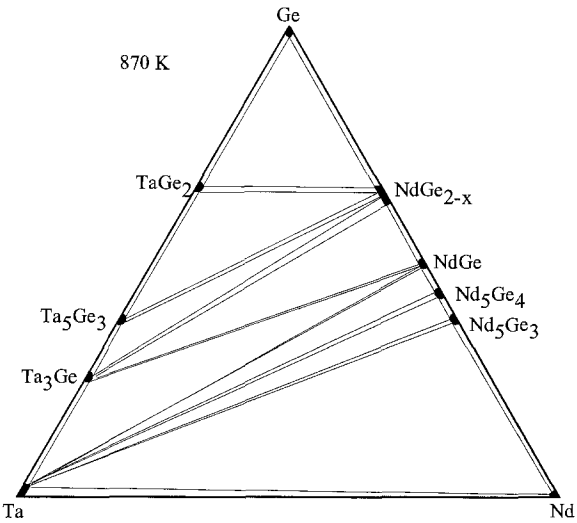

Fig. 69. Nd–Ta–Ge, isothermal section at 870 K.

4.6.18. *Nd–Re–Ge*

No ternary compounds were found in the ternary Nd–Re–Ge system at 870 K (fig. 71) (Salamakha 1997). For sample preparation, see Nd–V–Ge.

4.6.19. *Nd–Os–Ge*

The partial isothermal section of the Nd–Os–Ge system at 870 K is shown in fig. 72, after Salamakha et al. (1996e). Samples were prepared in the same manner as for the

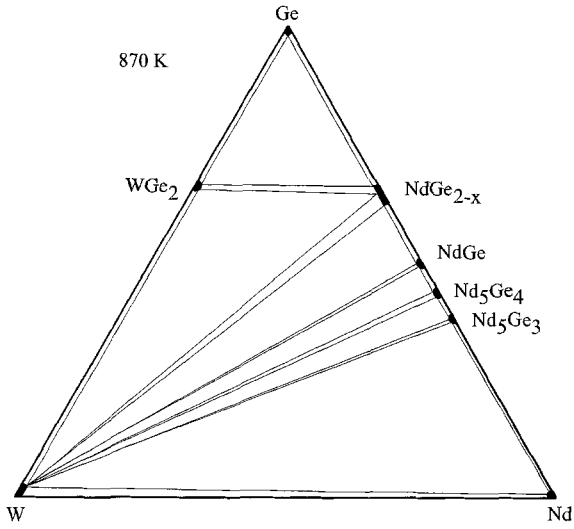

Fig. 70. Nd–W–Ge, isothermal section at 870 K.

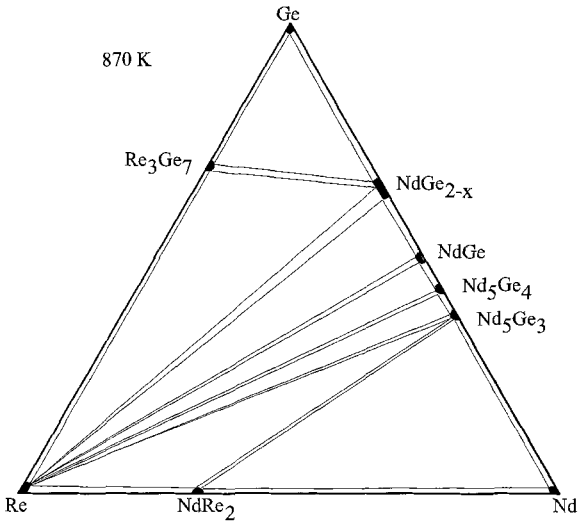

Fig. 71. Nd–Re–Ge, isothermal section at 870 K.

investigation of the Nd–Ru–Ge system. Two ternary compounds were found to exist within the concentration region under investigation.

The $Nd_3Os_4Ge_{13}$ (1) compound has been found to crystallize with $Y_3Co_4Ge_{13}$ type at 870 K, $a = 0.9080$ nm (Salamakha et al. 1989a) whereas at 1170 K the $Yb_3Rh_4Sn_{13}$ type has been realized (Segre et al. 1981b).

The crystal structure of the ~Nd_3OsGe_6 (2) compound has not been determined.

The $Nd_2Os_3Ge_5$ compound was established to crystallize with the $U_2Co_3Si_5$-type structure from X-ray powder diffraction of an as-cast specimen (Salamakha et al. 1996e).

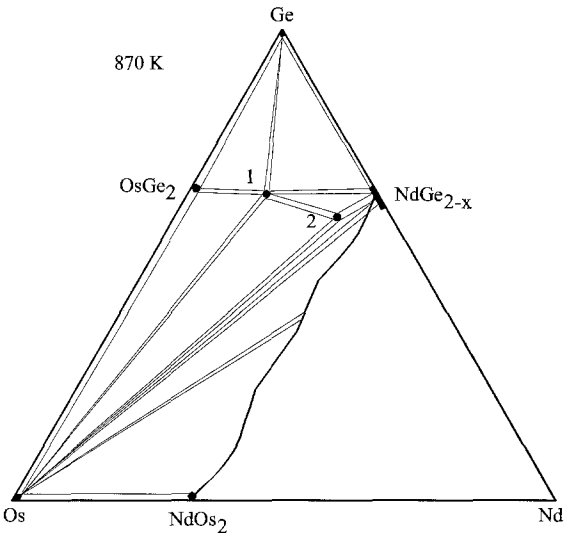

Fig. 72. Nd–Os–Ge, partial isothermal section at 870 K (0–33 at.% Nd).

4.6.20. *Nd–Ir(Pt)–Ge*

No ternary phase diagrams have been established for the Nd–Ir(Pt)–Ge systems, but the crystal structures of ternary compounds have been characterized by various authors (see table 25).

Table 25
Crystallographic data for the ternary Nd–Ir(Pt)–Ge compounds

Compound	Structure	Lattice parameters (nm)			Reference
		a	*b*	*c*	
$NdIr_2Ge_2$	$CaBe_2Ge_2$	0.4222		1.0032	Francois et al. (1985)
$Nd_2Ir_3Ge_5$	$U_2Co_3Si_5$	1.0172	1.1881	0.6030	Venturini et al. (1986b)
$Nd_3Ir_4Ge_{13}$	$Yb_3Rh_4Sn_{13}$	0.9042			Venturini et al. (1985b)
NdIrGe	TiNiSi	0.7302	0.4448	0.7335	Hovestreydt et al. (1982)
$NdIr_{0.5}Ge_{1.5}$	AlB_2	0.4229		0.4125	Salamakha et al. (1989a)
Nd_2IrGe_2	Sc_2CoSi_2	1.0840	0.4352	1.0545	Salamakha et al. (1989a)
			$\beta = 117.23°$		
$NdIrGe_2$	$YIrGe_2$	0.4358	0.8809	1.6153	Salamakha et al. (1989b)
$Nd_4Ir_{13}Ge_9$	$Ho_4Ir_{13}Ge_9$				Verniere et al. (1995)
$NdPt_2Ge_2$	$CeGa_2Al_2$	0.4380		0.9865	Rossi et al. (1979)
	$LaPt_2Ge_2$	0.4363	0.4389	0.9779	Venturini et al. (1989a)
			$\beta = 90.88°$		
Nd_2PtGe_6	Ce_2CuGe_6	0.4120	0.4063	2.2007	Sologub et al. (1995a)
$NdPtGe_2$	$YIrGe_2$	0.4398	0.8770	1.6418	Salamakha et al. (1989b)
NdPtGe	KHg_2	0.4428	0.7245	0.7599	Hovestreydt et al. (1982)
$NdPt_{0.6}Ge_{1.4}$	AlB_2	0.4227		0.4181	Salamakha et al. (1989a)

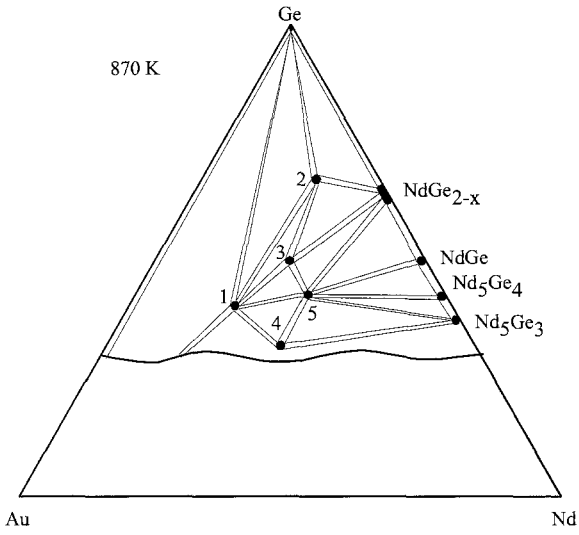

Fig. 73. Nd–Au–Ge, partial isothermal section at 870 K (33–100 at.% Ge)..

Table 26
Crystallographic data for the ternary Nd–Au–Ge compounds

No.	Compound	Structure	Lattice parameters (nm)			Reference
			a	*b*	*c*	
1	$NdAu_2Ge_2$	$CeGa_2Al_2$	0.4411		1.0559	Salamakha (1997)
2	Nd_2AuGe_6	Ce_2CuGe_6	0.42265	0.41272	2.1689	Sologub et al. (1995a)
3	$NdAuGe_2$	unknown				Salamakha (1997)
4	NdAuGe	LiGaGe	0.4439		0.7718	Salamakha (1997)
			0.4447		0.7702	Rossi et al. (1992)
5	$NdAu_{0.7}Ge_{1.3}$	AlB_2	0.4369		0.4278	Salamakha (1997)

4.6.21. *Nd–Au–Ge*

A partial isothermal section of the Nd–Au–Ge system at 870 K is shown in fig. 73, after Salamakha (1997). The phase relations are characterized by the formation of five ternary neodymium germanides of gold. Their crystallographic data are listed in table 26. For the details of sample preparation, see Nd–Ag–Ge.

4.7. *Sm–d element–Ge systems*

4.7.1. *Sm–Mn–Ge*

No phase diagram is available for the system Sm–Mn–Ge, however, a series of ternary compounds have been observed and characterized.

The $SmMn_2Ge_2$ compound has been prepared and studied by Rossi et al. (1978b). It was found to be of $CeGa_2Al_2$ type with lattice parameters $a = 0.4062$, $c = 1.0896$. For sample preparation, see $LaMn_2Ge_2$ under La–Mn–Ge.

SmMnGe with PbFCl-type was observed by Welter et al. (1995), $a = 0.4134$, $c = 0.7375$. The compound was prepared from commercially available high-purity elements. A compacted pellet of stoichiometric mixture was sealed under argon (100 mmHg) in a silica tube, heated at 1273 K as a preliminary homogenization treatment and then melted in an induction furnace. The resulting ingot was annealed for 2 weeks at 1173 K.

$SmMn_6Ge_6$ was found to crystallize in the YCo_6Ge_6-type structure by Venturini et al. (1992), $a = 0.5245$, $c = 0.8187$ (X-ray powder diffraction data). The alloy was synthesized by powder metallurgical reaction in an evacuated silica tube at 1073 K for 14 days.

Francois et al. (1990) investigated the occurrence of $CeNiSi_2$ type for samarium–manganese–germanium combinations for alloys annealed at 1173 K ($SmMn_{0.40}Ge_2$; $a = 0.4194$, $b = 1.633$, $c = 0.4062$).

4.7.2. *Sm–Fe–Ge*

Phase equilibria in the isothermal sections at 870 K (0–40 at.% Sm) and 670 K (40–100 at.% Sm) have been determined by Mruz (1988) using X-ray powder diffraction and partly microstructural analyses of 202 ternary alloys synthesized by arc melting ingots of Sm (99.77 mass%), Fe (99.90 mass%) and Ge (99.99 mass%); the alloys were then annealed in evacuated quartz tubes for 500–900 hours. The total number of compounds observed was nine. The Sm_5Ge_3 binary compound was found to dissolve up to 8 at.% Fe. Solubility of the third component in the binary compounds was reported to be negligible. Phase equilibria in the isothermal sections at 870 K and 670 K are presented in fig. 74.

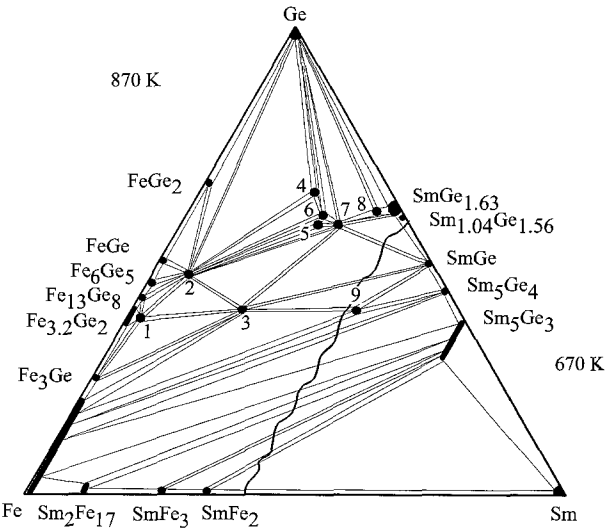

Fig. 74. Sm–Fe–Ge, isothermal sections at 870 K (0–40 at.% Sm) and 670 K (40–100 at.% Sm).

The $SmFe_6Ge_6$ (2) compound was observed and studied by Mruz et al. (1984). It was found to crystallize with YCo_6Ge_6 type with lattice parameters $a = 0.5135$, $c = 0.4091$ by X-ray powder diffraction of an arc melted alloy annealed at 870 K.

The formation and crystal structure of $SmFe_2Ge_2$ (3) was reported in an early investigation of samarium–iron–germanium combinations by Mruz et al. (1983): $CeGa_2Al_2$ type, $a = 0.4005$, $c = 1.0476$ (arc melted sample annealed at 870 K; X-ray powder diffraction data) later confirmed by Bara et al. (1990), $a = 0.4010$, $c = 1.0491$.

Pecharsky et al. (1989) investigated the formation and crystal structure of the $SmFe_{1-x}Ge_2$ (7) compound by X-ray single-crystal analysis of an arc melted sample annealed at 870 K. The $CeNiSi_2$-type structure was established with lattice parameters $a = 0.4188$–0.4198, $b = 1.6208$–1.6232, $c = 0.4058$–4079. Francois et al. (1990) confirmed the crystal structure of $SmFe_{0.52}Ge_2$ ($CeNiSi_2$ type, $a = 0.4195$, $b = 1.619$, $c = 0.4076$). The sample was prepared by powder metallurgical reaction and annealed in an evacuated silica tube at 1173 K.

The crystal structures of three compounds within the Sm–Fe–Ge system at 870 K were determined by Mruz (1988): $Sm_4Fe_{0.64}Ge_7$ (8) with Sm_4CoGe_7-type structure, $a = 0.4161$, $b = 0.4067$, $c = 3.021$; $Sm_{117}Fe_{52}Ge_{112}$ (9) with $Tb_{117}Fe_{52}Ge_{112}$-type structure, $a = 2.8989$; and ~$Sm_5Fe_3Ge_{12}$ (6) was found to adopt a new structure type $a = 0.4079$, $b = 2.5715$, $c = 0.4275$.

The crystal structures of three more germanides, ~$SmFe_{30}Ge_{19}$ (1), ~$Sm_3Fe_2Ge_9$ (4) and ~$Sm_3Fe_2Ge_7$ (5), have not been resolved.

The $SmFe_{0.67}Ge_{1.33}$ compound was found to adopt the AlB_2 type ($a = 0.4141$, $c = 0.4092$; X-ray powder diffraction) (Felner et al. 1972). This compound was not observed at 870 K by Mruz (1988) in the course of studying the phase equilibria in this system.

4.7.3. *Sm–Co–Ge*

Phase equilibria in the isothermal sections at 870 K (0–40 at.% Sm) and 670 K (40–100 at.% Sm) have been determined by Mruz (1988) using X-ray powder diffraction and microstructural analyses of 342 ternary alloys synthesized by arc melting ingots of Sm (99.77 mass%), Co (99.90 mass%) and Ge (99.99 mass%). The alloys were annealed in evacuated quartz tubes for 500–900 hours. The phase relations are characterized by the formation of eighteen ternary compounds and by the existence of rather extended solid solutions originating at Sm_5Ge_3 (up to 17.5 at.% Co), $SmCo_5$ (up to 15 at.% Ge) and $SmCo_3$ (up to 10 at.% Ge). Phase equilibria in the isothermal sections at 870 K and 670 K are presented in fig. 75.

Méot-Meyer et al. (1985a) reported the crystal structure of $SmCo_{0.71}Ge_2$ (8) ($CeNiSi_2$ type, $a = 0.4169$, $b = 1.649$, $c = 0.4097$). The sample was prepared by powder metallurgical reaction and annealed in evacuated silica tube at 1173 K. Pecharsky et al. (1989) investigated the formation and crystal structure of the $SmCo_{0.72-0.56}Ge_2$ compound by X-ray powder analysis of arc melted alloys annealed at 870 K alloys. The $CeNiSi_2$-type structure was confirmed ($a = 0.4174$–0.4169, $b = 1.6542$–1.6395, $c = 0.4122$–0.4069).

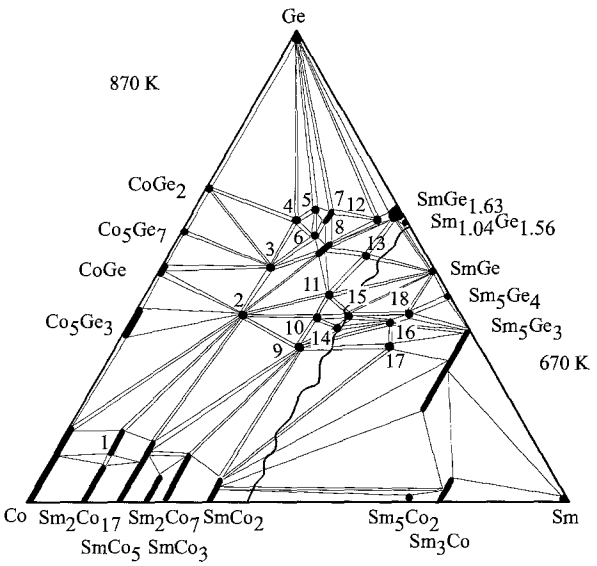

Fig. 75. Sm–Co–Ge, isothermal sections at 870 K (0–40 at.% Sm) and 670 K (40–100 at.% Sm).

The formation and crystal structure of $SmCo_2Ge_2$ (2) was reported in an early investigation of samarium–cobalt–germanium combinations by Mruz et al. (1983): $CeGa_2Al_2$ type, $a = 0.4016$, $c = 1.0133$ (arc melted sample annealed at 870 K; X-ray single-crystal diffraction data).

$Sm_2Co_3Ge_5$ (3) was found to crystallize with the $Lu_2Co_3Si_5$-type ($a = 1.1244$, $b = 1.193$, $c = 0.5768$, $\gamma = 120.2°$) by Venturini et al. (1986b) from X-ray powder analysis.

Gorelenko et al. (1984) reported the crystal structure of SmCoGe (9) (TiNiSi type, $a = 0.7137$, $b = 0.4319$, $c = 0.7133$; X-ray powder analysis). The alloy was obtained by arc melting and annealing in an evacuated quartz tube at 870 K for 350 hours.

$Sm_3Co_2Ge_4$ (11) crystallizes with the $Tb_3Co_2Ge_4$ type structure, $a = 1.0846$, $b = 0.8138$, $c = 0.4185$, $\gamma = 107.70°$. The sample was prepared by arc melting and annealing at 873 K for 1450 hours. The starting materials were Sm >99.9 mass%, Co 99.99 mass%, Ge 99.999 mass% (Mruz et al. 1989).

Bodak et al. (1986) reported the crystal structure for Sm_2CoGe_2 (15) (Sc_2CoSi_2 type, $a = 1.0818$, $b = 1.0343$, $c = 0.4254$, $\gamma = 118.53°$; X-ray powder diffraction) from an arc melted sample annealed at 870 K.

Investigating the isothermal section of the Sm–Co–Ge system, Mruz et al. (1987a) observed the $Sm_4Co_{0.64}Ge_7$ (12) compound which belonged to a new structure type. The crystal structure was investigated by a single-crystal method, the lattice parameters were obtained as $a = 0.4166$, $b = 0.4083$, $c = 3.018$.

The crystal structure of three compounds within the Sm–Co–Ge system at 870 K was determined by Mruz (1988): $Sm_2Co_{15.1-14.1}Ge_{1.9-2.9}$ (1) belongs to the Th_2Zn_{17} type, $a = 0.8425$–0.8433, $c = 1.2336$–1.2368; $SmCoGe_3$ (4) crystallizes with the $BaNiSn_3$ type, $a =$

0.4277, $c = 0.9799$; and $Sm_5Co_{3-2.5}Ge_{12-12.5}$ (7) was observed to form a new structure type with lattice parameters $a = 0.4143$–0.4174, $b = 2.5534$–2.5597, $c = 0.4216$–0.4221.

The crystal structures of eight more germanides, ~$Sm_3Co_2Ge_8$ (5), ~$Sm_3Co_2Ge_7$ (6), ~$Sm_5Co_4Ge_6$ (10), ~$Sm_{2.9}Co_{0.9}Ge_{4.2}$ (13), ~$Sm_3Co_2Ge_3$ (14), ~$Sm_{14}Co_4Ge_{11}$ (16), ~Sm_3CoGe_2 (17), ~Sm_5CoGe_4 (18) have not been solved yet.

Mruz (1988) observed the existence of the $Sm_{117}Co_{52}Ge_{112}$ compound at 870 K ($Tb_{117}Fe_{52}Ge_{112}$ type, $a = 2.8928$) which was found to decompose at 670 K. This compound is not shown in fig. 75, since it contains ~42 at.% Sm and thus is outside of the composition range of the 870 K isothermal section (0–40 at.% Sm), and as it does not exist at 670 K it does not appear in this isothermal section.

Venturini et al. (1985b) reported an X-ray powder diffraction study of the $Sm_3Co_4Ge_{13}$ compound from a sample prepared by heating a mixture of the starting components in an evacuated quartz tube and homogenizing at 1073 K. Finally the sample was quenched in water. The crystal structure was found to adopt the $Yb_3Rh_4Sn_{13}$ type, $a = 0.8814$. The purity of the starting components was Sm 99.9 mass%, Co 99.99 mass% and Ge 99.99 mass%.

4.7.4. *Sm–Ni–Ge*

Phase equilibria in the isothermal sections at 870 K (0–40 at.% Sm) and 670 K (40–100 at.% Sm) have been established by Mruz (1988) using X-ray powder diffraction and microstructural analyses of 247 ternary alloys synthesized by arc melting ingots of Sm (99.77 mass%), Ni (99.99 mass%) and Ge (99.99 mass%); the alloys were then annealed in evacuated quartz tubes for 500–900 hours. The phase relations are characterized by the formation of twelve ternary compounds and by the existence of rather extended solid solutions originating at Sm_5Ge_3 (dissolves up to 12.5 at.% Ni), $SmNi_5$ (15 at.% Ge) and Sm_2Ni_{17} (15 at.% Ge). Phase equilibria in the isothermal sections at 870 K and 670 K are presented in fig. 76.

$SmNi_5Ge_3$ (3) was reported to crystallize with the YNi_5Si_3 type, $a = 1.9196$, $b = 0.38981$, $c = 0.67917$ by Mruz (1988). The arc melted alloy was annealed at 870 K and investigated by X-ray powder diffraction analysis.

The $SmNi_2Ge_2$ (5) compound was found to adopt the $CeGa_2Al_2$-type of structure, $a = 0.4091$, $c = 0.9814$ (Rieger and Parthé 1969b).

$SmNiGe_3$ (7) with its own structure type ($a = 2.1657$, $b = 0.4102$, $c = 0.4092$, X-ray single-crystal analysis) was reported by Bodak et al. (1985). For details of sample preparation and purity of starting materials, see above.

Sm_2NiGe_6 (8) has been found by Mruz (1988) from X-ray powder diffraction to be isostructural with the Ce_2CuGe_6 type ($a = 0.4062$, $b = 0.3995$, $c = 2.1496$). The sample was prepared by arc melting ingots of the constituting elements and annealing at 870 K for 700 hours. For the purity of starting materials, see above.

Pecharsky et al. (1989) investigated the formation and crystal structure of the $SmNi_{1-0.75}Ge_2$ (9) compound by X-ray powder analysis of arc melted alloys annealed at 870 K ($CeNiSi_2$ type, $a = 0.4147$–0.4168, $b = 1.6701$–1.6589, $c = 0.4147$–0.4105).

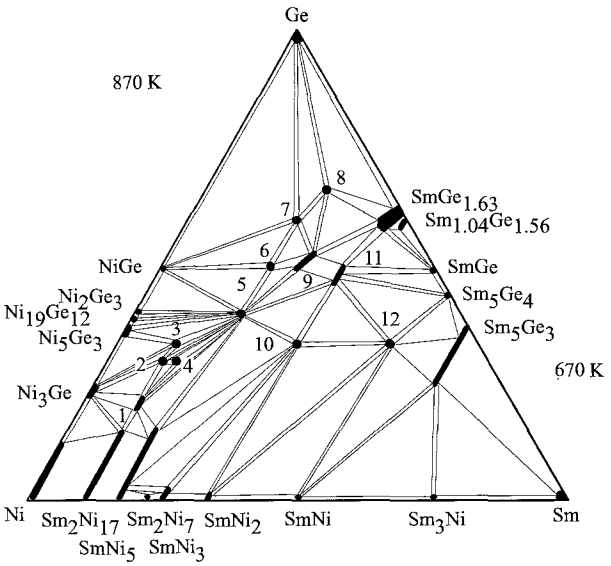

Fig. 76. Sm–Ni–Ge, isothermal sections at 870 K (0–40 at.% Sm) and 670 K (40–100 at.% Sm).

Mruz et al. (1987b) reported the crystal structure of SmNiGe (10) (TiNiSi type, $a=0.7100$, $b=0.4275$, $c=0.7301$; X-ray powder analysis). The alloy was obtained by arc melting and annealing in an evacuated quartz tube at 870 K for 500 hours.

An early investigation of the interaction of germanium with samarium and nickel has shown the existence of the $SmNi_{0.6-0.5}Ge_{1.4-1.5}$ (11) compound with AlB_2 type, $a=0.4125$–0.4114, $c=0.4101$–0.4127 (Gladyshevsky and Bodak 1965; X-ray powder diffraction).

The crystal structures of five germanides, ~$SmNi_7Ge_2$ (1), ~$SmNi_6Ge_2$ (2), ~$Sm_2Ni_9Ge_5$ (4), ~$Sm_2Ni_3Ge_5$ (6), ~Sm_3NiGe_2 (12) have not been evaluated (Mruz 1988).

One more ternary compound was reported by Bodak et al. (1982) who investigated the crystal structure of Sm_3NiGe_2 compound (La_3NiGe_2 type, $a=1.1605$, $b=0.4242$, $c=1.1470$) by the powder X-ray diffraction method. Apparently this compound does not exist at 870 K. For sample preparation and purity of starting elements, see Y_3NiGe_2 under Y–Ni–Ge.

The $SmNi_3Ge_3$ compound was investigated by the single-crystal method (own structure type, $a=0.4070$, $c=2.5137$). The single crystal was obtained from "as-cast" alloy (Mruz 1988). This compound was not observed at 870 K.

4.7.5. *Sm–Cu–Ge*

No phase diagram is available for the Sm–Cu–Ge system, but five ternary compounds have been found.

Rieger and Parthé (1969a) investigated the occurrence of the AlB_2-type structure by means of X-ray powder diffraction of arc melted alloys. The data presented were

$SmCu_{1-0.67}Ge_{1-1.33}$ with $a = 0.4255$–0.4152, $c = 0.3847$–0.4101. Iandelli (1993) confirmed the AlB_2 type ($a = 0.4259$ $c = 0.3810$, X-ray powder analysis) from the SmCuGe alloy which was prepared from filings or powders of the metals (samarium 99.7 mass%, copper and germanium 99.99 mass%) mixed and sealed in a tantalum crucible under argon, followed by melting in an induction furnace; afterwards the sample was annealed for 10 days at 1023 K.

Sologub et al. (1995a) reported on the crystal structure of Sm_2CuGe_6 alloy prepared by arc melting under argon and annealing at 870 K in an evacuated quartz tube for one week. From X-ray powder analysis, it was shown that this compound has the Ce_2CuGe_6-type structure with $a = 0.41496$, $b = 0.40275$, $c = 2.1221$.

Rieger and Parthé (1969b) prepared $SmCu_2Ge_2$ with the $CeGa_2Al_2$-type of structure, $a = 0.4088$, $c = 1.0223$.

Francois et al. (1990) reported the crystal structure of the $SmCu_{0.55}Ge_2$ ($CeNiSi_2$ type, $a = 0.4163$, $b = 1.690$, $c = 0.4028$). For sample preparation, see $LaFeGe_2$ under La–Fe–Ge.

$Sm_6Cu_8Ge_8$ crystallizes with the $Gd_6Cu_8Ge_8$-type and lattice parameters $a = 1.412$, $b = 0.668$, $c = 0.426$ (Hanel and Nowotny 1970).

4.7.6. *Sm–Zn–Ge*

No isothermal section is available for the ternary Sm–Zn–Ge system, however one ternary compound was observed and characterized by Rossi and Ferro (1996). $SmZn_{1.5}Ge_{0.5}$ was found to crystallize with the AlB_2 type, $a = 0.4412$, $c = 0.3737$ from X-ray powder diffraction of an induction melted alloy which was annealed at 1070 K for one week. An electronic micrographic examination, as well as microprobe microanalysis, was carried out. The metals employed in the synthesis of samples had a nominal purity of 99.9 mass% for samarium, and 99.999 mass% for other metals.

4.7.7. *Sm–Ru–Ge*

The phase equilibria in the Sm–Ru–Ge system have been investigated by Morozkin et al. (1996) by means of X-ray phase and local X-ray spectral analyses of ternary alloys, which were arc melted and subsequently annealed in evacuated silica tubes at 870 K for 1000 hours and finally quenched in water. Starting materials were Sm 99.98 mass%, Ru 99.99 mass%, Ge 99.99 mass%. According to the phase diagram, six ternary compounds exist within the Sm–Ru–Ge system at 870 K (fig. 77). The system contains an extended region of ternary solid solution based at $SmRu_2$.

Early investigations of the $SmRu_2Ge_2$ (1) compound showed that it had the $CeGa_2Al_2$-type structure: $a = 0.4236$, $c = 0.9944$, after Felner and Nowik (1985) from X-ray powder analysis of an induction melted alloy; and $a = 0.4238$, $c = 0.9953$ (Francois et al. 1985) from X-ray powder analysis of alloy obtained by powder metallurgical reaction at 1273 K. The starting components were Sm (3N), Ru (4N) and Ge (4N). The crystal structure type was confirmed by Morozkin et al. (1996): $a = 0.4237$, $c = 0.9918$ from arc melted alloy annealed at 870 K.

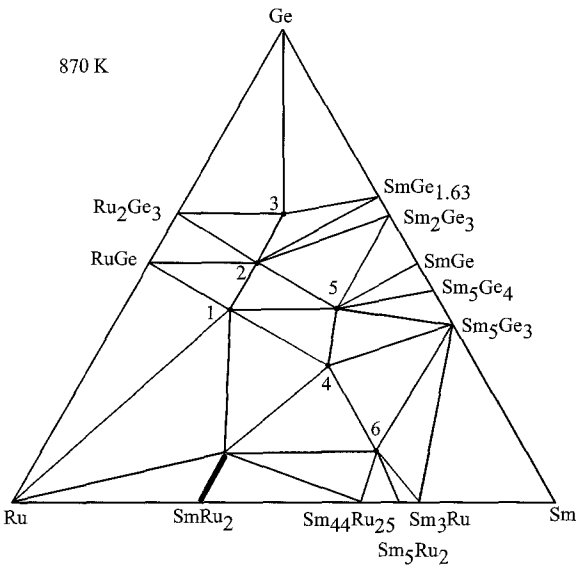

Fig. 77. Sm–Ru–Ge, isothermal section at 870 K.

Venturini et al. (1986b) and Morozkin et al. (1996) reported that the $Sm_2Ru_3Ge_5$ (2) compound crystallizes with the $U_2Co_3Si_5$-type structure. Lattice parameters were reported as $a=0.9867$, $b=1.244$, $c=0.5790$ (Venturini et al. 1986b; X-ray powder diffraction; for sample preparation, see $La_2Ru_3Ge_5$ under La–Ru–Ge) and $a=0.9880$, $b=1.2403$, $c=0.5778$ (Morozkin et al. 1996).

The $Pr_3Rh_4Sn_{13}$-type structure was reported for the $Sm_3Ru_4Ge_{13}$ compound ($a=0.9018$) by Segre et al. (1981a) from X-ray powder analysis of arc melted samples annealed at 1523 K for 1 day and at 1273 K for 7 days. The starting materials were Sm (3N), Ru (3N), Ge (6N). At variance with these data, Morozkin et al. (1996) observed the $SmRuGe_3$ (3) compound with the same structure type and lattice parameters $a=0.9012$ from X-ray powder analysis of arc melted alloy annealed at 870 K.

$Sm_3Ru_2Ge_2$ (4) was found to crystallize with the $La_3Ni_2Ga_2$-type structure ($a=0.5611$, $b=0.7818$, $c=1.3473$, X-ray powder diffraction) from arc melted samples annealed at 870 K (Bodak et al. 1989a). Morozkin et al. (1996) observed the same structure type and determined the lattice parameters $a=0.5595$, $b=0.7799$, $c=1.3527$.

The crystal structure of the Sm_2RuGe_2 (5) compound belongs to the Zr_2CoSi_2 type, $a=1.0713$, $b=1.114$, $c=0.413$, $\gamma=129.3°$ (Morozkin et al. 1996).

A compound of unknown structure, $Sm_{0.62}Ru_{0.28}Ge_{0.10}$ (6), was observed by Morozkin et al. (1996) from a sample annealed at 870 K.

The crystal structure of the SmRuGe compound was investigated by Welter et al. (1993b). It was found to adopt the PbFCl type, $a=0.4244$, $c=0.6711$ (X-ray powder diffraction). The compound was prepared from commercially available high-purity elements. A compacted stoichiometric mixture under argon in a sealed silica tube was

heated to 1173 K for preliminary homogenization and then melted in an induction furnace. This compound apparently does not exist at 870 K.

4.7.8. *Sm–Rh–Ge*

The phase equilibria in the Sm–Rh–Ge system have been investigated by Morozkin et al. (1996) by means of X-ray phase and local X-ray spectral analyses of ternary alloys, which were arc melted and subsequently annealed in evacuated silica tubes at 870 K for 1000 hours and finally quenched in water. The starting materials were Sm 99.98 mass%, Rh 99.99 mass%, Ge 99.99 mass% pure. Fourteen ternary compounds were found to exist within the Sm–Rh–Ge system at 870 K (fig. 78). The system contains an extended region of ternary solid solution based at $SmRh_2$.

Venturini et al. (1985b) reported an X-ray powder diffraction study of the $Sm_3Rh_4Ge_{13}$ compound from a sample which was prepared by heating a mixture of starting components in an evacuated quartz tube and homogenized at 1073 K. Finally the sample was quenched in water. The crystal structure was found to adopt the $Yb_3Rh_4Sn_{13}$ type, $a = 0.8985$. The purity of the starting components was Sm 99.9 mass%, Rh 99.99 mass% and Ge 99.99 mass%. Morozkin et al. (1996) observed the homogeneity field for this compound which includes the $SmRhGe_3$ composition: $Sm_{3+x}Rh_4Ge_{13-x}$ ($x = 0$–1) (4), $a =$ 0.8969–0.8976 from X-ray powder analysis of arc melted alloy annealed at 870 K.

Early investigations of the $SmRh_2Ge_2$ (2) compound determined the $CeGa_2Al_2$ type: $a = 0.4126$, $c = 1.037$ (Francois et al. 1985). For sample preparation, see $CeRu_2Ge_2$ under Ce–Ru–Ge. The structure type for this compound was confirmed later by Morozkin et al. (1996), $a = 0.4101$, c 1.0310 from arc melted alloy annealed at 870 K.

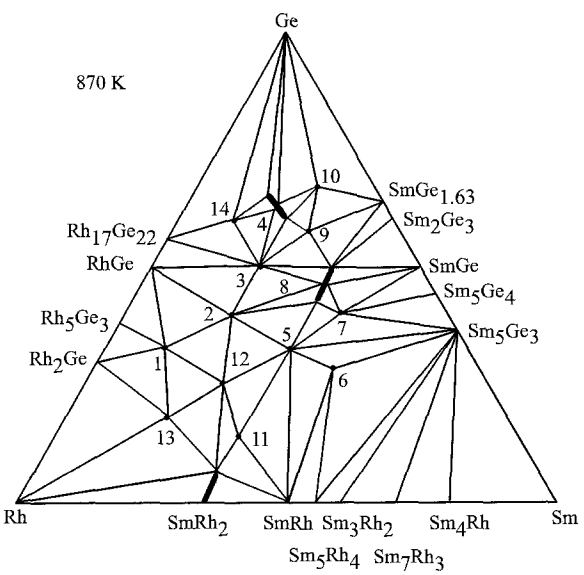

Fig. 78. Sm–Rh–Ge, isothermal section at 870 K.

$Sm_2Rh_3Ge_5$ (3) was found to crystallize with the $Lu_2Co_3Si_5$ type ($a=1.0005$, $b=1.2084$, $c=0.5894$, $\beta=120.2°$) by Venturini et al. (1986b) from X-ray powder analysis.

Hovestreydt et al. (1982) reported the crystal structure of the SmRhGe (5) compound (TiNiSi type, $a=0.7074$, $b=0.4371$, $c=0.7468$; X-ray powder data) from an arc melted sample annealed at 1270 K for 1–2 weeks. The starting components were Sm (3N), Rh (4N) and Ge (5N). Morozkin et al. (1996) observed the TiNiSi type for the sample annealed at 870 K ($a=0.7060$, $b=0.4360$, $c=0.7448$).

Gladyshevsky et al. (1991a) reported on the crystal structure for the $Sm_3Rh_2Ge_2$ (6) compound ($La_3Ni_2Ge_2$ type, $a=0.5608$, $b=0.7933$, $c=1.3332$; X-ray powder diffraction). For the details of sample preparation, see $La_3Rh_2Ge_2$ under La–Rh–Ge. Morozkin et al. (1996) observed the same structure type and lattice parameters $a=0.5592$, $b=0.7895$,$c=1.3293$ from X-ray powder diffraction.

Studying this phase diagram, Morozkin et al. (1996) established the crystal structure for $SmRh_5Ge_3$ (1) (UCo_5Si_3 type, $a=1.5848$, $c=0.3679$), $SmRh_{1-x}Ge_{2+x}$ (9) ($CeRh_{1-x}Ge_{2+x}$ type, $a=0.4225$, $b=0.4304$, $c=1.507$), $Sm_{33}Rh_{25-20}Ge_{42-47}$ (8) (AlB_2 type, $a=0.4219$–0.4208, $c=0.4017$–0.4025), Sm_2RhGe_2 (7) (Zr_2CoSi_2 type, $a=1.065$, $b=1.118$, $c=0.4106$, $\gamma=129.96°$) and for Sm_2RhGe_6 (10) (Ce_2CuGe_6 type, $a=0.4060$, $b=0.4008$, $c=2.190$). In addition they observed four compounds with an unknown structure: ~$Sm_{0.33}Rh_{0.53}Ge_{0.14}$ (11), ~$SmRh_2Ge$ (12), ~$Sm_{0.18}Rh_{0.64}Ge_{0.18}$ (13), ~$SmRh_3Ge_6$ (14).

Verniere et al. (1995) mentioned the existence of $Sm_4Rh_{13}Ge_9$ compound with the $Ho_4Ir_{13}Ge_9$ type. No lattice parameters were given. For the experimental procedure, see $La_4Ir_{13}Ge_9$ under La–Ir–Ge. This compound was not observed by Morozkin et al. (1996) in the investigation of phase equilibria in the Sm–Rh–Ge system at 870 K.

4.7.9. *Sm–Pd–Ge*

A systematic study of the Sm–Pd–Ge system at 870 K was performed by Barakatova (1994) over the whole concentration region by means of X-ray powder and single-crystal analyses as well as using metallography and microprobe analyses. The samples were prepared by arc melting under argon and annealing in evacuated quartz ampoules at 870 K for 1000 hours.

The phase-field distribution in the isothermal section at 870 K (fig. 79) is characterized by existence of ten ternary compounds. Maximum solubilities of germanium in the binary compounds of the Sm–Pd system are 10 at.% for SmPd and 5 at.% for $SmPd_{3-2.3}$. Solubility of samarium in the palladium germanides was found to be negligible. As reported by Barakatova (1994), $SmPd_2Ge_2$ (2) and $Sm(Pd,Ge)_2$ (9) dissolve 15 at.% Ge and 10 at.% Ge respectively.

According to an X-ray powder diffraction analysis reported by Hovestreydt et al. (1982), the compound SmPdGe (8) adopts the KHg_2-type of structure, $a=0.44263$, $b=0.7110$, $c=0.7606$. For sample preparation, see LaPdGe under La–Pd–Ge. The starting materials were Sm (3N), Pd (4N) and Ge (5N). The existence of SmPdGe was later confirmed by Barakatova (1994) (KHg_2 type, $a=0.4426$, $b=0.7110$, $c=0.7606$; X-ray powder data).

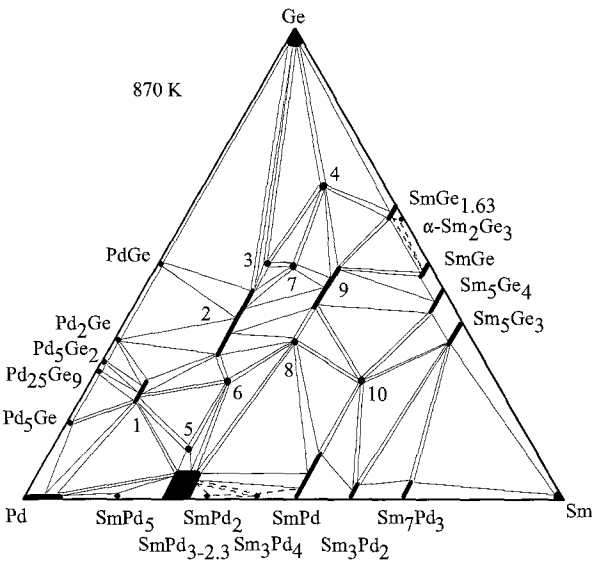

Fig. 79. Sm–Pd–Ge, isothermal section at 870 K.

The crystal structure of the compound $SmPd_2Ge$ (6) was found to be of the YPd_2Si type ($a=0.7501$, $b=0.6996$, $c=0.5673$; X-ray powder diffraction) by Jorda et al. (1983). For the experimental procedure, see $LaPd_2Ge$ under La–Pd–Ge. The starting materials were palladium 99.99 mass%; germanium, specpure quality; samarium 99.9 mass%. Barakatova (1994) confirmed the structure type and determined the lattice parameters $a=0.7504$, $b=0.6995$, $c=0.5680$ from X-ray powder analysis.

Sologub et al. (1995a) reported on the X-ray powder analysis of the Sm_2PdGe_6 (4) compound which was found to crystallize with the Ce_2CuGe_6-type structure, $a=0.4116$, $b=0.4044$, $c=2.170$. For the experimental procedure, see La_2PdGe_6 under La–Pd–Ge. The starting materials used were obtained from Johnson & Matthey, UK (99.9 mass%). The structure type after Barakatova (1994) is the same and lattice parameters are $a=0.4115$, $b=0.4031$, $c=2.164$.

During the phase investigation in the Sm–Pd–Ge system, Barakatova (1994) established the crystal structure for $Sm_3Pd_{20}Ge_6$ (1) ($Ce_3Pd_{20}Ge_6$ type, $a=1.242$–1.245); $SmPd_{2.5-1.75}Ge_{1.5-2.25}$ (2) ($BaAl_4$ type, $a=0.4238$–0.4258, $c=0.9971$–1.0066); $Sm_2Pd_3Ge_5$ (3) ($U_2Co_3Si_5$ type, $a=1.0136$, $b=1.2203$, $c=0.5983$); $Sm_{0.25}Pd_{0.65}Ge_{0.10}$ (5) ($CaTiO_3$ type, $a=0.4158$); $SmPdGe_2$ (7) ($YIrGe_2$ type, $a=0.4345$, $b=0.8762$, $c=1.6558$); $SmPd_{0.8-0.5}Ge_{1.2-1.5}$ (9) (AlB_2 type, $a=0.4276$–0.4216, $c=0.3669$–0.4115); and Sm_2PdGe (10) (FeB type, $a=0.8453$, $b=0.3732$, $c=0.5582$).

4.7.10. *Sm–Ag–Ge*

Information on interaction of samarium with silver and germanium is due to the work of three groups of authors (Sologub et al. 1995a, Protsyk 1994, Gibson et al. 1996). The

phase diagram of the Sm–Ag–Ge system is not available; three ternary compounds have been observed and analyzed.

The crystal structure of Sm_2AgGe_6 was found to be isotypic with Ce_2CuGe_6, $a = 0.42394$, $b = 0.40956$, $c = 2.1346$ by Sologub et al. (1995a) who employed X-ray powder diffraction analysis of an arc melted sample which was homogenized by annealing at 873 K for 150 hours.

Protsyk (1994) reported the $SmAg_2Ge_2$ compound with the $CeGa_2Al_2$-type structure, $a = 0.4223$, $c = 1.1048$. For sample preparation, see Ce–Ag–Ge.

The crystal structure of the SmAgGe compound was investigated by Gibson et al. (1996) with X-ray powder diffraction. It was found to adopt the ZrNiAl type with lattice parameters $a = 0.72005$, $c = 0.42692$. The alloy was arc melted and annealed at 970 K for 10 days.

4.7.11. *Sm–Os–Ge*

No phase diagram is available at present for the system Sm–Os–Ge, however, one ternary germanide has been observed and characterized by Segre et al. (1981a). $Sm_3Os_4Ge_{13}$ was found to crystallize with the $Pr_3Rh_4Sn_{13}$ type, $a = 0.9043$. For sample preparation, see $Ce_3Ru_4Ge_{13}$ under Ce–Ru–Ge.

4.7.12. *Sm–Ir–Ge*

Phase relations have not been established for the Sm–Ir–Ge system; information concerning the formation of compounds and their crystal structure is due to the work of different groups of authors.

Francois et al. (1987) reported the crystal structure of $SmIrGe_2$ ($YIrGe_2$ type, $a = 0.4314$, $b = 1.603$, $c = 0.8871$). The sample was prepared by heating a mixture of powders of the starting components (Sm 3N, Ir 3N and Ge 3N) in an evacuated silica tube at 1173 K.

According to an X-ray powder diffraction analysis reported by Hovestreydt et al. (1982), the compound SmIrGe adopts the TiNiSi-type structure, $a = 0.7017$, $b = 0.4346$, $c = 0.7557$. For the experimental procedure, see LaIrGe under La–Ir–Ge.

$SmIr_2Ge_2$ was found to crystallize in the P4/nmm space group with lattice parameters $a = 0.4203$, $c = 1.0084$ (Francois et al. 1985).

$Sm_2Ir_3Ge_5$ was found to adopt the $U_2Co_3Si_5$-type structure ($a = 1.0151$, $b = 1.182$, $c = 0.6005$) by Venturini et al. (1986b) from X-ray powder analysis.

Verniere et al. (1995) observed the existence of $Sm_4Ir_{13}Ge_9$ with $Ho_4Ir_{13}Ge_9$-type. The lattice parameters have not been established. For the experimental details, see $La_4Ir_{13}Ge_9$ under La–Ir–Ge.

Venturini et al. (1985b) reported on the X-ray powder diffraction study of the $Sm_3Ir_4Ge_{13}$ compound from a sample which was prepared by heating a mixture of the starting components (Sm 3N, Ir 4N, Ge 4N) in an evacuated quartz tube and homogenizing at 1073 K. The crystal structure was found to adopt the $Yb_3Rh_4Sn_{13}$ type, $a = 0.9012$.

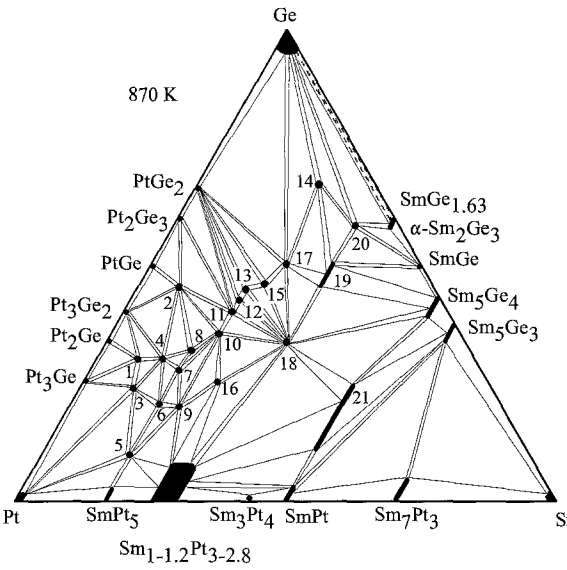

Fig. 80. Sm–Pt–Ge, isothermal section at 870 K.

4.7.13. *Sm–Pt–Ge*

A systematic study of the Sm–Pt–Ge system at 870 K was performed by Barakatova (1994) over the whole concentration region by means of X-ray powder and single-crystal analyses as well as using metallography and microprobe analyses of 158 alloys. The samples were prepared by arc melting under argon and annealing in evacuated quartz ampoules at 870 K for 1000 hours.

The phase-field distribution in the isothermal section at 870 K (fig. 80) is characterized by the existence of 21 ternary compounds. The maximum solubility of germanium in the binary compounds of Sm–Pt is not indicated by the author. The solubility of samarium in the palladium germanides was found to be negligible.

According to an X-ray powder diffraction analysis reported by Hovestreydt et al. (1982), the compound SmPtGe (18) adopts the TiNiSi-type of structure, $a = 0.7144$, $b = 0.4396$, $c = 0.7585$. For sample preparation, see LaPdGe under La–Pd–Ge. The starting materials were Sm (3N), Pt (4N) and Ge (5N). At variance with these data, Barakatova (1994) observed the SmPtGe compound with the KHg_2 type, lattice parameters $a = 0.4377$, $b = 0.7114$, $c = 0.7573$, from X-ray powder analysis of arc melted alloy annealed at 870 K.

Sologub et al. (1995a) reported on the X-ray powder analysis of the Sm_2PtGe_6 (14) compound which was found to crystallize with the Ce_2CuGe_6 type, $a = 0.40955$, $b = 0.40412$, $c = 2.1871$. For the experimental procedure, see La_2PdGe_6 under La–Pd–Ge. The starting materials used were obtained from Johnson & Matthey, UK (99.9 mass%).

Venturini et al. (1989a) investigated the crystal structure of $SmPt_2Ge_2$ (11) from an arc melted sample annealed at 1273 K for 5 days. The crystal structure was found to

belong to the $LaPt_2Ge_2$ type, $a=0.4345$, $b=0.4378$, $c=0.9751$, $\beta=91.02°$. The starting materials were Sm (3N), Pt (4N) and Ge (4N).

Francois et al. (1987) mentioned the existence of $SmPtGe_2$ (17) with the $YIrGe_2$-type of structure. No lattice parameters were given. Barakatova (1994) confirmed the crystal structure and established the lattice parameters $a=0.4367$, $b=0.8720$, $c=1.6332$ by X-ray powder analysis.

In the course of phase equilibrium investigation in the Sm–Pt–Ge system, Barakatova (1994) established the crystal structure for $Sm_{0.165}Pt_{0.735}Ge_{0.1}$ (5) ($CaCu_5$ type, $a=0.5296$, $c=0.4413$), $SmPt_{2.25}Ge_{1.75}$ (10) ($CaBe_2Ge_2$ type, $a=0.4288$, $c=0.9975$), $SmPt_{1.87}Ge_{2.13}$ (12) ($CaBe_2Ge_2$ type, $a=0.4325$, $c=0.9909$), $Sm_2Pt_3Ge_5$ (13) ($U_2Co_3Ge_5$ type, $a=0.9874$, $b=1.1987$, $c=0.5731$), $Sm_3Pt_4Ge_6$ (15) ($Ce_3Pt_4Ge_6$ type, $a=0.4351$, $b=0.4359$, $c=2.5886$), $SmPt_2Ge$ (16) (Fe_3C type, $a=0.7436$, $b=0.6901$, $c=0.5585$), $SmPt_{0.35-0.65}Ge_{1.65-1.35}$ (19) (AlB_2 type, $a=0.4252$–0.4185, $c=0.4022$–0.4157), $SmPt_{0.24}Ge_{1.76}$ (20) (α-$ThSi_2$ type, $a=0.4147$, $c=1.4131$) and $Sm_2Pt_{1-1.6}Ge_{1-0.4}$ (21) (CrB type, $a=0.4033$–0.3894, $b=1.0884$–1.0760, $c=0.4287$–0.4415).

The formation of eight more ternary phases with unknown structures has been observed by Barakatova (1994) while investigating the isothermal section of the Sm–Pt–Ge system at 870 K. They exist at compositions close to $Sm_{0.075}Pt_{0.625}Ge_{0.30}$ (1), $Sm_{0.075}Pt_{0.475}Ge_{0.45}$ (2), $Sm_{0.10}Pt_{0.665}Ge_{0.235}$ (3), $Sm_{0.12}Pt_{0.58}Ge_{0.30}$ (4), $Sm_{0.165}Pt_{0.635}Ge_{0.20}$ (6), $Sm_{0.165}Pt_{0.57}Ge_{0.265}$ (7), $Sm_{0.165}Pt_{0.525}Ge_{0.32}$ (8) and $Sm_{0.20}Pt_{0.60}Ge_{0.20}$ (9).

4.7.14. *Sm–Au–Ge*

Information on interaction of samarium with gold and germanium is due to the work of two groups of authors (Sologub et al. 1995a and Rossi et al. 1992). The phase diagram of the Sm–Au–Ge system is not available; two ternary compounds have been observed and analyzed.

Sologub et al. (1995a) employed X-ray powder diffraction analysis for investigation the crystal structure of the Sm_2AuGe_6 compound from an arc melted sample, which was homogenized by annealing at 873 K for 150 hours. The crystal structure was found to be isotypic with Ce_2CuGe_6, $a=0.42394$, $b=0.40956$, $c=2.1346$.

A ternary compound of samarium with gold and germanium in the stoichiometric ratio 1:1:1 has been identified and studied by means of X-ray and metallographic analyses by Rossi et al. (1992). The SmAuGe compound was found to adopt the LiGaGe type with lattice parameters $a=0.4434$, $c=0.7533$. The sample was prepared by melting the metals (about 99.9 mass% for samarium and 99.99 mass% for gold and germanium) in an induction furnace and annealing at 1070 K for one week.

4.8. *Eu–d element–Ge systems*

4.8.1. *Eu–Mn–Ge*

No phase diagram exists for the system Eu–Mn–Ge, and only one ternary compound has been observed from induction melted alloy by Felner and Novik (1978). According

to X-ray powder diffraction analysis, the $EuMn_2Ge_2$ compound crystallizes with the $CeGa_2Al_2$ type, $a = 0.4244$, $c = 1.075$.

4.8.2. *Eu–Fe–Ge*

Information on the phase equilibria in the ternary Eu–Fe–Ge system is due to the work of Belan (1988) who employed X-ray powder diffraction on samples prepared by arc melting of pure components. The resulting alloys were annealed at 670 K for 300 hours. The equilibrium phase diagram is shown in fig. 81. No ternary compounds were observed.

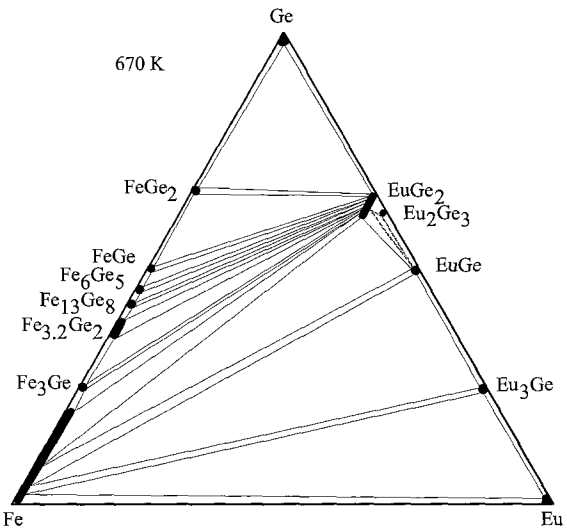

Fig. 81. Eu–Fe–Ge, isothermal section at 670 K.

4.8.3. *Eu–Co–Ge*

The isothermal section of the Eu–Co–Ge phase diagram at 670 K was constructed by Oniskovetz et al. (1985). The phase relations are characterized by the formation of three ternary compounds (fig. 82). For details of sample preparation, see Eu–Fe–Ge.

The crystal structures of two compounds have been studied by Oniskovetz et al. (1985). $EuCo_{2.5}Ge_{1.5}$ (1) belongs to the $BaAl_4$ type, $a = 0.4035$, $c = 0.9746$; $EuCoGe_3$ (2) crystallizes with the $BaNiSn_3$ type, $a = 0.4345$, $c = 0.9953$ (powder X-ray diffraction data). Venturini et al. (1985b) confirmed the crystal structure for the $Eu_3Co_4Ge_{13}$ compound from a sample prepared by heating a mixture of the starting components in an evacuated quartz tube and homogenizing at 1073 K. Finally the sample was quenched in water. It was found to adopt the $Yb_3Rh_4Sn_{13}$-type structure, $a = 0.8814$ (X-ray powder diffraction data). The purity of the starting components was Eu 99.9 mass%, Co 99.99 mass%, Ge 99.99 mass%.

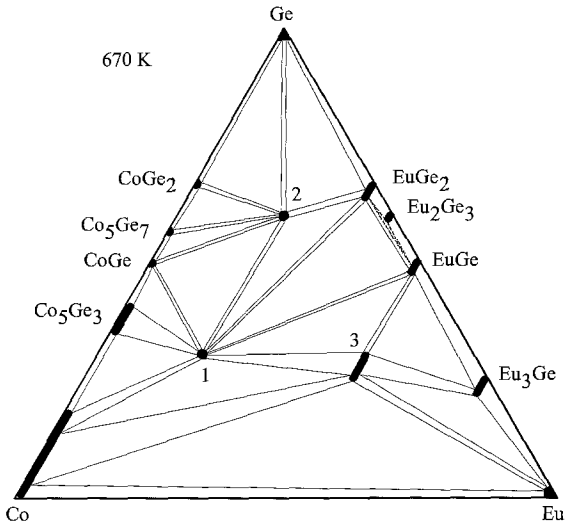

Fig. 82. Eu–Co–Ge, isothermal section at 670 K.

One more ternary compound with an unknown structure has been observed by Oniskovetz et al. (1985) in the course of phase equilibrium investigation in the Eu–Co–Ge system: $Eu_2Co_{1-1.2}Ge_{1-0.8}$ (3).

Felner and Novik (1978) observed the formation of the $EuCo_2Ge_2$ compound and investigated its crystal structure: $CeGa_2Al_2$ type, $a = 0.4035$, $c = 1.046$. The sample was melted in an induction furnace at about 1870 K under a protective argon atmosphere; afterwards the alloy was homogenized by annealing in the induction furnace at the melting temperature for about 30 min. Starting materials were Eu 99.9 mass%, Co 99.95 mass% and Ge 99.99 mass%. This phase was not observed by Oniskovetz et al. (1985) in the course of phase equilibrium studies in the Eu–Co–Ge system at 670 K.

4.8.4. *Eu–Ni–Ge*

Phase equilibria in the isothermal sections at 670 K have been determined by Belan (1988) using X-ray powder diffraction of alloys which were synthesized by arc melting ingots of Eu (99.81 mass%), Ni (99.99 mass%) and Ge (99.99 mass%); the alloys were then annealed in evacuated quartz tubes at 670 K for 300 hours. The phase relations are characterized by the formation of six ternary compounds and by the existence of rather extended solid solutions originating at Eu_2Ni_{17} (up to 18 at.% Ge), $EuNi_5$ (up to 20 at.% Ge) and Eu_3Ge (up to 12 at.% Ni). The phase equilibria in the isothermal section at 670 K are presented in fig. 83.

The formation and crystal structure of $EuNi_2Ge_2$ (2) was reported in an early investigation of europium–nickel–germanium combinations by Bodak et al. (1966): $CeGa_2Al_2$ type, $a = 0.4086$, $c = 0.9809$ (arc melted and annealed at 670 K sample; X-ray powder diffraction data). Belan (1988) confirmed the crystal structure and determined the lattice parameters $a = 0.4133$, $c = 1.0126$.

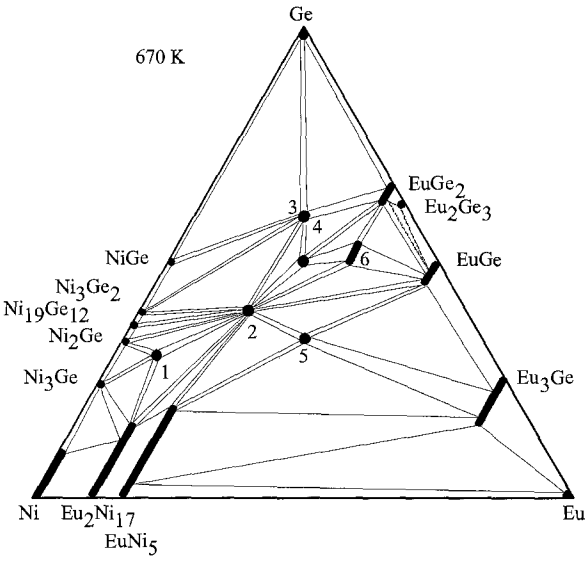

Fig. 83. Eu–Ni–Ge, isothermal section at 670 K.

According to Oniskovetz et al. (1987), EuNiGe (5) crystallizes with a new structure type, $a = 0.6996$, $b = 0.7581$, $c = 0.6187$, $\gamma = 130.22°$ (X-ray single-crystal data). The alloy was obtained by arc melting of the proper amounts of pure components (Eu 99.81 mass%; Ni 99.99 mass%, Ge 99.99 mass%) followed by annealing in an evacuated quartz tube at 670 K for 300 hours.

Crystal structures for four more ternary compounds have been established by Oniskovetz (1984) and Belan (1988) while investigating the Eu–Ni–Ge isothermal section: $EuNi_9Ge_4$ (1) ($CeNi_{8.5}Si_{4.5}$ type, $a = 0.7957$, $c = 1.1793$); $EuNiGe_3$ (3) ($BaNiSn_3$ type, $a = 0.4437$, $c = 0.9891$); $EuNiGe_2$ (4) ($CeNiSi_2$ type, $a = 0.4244$, $b = 1.691$, $c = 0.4228$); $EuNi_{0.5-0.35}Ge_{1.5-1.65}$ (6) (AlB_2 type, $a = 0.4184$–0.4169, $c = 0.4485$–0.4480).

4.8.5. *Eu–Cu–Ge*

A systematic study of the Eu–Cu–Ge system at 670 K was performed by Belan (1988). For sample preparation, see Eu–Ni–Ge. The starting materials were Eu 99.81 mass%, Cu 99.99 mass% and Ge 99.99 mass%. Four ternary compounds were found; two of them are characterized by the formation of extended homogeneity fields (see fig. 84).

Belan (1988) observed and characterized three of the four existing ternary compounds: $EuCu_{2.5-1.65}Ge_{1.5-2.35}$ (1) crystallizes with the $CeGa_2Al_2$ type, $a = 0.4187$–0.4212, $c = 1.0116$–1.0336; $EuCu_{0.8-0.5}Ge_{1.2-1.5}$ (3) was found to adopt the AlB_2 type, $a = 0.4217$–0.4218, $c = 0.4432$–0.4460; EuCuGe (2) belongs to the TiNiSi type, $a = 0.7342$, $b = 0.4372$, $c = 0.7550$. In contrast, Iandelli (1993) reported a CaCuGe type with $a = 2.209$, $b = 0.7543$, $c = 0.4453$ from X-ray powder diffraction. For the experimental details, see SmCuGe under Sm–Cu–Ge.

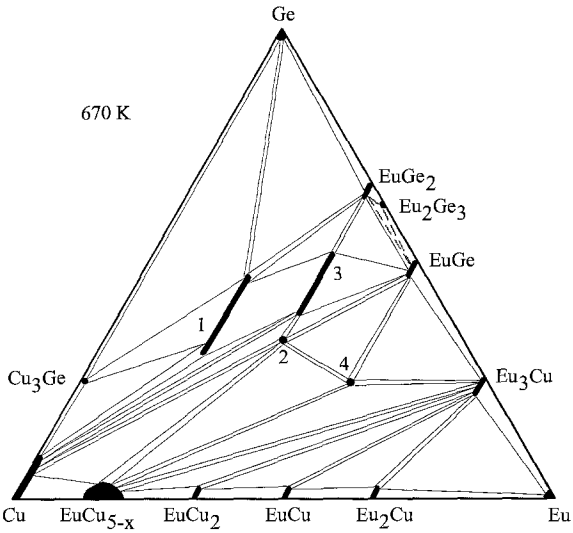

Fig. 84. Eu–Cu–Ge, isothermal section at 670 K.

The crystal structure for the Eu_2Cu_2Ge (4) compound has not yet been resolved (Belan 1988).

4.8.6. *Eu–Zn–Ge*

The only information on the interaction of europium with zinc and germanium is due to the work of Pöttgen (1996) who reported the crystal structure of EuZnGe (ZrBeSi type, $a = 0.4372$, $c = 0.8604$; X-ray powder diffraction).

4.8.7. *Eu–Ru–Ge*

$EuRu_2Ge_2$ was found to crystallize with the $CeGa_2Al_2$ type structure. The lattice parameters were reported as $a = 0.4276$, $c = 1.0204$ (Francois et al. 1985).

4.8.8. *Eu–Rh–Ge*

No phase diagram is available for the system Eu–Rh–Ge, and so far, only two ternary compounds have been observed and characterized.

According to Venturini et al. (1985b), the $EuRhGe_3$ compound crystallizes with the $BaNiSn_3$ type, $a = 0.4410$, $c = 1.0064$ (X-ray powder diffraction analysis). For sample preparation and purity of starting components, see $EuCoGe_3$ under Eu–Co–Ge.

$EuRh_2Ge_2$ was found to crystallize with the $CeGa_2Al_2$ type, $a = 0.4164$, $c = 1.0601$ (Francois et al. 1985).

4.8.9. *Eu–Pd–Ge*

Little information exists on the Eu–Pd–Ge system; two compounds have been observed and characterized so far.

According to Belan (1988), the EuPdGe crystallizes with the EuNiGe type, $a=0.6132$, $b=0.7934$, $c=0.7441$, $\gamma=132.64°$ (X-ray powder diffraction data). The alloy was obtained by arc melting the proper amounts of pure components (Eu 99.81 mass%; Pd 99.99 mass%, Ge 99.99 mass%) followed by annealing in an evacuated quartz tube at 670 K for 300 hours and finally quenching in cold water.

The crystal structure of the compound $EuPd_2Ge$ was found to be of the YPd_2Si type ($a=0.7582$, $b=0.6981$, $c=0.5834$; X-ray powder diffraction) by Jorda et al. (1983). The sample was obtained by induction heating the pressed powder compacts in a levitation coil under an argon atmosphere, pressure 4 atm. After the rapid reaction in the liquid state the molten sample was dropped into a boron nitride crucible. The alloy was annealed in an evacuated quartz tube for 10 days at 1173 K. Starting materials were palladium 99.99 mass%, germanium in specpure quality, and europium 99.9 mass%.

4.8.10. *Eu–Ag–Ge*

The phase equilibria for Eu–Ag–Ge in the isothermal section at 670 K have been determined by Protsyk (1994) using X-ray powder diffraction analysis of 80 ternary alloys, which were synthesized by arc melting ingots of Eu (98.9 mass%), Ag (99.9 mass%) and Ge (99.99 mass%). The alloys were annealed in evacuated quartz tubes for 400 hours. The total number of compounds observed was three. The $EuAg_2$ binary compound was observe to dissolve up to 15 at.% Ge. The solubility of the third component in other binary compounds was reported to be negligible. The phase equilibria in the isothermal sections at 670 K are presented in fig. 85.

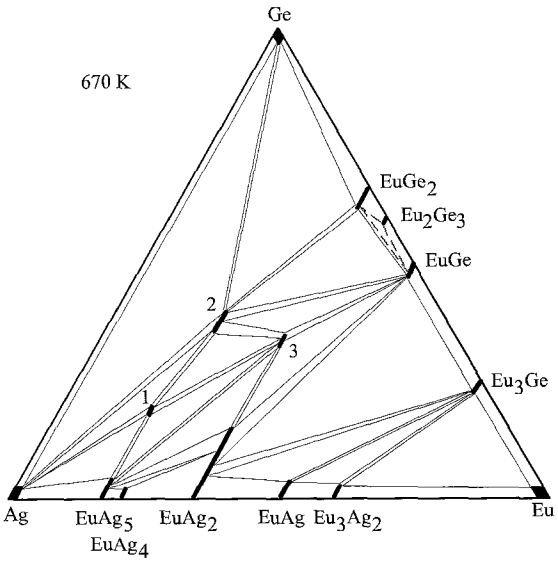

Fig. 85. Eu–Ag–Ge, isothermal section at 670 K.

The $EuAg_{2.00-2.25}Ge_{2.00-1.75}$ (2) compound was observed and studied by Protsyk (1994). It was found to crystallize with the $CeGa_2Al_2$ type, lattice parameters $a = 0.4300–0.4405$, $c = 1.0787–1.0835$, by X-ray powder diffraction of arc melted alloys annealed at 470 K.

The formation and crystal structure of the EuAgGe (3) compound was investigated by Protsyk (1994): AlB_2 type, $a = 0.4364$, $c = 0.4373$ (arc melted sample annealed at 670 K; X-ray powder diffraction data). Merlo et al. (1996) reported a dependence of the crystal structure of the EuAgGe system on the thermal treatment. According to micrographic and microprobe analyses, the as-cast sample, prepared on the 1:1:1 formula, contained two phases in nearly equal quantities, with approximate compositions $EuAg_{1.1}Ge_{0.9}$ and $EuAg_{0.8}Ge_{1.1}$. The X-ray powder pattern was completely indexed as a mixture of reflections of the $CeCu_2$-type cell and an AlB_2-type phase. The same sample, annealed at 970 K, showed a prevailing phase with composition $EuAgGe_{0.9}$. Nearly all reflections of the powder pattern were indexed on the basis of the $CeCu_2$-type cell, while some weak lines were ascribed to the AlB_2-type cell. The Ag-rich formulae ($EuAg_{1.1}Ge_{0.9}$) and Ge-rich formulae ($EuAg_{0.8}Ge_{1.1}$) were assigned to the $CeCu_2$ type ($a = 0.4675$, $b = 0.7395$, $c = 0.7981$) and the AlB_2 type ($a = 0.4390$, $c = 0.4360$), respectively.

The crystal structure of $Eu_{0.166}Ag_{0.654}Ge_{0.18}$ (1) has not been resolved yet (Protsyk 1994).

4.8.11. *Eu–Os–Ge*

No phase diagram is available at present for the system Eu–Os–Ge, however, one ternary gemanide has been observed and characterized by Segre et al. (1981a). $Eu_3Os_4Ge_{13}$ was found to crystallize with the $Pr_3Rh_4Sn_{13}$ type, $a = 0.9057$ (Segre et al. 1981a). For sample preparation, see $Ce_3Ru_4Ge_{13}$ under Ce–Ru–Ge.

4.8.12. *Eu–Ir–Ge*

Phase equilibria for the ternary Eu–Ir–Ge system have not been derived, however, the formation of two compounds has been observed.

The existence of $EuIrGe_3$ has been established by Venturini et al. (1985b). Crystallographic data reported are $BaNiSn_3$ type, $a = 0.4436$, $c = 1.0033$ (X-ray powder diffraction). For details of the experimental procedure, see $LaCoGe_3$ under La–Co–Ge.

$EuIr_2Ge_2$ was found to crystallize with the $CeGa_2Al_2$ type, $a = 0.4172$, $c = 1.0543$ (Francois et al. 1985).

4.8.13. *Eu–Pt–Ge*

Information on the interaction of europium and platinum with germanium is due to the work of two research groups who employed X-ray powder as well as single-crystal analyses for the investigation of alloys with specific compositions. The phase diagram of the Eu–Pt–Ge system is not available.

Venturini et al. (1989a) investigated the crystal structure of $EuPt_2Ge_2$ from an arc melted sample annealed at 1273 K for 5 days. The crystal structure was found to

belong to the $LaPt_2Ge_2$ type, $a = 0.4417$, $b = 0.4456$, $c = 0.9751$, $\beta = 91.27°$ (X-ray powder diffraction data). The starting materials were Eu (3N), Pt (4N) and Ge (4N).

Pöttgen et al. (1996b) investigated the crystal structure of EuPtGe: ZrOS type, $a =$ 0.65463 (single-crystal X-ray data). The starting materials for the preparation were ingots of europium (Johnson & Matthey), platinum powder (Degussa) and germanium lumps (Wacker), all with stated purity greater than 99.9 mass%. The elements were mixed in the ideal atomic ratio and sealed in a tantalum tube under an argon pressure of about 800 mbar. The tantalum tube was sealed in a quartz ampoule and heated at 1320 K for five days, then cooled to 1170 K and annealed for an additional four weeks.

4.8.14. *Eu–Au–Ge*

Phase relations have not been established for the ternary system Eu–Au–Ge; only one ternary compound has been reported: EuAuGe crystallizes in a new ternary ordered version of the $CeCu_2$ type, $a = 0.4601$, $b = 0.7371$, $c = 0.7881$ (single-crystal X-ray data; Pöttgen 1995). For sample preparation, see EuPtGe under Eu–Pt–Ge.

4.9. *Gd–d element–Ge systems*

4.9.1. *Gd–Mn–Ge*

Phase equilibria in the isothermal section at 970 K have been established by Markiv et al. (1993) using X-ray powder diffraction analysis of 103 ternary alloys which were synthesized by arc melting ingots of Gd (99.85 mass%), Mn (99.9 mass%) and Ge (99.999 mass%); the alloys were then annealed in evacuated quartz tubes for 450–550 hours. In some cases the alloys were preliminary homogenized at 1270 K and 1170 K for 10–30 hours. The phase relations are characterized by the formation of nine ternary compounds and by the existence of a solid solution originating at $GdMn_2$. Phase equilibria in the isothermal sections at 970 K are presented in fig. 86.

Information concerning the formation of compounds in the ternary Gd–Mn–Ge system is due to the work of several groups of authors; nine ternary compounds have been reported for the various gadolinium–manganese–germanium combinations.

Rossi et al. (1978b) reported on the crystal structure of the $GdMn_2Ge_2$ (4) compound ($CeGa_2Al_2$ type, $a = 0.4029$, $c = 1.0895$; X-ray powder method). The alloy was obtained by melting under argon in an induction furnace and was annealed at 770 K for one week. The metals used were of purity greater than 99.9 mass% for Gd, and greater than 99.99 mass% for Mn and Ge. The $CeGa_2Al_2$ structure type was confirmed by Belyavina et al. (1993) from X-ray powder diffraction of an arc melted alloy annealed at 970 K ($a = 0.4026$, $c =$ 1.0887).

$GdMn_6Ge_6$ (1) was found to crystallize with the $HfFe_6Ge_6$-type structure by Venturini et al. (1992), $a = 0.5242$, $c = 0.8184$ (X-ray powder diffraction data). The alloy was synthesized by a powder metallurgical reaction in an evacuated silica tube at 1073 K for 14 days. Belyavina et al. (1993) suggested a new structure type for the $GdMn_6Ge_6$ compound, which is a derivative from the $LiCo_6Ge_6$ type but with nearly the same lattice parameters: $a = 0.52333$, $c = 0.81806$.

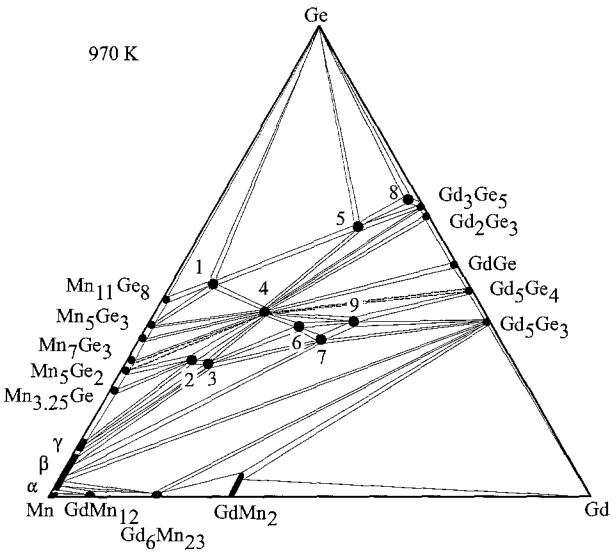

Fig. 86. Gd–Mn–Ge, isothermal section at 970 K.

Francois et al. (1990) investigated the occurrence of the $CeNiSi_2$ structure type for several gadolinium–manganese–germanium combinations from alloys annealed at 1173 K: $GdMn_{0.26-0.38}Ge_2$ (5); $a = 0.4138$–0.4163, $b = 1.606$–1.613, $c = 0.4000$–0.4036. Belyavina et al. (1993) studied the formation and crystal structure for the $GdMn_{0.39}Ge_2$ compound: $CeNiSi_2$ type, $a = 0.41590$, $b = 1.6130$, $c = 0.4039$.

Six more ternary compounds were observed and investigated by Belyavina et al. (1993) using X-ray powder diffraction of arc melted alloys annealed at 970 K: $GdMn_4Ge_2$ (3), $ZrFe_4Si_2$ type, $a = 0.76419$, $c = 0.39467$; $Gd_6Mn_8Ge_8$ (6), $Gd_6Cu_8Ge_8$ type, $a = 1.4015$, $b = 0.7118$, $c = 0.42027$; GdMnGe (7), TiNiSi type, $a = 0.7138$, $b = 0.41698$, $c = 0.8191$; $Gd_4Mn_{0.64}Ge_7$ (8), $Sm_4Co_{0.64}Ge_7$ type, $a = 0.4135$, $b = 0.4045$, $c = 3.0030$; $GdMn_6Ge_3$ (2), unknown structure; and $Gd_3Mn_2Ge_3$ (9), unknown structure.

4.9.2. *Gd–Fe–Ge*

Four ternary compounds were found in the Gd–Fe–Ge system.

$GdFe_6Ge_6$ was reported to be isotypic with the crystal structure of YCo_6Ge_6, with lattice parameters $a = 0.5118$, $c = 0.4056$ (Starodub and Mruz 1983). The sample was prepared by arc melting the proper amounts of the starting components followed by annealing at 870 K for two weeks. At variance with the data presented by Starodub and Mruz (1983), Venturini et al. (1992), using X-ray powder diffraction data, found that $GdFe_6Ge_6$ crystallized with a new structure type, Pnma space group, $a = 6.143$, $b = 0.8137$, $c = 7.979$. The alloy was obtained by powder metallurgical reaction in an evacuated silica tube at 1173 K for two weeks.

Pecharsky et al. (1989) reported $GdFe_{0.33}Ge_2$ to crystallize with the $CeNiSi_2$ type (a = 0.4140, b = 1.6017, c = 0.4021; X-ray powder analysis). The alloy was arc melted and annealed at 870 K. The purity of the starting materials was greater than 99.9 mass%. Later Francois et al. (1990) investigated the occurrence of the $CeNiSi_2$ structure type for several gadolinium–iron–germanium combinations from alloys obtained by powder metallurgical reaction which were afterwards annealed at 1173 K: $GdFe_{0.25-0.46}Ge_2$, $CeNiSi_2$ type, a = 0.4124–0.4156, b = 1.606–1.608, c = 0.3998–0.4046.

The $GdFe_2Ge_2$ compound was investigated by Rossi et al. (1978a) ($CeGa_2Al_2$ type, a = 0.3989, c = 1.0485) by means of X-ray diffraction. The alloy was obtained by melting under argon in an induction furnace and annealing at 770 K for one week. The metals used were of purity greater than 99.9 mass% (Gd, Fe) and greater than 99.99 mass% (Ge).

Oleksyn (1990) investigated the crystal structure of $Gd_{117}Fe_{52}Ge_{112}$ by the X-ray powder method ($Tb_{117}Fe_{52}Ge_{112}$ type, a = 2.8656). The alloy was synthesized by arc melting followed by annealing at 1070 K for 350 h. The starting materials were Gd 99.83 mass%, Fe 99.9 mass%, Ge 99.99 mass%.

4.9.3. *Gd–Co–Ge*

The phase diagram of the Gd–Co–Ge system has not been established; nine ternary compounds have been identified for gadolinium–cobalt–germanium combinations.

Méot-Meyer et al. (1985a) reported the crystal structure of $GdCo_{1-x}Ge_2$, x = 0.36 ($CeNiSi_2$ type, a = 0.4139, b = 1.627, c = 0.4062). The sample was prepared by powder metallurgical reaction and annealed in evacuated silica tube at 1173 K. Pecharsky et al. (1989) investigated the formation and crystal structure of the $GdCo_{1-x}Ge_2$ compound by X-ray powder analysis of arc melted alloys annealed at 870 K. The $CeNiSi_2$-type structure was confirmed, and the existence of an extended homogeneity region was established: $0.3 < x < 0.7$ (a = 0.4128–0.4165, b = 1.6157–1.6398, c = 0.4024–0.4077). Francois et al. (1990) confirmed the existence of the homogeneity field with a slight deviation in concentration ratio: $GdCo_{0.24-0.64}Ge_2$, $CeNiSi_2$ type, a = 0.4113–0.4139, b = 1.608–1.627, c = 0.3986–0.4062. For sample preparation, see $GdFe_{0.25-0.46}Ge_2$ under Gd–Fe–Ge.

The crystal structure of $Gd_3Co_4Ge_{13}$ ($Yb_3Rh_4Sn_{13}$ type, a = 0.8780; X-ray powder diffraction) was investigated by Venturini et al. (1985b) from a sample which was prepared by heating the a compacted mixture of the starting materials (Gd in pieces, 99.9 mass%; Co and Ge in powder, 99.99 mass%) in an evacuated quartz tube at 1073 K. Bodak et al. (1987) reported the $Y_3Co_4Ge_{13}$-type structure for the $Gd_3Co_4Ge_{13}$ compound (a = 0.8769; X-ray powder data) from arc melted alloy annealed at 870 K.

Rieger and Parthé (1969b) investigated the formation of the $GdCo_2Ge_2$ compound ($CeGa_2Al_2$ type, a = 0.3996, c = 1.0096; X-ray powder diffraction).

From X-ray powder analysis of an alloy obtained by powder metallurgical reaction and annealed at 1173 K, $Gd_2Co_3Ge_5$ was reported to adopt the $Lu_2Co_3Si_5$-type structure, a = 0.9683, b = 1.183, c = 0.5750, β = 91.65° (Venturini et al. 1986b).

The crystal structure of the $GdCo_6Ge_6$ compound was reported by Buchholz and Schuster (1981): YCo_6Ge_6 type, a = 0.5016, c = 0.3931. The sample was melted under argon in a corundum crucible at 1073–1273 K.

Gorelenko et al. (1984) reported the crystal structure of GdCoGe: TiNiSi type, $a = 0.6995$, $b = 0.4269$, $c = 0.7253$; X-ray powder analysis. The alloy was obtained by arc melting and annealing in an evacuated quartz tube at 870 K for 350 hours.

$Gd_3Co_2Ge_4$ crystallizes with the $Tb_3Co_2Ge_4$-type of structure, $a = 1.0472$, $b = 0.8057$, $c = 0.4177$, $\gamma = 107.84°$. The sample was prepared by arc melting and annealing at 873 K for 1450 h. The starting materials were Gd >99.9 mass%, Co 99.99 mass%, Ge 99.999 mass% (Mruz et al. 1989).

Gd_2CoGe_6 is isotypic with Ce_2CuGe_6, $a = 0.3952$, $b = 0.4019$, $c = 2.1471$ (Oleksyn et al. 1991; X-ray powder diffraction data). The sample was melted in an arc furnace and annealed at 1070 K in an evacuated quartz capsule for 400 h. The purity of the starting materials was greater than 99.9 mass%.

Bodak et al. (1986) reported the crystal structure for Gd_2CoGe_2 (Sc_2CoSi_2 type, $a = 1.0647$, $b = 1.0259$, $c = 0.4224$, $\gamma = 118.48°$; X-ray powder diffraction) from an arc melted sample annealed at 870 K.

4.9.4. *Gd–Ni–Ge*

$GdNi_5Ge_3$ was reported to crystallize with the YNi_5Si_3 type, $a = 1.9072$, $b = 0.3880$, $c = 0.6792$, by Fedyna et al. (1987). The arc melted alloy, annealed at 870 K, was investigated by X-ray powder diffraction analysis. The starting materials were Gd 99.83 mass%, Ni 99.99 mass% and Ge 99.99 mass%.

The $GdNi_2Ge_2$ compound was found to adopt the $CeGa_2Al_2$-type structure, $a = 0.4063$, $c = 0.9783$ (Rieger and Parthé 1969b).

$GdNiGe_3$ with the $SmNiSi_3$-type of structure ($a = 2.1545$, $b = 0.4079$, $c = 0.4073$, X-ray powder diffraction analysis) was reported by Bodak et al. (1985). For details of sample preparation and purity of starting materials, see $GdNi_5Ge_3$ under Gd–Ni–Ge.

Bodak et al. (1982) reported on the crystal structure of Gd_3NiGe_2 from X-ray powder diffraction (La_3NiGe_2 type, $a = 1.1450$, $b = 0.4220$, $c = 1.1355$). The proper amounts of starting components were arc melted and annealed at 870 K.

Gd_2NiGe_6 has been found by Oleksyn (1990) from X-ray powder diffraction to be isostructural with Ce_2CuGe_6 ($a = 0.3976$, $b = 0.4029$, $c = 2.133$). The sample was prepared by arc melting ingots of the constituting elements and annealing at 1070 K for 700 h. For the purity of starting materials, see $GdNi_5Ge_3$ under Gd–Ni–Ge.

Pecharsky et al. (1989) investigated the formation and crystal structure of the $GdNi_{0.95}Ge_2$ compound by X-ray powder analysis of arc melted alloys annealed at 870 K ($CeNiSi_2$ type, $a = 0.4128$, $b = 1.674$, $c = 0.4129$). For sample preparation, see $GdFe_{1-x}Ge_2$ under Gd–Fe–Ge. Francois et al. (1990) observed the formation of a homogeneity field for this compound: $GdNi_{0.40-0.95}Ge_2$, $CeNiSi_2$ type, $a = 0.4124$–0.4128, $b = 1.628$–1.674, $c = 0.4009$–0.4129.

$GdNi_{0.7-0.6}Ge_{1.3-1.4}$ crystallizes with the AlB_2 type, $a = 0.4111$–0.4101, $c = 0.4033$–0.4053 (Contardi et al. 1977).

Gorelenko et al. (1984) reported the crystal structure of GdNiGe: TiNiSi type, $a = 0.7009$, $b = 0.4280$, $c = 0.7283$; X-ray powder analysis. The alloy was obtained by arc melting and annealing in an evacuated quartz tube at 870 K for 350 hours.

4.9.5. *Gd–Cu–Ge*

Five ternary compounds have been found in the Gd–Cu–Ge system.

Rieger and Parthé (1969a) investigated the occurrence of the AlB_2-type structure by means of X-ray powder diffraction of arc melted alloys. The data presented were for a series of alloys $GdCu_{1-0.67}Ge_{1-1.33}$ with $a = 0.4228$–0.4136, $c = 0.3796$–0.4041. Iandelli (1993) confirmed the structure type for a GdCuGe sample (AlB_2 type, $a = 0.4241$, $c = 0.3755$, X-ray powder analysis). The alloy was prepared from turnings or powders of metals (gadolinium 99.7 mass%, copper and germanium 99.99 mass%) which were mixed and sealed in a tantalum crucible under argon, melted by induction heating and annealed for 10 days at 1023 K.

$Gd_6Cu_8Ge_8$ crystallizes with it own structure type; the lattice parameters are $a = 1.4000$, $b = 0.6655$, $c = 0.4223$ (Rieger 1970).

Konyk et al. (1988) investigated the crystal structure of Gd_2CuGe_6 alloy prepared by arc melting under argon and annealed at 870 K in an evacuated quartz tube for 720 h. From X-ray powder analysis a Ce_2CuGe_6-type was claimed, $a = 0.4003$, $b = 0.4120$, $c = 2.1096$.

Rieger and Parthé (1969b) prepared $GdCu_2Ge_2$ with the $CeGa_2Al_2$-type structure, $a = 0.4057$, $c = 1.0248$.

Francois et al. (1990) reported the crystal structure of the $GdCu_{0.32-0.47}Ge_2$ ($CeNiSi_2$ type, $a = 0.4118$–4133, $b = 1.644$–1670, $c = 0.3999$–0.4005). For sample preparation, see $GdFeGe_2$ under Gd–Fe–Ge.

4.9.6. *Gd–Nb–Ge*

The phase diagram of the Gd–Nb–Ge system has not been established.

The existence of a compound $Gd_2Nb_3Ge_5$ with the $Ce_2Sc_3Si_4$ type ($a = 0.6998$, $b = 1.3552$, $c = 0.7184$) was reported by Le Bihan et al. (1996a) from X-ray powder diffraction data of arc melted alloy. The starting materials were: Gd and Nb 99.99 mass%, Ge 99.999 mass%.

4.9.7. *Gd–Ru–Ge*

Early investigations of the $GdRu_2Ge_2$ compound determined the $CeGa_2Al_2$ type with $a = 0.4057$, $c = 0.9895$ (Francois et al. 1985) from X-ray powder analysis of alloy obtained by powder metallurgical reaction at 1273 K. The starting components were Gd (3N), Ru (4N) and Ge (4N).

Venturini et al. (1986b) reported that the $Gd_2Ru_3Ge_5$ compound crystallizes as the $U_2Co_3Si_5$-type. The lattice parameters were established as $a = 0.9840$, $b = 1.241$, $c = 0.5767$ (X-ray powder diffraction data; for sample preparation, see $La_2Ru_3Ge_5$ under La–Ru–Ge).

$Pr_3Rh_4Sn_{13}$ type was announced for the $Gd_3Ru_4Ge_{13}$ compound ($a = 0.8995$) by Segre et al. (1981a) from X-ray powder analysis of an arc melted sample annealed at 1523 K for 1 day and at 1273 K for 7 days. The starting materials were Gd (3N), Ru (3N) and Ge (6N).

Francois et al. (1990) reported the crystal structure of $GdRu_{0.23-0.36}Ge_2$ ($CeNiSi_2$ type, $a = 0.4146–4170$, $b = 1.606–1613$, $c = 0.4030–0.4064$). For sample preparation, see $GdFeGe_2$ under Gd–Fe–Ge.

4.9.8. *Gd–Rh–Ge*

Venturini et al. (1985b) reported an X-ray powder diffraction study of the $Gd_3Rh_4Ge_{13}$ compound from a sample which was prepared by heating mixture of starting components (La 3N, Ru 4N, Ge 4N) in an evacuated quartz tube at 1073 K. The crystal structure was found to adopt the $Yb_3Rh_4Sn_{13}$ type, $a = 0.8968$.

Early investigations of the $GdRh_2Ge_2$ compound determined it to have the $CeGa_2Al_2$-type structure: $a = 0.4127$, $c = 1.0142$ (Rossi et al. (1979)).

$Gd_2Rh_3Ge_5$ was found to crystallize with the $Lu_2Co_3Si_5$ type ($a = 0.9993$, $b = 1.2062$, $c = 0.5875$, $\beta = 91.7°$; X-ray powder diffraction data) by Venturini et al. (1986b) from a sample prepared by a powder metallurgical reaction at 1173 K. The purity of the starting materials was greater than 99.9 mass%.

Hovestreydt et al. (1982) reported the crystal structure of the GdRhGe compound (TiNiSi type, $a = 0.6993$, $b = 0.4329$, $c = 0.7511$; X-ray powder data) from an arc melted sample annealed at 1270 K for 1–2 weeks. The starting components were Gd (3N), Rh (4N) and Ge (5N).

Gladyshevsky et al. (1991a) reported on the crystal structure for the $Gd_3Rh_2Ge_2$ compound: $La_3Ni_2Ge_2$ type, $a = 0.5589$, $b = 0.7856$, $c = 1.3289$ (X-ray powder diffraction data). For the details of sample preparation, see $La_3Rh_2Ge_2$ under La–Rh–Ge.

Verniere et al. (1995) observed the existence of $Gd_4Rh_{13}Ge_9$ with $Ho_4Ir_{13}Ge_9$-type structure. No lattice parameters were reported. For details of sample preparation, see $La_4Ir_{13}Ge_4$ under La–Ir–Ge.

Francois et al. (1990) found a homogeneity field for the compound $GdCo_{0.24-0.37}Ge_2$, $CeNiSi_2$ type, $a = 0.4145–0.4169$, $b = 1.610–1.622$, $c = 0.4010–0.4054$. For sample preparation, see $GdFe_{0.25-0.46}Ge_2$ under Gd–Fe–Ge.

Venturini et al. (1984) observed the existence of the $Gd_5Rh_4Ge_{10}$ compound with the $Sc_5Co_4Si_{10}$ type from a sample which was obtained by heating in an evacuated tube at 1073 K.

4.9.9. *Gd–Pd–Ge*

No systematic study of the Gd–Pd–Ge system has been performed, but the existence of five ternary compounds has been established by different groups of authors.

The existence of the $GdPd_2Ge_2$ compound ($CeGa_2Al_2$ type, $a = 0.4255$, $c = 1.0035$) was reported by Rossi et al. (1979). Details of sample preparation are the same as for $LaPt_2Ge_2$.

Sologub et al. (1995a) reported on the X-ray powder analysis of the Gd_2PdGe_6 compound which was found to crystallize with the Ce_2CuGe_6 type, $a = 0.40953$, $b = 0.40320$, $c = 2.1624$. For the experimental procedure, see La_2PdGe_6 under La–Pd–Ge. The starting materials used were obtained from Johnson & Matthey, UK (99.9 mass%).

The crystal structure of the compound $GdPd_2Ge$ was observed to be of the YPd_2Si type, $a=0.7431$, $b=0.7014$, $c=0.5607$ (X-ray powder diffraction), by Jorda et al. (1983). For the experimental procedure, see $LaPd_2Ge$ under La–Pd–Ge. The starting materials were palladium 99.99 mass%; germanium in specpure quality, and gadolinium 99.9 mass%.

According to an X-ray powder diffraction analysis reported by Hovestreydt et al. (1982), the compound GdPdGe adopts the KHg_2-type structure, $a=0.44406$, $b=0.7054$, $c=0.7577$. For sample preparation, see LaPdGe under La–Pd–Ge. The starting materials were Gd (3N), Pd (4N) and Ge (5N).

Francois et al. (1990) observed the existence of a homogeneity field for the $GdPd_{0.30-0.43}Ge_2$ compound ($CeNiSi_2$ type, $a=0.4131$–0.4154, $b=1.630$–1.648, $c=0.4033$–0.4063). For sample preparation, see $GdFe_{0.25-0.46}Ge_2$ under Gd–Fe–Ge.

4.9.10. *Gd–Ag–Ge*

No ternary phase diagram has been established for the Gd–Ag–Ge system, however five ternary compounds have been characterized.

$GdAgGe_3$ was found to crystallize with a new structure type ($a=3.478$, $b=0.8313$, $c=0.8113$; X-ray single-crystal method) by Anisimova et al. (1992). The single crystal was isolated from a sample which was arc melted and annealed at 870 K for two weeks. The purity of the starting materials was greater than 99.9 mass%.

Sologub et al. (1995a) reported on the X-ray powder analysis of the Gd_2AgGe_6 compound which was found to crystallize with the Ce_2CuGe_6 type, $a=0.41946$, $b=0.40583$, $c=2.1166$. For the experimental procedure, see La_2AgGe_6 under La–Ag–Ge. The starting materials used were obtained from Johnson & Matthey, UK (99.9 mass%).

Anisimova et al. (1992, 1995) reported the existence of the $Gd_6Ag_8Ge_8$ ($Gd_6Cu_8Ge_8$ type) and $GdAg_2Ge_2$ ($CeGa_2Al_2$ type) compounds. No lattice parameters were given.

The crystal structure of the GdAgGe compound was first investigated by Zanicchi et al. (1983) by X-ray powder diffraction. It was found to adopt the ZrNiAl type with lattice parameters $a=0.7164$, $c=0.4241$. Gibson et al. (1996) reported a single-crystal investigation of this compound. The crystal structure was confirmed and lattice parameters were obtained as $a=0.7154$, $c=0.4237$ using a single crystal which was extracted from an arc melted sample annealed at 970 K for 10 days.

4.9.11. *Gd–Re–Ge*

The only information on the system Gd–Re–Ge is due to Francois et al. (1990) who investigated the occurrence of the compound with a $CeNiSi_2$ type; no phase diagram is available. The $GdRe_{0.25}Ge_2$ compound was found to adopt the $CeNiSi_2$ type with lattice parameters $a=0.4162$, $b=1.607$, $c=0.4056$ (X-ray powder diffraction data). For sample preparation, see $GdFe_{0.25-0.46}Ge_2$ under Gd–Fe–Ge.

4.9.12. *Gd–Os–Ge*

No phase diagram exists for the ternary Gd–Os–Ge system; one ternary compound has been observed and studied. The $Pr_3Rh_4Sn_{13}$-type structure was announced for the

$Gd_3Os_4Ge_{13}$ compound ($a = 0.9025$) by Segre et al. (1981a) from X-ray powder analysis of an arc melted sample annealed at 1523 K for 1 day and at 1273 K for 7 days. The starting materials were Gd (3N), Os (3N) and Ge (6N).

4.9.13. *Gd–Ir–Ge*

No ternary phase diagram has been established for the Gd–Ir–Ge system, however seven ternary compounds have been characterized.

Venturini et al. (1984) observed the $Gd_5Ir_4Ge_{10}$ compound with $Sc_5Co_4Si_{10}$-type structure from a sample obtained by heating a mixture of the starting components in an evacuated silica tube at 1073 K.

$Gd_2Ir_3Ge_5$ was found to crystallize with the $U_2Co_3Si_5$ type ($a = 1.0127$, $b = 1.178$, $c = 0.5980$, X-ray powder diffraction method) by Venturini et al. (1986b) from a sample prepared by a powder metallurgical reaction at 1173 K. The purity of the starting materials was greater than 99.9 mass%.

Venturini et al. (1985b) reported an X-ray powder diffraction study of the $Gd_3Ir_4Ge_{13}$ compound from a sample which was synthesized by heating a mixture of the starting components (Gd 3N, Ir 4N, Ge 4N) in an evacuated quartz tube at 1073 K. The crystal structure was found to adopt the $Yb_3Rh_4Sn_{13}$-type structure, $a = 0.8981$.

$GdIr_2Ge_2$ was found to crystallize in an orthorhombic structure with lattice parameters $a = 0.4113$, $b = 0.4207$, $c = 1.0167$ (Francois et al. 1985).

Hovestreydt et al. (1982) reported the crystal structure of the GdIrGe compound (TiNiSi type, $a = 0.6933$, $b = 0.4308$, $c = 0.7596$; X-ray powder data) from an arc melted sample annealed at 1270 K for 1–2 weeks. The starting components were Gd (3N), Ir (4N) and Ge (5N).

Verniere et al. (1995) have mentioned the existence of $Gd_4Ir_{13}Ge_9$ with $Ho_4Ir_{13}Ge_9$ type. No lattice parameters were given. For the experimental procedure, see $La_4Ir_{13}Ge_9$ under La–Ir–Ge.

Francois et al. (1987) reported the crystal structure of the $GdIrGe_2$ ($YIrGe_2$ type, $a = 0.4287$, $b = 1.600$, $c = 0.8845$). The sample was prepared by heating mixture of powders of starting components (Gd 3N, Ir 3N, Ge 3N) in an evacuated silica tube at 1173 K.

4.9.14. *Gd–Pt–Ge*

No phase diagram has been established for the Gd–Pt–Ge system. Four ternary compounds were observed by different authors.

According to an X-ray powder diffraction analysis Hovestreydt et al. (1982) reported the compound GdPtGe to adopt the TiNiSi-type structure, $a = 0.7071$, $b = 0.4370$, c 0.7571. For sample preparation, see LaPdGe under La–Pd–Ge.

The existence of the $GdPt_2Ge_2$ compound ($CeGa_2Al_2$ type, $a = 0.436$, $c = 0.977$) was reported by Rossi et al. (1979). For sample preparation see $LaMn_2Ge_2$ under La–Mn–Ge. Venturini et al. (1989a) investigated the crystal structure of $GdPt_2Ge_2$ from an arc melted sample annealed at 1273 K for 5 days. It was found to belong to the $LaPt_2Ge_2$ structure type, $a = 0.4324$, $b = 0.4362$, $c = 0.9717$, $\beta = 91.13°$. The starting materials were Gd (3N), Pt (4N) and Ge (4N).

Sologub et al. (1995a) reported an X-ray powder analysis of the Gd_2PtGe_6 compound which was found to crystallize with the Ce_2CuGe_6-type structure, $a=0.40693$, $b=0.40239$, $c=2.1793$. For sample preparation, see La_2PdGe_6 under La–Pd–Ge.

Francois et al. (1987) reported on the existence of the $GdPtGe_2$ with $YIrGe_2$-type. No lattice parameters were given. The sample was prepared by heating mixture of powders of starting components (Gd 3N, Pt 3N, Ge 3N) in evacuated silica tube at 1173 K.

4.9.15. *Gd–Au–Ge*

Information on interaction of gadolinium with gold and germanium is due to the work of two groups of authors (Sologub et al. 1995a, Rossi et al. 1992). The phase diagram of the Gd–Au–Ge system is not yet available; two ternary compounds have been observed and analyzed.

Sologub et al. (1995a) employed X-ray powder diffraction analysis for investigation the crystal structure of the Gd_2AuGe_6 compound from arc melted samples, which was homogenized by annealing at 873 K for 150 hours. The crystal structure was found to be isotypic with Ce_2CuGe_6 compound, $a=0.41325$, $b=0.40234$, $c=2.1187$.

A ternary compound of gadolinium with gold and germanium in the stoichiometric ratio 1:1:1 has been identified and studied by means of X-ray and metallographic analyses by Rossi et al. (1992). GdAuGe was found to adopt the LiGaGe type structure with lattice parameters $a=0.4432$, $c=0.7418$. The sample was prepared by melting the metals (about 99.9 mass% for gadolinium and 99.99 mass% for gold and germanium) in an induction furnace and annealing at 1070 K for 1 week.

4.10. *Tb–d element–Ge systems*

4.10.1. *Tb–Cr–Ge*

Brabers et al. (1994) reported the existence of a compound $TbCr_6Ge_6$ with the $HfFe_6Ge_6$ type ($a=0.5167$, $c=0.8275$; X-ray powder diffraction). The sample was prepared by arc melting and subsequent annealing at 1073 K for three weeks in vacuum.

4.10.2. *Tb–Mn–Ge*

A systematic study of the Tb–Mn–Ge system at 870 K was performed by Starodub et al. (1996) over the whole concentration region by means of X-ray powder analysis (fig. 87). The samples were prepared by arc melting under argon and annealed in evacuated quartz ampoules at 870 K for 240 hours. The starting materials were Tb 99.99 mass%, Mn 99.98 mass% and Ge 99.999 mass%.

The phase-field distribution in the isothermal section at 870 K is characterized by existence of four ternary compounds and by the formation of a homogeneity field for the $TbMn_{1-x}Ge_2$ (3) compound. Maximum solubility of manganese in the $TbGe_{1.5}$ compound is 5 at.%.

$TbMn_6Ge_6$ (1) was found to crystallize in the $HfFe_6Ge_6$-type structure by Venturini et al. (1992) ($a=0.5232$, $c=0.8169$; X-ray powder diffraction data). The alloy was

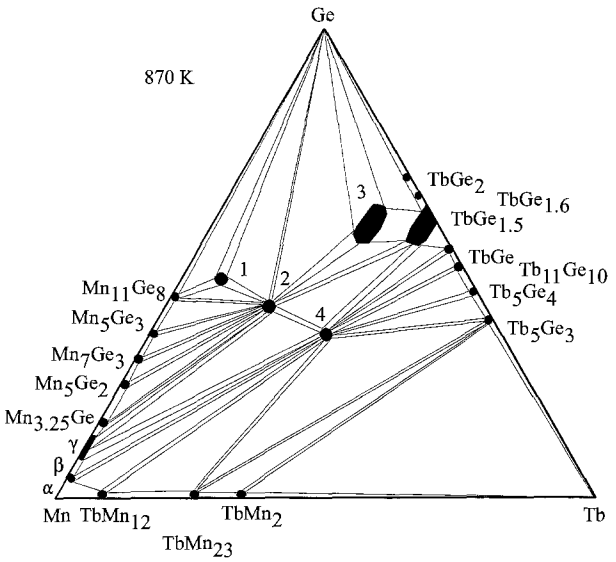

Fig. 87. Tb–Mn–Ge, isothermal section at 870 K.

synthesized by powder metallurgical reaction in evacuated silica tube at 1073 K for 14 days. Starodub et al. (1996) suggested the YCo_6Ge_6 type structure with lattice parameters $a = 0.5210$, $c = 0.4066$ (X-ray powder diffraction).

Rossi et al. (1978b) reported on investigation of the crystal structure of the $TbMn_2Ge_2$ (2) compound ($CeGa_2Al_2$ type, $a = 0.3999$, $c = 1.0850$; X-ray powder method). The alloy was obtained by melting under argon in an induction furnace and was annealed at 770 K for one week. The metals used were of purity greater than 99.9 mass% (Tb) and greater than 99.99 mass% (Mn, Ge). Starodub et al. (1996) confirmed the crystal structure and obtained slightly different lattice parameters: $a = 0.3998$, $c = 1.0775$.

$TbMn_{0.33}Ge_2$ (3) was found to adopt the $CeNiSi_2$ type with lattice parameters $a = 0.4135$, $b = 1.594$, $c = 0.4020$ by Francois et al. (1990) (X-ray powder diffraction data). For sample preparation, see $GdFe_{0.25-0.46}Ge_2$ under Gd–Fe–Ge. Starodub et al. (1996) confirmed the structure type and observed a homogeneity region for the compound with the $CeNiSi_2$ type: $TbMn_{0.30-0.35}Ge_2$, $a = 0.4114$–0.4202, $b = 1.5890$–1.6017, $c = 0.3994$–0.4160.

One more ternary compound was observed and investigated by Starodub et al. (1996): $Tb_9Mn_{10}Ge_{10}$ (4). It was found to adopt a $Tm_9Fe_{10}Ge_{10}$-type structure with lattice parameters $a = 0.5398$, $b = 1.3317$, $c = 1.3930$.

The crystal structures of TbMnGe (TiNiSi type, $a = 0.7077$, $b = 0.4132$, $c = 0.8166$), $Tb_3Mn_4Ge_4$ ($Gd_3Cu_4Ge_4$ type, $a = 1.3901$, $b = 0.7120$, $c = 0.4163$), and $TbMn_5Ge_3$ (YCo_5P_3 type, $a = 1.3050$, $b = 0.3904$, $c = 1.1408$) were derived using a single-crystal method (Venturini and Malaman 1997). Single crystals of TbMnGe and $Tb_3Mn_4Ge_4$ were extracted from ingots of the corresponding stoichiometry melted in an induction furnace.

The $TbMn_5Ge_3$ compound was synthesized from a stoichiometry mixture of commercially available high-purity elements compacted into pellets, sealed in a silica tube under argon and annealed at 1223 K for 5 days.

4.10.3. *Tb–Fe–Ge*

The phase diagram for the Tb–Fe–Ge system (fig. 88) was investigated by Starodub (1988) by means of metallographic and X-ray phase analyses. Alloys were prepared by arc melting followed by annealing at 870 K for 240 hours. The purity of the starting components was greater than 99.9 mass%. Six ternary compounds were observed.

$TbFe_6Ge_6$ (1) was reported to be isotypic with YCo_6Ge_6 with lattice parameters $a = 0.5106$, $c = 0.4055$ (Mruz et al. 1984). The sample was prepared by arc melting the proper amounts of starting components followed by annealing at 870 K for two weeks. At variance with these data, Venturini et al. (1992) using X-ray powder diffraction data found $TbFe_6Ge_6$ to crystallize with the $TbFe_6Sn_6$ type, $a = 0.8126$, $b = 1.776$, $c = 0.5125$. The alloy was obtained by powder metallurgical reaction in an evacuated silica tube at 1173 K for two weeks.

Pecharsky et al. (1989) reported $TbFe_{0.33}Ge_2$ (5) to crystallize with the $CeNiSi_2$-type structure ($a = 0.4123$, $b = 1.5830$, $c = 0.4006$; X-ray powder analysis). The alloy was arc melted and annealed at 870 K. The purity of the starting materials was greater than 99.9 mass%. Francois et al. (1990) confirmed the occurrence of the $CeNiSi_2$ type for terbium–iron–germanium combinations from the alloys annealed at 1173 K ($TbFe_{0.42}Ge_2$; $a = 0.4135$, $b = 1.591$, $c = 0.4026$).

Pecharsky et al. (1987) investigated the crystal structure of $Tb_{117}Fe_{52}Ge_{112}$ (6) by the X-ray single-crystal method (own structure type, $a = 2.8580$). The alloy was synthesized

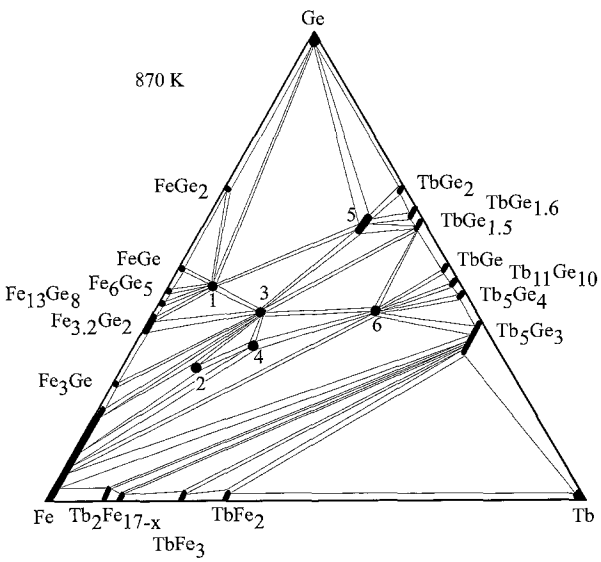

Fig. 88. Tb–Fe–Ge, isothermal section at 870 K.

by arc melting followed by annealing at 1070 K for 350 h. The starting materials were Tb 99.83 mass%, Fe 99.9 mass%, Ge 99.99 mass%.

According to X-ray powder diffraction data, $TbFe_2Ge_2$ (3) was found to be isostructural with the $CeGa_2Al_2$ type, with lattice parameters $a = 0.3966$, $c = 1.0470$ (Bara et al. 1990). The sample was synthesized by direct melting the high-purity constituent elements (Tb 4N, Fe 3N, Ge 5N) in an arc furnace. After melting, the sample was annealed at 1073 K for 1 week.

Two more ternary compounds with an unknown structure type were observed by Starodub (1988) at 870 K: $TbFe_4Ge_2$ (2) and $Tb_2Fe_4Ge_3$ (4).

4.10.4. *Tb–Co–Ge*

The isothermal section of the Tb–Co–Ge system at 870 K over the whole concentration region was derived by Starodub (1988) (fig. 89) employing X-ray and microstructural analyses of alloys which were prepared by arc melting the proper amounts of the high-purity constituent elements. The melted buttons were then annealed in evacuated silica tubes at 870 K for 300 hours. Ten ternary compounds were found to exist.

Méot-Meyer et al. (1985a) reported the crystal structure of $TbCo_xGe_2$, $x = 0.57$ (7) ($CeNiSi_2$ type, $a = 0.4117$, $b = 1.618$, $c = 0.4043$). The sample was prepared by powder metallurgical reaction and annealed in an evacuated silica tube at 1173 K. Pecharsky et al. (1989) confirmed the formation and crystal structure of the $TbCo_xGe_2$ compound from arc melted alloy annealed at 870 K ($a = 0.4110$–0.4122, $b = 1.5991$–1.6209, $c = 0.3999$–0.4050; X-ray powder analysis).

The crystal structure of $Tb_3Co_4Ge_{13}$ (2) ($Yb_3Rh_4Sn_{13}$ type, $a = 0.8764$; X-ray powder diffraction) was investigated by Venturini et al. (1985b) from a sample prepared by heating

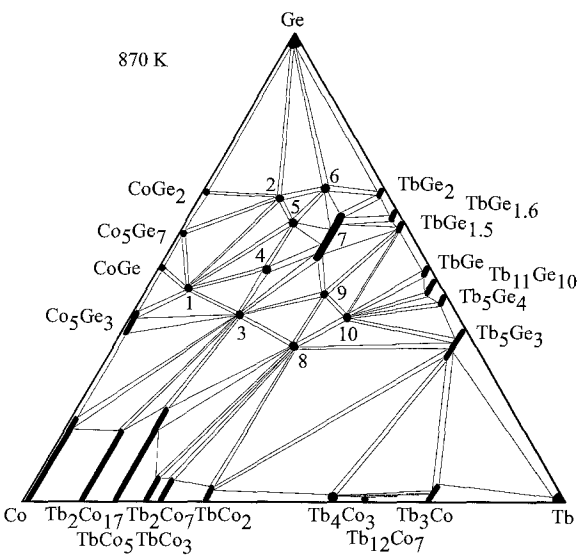

Fig. 89. Tb–Co–Ge, isothermal section at 870 K.

a compacted mixture of the starting materials (Tb in pieces, 99.9 mass%; Co and Ge in powder, 99.99 mass%) in an evacuated quartz tube at 1073 K. Bodak et al. (1987) reported the $Y_3Co_4Ge_{13}$ type for $Tb_3Co_4Ge_{13}$, $a = 0.8779$ (X-ray powder data) from arc melted alloy annealed at 870 K.

$TbCo_2Ge_2$ (3) was found to adopt the $CeGa_2Al_2$-type structure, $a = 0.3984$, $c = 1.0059$ (Starodub 1988; X-ray powder diffraction).

From X-ray powder analysis of an alloy annealed at 1173 K, $Tb_2Co_3Ge_5$ (4) was reported to adopt the $Lu_2Co_3Si_5$-type structure, $a = 0.9649$, $b = 1.183$, $c = 0.5715$, $\beta = 91.8°$ (Venturini et al. 1986b). Starodub (1988) announced the $U_2Co_3Si_5$-type structure with unknown lattice parameters for the $Tb_2Co_3Ge_5$ compound.

The crystal structure of the $TbCo_6Ge_6$ (1) compound was reported by Buchholz and Schuster (1981) (YCo_6Ge_6 structure type, $a = 0.5106$, c 0.4055). The sample was melted under argon in a corundum crucible at 1073–1273 K.

Gorelenko et al. (1984) reported the crystal structure of TbCoGe (8) (TiNiSi type, $a = 0.6955$, $b = 0.4242$, $c = 0.7271$; X-ray powder analysis). The alloy was obtained by arc melting and annealing in an evacuated quartz tube at 870 K for 350 hours.

$Tb_3Co_2Ge_4$ (9) crystallizes with a new type of structure, $a = 1.0692$, $b = 0.8067$, $c = 0.4164$, $\gamma = 107.72°$ (X-ray single-crystal data; Starodub et al. 1986). The sample was prepared by arc melting and annealing at 873 K for 240 h.

Tb_2CoGe_6 is isotypic with Ce_2CuGe_6 (6), $a = 0.3941$, $b = 0.4003$, $c = 2.1439$ (Oleksyn et al. 1991; X-ray powder diffraction data). The sample was melted in an arc furnace and annealed at 1070 K in an evacuated quartz capsule for 400 h. The purity of the starting materials was greater than 99.9 mass%.

Bodak et al. (1986) reported an X-ray single-crystal investigation of the compound Tb_2CoGe_2 (10): Sc_2CoSi_2 type, $a = 1.0569$, $b = 1.0209$, $c = 0.4212$, $\gamma = 118.18°$.

In the course of isothermal section studies, Starodub (1988) observed a compound $TbCoGe_3$ (5) with unknown structure.

4.10.5. *Tb–Ni–Ge*

Figure 90 represents the isothermal section of the Tb–Ni–Ge phase diagram at 870 K, which was studied by Starodub (1988). The isothermal section was constructed by means of X-ray powder analysis of 234 alloys which were arc melted and subsequently annealed in evacuated silica tubes for 400 h at 870 K and finally quenched in water. The starting materials were Tb 99.99 mass%, Ni 99.98 mass% and Ge 99.99 mass%.

The ternary phase equilibrium diagram is characterized by the existence of ten ternary compounds and by the formation of a substitutional exchange of Ge/Ni in the solid solutions $Tb_2(Ni_{1-x}Ge_x)_{17}$ and $Tb(Ni_{1-x}Ge_x)_5$ for $0 < x < 0.12$. This behavior corresponds to the solid solution range of Ge in nickel. Nonstoichiometry was observed for $TbNi_{1-x}Ge_2$. The binary Tb_2Ge_3 compound dissolves 12 at.% Ni.

$TbNi_5Ge_3$ (1) was reported to crystallize with the YNi_5Si_3 type, $a = 1.9068$, $b = 0.3871$, $c = 0.6790$ by Koterlyn et al. (1988). The arc melted alloy, annealed at 870 K, was investigated by X-ray powder diffraction analysis. The starting materials were Tb 99.83 mass%, Ni 99.99 mass% and Ge 99.99 mass%.

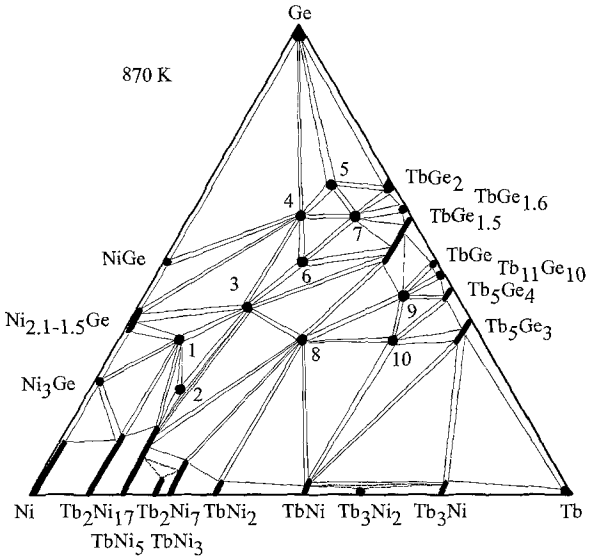

Fig. 90. Tb–Ni–Ge, isothermal section at 870 K

$Tb_3Ni_{11}Ge_4$ (2) belongs to the $Sc_3Ni_{11}Si_4$ type, $a = 0.8321$, $c = 0.8832$, after Koterlyn et al. (1988). The alloy was prepared in the same manner as $TbNi_5Ge_3$.

The $TbNi_2Ge_2$ (3) compound was found to adopt the $CeGa_2Al_2$-type structure, $a = 0.4044$, $c = 0.9782$ (Rieger and Parthé 1969b).

$TbNiGe_3$ (4) with the $ScNiSi_3$-type structure ($a = 2.1496$, $b = 0.4058$, $c = 0.4054$; X-ray powder diffraction analysis) was reported by Bodak et al. (1985). For the details of sample preparation and purity of starting materials, see $TbNi_5Ge_3$.

Tb_2NiGe_6 (5) has been found by Oleksyn (1990) from X-ray powder diffraction to be isostructural with Ce_2CuGe_6 ($a = 0.3955$, $b = 2.1224$, $c = 0.4001$). The sample was prepared by arc melting ingots of the constituting elements and annealing at 1070 K for 700 h. For the purity of starting materials, see $TbNi_5Ge_3$.

Pecharsky et al. (1989) investigated the formation and crystal structure of the $TbNi_{1-x}Ge_2$ (7) compound by X-ray powder analysis of an arc melted alloy annealed at 870 K ($CeNiSi_2$ type, $a = 0.4105$, $b = 1.621$, $c = 0.3993$). For sample preparation, see $TbNi_5Ge_3$. Francois et al. (1990) confirmed the structure and reported the composition and lattice parameters as $TbNi_{0.94}Ge_2$, $a = 0.4096$, $b = 1.637$, $c = 0.4086$ (X-ray powder diffraction) from a sample obtained by a powder metallurgical reaction at 1173 K.

Gorelenko et al. (1984) reported the crystal structure of TbNiGe (8) (TiNiSi type, $a = 0.6949$, $b = 0.4196$, $c = 0.7303$; X-ray powder analysis). The alloy was obtained by arc melting and annealing in an evacuated quartz tube at 870 K for 350 hours.

Bodak et al. (1982) reported on the crystal structure of Tb_3NiGe_2 (10) from X-ray powder diffraction (La_3NiGe_2 type, $a = 1.1381$, $b = 0.4222$, $c = 1.1257$). The proper amounts of starting components were arc melted and annealed at 870 K.

The crystal structures of two ternary compounds, $TbNiGe_2$ (6) and $Tb_{4.75}NiGe_{4.25}$ (9), have not been evaluated (Starodub 1988).

4.10.6. *Tb–Cu–Ge*

The isothermal section of the Tb–Cu–Ge system at 870 K was constructed by Starodub (1988) (fig. 91) as a result of an X-ray powder analysis of 125 alloys. Samples were obtained by arc melting the proper amounts of constituent elements (purity greater than 99.8 mass%) followed by annealing in evacuated quartz tubes at 870 K for 350 h. Finally samples were quenched in ice water. Phase relations are characterized by formation of four ternary compounds. The binary compound $TbCu_2$ dissolves about 15 at.% Ge. The existence of an extensive terminal solid solution of $TbGe_{1.5}$ which dissolves ~20 at.% Cu, and then shifts in stoichiometry from 1:1.5 to 1:2 as an additional ~10 at.% Cu is added, was observed during the investigation of the phase relations by Starodub (1988).

Rieger and Parthé (1969a) investigated the occurrence of the AlB_2 type structure by means of X-ray powder diffraction of arc melted alloys. The data presented are $TbCu_{1-0.67}Ge_{1-1.33}$ (4) with $a = 0.4122$–0.4218, $c = 0.3976$–0.3744. At variance with these data, Iandelli (1993) reported that TbCuGe had the $CaIn_2$-type structure ($a = 0.4247$, $c = 0.7336$, X-ray powder analysis). The alloy was prepared from turnings or powders of the metals (terbium 99.7 mass%, copper and germanium 99.99 mass%), which were mixed and sealed in a tantalum crucible under argon, melted by induction heating and annealed for 10 days at 1023 K. Starodub (1988) observed the AlB_2 type for the compound $TbCu_{1.0-1.2}Ge_{1.0-0.8}$ (4), $a = 0.4234$–0.4225, $c = 0.3688$–0.3658.

$Tb_6Cu_8Ge_8$ (2) crystallizes with the $Gd_6Cu_8Ge_8$ type, and the lattice parameters are $a = 1.392$, $b = 0.664$, $c = 0.420$ (Hanel and Nowotny 1970). Starodub (1988) confirmed the

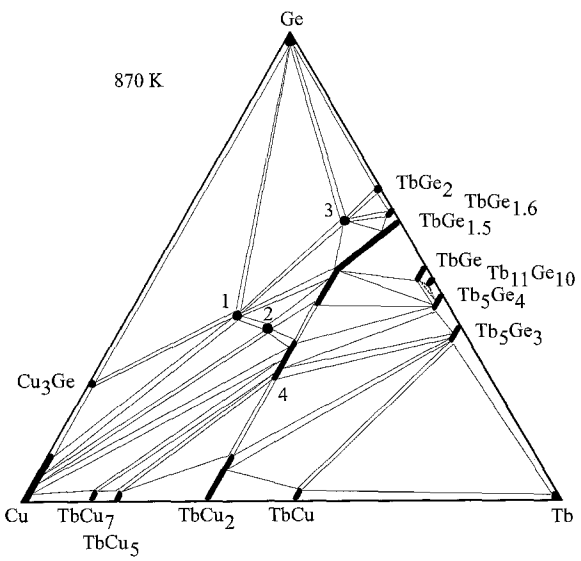

Fig. 91. Tb–Cu–Ge, isothermal section at 870 K.

crystal structure of the $Tb_6Cu_8Ge_8$ compound ($a = 1.3900$, $b = 0.6618$, $c = 0.4191$; X-ray powder diffraction) from an arc melted sample annealed at 870 K.

Konyk et al. (1988) investigated the crystal structure of Tb_2CuGe_6 (3) alloy prepared by arc melting under argon and annealed at 870 K in an evacuated quartz tube for 720 h. From X-ray powder analysis the authors concluded that this phase has Ce_2CuGe_6-type structure, $a = 0.4000$, $b = 0.4113$, $c = 2.1010$.

Rieger and Parthé (1969b) prepared $TbCu_2Ge_2$ (1) with the $CeGa_2Al_2$-type of structure, $a = 0.4044$, $c = 1.0248$. The existence and crystal structure of this compound was confirmed by Starodub (1988) from an arc melted sample annealed at 870 K.

Francois et al. (1990) observed the $CeNiSi_2$ type for the $TbCu_{0.39}Ge_2$ compound and reported lattice parameters $a = 0.4100$, $b = 1.648$, $c = 0.3995$ (X-ray powder diffraction) from the sample obtained by the powder metallurgical reaction at 1173 K. Apparently this phase does not exist at 870 K.

4.10.7. *Tb–Nb–Ge*

The phase diagram of the Tb–Nb–Ge system has not been established. However, the existence of the compound $Tb_2Nb_3Ge_4$ with the $Ce_2Sc_3Si_4$-type structure ($a = 0.6981$, $b = 1.3515$, $c = 0.7156$) was reported by Le Bihan et al. (1996a) from X-ray powder diffraction data of an arc melted alloy. Starting materials were Tb and Nb 99.99%, Ge 99.999%.

4.10.8. *Tb–Mo–Ge*

No phase diagram exists for the Tb–Mo–Ge system; only one compound was observed and investigated. $Tb_2Mo_3Ge_4$ was reported to crystallize with the $Ce_2Sc_3Si_4$-type structure ($a = 0.6921$, $b = 1.3149$, $c = 0.7062$) by Le Bihan et al. (1996b) from X-ray powder diffraction of an arc melted alloy. The starting materials were Tb and Mo 99.99 mass%, Ge 99.999 mass%.

4.10.9. *Tb–Ru–Ge*

Early investigations on the $TbRu_2Ge_2$ compound determined that it had the $CeGa_2Al_2$-type structure with $a = 0.4221$, $c = 0.9879$ (Francois et al. 1985) from X-ray powder analysis of an alloy obtained by powder metallurgical reaction at 1273 K. The starting components were Tb (3N), Ru (4N) and Ge (4N).

Venturini et al. (1986b) reported that the $Tb_2Ru_3Ge_5$ compound crystallizes with the $U_2Co_3Si_5$-type structure. The lattice parameters were reported as $a = 0.9793$, $b = 1.241$, $c = 0.5742$ (X-ray powder diffraction data). For sample preparation, see $La_2Ru_3Ge_5$ under La–Ru–Ge.

The $Pr_3Rh_4Sn_{13}$ type was announced for the $Tb_3Ru_4Ge_{13}$ compound ($a = 0.8965$) by Segre et al. (1981a) from X-ray powder analysis of an arc melted sample annealed at 1523 K for 1 day and at 1273 K for 7 days. The starting materials were Tb (3N), Ru (3N), Ge (6N).

4.10.10. *Tb–Rh–Ge*

Venturini et al. (1985b) reported an X-ray powder diffraction study of the $Tb_3Rh_4Ge_{13}$ compound from a sample which was prepared by heating a mixture of the starting components (Tb 3N, Rh 4N, Ge 4N) in an evacuated quartz tube at 1073 K. The crystal structure was found to adopt the $Yb_3Rh_4Sn_{13}$ type, $a = 0.8950$.

Francois et al. (1985) determined the $CeGa_2Al_2$ type for the $TbRh_2Ge_2$ compound, $a = 0.4118$, $c = 1.0280$.

$Tb_2Rh_3Ge_5$ was found to crystallize with $Lu_2Co_3Si_5$-type structure ($a = 0.9951$, $b = 1.2046$, $c = 0.5849$, $\beta = 91.9°$; X-ray powder diffraction data) by Venturini et al. (1986b) from a sample prepared by powder metallurgical reaction at 1173 K. The purity of the starting materials was greater than 99.9 mass%.

Hovestreydt et al. (1982) reported the crystal structure of the TbRhGe compound (TiNiSi type, $a = 0.6933$, $b = 0.4302$, $c = 0.7506$; X-ray powder data) from an arc melted sample annealed at 1270 K for 1–2 weeks. The starting components were Tb (3N), Rh (4N) and Ge (5N).

Gladyshevsky et al. (1991a) reported on the crystal structure for the $Tb_3Rh_2Ge_2$ compound ($La_3Ni_2Ge_2$ type, $a = 0.55627$, $b = 0.7808$, $c = 1.3233$; X-ray powder diffraction data). For the details of sample preparation, see $La_3Rh_2Ge_2$ under La–Rh–Ge.

Verniere et al. (1995) established that the compound $Tb_4Rh_{13}Ge_9$ formed the $Ho_4Ir_{13}Ge_9$-type structure. No lattice parameters were given. For experimental details, see $La_4Ir_{13}Ge_9$ under La–Ir–Ge.

Venturini et al. (1984) observed the existence of the $Tb_5Rh_4Ge_{10}$ compound with $Sc_5Co_4Si_{10}$-type structure ($a = 1.2970$, $c = 0.4285$; X-ray powder diffraction) from a sample obtained by heating a mixture of powders in an evacuated tube at 1073 K.

4.10.11. *Tb–Pd–Ge*

No systematic study of the Tb–Pd–Ge system has been performed, but the existence of three ternary compounds has been established by different groups of authors.

Sologub et al. (1995a) reported on the X-ray powder analysis of the Tb_2PdGe_6 compound which was found to crystallize with the Ce_2CuGe_6-type structure, $a = 0.40830$, $b = 0.40227$, $c = 2.1530$. For the experimental procedure, see La_2PdGe_6 under La–Pd–Ge. The starting materials used were obtained from Johnson & Matthey, UK (99.9 mass%).

The crystal structure of the compound $TbPd_2Ge$ was found to be of the YPd_2Si type ($a = 0.7390$, $b = 0.7028$, $c = 0.5598$; X-ray powder diffraction) by Jorda et al. (1983). For the experimental procedure, see $LaPd_2Ge$ under La–Pd–Ge. The starting materials were palladium 99.99 mass%, germanium in specpure quality, and terbium 99.9 mass%.

According to an X-ray powder diffraction analysis reported by Hovestreydt et al. (1982), the compound TbPdGe adopts the KHg_2-type of structure, $a = 0.4381$, $b = 0.7000$, $c = 0.7573$. For sample preparation, see LaPdGe under La–Pd–Ge. The starting materials were Tb (3N), Pd (4N) and Ge (5N).

4.10.12. *Tb–Ag–Ge*

No ternary phase diagram has been established for the Tb–Ag–Ge system, however two ternary compounds have been characterized.

The crystal structure of the $TbAg_{0.33}Ge_{1.67}$ compound has been investigated by Protsyk (1994) by means of X-ray analysis from alloy which was arc melted and annealed in an evacuated silica tube for 500 h at 770 K and finally quenched in water. The starting materials were Tb 99.85 mass%, Ag 99.9 mass% and Ge 99.99 mass%. It was found to adopt the α-$ThSi_2$-type structure with lattice parameters $a = 0.4066$, $c = 1.3783$.

Gibson et al. (1996) reported an X-ray single-crystal investigation of the TbAgGe compound. It was found to adopt the ZrNiAl type, $a = 0.71277$, $c = 0.42103$. The single crystal was extracted from an arc melted sample annealed at 970 K for 10 days.

4.10.13. *Tb–Os–Ge*

No phase diagram exists for the ternary Tb–Os–Ge system, but two ternary compounds have been observed.

$Pr_3Rh_4Sn_{13}$-type was announced for the $Tb_3Os_4Ge_{13}$ compound ($a = 0.9002$) by Segre et al. (1981a) from X-ray powder analysis of an arc melted sample annealed at 1523 K for 1 day and at 1273 K for 7 days. The starting materials were Tb (3N), Os (3N) and Ge (6N).

Venturini et al. (1986b) observed the existence of the $Tb_2Os_3Ge_5$ compound with $Sc_5Co_4Si_{10}$ type structure from a sample obtained by heating a mixture of the starting components in an evacuated quartz tube at 1173 K.

4.10.14. *Tb–Ir–Ge*

No ternary phase diagram has been established for the Tb–Ir–Ge system, however eight ternary compounds have been characterized.

Venturini et al. (1984) observed the existence of the $Tb_5Ir_4Ge_{10}$ compound with $Sc_5Co_4Si_{10}$ type, $a = 1.2935$, $c = 0.4318$, from a sample obtained by heating a mixture of the starting components in an evacuated quartz tube at 1073 K.

$Tb_2Ir_3Ge_5$ was found to crystallize with $U_2Co_3Si_5$-type structure ($a = 1.0122$, $b = 1.276$, $c = 0.5790$, X-ray powder diffraction method) by Venturini et al. (1986b) from a sample prepared by powder metallurgical reaction at 1173 K. The purity of the starting materials was greater than 99.9 mass%.

Venturini et al. (1985b) reported on the X-ray powder diffraction study of the $Tb_3Ir_4Ge_{13}$ compound from an alloy which was synthesized by heating a mixture of the starting components (Tb 3N, Ir 4N, Ge 4N) in an evacuated quartz tube at 1073 K. The crystal structure was found to adopt the $Yb_3Rh_4Sn_{13}$ type, $a = 0.8962$.

$TbIr_2Ge_2$ was found to adopt a tetragonal structure with lattice parameters $a = 0.4144$, $c = 1.0222$ (Francois et al. 1985).

Hovestreydt et al. (1982) reported the crystal structure for the TbIrGe compound (TiNiSi type, $a = 0.6871$, $b = 0.4280$, $c = 0.7591$; X-ray powder data) from an arc melted

sample annealed at 1270 K for 1–2 weeks. The starting components were Tb (3N), Ir (4N) and Ge (5N).

Verniere et al. (1995) announced the $Ho_4Ir_{13}Ge_9$-type structure for $Tb_4Ir_{13}Ge_9$. No lattice parameters were given. For the experimental procedure, see $La_4Ir_{13}Ge_9$ under La–Ir–Ge.

Francois et al. (1987) reported the crystal structure of $TbIrGe_2$ ($NdIrGe_2$ type, $a = 0.4266$, $b = 1.595$, $c = 0.8829$). The sample was prepared by heating a mixture of powders of the starting components (Tb 3N, Ir 3N and Ge 3N) in an evacuated silica tube at 1173 K.

$Tb_4Ir_7Ge_6$ was reported to adopt the $U_4Re_7Si_6$-type structure ($a = 0.8345$; Francois et al. 1985) from a sample obtained by heating a mixture of powders of the starting materials (Tb 3N, Os and Ge 4N) in an evacuated quartz tube at 1273 K.

4.10.15. *Tb–Pt–Ge*

No phase diagram has been established for the Tb–Pt–Ge system. Four ternary compounds were observed by different authors.

According to an X-ray powder diffraction analysis reported by Hovestreydt et al. (1982), the compound TbPtGe adopts the TiNiSi-type of structure, $a = 0.7020$, $b = 0.4354$, $c = 0.7564$. For sample preparation, see LaPdGe under La–Pd–Ge.

The existence of the $TbPt_2Ge_2$ compound ($CeGa_2Al_2$ type, $a = 0.436$, $c = 0.977$) was reported by Rossi et al. (1979). For sample preparation see $LaMn_2Ge_2$ under La–Mn–Ge. Venturini et al. (1989a) investigated the crystal structure of $TbPt_2Ge_2$ from an arc melted sample annealed at 1273 K for 5 days. The crystal structure was found to belong to the $LaPt_2Ge_2$ type, $a = 0.4311$, $b = 0.4351$, $c = 0.9711$, $\beta = 91.09°$. The starting materials were Tb (3N), Pt (4N) and Ge (4N).

Sologub et al. (1995a) reported on the X-ray powder analysis of the Tb_2PtGe_6 compound which was found to crystallize with the Ce_2CuGe_6 type, $a = 0.40634$, $b = 0.40155$, $c = 2.1648$. For sample preparation, see La_2PdGe_6 under La–Pd–Ge.

Francois et al. (1987) mentioned the existence of $TbPtGe_2$ with $YIrGe_2$-type structure. No lattice parameters were given. The sample was prepared by heating a mixture of powders of the starting components (Gd 3N, Ir 3N, Ge 3N) in an evacuated silica tube at 1173 K.

4.10.16. *Tb–Au–Ge*

Information on interaction of terbium with gold and germanium is due to the work of two groups of authors (Sologub et al. 1995a and Rossi et al. 1992). The phase diagram of the Tb–Au–Ge system is not yet available; two ternary compounds have been observed and their structures were determined.

Sologub et al. (1995a) employed X-ray powder diffraction analysis for studying the crystal structure of Tb_2AuGe_6. It was found to be isotypic with Ce_2CuGe_6, $a = 0.41325$, $b = 0.40234$, $c = 2.1187$. For the details of sample preparation, see Gd_2AuGe_6 under Gd–Au–Ge.

A ternary compound of terbium with gold and germanium in the stoichiometric ratio 1:1:1 has been identified and studied by means of X-ray and metallographic analyses by Rossi et al. (1992). TbAuGe was found to adopt the LiGaGe type with lattice parameters $a = 0.4416$, $c = 0.7335$. For the experimental procedure see GdAuGe under Gd–Au–Ge.

4.11. *Dy–d element–Ge systems*

4.11.1. *Dy–Cr–Ge*

The only reference on the Dy–Cr–Ge system is due to Brabers et al. (1994) who reported the existence of a compound $DyCr_6Ge_6$ with the $HfFe_6Ge_6$ type ($a = 0.5162$, $c = 0.8272$; X-ray powder diffraction). The sample was prepared by arc melting and subsequent annealing at 1073 K for three weeks in vacuum.

4.11.2. *Dy–Mn–Ge*

No ternary phase diagram of the Dy–Mn–Ge system is available. Two ternary compounds have been reported for various dysprosium manganese germanium combinations.

$DyMn_6Ge_6$ was found to crystallize in the $HfFe_6Ge_6$-type structure by Venturini et al. (1992), $a = 0.5228$, $c = 0.8163$ (X-ray powder diffraction data). The alloy was synthesized by a powder metallurgical reaction in an evacuated silica tube at 1073 K for 14 days.

Rossi et al. (1978b) reported on the crystal structure of the $DyMn_2Ge_2$ compound ($CeGa_2Al_2$ type, $a = 0.3980$, $c = 1.0737$; X-ray powder method). The alloy was obtained by melting under argon in an induction furnace and annealing at 770 K for a week. The metals used were of purity greater than 99.9 mass% for Dy, and greater than 99.99 mass% for Mn and Ge.

The $DyMn_{0.33}Ge_2$ compound was found to adopt the $CeNiSi_2$-type structure with lattice parameters $a = 0.4118$, $b = 1.583$, $c = 0.4000$ by Francois et al. (1990) (X-ray powder diffraction data). For sample preparation, see $GdFe_{0.25-0.46}Ge_2$ under Gd–Fe–Ge.

4.11.3. *Dy–Fe–Ge*

No phase diagram has been constructed for the Dy–Fe–Ge system, but six ternary compounds have been found and characterized by different authors.

$DyFe_6Ge_6$ was reported to be isotypic with YCo_6Ge_6 with lattice parameters $a = 0.5108$, $c = 0.4044$ (Mruz et al. 1984). The sample was prepared by arc melting of the proper amounts of the starting components followed by annealing at 870 K for two weeks. At variance with these data, $DyFe_6Ge_6$ was found to crystallize with the $TbFe_6Sn_6$ type, $a = 0.8111$, $b = 1.766$, $c = 0.5116$ by Venturini et al. (1992) from X-ray powder diffraction data. The alloy was obtained by a powder metallurgical reaction in an evacuated silica tube at 1173 K for two weeks.

Pecharsky et al. (1989) reported $DyFe_{0.33}Ge_2$ to crystallize with the $CeNiSi_2$-type structure ($a = 0.4118$, $b = 1.5903$, $c = 0.4002$; X-ray powder analysis). The alloy was arc melted and annealed at 870 K. The purity of the starting materials was greater than

99.9 mass%. Francois et al. (1990) confirmed the crystal structure of this compound, a = 0.4121, b = 1.581, c = 0.4011 (X-ray powder diffraction data). For sample preparation, see $GdFe_{0.25-0.46}Ge_2$ under Gd–Fe–Ge.

$DyFe_4Ge_2$ is isotypic with the crystal structure of $ZrFe_4Si_2$; a = 0.7303, c = 0.3865 according to Fedyna (1988). The alloy was prepared by arc melting the proper amounts of the starting components followed by annealing at 870 K for 400 hours.

Oleksyn (1990) investigated the crystal structure of $Dy_{117}Fe_{52}Ge_{112}$ compound by the X-ray powder method ($Tb_{117}Fe_{52}Ge_{112}$ type, a = 2.8382). The alloy was synthesized by arc melting followed by annealing at 1070 K for 350 h. The starting materials were Dy 99.83 mass%, Fe 99.9 mass%, Ge 99.99 mass%.

According to X-ray powder diffraction, $DyFe_2Ge_2$ was found to be isostructural with the $CeGa_2Al_2$ type, a = 0.3957, c = 1.0446 (Rossi et al. 1978a).

$Dy_6Fe_8Ge_8$ has the $Gd_6Cu_8Ge_8$ type structure, a = 1.3528, b = 0.6793, c = 0.4135 (X-ray powder diffraction; Fedyna et al. 1994).

4.11.4. *Dy–Co–Ge*

The phase diagram for the Dy–Co–Ge system has not been established. Nine ternary compounds have been identified for various dysprosium–cobalt–germanium combinations.

Méot-Meyer et al. (1985a) reported the crystal structure of the $DyCo_{1-x}Ge_2$, x = 0.44 ($CeNiSi_2$ type, a = 0.4098, b = 1.607, c = 0.4020). Samples were prepared by powder metallurgical reaction and annealed in an evacuated silica tube at 1173 K. Pecharsky et al. (1989) investigated the formation and crystal structure of the $DyCo_{1-x}Ge_2$ compound by X-ray powder analysis of arc melted alloys annealed at 870 K. The $CeNiSi_2$-type structure was confirmed with lattice parameters a = 0.4130–0.4135, b = 1.6045–1.6057, c = 0.4026–0.4028.

The crystal structure of $Dy_3Co_4Ge_{13}$ ($Yb_3Rh_4Sn_{13}$ type, a = 0.8744; X-ray powder diffraction) was investigated by Venturini et al. (1985b) from a sample which was prepared by heating a compacted mixture of the starting materials (Dy in pieces, 99.9 mass%; Co and Ge in powder, 99.99 mass%) in an evacuated quartz tube at 1073 K. Bodak et al. (1987) reported the $Y_3Co_4Ge_{13}$ type for the $Dy_3Co_4Ge_{13}$ compound (a = 0.8750; X-ray powder data) from arc melted alloy annealed at 870 K.

From X-ray powder analysis of an alloy annealed at 1173 K, $Dy_2Co_3Ge_5$ was reported to adopt $Lu_2Co_3Si_5$-type structure, a = 0.9627, b = 1.180, c = 0.5707, β = 91.0° (Venturini et al. 1986b).

The crystal structure of the $DyCo_6Ge_6$ compound was reported by Buchholz and Schuster (1981) (YCo_6Ge_6 structure type, a = 0.5081, c = 0.3918). The sample was melted under argon in a corundum crucible at 1073–1273 K.

Gorelenko et al. (1984) reported the crystal structure of DyCoGe (TiNiSi type, a = 0.6886, b = 0.4204, c = 0.7256; X-ray powder analysis). The alloy was arc melted and annealed in an evacuated quartz tube at 870 K for 350 hours.

$Dy_3Co_2Ge_4$ crystallizes with the $Tb_3Co_2Ge_4$ type structure, a = 1.0590, b = 0.8114, c = 0.4135, γ = 107.83°. The sample was prepared by arc melting and annealing at

873 K for 1450 h. The starting materials were: Dy >99.9 mass%, Co 99.99 mass%, Ge 99.999 mass% (Mruz et al. 1989).

Dy_2CoGe_6 is isotypic with Ce_2CuGe_6, $a = 0.3931$, $b = 0.3983$, $c = 2.1341$ (Oleksyn et al. 1991, X-ray powder diffraction data). The sample was melted in an arc furnace and annealed at 1070 K in an evacuated quartz capsule for 400 hours. The purity of the starting materials was greater than 99.9 mass%.

Bodak et al. (1986) reported the crystal structure for Dy_2CoGe_2 (Sc_2CoSi_2 type, $a = 1.0467$, $b = 1.0132$, $c = 0.4178$, $\gamma = 117.33°$; X-ray powder diffraction) from an arc melted sample annealed at 870 K.

4.11.5. *Dy–Ni–Ge*

Figure 92 represents the isothermal section of the Dy–Ni–Ge phase diagram at 870 K, which was studied by Koterlyn et al. (1988). The isothermal section was constructed by means of X-ray powder analysis of alloys, which were arc melted, subsequently annealed in evacuated silica tubes for 400 h at 870 K, and finally quenched in ice water. The starting materials were Dy 99.99 mass%, Ni 99.98 mass% and Ge 99.99 mass%.

The ternary phase diagram is characterized by the existence of ten ternary compounds and by the formation of a substitutional exchange of Ge/Ni in the Ni terminal solid solutions $Dy_2(Ni_{1-x}Ge_x)_{17}$ and $Dy(Ni_{1-x}Ge_x)_5$. Nonstoichiometry and a homogeneity range were observed for $DyNi_{1-x}Ge_2$ (7). The binary Dy_2Ge_3 compound dissolves 20 at.% Ni.

$DyNi_5Ge_3$ (1) was reported to crystallize with the YNi_5Si_3 type, $a = 1.9065$, $b = 0.3864$, $c = 0.6787$, by Fedyna (1988). The arc melted alloy, annealed at 870 K, was investigated

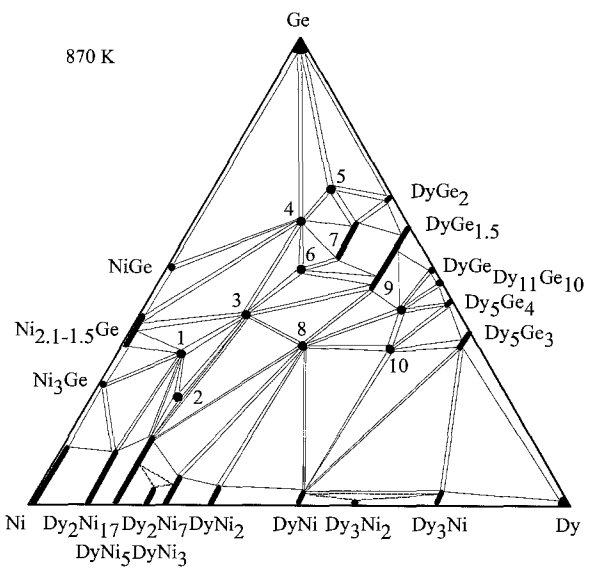

Fig. 92. Dy–Ni–Ge, isothermal section at 870 K.

by X-ray powder diffraction analysis. The starting materials were Dy 99.83 mass%, Ni 99.99 mass%, and Ge 99.99 mass%.

$Dy_3Ni_{11}Ge_4$ (2) belongs to the $Sc_3Ni_{11}Si_4$ type, $a = 0.8317$, $c = 0.8807$, after Fedyna (1988). For sample preparation, see $DyNi_5Ge_3$ under Dy–Ni–Ge.

The $DyNi_2Ge_2$ (3) compound was found to adopt the $CeGa_2Al_2$-type structure, $a = 0.4035$, $c = 0.9758$ (Rieger and Parthé 1969b).

$DyNiGe_3$ (4) with the $ScNiSi_3$-type structure ($a = 2.1430$, $b = 0.4054$, $c = 0.4042$, X-ray powder diffraction analysis) was reported by Bodak et al. (1985). For the details of sample preparation and purity of starting materials, see $DyNi_5Ge_3$, above.

Dy_2NiGe_6 (5) has been found by Oleksyn (1990) from X-ray powder diffraction to be isostructural with Ce_2CuGe_6 ($a = 0.3955$, b 2.1170, $c = 0.4007$). Samples were prepared by arc melting ingots of the constituting elements and annealing at 1070 K for 700 h. For the purity of starting materials, see $DyNi_5Ge_3$, above.

Pecharsky et al. (1989) investigated the formation and crystal structure of the $DyNi_{1-x}Ge_2$ (7) compound by X-ray powder analysis of an arc melted alloy annealed at 870 K ($CeNiSi_2$ type, $a = 0.4102$, $b = 1.6216$, $c = 0.4013$). For sample preparation, see $DyFe_{1-x}Ge_2$ under Dy–Fe–Ge. Francois et al. (1990) confirmed the structure and reported the composition and lattice parameters $DyNi_{0.80}Ge_2$, $a = 0.4093$, $b = 1.651$, $c = 0.4052$ (X-ray powder diffraction) from a sample obtained by a powder metallurgical reaction at 1173 K.

Gorelenko et al. (1984) reported the crystal structure for DyNiGe (8) (TiNiSi type, $a = 0.6963$, $b = 0.4213$, $c = 0.7285$; X-ray powder analysis). The alloy was obtained by arc melting and annealing in an evacuated quartz tube at 870 K for 350 hours.

Bodak et al. (1982) reported on the crystal structure for the Dy_3NiGe_2 (10) compound from X-ray powder diffraction (La_3NiGe_2-type structure, $a = 1.1272$, $b = 0.4207$, $c = 1.1218$). The proper amounts of starting components were arc melted and annealed at 870 K.

The crystal structure of two ternary compounds $DyNiGe_2$ (6) and $Dy_{4.75}NiGe_{4.25}$ (9) has not been evaluated yet (Koterlyn et al. 1988).

4.11.6. *Dy–Cu–Ge*

No isothermal section is available for the Dy–Cu–Ge system; four ternary compounds have been found and analyzed by various groups of authors.

Rieger and Parthé (1969a) investigated the occurrence of the AlB_2-type structure by means of X-ray powder diffraction of arc melted alloys. The data presented were $DyCu_{1-0.67}Ge_{1-1.33}$ with $a = 0.4221$–0.4038, $c = 0.3664$–0.3637. At variance with these data, Iandelli (1993) observed DyCuGe with the $CaIn_2$-type ($a = 0.4239$, $c = 0.7239$, X-ray powder analysis). The alloy was obtained from turnings or powders of metals (Dy 99.7 mass%, Cu and Ge 99.99 mass%), which were mixed and sealed in a tantalum crucible under argon, melted by induction heating and annealed for 10 days at 1023 K.

$Dy_6Cu_8Ge_8$ crystallizes with the $Gd_6Cu_8Ge_8$ type, lattice parameters $a = 1.3845$, $b = 0.6618$, $c = 0.4173$ (Rieger 1970).

Konyk et al. (1988) investigated the crystal structure of Dy_2CuGe_6 alloy synthesized by arc melting under argon and annealing at 870 K in an evacuated quartz tube for 720 h. From X-ray powder analysis a Ce_2CuGe_6-type structure was claimed for this phase, $a=0.3993$, $b=0.4100$, $c=2.0939$.

Rieger and Parthé (1969b) observed $DyCu_2Ge_2$ with the $CeGa_2Al_2$-type structure, $a=0.4029$, $c=1.0281$.

Francois et al. (1990) observed the $CeNiSi_2$ type for the $DyCu_{0.38}Ge_2$ compound and reported lattice parameters $a=0.4092$, $b=1.635$, $c=0.3968$ (X-ray powder diffraction) from a sample obtained by the powder metallurgical reaction at 1173 K.

4.11.7. *Dy–Nb–Ge*

A phase diagram for the Dy–Nb–Ge system has not been established. However, the existence of a compound $Dy_2Nb_3Ge_4$ with the $Ce_2Sc_3Si_4$-type ($a=0.6975$, $b=1.3510$, $c=0.7154$) was reported by Le Bihan et al. (1996a) from X-ray powder diffraction analysis of arc melted alloy. The starting materials were: Dy and Nb 99.99 mass%, Ge 99.999 mass%.

4.11.8. *Dy–Mo–Ge*

The existence of the $Dy_2Mo_3Ge_4$ compound with the $Ce_2Sc_3Si_4$ type ($a=0.6892$, $b=1.3112$, $c=0.7038$) was reported by Le Bihan et al. (1996b). For the sample preparation and purity of starting materials, see Dy–Nb–Ge.

4.11.9. *Dy–Ru(Rh, Pd)–Ge*

The ternary Dy–Ru(Rh, Pd)–Ge systems have been studied only with respect to the formation of compounds with specific composition and structure. Their crystallographic characteristics are listed in table 27.

4.11.10. *Dy–Ag–Ge*

No ternary phase diagram has been established for the Dy–Ag–Ge system, however one ternary compound has been characterized.

The crystal structure of the DyAgGe compound was firstly investigated by Zanicchi et al. (1983) using X-ray powder diffraction. It was found to adopt the ZrNiAl type with lattice parameters $a=0.7105$, $c=0.4198$. Gibson et al. (1996) reported the single-crystal investigation of this compound. The crystal structure was confirmed and lattice parameters were obtained as $a=0.71056$, $c=0.41960$. The single crystal was extracted from an arc melted sample annealed at 970 K for ten days.

4.11.11. *Dy–Os(Ir, Pt)–Ge*

No systematic studies have been performed for the ternary Dy–Os(Ir, Pt)–Ge systems. Interaction of dysprosium with osmium (irridium, platinum) and germanium has been studied only with respect to the formation of compounds with a specific composition and structure. The crystallographic characteristics are listed in table 28.

Table 27
Crystallographic data for the ternary Dy–Ru(Rh, Pd)–Ge compounds

Compound	Structure	Lattice parameters (nm)			Reference
		a	*b*	*c*	
$DyRu_2Ge_2$	$CeGa_2Al_2$	0.4219		0.9856	Francois et al. (1985)
$Dy_2Ru_3Ge_5$	$U_2Co_3Si_5$	0.9783	1.241	0.5723	Venturini et al. (1986b)
$Dy_3Ru_4Ge_{13}$	$Yb_3Rh_4Sn_{13}$	0.895			Segre et al. (1981a)
$DyRh_2Ge_2$	$CeGa_2Al_2$	0.4104		1.0253	Francois et al. (1985)
$Dy_2Rh_3Ge_5$	$Lu_2Co_3Si_5$	0.9940	1.2035 $\beta = 92.0°$	0.5827	Venturini et al. (1986b)
$Dy_5Rh_4Ge_{10}$	$Sc_5Co_4Si_{10}$				Méot-Meyer et al. (1985b)
$Dy_4Rh_7Ge_6$	$U_4Re_7Si_6$	0.8326			Francois et al. (1985)
$Dy_3Rh_4Ge_{13}$	$Yb_3Rh_4Sn_{13}$	0.8928			Venturini et al. (1985b)
$Dy_4Rh_{13}Ge_9$	$Ho_4Ir_{13}Ge_9$				Verniere et al. (1995)
DyRhGe	TiNiSi	0.6899	0.4289	0.7521	Hovestreydt et al. (1982)
$DyPd_2Ge$	YPd_2Si	0.7355	0.7033	0.5565	Jorda et al. (1983)
Dy_2PdGe_6	Ce_2CuGe_6	0.4073	0.4016	2.1485	Sologub et al. (1995a)
$DyPd_2Ge_2$	$CeGa_2Al_2$	0.4035		0.9758	Rossi et al. (1979)
DyPdGe	KHg_2	0.4366	0.6963	0.7556	Hovestreydt et al. (1982)

Table 28
Crystallographic data for the ternary Dy–Os(Ir, Pt)–Ge compounds

Compound	Structure	Lattice parameters (nm)			Reference
		a	*b*	*c*	
$Dy_5Os_4Ge_{10}$	$Sc_5Co_4Si_{10}$				Méot-Meyer et al. (1985b)
$Dy_3Os_4Ge_{13}$	$Yb_3Rh_4Sn_{13}$	0.8986			Segre et al. (1981a)
$DyIrGe_2$	$NdIrGe_2$	0.4256	1.593	0.8815	Francois et al. (1987)
$Dy_2Ir_3Ge_5$	$U_2Co_3Si_5$	1.0122	1.171	0.5950	Venturini et al. (1986b)
$Dy_4Ir_7Ge_6$	$U_4Re_7Si_6$	0.8322			Francois et al. (1985)
$Dy_5Ir_4Ge_{10}$	$Sc_5Co_4Si_{10}$				Méot-Meyer et al. (1985b)
$Dy_3Ir_4Ge_{13}$	$Yb_3Rh_4Sn_{13}$	0.8937			Venturini et al. (1985b)
$Dy_4Ir_{13}Ge_9$	$Ho_4Ir_{13}Ge_9$				Verniere et al. (1995)
DyIrGe	TiNiSi	0.6838	0.4266	0.7597	Hovestreydt et al. (1982)
$DyPtGe_2$	$NdIrGe_2$				Francois et al. (1987)
$DyPt_2Ge_2$	$CeGa_2Al_2$	0.434		0.975	Rossi et al. (1979)
	$LaPt_2Ge_2$	0.4301	0.4346 $\beta = 91.26°$	0.9682	Venturini et al. (1989a)
DyPtGe	TiNiSi	0.6983	0.4340	0.7554	Hovestreydt et al. (1982)
Dy_2PtGe_6	Ce_2CuGe_6	0.4043	0.4005	2.1672	Sologub et al. (1995a)

4.11.12. *Dy–Au–Ge*

No ternary phase diagram exists for the Dy–Au–Ge system, however, a ternary compound of dysprosium with gold and germanium in the stoichiometric ratio 1:1:1 has been identified and studied by means of X-ray and metallographic analyses by Rossi et al. (1992). DyAuGe was found to adopt the LiGaGe type with lattice parameters $a = 0.4411$, $c = 0.7287$. The sample was prepared by melting the metals (around 99.9 mass% for dysprosium and 99.99 mass% for gold and germanium) in an induction furnace and annealing at 1070 K for one week.

4.12. *Ho–d element–Ge systems*

4.12.1. *Ho–Cr–Ge*

Brabers et al. (1994) reported the existence of the compound $HoCr_6Ge_6$ with the $HfFe_6Ge_6$ type structure ($a = 0.5158$, $c = 0.8269$; X-ray powder diffraction). The sample was prepared by arc melting and subsequent annealing at 1073 K for three weeks in a vacuum.

4.12.2. *Ho–Mn–Ge*

No phase diagram is available for the ternary Ho–Mn–Ge system; however three ternary compounds have been observed and characterized by different authors.

Venturini et al. (1992) reported the existence of the compound $HoMn_6Ge_6$ with the $HfFe_6Ge_6$ type ($a = 0.5230$, $c = 0.8155$; X-ray powder diffraction). The sample was synthesized from a mixture of stoichiometric amounts of the elements, which was compacted and sealed in a silica tube under argon followed by annealing at 1073 K for two weeks.

Rossi et al. (1978b) reported an investigation of the crystal structure of the $HoMn_2Ge_2$ compound ($CeGa_2Al_2$ type, $a = 0.3977$, $c = 1.0845$; X-ray powder method). The alloy was obtained by melting under argon in an induction furnace and was annealed at 770 K for one week. The metals used were of purity greater than 99.9 mass% for Ho, and greater than 99.99 mass% for Mn and Ge.

$HoMn_{0.25}Ge_2$ was found to adopt the $CeNiSi_2$ type structure with lattice parameters $a = 0.4097$, $b = 1.574$, $c = 0.3983$ by Francois et al. (1990) (X-ray powder diffraction data). For sample preparation see $GdFe_{0.25-0.46}Ge_2$ under Gd–Fe–Ge.

4.12.3. *Ho–Fe–Ge*

The phase diagram for the Ho–Fe–Ge system was investigated by Salamakha et al. (1996g) by means of X-ray analysis (fig. 93). Alloys for investigation were prepared by arc melting proper amounts of the constituent elements. The starting materials were used in the form of ingots of holmium (99.9 mass%), iron (99.99 mass%) and germanium (99.999 mass%). The samples were annealed at 870 K for two weeks. Six ternary compounds have been observed and characterized.

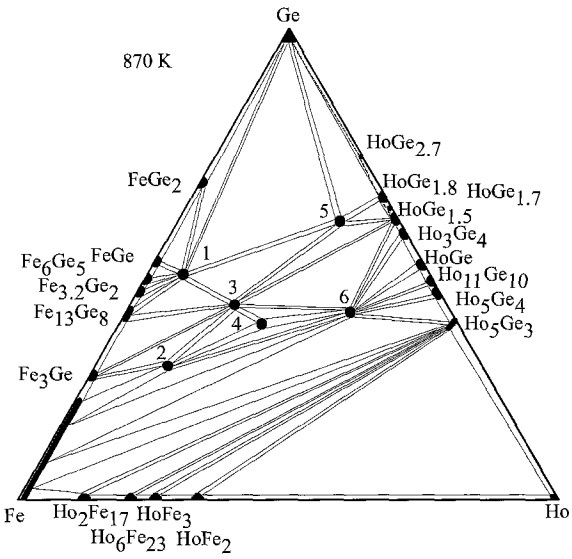

Fig. 93. Ho–Fe–Ge, isothermal section at 870 K.

$HoFe_6Ge_6$ (1) was reported to be isotypic with YCo_6Ge_6, lattice parameters $a = 0.5110$, $c = 0.4056$ (Mruz et al. 1984). The sample was prepared by arc melting the proper amounts of the starting components, followed by annealing at 870 K for two weeks and finally quenching in cold water. At variance with these data, $HoFe_6Ge_6$ was found to crystallize with the $TbFe_6Sn_6$ type, $a = 0.8111$, $b = 1.766$, $c = 0.5116$ by Venturini et al. (1992) from X-ray powder diffraction data. The alloy was obtained by powder metallurgical reaction in an evacuated silica tube at 1173 K for two weeks. This suggests that $HoFe_6Ge_6$ may be polymorphic.

Pecharsky et al. (1989) reported $HoFe_{0.33}Ge_2$ (5) to crystallize with the $CeNiSi_2$-type ($a = 0.4102$, $b = 1.5689$, $c = 0.3986$; X-ray powder analysis). The alloy was arc melted and annealed at 870 K. The purity of the starting materials was greater than 99.9 mass%. Francois et al. (1990) confirmed the occurrence of $CeNiSi_2$ type for holmium–iron–germanium combinations from the alloys annealed at 1173 K ($HoFe_{0.38}Ge_2$; $a = 0.4105$, $b = 1.572$, $c = 0.3999$).

Salamakha et al. (1996g) investigated the crystal structure of $Ho_{117}Fe_{52}Ge_{112}$ (6) by X-ray powder diffraction ($Tb_{117}Fe_{52}Ge_{112}$ type, $a = 2.8238$). The alloy was synthesized by arc melting and annealing at 870 K for two weeks. The starting materials were Ho 99.9 mass%, Fe 99.9 mass%, and Ge 99.99 mass%.

According to X-ray powder diffraction data, $HoFe_2Ge_2$ (3) was found to be isostructural with the $CeGa_2Al_2$ type, with lattice parameters $a = 0.3949$, $c = 1.0430$ (Rossi et al. 1978a).

Fedyna (1988) reported on the X-ray powder investigation of the crystal structure of $HoFe_4Ge_2$ (2) ($ZrFe_4Si_2$ type, $a = 0.7255$, $c = 0.3852$) from an arc melted alloy annealed at 870 K alloy.

$Ho_6Fe_8Ge_8$ (4) belongs to the $Gd_6Cu_8Ge_8$ type, $a = 1.3450$, $b = 0.6781$, $c = 0.4117$, after Fedyna et al. (1994).

4.12.4. *Ho–Co–Ge*

The isothermal section of the Ho–Co–Ge system at 870 K over the whole concentration region was derived by Aslan (1990) (fig. 94) employing X-ray and microstructural analyses of 212 alloys which were prepared by arc melting the proper amounts of the constituent elements of high purity. The melted buttons were then annealed in evacuated silica tubes at 870 K for 720 hours.

The ternary phase diagram is characterized by the existence of eleven ternary compounds and by the formation of solid solutions based at the Ho_2Co_{17} and $HoCo_5$ binary compounds where the maximum solubility of germanium is 10 at.%. The Ho_5Ge_3 phase dissolves 8 at.% Co.

Méot-Meyer et al. (1985a) reported the crystal structure of $HoCo_xGe_2$ (8), $x = 0.48$ ($CeNiSi_2$ type, $a = 0.4094$, $b = 1.595$, $c = 0.4009$). The sample was prepared by powder metallurgical reaction and annealed in an evacuated silica tube at 1173 K. Pecharsky et al. (1989) confirmed the formation and crystal structure of the $HoCo_{1-x}Ge_2$ compound and additionally observed the existence of a homogeneity field from arc melted alloys annealed at 870 K ($a = 0.4080$–0.4093, $b = 1.583$–1.592, $c = 0.3953$–0.4008; X-ray powder analysis).

The crystal structure of $Ho_3Co_4Ge_{13}$ (3) ($Yb_3Rh_4Sn_{13}$ type, $a = 0.8735$; X-ray powder diffraction) was investigated by Venturini et al. (1985b) from a sample which was prepared by heating a compacted mixture of the starting materials (Ho in pieces, 99.9 mass%; Co and Ge in powder, 99.99 mass%) in an evacuated quartz tube at 1073 K. Bodak et al.

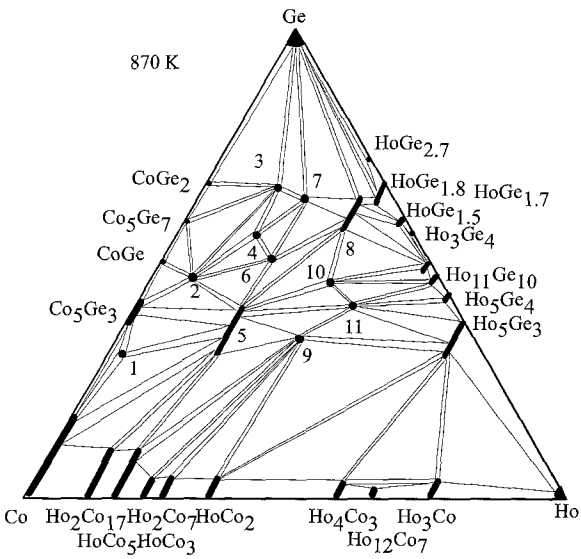

Fig. 94. Ho–Co–Ge, isothermal section at 870 K.

(1987) reported the $Y_3Co_4Ge_{13}$-type for the $Ho_3Co_4Ge_{13}$ compound ($a = 0.8742$; X-ray powder data) from arc melted alloy annealed at 870 K.

$HoCo_2Ge_2$ (5) was found to adopt the $CeGa_2Al_2$ type, $a = 0.3957$, $c = 1.0077$ (Szytuła et al. 1980; X-ray powder diffraction). Aslan (1990) confirmed the crystal structure and observed the existence of a homogeneity field for $HoCo_{2.0+x}Ge_{2-x}$ ($x = 0.5$).

From an X-ray powder analysis of alloy annealed at 1173 K, $Ho_2Co_3Ge_5$ (6) was reported to adopt the $Lu_2Co_3Si_5$-type structure, $a = 0.9618$, $b = 1.1805$, $c = 0.5691$, $\beta = 91.9°$ (Venturini et al. 1986b).

The crystal structure of the $HoCo_6Ge_6$ (2) compound was reported by Buchholz and Schuster (1981) (YCo_6Ge_6 structure type, $a = 0.5074$, c 0.3910). The sample was melted under argon in a corundum crucible at 1073–1273 K.

Gorelenko et al. (1984) reported the crystal structure of HoCoGe (9) (TiNiSi type, $a = 0.6851$, $b = 0.4198$, $c = 0.7253$; X-ray powder analysis). The alloy was arc melted, and annealed in an evacuated quartz tube at 870 K for 350 hours.

$Ho_3Co_2Ge_4$ (10) crystallizes with a $Tb_3Co_2Ge_4$-type of structure, $a = 1.0523$, $b = 0.7958$, c 0.4152, $\gamma = 107.36°$ (X-ray powder data; Mruz et al. 1989). The sample was prepared by arc melting and annealing at 873 K for 240 h.

Ho_2CoGe_6 (7) is isotypic with Ce_2CuGe_6, $a = 0.3923$, $b = 0.3974$, $c = 2.131$ (Oleksyn et al. 1991; X-ray powder diffraction data). The sample was melted in an arc furnace and annealed at 1070 K in an evacuated quartz capsule for 400 h. The purity of the starting materials was greater than 99.9 mass%.

Bodak et al. (1986) reported on the X-ray powder investigation of the compound Ho_2CoGe_2 (11), Sc_2CoSi_2 type, $a = 1.0408$, $b = 1.0109$, $c = 0.4166$, $\gamma = 117.45°$.

Investigating the isothermal section, Aslan (1990) observed two compounds with unknown structures: ~$Ho_3Co_{65}Ge_{32}$ (1) and ~$HoCo_2Ge_5$ (4).

4.12.5. *Ho–Ni–Ge*

Figure 95 represents the isothermal section of the Ho–Ni–Ge phase diagram at 870 K, which was studied by Aslan (1990). The isothermal section was constructed by means of X-ray powder and partly microstructural analyses of 158 alloys which were arc melted, subsequently annealed in evacuated silica tubes for 720 h at 870 K, and finally quenched in cold water. The starting materials were Ho 99.9 mass%, Ni 99.98 mass%, and Ge 99.99 mass%.

The ternary phase diagram is characterized by the existence of ten ternary compounds and by the formation of substitutional solid solutions originating at Ho_2Ni_{17} and $HoNi_5$ binary compounds where the maximum solubility of germanium is 17 at.%. The binary $HoGe_{1.5}$ compound dissolves 15 at.% Ni.

$HoNi_5Ge_3$ (1) was reported to crystallize with the YNi_5Si_3 type, $a = 1.9050$, $b = 0.3856$, $c = 0.6785$, by Fedyna et al. (1987). The arc melted alloy, annealed at 870 K, was investigated by X-ray powder diffraction analysis. The starting materials were Ho 99.9 mass%, Ni 99.99 mass%, and Ge 99.999 mass%.

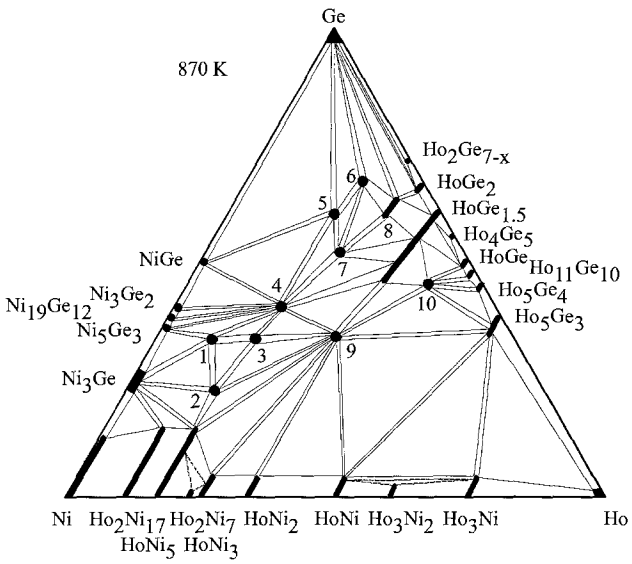

Fig. 95. Ho–Ni–Ge, isothermal section at 870 K.

$Ho_3Ni_{11}Ge_4$ (2) belongs to the $Sc_3Ni_{11}Si_4$ type, $a = 0.8292$, $c = 0.8682$, after Fedyna et al. (1987). An alloy was prepared in the same manner as $HoNi_5Ge_3$.

The $HoNi_2Ge_2$ (4) compound was found to adopt the $CeGa_2Al_2$-type structure, $a = 0.4021$, $c = 0.9757$ (Rieger and Parthé 1969b).

$HoNiGe_3$ (5) with the $SmNiGe_3$-type structure ($a = 2.1476$, $b = 0.4063$, $c = 0.4054$, X-ray powder diffraction analysis) was reported by Bodak et al. (1985). For the details of sample preparation and purity of starting materials, see $HoNi_5Ge_3$, above.

Ho_2NiGe_6 (6) has been found by Oleksyn (1990) from X-ray powder diffraction to be isostructural with Ce_2CuGe_6 ($a = 0.3941$, b 2.1108, $c = 0.3991$). The sample was prepared by arc melting ingots of the constituting elements and annealing at 1070 K for 700 h. For the purity of starting materials, see $HoNi_5Ge_3$, above.

Pecharsky et al. (1989) investigated the formation and crystal structure of the $HoNi_{1-x}Ge_2$ (8) compound by X-ray powder analysis of arc melted alloy annealed at 870 K ($CeNiSi_2$ type, $a = 0.4059$–0.4079, $b = 1.5809$–1.5796, $c = 0.3934$–0.3952). Francois et al. (1990) confirmed the structure and reported the composition and lattice parameters $HoNi_{0.71}Ge_2$, $a = 0.4084$, $b = 1.629$, $c = 0.4091$ (X-ray powder diffraction) from a sample obtained by powder metallurgical reaction at 1173 K.

Gorelenko et al. (1984) reported the crystal structure of HoNiGe (9) (TiNiSi type, $a = 0.6856$, $b = 0.4204$, $c = 0.7256$; X-ray powder analysis). For the experimental details, see HoCoGe under Ho–Co–Ge.

The crystal structure of $HoNiGe_2$ (7) was reported by Oleksyn (1990): $NdIrGe_2$ type, $a = 0.4136$, $b = 0.8430$, $c = 1.5792$ (X-ray powder diffraction). The sample was prepared by arc melting ingots of the constituting elements and annealing at 1070 K for 700 h.

Bodak et al. (1982) reported on the crystal structure of Ho_3NiGe_2 from X-ray powder diffraction (La_3NiGe_2 type, $a = 1.1195$, $b = 0.4197$, $c = 1.1192$). This compound, however, apparently does not exist at 870 K.

The crystal structures of two more ternary compounds ~$HoNi_3Ge_2$ (3) and ~Ho_4NiGe_4 (10) have not yet been evaluated (Aslan 1990).

4.12.6. *Ho–Cu–Ge*

No phase diagram is available for the Ho–Cu–Ge system; however the crystal structures for five ternary compounds are reported by different groups of authors.

Rieger and Parthé (1969a) investigated the occurrence of the AlB_2-type structure by means of X-ray powder diffraction of arc melted alloys. The data presented are $HoCu_{1-0.67}Ge_{1-1.33}$ with $a = 0.4225$–0.400, $c = 0.3608$–0.402. At variance with these data, Iandelli (1993) observed HoCuGe with the $CaIn_2$-type structure ($a = 0.4232$, $c = 0.7188$, X-ray powder analysis). The alloy was prepared from filings or powders of metals (Ho 99.7 mass%, Cu and Ge 99.99 mass%), which were mixed and sealed in a tantalum crucible under argon, melted by induction heating, and annealed for 10 days at 1023 K.

$Ho_6Cu_8Ge_8$ crystallizes with the $Gd_6Cu_8Ge_8$ type, lattice parameters $a = 1.384$, $b = 0.662$, $c = 0.417$ (Hanel and Nowotny 1970).

Konyk et al. (1988) investigated the crystal structure of Ho_2CuGe_6 alloy prepared by arc melting under argon and annealing at 870 K in an evacuated quartz tube for 720 h. From X-ray powder analysis a Ce_2CuGe_6-type was claimed, $a = 0.4011$, $b = 0.4129$, $c = 2.1104$.

Rieger and Parthé (1969b) prepared $HoCu_2Ge_2$ with the $CeGa_2Al_2$-type structure, $a = 0.4016$, $c = 1.0302$.

Francois et al. (1990) observed the $CeNiSi_2$ type structure for the $HoCu_{0.33}Ge_2$ compound and reported lattice parameters $a = 0.4074$, $b = 1.618$, $c = 0.3950$ (X-ray powder diffraction) from a sample obtained by powder metallurgical reaction at 1173 K.

4.12.7. *Ho–Nb–Ge*

The phase diagram of the Ho–Nb–Ge system has not been established, but at least one ternary phase is known. The existence of the compound $Ho_2Nb_3Ge_5$ with the $Ce_2Sc_3Si_4$-type structure ($a = 0.6956$, $b = 1.3479$, $c = 0.7131$) was reported by Le Bihan et al. (1996a) from X-ray powder diffraction data of an arc melted alloy. The starting materials were: Ho and Nb 99.99 mass%, Ge 99.999 mass%.

4.12.8. *Ho–Mo–Ge*

No phase diagram is available for the Ho–Mo–Ge system, and only one compound was observed and investigated. $Ho_2Mo_3Ge_4$ was reported to crystallize with the $Ce_2Sc_3Si_4$-type structure ($a = 0.6868$, $b = 1.3079$, $c = 0.7032$) by Le Bihan et al. (1996b) from X-ray powder diffraction of an arc melted alloy. The starting materials were: Ho and Mo 99.99 mass%, Ge 99.999 mass%.

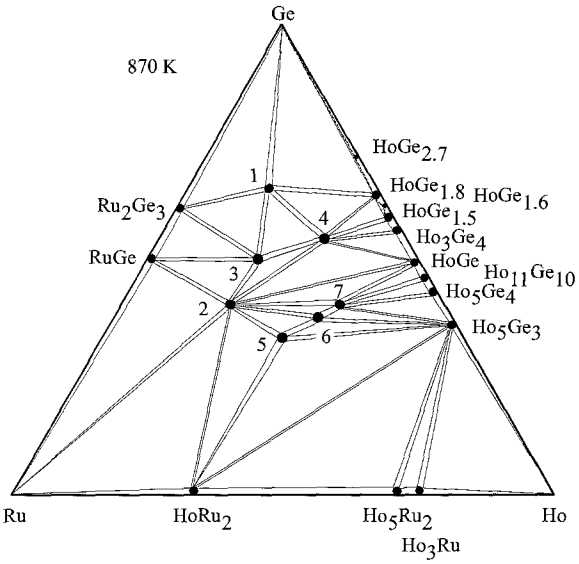

Fig. 96. Ho–Ru–Ge, isothermal section at 870 K.

4.12.9. *Ho–Ru–Ge*

The isothermal section for Ho–Ru–Ge was constructed by Sologub (1995) at 870 K by means of X-ray diffraction (fig. 96). The samples were prepared by direct arc melting of pieces of high purity components (greater than 99.9 mass%), annealed at 870 K for two weeks in evacuated quartz ampoules and quenched in cold water. The phase-field distribution is characterized by the formation of seven compounds.

Early investigations of the $HoRu_2Ge_2$ (2) compound showed that it had the $CeGa_2Al_2$-type structure with $a=0.4211$, $c=0.9790$ (Francois et al. 1985) from X-ray powder analysis of an alloy obtained by powder metallurgical reaction at 1273 K. The starting components were Ho (3N), Ru (4N), and Ge (4N). Sologub et al. (1995b) confirmed the crystal structure and obtained the lattice parameters $a=0.4218$, $c=0.9805$.

Venturini et al. (1986b) reported the structure for the $Ho_2Ru_3Ge_5$ (3) compound, which crystallizes with the $U_2Co_3Si_5$-type of structure. The lattice parameters were reported as $a=0.9771$, $b=1.241$, $c=0.5706$ (X-ray powder diffraction data). For sample preparation, see $La_2Ru_3Ge_5$ under La–Ru–Ge.

The $Pr_3Rh_4Sn_{13}$-type structure was announced for the $Ho_3Ru_4Ge_{13}$ (1) compound ($a=$ 0.8945) by Segre et al. (1981a) from an X-ray powder analysis of an arc melted sample annealed at 1523 K for 1 day and at 1273 K for 7 days. The starting materials were Ho (3N), Ru (3N), and Ge (6N).

Francois et al. (1990) reported the crystal structure of $HoRu_{0.27}Ge_2$ (4) ($CeNiSi_2$ type, $a=0.4116$, $b=1.577$, $c=0.4007$). For sample preparation, see $GdFeGe_2$ under Gd–Fe–Ge. Sologub et al. (1995b) confirmed the formation and crystal structure for this compound, $a=0.4105$, $b=1.5701$, $c=0.4008$ (X-ray powder diffraction).

Sologub et al. (1994a) reported on a single-crystal investigation of two compounds: HoRuGe (5), TiNiSi type, $a=0.6980$, $b=0.4351$, $c=0.7281$, and $Ho_3Ru_2Ge_3$ (6), $Hf_3Ni_2Si_3$ type, $a=0.4242$, $b=1.0731$, $c=1.3840$. The single crystals were obtained from samples which were arc melted and annealed at 870 K for 400 h.

Ho_2RuGe_2 (7) was found to crystallize with the Sc_2CoSi_2-type structure, $a=1.0643$, $b=0.4259$, $c=1.0203$, $\beta=118.0°$ by Sologub et al. (1995b).

4.12.10. *Ho–Rh–Ge*

The phase relations in the ternary Ho–Rh–Ge system (0–50 at.% Rh) at 870 K were investigated by Sologub (1995) (fig. 97). Fourteen ternary compounds were found to exist within the concentration region investigated. For experimental procedures, see Ho–Ru–Ge.

Venturini et al. (1985b) reported an X-ray powder diffraction study of the $Ho_3Rh_4Ge_{13}$ (1) compound from a sample prepared by heating a mixture of starting components (Ho 3N, Rh 4N, Ge 4N) in an evacuated quartz tube at 1073 K. The crystal structure was found to be of the $Yb_3Rh_4Sn_{13}$ type, $a=0.8916$.

Francois et al. (1985) determined the $CeGa_2Al_2$-type structure for the $HoRh_2Ge_2$ (3) compound, $a=0.4101$, $c=1.0196$.

$Ho_2Rh_3Ge_5$ (4) was found to crystallize with $Lu_2Co_3Si_5$-type structure (a=1.1353, b=1.1976, $c=0.5813$, $\beta=119.05°$; X-ray single-crystal data) by Venturini et al. (1986b) from a sample synthesized by powder metallurgical reaction at 1173 K. The purity of the starting materials was greater than 99.9 mass%.

Hovestreydt et al. (1982) reported the crystal structure of the HoRhGe (8) compound (TiNiSi type, $a=0.6964$, $b=0.4272$, $c=0.7516$; X-ray powder data) from an arc melted

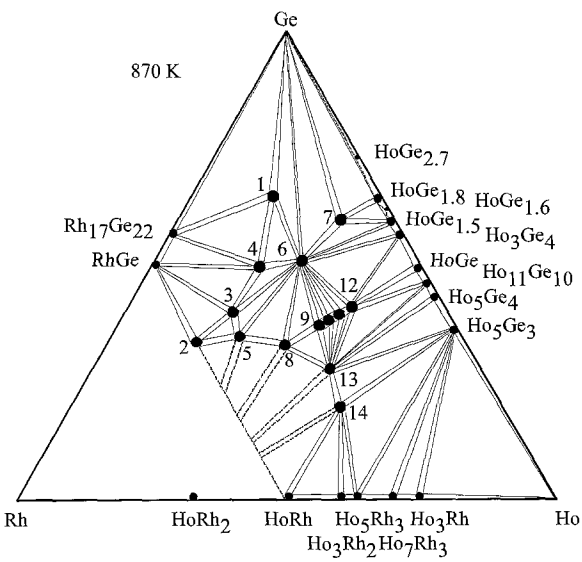

Fig. 97. Ho–Rh–Ge, partial isothermal section at 870 K (0–50 at.% Rh).

sample annealed at 1270 K for 1–2 weeks. The starting components were Ho (3N), Rh (4N), and Ge (5N).

Salamakha and Sologub (1999) reported on the crystal structure of the $Ho_3Rh_2Ge_2$ (13) compound ($La_3Ni_2Ga_2$ type, $a = 0.55367$, $b = 0.7726$, $c = 1.3165$; X-ray powder diffraction data). For the details of sample preparation, see $La_3Rh_2Ge_2$ under La–Rh–Ge.

Sologub (1995) established the $Ho_4Ir_{13}Ge_9$-type for the $Ho_4Rh_{13}Ge_9$ (2) compound, $a = 0.3962$, $b = 1.1034$, $c = 1.9203$. For sample preparation, see Ho–Ru–Ge.

Venturini et al. (1984) observed the existence of the $Ho_5Rh_4Ge_{10}$ (6) compound with $Sc_5Co_4Si_{10}$ type ($a = 1.2902$, $c = 0.4242$; X-ray powder diffraction) from a sample obtained by heating amixture of powders in an evacuated tube at 1073 K. Salamakha and Sologub (1999) confirmed the $Sc_5Co_4Si_{10}$-type of structure by a single-crystal method, $a = 1.29336$, $c = 0.42596$. The single crystal was taken from an arc melted sample annealed at 870 K.

$Ho_4Rh_7Ge_6$ (5) was reported to adopt the $U_4Re_7Si_6$ type structure, $a = 0.8305$ (Francois et al. 1985) from a sample which was obtained by heating a mixture of powders of the starting materials (Ho 3N, Rh 4N, Ge 4N) in evacuated quartz tubes at 1273 K.

Francois et al. (1990) reported the crystal structure of $HoRh_{0.28}Ge_2$ (7) ($CeNiSi_2$ type, $a = 0.4107$, $b = 1.584$, $c = 0.3988$). For sample preparation, see $GdFeGe_2$ under Gd–Fe–Ge.

Four more ternary compounds were observed and investigated by Sologub (1995) using an X-ray single-crystal method: $Ho_3Rh_2Ge_3$ (9), $Hf_3Ni_2Si_3$ type, $a = 0.425$, $b = 1.026$, $c = 1.488$; $\sim Ho_{3+x}Rh_2Ge_{3+x}$ (10), orthorhomb., $a = 0.423$, $b = 1.024$, $c = 10.2$; Ho_2RhGe_2 (11), Sc_2CoSi_2 type, $a = 1.0465$, $b = 0.42670$, $c = 1.02203$, $\beta = 117.2°$; $\sim Ho_{2+x}RhGe_{2+x}$ (12), monoclinic, $a = 1.042$, $b = 0.428$, $c = 6.3$, $\beta = 117°$.

The crystal structure of $\sim Ho_5Rh_3Ge_2$ (14) has not been evaluated (Sologub 1995).

4.12.11. *Ho–Pd–Ge*

A systematic study of the Ho–Pd–Ge system at 870 K was performed by Sologub (1995) over the whole concentration region by means of X-ray powder analysis (fig. 98). The samples were prepared by arc melting under an argon atmosphere and annealed in evacuated quartz ampoules at 870 K for 500 hours. The starting materials were 99.8 mass% pure or better.

Phase relations are characterized by the existence of ten ternary compounds and by the formation of an extended solid solution originating at the $HoPd_3$ binary compound. The maximum solubility of Ge in $HoPd_3$ was observed as 12 at.%. The solubility of the third component in other binary compounds was found to be negligible.

The existence of the $HoPd_2Ge_2$ (2) compound ($CeGa_2Al_2$ type, $a = 0.4220$, $c = 1.0018$) was reported by Bodak and Sologub (1991a). The sample was prepared in the same manner as the Ho–Pd–Ge alloys.

Bodak and Sologub (1991a) reported on the X-ray powder analysis of the Ho_2PdGe_6 (3) compound which was found to crystallize with the Ce_2CuGe_6 type, $a = 0.4080$, $b = 0.4007$, $c = 2.140$. For the experimental procedure, see Ho–Pd–Ge.

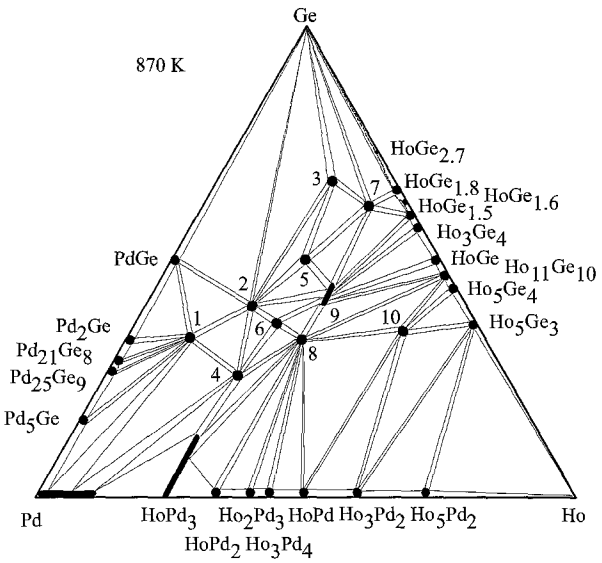

Fig. 98. Ho–Pd–Ge, isothermal section at 870 K.

The crystal structure of the compound $HoPd_2Ge$ (4) was found to be of the YPd_2Si type ($a = 0.7318$, $b = 0.6036$, $c = 0.5553$; X-ray powder diffraction) by Jorda et al. (1983). For the experimental procedure, see $LaPd_2Ge$ under La–Pd–Ge. The starting materials were Pd 99.99 mass%, Ge specpure quality, and Ho 99.9 mass%. Sologub (1995) confirmed the structure of $HoPd_2Ge$ and reported similar lattice parameters ($a = 0.7321$, $b = 0.6045$, $c = 0.5563$; X-ray powder diffraction).

According to an X-ray powder diffraction analysis reported by Hovestreydt et al. (1982), the compound HoPdGe (8) adopts the KHg_2-type of structure, $a = 0.4360$, $b = 0.6938$, $c = 0.7547$. For sample preparation, see LaPdGe under La–Pd–Ge. The starting materials were Ho (3N), Pd (4N), and Ge (5N). Sologub (1995) reported a single-crystal investigation of HoPdGe from an arc melted specimen annealed at 870 K for 500 h (KHg_2 type, $a = 0.4358$, $b = 0.6922$, $c = 0.7546$).

Francois et al. (1990) investigated the crystal structure of the $HoPd_{0.33}Ge_2$ (7) compound ($CeNiSi_2$ type, $a = 0.4118$, $b = 1.593$, $c = 0.4002$). In the course of studying the phase equilibria in the Ho–Pd–Ge system at 870 K, Sologub (1995) confirmed the existence of the compound with the $CeNiSi_2$ type structure and obtained similar lattice parameters: $a = 0.4107$, $b = 1.5924$, $c = 0.3979$.

Sologub (1995) studied the crystal structures of $HoPdGe_2$ (5) ($NdIrGe_2$ type, $a = 0.4234$, $b = 1.597$, $c = 0.8715$) and $HoPd_{0.8-0.6}Ge_{1.2-1.4}$ (9) (AlB_2 type, $a = 0.4237$–0.4276, $c = 0.3828$–0.3721) by X-ray powder diffraction. The experimental details are given above (Ho–Pde–Ge isothermal section).

$Ho_6Pd_8Ge_8$ (6) was found to crystallize with the $Gd_6Cu_8Ge_8$-type structure, $a = 0.42348$, $b = 0.68373$, $c = 1.4093$ (Gladyshevsky et al. 1991b; X-ray single-crystal data).

Sologub et al. (1994b) investigated $Ho_{26}Pd_4(Pd, Ge)_{19-x}$ (10) by an X-ray single-crystal method: own structure type, $a = 1.4523$, $c = 1.0318$. The alloy was arc melted and annealed at 870 K for 500 h.

The crystal structure of the ~$HoPd_5Ge_3$ (1) compound has not yet been established (Sologub 1995).

4.12.12. *Ho–Ag–Ge*

The isothermal section of the Ho–Ag–Ge system at 870 K was reported by Sologub and Protsyk (1991) from an X-ray powder analysis of 54 alloys (fig. 99). The samples were obtained by arc melting the components in purified argon and annealing at 870 K for 500 h in evacuated quartz tubes. Finally the alloys were water quenched. The purity of the starting components was Ho 99.8 mass%, Ag 99.9 mass%, and Ge 99.999 mass%. One ternary compound was found to exist in this system at 870 K.

Sologub and Protsyk (1991) reported on the crystal structure of the HoAgGe compound. It was found to adopt the ZrNiAl-type structure, $a = 0.7084$, $c = 0.41793$ (X-ray powder diffraction). Gibson et al. (1996) confirmed the crystal structure from X-ray powder diffraction of an arc melted alloy annealed at 970 K for ten days, and presented the lattice parameters $a = 0.70783$, $c = 0.41826$.

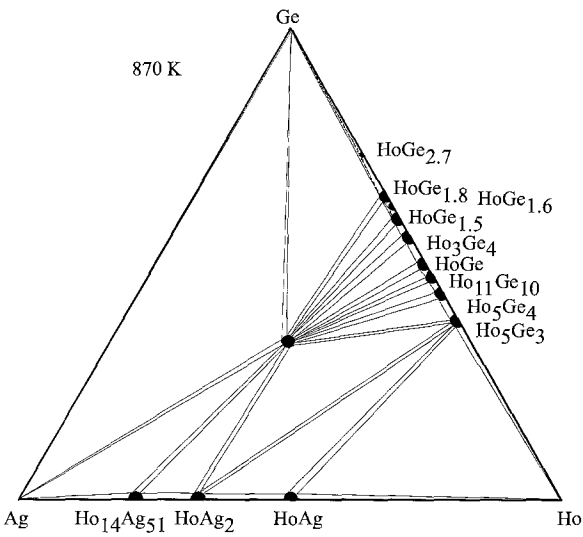

Fig. 99. Ho–Ag–Ge, isothermal section at 870 K.

4.12.13. *Ho–Re–Ge*

The only information on the system Ho–Re–Ge is due to Francois et al. (1990) who investigated the occurrence of the compound with the $CeNiSi_2$ type; no phase diagram is available. The $HoRe_{0.25}Ge_2$ compound was found to adopt the $CeNiSi_2$-type structure with lattice parameters $a = 0.4128$, $b = 1.578$, $c = 0.4028$ by Francois et al. (1990) (X-ray

powder diffraction data). The alloy was prepared from a mixture of the proper amounts of the components with purity 99.9 mass% by metallurgical reaction in a quartz tube at 1173 K.

4.12.14. *Ho–Os–Ge*

Bodak and Sologub (1991b) were the first to investigate, by X-ray powder diffraction, the phase equilibria within the Ho–Os–Ge system at 870 K over the whole concentration region; samples were prepared as described under Ho–Ru–Ge. The phase relations are characterized by the existence of three ternary compounds (fig. 100).

Bodak et al. (1991) indicated a $Sc_5Co_4Si_{10}$-type structure for $Ho_5Os_4Ge_{10}$ (2) from X-ray single-crystal diffraction and reported the lattice parameters $a = 1.2984$, $c = 0.42820$.

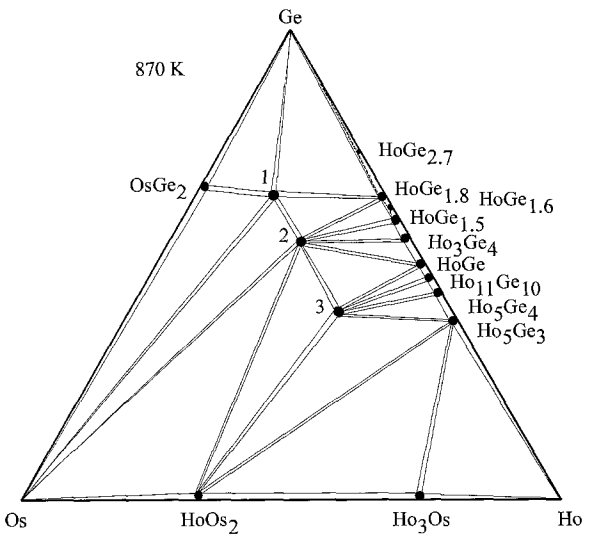

Fig. 100. Ho–Os–Ge, isothermal section at 870 K.

$Pr_3Rh_4Sn_{13}$-type structure was announced for the $Ho_3Os_4Ge_{13}$ compound (1) ($a = 0.8977$) by Segre et al. (1981a) from X-ray powder analysis of an arc melted sample annealed at 1523 K for 1 day and at 1273 K for 7 days. The starting materials were Ho (3N), Os (3N), and Ge (6N). At variance with these data, Bodak and Sologub (1991b) observed the $Y_3Co_4Ge_{13}$ type for a $Ho_3Os_4Ge_{13}$ alloy which was arc melted and annealed at 870 K for 500 hours ($a = 0.89737$; X-ray powder diffraction).

Ho_2OsGe_2 (3) was found to adopt the Sc_2CoSi_2 type structure, $a = 1.0691$, $b = 0.42618$, $c = 1.0050$, $\beta = 118.07°$ (X-ray single-crystal analyses; Gladyshevsky et al. 1991b).

4.12.15. *Ho–Ir–Ge*

The partial isothermal section for the Ho–Ir–Ge system at 870 K (0–50 at.% Ir) was established by Sologub (1995) (fig. 101). For sample preparation, see Ho–Ru–Ge. Five

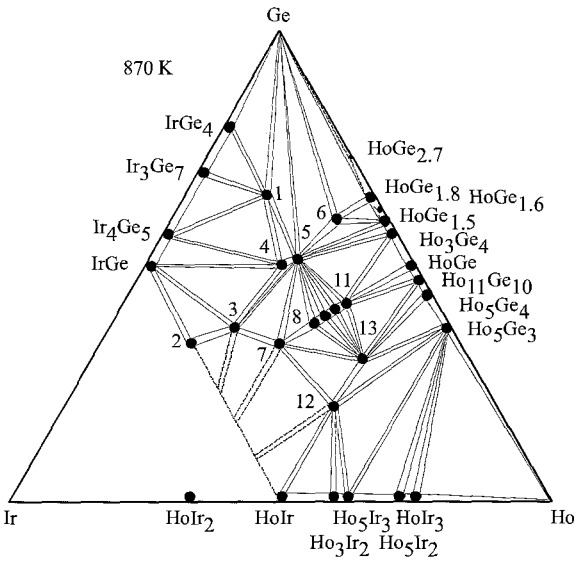

Fig. 101. Ho–Ir–Ge, partial isothermal section at 870 K (0–50 at.% Ir).

ternary compounds were confirmed and eight ternary phases were observed for the first time. No homogeneous ranges were encountered for the ternary compounds.

Venturini et al. (1984) observed the existence of the $Ho_5Ir_4Ge_{10}$ (5) compound with $Sc_5Co_4Si_{10}$-type structure from X-ray powder diffraction of a sample obtained by heating the starting components in an evacuated tube at 1073 K, $a = 1.2878$, $c = 0.4286$.

Venturini et al. (1985b) reported on an X-ray powder diffraction study of the $Ho_3Ir_4Ge_{13}$ (1) compound from a sample prepared by heating a mixture of the starting components (Ho 3N, Ir 4N, Ge 4N) in an evacuated quartz tube at 1073 K. The crystal structure was found to adopt the $Yb_3Rh_4Sn_{13}$ type, $a = 0.8931$.

Hovestreydt et al. (1982) reported the crystal structure of the HoIrGe (7) compound (TiNiSi type, $a = 0.6801$, $b = 0.4252$, $c = 0.7595$; X-ray powder data) from an arc melted sample annealed at 1270 K for 1–2 weeks. The starting components were Ho (3N), Ir (4N), and Ge (5N).

Francois et al. (1987) reported the crystal structure of $HoIrGe_2$ (4) ($NdIrGe_2$ type, $a = 0.4244$, $b = 1.595$, $c = 0.8804$). The sample was prepared by heating mixtures of powders of the starting components (Ho 3N, Ir 3N, Ge 3N) in an evacuated silica tube at 1173 K.

$HoIr_{0.28}Ge_2$ (6) was found to crystallize with a $CeNiSi_2$ type, $a = 0.4108$, $b = 1.585$, $c = 0.3988$ (X-ray powder diffraction; Sologub 1995). For sample preparation, see Ho–Ru–Ge.

$Ho_4Ir_7Ge_6$ (3) was reported to adopt the $U_4Re_7Si_6$ type ($a = 0.8311$; Francois et al. 1985) from a sample obtained by heating a mixture of powders of the starting materials (Ho 3N, Os 4N, Ge 4N) in an evacuated quartz tube at 1273 K.

Five other ternary compounds were observed and characterized by an X-ray single-crystal method by Sologub et al. (1993) and Sologub (1995): $Ho_4Ir_{13}Ge_9$ (2) belongs to a

new structure type, $a = 0.3954$, $b = 1.1186$, $c = 1.9301$ (Sologub et al. 1993); $Ho_3Ir_2Ge_3$ (8) adopts $Hf_3Ni_2Si_3$-type structure with $a = 0.423$, $b = 1.024$, $c = 1.485$ (Sologub 1995); $\sim Ho_{3+x}Ir_2Ge_{3+x}$ (9) is orthorhombic, $a = 0.424$, $b = 1.025$, $c = 10.25$ (Sologub 1995); Ho_2IrGe_2 (10) crystallizes with the Sc_2CoSi_2-type structure, $a = 1.047$, $b = 0.428$, $c = 1.079$, $\beta = 118°$ (Sologub 1995); $\sim Ho_{2+x}IrGe_{2+x}$ (11) is monoclinic, $a = 1.042$, $b = 0.428$, $c = 6.3$, $\beta = 117°$ (Sologub 1995). The alloys for this investigation were prepared in the same manner as Ho–Ru–Ge.

Two more compounds with unknown structures were observed by Sologub (1995): $\sim Ho_5Ir_3Ge_2$ (12) and $\sim Ho_5Ir_2Ge_3$ (13).

4.12.16. *Ho–Pt–Ge*

The phase equilibria in the Ho–Pt–Ge system (fig. 102) have been investigated by Sologub (1995) by means of an X-ray analysis of 90 alloys which were arc melted and subsequently annealed in evacuated silica tubes for 500 h at 870 K and finally quenched in water. The starting materials were Ho 99.8 mass%, Pt 99.99 mass% and Ge 99.999 mass%. One ternary compound was confirmed and ten ternary phases were observed for the first time.

According to an X-ray powder diffraction analysis reported by Hovestreydt et al. (1982), the compound HoPtGe (8) adopts the TiNiSi-type structure, $a = 0.6949$, $b = 0.4328$, $c = 0.7535$. For sample preparation, see LaPdGe under La–Pd–Ge.

Sologub et al. (1995a) reported on the X-ray powder analysis of the Ho_2PtGe_6 (3) compound which was found to crystallize with the Ce_2CuGe_6-type structure, $a = 0.40441$, $b = 0.40026$, $c = 2.1571$. For sample preparation, see La_2PdGe_6 under La–Pd–Ge.

X-ray single-crystal analysis was employed to investigate the crystal structure of the

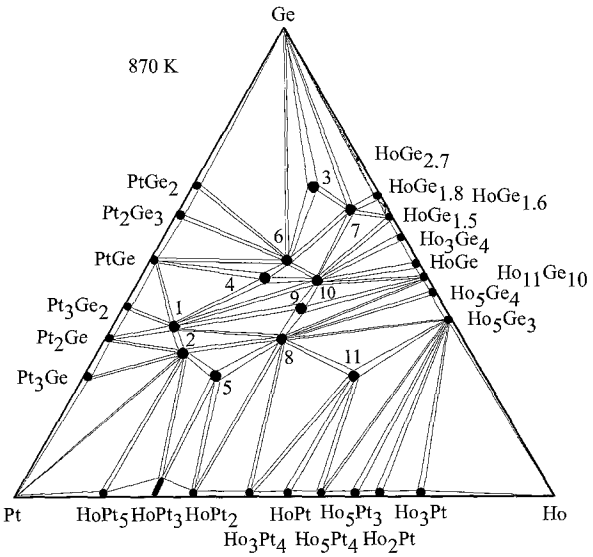

Fig. 102. Ho–Pt–Ge, isothermal section at 870 K.

$HoPtGe_2$ (6) compound, $NdIrGe_2$ type, $a = 0.4292$, $b = 0.8702$, $c = 1.6172$ (Salamakha and Sologub 1998). The single crystal was obtained from an arc melted sample annealed at 870 K for 500 h.

Five more ternary compounds in the Ho–Pt–Ge system at 870 K were observed and characterized by Sologub (1995) in the course of phase equilibrium studies using X-ray powder diffraction: $Ho_2Pt_7Ge_4$ (2), $Ce_2Pt_7Ge_4$-type structure, $a = 1.984$, $b = 0.4062$, $c = 1.1427$; $HoPt_2Ge$ (5), YPd_2Si-type structure, $a = 0.7218$, $b = 0.6036$, $c = 0.5453$; $HoPt_{0.22}Ge_2$ (7), $CeNiSi_2$-type structure, $a = 0.4102$, $b = 1.592$, $c = 0.3951$; $Ho(Pt,Ge)_2$ (10), AlB_2-type structure, $a = 0.4227$, $c = 0.3822$; Ho_2PtGe (11), CrB-type structure, $a = 0.4022$, $b = 1.0864$, $c = 0.4282$.

Three ternary compounds with unknown structure types were observed by X-ray powder diffraction at 870 K: ~$HoPt_5Ge_3$ (1), ~$Ho_3Pt_4Ge_6$ (4) and ~$Ho_3Pt_2Ge_4$ (9) (Sologub 1995).

4.12.17. *Ho–Au–Ge*

Information on interaction of holmium with gold and germanium is due to the work of two groups of authors (Sologub 1995 and Rossi et al. 1992). A phase diagram of the Ho–Au–Ge system is not available, however, one ternary compound has been observed and characterized.

A ternary compound of holmium with gold and germanium in the stoichiometric ratio 1:1:1 has been identified and studied by means of X-ray and metallographic analyses by Rossi et al. (1992). HoAuGe was found to adopt the LiGaGe type with lattice parameters $a = 0.4416$, $c = 0.7335$. Samples were prepared by melting the metals in an induction furnace, and annealing the resulting alloys at 1070 K for one week. The metal used had a purity of about 99.9 mass% for holmium and 99.99 mass% for gold and germanium. Sologub (1995) confirmed the structure type from X-ray powder diffraction of an alloy with equiatomic composition which was obtained by arc melting the metals and annealing the resulting button at 870 K for 500 h: $a = 0.44015$, $b = 0.7231$.

4.13. *Er–d element–Ge systems*

4.13.1. *Er–Cr–Ge*

Brabers et al. (1994) reported the existence of a compound $ErCr_6Ge_6$ with the $HfFe_6Ge_6$-type structure ($a = 0.5150$, $c = 0.8258$; X-ray powder diffraction). For sample preparation, see $TbCr_6Ge_6$ under Tb–Cr–Ge.

4.13.2. *Er–Mn–Ge*

No systematic study of the Er–Mn–Ge system has been carried out so far; however two ternary compounds were observed and investigated by two groups of authors (Rossi et al. 1978b, Venturini et al. 1992).

$ErMn_6Ge_6$ was found to crystallize in the $HfFe_6Ge_6$-type structure by Venturini et al. (1992), $a = 0.5221$, $c = 0.8142$ (X-ray powder diffraction data). For sample preparation, see $TbMn_6Ge_6$ under Tb–Mn–Ge.

Rossi et al. (1978b) reported an investigation of the crystal structure of the $ErMn_2Ge_2$ compound ($CeGa_2Al_2$-type structure, $a=0.3963$, $c=1.0835$; X-ray powder method). For the experimental details, see $TbMn_2Ge_2$ under Tb–Mn–Ge.

4.13.3. *Er–Fe–Ge*

The isothermal section of the Er–Fe–Ge system at 1070 K (fig. 103) was investigated by Oleksyn (1990) by means of metallographic, X-ray and microprobe analyses. Alloys for investigation were prepared by arc melting followed by annealing at 1070 K for 350 hours. The purity of the starting components was Er 99.82 mass%, Fe 99.90 mass%, and Ge 99.99 mass%. Eight ternary compounds were found to exist. The solubility of germanium in iron was established as 18 at.%.

$ErFe_6Ge_6$ (1) was reported to be isotypic with the crystal structure of YCo_6Ge_6 with lattice parameters $a=0.5100$, $c=0.4041$ by Mruz et al. (1984) (X-ray powder diffraction; for sample preparation, see $TbFe_6Ge_6$ under Tb–Fe–Ge); and $a=0.51086$, $c=0.4048$ by Oleksyn (1990) (X-ray powder diffraction). At variance with these data, Venturini et al. (1992) reported the $HoFe_6Sn_6$-type structure for $ErFe_6Ge_6$, $a=0.8103$, $b=2.652$, $c=0.5108$ from X-ray powder diffraction data. The alloy was obtained by powder metallurgical reaction in an evacuated silica tube at 1173 K for two weeks.

Pecharsky et al. (1989) reported $ErFe_xGe_{2-x}$ (6) to crystallize with the $CeNiSi_2$-type structure ($a=0.4079$–0.4086, $b=1.5609$–1.5930, $c=0.3967$–0.3976; X-ray powder analysis). The alloy was arc melted and annealed at 870 K. The purity of the starting materials was greater than 99.9 mass%. Oleksyn (1990) determined the homogeneity region for the $ErFe_{0.06-0.30}Ge_{1.94-1.70}$ ($CeNiSi_2$-type) compound and obtained lattice parameters $a=0.4083$–0.4080, $b=1.5630$–1.5616, $c=0.3982$–0.3974. Francois et al.

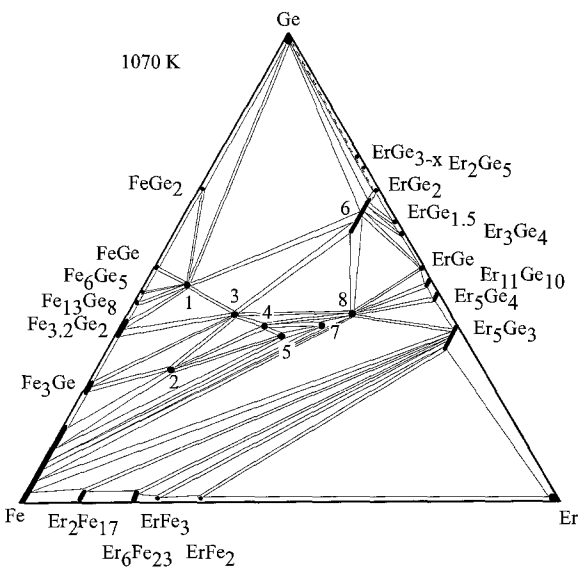

Fig. 103. Er–Fe–Ge, isothermal section at 1070 K.

(1990) confirmed the occurrence of the $CeNiSi_2$-type structure for erbium–iron–germanium combinations from alloys annealed at 1173 K ($ErFe_{0.36}Ge_2$; $a = 0.4098$, $b = 1.565$, $c = 0.3987$).

According to X-ray powder diffraction data, $ErFe_2Ge_2$ (3) is isostructural with $CeGa_2Al_2$, lattice parameters $a = 0.3945$, $c = 1.0435$ (Bara et al. 1990). For the experimental procedure, see $TbFe_2Ge_2$ under Tb–Fe–Ge. The crystal structure was also confirmed by Oleksyn (1990) from X-ray powder diffraction, $a = 0.3932$, $c = 1.0417$.

$ErFe_4Ge_2$ (2) was observed to adopt the $ZrFe_4Si_2$-type of structure, $a = 0.7229$, $c = 0.3842$, from X-ray powder diffraction of an arc melted sample annealed at 870 K (Fedyna 1988). The crystallographic characteristics obtained by Oleksyn (1990) for $ErFe_4Ge_2$ are in good agreement: $ZrFe_4Si_2$ type, $a = 0.7246$, $c = 0.3864$.

Four more ternary compounds were observed for the first time and characterized by Oleksyn (1990): $Er_6Fe_8Ge_8$ (4), $Gd_6Cu_8Ge_8$ type, $a = 1.3460$, $b = 0.6815$, $c = 0.41057$ (X-ray powder diffraction); $Er_9Fe_{10}Ge_{10}$ (5), $Tm_9Fe_{10}Ge_{10}$ type, $a = 0.5393$, $b = 1.3343$, $c = 1.3949$ (X-ray single-crystal data); $Er_3Fe_2Ge_3$ (7), $Hf_3Ni_2Si_3$ type, $a = 0.41491$, $b = 1.0591$, $c = 1.3758$ (X-ray powder diffraction); $Er_{117}Fe_{52}Ge_{112}$ (8), $Tb_{117}Fe_{52}Ge_{112}$ type, $a = 0.2838$ (X-ray powder diffraction).

Two compounds were observed from arc melted samples investigated by Oleksyn (1990) using a single-crystal method: $Er_{6-x}Fe_6Ge_4$, new structure type, $a = 0.5086$, $c = 0.7851$, and Er_3FeGe_3, W_3CoB_3 type, $a = 0.4005$, $b = 1.0544$, $c = 1.4135$. Apparently these phases are not stable equilibrium phases at 1070 K.

4.13.4. *Er–Co–Ge*

The isothermal section of the Er–Co–Ge system at 1070 K over the whole concentration region was derived by Oleksyn (1990) (fig. 104) employing X-ray phase and microstructural and microprobe analyses of alloys prepared by arc melting proper amounts of the constituent elements (Er 99.82 mass%, Co 99.90 mass%, Ge 99.99 mass%). The melted buttons were then annealed in evacuated silica tubes at 1070 K for 350 hours. Sixteen ternary compounds were found to exist. Extensive solid solubility regions of Ge in Fe (10 at.%) and in Er_2Co_{17-x} (10 at.%) were observed.

The crystal structure of the $ErCo_6Ge_6$ (2) compound was reported by Buchholz and Schuster (1981) (YCo_6Ge_6 structure type, $a = 0.5074$, c 0.3910). For experimental details see $ErCo_6Ge_6$ under Er–Co–Ge.

Méot-Meyer et al. (1985a) reported the crystal structure of $ErCo_xGe_2$ (13) ($CeNiSi_2$ type, $a = 0.4078$, $b = 1.586$, $c = 0.3985$). Samples were prepared by powder metallurgical reaction and annealed in an evacuated silica tube at 1173 K. Pecharsky et al. (1989) confirmed the formation and crystal structure of the $ErCo_xGe_2$ compound from arc melted alloys annealed at 870 K ($a = 0.3983$–0.4089, $b = 1.5706$–1.5805, $c = 0.3955$–0.3986; X-ray powder analysis). Oleksyn (1990) established the homogeneity region for the compound with $CeNiSi_2$ type: $ErCo_{0.09-0.33}Ge_{1.91-1.67}$, $a = 0.4058$–0.4003, $b = 1.5743$–1.5766, $c = 0.3964$–0.3932 (X-ray powder diffraction).

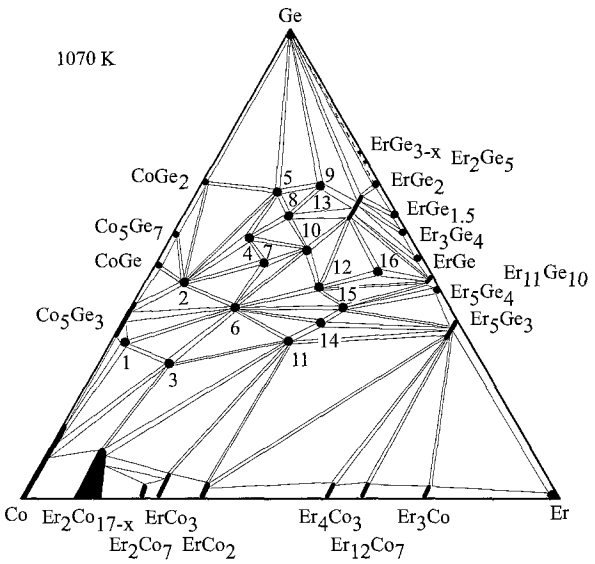

Fig. 104. Er–Co–Ge, isothermal section at 1070 K.

Fedyna (1988) reported the $ErCo_4Ge_2$ (3) compound to have $ZrFe_4Si_2$-type structure, $a = 0.7217$, $c = 0.3743$ (X-ray powder diffraction).

The crystal structure of $Er_3Co_4Ge_{13}$ (5) ($Yb_3Rh_4Sn_{13}$ type, $a = 0.8726$; X-ray powder diffraction) was investigated by Venturini et al. (1985b) from a sample which was prepared by heating a compacted mixture of the starting materials (Er in pieces, 99.9 mass%; Co and Ge in powder, 99.99 mass%) in an evacuated quartz tube at 1073 K. Bodak et al. (1987) reported $Y_3Co_4Ge_{13}$ type for the $Er_3Co_4Ge_{13}$ compound ($a = 0.8731$; X-ray powder data) from arc melted alloy annealed at 870 K.

$ErCo_2Ge_2$ (6) was found to adopt the $CeGa_2Al_2$-type structure, $a = 0.3959$, $c = 1.0057$ (Oleksyn 1990; X-ray powder diffraction).

From X-ray powder analysis of an alloy annealed at 1173 K, $Er_2Co_3Ge_5$ (7) was reported to adopt $Lu_2Co_3Si_5$-type structure, $a = 0.9601$, $b = 1.178$, $c = 0.5680$, $\beta = 91.9°$ (Venturini et al. 1986b).

Gorelenko et al. (1984) reported the crystal structure of ErCoGe (11) (TiNiSi type, $a = 0.6815$, $b = 0.4181$, $c = 0.7245$; X-ray powder analysis). The alloy was obtained by arc melting and annealing in an evacuated quartz tube at 870 K for 350 hours.

$Er_3Co_2Ge_4$ (12) crystallizes with the $Tb_3Co_2Ge_4$-type structure, $a = 1.0459$, $b = 0.7938$, $c = 0.4148$, $\gamma = 107.20°$ (X-ray powder diffraction; Mruz et al. 1989).

Bodak et al. (1986) reported an X-ray powder investigation of the compound Er_2CoGe_2 (15): Sc_2CoSi_2 type, $a = 1.0359$, $b = 1.0181$, $c = 0.4142$, $\gamma = 116.89°$.

Er_2CoGe_6 is isotypic with Ce_2CuGe_6 (9), $a = 0.39777$, $b = 0.39331$, $c = 2.1386$ (Oleksyn et al. 1991; X-ray powder diffraction data). The sample was melted in an arc furnace and annealed at 1070 K in an evacuated quartz capsule for 400 h. The purity of the starting materials was greater than 99.9 mass%.

$Er_5Co_4Ge_{10}$ (10) was found to adopt the $Sc_5Co_4Si_{10}$-type structure, $a = 1.2663$, $c = 0.41504$ (Oleksyn 1990; X-ray powder diffraction).

$Er_3Co_2Ge_3$ (14) crystallizes with the $Hf_3Ni_2Si_3$ type structure, $a = 0.4145$, $b = 1.0337$, $c = 1.3784$ (Oleksyn 1990; X-ray powder diffraction).

Four compounds with unknown structures were observed by Oleksyn (1990) in the Er–Co–Ge system at 1070 K: ~$Er_{0.03}Co_{0.65}Ge_{0.32}$ (1), ~$Er_{0.15}Co_{0.30}Ge_{0.55}$ (4), ~$Er_{0.20}Co_{0.20}Ge_{0.60}$ (8) and ~$Er_{0.42}Co_{0.10}Ge_{0.48}$ (16).

One more compound was observed from an arc melted sample and investigated by Oleksyn (1990) using single-crystal method: $Er_{6-x}Co_6Ge_4$, new structure type, $a = 0.5091$, $c = 0.7861$.

4.13.5. *Er–Ni–Ge*

Figure 105 presents the isothermal section of the Er–Ni–Ge phase diagram at 1070 K, studied by Oleksyn (1990). The isothermal section was constructed by means of X-ray powder microprobe and microstructural analyses of 240 alloys which were arc melted, subsequently annealed in evacuated silica tubes for 350 h at 1070 K, and finally quenched in water. The starting materials were Er 99.82 mass%, Ni 99.99 mass%, and Ge 99.99 mass%.

The ternary phase diagram is characterized by the existence of fourteen ternary compounds and by the formation of substitutional solid solutions originating at Er_2Ni_{17} and $ErNi_5$ (10 at.% Ge) as well as Er_5Ge_3 (13 at.% Ni). Nonstoichiometry was observed for $ErNi_{1-x}Ge_2$.

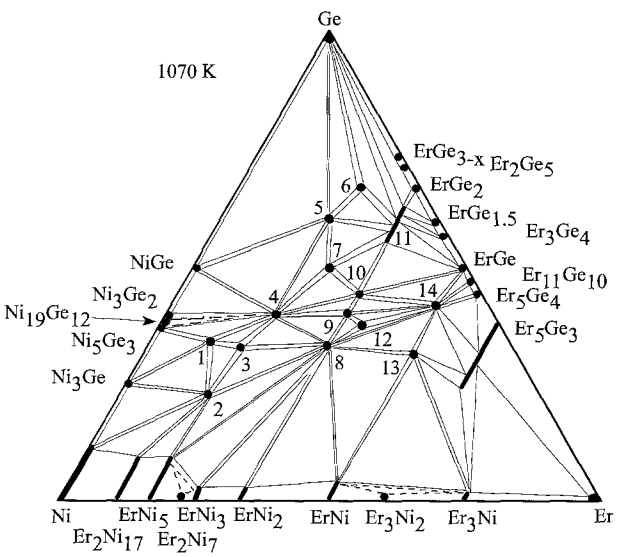

Fig. 105. Er–Ni–Ge, isothermal section at 1070 K.

$ErNi_5Ge_3$ (1) was reported to crystallize with the YNi_5Si_3 type, $a = 1.903$, $b = 0.3847$, $c = 0.6783$ by Fedyna et al. (1987). The arc melted alloy, annealed at 1070 K, was investigated by X-ray powder diffraction analysis. The starting materials were Er 99.82 mass%, Ni 99.99 mass%, and Ge 99.99 mass%.

$Er_3Ni_{11}Ge_4$ (2) belongs to the $Sc_3Ni_{11}Si_4$-type family of compounds, $a = 0.8273$, $c = 0.8680$, after Fedyna et al. (1987). For the preparation of the alloy, see $ErNi_5Ge_3$.

Oleksyn and Bodak (1994) used X-ray powder diffraction to investigate the crystal structure of $ErNi_3Ge_2$ (3) which forms a new structure type, $a = 1.79662$, $c = 0.379410$. For alloy synthesis, see Er–Ni–Ge.

The $ErNi_2Ge_2$ (4) compound was found to adopt the $CeGa_2Al_2$-type structure, $a = 0.4016$, $c = 0.9733$ (Rieger and Parthé 1969b).

$ErNiGe_3$ (5) with the $SmNiGe_3$-type structure ($a = 0.4013$, $b = 0.4031$, $c = 2.1396$, X-ray powder diffraction analysis) was reported by Bodak et al. (1985). For the details of sample preparation and purity of starting materials, see $SmNiGe_3$ under Sm–Ni–Ge.

Er_2NiGe_6 (6) was found to be isostructural with the Ce_2CuGe_6-type structure ($a = 0.39492$, $b = 2.1148$, $c = 0.39957$) by Oleksyn (1990) from X-ray powder diffraction. The sample was prepared by arc melting ingots of the constituting elements and annealing the resulting button at 1070 K for 700 h.

The crystal structure of the $ErNiGe_2$ (7) compound was investigated by Oleksyn (1990) from X-ray powder diffraction of arc melted alloys annealed at 1070 K for 350 h. It was found to adopt a $NdIrGe_2$-type structure with lattice parameters $a = 0.4125$, $b = 0.8451$, $c = 1.5792$.

Gorelenko et al. (1984) reported the crystal structure of ErNiGe (8) (TiNiSi type, $a = 0.6818$, $b = 0.4188$, $c = 0.7239$; X-ray powder analysis). The alloy was obtained by arc melting and annealing in an evacuated quartz tube at 870 K for 350 hours.

$ErNi_{0.4}Ge_{1.6}$ (10) was said to crystallize with the AlB_2 type structure, $a = 0.40737$, $c = 0.39284$ (Oleksyn 1990; X-ray powder diffraction).

Pecharsky et al. (1989) investigated the formation and crystal structure of the $ErNi_{1-x}Ge_2$ (11) compound by X-ray powder analysis of arc melted alloy annealed at 870 K ($CeNiSi_2$ type, $a = 0.3970$, $b = 1.5938$, $c = 0.3980$). Francois et al. (1990) confirmed the structure and reported the composition and lattice parameters $ErNi_{0.65}Ge_2$, $a = 0.4068$, $b = 1.612$, $c = 0.3922$ (X-ray powder diffraction) from a sample obtained by powder metallurgical reaction at 1173 K. Oleksyn (1990) described the limits of the homogeneity field for the compound with the $CeNiSi_2$ type structure with the formula $ErNi_{0.12-0.36}Ge_{1.88-1.64}$, $a = 0.4078$–0.4052, $b = 1.621$–1.578, $c = 0.4000$–0.3924.

$Er_3Ni_2Ge_3$ (12) belongs to the $Hf_3Ni_2Si_3$ type, $a = 0.41435$, $b = 1.0266$, $c = 1.3863$ (Oleksyn 1990; X-ray powder diffraction).

Bodak et al. (1982) reported on the crystal structure of the Er_3NiGe_2 (13) compound from X-ray powder diffraction (La_3NiGe_2 type, $a = 1.1180$, $b = 0.4181$, $c = 1.1124$). The proper amounts of starting components were arc melted and annealed at 870 K.

The crystal structures of two ternary compounds have not been evaluated (Oleksyn 1990): $Er_{0.333}Ni_{0.25}Ge_{0.417}$ (9), $Er_{0.48}Ni_{0.10}Ge_{0.42}$ (14).

4.13.6. *Er–Cu–Ge*

No phase diagram is available for the ternary Er–Cu–Ge system, however five ternary compounds were observed and characterized by different groups of authors.

Rieger and Parthé (1969a) investigated the occurrence of the AlB_2-type structure by means of X-ray powder diffraction of arc melted alloys. The data presented are $ErCu_{0.67}Ge_{1.33}$ with $a = 0.398$, $c = 0.404$. Iandelli (1993) observed ErCuGe with the $CaIn_2$ type ($a = 0.4227$, $c = 0.7108$, X-ray powder analysis). The alloy was prepared from filings or powders of metals (Er 99.7%, Cu and Ge 99.99%), which were mixed and sealed in a tantalum crucible under argon, melted by induction heating, and annealed for 10 days at 1023 K.

$Er_6Cu_8Ge_8$ crystallizes with the $Gd_6Cu_8Ge_8$-type structure, lattice parameters $a = 1.3790$, $b = 0.6617$, $c = 0.4153$ (Rieger 1970).

Konyk et al. (1988) investigated the crystal structure of Er_2CuGe_6 alloy prepared by arc melting under argon and annealing at 870 K in an evacuated quartz tube for 720 h. From X-ray powder analysis the compound was claimed to have the Ce_2CuGe_6-type structure, $a = 0.3977$, $b = 0.4080$, $c = 2.0837$.

Rieger and Parthé (1969b) observed $ErCu_2Ge_2$ with the $CeGa_2Al_2$-type of structure, $a = 0.4003$, $c = 1.0317$.

Francois et al. (1990) observed the $CeNiSi_2$ type for the $ErCu_{0.39}Ge_2$ compound and reported the lattice parameters $a = 0.4066$, $b = 1.602$, $c = 0.3941$ (X-ray powder diffraction) from a sample obtained by a powder metallurgical reaction at 1173 K.

4.13.7. *Er–Nb–Ge*

The phase diagram of the Er–Nb–Ge system has not been yet established. The existence of the compound $Er_2Nb_3Ge_4$ with the $Ce_2Sc_3Si_4$-type structure ($a = 0.6927$, $b = 1.3465$, $c = 0.7116$) was reported by Le Bihan et al. (1996a) from X-ray powder diffraction data of an arc melted alloy. The starting materials were: Er and Nb 99.99 mass%, Ge 99.999 mass%.

4.13.8. *Er–Mo–Ge*

No phase diagram is available for the Er–Mo–Ge system; only one compound was observed and characterized. $Er_2Mo_3Ge_4$ was reported to crystallize with the $Ce_2Sc_3Si_4$-type structure ($a = 0.6863$, $b = 1.3070$, $c = 0.7028$) by Le Bihan et al. (1996b) from X-ray powder diffraction of an arc melted alloy. The starting materials were: Er and Mo 99.99 mass%, Ge 99.999 mass%.

4.13.9. *Er–Ru–Ge*

Early investigations of the $ErRu_2Ge_2$ compound determined that it had the $CeGa_2Al_2$-type structure with $a = 0.4211$, $c = 0.9801$ (Francois et al. 1985) from X-ray powder analysis of an alloy obtained by a powder metallurgical reaction at 1273 K. The starting components were Er (3N), Ru (4N), and Ge (4N).

Venturini et al. (1986b) reported the $Er_2Ru_3Ge_5$ compound to crystallize with the $U_2Co_3Si_5$-type structure, lattice parameters $a=0.9752$, $b=1.240$, $c=0.5696$ (X-ray powder diffraction data). For sample preparation, see $La_2Ru_3Ge_5$ under La–Ru–Ge.

$Pr_3Rh_4Sn_{13}$ type was announced for the $Er_3Ru_4Ge_{13}$ compound ($a=0.8945$) by Segre et al. (1981a) from X-ray powder analysis of an arc melted sample annealed at 1523 K for 1 day and at 1273 K for 7 days. The starting materials were Er (3N), Ru (3N), and Ge (6N).

4.13.10. *Er–Rh–Ge*

Venturini et al. (1985b) reported an X-ray powder diffraction study of the $Er_3Rh_4Ge_{13}$ compound from a sample prepared by heating a mixture of the starting components (Er 3N, Rh 4N, Ge 4N) in an evacuated quartz tube at 1073 K. The crystal structure was found be of the $Yb_3Rh_4Sn_{13}$ type, $a=0.8904$.

$Er_2Rh_3Ge_5$ was found to crystallize with $Lu_2Co_3Si_5$-type ($a=0.9933$, $b=1.2025$, $c=0.5808$, $\beta=92.1°$; X-ray powder diffraction data) by Venturini et al. (1986b) from an alloy which was synthesized by a powder metallurgical reaction at 1173 K. The purity of the starting materials was greater than 99.9 mass%.

$Er_4Rh_7Ge_6$ was reported to adopt $U_4Re_7Si_6$-type structure ($a=0.8296$; Francois et al. 1985) from a sample which was obtained by heating a mixture of powders of the starting materials (Er 3N, Rh 4N, Ge 4N) in an evacuated quartz tube at 1273 K.

Gladyshevsky et al. (1991a) reported on the crystal structure of the $Er_3Rh_2Ge_2$ compound ($La_3Ni_2Ge_2$ type, $a=0.55207$, $b=0.7683$, $c=1.3138$; X-ray powder diffraction data). For the details of sample preparation, see $La_3Rh_2Ge_2$ under La–Rh–Ge.

Verniere et al. (1995) established that the compound $Er_4Rh_{13}Ge_9$ is of the $Ho_4Ir_{13}Ge_9$ type. No lattice parameters were given. For sample preparation, see $La_4Ir_{13}Ge_9$ under La–Ir–Ge.

Er_2Rh_3Ge crystallizes with the Y_2Rh_3Ge-type of structure, lattice parameters $a=0.5523$, $c=1.1762$ (Cenzual et al. 1987). The sample was obtained by arc melting under argon and annealing at 1273 K for 7 days.

Méot-Meyer et al. (1985b) reported the existence of the $Er_5Rh_4Ge_{10}$ compound with $Sc_5Co_4Si_{10}$-type structure, but no lattice parameters were given.

Francois et al. (1985) determined the $CeGa_2Al_2$ type for the $ErRh_2Ge_2$ compound, $a=0.4094$, $c=1.0170$.

Hovestreydt et al. (1982) reported the crystal structure of the ErRhGe compound (TiNiSi type, $a=0.6827$, $b=0.4257$, $c=0.7507$; X-ray powder data) from an arc melted sample annealed at 1270 K for 1–2 weeks. The starting components were Er (3N), Rh (4N), and Ge (5N).

4.13.11. *Er–Pd–Ge*

No systematic study of the Er–Pd–Ge system has been performed; the existence of three ternary compounds has been observed by different groups of authors.

Sologub et al. (1995a) reported an X-ray powder analysis of the Er_2PdGe_6 compound which was found to crystallize with the Ce_2CuGe_6-type structure, $a = 0.40574$, $b = 0.40051$, $c = 2.1402$. For the experimental procedure, see La_2PdGe_6 under La–Pd–Ge. The starting materials used were obtained from Johnson & Matthey, UK (99.9%).

The crystal structure of the compound $ErPd_2Ge$ was found to be of the YPd_2Si type ($a = 0.7296$, $b = 0.7038$, $c = 0.5551$; X-ray powder diffraction) by Jorda et al. (1983). For the experimental procedure, see $LaPd_2Ge$ under La–Pd–Ge. The starting materials were Pd 99.99 mass%, Ge specpure quality, and Er 99.9 mass%.

According to an X-ray powder diffraction analysis reported by Hovestreydt et al. (1982), the compound ErPdGe adopts the KHg_2-type structure, $a = 0.4348$ $b = 0.6900$, $c = 0.7536$. For sample preparation, see LaPdGe under La–Pd–Ge. The starting materials were Er (3N), Pd (4N), and Ge (5N).

4.13.12. *Er–Ag–Ge*

No ternary phase diagram has been established for the Er–Ag–Ge system, however one ternary compound has been characterized. Gibson et al. (1996) reported an X-ray single-crystal investigation of the ErAgGe compound. It was found to adopt the ZrNiAl type, $a = 0.70649$, $c = 0.41665$. The single crystal was isolated from an arc melted sample annealed at 970 K for ten days.

4.13.13. *Er–Os–Ge*

No phase diagram exists for the ternary Er–Os–Ge system; four ternary compounds have been observed and studied. The $Pr_3Rh_4Sn_{13}$-type was announced for the $Er_3Os_4Ge_{13}$ compound ($a = 0.8973$) by Segre et al. (1981a) from X-ray powder analysis of an arc melted sample annealed at 1523 K for 1 day and at 1273 K for 7 days. The starting materials were Er (3N), Os (3N), and Ge (6N).

Méot-Meyer et al. (1985b) observed the existence of the $Er_5Os_4Ge_{10}$ compound with $Sc_5Co_4Si_{10}$-type structure from X-ray powder diffraction of a sample obtained by heating in an evacuated tube at 1073 K. However, no lattice parameters were reported.

$Er_4Os_7Ge_6$ was reported to adopt the $U_4Re_7Si_6$-type structure ($a = 0.8314$; Francois et al. 1985) from a sample obtained by heating a mixture of powders of the starting materials (Er 3N, Os 4N, Ge 4N) in an evacuated quartz tube at 1273 K.

$ErOsGe_2$ belongs to the $TiMnSi_2$-type, $a = 0.957$, $b = 1.055$, $c = 0.829$ (Venturini et al. 1985b; X-ray powder diffraction). The alloy was synthesized by a powder metallurgical reaction and annealed at 1073 K.

4.13.14. *Er–Ir–Ge*

No ternary phase diagram has been established for the Er–Ir–Ge system, however six ternary compounds have been characterized.

Venturini et al. (1985b) reported an X-ray powder diffraction study of the $Er_3Ir_4Ge_{13}$ compound from a sample which was prepared by heating a mixture of the starting

components (Er 3N, Ir 4N, Gea 4N) in an evacuated quartz tube at 1073 K. The crystal structure was found to be of the $Yb_3Rh_4Sn_{13}$ type, $a = 0.8923$.

Verniere et al. (1995) reported the $Ho_4Ir_{13}Ge_9$-type structure for the $Er_4Ir_{13}Ge_9$ compound. No lattice parameters were given. For the experimental procedure, see $La_4Ir_{13}Ge_9$ under La–Ir–Ge.

Hovestreydt et al. (1982) reported the crystal structure of the ErIrGe compound (TiNiSi type, $a = 0.6766$, $b = 0.4238$, $c = 0.7593$; X-ray powder data) from an arc melted sample annealed at 1270 K for 1–2 weeks. The starting components were Er (3N), Ir (4N), and Ge (5N).

Francois et al. (1987) reported the crystal structure of $ErIrGe_2$ ($NdIrGe_2$ type, $a = 0.4227$, $b = 1.594$, $c = 0.8783$). The sample was prepared by heating a mixture of powders of the starting components (Er 3N, Ir 3N, Ge 3N) in an evacuated silica tube at 1173 K.

Méot-Meyer et al. (1985b) observed the existence of the $Er_5Ir_4Ge_{10}$ compound with $Sc_5Co_4Si_{10}$ type from a sample obtained by heating in an evacuated tube at 1073 K. However, no lattice paramenters were given.

$Er_4Ir_7Ge_6$ was reported to adopt $U_4Re_7Si_6$-type structure ($a = 0.8295$; Francois et al. 1985) from a sample which was obtained by heating a mixture of powders of the starting materials (Er 3N, Ir 4N, Ge 4N) in an evacuated quartz tube at 1273 K.

4.13.15. *Er–Pt–Ge*

No phase diagram has been established for the Er–Pt–Ge system. Two ternary compounds were observed by different authors.

According to an X-ray powder diffraction analysis reported by Hovestreydt et al. (1982), the compound ErPtGe adopts the TiNiSi-type structure, $a = 0.6917$, $b = 0.4319$, $c = 0.7527$. For sample preparation, see LaPdGe under La–Pd–Ge.

Sologub et al. (1995a) reported an X-ray powder analysis of the Er_2PtGe_6 compound which was found to crystallize with the Ce_2CuGe_6-type structure, $a = 0.40315$, $b = 0.39977$, $c = 2.1573$. For sample preparation, see La_2PdGe_6 under La–Pd–Ge.

4.13.16. *Er–Au–Ge*

Information on interaction of erbium with gold and germanium is due to Rossi et al. 1992). The phase diagram of the Er–Au–Ge system is not available. A ternary compound of erbium with gold and germanium of the stoichiometric 1:1:1 ratio has been identified and studied by means of X-ray and metallographic analyses by Rossi et al. (1992). ErAuGe was found to adopt the LiGaGe type with lattice parameters $a = 0.4397$, $c = 0.7203$. For the experimental procedure, see GdAuGe under Gd–Au–Ge.

4.14. *Tm–d element–Ge systems*

4.14.1. *Tm–Mn–Ge*

No systematic study has been performed for the Tm–Mn–Ge system; however, the formation of two ternary compounds has been reported so far.

$TmMn_6Ge_6$ was found to crystallize in the $HfFe_6Ge_6$-type structure by Venturini et al. (1992), $a = 0.5219$, $c = 0.8139$ (X-ray powder diffraction data). The alloy was synthesized by a powder metallurgical reaction in an evacuated silica tube at 1073 K for 14 days.

$TmMn_{0.25}Ge_2$ compound was found to adopt the $CeNiSi_2$-type structure with lattice parameters $a = 0.4073$, $b = 1.557$, $c = 0.3966$ by Francois et al. (1990) (X-ray powder diffraction data). For sample preparation, see $GdFe_{0.25-0.46}Ge_2$ under Gd–Fe–Ge.

4.14.2. *Tm–Fe–Ge*

The phase diagram of the Tm–Fe–Ge system was investigated by Fedyna (1988) by means of metallographic and X-ray phase analyses (fig. 106). Alloys for investigation were prepared by arc melting followed by annealing at 870 K for 500 hours. The purity of the starting components was greater than 99.9 mass%. Ten ternary compounds were observed.

$TmFe_6Ge_6$ (1) was reported to be isotypic with the crystal structure of YCo_6Ge_6, lattice parameters $a = 0.5143$, $c = 0.4098$ (Mruz et al. 1984). The sample was prepared by arc melting the proper amounts of the starting components followed by annealing at 870 K for two weeks. At variance with these data, $TmFe_6Ge_6$ was found to crystallize with the $HoFe_6Sn_6$-type structure, $a = 0.8095$, $b = 2.653$, $c = 0.5107$, by Venturini et al. (1992) from X-ray powder diffraction data. The alloy was obtained by powder metallurgical reaction in an evacuated silica tube at 1173 K for two weeks. These results suggest that $TmFe_6Ge_6$ may be polymorphic.

$TmFe_4Ge_2$ (2) was found to crystallize in the $ZrFe_4Si_2$-type structure, $a = 0.72228$, $c = 0.37456$, by Fedyna (1988) in the course of a phase diagram investigation employing X-ray powder diffraction.

According to X-ray powder diffraction data, $TmFe_2Ge_2$ (4) is isostructural with

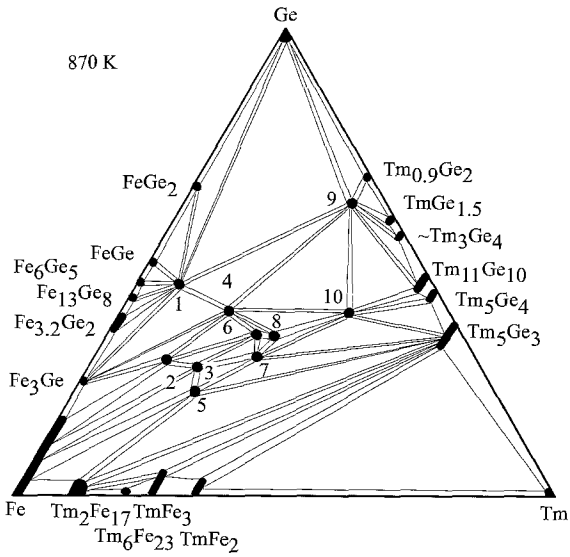

Fig. 106. Tm–Fe–Ge, isothermal section at 870 K.

$CeGa_2Al_2$, lattice parameters $a=0.39301$, $c=1.04184$ (Fedyna 1988; X-ray powder diffraction).

Fedyna (1988) investigated the crystal structure of $Tm_9Fe_{10}Ge_{10}$ (8) by a single-crystal method. It was found to crystallize with a new structure type, $a=0.5386$, $b=1.3306$, $c=1.3913$. The single crystal was isolated from an alloy which was arc melted and annealed at 870 K.

Pecharsky et al. (1989) reported $TmFe_{1-x}Ge_2$ (9) to crystallize with the $CeNiSi_2$-type structure ($a=0.4061$–0.4066, $b=1.5532$–1.5610, $c=0.3959$–0.3961; X-ray powder analysis). The alloy was arc melted and annealed at 870 K. The purity of the starting materials was greater than 99.9 mass%. Francois et al. (1990) confirmed the occurrence of the $CeNiSi_2$ type for thulium–iron–germanium combinations from alloys annealed at 1173 K ($TmFe_{0.35}Ge_2$; $a=0.4082$, $b=1.558$, $c=0.3973$).

Fedyna (1988) investigated the crystal structure of the $Tm_{117}Fe_{52}Ge_{112}$ (10) compound by X-ray powder diffraction ($Tb_{117}Fe_{52}Ge_{112}$ structure type, $a=2.7964$). The alloy was synthesized by arc melting and annealing a melted button at 870 K for 350 h. The starting materials were Tm 99.83 mass%, Fe 99.9 mass%, and Ge 99.99 mass%.

Four more ternary compounds with unknown structure were observed by Fedyna (1988) at 870 K: ~$Tm_{0.20}Fe_{0.53}Ge_{0.27}$ (3), ~$Tm_{0.225}Fe_{0.55}Ge_{0.225}$ (5), ~$Tm_{0.275}Fe_{0.375}Ge_{0.35}$ (6) and ~$Tm_{0.30}Fe_{0.40}Ge_{0.30}$ (7).

4.14.3. *Tm–Co–Ge*

Isothermal sections of the Tm–Co–Ge system at 870 K (33–100 at.% Tm) and at 1070 K (0–33 at.% Tm) were derived by Fedyna (1988) (fig. 107) employing X-ray phase and

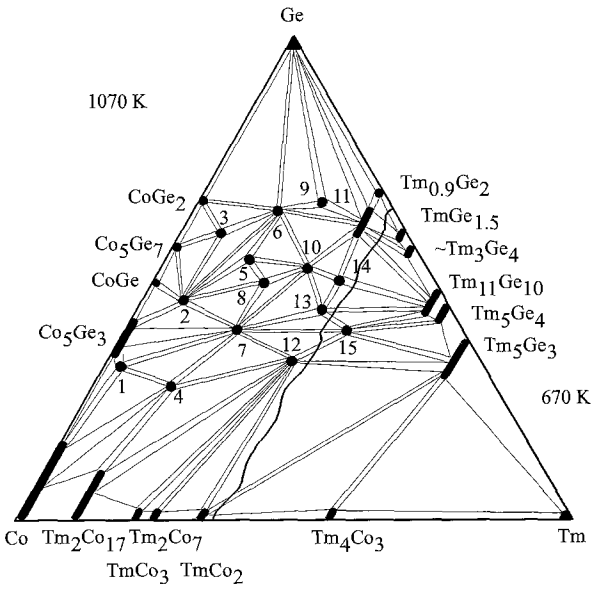

Fig. 107. Tm–Co–Ge, isothermal sections at 1070 K (0–33 at.% Tm) and at 670 K (33–100 at.% Tm).

microstructural analyses of 145 alloys prepared by arc melting the proper amounts of the constituent elements of high purity. The melted buttons were then annealed in evacuated silica tubes for 500 hours. Fifteen ternary compounds were found to exist.

The crystal structure of the $TmCo_6Ge_6$ (2) compound was reported by Buchholz and Schuster (1981) (YCo_6Ge_6 structure type, $a = 0.5098$, c 0.3912). The sample was melted under argon in a corundum crucible at 1073–1273 K.

$TmCo_4Ge_2$ (4) was found to form the $ZrFe_4Si_2$-type structure, $a = 0.72285$, $c = 0.37456$, by Fedyna (1988) employing X-ray powder diffraction.

Méot-Meyer et al. (1985a) reported the crystal structure of $TmCo_xGe_2$ (11), $x = 0.42$ ($CeNiSi_2$ type, $a = 0.4070$, $b = 1.578$, $c = 0.3988$). The sample was prepared by a powder metallurgical reaction and annealed in an evacuated silica tube at 1173 K. Pecharsky et al. (1989) confirmed the formation and crystal structure of the $TmCo_xGe_2$ compound from arc melted alloys annealed at 870 K ($a = 0.4062$–0.4079, $b = 1.5613$–1.5760, $c = 0.3965$–0.3977; X-ray powder analysis).

The crystal structure of $Tm_3Co_4Ge_{13}$ (6) ($Yb_3Rh_4Sn_{13}$ type, $a = 0.8715$; X-ray powder diffraction) was investigated by Venturini et al. (1985b) from a sample which was prepared by heating a compacted mixture of the starting materials (Tm in pieces, 99.9 mass%; Co and Ge in powder, 99.99 mass%) in an evacuated quartz tube at 1073 K. Bodak et al. (1987) reported the $Y_3Co_4Ge_{13}$-type structure for the $Tm_3Co_4Ge_{13}$ compound ($a = 0.87156$; X-ray powder data) from an arc melted alloy annealed at 870 K.

$TmCo_2Ge_2$ (7) was found to adopt the $CeGa_2Al_2$-type structure, $a = 0.4259$, $c = 1.1060$ (Fedyna 1988; X-ray powder diffraction).

Tm_2CoGe_6 is isotypic with Ce_2CuGe_6 (9), $a = 0.3909$, $b = 0.3951$, $c = 2.1252$ (Oleksyn et al. 1991; X-ray powder diffraction data). The sample was melted in an arc furnace and annealed at 1070 K in an evacuated quartz capsule for 400 h. The purity of the starting materials was greater than 99.9 mass%.

$Tm_5Co_4Ge_{10}$ (10) has the $Sc_5Co_4Si_{10}$-type structure, $a = 1.2622$, $c = 0.4139$, after Venturini et al. (1984).

Gorelenko et al. (1984) reported the crystal structure of TmCoGe (12) (TiNiSi type, $a = 0.6775$, $b = 0.4168$, $c = 0.7224$; X-ray powder analysis). The alloy was obtained by arc melting and annealing in an evacuated quartz tube at 870 K for 350 hours.

$Tm_3Co_2Ge_4$ (13) crystallizes with the $Tb_3Co_2Ge_4$-type structure, $a = 1.0410$, $b = 0.7904$, $c = 0.4143$, $\gamma = 107.04°$ (X-ray powder diffraction data; Mruz et al. (1989). The sample was prepared by arc melting and annealing at 873 K for 240 h.

Bodak et al. (1986) reported an X-ray powder investigation of the compound Tm_2CoGe_2 (15): Sc_2CoSi_2-type structure, $a = 1.0326$, $b = 1.0125$, $c = 0.4119$, $\gamma = 117.00°$.

In the course of phase diagram studies, Fedyna (1988) observed five more ternary compounds with unknown structures: ~$Tm_{0.03}Co_{0.65}Ge_{0.32}$ (1), ~$Tm_{0.07}Co_{0.33}Ge_{0.60}$ (3), ~$Tm_{0.15}Co_{0.30}Ge_{0.55}$ (5), ~$Tm_{0.20}Co_{0.30}Ge_{0.50}$ (8) and ~$Tm_{0.33}Co_{0.17}Ge_{0.50}$ (14).

4.14.4. *Tm–Ni–Ge*

Figure 108 represents the isothermal sections of the Tm–Ni–Ge system at 870 K (0–50 at.% Tm) and at 670 K (50–100 at.% Tm), studied by Fedyna (1988). The isothermal

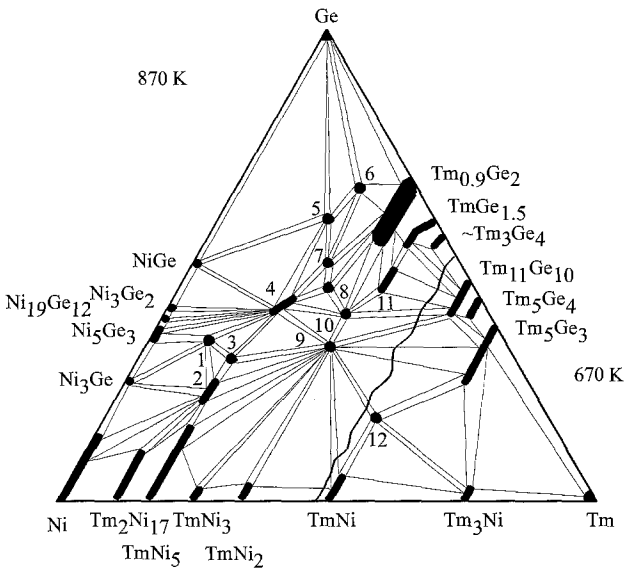

Fig. 108. Tm–Ni–Ge, isothermal sections at 870 K (0–50 at.% Tm) and at 670 K (50–100 at.% Tm).

sections were constructed by means of X-ray powder and metallographic analyses of 200 alloys which were arc melted, subsequently annealed in evacuated silica tubes for 900 h, and finally quenched in water. The starting materials were Tm 99.82 mass%, Ni 99.98 mass% and Ge 99.99 mass%.

The ternary phase diagram is characterized by the existence of twelve ternary compounds and by the formation of substitutional solid solutions based at Tm_2Ni_{17} (10 at.% Ge) and $TmNi_5$ (15 at.% Ge). The binary compounds Tm_5Ge_3 and $Tm_{11}Ge_{10}$ dissolve 13 and 8 at.% Ni, respectively.

$TmNi_5Ge_3$ (1) was reported to crystallize with the YNi_5Si_3 type, $a = 1.90183$, $b = 0.38398$, $c = 0.67867$, by Fedyna (1988). The arc melted alloy, annealed at 870 K, was investigated by X-ray powder diffraction analysis. The starting materials were Tm 99.82 mass%, Ni 99.99 mass%, and Ge 99.99 mass%.

$Tm_3Ni_{11}Ge_4$ (2) belongs to the $Sc_3Ni_{11}Si_4$-type structure group of compounds, $a = 0.8279$, $c = 0.8690$, after Fedyna et al. (1987). The alloy was prepared in the same manner as $TmNi_5Ge_3$.

The $TmNi_{2-1.56}Ge_{2-2.20}$ (4) compound was found to adopt the $CeGa_2Al_2$-type structure, $a = 0.4003$–0.3985, $c = 0.9724$–0.9596 (Fedyna 1988).

$TmNiGe_3$ (5) with the $ScNiSi_3$-type structure ($a = 2.1372$, $b = 0.4019$, $c = 0.4003$, X-ray powder diffraction analysis) was reported by Bodak et al. (1985). For the details of sample preparation and the purity of the starting materials, see $TmNi_5Ge_3$.

Tm_2NiGe_6 (6) has been found by Oleksyn (1990) from X-ray powder diffraction to be isostructural with Ce_2CuGe_6-type structure ($a = 0.3931$, $b = 2.1031$, $c = 0.3979$). The

sample was prepared by arc melting ingots of the constituting elements and annealing at 1070 K for 700 h. For the purity of starting materials, see $TmNi_5Ge_3$.

Oleksyn (1990) reported the crystal structure of the $TmNiGe_2$ (7) compound, $NdIrGe_2$ type, $a = 0.4095$, $b = 0.8405$, $c = 1.5779$, from X-ray powder diffraction analysis. For the experimental procedure, see Tm_2NiGe_6.

Gorelenko et al. (1984) investigated the crystal structure of TmNiGe (9) (TiNiSi type, $a = 0.6790$, $b = 0.4183$, $c = 0.7235$; X-ray powder analysis). The alloy was obtained by arc melting and annealing in an evacuated quartz tube at 870 K for 350 hours. According to DTA, this phase exhibits polymorphism at 1630 K (Koterlyn et al. 1994).

$Tm(Ni_{0.23-0.165}Ge_{0.60-0.665})_{2-x}$ (11), $x = 0.34$, was said to form an AlB_2 type, $a =$ 0.40795–0.40706, $c = 0.39238$–0.40084 (Fedyna 1988; X-ray powder diffraction).

Four more ternary compounds with unknown structures were observed by Fedyna (1988) in the Tm–Ni–Ge system: $\sim Tm_{0.17}Ni_{0.53}Ge_{0.30}$ (3), $\sim Tm_{0.27}Ni_{0.28}Ge_{0.45}$ (8), $\sim Tm_{0.33}Ni_{0.27}Ge_{0.40}$ (10) and $\sim Tm_{0.50}Ni_{0.32}Ge_{0.18}$ (12).

Pecharsky et al. (1989) investigated the formation and crystal structure of the $TmNi_{1-x}Ge_2$ compound by X-ray powder analysis of arc melted alloy annealed at 870 K ($CeNiSi_2$ type, $a = 0.4015$–0.4071, $b = 1.5728$–1.6023, $c = 0.3881$–0.3979). For sample preparation, see $TmNi_5Ge_3$. Francois et al. (1990) confirmed the structure and reported the composition and lattice parameters $TmNi_{0.42}Ge_2$, $a = 0.4070$, $b = 1.578$, $c = 0.3988$ (X-ray powder diffraction) from a sample obtained by powder metallurgical reaction at 1173 K.

4.14.5. *Tm–Cu–Ge*

No isothermal section is available for the ternary Tm–Cu–Ge system; however five ternary compounds were observed and characterized by different groups of authors.

Rieger and Parthé (1969a) investigated the occurrence of the AlB_2-type structure by means of X-ray powder diffraction of arc melted alloys. The data presented were $TmCu_{1-0.67}Ge_{1-1.33}$ with $a = 0.4220$–0.397, $c = 0.3545$–0.397. At variance with the data of Rieger and Parthé (1969a), Iandelli (1993) observed TmCuGe with the $CaIn_2$-type ($a = 0.4225$, $c = 0.7045$, X-ray powder analysis). The alloy was prepared from turnings or powders of metals (thulium 99.7 mass%, copper and germanium 99.99 mass%), which were mixed and sealed in a tantalum crucible under argon, melted by induction heating, and annealed for 10 days at 1023 K.

$Tm_6Cu_8Ge_8$ crystallizes with the $Gd_6Cu_8Ge_8$-type structure, lattice parameters $a =$ 1.374, $b = 0.660$, $c = 0.413$ (Hanel and Nowotny 1970).

Konyk et al. (1988) investigated the crystal structure of Tm_2CuGe_6 which had been prepared by arc melting the starting components under argon and annealing at 870 K in an evacuated quartz tube for 720 h. From X-ray powder analysis the Ce_2CuGe_6-type structure was claimed for this compound, $a = 0.4065$, $b = 0.3963$, $c = 2.0767$.

Rieger and Parthé (1969b) prepared $TmCu_2Ge_2$ with the $CeGa_2Al_2$-type structure, $a =$ 0.3994, $c = 1.0307$.

Francois et al. (1990) observed the $CeNiSi_2$-type structure for the $TmCu_{0.20}Ge_2$ compound and reported the lattice parameters $a = 0.4055$, $b = 1.585$, $c = 0.3931$ (X-ray

powder diffraction) from a sample obtained by a powder metallurgical reaction at 1173 K.

4.14.6. *Tm–Nb–Ge*

The phase diagram of the Tm–Nb–Ge system has not been established. The existence of the compound $Tm_2Nb_3Ge_4$ with the $Ce_2Sc_3Si_4$ type ($a=0.6917$, $b=1.3416$, $c=0.7092$) was reported by Le Bihan et al. (1996a) from X-ray powder diffraction data of arc melted alloy. Starting materials were: Tm and Nb 99.99 mass%, Ge 99.999 mass%.

4.14.7. *Tm–Mo–Ge*

No phase diagram is available for the Tm–Mo–Ge system, and only one compound was observed and investigated. $Tm_2Mo_3Ge_4$ was reported to crystallize with the $Ce_2Sc_3Si_4$-type structure ($a=0.6840$, $b=1.3041$, $c=0.7009$) by Le Bihan et al. (1996b) from X-ray powder diffraction of an arc melted alloy. The starting materials were: Tm and Mo 99.99 mass%, Ge 99.999 mass%.

4.14.8. *Tm–Ru–Ge*

X-ray powder analysis of an alloy with the $TmRu_2Ge_2$ composition showed that it had the $CeGa_2Al_2$-type structure with $a=0.4202$, $c=0.9797$ (Francois et al. 1985). The sample was obtained by a powder metallurgical reaction at 1273 K. The starting components were Tm (3N), Ru (4N), and Ge (4N).

Venturini et al. (1986b) reported on $Tm_2Ru_3Ge_5$ crystallizing with the $U_2Co_3Si_5$ type. Lattice parameters were reported as $a=0.9725$, $b=1.239$, $c=0.5676$ (X-ray powder diffraction data). For sample preparation, see $La_2Ru_3Ge_5$ under La–Ru–Ge.

$Yb_3Rh_4Sn_{13}$ type was reported for the $Tm_3Ru_4Ge_{13}$ compound ($a=0.8925$) by Segre et al. (1981a) from X-ray powder analysis of an arc melted sample annealed at 1523 K for 1 day and at 1273 K for 7 days. The starting materials were Tm (3N), Ru (3N), and Ge (6N).

4.14.9. *Tm–Rh–Ge*

Venturini et al. (1985b) reported an X-ray powder diffraction study of the crystal structure of $Tm_3Rh_4Ge_{13}$ from an alloy which was prepared by heating a mixture of the starting components (Tm 3N, Rh 4N, Ge 4N) in an evacuated quartz tube at 1073 K. It was found to adopt the $Yb_3Rh_4Sn_{13}$-type structure, $a=0.8899$.

Francois et al. (1985) determined the $CeGa_2Al_2$ type for the $TmRh_2Ge_2$ compound, $a=0.4062$, $c=1.0129$.

$Tm_2Rh_3Ge_5$ was found to crystallize with $Lu_2Co_3Si_5$-type structure ($a=0.9903$, $b=1.2009$, $c=0.5781$, $\beta=92.4°$; X-ray powder diffraction data) by Venturini et al. (1986b) from a sample prepared by a powder metallurgical reaction at 1173 K. The purity of the starting materials was greater than 99.9 mass%.

Gladyshevsky et al. (1991a) reported on the crystal structure of the $Tm_3Rh_2Ge_2$ compound ($La_3Ni_2Ge_2$ type, $a=0.550897$, $b=0.7654$, $c=1.3097$; X-ray powder diffraction data). For the details of sample preparation, see $La_3Rh_2Ge_2$ under La–Rh–Ge.

Verniere et al. (1995) observed that the compound $Tm_4Rh_{13}Ge_9$ belonged to the $Ho_4Ir_{13}Ge_9$-type structure. No lattice parameters were reported. For sample preparation, see $La_4Ir_{13}Ge_9$ under La–Ir–Ge.

Venturini et al. (1984) established the existence of the $Tm_5Rh_4Ge_{10}$ compound with $Sc_5Co_4Si_{10}$-type structure, $a=1.2868$, $c=0.4230$, from X-ray powder analysis of a sample obtained by heating a mixture of powders in an evacuated tube at 1073 K.

$Tm_4Rh_7Ge_6$ belongs to the $U_4Re_7Si_6$-type structure group, $a=0.8276$ (Francois et al. 1985; X-ray powder diffraction). The alloy was synthesized by heating a mixture of powders of the constituent elements in an evacuated quartz tube at 1273 K. The starting components were Tm (3N), Rh (4N), and Ge (4N).

4.14.10. *Tm–Pd–Ge*

No systematic study of the Tm–Pd–Ge system has been performed, but the existence of three ternary compounds has been observed by different groups of authors.

Sologub et al. (1995a) reported an X-ray powder analysis of the Tm_2PdGe_6 compound which was found to crystallize with the Ce_2CuGe_6-type structure, $a=0.4047$, $b=0.3995$, $c=2.1346$. For the experimental procedure, see La_2PdGe_6 under La–Pd–Ge. The purity of the starting materials used was 99.9 mass%.

The crystal structure of the compound $TmPd_2Ge$ was found to be of the YPd_2Si type ($a=0.7254$, $b=0.7045$, $c=0.5523$; X-ray powder diffraction) by Jorda et al. (1983). For the experimental procedure, see $LaPd_2Ge$ under La–Pd–Ge. The starting materials were Pd 99.99 mass%, Ge specpure quality, and Tm 99.9 mass%.

According to an X-ray powder diffraction analysis reported by Hovestreydt et al. (1982), the compound TmPdGe adopts the KHg_2-type structure, $a=0.4337$, $b=0.6855$, $c=0.7524$. For sample preparation, see LaPdGe under La–Pd–Ge. The starting metals were Tm (3N), Pd (4N), and Ge (5N).

4.14.11. *Tm–Ag–Ge*

No ternary phase diagram has been established for the Tm–Ag–Ge system, however one ternary compound has been characterized. Gibson et al. (1996) reported an X-ray powder investigation of the TmAgGe compound. It was found to adopt the ZrNiAl-type structure, $a=0.70415$, $c=0.41570$. The sample was arc melted and annealed at 970 K for ten days.

4.14.12. *Tm–Os–Ge*

No phase diagram is available for the ternary Tm–Os–Ge system; four ternary compounds have been observed. $Tm_4Os_7Ge_6$ belongs to the $U_4Re_7Si_6$-type structure group of compounds, $a=0.8297$ (Francois et al. 1985; X-ray powder diffraction). The alloy was synthesized by heating a mixture of powders of the constituent elements in an evacuated quartz tube at 1273 K. The starting components were Tm (3N), Os (4N), and Ge (4N).

The $Pr_3Rh_4Sn_{13}$-type structure was reported for the $Tm_3Os_4Ge_{13}$ compound (a= 0.8955) by Segre et al. (1981a) from X-ray powder analysis of an arc melted sample annealed at 1523 K for 1 day and at 1273 K for 7 days. The starting materials were Tm (3N), Os (3N), and Ge (6N).

Venturini et al. (1984) observed the existence of the $Tm_5Os_4Ge_{10}$ compound with $Sc_5Co_4Si_{10}$-type structure, a = 1.2929, c = 0.4253, from a sample obtained by heating a compacted mixture of powders of the starting metals in an evacuated tube at 1073 K.

$TmOsGe_2$ is isostructural with $TiMnSi_2$, a = 0.953, b = 1.052, c = 0.827 (Venturini et al. 1985b; X-ray powder diffraction). The alloy was obtained by a powder metallurgical reaction and annealed at 1073 K.

4.14.13. *Tm–Ir–Ge*

No ternary phase diagram has been established for the Tm–Ir–Ge system, however five ternary compounds have been characterized.

Méot-Meyer et al. (1985b) observed the existence of the $Tm_5Ir_4Ge_{10}$ compound with $Sc_5Co_4Si_{10}$-type structure from samples obtained by heating compacted mixtures of the proper amounts of the starting metals in evacuated tubes at 1073 K.

Venturini et al. (1985b) reported an X-ray powder diffraction study of the $Tm_3Ir_4Ge_{13}$ compound from a sample which was prepared in the same way as $Tm_5Ir_4Ge_{10}$. The starting components were Tm (3N), Ir (4N), and Ge (4N). The crystal structure was found to be of the $Yb_3Rh_4Sn_{13}$ type, a = 0.8912.

Hovestreydt et al. (1982) reported the crystal structure of the TmIrGe compound (TiNiSi type, a = 0.6736, b = 0.4227, c = 0.7591; X-ray powder data) from an arc melted sample annealed at 1270 K for 1–2 weeks. The starting components were Tm (3N), Ir (4N), and Ge (5N).

Verniere et al. (1995) suggested the $Ho_4Ir_{13}Ge_9$-type structure for the $Tm_4Ir_{13}Ge_9$ compound. No lattice parameters were given. For the experimental procedure, see $La_4Ir_{13}Ge_9$ under La–Ir–Ge.

$Tm_4Ir_7Ge_6$ was reported to adopt the $U_4Re_7Si_6$-type structure (a = 0.8273; Francois et al. 1985) from a sample which was obtained by heating a mixture of powders of the starting materials (Tm 3N, Ir 3N, Ge 4N) in an evacuated quartz tube at 1273 K.

4.14.14. *Tm–Pt–Ge*

No phase diagram has been established for the Tm–Pt–Ge system. Three ternary compounds were observed by different scientific groups.

According to an X-ray powder diffraction analysis reported by Hovestreydt et al. (1982), the compound TmPtGe adopts the TiNiSi-type structure, a = 0.6880, b = 0.4306, c = 0.7517. For sample preparation, see LaPdGe under La–Pd–Ge.

Sologub et al. (1995a) reported an X-ray powder analysis of the Tm_2PtGe_6 compound which was found to crystallize with the Ce_2CuGe_6-type structure, a = 0.4048, b = 0.3993, c = 2.1539. For sample preparation, see La_2PdGe_6 under La–Pd–Ge.

Francois et al. (1987) observed the existence of $TmPtGe_2$ with the $NdIrGe_2$-type structure. The lattice parameters were measured as $a = 0.4263$, $b = 1.620$, $c = 0.8657$. The sample was prepared by heating a mixture of powders of the starting components (Tm 3N, Pt 3N, Ge 3N) in an evacuated silica tube at 1173 K.

4.14.15. *Tm–Au–Ge*

The only information on the interaction of components in the ternary Tm–Au–Ge system is due to Pöttgen et al. (1996a) who observed and characterized the TmAuGe compound. The LiGaGe-type structure was claimed with lattice parameters $a = 0.43907$, $c = 0.71659$ (X-ray single-crystal data). The sample was obtained by melting a mixture of the metals in an arc furnace and annealing at 1070 K for one week.

4.15. *Yb–d element–Ge systems*

4.15.1. *Yb–Mn–Ge*

The isothermal section for the Yb–Mn–Ge system at 670 K was established by Dzianii (1995) who employed X-ray powder analysis of 84 samples obtained by arc melting the proper amounts of starting components and annealing at 670 K for twenty days. The phase-field relations are characterized by the existence of three ternary compounds (fig. 109). The solubility of a third component in the binary compounds was found to be negligible.

$YbMn_6Ge_6$ (1) was found to crystallize with the $HfFe_6Ge_6$-type structure by Venturini et al. (1992), $a = 0.5212$, $c = 0.8132$ (X-ray powder diffraction data). The alloy was synthesized by powder metallurgical reaction in an evacuated silica tube at 1073 K for 14 days.

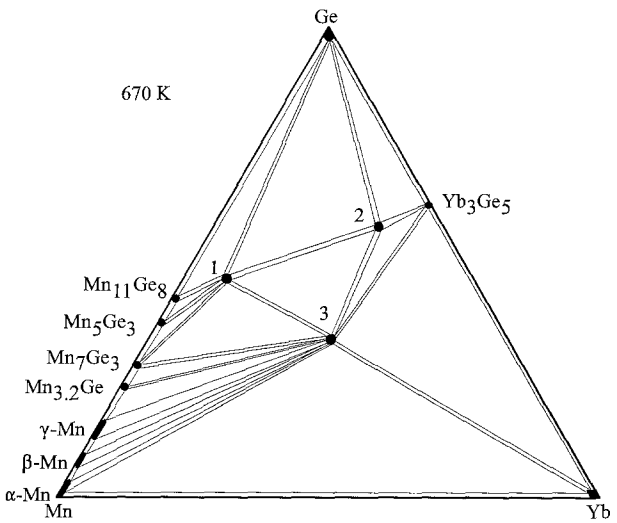

Fig. 109. Yb–Mn–Ge, isothermal section at 670 K.

Dzianii (1995) reported on the existence of the $YbMn_{0.52}Ge_2$ (2) compound: $CeNiSi_2$ type, $a=0.4071$, $b=1.5503$, $c=0.3964$ (X-ray powder diffraction).

One more ternary compound with an unknown structure was observed by Dzianii (1995) in the course of studying the phase equilibria in the Yb–Mn–Ge system at 670 K; ~$Yb_9Mn_{10}Ge_{10}$ (3).

Rossi et al. (1978b) investigated the crystal structure of the $YbMn_2Ge_2$ compound by X-ray powder diffraction. The $CeGa_2Al_2$-type structure was announced for this phase with lattice parameters $a=0.4067$, $c=1.0871$. For sample preparation, see $TbMn_2Ge_2$ under Tb–Mn–Ge. Apparently this phase does not exist at 670 K.

4.15.2. *Yb–Fe–Ge*

The phase diagram of the Yb–Fe–Ge system (fig. 110) was investigated by Dzianii (1995) by means of X-ray phase analysis of 90 samples. The alloys for investigation were prepared by arc melting. The samples were homogenized by annealing at 670 K for 480 hours. The purity of the starting components was Yb 99.8 mass%, Fe 99.9 mass%, and Ge 99.99 mass%. Five ternary compounds were observed.

$YbFe_6Ge_6$ (1) was found to crystallize with the $HfFe_6Ge_6$-type structure, $a=0.5097$, $c=0.8092$, by Venturini et al. (1992) from X-ray powder diffraction data. The alloy was obtained by a powder metallurgical reaction in an evacuated silica tube at 1173 K for two weeks. At variance with these data, $YbFe_6Ge_6$ was reported to be isotypic with the crystal structure of YCo_6Ge_6 with lattice parameters $a=0.5098$, $c=0.4049$ (Dzianii et al. 1995a). The sample was prepared by arc melting the proper amounts of starting components followed by annealing at 670 K for two weeks.

$YbFe_4Ge_2$ (2) was found to crystallize with the $ZrFe_4Si_2$ type structure, $a=0.72279$, $c=0.38764$, by Dzianii et al. (1995b). For the experimental procedure, see Yb–Fe–Ge.

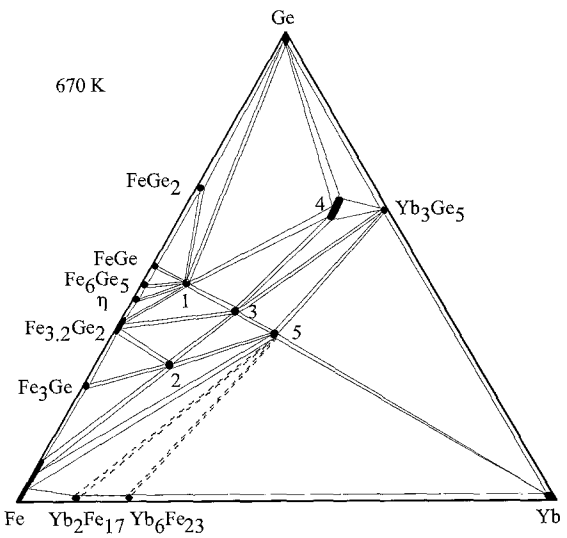

Fig. 110. Yb–Fe–Ge, isothermal section at 670 K.

According to X-ray powder diffraction data, $YbFe_2Ge_2$ (3) is isostructural with the $CeGa_2Al_2$ type, lattice parameters $a = 0.3924$, $c = 1.0503$ (Rossi et al. 1978a; X-ray powder diffraction).

Dzianii (1995) reported $Yb(Fe_{0.43-0.25}Ge_{0.25-0.39})Ge_2$ (4) to crystallize with the $CeNiSi_2$-type structure ($a = 0.4070$, $b = 1.5475$, $c = 0.3961$; X-ray powder analysis).

One more ternary compound with an unknown structure was observed in the course of phase equilibrium studies of the ternary Yb–Fe–Ge system at 670 K by Dzianii (1995) employing X-ray powder diffraction: $\sim Yb_9Fe_{10}Ge_{10}$ (5).

4.15.3. *Yb–Co–Ge*

The isothermal section of the Yb–Co–Ge system at 670 K was derived by Dzianii et al. (1995c) (fig. 111) using X-ray analysis of 99 alloys prepared by arc melting the proper amounts of high-purity constituent elements. The melted buttons were then annealed in evacuated silica tubes for 500 hours. Seven ternary compounds were found to exist.

The crystal structure of the $YbCo_6Ge_6$ (1) compound was reported by Buchholz and Schuster (1981): YCo_6Ge_6 structure type, $a = 0.5078$, $c = 0.3910$. The sample was melted under argon in a corundum crucible at 1073–1273 K.

$YbCo_4Ge_2$ (2) was found to adopt the $ZrFe_4Si_2$-type structure, $a = 0.7236$, $c = 0.3716$, by Fedyna (1988) employing X-ray powder diffraction method. For sample preparation, see Pr–Fe–Ge.

The crystal structure of the $Yb_3Co_4Ge_{13}$ (3) compound ($Yb_3Rh_4Sn_{13}$ type, $a = 0.8705$; X-ray powder diffraction) was investigated by Venturini et al. (1985b) from a sample which was prepared by heating a compacted mixture of the starting materials (Yb in pieces, 99.9 mass%; Co and Ge in powder, 99.99 mass%) in an evacuated quartz tube

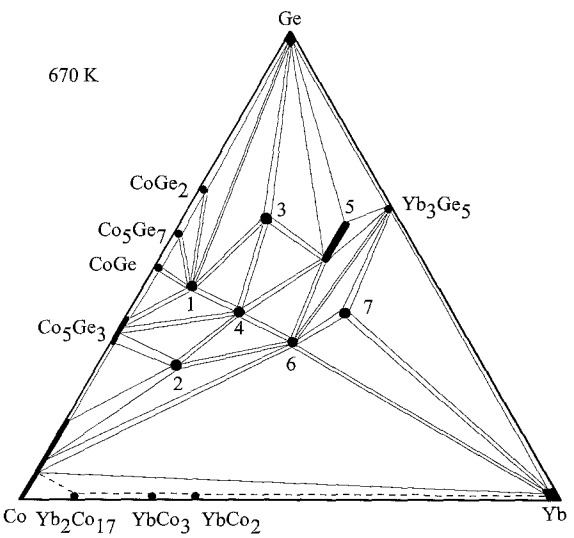

Fig. 111. Yb–Co–Ge, isothermal section at 670 K.

at 1073 K. Bodak et al. (1987) reported the $Y_3Co_4Ge_{13}$-type structure for the $Yb_3Co_4Ge_{13}$ compound ($a = 0.8725$; X-ray powder data) from an arc melted alloy annealed at 870 K.

$YbCo_2Ge_2$ (4) was found to adopt the $CeGa_2Al_2$-type structure, $a = 0.3996$, $c = 1.0123$ (Dzianii 1995; X-ray powder diffraction).

Méot-Meyer et al. (1985a) reported the crystal structure of $YbCo_xGe_2$ (5), $x = 0.37$ ($CeNiSi_2$ type, $a = 0.4077$, $b = 1.563$, $c = 0.3967$). The sample was prepared by a powder metallurgical reaction and annealed in an evacuated silica tube at 1173 K. Pecharsky et al. (1989) confirmed the formation and crystal structure of the $YbCo_xGe_2$ compound from arc melted alloys annealed at 870 K ($a = 0.4045$, $b = 1.5512$, $c = 0.3948$; X-ray powder analysis).

In the course of phase diagram studies, two more ternary compounds with unknown structures were observed by Dzianii (1995): ~YbCoGe (6) and ~Yb_2CoGe_2 (7).

$Yb_5Co_4Ge_{10}$ was observed to crystallize with the $Sc_5Co_4Si_{10}$-type structure by Méot-Meyer et al. (1985b). For experimental details, see $YbCo_xGe_2$ under Yb–Co–Ge. Apparently this phase does not exist at 670 K.

4.15.4. *Yb–Ni–Ge*

Figure 112 represents the isothermal section of the Yb–Ni–Ge system at 670 K, studied by Dzianii (1995). The isothermal section was constructed by means of X-ray powder analysis of 110 alloys which were arc melted and subsequently annealed in evacuated silica tubes for 480 h and finally quenched in water. The starting materials were Yb 99.8 mass%, Ni 99.9 mass%, and Ge 99.99 mass%.

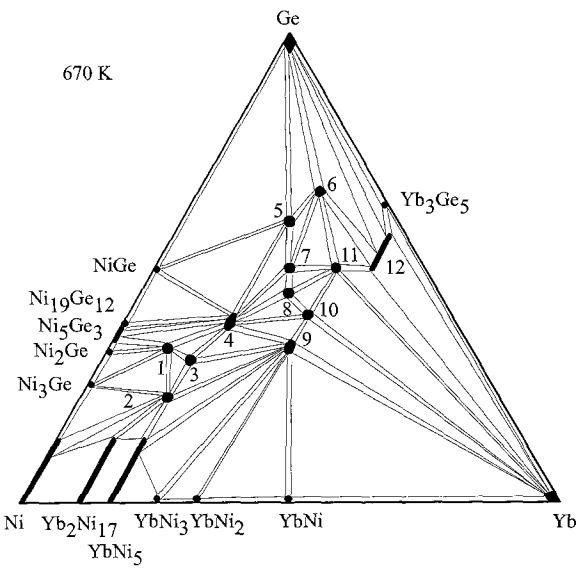

Fig. 112. Yb–Ni–Ge, isothermal section at 670 K.

The ternary phase diagram is characterized by the existence of twelve ternary compounds and by the formation of substitutional solid solutions based at Tm_2Ni_{17} and $TmNi_5$, which dissolve 15 at.% Ge.

$YbNi_5Ge_3$ (1) was reported to crystallize with the YNi_5Si_3- type structure, $a = 1.8892$, $b = 0.3830$, $c = 0.6779$, by Fedyna et al. (1987). The arc melted alloy, annealed at 870 K, was investigated by X-ray powder diffraction analysis. The starting materials were Yb 99.8 mass%, Ni 99.99 mass%, and Ge 99.99 mass%.

$Yb_3Ni_{11}Ge_4$ (2) belongs to the $Sc_3Ni_{11}Si_4$-type structure group, $a = 0.8259$, $c = 0.8648$, after Fedyna et al. (1987). The alloy was prepared in the same manner as $TmNi_5Ge_3$.

The $YbNi_2Ge_2$ (4) compound was found to adopt the $CeGa_2Al_2$-type structure, $a = 0.4001$, $c = 0.9733$ (Rieger and Parthé 1969b).

$YbNiGe_3$ (5) with the $ScNiSi_3$-type structure ($a = 0.4067$, $b = 2.1548$, $c = 0.4067$, X-ray powder diffraction analysis) was reported by Dzianii (1995). For the details of sample preparation and the purity of starting materials, see Yb–Ni–Ge.

Yb_2NiGe_6 (6) has been found by Dzianii (1995) from X-ray powder diffraction to be isostructural with Ce_2CuGe_6 ($a = 0.3948$, b 2.100, $c = 0.3960$). The sample was prepared by arc melting ingots of the constituting elements and annealing the resulting button at 670 K for 480 h. For the purity of starting materials, see Yb–Ni–Ge.

Gorelenko et al. (1984) investigated the crystal structure of YbNiGe (9) (TiNiSi type, $a = 0.6740$, $b = 0.4162$, $c = 0.7217$; X-ray powder analysis). The proper amounts of starting materials were arc melted, and the resulting alloy was annealed in an evacuated quartz tube at 870 K for 350 hours.

$YbNi_{0.6}Ge_{1.4}$ (12) was said to adopt the AlB_2-type structure, $a = 0.4193$, $c = 0.3965$ (Contardi et al. 1977; X-ray powder diffraction). Dzianii (1995) observed a homogeneity field for the compound with AlB_2 structure and obtained significantly different lattice parameters: $Yb_2(Ni,Ge)_3$, $a = 0.3405$–0.3764, $c = 0.3942$–0.4009 (X-ray powder diffraction).

Five more ternary compounds with unknown structure were observed by Dzianii (1995) in the Yb–Ni–Ge system: ~$Yb_{0.17}Ni_{0.53}Ge_{0.30}$ (3), ~$Yb_{0.25}Ni_{0.25}Ge_{0.50}$ (7), ~$Yb_{0.27}Ni_{0.28}Ge_{0.45}$ (8), ~$Yb_{0.33}Ni_{0.27}Ge_{0.40}$ (10), ~$Yb_{0.33}Ni_{0.17}Ge_{0.50}$ (11).

4.15.5. *Yb–Cu–Ge*

The isothermal section for the ternary Yb–Cu–Ge system over the whole concentration region (fig. 113) was established by Salamakha et al. (1996a). Four ternary compounds were observed and characterized by employing X-ray powder analysis of arc melted alloys annealed at 670 K. The starting materials were used in the form of ingots of high-purity elements: Yb 99.9 mass%, Cu 99.99 mass%, and Ge 99.999 mass%.

Iandelli (1993) observed YbCuGe (4) with the $CaIn_2$-type structure ($a = 0.4213$, $c = 0.7036$, X-ray powder analysis). The alloy was prepared from filings or powders of the metals (Yb 99.7 mass%, Cu and and Ge 99.99 mass%), which were mixed, sealed in a tantalum crucible under argon, melted by induction heating, and annealed for 10 days at

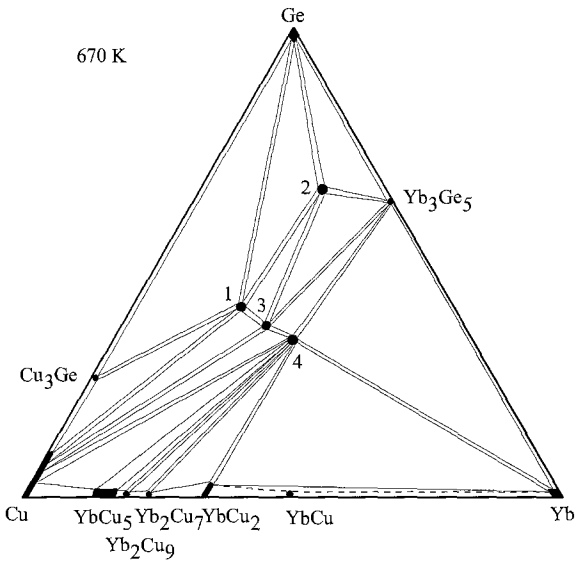

Fig. 113. Yb–Cu–Ge, isothermal section at 670 K.

1023 K. The crystal structure of this compound was confirmed by Dzianii et al. (1995d), $a = 0.4186$, $c = 0.6988$. For the experimental details, see the preceding paragraph.

$Yb_6Cu_8Ge_8$ (3) crystallizes with the $Gd_6Cu_8Ge_8$-type structure, lattice parameters $a = 1.371$, $b = 0.659$, $c = 0.413$ (Hanel and Nowotny 1970). The crystal structure was confirmed for the $Yb_6Cu_8Ge_8$ compound by Dzianii (1995) from X-ray powder diffraction data, $a = 1.414$, $b = 0.6637$, $c = 0.4201$.

Konyk et al. (1988) investigated the crystal structure of Yb_2CuGe_6 (2), which was prepared by arc melting under argon and annealing at 870 K in an evacuated quartz tube for 720 h. From X-ray powder analysis, the Ce_2CuGe_6-type structure was claimed, $a = 0.3994$, $b = 0.4082$, $c = 2.1018$.

Rieger and Parthé (1969b) prepared $YbCu_2Ge_2$ (1) with the $CeGa_2Al_2$-type structure, $a = 0.4045$, $c = 1.0228$.

4.15.6. *Yb–Nb–Ge*

The phase diagram of the Yb–Nb–Ge system has not been established yet. However, the existence of a compound $Yb_2Nb_3Ge_4$ with the $Ce_2Sc_3Si_4$-type structure ($a = 0.6937$, $b = 1.3449$, $c = 0.7109$) was reported by Le Bihan et al. (1996a) from X-ray powder diffraction data of an arc melted alloy. The starting materials were: Yb and Nb 99.99 mass%, Ge 99.999 mass%.

4.15.7. *Yb–Ru–Ge*

X-ray powder analysis of an alloy of the $YbRu_2Ge_2$ composition indicated that it had the $CeGa_2Al_2$-type structure with $a = 0.4203$, $c = 0.9763$ (Francois et al. 1985). The sample

was obtained by a powder metallurgical reaction at 1273 K. The starting components were Yb (3N), Ru (4N), and Ge (4N).

$Yb_3Rh_4Sn_{13}$-type structure was reported for the $Yb_3Ru_4Ge_{13}$ compound ($a=0.8911$) by Segre et al. (1981a) from X-ray powder analysis of an arc melted sample annealed at 1523 K for 1 day and at 1273 K for 7 days. The starting materials were Yb (3N), Ru (3N), and Ge (6N).

4.15.8. *Yb–Rh–Ge*

Venturini et al. (1985b) reported an X-ray powder diffraction study of the $Yb_3Rh_4Ge_{13}$ compound from a sample which was prepared by heating a mixture of the starting components (Yb 3N, Rh 4N, Ge 4N) in an evacuated quartz tube at 1073 K. The crystal structure was found to be of the $Yb_3Rh_4Sn_{13}$ type, $a=0.8941$.

Francois et al. (1985) determined the $CeGa_2Al_2$-type structure for the $YbRh_2Ge_2$ compound, $a=0.4062$, $c=1.0065$.

Venturini et al. (1984) established the existence of the $Yb_5Rh_4Ge_{10}$ compound with $Sc_5Co_4Si_{10}$-type structure and lattice parameters $a=1.2886$, $c=0.4234$ from X-ray powder analysis of a sample obtained by heating a mixture of powders in an evacuated tube at 1073 K.

$Yb_4Rh_7Ge_6$ belongs to the $U_4Re_7Si_6$-type structure family, $a=0.8254$, according to Francois et al. 1985 (X-ray powder diffraction). The alloy was synthesized by heating a mixture of powders of the constituent elements in an evacuated quartz tube at 1273 K. Starting components were Yb (3N), Rh (4N), and Ge (4N).

4.15.9. *Yb–Pd–Ge*

A systematic study of the Yb–Pd–Ge system (fig. 114) has been performed by Seropegin et al. (1994) employing X-ray phase analysis, microstructural and local X-ray spectral analyses of 152 samples which were arc melted and annealed at 870 K for 600 h. The existence of one ternary compound was confirmed and formation of nine other ternary phases was observed for the first time. The purity of the metals used for the synthesis of the alloys was Yb 99.98 mass%, Pd and Ge 99.99 mass%.

According to X-ray powder diffraction analysis, $YbPd_2Ge_2$ (3) was reported to adopt the $CeGa_2Al_2$-type structure, $a=0.4287$, $c=1.0020$ (Rossi et al. 1979). Seropegin et al. (1994) confirmed the existence and structure of this compound with $a=0.42841$, $c=1.0001$.

Seropegin et al. (1994) reported an X-ray powder analysis of the Yb_2PdGe_6 (4) compound which was found to crystallize with the Ce_2CuGe_6-type structure, $a=0.3974$, $b=2.1834$, $c=0.40689$. For the experimental procedure, see the Yb–Pd–Ge isothermal section. Sologub et al. (1995a) confirmed the formation of Yb_2PdGe_6 with the Ce_2CuGe_6-type structure and obtained $a=0.40755$, $b=0.39934$, $c=2.1851$. For the experimental procedure, see La_2PdGe_6 under La–Pd–Ge. The starting materials used were of purity 99.9 mass%.

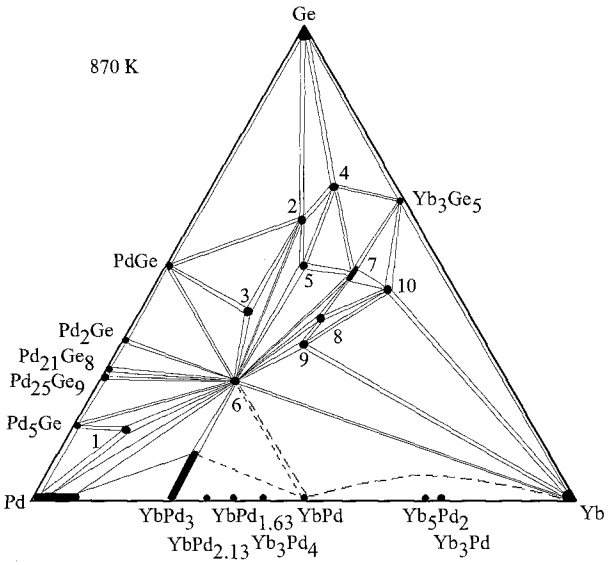

Fig. 114. Yb–Pd–Ge, isothermal section at 870 K.

In the course of the phase equilibria investigation, three more compounds were observed and characterized: $YbPdGe_2$ (5), $NdIrGe_2$ type, $a = 0.4336$, $b = 0.8626$, $c = 1.6071$ (X-ray powder diffraction); $YbPd_{0.5-0.62}Ge_{1.5-1.38}$ (7), AlB_2 type, $a = 0.42276$–0.42263, $c = 0.40686$–0.40649 (X-ray powder diffraction); YbPdGe (9), KHg_2 type, $a = 0.4344$, $b = 0.6839$, $c = 0.7522$ (X-ray powder diffraction).

The crystal structures of the compounds ~$Yb_{10}Pd_{75}Ge_{15}$ (1) (Seropegin et al. 1994), ~$Yb_{20}Pd_{20}Ge_{60}$ (2) (Seropegin et al. 1994), ~$YbPd_2Ge$ (6) (Jorda et al. 1983), ~$Yb_{33.3}Pd_{28}Ge_{38.7}$ (8) (Seropegin et al. 1994) and ~$Yb_{42}Pd_{13}Ge_{45}$ (10) (Seropegin et al. 1994) have not been determined.

4.15.10. *Yb–Ag–Ge*

No ternary phase diagram has been established for the Yb–Ag–Ge system, however one ternary compound has been characterized. Gibson et al. (1996) reported an X-ray powder investigation of the YbAgGe compound. It was found to adopt the ZrNiAl-type structure, $a = 0.70524$, $c = 0.41387$. The sample was arc melted and annealed at 970 K for ten days.

4.15.11. *Yb–Os–Ge*

No phase diagram is available for the ternary Yb–Os–Ge system, but two ternary compounds have been observed.

$Yb_4Os_7Ge_6$ belongs to the $U_4Re_7Si_6$-type structure family, $a = 0.8288$ (Francois et al. 1985; X-ray powder diffraction). The alloy was synthesized by heating a mixture of powders of the constituent elements in an evacuated quartz tube at 1273 K. The starting components were Yb (3N), Os (4N), and Ge (4N).

The $Pr_3Rh_4Sn_{13}$-type structure was announced for the $Yb_3Os_4Ge_{13}$ compound (a = 0.8941) by Segre et al. (1981a) from X-ray powder analysis of an arc melted sample annealed at 1523 K for 1 day and at 1273 K for 7 days sample. The starting materials were Yb (3N), Os (3N), and Ge (6N).

4.15.12. *Yb–Ir–Ge*

No ternary phase diagram has been established for the Yb–Ir–Ge system, however three ternary compounds have been characterized.

Méot-Meyer et al. (1985b) observed the $Yb_5Ir_4Ge_{10}$ compound with $Sc_5Co_4Si_{10}$-type structure from a sample which was obtained by heating a compacted mixture of powders in evacuated tube at 1073 K. No lattice parameters were given.

Venturini et al. (1985b) reported an X-ray powder diffraction study of the $Yb_3Ir_4Ge_{13}$ compound from a sample which was prepared from the pure components (Yb 3N, Ir 4N, Ge 4N) by a powder metallurgical reaction at 1073 K. The crystal structure was found to be of the $Yb_3Rh_4Sn_{13}$ type, a = 0.8936.

$Yb_4Ir_7Ge_6$ was reported to adopt $U_4Re_7Si_6$-type structure (a = 0.8262; Francois et al. 1985) from a sample which was obtained by heating a mixture of powders of the starting materials (Yb 3N, Ir 4N, Ge 4N) in an evacuated quartz tube at 1273 K.

4.15.13. *Yb–Pt–Ge*

A systematic study of the Yb–Pt–Ge system (fig. 115) has been performed by Borisenko (1993) employing X-ray phase analysis as well as microstructural and local X-ray spectral analyses of 72 samples which were arc melted and annealed at 870 K for 600 h. The

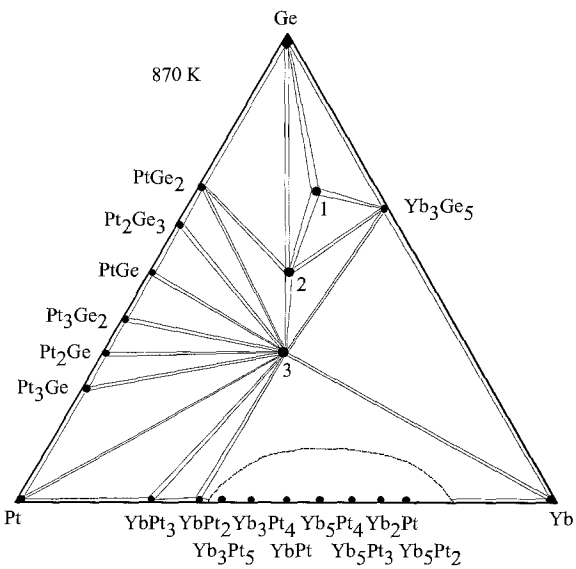

Fig. 115. Yb–Pt–Ge, isothermal section at 870 K.

existence of three ternary compounds was observed. The purity of the metals used for the synthesis of the alloys was Yb 99.98 mass%, Pt and Ge 99.99 mass%.

Borisenko (1993) reported an X-ray powder analysis of the Yb_2PtGe_6 (1) compound which was found to crystallize with the Ce_2CuGe_6-type structure, $a = 0.3949$, $b = 2.186$, $c = 0.4091$. For the experimental procedure, see the preceding paragraph. Sologub et al. (1995a) confirmed the formation of Yb_2PtGe_6 with the Ce_2CuGe_6-type structure and obtained $a = 0.40482$, $b = 0.39771$, $c = 2.1940$. For the experimental procedure, see La_2PdGe_6 under La–Pd–Ge. The purity of the starting materials used was 99.9 mass%.

In the course of phase equilibrium studies, two more compounds were observed and characterized by X-ray powder diffraction: $YbPtGe_2$ (2), $NdIrGe_2$ type, $a = 0.4337$, $b = 0.8734$, $c = 1.6134$; and YbPtGe (3), TiNiSi type, $a = 0.6897$, $b = 0.4325$, $c = 0.7542$.

4.15.14. *Yb–Au–Ge*

Only one report exists on the interaction of components in the ternary Yb–Au–Ge system: Rossi et al. (1992) observed and characterized the YbAuGe compound as having the LiGaGe-type structure with lattice parameters $a = 0.4475$, $c = 0.7163$ (X-ray powder diffraction). The sample was obtained by melting the metals in an induction furnace and annealing at 1070 K for one week. The metals used had a purity of around 99.9 mass.% for Yb and 99.99 mass.% for Au and Ge.

4.16. *Lu–d element–Ge systems*

4.16.1. *Lu–Mn–Ge*

No ternary phase diagram for the Lu–Mn–Ge system is available. Three ternary compounds have been reported for various luthetium–manganese–germanium combinations.

$LuMn_6Ge_6$ was found to crystallize in the $HfFe_6Ge_6$-type structure by Venturini et al. (1992), $a = 0.5211$, $c = 0.8134$ (X-ray powder diffraction data). The alloy was synthesized by a powder metallurgical reaction in an evacuated silica tube at 1073 K for 14 days.

$LuMn_{0.27-0.12}Ge_2$ was found by Francois et al. (1990) to adopt the $CeNiSi_2$-type structure with lattice parameters $a = 0.4053$–0.4028, $b = 1.543$–1.558, $c = 0.3956$–0.3897 (X-ray powder diffraction data). For sample preparation, see $GdFe_{0.25-0.46}Ge_2$ under Gd–Fe–Ge.

Meyer et al. (1983) investigated the crystal structure of the $LuMnGe_2$ compound, and found it had a new structure type, $a = 0.5466$, $b = 1.8519$, $c = 0.8173$ (X-ray single-crystal method) from an alloy obtained by heating the proper amounts of the metals in a quartz tube under argon and annealing at 1173 K.

4.16.2. *Lu–Fe–Ge*

No phase diagram has been constructed for the Lu–Fe–Ge system; six ternary compounds have been found and characterized by different groups of authors.

$LuFe_6Ge_6$ was reported to be isotypic with YCo_6Ge_6, lattice parameters $a = 0.5087$, $c = 0.4034$ (Mruz et al. 1984). The sample was prepared by arc melting the proper amounts

of the starting components followed by annealing at 870 K for two weeks. At variance with these data, $LuFe_6Ge_6$ was found to crystallize with the $HfFe_6Ge_6$-type structure, $a = 0.5096$, $c = 0.8081$, by Venturini et al. (1992) from X-ray powder diffraction data. The alloy was obtained by a powder metallurgical reaction in an evacuated silica tube at 1173 K for two weeks.

Pecharsky et al. (1989) reported $LuFe_xGe_2$ to crystallize with the $CeNiSi_2$-type structure ($a = 0.4042$, $b = 1.5431$, $c = 0.3947$; X-ray powder analysis). The alloy was arc melted and annealed at 870 K. The purity of the starting materials was greater than 99.9 mass%. Francois et al. (1990) confirmed the structure of this compound and established the composition as $LuFe_{0.33-0.11}Ge_2$, $a = 0.4121$, $b = 1.581$, $c = 0.4011$ (X-ray powder diffraction data). For sample preparation, see $GdFe_{0.25-0.46}Ge_2$ under Gd–Fe–Ge.

$LuFe_4Ge_2$ is isotypic with $ZrFe_4Si_2$, lattice parameters $a = 0.7200$, $c = 0.3854$, after Fedyna (1988). The alloy was prepared by arc melting the proper amounts of the starting components followed by annealing at 870 K for 400 hours.

Oleksyn (1990) investigated the crystal structure of the $Lu_{117}Fe_{52}Ge_{112}$ compound by the X-ray powder method ($Tb_{117}Fe_{52}Ge_{112}$ type, $a = 2.792$). The alloy was synthesized by arc melting and annealing at 1070 K for 350 h. The starting materials were Lu 99.83 mass%, Fe 99.9 mass%, and Ge 99.99 mass%.

$Lu_6Fe_8Ge_8$ belongs to the $Gd_6Cu_8Ge_8$-type structure family, $a = 1.3280$, $b = 0.6805$, $c = 0.4038$ (X-ray powder diffraction; Fedyna et al. 1994).

Fedyna and Zavodnik (1988) reported a single-crystal investigation of the $Lu_3Fe_2Ge_3$ compound, showing that it had the $Hf_3Ni_2Si_3$-type structure, $a = 0.41272$, $b = 1.047$, $c = 1.3611$. The single crystal was isolated from an arc melted alloy.

4.16.3. *Lu–Co–Ge*

The phase diagram of the Lu–Co–Ge system has not yet been established; seven ternary compounds have been identified and characterized for various lutetium–cobalt–germanium combinations.

Méot-Meyer et al. (1985a) reported that $LuCo_{1-x}Ge_2$, $x = 0.34$, has the $CeNiSi_2$-type structure with $a = 0.4038$, $b = 1.554$, $c = 0.3939$. The sample was prepared by a powder metallurgical reaction and annealed in an evacuated silica tube at 1173 K. Pecharsky et al. (1989) also investigated the formation and crystal structure of the $LuCo_{1-x}Ge_2$ compound by X-ray powder analysis of an arc melted alloy annealed at 870 K: $CeNiSi_2$ type, $a = 0.4038$–0.4040, $b = 1.5512$–1.5551, $c = 0.3948$–0.3949).

The crystal structure of $Lu_3Co_4Ge_{13}$ ($Yb_3Rh_4Sn_{13}$ type, $a = 0.8700$; X-ray powder diffraction) was investigated by Venturini et al. (1985b) from a sample which was prepared by heating a compacted mixture of the starting materials (Lu in pieces, 99.9 mass%; Co and Ge in powder, 99.99 mass%) in an evacuated quartz tube at 1073 K. Bodak et al. (1987) reported the $Y_3Co_4Ge_{13}$ type for the $Lu_3Co_4Ge_{13}$ compound ($a = 0.8694$; X-ray powder data) from an arc melted alloy annealed at 870 K.

Gorelenko et al. (1984) reported the crystal structure of LuCoGe (TiNiSi type, $a = 0.6720$, $b = 0.4140$, $c = 0.7226$; X-ray powder analysis). The alloy was obtained by arc melting and annealing in an evacuated quartz tube at 870 K for 350 hours.

Lu_2CoGe_6 is isotypic with Ce_2CuGe_6, $a = 0.3904$, $b = 0.3936$, $c = 2.1192$ (Oleksyn et al. 1991; X-ray powder diffraction data). The sample was melted in an arc furnace and annealed at 1070 K in evacuated quartz capsule for 400 h. The purity of the starting materials was greater than 99.9 mass%.

Koterlyn (1996) investigated the crystal structure of the $LuCo_{3.8}Ge_{1.2}$ compound which belongs to the $CaCu_5$-type structure, $a = 0.48823$, $c = 0.40301$ (X-ray powder diffraction).

Bodak et al. (1986) reported the crystal structure for Lu_2CoGe_2 (Sc_2CoSi_2 type, $a = 1.0234$, $b = 1.0049$, $c = 0.4109$, $\gamma = 117.31°$; X-ray powder diffraction) from an arc melted sample annealed at 870 K.

$LuCo_4Ge_2$ is isotypic with $ZrFe_4Si_2$, lattice parameters $a = 0.7199$, $c = 0.3735$, after Fedyna (1988). The alloy was prepared by arc melting the proper amounts of the starting components and annealing at 870 K for 400 hours.

4.16.4. *Lu–Ni–Ge*

No isothermal section for the Lu–Ni–Ge system is available; eight ternary compounds were observed and characterized by different groups of authors.

$LuNi_5Ge_3$ was reported to crystallize with the YNi_5Si_3-type structure, $a = 1.8973$, $b = 0.3826$, $c = 0.6775$, by Fedyna et al. (1987). An arc melted alloy, annealed at 870 K, was investigated by X-ray powder diffraction analysis. The starting materials were Lu 99.83 mass%, Ni 99.99 mass%, and Ge 99.99 mass%.

$Lu_3Ni_{11}Ge_4$ belongs to the $Sc_3Ni_{11}Si_3$-type structure, $a = 0.8249$, $c = 0.8641$, after Fedyna et al. (1987). For sample preparation, see the preceding paragraph.

The $LuNi_2Ge_2$ compound was found to adopt the $CeGa_2Al_2$-type structure, $a = 0.39975$, $c = 0.97538$ (Bodak and Koterlyn 1995).

$LuNiGe_3$ with the $SmNiGe_3$-type structure ($a = 2.1305$, $b = 0.3932$, $c = 0.3982$, X-ray powder diffraction analysis) was reported by Bodak et al. (1985). For the details of sample preparation and the purity of the starting materials, see $LuNi_5Ge_3$.

Lu_2NiGe_6 has been found by Oleksyn (1990) from X-ray powder diffraction to be isostructural with Ce_2CuGe_6 ($a = 0.3908$, $b = 0.4007$, $c = 2.1265$). The sample was prepared by arc melting ingots of the constituting elements and annealing at 1070 K for 700 h. For the purity of starting materials, see $LuNi_5Ge_3$.

Pecharsky et al. (1989) investigated the formation and crystal structure of the $LuNi_{1-x}Ge_2$ compound by X-ray powder analysis of an arc melted alloy annealed at 870 K ($CeNiSi_2$ type, $a = 0.3993$–0.4045, $b = 1.5566$–1.5690, $c = 0.3852$–0.3929). For sample preparation, see $LuFe_{1-x}Ge_2$ under Lu–Fe–Ge. Francois et al. (1990) confirmed the structure and reported the composition and lattice parameters $LuNi_{0.48-0.19}Ge_2$, $a = 0.4037$–0.4015, $b = 1.535$–1.558, $c = 0.3945$–0.3898 (X-ray powder diffraction) from a sample obtained by a powder metallurgical reaction at 1173 K.

Gorelenko et al. (1984) reported the crystal structure of LuNiGe (TiNiSi type, $a = 0.6727$, $b = 0.4147$, $c = 0.7229$; X-ray powder analysis). The alloy was obtained by arc melting and annealing in an evacuated quartz tube at 870 K for 350 hours. Koterlyn et al. (1994) investigated a single crystal which was extracted from an arc melted LuNiGe alloy. A new structure type was observed, $a = 0.4116$, $b = 0.9194$, $c = 2.2334$. According to DTA, this phase exists above 1570 K.

Oleksyn (1990) reported on the crystal structure of $LuNiGe_2$ from X-ray powder diffraction ($NdIrGe_2$ type, $a = 0.4082$, $b = 0.8893$, $c = 1.5795$). The proper amounts of the starting components were arc melted and annealed at 1070 K.

4.16.5. *Lu–Cu–Ge*

No isothermal section is available for the Lu–Cu–Ge system; four ternary compounds have been found and analyzed by various groups of authors.

Rieger and Parthé (1969a) investigated the occurrence of the AlB_2-type structure by means of X-ray powder diffraction of arc melted alloys. The data presented indicated a compound of $LuCu_{0.67}Ge_{1.33}$ stoichiometry with $a = 0.383$, $c = 0.405$.

Iandelli (1993) observed LuCuGe with the $CaIn_2$ type ($a = 0.4212$, $c = 0.6962$, X-ray powder analysis). The alloy was prepared from turnings or powders of the metals (lutetium 99.7 mass%, copper and germanium 99.99 mass%), which were mixed and sealed in a tantalum crucible under argon, melted by induction heating, and annealed for 10 days at 1023 K.

$Lu_6Cu_8Ge_8$ crystallizes with the $Gd_6Cu_8Ge_8$-type structure, lattice parameters $a = 1.3661$, $b = 0.6581$, $c = 0.4113$ (Rieger 1970).

Francois et al. (1990) observed the $CeNiSi_2$-type structure for the $LuCu_{0.14}Ge_2$ compound and reported lattice parameters $a = 0.4029$, $b = 1.567$, $c = 0.3903$ (X-ray powder diffraction) from a sample obtained by a powder metallurgical reaction at 1173 K.

4.16.6. *Lu–Nb–Ge*

The phase diagram of the Lu–Nb–Ge system has not been established yet. The existence of the compound $Lu_2Nb_3Ge_4$ with the $Ce_2Sc_3Si_4$-type structure ($a = 0.6895$, $b = 1.3392$, $c = 0.7071$) was reported by Le Bihan et al. (1996a) from X-ray powder diffraction data of an arc melted alloy. The starting materials were: Lu and Nb 99.99 mass%, Ge 99.999 mass%.

4.16.7. *Lu–Mo–Ge*

The existence of $Lu_2Mo_3Ge_4$ with the $Ce_2Sc_3Si_4$-type structure ($a = 0.6789$, $b = 1.3012$, $c = 0.6990$) was reported by Le Bihan et al. (1996b). For sample preparation and purity of starting materials, see Lu–Nb–Ge.

Table 29
Crystallographic data for the ternary Lu–Ru(Rh, Pd)–Ge compounds

Compound	Structure	Lattice parameters (nm)			Reference
		a	*b*	*c*	
$Lu_4Ru_7Ge_6$	$U_4Re_7Si_6$	0.8256		0.9856	Francois et al. (1985)
$LuRu_{0.25}Ge_2$	$CeNiSi_2$	0.4076	1.549	0.3980	Francois et al. (1990)
$LuRuGe_2$	$TiMnSi_2$	0.953	1.049	0.823	Venturini et al. (1985a)
$Lu_3Ru_4Ge_{13}$	$Yb_3Rh_4Sn_{13}$	0.8911			Segre et al. (1981a)
$Lu_5Rh_4Ge_{10}$	$Sc_5Co_4Si_{10}$				Méot-Meyer et al. (1985b)
$Lu_3Rh_2Ge_2$	$La_3Ni_2Ga_2$	0.54917	0.7593	1.3051	Gladyshevsky et al. (1991a)
$Lu_4Rh_7Ge_6$	$U_4Re_7Si_6$	0.8243			Francois et al. (1985)
$Lu_3Rh_4Ge_{13}$	$Yb_3Rh_4Sn_{13}$	0.8900			Venturini et al. (1985b)
$Lu_4Rh_{13}Ge_9$	$Ho_4Ir_{13}Ge_9$				Verniere et al. (1995)
$LuRh_{0.23}Ge_2$	$CeNiSi_2$	0.4054	1.555	0.3962	Francois et al. (1990)
$LuPd_2Ge$	YPd_2Si	0.7189	0.7049	0.5512	Jorda et al. (1983)
$LuPd_{0.16}Ge_2$	$CeNiSi_2$	0.4059	1.561	0.3934	Francois et al. (1990)

4.16.8. *Lu–Ru(Rh, Pd)–Ge*

The ternary Lu–Ru(Rh, Pd)–Ge systems have been studied only with respect to the formation of compounds with specific compositions and structures. Their crystallographic characteristics are listed in table 29.

4.16.9. *Lu–Ag–Ge*

Protsyk (1994) constructed the equilibrium phase diagram for the Lu–Ag–Ge system at 770 K (fig. 116) by means of X-ray powder phase analysis of 65 alloys. The samples

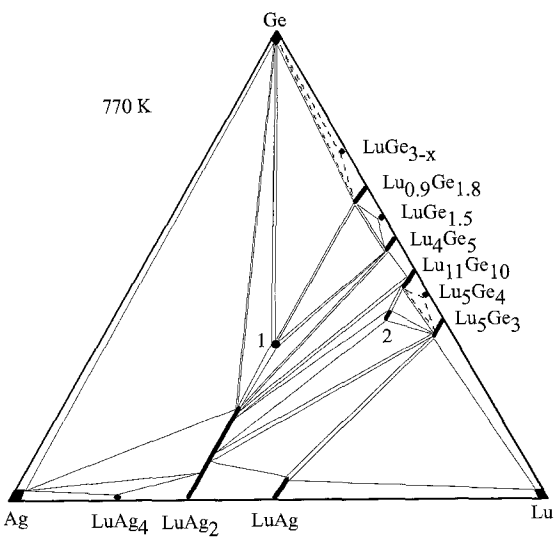

Fig. 116. Lu–Ag–Ge, isothermal section at 770 K.

were arc melted and annealed for 500 h. Two ternary compounds were observed. $LuAg_2$ dissolves 20 at.% Ge.

The crystal structure of the LuAgGe (1) compound was investigated by Protsyk (1994) by X-ray powder diffraction method. It was found to adopt the ZrNiAl-type structure with lattice parameters $a = 0.7006$, $c = 0.4129$. The crystal structure was confirmed by Gibson et al. (1996), with lattice parameters $a = 0.71025$, $c = 0.41337$ (X-ray powder diffraction).

The crystal structure of ~$Lu_5(Ag,Ge)_4$ (2) was not resolved (Protsyk 1994).

4.16.10. *Lu–Re–Ge*

The only information on the system Lu–Re–Ge is due to Francois et al. (1990) who investigated the occurrence of the compound with a $CeNiSi_2$ type; no phase diagram is available.

$LuRe_{0.12}Ge_2$ was found by Francois et al. (1990) to crystallize with the $CeNiSi_2$-type structure with lattice parameters $a = 0.4085$, $b = 1.551$, $c = 0.3991$ (X-ray powder diffraction data). The alloy was prepared from a mixture of the proper amounts of the components with purity of 99.9 mass% by a metallurgical reaction in a quartz tube at 1173 K.

4.16.11. *Lu–Os(Ir)–Ge*

The ternary Lu–Os(Ir)–Ge systems have been studied only with respect to the formation of compounds with specific compositions and structures. Their crystallographic characteristics are listed in table 30.

Table 30
Crystallographic data for the ternary Lu–Os(Ir,Pt)–Ge compounds

Compound	Structure	Lattice parameters (nm)			Reference
		a	*b*	*c*	
$LuOsGe_2$	$TiMnSi_2$	0.951	1.048	0.827	Venturini et al. (1985a)
$Lu_3Os_4Ge_{13}$	$Yb_3Rh_4Sn_{13}$	0.8941			Segre et al. (1981a)
$Lu_4Os_7Ge_6$	$U_4Re_7Si_6$	0.8276			Francois et al. (1985)
$Lu_4Ir_7Ge_6$	$U_4Re_7Si_6$	0.8258			Francois et al. (1985)
$Lu_5Ir_4Ge_{10}$	$Sc_5Co_4Si_{10}$				Méot-Meyer et al. (1985b)
$Lu_3Ir_4Ge_{13}$	$Yb_3Rh_4Sn_{13}$	0.8898			Venturini et al. (1985b)

4.16.12. *Lu–Au–Ge*

No ternary phase diagram exists for the Lu–Au–Ge system, however, a ternary compound of luthetium with gold and germanium in the stoichiometric ratio 1:1:1 has been identified and studied by means of X-ray analysis by Pöttgen et al. (1996a). LuAuGe was found to adopt the LiGaGe type with lattice parameters $a = 0.43775$, $c = 0.71138$. The sample was prepared by melting a mixture of the metals in an arc furnace and annealing at 1070 K.

5. Rare earth–f element–germanium systems

5.1. *Sc–R′–Ge systems*

5.1.1. *Sc–Y–Ge*

The phase equilibria in the Sc–Y–Ge system (fig. 117) were investigated by Shpyrka and Mokra (1991) by means of X-ray phase and microstructural analyses of alloys which were arc melted and subsequently annealed in evacuated silica tubes for 350 h at 870 K and finally quenched in water. The starting materials were Sc 99.92 mass%, Y 99.90 mass%, and Ge 99.99 mass%. The phase relations are characterized by the existence of three ternary compounds and the formation of a continuous solid solution $(Sc,Y)_5Ge_3$ originating at the isotypic binary compounds. The binary compounds $ScGe_2$, Y_2Ge_3 and $Sc_{11}Ge_{10}$ dissolve 18, 10 and 8 at.% of third component, respectively.

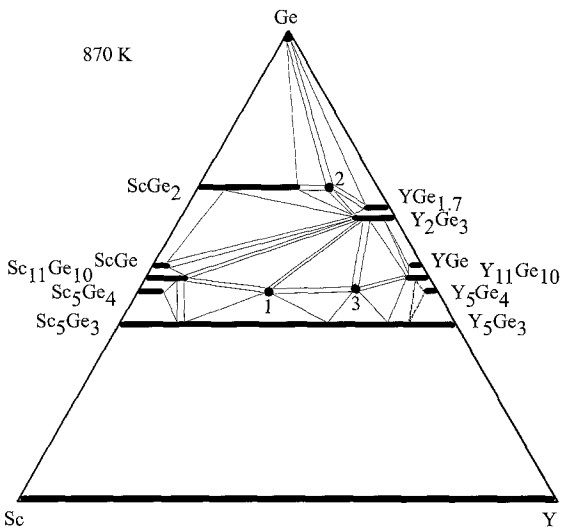

Fig. 117. Sc–Y–Ge, isothermal section at 870 K.

In the course of a phase equilibrium study, three ternary compounds were observed by Shpyrka and Mokra (1991): $Sc_{2.7}Y_{2.3}Ge_4$ (1) was found to be isotypic with Sm_5Ge_4, $a=0.7283$, $b=1.418$, $c=0.7461$; $Sc_{1.35}Y_{3.65}Ge_4$ (3) belongs to the Sm_5Ge_4-type structure family, $a=0.7440$, $b=1.431$, $c=0.7578$; and $\sim Sc_{0.3}Y_{0.7}Ge_2$ (2) crystallizes with an unknown structure type.

5.1.2. *Sc–La–Ge*

No phase diagram is available for the Sc–La–Ge system; however two ternary compounds were observed and characterized in the course of searching for isostructural series of compounds.

$Sc_3La_{1.22}Ge_4$ was found to be isotypic with $Sc_3Ce_2Si_4$, $a=0.7252$, $b=1.4350$, $c=0.7652$ (X-ray powder diffraction; Shpyrka et al. 1990). ScLaGe belongs to the

ScCeSi type, $a = 0.4351$, $c = 1.6067$ (X-ray powder diffraction; Shpyrka 1990). For the experimental details, see Sc–Y–Ge.

Shpyrka (1990) investigated the phase formation in the section $ScGe_2$–$LaGe_2$, and no ternary compounds were observed.

5.1.3. *Sc–Ce–Ge*

Phase relations in the isothermal section of the Sc–Ce–Ge system at 870 K (fig. 118) were determined by Bodak and Kokhan (1983) from X-ray powder diffraction and microstructural analyses of 120 alloys prepared by arc melting Sc (99.92 mass%), Ce (99.56 mass%) and Ge (99.99 mass%) ingots. The melted buttons were then annealed at 870 K for 400 h in evacuated silica tubes. Four ternary compounds were found to exist. Up to 4 at.% Sc and 8 at.% Sc dissolve in $CeGe_{2-1.78}$ and $CeGe_{1.6-1.56}$. The solubilities of third component in other binary compounds were reported to be negligible.

The crystal structures of $Sc_3Ce_{1.22}Ge_4$ (2) ($Sc_3Ce_2Si_4$ type; $a = 0.7188$, $b = 1.339$, $c = 0.7416$) and ScCeGe (3) (ScCeSi type; $a = 0.4314$, $c = 1.5913$) were investigated by Shpyrka et al. (1990) and Shpyrka (1990), respectively, employing an X-ray single-crystal method. The samples were prepared in the same manner as for the investigation of the isothermal section of this system.

The crystal structures of ~$Sc_5Ce_{0.5}Ge_{4.5}$ (1) and ~$Sc_2Ce_5Ge_6$ (4) are not determined.

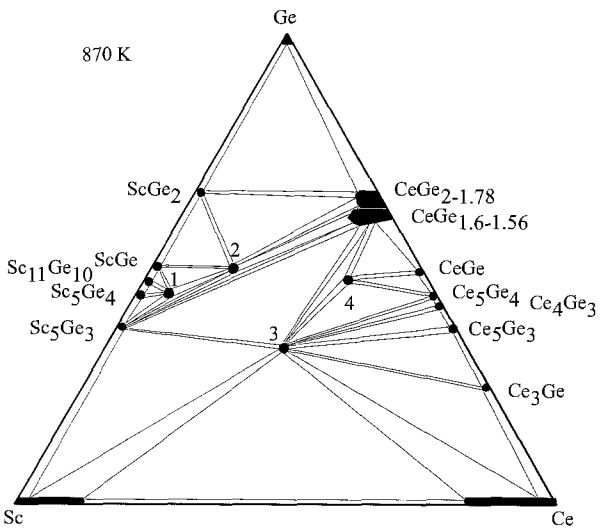

Fig. 118. Sc–Ce–Ge, isothermal section at 870 K.

5.1.4. *Sc–Pr–Ge*

At present, the phase relations are unknown for the system Sc–Pr–Ge. The formation of two ternary germanides was observed in the course of searching for isostructural series of compounds.

$Sc_3Pr_{1.22}Ge_4$ was found to be isotypic with $Sc_3Ce_2Si_4$, $a=0.7116$, $b=1.4059$, $c=0.7576$ (X-ray powder diffraction; Shpyrka et al. 1990). ScPrGe belongs to the ScCeSi type, $a=0.4325$, $c=1.5874$ (X-ray powder diffraction; Shpyrka 1990). For the experimental details, see Sc–Y–Ge.

5.1.5. *Sc–Nd–Ge*

The isothermal section for the Sc–Nd–Ge system at 870 K (fig. 119) was constructed by Shpyrka (1990) employing X-ray phase and microstructural analyses of 112 alloys which were arc melted and annealed for 400 h in sealed quartz ampoules. The phase relations within the Sc–Nd–Ge system at 870 K are characterized by the existence of three ternary compounds and by the formation of substitutional solid solutions originating at Nd_5Ge_3

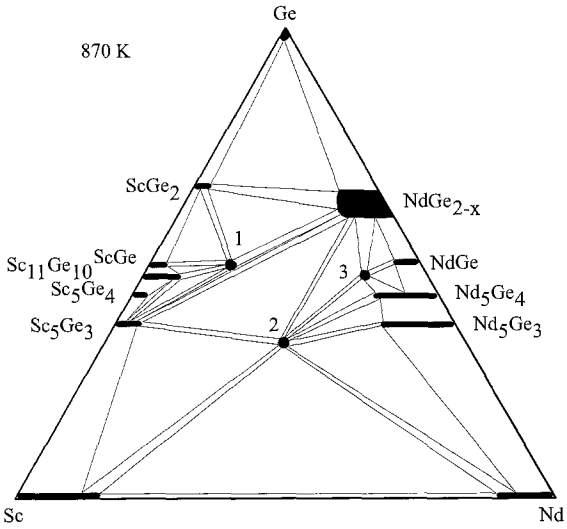

Fig. 119. Sc–Nd–Ge, isothermal section at 870 K.

(dissolves 12.5 at.% Sc), Nd_5Ge_4 (10 at.% Sc), NdGe (5 at.% Sc), $NdGe_{2-x}$ (8 at.% Sc), $Sc_{11}Ge_{10}$ (8 at.% Nd), and Sc_5Ge_3 (5 at.% Nd). The purity of the starting metals was Sc 99.92 mass%, Nd 99.44 mass%, and Ge 99.99 mass%. The solubilities of third component in other binary compounds were reported to be <5 at.%.

The crystal structures of $Sc_3Nd_{1.22}Ge_4$ (1) ($Sc_3Ce_2Ge_4$ type; $a=0.7119$, $b=1.4065$, $c=0.7574$) and ScNdGe (2) (ScCeSi type; $a=0.43106$, $c=1.5823$) were investigated by Shpyrka et al. (1990) and Shpyrka (1990), respectively, employing X-ray powder diffraction. For experimental details, see Sc–Nd–Ge, isothermal section.

The crystal structure of ~$Sc_2Nd_5Ge_6$ (3) was not investigated.

5.1.6. *Sc–Sm–Ge*

No phase diagram is available for the Sc–Sm–Ge system; however two ternary compounds were observed and characterized.

$Sc_3Sm_{1.22}Ge_4$ was found to be isotypic with $Sc_3Ce_2Si_4$, $a=0.7102$, $b=1.4020$, $c=0.7546$ (X-ray powder diffraction; Shpyrka et al. 1990). ScSmGe belongs to the ScCeSi type, $a=0.4264$, $c=1.5623$ (X-ray powder diffraction; Shpyrka 1990). For the experimental details, see Sc–Y–Ge.

The phase relations along the section $ScGe_2$-$SmGe_2$ were investigated by Shpyrka (1990); the formation of a ternary compound $Sc_{0.12}Sm_{0.22}Ge_{0.66}$ with an unknown structure type was observed.

5.1.7. *Sc–Eu–Ge*

Little information exists about the Sc–Eu–Ge system; only one ternary germanide was characterized. ScEuGe was found to be isotypic with a ScCeSi type, $a=0.4270$, $c=1.5636$ (X-ray powder diffraction; Shpyrka 1990). For the experimental details, see Sc–Y–Ge.

5.1.8. *Sc–Gd–Ge*

No complete phase diagram is available for the Sc–Gd–Ge system; phase relations along $ScGe_2$–$GdGe_2$ were studied by Shpyrka (1990). From X-ray powder diffraction data for arc melted alloys annealed at 870 K, the solubility of $ScGe_2$ in $GdGe_2$ was found to extend up to 8 at.% Sc.

5.1.9. *Sc–Tb–Ge*

The only phase diagram information on the system Sc–Tb–Ge is due to Shpyrka (1990) who investigated ternary arc melted alloys annealed at 870 K in the $ScGe_2$–$TbGe_2$ quasibinary system by means of X-ray powder diffraction. The solubility of $ScGe_2$ in $TbGe_2$ extends to 6 at.% Sc.

5.1.10. *Sc–Dy–Ge*

The phase equilibria in the Sc–Dy–Ge system (fig. 120) were investigated by Shpyrka and Mokra (1991) using X-ray phase and microstructural analyses of alloys which were arc melted and subsequently annealed in evacuated silica tubes for 350 h at 870 K and finally quenched in water. The starting materials were Sc 99.92 mass%, Dy 99.90 mass% and Ge 99.99 mass%. The phase relations are characterized by the existence of three ternary compounds and the formation of continuous solid solution $(Sc,Dy)_5Ge_3$ originating at the isotypic binary compounds. The binary compounds $DyGe_{1.33}$, $ScGe_2$, $Sc_{11}Ge_{10}$ and $Dy_{11}Ge_{10}$ dissolve 20, 18, 8 and 8 at.% of the third component, respectively.

The three compounds observed by Shpyrka and Mokra (1991) were $Sc_{1.8}Dy_{3.2}Ge_4$ (1) (Sm_5Ge_4 type, $a=0.7346$, $b=1.4295$, $c=0.7555$); $Sc_{2.7}Dy_{2.3}Ge_4$ (3) (isotypic with Sm_5Ge_4, $a=0.7260$, $b=1.4151$, $c=0.7477$); and ~$ScDy_2Ge_6$ (2) which crystallizes with an unknown structure type.

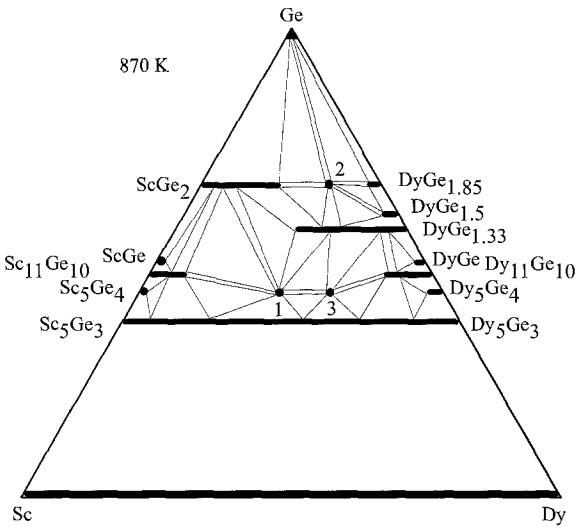

Fig. 120. Sc–Dy–Ge, isothermal section at 870 K.

5.2. *Y–R′–Ge systems*

5.2.1. *Y–Ce–Ge*

The isothermal section of the Y–Ce–Ge phase diagram at 870 K (fig. 121) was constructed by Shpyrka (1990) using X-ray powder diffraction data of 163 arc melted alloys annealed for 400 h. The purity of the starting components was Y 99.90 mass%, Ce 99.56 mass%, and Ge 99.99 mass%. The phase relations are characterized by the existence of two ternary compounds and by the formation of two continuous solid solutions between binary

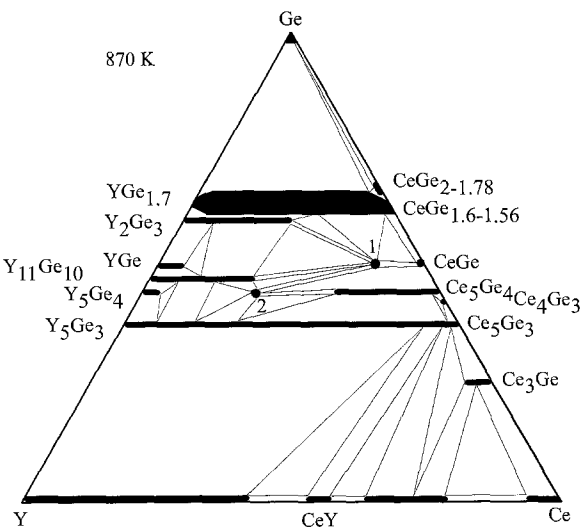

Fig. 121. Y–Ce–Ge, isothermal section at 870 K.

RGe_{2-x} and R_5Ge_3 compounds. Three solid solution ranges were found to exist within the Y–Ce–Ge system at 870 K: Ce in Y_2Ge_3 (up to 20 at.%), Ce in $Y_{11}Ge_{10}$ (up to 18 at.%) and Y in Ce_5Ge_4 (up to 20 at.%).

$Y_{0.2}Ce_{0.8}Ge$ (1) was said to crystallize with CrB type structure, $a = 0.447$, $b = 1.1095$, $c = 0.4064$ (Shpyrka 1990; X-ray powder diffraction).

$Y_{3.2}Ce_{1.8}Ge_4$ (2) belongs to the Sm_5Ge_4 type structure, $a = 0.760$, $b = 1.463$, $c = 0.756$ (Shpyrka 1990; X-ray powder diffraction).

5.3. *La–R′–Ge systems*

5.3.1. *La–Ce–Ge*

The phase equilibria in the La–Ce–Ge system at 870 K (fig. 122) were investigated by Shpyrka (1988) by means of X-ray phase analysis and partly microstructural analysis of alloys which were arc melted and subsequently annealed in evacuated silica tubes for 350 h and finally quenched in water. The starting materials were La 99.79 mass%, Ce 99.56 mass%, and Ge 99.99 mass%. The phase relations are characterized by the formation of continuous solid solutions originating at the isotypic binary compounds.

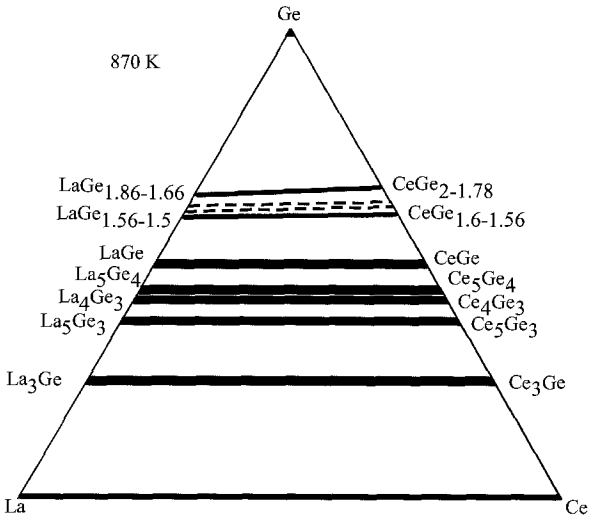

Fig. 122. La–Ce–Ge, isothermal section at 870 K.

5.3.2. *La–Gd–Ge*

The phase relations in the La–Gd–Ge ternary system at 873 K within 40–100 at.% Ge were investigated by Stetskiv et al. (1995) using X-ray powder and partly microstructural analyses. Samples were obtained by arc melting, and homogenized at 873 K for 500 h. The formation of the continuous solid solution $(La, Gd)Ge_{2-x}$ (α-$ThSi_2$ structure type) was found and solubility of Gd (~10 at.%) in $LaGe_{2-x}$ (α-$GdSi_2$ structure type) was determined.

5.4. *Ce–R′–Ge systems*

5.4.1. *Ce–Gd–Ge*

The phase equilibria in the Ce–Gd–Ge system (fig. 123) were investigated by Shpyrka et al. (1986) by means of X-ray phase analysis of 170 alloys which were arc melted and subsequently annealed in evacuated silica tubes for 350 h at 870 K and finally quenched in water. The starting materials were Ce 99.56 mass%, Gd 99.85 mass%, and Ge 99.99 mass%. The phase relations are characterized by the formation of three continuous solid solutions between isotypic binary compounds: $(Ce,Gd)Ge_{2-x}$, $(Ce,Gd)_5Ge_4$ and $(Ce,Gd)_5Ge_3$. The binary compounds GdGe, Ce_3Ge and $Gd_{1.04}Ge_{1.56}$ dissolve 40, 20 and 16 at.% of the third component, respectively.

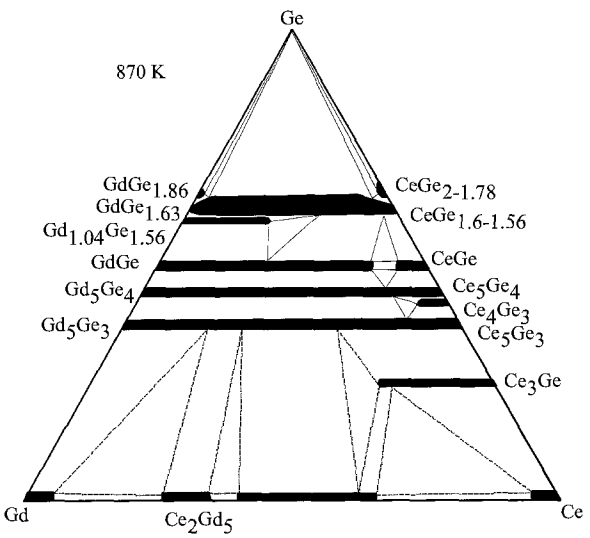

Fig. 123. Ce–Gd–Ge, isothermal section at 870 K.

5.4.2. *Ce–Dy–Ge*

Little information exists about the Ce–Dy–Ge system; only one ternary germanide was characterized. $Ce_{0.8}Dy_{0.2}Ge$ was found to be isotypic with CrB, $a = 0.4465$, $b = 1.1064$, $c = 0.4050$ (X-ray powder diffraction; Shpyrka 1990). For the experimental details, see Y–Ce–Ge.

5.4.3. *Ce–Ho–Ge*

No phase diagram is available for the Ce–Ho–Ge system; however one ternary compound was observed and characterized in the course of searching for isostructural series of compounds. $Ce_{0.8}Ho_{0.2}Ge$ was reported to be isotypic with CrB, $a = 0.4475$, $b = 1.1092$, $c = 0.4063$ (X-ray powder diffraction; Shpyrka et al. 1990). For the experimental details, see Y–Ce–Ge.

5.4.4. *Ce–Er–Ge*

At present, phase relations are unknown for the system Ce–Er–Ge; the formation of one ternary germanide was observed. Shpyrka (1990) reported the crystallographic characteristics for $Ce_{0.8}Er_{0.2}Ge$: CrB-type structure, $a = 0.4470$, $b = 1.1104$, $c = 0.4072$ (X-ray powder diffraction). For experimental details, see Y–Ce–Ge.

5.4.5. *Ce–Tm–Ge*

No phase diagram is available for the Ce–Tm–Ge system; however one ternary compound was observed and characterized by Shpyrka (1990): $Ce_{0.8}Tm_{0.2}Ge$, CrB-type structure, $a = 0.4485$, $b = 1.1110$, $c = 0.4073$ (X-ray powder diffraction). For experimental details, see Y–Ce–Ge.

5.4.6. *Ce–Lu–Ge*

The phase equilibria in the Ce–Lu–Ge system at 870 K (fig. 124) were investigated by Shpyrka (1990) by means of X-ray phase and microstructural analyses of 143 alloys which were arc melted and subsequently annealed in evacuated silica tubes for 350 h and finally quenched in water. The starting materials were Ce 99.56 mass%, Lu 99.98 mass%, and Ge 99.99 mass%. The phase relations are characterized by the existence of two ternary compounds and the formation of continuous solid solution $(Ce,Lu)_5Ge_3$ between the isotypic binary compounds. The binary compounds Ce_3Ge, $Lu_{0.9}Ge_2$ and $LuGe_{1.5}$ dissolve 12.5, 10 and 10 at.% of third component, respectively.

The two ternary compounds observed by Shpyrka (1990) were $Ce_{0.45-1.35}Lu_{4.55-3.65}Ge_4$ (1) ($a = 0.7389$–0.7469, $b = 1.4305$–1.4436, $c = 0.7607$–0.7649) and $Ce_{3.25}Lu_{1.75}Ge_4$ (2) ($a = 0.7666$, $b = 1.4925$, $c = 0.7649$). Both phases are isotypic with Sm_5Ge_4.

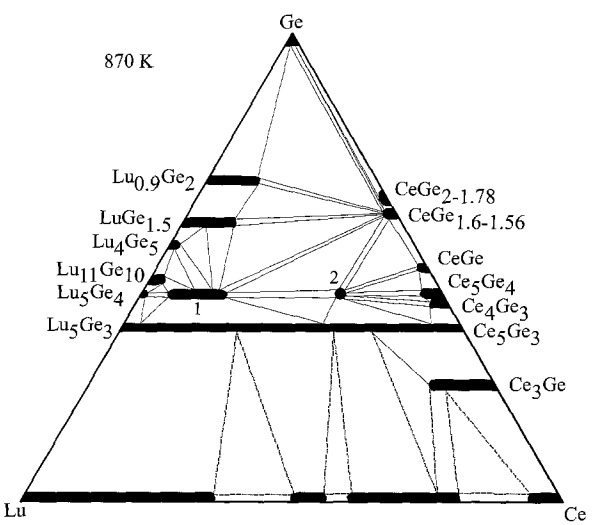

Fig. 124. Ce–Lu–Ge, isothermal section at 870 K.

5.5. *Sm–R′–Ge systems*

5.5.1. *Sm–Lu–Ge*

Shpyrka investigated the phase formation within the $SmGe_2$–$LuGe_2$ section at 870 K; three ternary phases were observed: ~$Sm_{26}Lu_8Ge_{66}$ (unknown type), ~$Sm_{24}Lu_{10}Ge_{66}$ ($DyGe_{1.85}$ type) and ~$Sm_{22}Lu_{12}Ge_{66}$ ($HoGe_2$ type). For sample preparation, see Ce–Lu–Ge.

5.6. *Dy–R′–Ge systems*

5.6.1. *Dy–Ho–Ge*

The only information on the phase relations in the Dy–Ho–Ge system is due to Shpyrka (1990) who investigated the $DyGe_2$–$HoGe_2$ section by means of X-ray powder diffraction. The samples were prepared by arc melting followed by annealing at 870 K for 400 h. The purity of the starting materials was Dy 99.83 at.%, Ho 99.50 at.%, and Ge 99.99 at.%. The solubility of $HoGe_2$ in $DyGe_2$ extends to 15 at.% Ho. One ternary compound $Dy_{0.19-0.17}Ho_{0.19-0.21}Ge_{0.66}$ with unknown structure was observed. The solubility of $DyGe_2$ in $HoGe_2$ extends to 8.5 at.% Ho.

5.7. *Er–R′–Ge systems*

5.7.1. *Er–Tm–Ge*

No ternary phase diagram exists for the Er–Tm–Ge system; however the formation of a ternary compound ~$Er_{0.24}Tm_{0.12}Ge_{0.66}$ with an unknown structure was reported from an X-ray investigation of the $ErGe_2$–$TmGe_2$ section. The solubility of $TmGe_2$ in $ErGe_2$ extends to 3 at.% Tm, whereas the solubility of $ErGe_2$ in $TmGe_2$ extends to 20 at.% Er.

6. Discussion

6.1. *Peculiarities of the interactions in the R–s element–Ge systems*

6.1.1. *R–Li–Ge systems*

From 16 rare-earth ternary systems with lithium and germanium the isothermal sections for 10 systems have been established over the whole concentration region.

The main peculiarity of all ternary systems with rare-earth metals concerns the influence which the component interaction in the terminal binary systems has on the ternary systems. The binary immiscibility region R–Li always extends into the ternaries up to a maximum content of 17–26 at.% Ge. As a consequence, a small number of ternary compounds is formed, with a maximum observed for the Ho–Li–Ge system (7 intermetallics). All ternary compounds, as a rule, have a narrow homogeneity range, which is connected with the pronounced difference in characteristic alloying parameters of the interacting components.

Table 31
Isotypic compounds of the ternary R–Li–Ge systems[a]

Structure type	La	Ce	Pr	Nd	Sm	Eu	Gd	Tb	Dy	Ho	Er	Tm	Yb	Lu	Y
$Ce_2Li_2Ge_3$	+	+	+	+	+		−			−	−	−	−	−	
Ce_2MnGe_5		+	+	+	+		−			−	−	−	−	−	
$AlCr_2C$	+	+	+	+	−		−			−	−	−	−	−	
Pr_2LiGe_6		+	+	−	−		−			−	−	−	−	−	
$CaLiSi_2$	+	+	+	+	+	+	+			−	−	−	−	−	
ZrNiAl		−	+	+	+		+	+	+	+	+	+	+	+	+
Tm_4LiGe_4		−	−	−	−		+	+	+	+	+	+	+	+	+
$Hf_3Ni_2Si_3$		−	−	−	−		−	+	+	+	+	+	−	+	+
$TmLi_{1-x}Ge_2$		−	−	−	−		−			+	+	+	−	+	

[a]An empty cell means that the alloy of this composition was not investigated; a plus sign means that the compound exists, a minus sign that it was not observed.

Analysis of the compositions and crystal structures of the experimentally observed ternary intermetallics established a sharp differentiation between systems belonging to the ceric or to the yttric subgroup. This situation is illustrated by table 31.

From the investigated series of isostructural compounds, intermetallics of equiatomic composition with ZrNiAl structure are typical for both the ceric and the yttric subgroups. Other series exist either in the ceric subgroup (RLi_2Ge, R_2LiGe_6, R_2LiGe_5, $R_2Li_2Ge_3$) or in the yttric subgroup (R_4LiGe_4, $R_3Li_2Ge_3$, $RLi_{1-x}Ge_2$). The system Gd–Li–Ge occupies the intermediate position with compounds crystallizing in structural types typical for the ceric subgroup ($CaLiSi_2$), as well as types typical for the yttric subgroup (Tm_4LiGe_4) or for both subgroups (ZrNiAl). However the systems of a particular subgroup are not complete analogues. For example, in the Ce–Li–Ge system, a compound of composition $Ce_{26}Li_5Ge_{22}$ exists which has not been found in the corresponding systems of this subgroup. Also the intermetallic of equiatomic composition with the ZrNiAl structure does not form with cerium. In the systems with Nd and Sm the homologous compounds with Pr_2LiGe_6 structure, which are formed with cerium and praseodymium, have not been found. Also, in the Sm–Li–Ge system there is no compound with $AlCr_2C$ structure.

For the yttric subgroup the biggest differences are observed for the Yb–Li–Ge system. The formation of two compounds (Yb_8LiGe_{13} and $Yb_5Li_4Ge_4$) with new structure types which do not occur within any other system of this subgroup has been found for the ytterbium–lithium–germanium combinations. This is probably due to the tendency of ytterbium to be divalent or mixed-valent.

Compounds of equiatomic composition with rare-earth metals of the yttric and cerium subgroups crystallize with the ZrNiAl type whereas scandium germanide of equiatomic composition forms the MgAgAs type.

Due to a noticeable lack of information on ternary R–Li–Ge systems, it is still difficult to establish a relation between the number of compounds formed per individual system

and the chemical nature of the interacting elements. From the data available, one can distinguish some established regularities:

(i) the number of compounds formed per system increases with increasing differences in atom size, electronegativity, electronic structure and thermodynamic properties;
(ii) a separation of systems into ceric and yttric subgroups is observed; the Gd–Li–Ge system occupies an intermediate position between these subgroups;
(iii) binary immiscibility always extends into the corresponding ternary system.

6.1.2. *R–Mg–Ge*

Interaction of rare earths with magnesium and germanium has not been studied sufficiently; few ternary compounds were observed and investigated (EuMgGe, YbMgGe and $EuMg_3Ge_3$). Therefore it is impossible to draw any conclusions with respect to the alloying behavior of these metals.

6.2. *Peculiarities of the interactions in the R–p element–Ge systems*

6.2.1. *R–B–Ge systems*

The characteristic features of the interaction of boron and germanium with the rare earths is the absence of ternary compounds and the lack of solid solubility of the third component in the binary phases.

6.2.2. *R–Al–Ge systems*

In spite of the fact that the partial isothermal sections (0–33 at.% R) have been investigated only for four ternary systems, it is possible to draw some conclusions on the interaction of components in these systems (see table 32). Similarly to the ternary R–Li–Ge combinations, a differentiation exists between ternary systems containing light and heavy lanthanides; the Gd–Al–Ge system occupies an intermediate position between ceric and yttric subgroups:

Table 32
Isotypic compounds of the ternary R–Al–Ge systems

Structure type	La	Ce	Pr	Nd	Sm	Eu	Gd	Tb	Dy	Ho	Er	Tm	Yb	Lu	Y	Sc
$CaAl_2Si_2$	+	+	+	+	+	+	+	+	+	+	+	+	+	+	+	–
$Ba_2Cd_3Bi_4$	+	+	+	+	+	–	+	+	+	+	+	–	–	–	–	–
La_2AlGe_6	+	+	+	+	+	–	+	–	–	–	–	–	–	–	–	–
α-$ThSi_2$	+	+	+	+	+	+	+	–	–	–	–	–	–	–	–	–
YAlGe	–	–	–	–	–	–	+	+	+	+	+	+	+	+	+	+
AlB_2	+	+		+			–								–	

[a]An empty cell means that the alloy of this composition was not investigated; a plus sign means that the compound exists, a minus sign that it was not observed.

(i) the R_2AlGe_6 and α-$ThSi_2$ structures are typical for the ceric subgroup, and the Gd-containing compounds are the ending members of these isotypic series;
(ii) the YAlGe structure is typical for the yttric subgroup, and the Gd-containing compound is the first member of this isostructural series;
(iii) the $CaAl_2Si_2$ type occurs in all systems except of for scandium;
(iv) the GdAlGe compound has two polymorphic modifications, α-$ThSi_2$ and YAlGe.

6.2.3. *R–Ga(In, C)–Ge systems*

Little information exists on the interaction of gallium (indium, carbon) with germanium and the rare earths. From the available data, one notices that for the gallium-containing compounds the most typical structures are the AlB_2-, $ThSi_2$- and Ce_2GaGe_6-types. Only one series of isotypic compounds was observed both for the rare-earth–indium–germanium combinations (Mo_2NiB_2) and for the carbon-containing ternary alloys (R_5CGe_3).

6.2.4. *R–Si–Ge systems*

The R–Si–Ge systems are characterized by the presence of two components with similar crystallochemical behavior. This is the main reason why limited or continuous solid solutions are formed between the isotypic binary compounds. These solid solutions often show various deviations from linearity in the unit cell volume versus concentration plots.

Two ternary compounds were found only in the Y–Si–Ge system. They have the crystal structures of binary YSi_2 and YGe_2 compounds.

6.3. *Peculiarities of the interactions in the R–d element–Ge systems*

The majority of experimental investigations deals with Fe, Co, Ni and Cu. Therefore, our discussion will be based on the interaction peculiarities of rare earths and germanium with the above-mentioned elements and their electronic analogues.

6.3.1. *R–Fe–Ge systems*

From the results reviewed in this chapter, some common regularities of the interaction of rare-earth metals with iron and germanium can be drawn. The number of ternary compounds formed with light rare-earth elements, iron and germanium monotonously increases from lanthanum to samarium. No ternary compounds were found with europium, which is probably due to its divalent nature, compared to trivalency for the other rare earths. Among the heavy lanthanides, Tm forms the largest number of ternary compounds with iron and germanium.

The ternary systems R–Fe–Ge are characterized by various stoichiometries and crystal structures of the existing ternary compounds, depending on the rare-earth metal (table 33). As one can see, the most prevailing structure types are $CeGa_2Al_2$ and $CeNiSi_2$. Compounds with AlB_2-, $BaNiSn_3$-, $Nd_6Fe_{13}Si$- and $Sm_4Co_{1-x}Ge_7$-type structures were observed in ternary systems containing light lanthanides; compounds with $CeGa_2Al_2$-,

Table 33
Isotypic compounds in the ternary R–Fe–Ge systems[a]

Structure type	La	Ce	Pr	Nd	Sm	Eu	Gd	Tb	Dy	Ho	Er	Tm	Yb	Lu	Y	Sc
$CeGa_2Al_2$	+	+	+	+	+	–	+	+	+	+	+	+	+	+	+	–
$CeNiSi_2$	–	+	+	+	+	–	+	+	+	+	+	+	+	+	+	–
YCo_6Ge_6	–	–	+	+	+	–	+	+	+	+	+	+	+	+	+	–
$Tb_{117}Fe_{52}Ge_{112}$		–	+	–	+	–		+	+	+	+	+	–	+	+	–
$ZrFe_4Si_2$		–	–	–	–	–	–	+	+	+	+	+	+	+	+	–
$Gd_6Cu_8Ge_8$		–	–	–	–	–	–	–	+	+	+	+	–	+	–	–
$Hf_3Ni_2Si_3$		–	–	–	–	–		–		–	+	–	–	+		–
$Tm_9Fe_{10}Ge_{10}$		–	–	–	–	–		–		–	+	+	+			–
$BaNiSn_3$		+	+	–	–	–		–		–	–	–	–			–
AlB_2	+	–	–	+	+	–		–		–	–	–	–			–
$Nd_6Fe_{13}Si$		–	+	+	–	–		–		–	–	–	–			–
$Sm_4Co_{1-x}Ge_7$		–	+	+	+	–		–		–	–	–	–			–

[a]An empty cell means that the alloy of this composition was not investigated; a plus sign means that the compound exists, a minus sign that it was not observed.

$CeNiSi_2$-, YCo_6Ge_6- and $Tb_{117}Fe_{52}Ge_{112}$-type structures are found for both the light and heavy rare-earth elements; and $ZrFe_4Si_2$-, $Gd_6Cu_8Ge_8$-, $Tm_9Fe_{10}Ge_{10}$- and $Hf_3Ni_2Si_3$-type structures are typical only for the heavy lanthanides.

The range of formation of ternary R–Fe–Ge compounds is restricted to concentrations of less than ~42 at.% rare-earth metal; $R_{117}Fe_{52}Ge_{112}$ ($Tb_{117}Fe_{52}Ge_{112}$ type) is the terminal R-rich phase. Ternary compounds with light lanthanides are found predominantly in the range 40–70 at.% Ge, whereas the heavy rare-earth elements form compounds primarily in the concentration region from 28 to 50 at.% Ge.

6.3.2. *R–Co–Ge systems*

Interactions of R with cobalt and germanium have been sufficiently studied to draw some conclusions, i.e. the phase diagrams for 12 ternary R–Co–Ge systems have been established. Most of them are characterized by a large number of ternary compounds. Substitution of an R element essentially affects the alloying behaviour of elements that is displayed in the number of compounds formed. The maximum number of ternary phases (20) has been observed for the samarium-containing system. The Eu–Co–Ge system strongly differs from all other R–Co–Ge systems by the number of ternary compounds. The isotypic series of compounds which are observed in these systems are listed in table 34.

Dimorphism phenomena are characteristic for the $R_2Co_3Ge_5$ compounds ($Lu_2Co_3Si_5$-type $\leftrightarrow$ $U_2Co_3Si_5$-type) (R = Ce–Sm, Gd). Morphotropic transformation was noticed for

Table 34
Isotypic compounds of the ternary R–Co–Ge systems[a]

	La	Ce	Pr	Nd	Sm	Eu	Gd	Tb	Dy	Ho	Er	Tm	Yb	Lu	Y	Sc
$CeGa_2Al_2$	+	+	+	+	+	+	+	+	+	+	+	+	+		+	–
$CeNiSi_2$	+	+	+	+	+	–	+	+	+	+	+	+	+	+	+	–
Sc_2CoSi_2		–	–	+	+	–	+	+	+	+	+	+	+	+	+	+
$Tb_3Co_2Ge_4$		–	–	–	+	–	+	+	+	+	+	+	–	–	+	–
TiNiSi		–	–	–	+	–	+	+	+	+	+	+	+	+	+	+
$Y_3Co_4Ge_{13}$		–	–	–	–	–	+	+	+	+	+	+	+	+	+	–
YCo_6Ge_6		–	–	–	–	–	+	+	+	+	+	+	+	+	+	–
Ce_2CuGe_6		–	–	–	–	–	+	+	+	+	+	+	–	+	+	–
$ZrFe_4Si_2$		–	–	–	–	–		–		–	+	+	+	+		–
$Sc_5Co_4Si_{10}$		–	–	–	–	–		–		–	+	+	+		+	–
$BaNiSn_3$		+	+	+	+	+		–		–	–	–				–
AlB_2		+	+	+				–		–	–	–				–
PbFCl		+	+	+				–		–	–	–				–
La_3NiGe_2		+	+	+				–		–	–	–				–
$Tb_{117}Fe_{52}Ge_{112}$		–	+	+	+	–		–		–	–	–				–
$U_2Co_3Si_5$		+	+	+	–	–		+					–	–	+	–
$Lu_2Co_3Si_5$		+	+	+	+		+		+	+	+		–	–		–

[a]An empty cell means that the alloy of this composition was not investigated; a plus sign means that the compound exists, a minus sign that it was not observed.

the RCoGe compounds: from structure type PbFCl (CeCoGe, PrCoGe, NdCoGe) to structure type TiNiSi (SmCoGe, GdCoGe). No compound of equiatomic composition was observed within the Eu–Co–Ge system.

The maximum number of ternary compounds in the R–3d element–Ge systems with Pr, Nd, Sm, Tb, Ho, Er, Tm is formed with cobalt.

6.3.3. *R–Ni–Ge systems*

The primary intention of this section is to discuss and compare the interaction of the components in the R–Ni–Ge systems. According to sect. 4, the phase equilibria have been investigated for 12 ternary systems.

Concerning the number and the composition of compounds formed, the interaction of the components in the ternary systems R–Ni–Ge is rather complicated and varies considerably.

In this respect the most significant differences are observed in the light rare-earth group, between Ce and Eu. The ternary nickel germanides with cerium (20 compounds) exist within a wide concentration region from 7.5 to 62.5 at.% Ce, whereas the ternary phases in the Eu–Ni–Ge system (six compounds) occur between 7.5 and 33.3 at.% Eu.

Table 35
Isotypic compounds of the ternary R–Ni–Ge systems[a]

Structure type	La	Ce	Pr	Nd	Sm	Eu	Gd	Y	Tb	Dy	Ho	Er	Tm	Yb	Lu	Sc
$CeGa_2Al_2$	+	+	+	+	+	+	+	+	+	+	+	+	+	+	+	–
$CeNiSi_2$	+	+	+	+	+	+	+	+	+	+	+	+	+		+	–
AlB_2	+	+	+	+	+	+	+	+	+	+	+	+	+	+		–
$SmNiGe_3$		+	+	+	+	–	+	+	+	+	+	+	+	–	+	–
TiNiSi		+	+	+	+	–	+	+	+	+	+	+	+	+	+	+
Ce_2CuGe_6		+	+	+	+	–	+	+	+	+	+	+	+	+	+	–
La_3NiGe_2	+	+	+	+	+	–	+	+	+	+	+	+	–	–	–	–
YNi_5Si_3		–	–	–	+	–	+	+	+	+	+	+	+	+	+	–
$Sc_3Ni_{11}Si_4$		–	–	–	–	–		+	+	+	+	+	+	+	+	+
$NdIrGe_2$	–	–	–	–	–	–		?	?	?	+	+	+	?	+	–
LuNiGe		–	–	–	–	–		–	–	–	–	–	+	–	+	–
$La_{11}NiGe_6$	+	+	–	–	–	–		–	–	–	–	–	–	–		–
$U_3Ni_4Si_4$	+	+	+	–	–	–		–	–	–	–	–	–	–		–
$U_2Co_3Si_5$		+	+	?	?	–		–	–	–	–	–	–	–		–
$CeNi_{8.5}Si_{4.5}$	–	+	+	+	–	+		–	–	–	–	–	–	–		–

[a]An empty cell means that the alloy of this composition was not investigated; a plus sign means that the compound exists, a minus sign that it was not observed.

The maximum rare-earth concentration in the ternary nickel germanides of Pr (Nd, Sm) is approximately 50 at.%.

The formation of ternary phases with the rare-earth elements from Tb through Tm (including Y) exhibits a close resemblance between systems. Moreover, the Y(Tb, Dy)–Ni–Ge systems are identical. This is also true for the Ho(Er, Tm)–Ni–Ge systems.

It should be noted, that the concentration region spanned by the compounds formed for the R elements from Tb through Tm (including Y) is somewhat narrower in comparison with R–Ni–Ge systems, where R = Ce, Pr, Nd, Sm, Eu (from 11 to 50 at.% R). The maximum Ge concentration in the ternary nickel germanides of the light rare-earth elements as well as of the heavy rare earths is 66.6 at.% (in the R_2NiGe_6 compounds).

Another interesting feature of the R–Ni–Ge systems is the solubility of Ge in the Ni-rich binary compounds R_2Ni_{17} and RNi_5.

Table 35 gives a survey of the isotypic series of the compounds in the R–Ni–Ge systems. The compounds of the $CeGa_2Al_2$-, $CeNiSi_2$-, AlB_2-, Ce_2CuGe_6-, La_3NiGe_2-, TiNiSi- and $SmNiGe_3$-type structures are found for both the light and the heavy rare-earth elements. The compounds of the $CeNi_{8.5}Si_{4.5}$-, $U_2Co_3Si_5$-, $U_3Ni_4Si_4$- and $La_{11}Ni_4Ge_6$-type structures are observed in ternary systems containing light lanthanides. The $Sc_3Ni_{11}Si_4$-, $NdIrGe_2$- and LuNiGe-type structures occur typically only for the

heavy lanthanides. The RNi_5Ge_3 compounds of YNi_5Si_3 structure type, unexpectedly, occur solely with samarium and with the heavy rare-earth elements. In addition to the compounds listed in table 35, the crystal structure has been solved for the following germanides: La_2NiGe (space group I4/mcm), La_8NiGe_5 (space group Pmmn), $La(Ni,Ge)_{13}$ (space group Fm3c), Ce_5NiGe_2 (space group P4/ncc), $SmNi_3Ge_3$ (space group I4/mmm), EuNiGe (space group $P2_1/b$), $EuNiGe_3$ (space group I4mm) and $Er_3Ni_2Ge_3$ (space group Cmcm). All these compounds are the unique representatives of the indicated structure types in the R–Ni–Ge systems.

As one can see from table 35, a few morphotropic transformations have been observed in the systems under discussion. A brief description follows:

(i) The $RNiGe_2$ compounds. The compounds with 1:1:2 composition when R is a light rare-earth element crystallize in the $CeNiSi_2$-type structure. The compounds of the same structure type for the heavy rare-earth elements have been found to form with a nonstoichiometric composition and are defective of Ni atoms. Furthermore, the compounds of stoichiometric composition with Ho, Er, Tm and Lu have been found to crystallize with the $NdIrGe_2$-type structure.

(ii) The $R(Ni,Ge)_{13}$ compounds. The following morphotropic transformation has been observed for the light rare-earth elements: from $La(Ni,Ge)_{13}$ ($NaZn_{13}$ type, space group Fm3c) to $R(Ni,Ge)_{13}$ (R = Ce–Nd, Eu, $CeNi_{8.5}Si_{4.5}$ type, space group I4/mcm).

(iii) The $RNiGe_3$ compounds. In this series the $SmNiGe_3$ structure type (space group Cmmm) was observed for the compounds of the lanthanides except Eu and Yb. The $EuNiGe_3$ compound crystallizes in the $BaNiSn_3$ type (space group I4mm).

(iv) The RNiGe compounds. A similar transformation, which also is caused, probably, by the peculiar behavior of the Eu atom has been observed in the RNiGe series of compounds: Ce(Pr–Sm)NiGe (TiNiSi-type) to EuNiGe (own structure type) → Gd(Tb–Lu)NiGe (TiNiSi-type).

The TmNiGe and LuNiGe compounds exhibit dimorphism. The TiNiSi type ↔ LuNiGe type transition temperature is 1630 K for TmNiGe and 1570 K for LuNiGe.

The compound Ce_5NiGe_2 also occurs in two modifications: the compound in its own structure type (high-temperature modification) transforms into a compound of unknown structure type (low-temperature modification).

Thus, the comparison of the R–Ni–Ge systems, carried out above, shows a similarity in the interaction of rare-earth metals with nickel and germanium with the exception of europium, which forms a considerably smaller number of compounds. This is consistent with europium's divalent character, and its similar behavior observed in the other Eu–3d element–Ge systems. At the same time, the type of interaction and the crystal structures of compounds formed are different for the elements of the light and heavy lanthanides. The only two ternary germanides of scandium, which are isotypic with lanthanide-containing compounds, are ScNiGe (structure type TiNiSi) and $Sc_3Ni_{11}Ge_4$ (structure type $Sc_3Ni_{11}Ge_4$).

6.3.4. *R–Cu(Ag, Au)–Ge systems*

In contradiction to earlier reviewed R–Fe(Co, Ni)–Ge systems with a brightly pronounced distinction between systems containing light rare earths and systems containing heavy rare earths, the alloying behavior in R–Cu(Ag, Au)–Ge systems is of an analogous type.

The predominant majority of ternary compounds exists within the narrow concentration region from 20 to 33 at.% R.

Table 36 lists the isotypic series of the compounds in the R–Cu(Ag, Au)–Ge systems. Ternary phases of $Ce_2Cu_3Ge_3$- and $CeNiSi_2$-type structures are found only in the R–Cu–Ge system and are not included in table 36.

Table 36
Isotypic compounds of the ternary R–Cu(Ag, Au)–Ge systems[a]

Structure type		La	Ce	Pr	Nd	Sm	Eu	Gd	Tb	Dy	Ho	Er	Tm	Yb	Lu	Y	Sc
$CeGa_2Al_2$	Cu	+	+	+	+	+	+	+	+	+	+	+	+	+		+	–
	Ag	+	+	+	+	+	+	+									–
	Au				+												–
Ce_2CuGe_6	Cu	+	+	+	+	+	–	+	+	+	+	+	+	+		+	–
	Ag	+	+	+	+	+	–	+			–				–		–
	Au	+	+	+	+	+	–	+			–						
AlB_2	Cu	+	+	+	+	+	+	+	+	+	+	+	+	–		+	–
	Ag	+	+	+	+						–				–		–
	Au				+						–						
$CaIn_2$ or	Cu	–	–	–	–	–	–	–	+	+	+	+	+	+	+	+	–
LiGaGe	Ag	+	+	+	–	–	–	–	–	–	–	–	–	–	–	–	–
	Au	+	+	+	+	+	–	+	+	+	+	+	+	+	+	+	+
Fe_2P or	Cu																+
ZrNiAl	Ag	–	–	+	+	+	+	–	+	+	+	+	+	+	+	+	+
	Au				–	–	–	–	–	–	–	–	–	–	–	–	–
$Gd_6Cu_8Ge_8$	Cu	–	–	+	+	+	–	+	+	+	+	+	+	+	+	+	+
	Ag	–	–	+	+	+	–	+			–				–		–
	Au				–												

[a]An empty cell means that the alloy of this composition was not investigated; a plus sign means that the compound exists, a minus sign that it was not observed.

The compounds of equiatomic composition are found to crystallize mainly in hexagonal basis. The following morphotropic transformation was observed in the RCuGe compounds: (La–Sm, Gd)CuGe (AlB_2 structure type) → (Y, Tb–Lu)CuGe ($CaIn_2$ structure type) → ScCuGe (ZrNiAl structure type). For the ternary RAgGe compounds the following structure types are characteristic: (La, Ce, Pr)AgGe (LiGaGe structure type) → EuAgGe (AlB_2 structure type) → (Gd–Lu, Sc)AgGe (ZrNiAl structure type). The RAuGe compounds crystallize with the LiGaGe structure type.

Unlike other lanthanides, europium forms equiatomic compounds with an orthorhombic structure: EuCuGe (structure types TiNiSi and CaCuGe), EuAgGe (structure type KHg_2) and EuAuGe (own structure type).

6.3.5. *R–platinum metals–Ge systems*

Although the isothermal sections are completely or partly constructed only for 18 ternary systems from 96 possible R–platinum metals–Ge combinations, one can see that with respect to the formation of compounds in the ternary R–M–Ge systems, Ru and Os show behavior similar to Rh and Ir (see table 37). Analysis of the compositions and crystal structures of the experimentally observed ternary germanides of platinum metals established a likeness between platinum- and palladium-containing systems (see table 38). Since information on the systematic investigations of the R–Pt–Ge systems is still lacking, only some regularities on the interaction of these components are observed.

Table 37
Isotypic compounds of the ternary R–Ru(Os, Rh, Ir)–Ge systems[a]

Structure type	La	Ce	Pr	Nd	Sm	Eu	Gd	Tb	Dy	Ho	Er	Tm	Yb	Lu	Y	Sc	
$Yb_3Rh_4Sn_{13}$	Ru	–	+	+	+	+	–	+	+	+	+	+	+	+	+	+	–
	Os	–	+	+	+	+	+	+	+	+	+	+	+	+	+	+	–
	Rh	–	+	–	+	+	–	+	+	+	+	+	+	+	+	+	–
	Ir	–	+	+	+	+	–	+	+	+	+	+	+	+	+	+	–
$CeGa_2Al_2$	Ru	+	+	+	+	+	+	+	+	+	+	+	+	+	+	+	–
	Rh	+	+	+	+	+	+	+	+	+	+	+	+	+	+	+	–
$CaBe_2Ge_2$	Ir	+	+	+	+	+	+	+	+	–	–	–	–	–	–	–	–
$U_2Co_3Si_5$ or	Ru	+	+	+	+	+	–	+	+	+	+	+	+	+	+	+	–
$Lu_2Co_3Si_5$	Rh	+	+	+	+	+	–	+	+	+	+	+	+	+	+	+	–
	Ir	+	+	+	+	+	–	+	+	+	–	–	–	–	–	–	–
$U_4Re_7Si_6$	Rh	–	–	–	–	–	–	–	–	+	+	+	+	+	+	+	+
	Ir	–	–	–	–	–	–	–	+	+	+	+	+	+	+	+	+
	Os	–	–	–	–	–	–	–	–	–	–	+	+	+	+	+	+
$NdIrGe_2$	Ir	–	–	+	+	+	–	+	+	+	+	+	–	–	–	+	–
$Sc_5Co_4Si_{10}$	Rh	–	–	–	–	–	–	+	+	+	+	+	+	+	+	+	–
	Ir	–	–	–	–	–	–	–	–	+	+	+	+	–	–	+	–
	Os	–	–	–	–	–	–	+	+	+	+	+	+	+	+	+	–
TiNiSi	Rh	+	+	+	+	+	–	+	+	+	+	+	+	+	+	+	+
	Ir	+	+	+	+	+	–	+	+	+	+	+	+	+	+	+	+
$La_3Ni_2Ga_2$	Ru	+	+	+	+	+	–	–	–	–	–	–	–	–	–	–	–
	Rh	+	+	+	+	+	–	+	+	+	+	+	+	–	+	+	–
$Ho_4Ir_{13}Ge_9$	Rh	+	+	+	+	+	–	+	+	+	+	+	+	+	+	+	–
	Ir	+	+	+	+	+	–	+	+	+	+	+	+	+	+	+	–

[a]An empty cell means that the alloy of this composition was not investigated; a plus sign means that the compound exists, a minus sign that it was not observed.

As one can see from table 37, the most prevailing structure type among the compounds within R–Ru(Os,Rh,Ir)–Ge systems is the $Yb_3Rh_4Sn_{13}$ type. In addition to the compounds listed in table 37, the crystal structure has been solved for a few germanides with the $TiMnSi_2$-, Sc_2CoSi_2-, $Hf_3Ni_2Si_3$-, $CeNiSi_2$- and $BaNiSn_3$-types of structure. Morphotropic transformations were observed for the RRuGe compounds: (La–Sm)RuGe (PbFCl structure type) → HoRuGe (TiNiSi structure type) → ScRuGe (ZrNiAl structure type).

Table 38
Isotypic compounds of the ternary R–Pd(Pt)–Ge systems[a]

Structure type		La	Ce	Pr	Nd	Sm	Eu	Gd	Tb	Dy	Ho	Er	Tm	Yb	Lu	Y	Sc	
KHg_2	Pd	+	+	+	+	+	+	−	+	+	+	+	+	+	+	+	+	−
	Pt	−	+	+	+	−	−	−	−	−	−	−	−	−	−		−	−
TiNiSi	Pt	−	−	−	−	−	+	−	+	+	+	+	+	+	+		+	+
YPd_2Si	Pd	+	+	+	+	+	+	−	+	+	+	+	+	+	+	+	+	−
$CeGa_2Al_2$	Pd	+	+	+	+	+	+	+	+	+	+	+	+	+	+	+	+	−
	Pt	+	+	+	+	+	+	+	+	+	+	−	+	−	−	−	+	−
$LaPt_2Ge_2$	Pt	+	+	+	+	+	+	+	+	+	+	−	−	−	−	−	+	−
$CeCuGe_6$	Pd	+	+	+	+	+			+	+	+	+	+	+	+		+	
	Pt	+	+	+	+	+			+	+	+	+	+	+	+		+	
$NdIrGe_2$	Pt	−	+	+	+	+	+	−	+	+	+	+	+	+	+	−	+	−

[a]An empty cell means that the alloy of this composition was not investigated; a plus sign means that the compound exists, a minus sign that it was not observed.

The RPt_2Ge_2 compounds crystallizes with two structure types, $CeGa_2Al_2$ and $LaPt_2Ge_2$ (see table 38). The $CePt_2Ge_2$ compound has three polymorphic modifications, $CeGa_2Al_2$, $CaBe_2Ge_2$ and $LaPt_2Ge_2$. Compounds of equiatomic composition with platinum crystallize with the following structure types: LaPtGe (LaPtSi structure type) → (Ce–Nd) PtGe (KHg_2 structure type) → SmPtGe (TiNiSi structure type) → EuPtGe (ZrOS structure type) → (Gd-Yb,Sc)PtGe (TiNiSi structure type).

6.4. *Peculiarities of the interactions in the R–R′–Ge systems*

An analysis of the interaction of the components in the ternary systems R–R′–Ge for which the isothermal sections have been constructed showed that they can be divided into three groups: (a) systems which are characterized by formation of ternary compounds; (b) systems which are characterized by formation of continuous solid solutions and limited solid solutions between binary germanides; (c) systems in which both ternary compounds and continuous and limited solid solutions are formed.

(a) The Sc–Ce(Nd)–Ge ternary systems are characterized by the formation of ternary compounds, comparatively small solubility of the third component in the binary

compounds, and the absence of continuous solid solutions. These are connected with the significant differences in the rare-earth metal atom structure (absence of 4f electron shell in Sc atom) and in atom size ($r_{Sc} = 0.164$ nm, $r_{Ce} = 0.183$ nm, $r_{Nd} = 0.182$ nm).

In comparing the considered systems with one another, it is necessary to indicate that at the transition from cerium to neodymium the number of ternary compounds decreases from 4 to 3 and the homogeneity range of the solid solutions on the base of the binary phases increases from 8 to 12.5 at.% Sc.

Concerning the formation of compounds, a common feature of these systems is the formation of the ternary phase with Ge content 33.3 at.% (ScRGe).

The $Ce_{0.5}Sc_{4.5}Ge_4$ compound has no equivalent in the Nd–Sc–Ge system. The $R_{1.25}Sc_3Ge_4$ compound exists with all the rare-earth metals of the cerium subgroup (La, Ce, Pr, Nd, Sm, Eu).

Considering the crystal structures of the compounds it is possible to conclude that the presence of scandium leads to the formation of various kinds of superstructures to the structure types of the binary compounds (Sm_5Ge_4, Ca_2As). RScGe ternary germanides are isostructural and are formed with the elements of the cerium subgroup (La, Ce, Pr, Nd, Sm, Eu), i.e. at the ratio r_R/r_{Sc} 1.1; for R = Y, Gd, Tb, Dy, Ho, Er, Tm, Yb, Lu the compounds of this composition are not observed.

(b) The existence of two components with close crystal chemical properties and a similar structure for most of the binary compounds determines the character of the interaction of the components in the Ce–La–Ge and Ce–Gd–Ge systems (absence of ternary compounds, formation of continuous and limited solid solutions between the isotypic binary compounds). As a consequence of the similar structure of all of the binary germanides, the Ce–La–Ge system is characterized by the formation of continuous solid solutions only (ratio $r_{Ce}/r_{La} = 0.997$). In the Ce–Gd–Ge system, the isotypic compounds were found to form continuous solid solutions as well, and on the basis of compounds which belong to different structure types, limited substitutional solid solution of different extension were observed. Extension of the solid solutions by the substitution of one rare-earth element by another is determined by the size of substituting atoms.

(c) The Sc–Y(Dy)–Ge and Ce–Y(Lu)–Ge systems occupy a special position among the R–R′–Ge systems. Both ternary compounds and continuous and limited solid solutions on the basis of binary compounds are found to exist. The peculiarity of the systems considered is the formation of continuous solid solutions between isostructural germanides with the composition R_5Ge_3 (Mn_5Si_3 structure type). One more continuous solid solution was observed in the system Ce–Y–Ge.

Another feature of the systems of this subgroup is the large extent of the limited solid solutions. Differences in the crystal chemistry characteristics of the rare-earth metals in the systems considered are insignificant, but they influence composition, structure and the number of ternary compounds. Ternary compounds with the composition $Sc_{0.3}R_{0.7}Ge_2$ (R = Y, Dy) were found to exist for the Sc and Ge ternaries with Y and Dy on the digermanide section. They have no equivalent in other

R–R′–Ge systems. The formation of compounds with the $Ce_{0.8}R_{0.2}Ge$ composition (structure type CrB) is characteristic of elements of the yttric subgroup (Y, Dy, Ho, Er, Tm). An increase in the volume of the unit cell in the series of the isostructural compounds is connected with the ability of the cerium atoms to adopt an intermediate state.

As one can see from the present review, rare-earth metals show very similar crystal chemistry that is displayed in the formation of continuous solid solutions as well as substitutional solid solutions. On the other hand, differences in electron configuration of the rare-earth atoms influence the interactions in the ternary systems, as shown by different compositions, structures and the number of ternary compounds.

References

Andrusyak, R.I., 1986, Visn. L'vivsk. Univer., Ser. Khim. **27**, 24.

Andrusyak, R.I., 1988, Ph.D. Chemistry Thesis (L'viv State University, L'viv) pp. 1–17.

Andrusyak, R.I., and B.Ya. Kotur, 1987, Kristallografiya **32**, 1018.

Andrusyak, R.I., and B.Ya. Kotur, 1989, Kristallografiya **34**, 740.

Andrusyak, R.I., and B.Ya. Kotur, 1991, Izv. Akad. Nauk SSSR, Met. **4**, 198.

Anisimova, E.V., E.I. Gladyshevsky, E.P. Marusin and V.K. Pecharsky, 1992, Crystal structure of compounds in the ternary systems Gd–Ag–Si(Ge), in: Tezisy VI Soveshch. po Kristallokh. Neorg. i Koord. Soedyneniy, Lv'iv, 1992, p. 160.

Anisimova, E.V., E.P. Marusin, V.K. Pecharsky and E.I. Gladyshevsky, 1995, Phase equilibria in the system Gd–Ag–Ge (range 0–40 at.% Gd) and crystal structure of the compound Gd_7Ge_{11}, in: Sixth Int. Conf. on Crystal Chemistry of Intermetallic Compounds, L'viv, Ukraine, 1995, Abstracts, p. 24.

Aslan, A.M., 1990, Phase equilibria, crystal structures and physical properties of the compounds in the ternary systems Ho,U–Co,Ni–Ge, Ph.D. Chemistry Thesis (Lv'iv State University, Lv'iv) pp. 1–17.

Bara, J.J., H.U. Hrynkiewicz, A. Milos and A. Szytuła, 1990, J. Less-Common Met. **161**, 185.

Barakatova, J.M., 1994, Physical chemistry interaction of palladium, platinum, silicon and germanium with samarium, Ph.D. Chemistry Thesis (Moscow State University, Moscow) pp. 1–21.

Belan, B.D., 1988, Phase equilibria, crystal structures and properties of compounds in the systems Eu–Fe,Co,Ni,Cu–Si,Ge, Ph.D. Chemistry Thesis (Lv'iv State University, Lv'iv) pp. 1–17.

Belsky, V.K., M.B. Konyk, V.K. Pecharsky and O.I. Bodak, 1987, Kristallografiya **32**, 241.

Belyavina, N.M., O.Ya. Beloborodova, V.Ya. Markiv and N.V. Alekseeva, 1993, Dopov. Akad. Nauk URSR **9**, 84.

Belyavina, N.M., V.Ya. Markiv and M.V. Speca, 1996, The phase equilibria and the alloys crystal structure in Y–Ge–Ga and Y–Si–Ga systems, in: Fifth Int. School "Phase Diagrams in Materials Science", 1996, Katsyvely, Crimea, Ukraine, Abstracts, p. 23.

Bodak, O.I., and E.I. Gladyshevsky, 1985, Ternary systems containing rare earth metals, Vyshcha shkola, Lvov, p. 328.

Bodak, O.I., and Z.M. Kokhan, 1983, Izv. Akad. Nauk SSSR, Neorg. Mater. **19**(7), 1094.

Bodak, O.I., and G.M. Koterlyn, 1995, Phase equilibria and crystal structure of compounds in the Lu–Ni–Ge system, in: Sixth Int. Conf. on Crystal Chemistry of Intermetallic Compounds, L'viv, Ukraine, 1995 (Abstracts) p. 26.

Bodak, O.I., and L.A. Muratova, 1979, Vestn. L'vov. Univers., Ser. Khim. **21**, 55.

Bodak, O.I., and L.A. Muratova, 1981, Vestn. L'vov. Univers., Ser. Khim. **23**, 67.

Bodak, O.I., and O.L. Sologub, 1991a, Izv. Akad. Nauk, Neorg. Mater. **27**, 2558.

Bodak, O.I., and O.L. Sologub, 1991b, Z. Neorg. Khim. **36**, 2401.

Bodak, O.I., E.I. Gladyshevsky and P.I. Kripyakevich, 1966, Izv. Akad. Nauk SSSR, Neorg. Mater. **2**(12), 2151.

Bodak, O.I., V.A. Bruskov and V.K. Pecharsky, 1982, Kristallografiya **27**, 896.

Bodak, O.I., V.K. Pecharsky, O.Ya. Mruz, V.E. Zavodnik, G.M. Vytvitska and P.S. Salamakha, 1985, Dopov. Akad. Nauk URSR, B **12**, 36.

Bodak, O.I., V.K. Pecharsky, P.K. Starodub, P.S. Salamakha, O.Ya. Mruz and V.A. Bruskov, 1986, Izv. Akad. Nauk SSSR, Met. **4**, 214.

Bodak, O.I., R.V. Skolozdra, M.F. Fedyna, V.K. Pecharsky and Yu.K. Gorelenko, 1987, Anomalous electrokinetical and magnetic properties of the $R_3Co_4Ge_{13}$ germanides, in: IV Vsesoyuzn. Konf. Fiz. Khim. Redkozem. Poluprovodnikov. Tezisy Dokl., Novosibirsk, 1987 (Nauka, Novosibirsk) p. 29.

Bodak, O.I., E.I. Gladyshevsky, P.S. Salamakha, V.K. Pecharsky and V.A. Bruskov, 1989a, Kristallografiya **34**, 1285.

Bodak, O.I., V.K. Pecharsky, O.L. Sologub and V.B. Rybakov, 1989b, Izv. Akad. Nauk SSSR, Met. **2**, 34.

Bodak, O.I., V.V. Pavlyuk, R.I. Andrusyak, B.Ya. Kotur, V.K. Pecharsky and V.A. Bruskov, 1990, Kristallografiya **35**, 223.

Bodak, O.I., O.L. Sologub, P.Yu. Zavalii and V.E. Zavodnik, 1991, Izv. Akad. Nauk, Met. **6**, 168.

Bodak, O.I., J. Deberitz, R. Ferro, M. Harmelin, H.L. Lukas, V.V. Pavlyuk, P. Rogl, R. Smidt-Fetzer and J.K. Schuster, 1995, Evaluated constitutional data, phase diagrams, crystal structures and applications of lithium alloy systems, in: Ternary Alloys, eds G. Effenberg, F. Aldinger and O.I. Bodak, Vol. 14–15 (MSI, VCH Verlagsgesellschaft).

Borisenko, O.L., 1993, Phase equilibria and some physical chemical properties of alloys in the Yb–(Pt,Pd)–(Si,Ge) systems, Ph.D. Chemistry Thesis (Moscow State University, Moscow) pp. 1–17.

Brabers, J.H.V.J., K.H.J. Buschow and F.R. de Boer, 1994, J. Alloys & Compounds **205**, 77.

Braun, H.F., K. Yvon and R.M. Braun, 1980, Acta Crystallogr. B **36**(10), 2397.

Bruskov, V.A., 1984, New structure types of rare earth germanides, Ph.D. Chemistry Thesis (Lv'iv State University, Lv'iv) pp. 1–17.

Bruskov, V.A., V.K. Pecharsky and O.I. Bodak, 1986, Izv. Akad. Nauk SSSR, Neorg. Mater. **22**, 1471.

Buchholz, W., and H.-U. Schuster, 1981, Z. Anorg. Allg. Chem. **482**, 40.

Cenzual, K., B. Chabot and E. Parthé, 1987, J. Solid State Chem. **70**, 229.

Contardi, V., R. Ferro, R. Marazza and D. Rossi, 1977, J. Less-Common Met. **51**, 277.

Czybulka, A., and H.-U. Schuster, 1979, Z. Naturforsch. **34b**, 1234.

Czybulka, A., G. Steinberg and H.-U. Schuster, 1979, Z. Naturforsch. **34b**, 1057.

Czybulka, A., W. Schauerte and H.-U. Schuster, 1990, Z. Anorg. Allg. Chem. **580**, 45.

Dommann, A., F. Hulliger and H.R. Ott, 1985, J. Less-Common Met. **110**, 331.

Dwight, A.E., W.C. Harper and C.W. Kimball, 1973, J. Less-Common Met. **30**, 1.

Dzianii, R.B., 1995, Phase equilibria, crystal structure and physical properties of compounds in the Yb–(Mn, Fe, Co, Ni, Cu)–Ge systems, Ph.D. Chemistry Thesis (L'viv State University, L'viv) pp. 1–21.

Dzianii, R.B., O.I. Bodak, L.G. Akselrud and V.V. Pavlyuk, 1995a, Neorg. Mater. **31**(7), 987.

Dzianii, R.B., O.I. Bodak and L.G. Akselrud, 1995b, Neorg. Mater. **31**(7), 988.

Dzianii, R.B., O.I. Bodak and V.V. Pavlyuk, 1995c, Neorg. Mater. **31**(7), 985.

Dzianii, R.B., O.I. Bodak and L.G. Akselrud, 1995d, Neorg. Mater. **31**(7), 990.

Engel, N., B. Chabot and E. Parthé, 1984, J. Less-Common Met. **96**, 291.

Fedyna, M.F., 1988, Phase equilibria, crystal structures and physical properties of compounds in the (Pr, Tm)–(Fe, Co, Ni)–Ge systems, Ph.D. Chemistry Thesis (L'viv State University, L'viv) pp. 1–17.

Fedyna, M.F., and V.E. Zavodnik, 1988, Vestn. Lvov. Univers., Ser. Khim. **29**, 29.

Fedyna, M.F., V.K. Pecharsky, P.K. Starodub, G.M. Koterlyn and O.I. Bodak, 1987, Ternary compounds with structure types YNi_5Si_3 and $Sc_3Ni_{11}Si_4$. Manuscript referred to Ukr. NIITI, 07.09.1987, Nr2306-Uk87, pp. 1–15.

Fedyna, M.F., O.Ya. Oleksyn, N.S. Bilonishko and O.V. Gulyak, 1994, Visn. L'viv Univers. **33**, 53.

Fedyna, M.F., O.V. Guljak and I.R. Mokra, 1995, Investigation of Pr–Cu–Ge system, in: Sixth Int. Conf. on Crystal Chemistry of Intermetallic Compounds, 1995, L'viv (Abstracts) p. 30.

Felner, I., and I. Novik, 1978, J. Phys. Chem. Solids **39**, 763.

Felner, I., and I. Nowik, 1985, J. Phys. Chem. Solids **46**(6), 681.

Felner, I., and M. Schieber, 1973, Solid State Commun. **13**, 457.

Felner, I., I. Mayer, A. Grill and M. Schieber, 1972, Solid State Commun. **11**(9), 1231.

Francois, M., G. Venturini, J.M. Mareche, B. Malaman and B. Roques, 1985, J. Less-Common Met. **113**, 231.

Francois, M., G. Venturini, E. McRae, B. Malaman and B. Roques, 1987, J. Less-Common Met. **128**, 249.

Francois, M., G. Venturini, B. Malaman and B. Roques, 1990, J. Less-Common Met. **160**, 197.

Ghosh, K., S. Ramakrishnan, S.K. Dhar, S.K. Malik, G. Chandra, V.K. Pecharsky, K.A. Gschneidner Jr, Z. Hu and W.B. Yelon, 1995, Phys. Rev., B **52**, 10, 7267.

Gibson, B., R. Pöttgen, R.K. Kremer, A. Simon and K. Ziebeck, 1996, J. Alloys & Compounds **239**, 34.

Gladyshevsky, E.I., and O.I. Bodak, 1965, Dopov. Akad. Nauk URSR, A **5**, 601.

Gladyshevsky, E.I., V.Ya. Markiv and Yu.B. Kuz'ma, 1962, Dopov. Akad. Nauk Ukr. RSR, Ser. A **5**, 481.

Gladyshevsky, R.E., J.T. Zhao and E. Parthé, 1991a, Acta Crystallogr. C **48**, 10.

Gladyshevsky, R.E., O.L. Sologub and E. Parthé, 1991b, J. Alloys & Compounds **176**, 329.

Gladyshevsky, R.E., K. Cenzual, J.T. Zhao and E. Parthé, 1992, Acta Crystallogr. C **48**, 221.

Golovata, N.V., V.Ya. Markiv and N.M. Belyavina, 1996, The phase equilibria and the alloys crystal structure in Gd–Ga–Ge and Gd–Ga–Si systems, in: Fifth Int. School "Phase Diagrams in Materials Science", 1996, Katsyvely, Crimea, Ukraine, Abstracts, p. 47.

Gorelenko, Yu.K., P.K. Starodub, V.A. Bruskov, R.V. Skolozdra, V.I. Yarovetz, O.I. Bodak and V.K. Pecharsky, 1984, Ukr. Fiz. Zh. **29**, 867.

Gribanov, A.V., 1994, Phase equilibria, crystal structure and physical properties of intermetallics in the ternary Ce–(Pd,Pt)–(Si,Ge) systems, Ph.D. Thesis (Moscow State University, Moscow) pp. 1–21.

Gribanov, A.V., O.L. Sologub, P.S. Salamakha, O.I. Bodak, Yu.D. Seropegin and V.K. Pecharsky, 1992a, J. Alloys & Compounds **179**, L7.

Gribanov, A.V., O.L. Sologub, P.S. Salamakha, O.I. Bodak, Yu.D. Seropegin, V.V. Pavlyuk and V.K. Pecharsky, 1992b, J. Alloys & Compounds **189**, L11.

Gribanov, A.V., Yu.D. Seropegin, O.I. Bodak, V.V. Pavlyuk, L.G. Akselrud, V.N. Nikiforov and A.A. Velikhovskii, 1993a, J. Alloys & Compounds **202**, 133.

Gribanov, A.V., Yu.D. Seropegin, O.I. Bodak, V.V. Pavlyuk, V.K. Pecharsky, O.L. Sologub and P.S. Salamakha, 1993b, J. Alloys & Compounds **198**, 39.

Gribanov, A.V., Yu.D. Seropegin and O.I. Bodak, 1994, J. Alloys & Compounds **204**, L9.

Gribanov, A.V., Yu.D. Seropegin, O.I. Bodak, V.N. Nikiforov, A.A. Velikhovskii and J. Mirkovic, 1996, J. Phase Equilibria **17**(3), 196.

Grund, I., 1985, Ternary compounds of Li with rare earth metals, Sc and Y and 4B- and 5B elements, Thesis (University of Cologne) pp. 1–77.

Grund, I., G. Zwiener and H.-U. Schuster, 1986, Z. Anorg. Allg. Chem. **535**, 7.

Gryniv, I.O., and O.R. Myakush, 1989, System Tm–Ga–Ge, in: V Vsesoyuzn. Konf. Kristallokh. Internet. Soed., Lvov, 1989, p. 80.

Gryniv, I.O., A.S. Noga and Yu.N. Grin', 1989, Ternary systems of gallium and germanium with rare earth (Ce) and transition (Mn) metals, in: V Vsesoyuzn. Soveshch. Diagr. Sost. metal. system., Tezisy Dokl., Zvenigorod, 1989, p. 154.

Hanel, G., and H. Nowotny, 1970, Monatsh. Chem. **101**, 463.

Haschke, H., H. Nowotny and F. Benesovsky, 1966, Monatsh. Chem. **97**, 1452.

Holtzberg, F., R.J. Gambino and T.R. McGuire, 1967, J. Phys. Chem. Solids **28**, 2283.

Hovestreydt, E., N. Engel, K. Klepp, B. Chabot and E. Parthé, 1982, J. Less-Common Met. **85**, 247.

Iandelli, A., 1993, J. Alloys & Compounds **198**, 141.

Jones, C.D.W., R.A. Gordon, F.J. DiSalvo, R. Pöttgen and R.K. Kremer, 1997, J. Alloys & Compounds **260**, 50.

Jorda, J.L., N. Ishikawa and E. Hovestreydt, 1983, J. Less-Common Met. **92**, 155.

Konyk, M.B., 1988, Visn. L'viv Univers., Ser. Khim. **29**, 25.

Konyk, M.B., 1989, Phase equilibria, crystal structure and physical properties of compounds in the Ce–(Mn,Fe,Co,Ni,Cu)–Ge systems, Ph.D. Thesis (Lv'iv State University, Lvov) p. 17.

Konyk, M.B., P.S. Salamakha, O.I. Bodak and V.K. Pecharsky, 1988, Kristallografiya **33**(4), 838.

Koterlyn, G.M., 1996, Visn. L'viv. Univers., Ser. Khim. **36**, 43.

Koterlyn, G.M., P.K. Starodub, G.I. Kyrchiv and O.I. Bodak, 1988, Visn. L'vivsk. Univ., Ser. Khim. **29**, 56.

Koterlyn, G.M., M.F. Fedyna and V.M. Baranyak, 1994, Visn. L'viv Univ., Ser. Khim. **33**, 37.

Kotur, B.Ya., 1986, Dopov. Akad. Nauk URSR, A **1**, 79.

Kotur, B.Ya., 1987, Izv. Akad. Nauk SSSR, Neorg. Mater. **4**, 558.

Kotur, B.Ya., 1991, Izv. Akad. Nauk SSSR, Met. **3**, 213.

Kotur, B.Ya., 1995, Metal chemistry of scandium and its intermetallic compounds, Dr.Sc. Chemistry Thesis (L'viv State University, L'viv) p. 43.

Kotur, B.Ya., and R.I. Andrusyak, 1984a, Dopov. Akad. Nauk Ukr. RSR, Ser. B **12**, 40.

Kotur, B.Ya., and R.I. Andrusyak, 1984b, Visn. L'vivsk. Univ., Ser. Khim. **25**, 35.

Kotur, B.Ya., and R.I. Andrusyak, 1991, Izv. Akad. Nauk SSSR, Neorg. Mater. **27**(7), 1433.

Kotur, B.Ya., and O.I. Bodak, 1988, Izv. Akad. Nauk SSSR, Met. **4**, 189.

Kotur, B.Ya., and O.I. Bodak, 1990, Izv. Akad. Nauk SSSR, Met. **6**, 200.

Kotur, B.Ya., and L.A. Boichuk, 1988, Vestn. Lvov Univ., Ser. Khim. **29**, 51.

Kotur, B.Ya., and M. Sikirica, 1982, J. Less-Common Met. **83**, 129.

Kotur, B.Ya., O.I. Bodak, M. Sikirica and M. Bruno, 1983, Dopov. Akad. Nauk Ukr. RSR, Ser. B **10**, 47.

Kotur, B.Ya., O.I. Bodak and V.E. Zavodnik, 1986, Kristallografiya **5**, 868.

Kotur, B.Ya., R.I. Andrusyak and V.E. Zavodnik, 1988a, Kristallografiya **1**, 240.

Kotur, B.Ya., A.B. Kravs and R.I. Andrusyak, 1988b, Izv. Akad. Nauk SSSR, Met. **6**, 198.

Kotur, B.Ya., O.M. Vozniak and O.I. Bodak, 1989, Izv. Akad. Nauk, Neorg. Mater. **25**(3), 399.

Le Bihan, T., K. Hiebl, P. Rogl and H. Noël, 1996a, J. Alloys & Compounds **235**, 80.

Le Bihan, T., H. Noël, K. Hiebl and P. Rogl, 1996b, J. Alloys & Compounds **232**, 142.

Markiv, V.Ya., O.Ya. Beloborodova, N.M. Belyavina and N.V. Alekseeva, 1993, Dopov. Akad. Nauk URSR **7**, 70.

Marko, M.A., and Yu.B. Kuz'ma, 1979, Izv. Akad. Nauk SSSR, Neorg. Mater. **15**(11), 2070.

Marko, M.A., M.S. Nalyvaiko and Yu.B. Kuz'ma, 1978, Izv. Akad. Nauk SSSR, Neorg. Mater. **14**(7), 1350.

Mayer, I., and I. Felner, 1974, J. Less-Common Met. **37**(1), 171.

Mayer, I., and I. Shidlowsky, 1969, Inorg. Chem. **8**(6), 1240.

McCall, W.M., K.S.V.L. Narasimhan and R.A. Butera, 1973a, J. Appl. Phys. **44**, 4724.

McCall, W.M., K.S.V.L. Narasimhan and R.A. Butera, 1973b, J. Appl. Cryst. **6**, 301.

Méot-Meyer, M., G. Venturini, B. Malaman and B. Roques, 1985a, Mater. Res. Bull. **20**, 1515.

Méot-Meyer, M., G. Venturini, E. McRae, J.F. Mareche, B. Malaman and B. Roques, 1985b, New ternary rare earth–transition metal germanides with $TiMnSi_2$, $Sc_5Co_5Si_{10}$ or $U_2Co_3Si_5$ type structures. Superconductivity in these compounds, in: VIII Int. Conf. on Solid Compounds of Transition Elements, Vienna (Extended Abstracts) P3B9, pp. 1–3.

Merlo, F., M. Pani and M.L. Fornasini, 1993, J. Alloys & Compounds **196**, 145.

Merlo, F., M. Pani and M.L. Fornasini, 1996, J. Alloys & Compounds **232**, 289.

Meyer, M., G. Venturini, B. Malaman, J. Steinmetz and B. Roques, 1983, Mater. Res. Bull. **18**, 1983.

Morozkin, A.V., Yu.D. Seropegin and O.I. Bodak, 1996, J. Alloys & Compounds **234**, 143.

Mruz, O.Ya., 1988, Ternary systems Sm–(Fe,Co,Ni)–Ge, Ph.D. Chemistry Thesis (Lv'iv State University, Lv'iv) pp. 1–17.

Mruz, O.Ya., V.K. Bel'sky, O.I. Bodak, B.Ya. Kotur and V.E. Zavodnik, 1983, Dopov. Akad Nauk URSR, B **6**, 41.

Mruz, O.Ya., P.K. Starodub and O.I. Bodak, 1984, Dopov. Akad. Nauk URSR, B **12**, 44.

Mruz, O.Ya., V.K. Pecharsky, O.I. Bodak and V.A. Bruskov, 1987a, Dopov. Akad. Nauk URSR, B **6**, 51.

Mruz, O.Ya., V.K. Bel'sky, Yu.K. Gorelenko, R.V. Skolozdra and O.I. Bodak, 1987b, Ukr. Phys. J. **32**(12), 1856.

Mruz, O.Ya., M.F. Fedyna, V.K. Pecharsky and O.I. Bodak, 1989, Izv. Akad. Nauk SSSR, Neorg. Mater. **25**(12), 2023.

Muratova, L.A., 1974, Visn. L'viv. Univers., Ser. Khim. **16**, 15.

Muratova, L.A., 1976, Ternary systems (yttrium, lanthanum, cerium, praseodymium, gadolinium)–germanium–silicon, Ph.D. Chemistry Thesis (Lv'iv University, Lv'iv) pp. 1–17.

Muratova, L.A., and O.I. Bodak, 1974, Ternary systems (Y, La, Ce, Pr, Gd)-Ge-Si, in: IInd All-Union Conference on Crystal Chemistry of Intermetallic Compounds, Abstracts, p. 33.

Muratova, L.A., O.I. Bodak and E.I. Gladyshevsky, 1974, Visn. L'viv. Univers., Ser. Khim. **15**, 43.

Muratova, L.A., O.I. Bodak and E.I. Gladyshevsky, 1975, Visn. L'viv. Univers., Ser. Khim. **17**, 30.

Muravyeva, A.A., and O.S. Zarechnyuk, 1970, Izv. Akad. Nauk SSSR, Neorg. Mater. **6**, 1066.

Muravyeva, A.A., O.S. Zarechnyuk and E.I. Gladyshevsky, 1971, Izv. Akad. Nauk SSSR, Neorg. Mater. 7, 38.

Oleksyn, O.Ya., 1990, Interaction of components in the Er–(Fe, Co, Ni)–Ge systems (phase equilibria, crystal structures and some physical properties of compounds), Ph.D. Chemistry Thesis (L'viv State University, L'viv) p. 17.

Oleksyn, O.Ya., and O.I. Bodak, 1994, J. Alloys & Compounds **215**, 45.

Oleksyn, O.Ya., M.F. Fedyna and G.M. Koterlyn, 1991, Visn. L'viv. Univers., Ser. Khim. **31**, 19.

Olenych, R.R., L.G. Akselrud and Ya.P. Yarmolyuk, 1981, Dopov. Akad. Nauk Ukr. RSR, Ser. A **2** 84.

Oniskovetz, B.D., 1984, Vestn. Lvov. Univers., Ser. Khim. **25**, 21.

Oniskovetz, B.D., V.V. Pavlyuk and O.I. Bodak, 1985, Dopov. Akad. Nauk URSR, B **10**, 40.

Oniskovetz, B.D., V.K. Belsky, V.K. Pecharsky and O.I. Bodak, 1987, Kristallografiya **32**, 888.

Opainych, I.M., 1996, Phase equilibria and crystal structure of compounds in the Ce–(Fe,Ni)–(Mg,Zn) and Ce–Zn–Ge systems, Ph.D. Chemistry Thesis (L'viv State University, Lviv) pp. 1–21.

Opainych, I.M., O.M. Sichevich and Yu.N. Grin', 1992, Crystal structure and magnetic properties of compounds in Nd–Ga–Ge system, in: IV Soveshch. Krist. Neorg. Koord. Soed., Tezisy Dokl., Lvov, 1992, p. 205.

Parthé, E., and B. Chabot, 1984, Crystal structures and crystal chemistry of ternary rare earth–transition metal borides, silicides and homologous, in: Handbook on the Physics and Chemistry of Rare Earths, Vol. 6, eds K.A. Gschneidner Jr and L. Eyring (North-Holland, Amsterdam) ch. 48, p. 113.

Pavlyuk, V.V., 1989, Interaction of Li with elements of the IVa Group and f(d)-metals, Ph.D. Chemistry Thesis (L'viv State University, L'viv) pp. 1–17.

Pavlyuk, V.V., 1993, Synthesis and crystal chemistry of the intermetallic compounds of lithium, Dr.Sc. Chemistry Thesis (L'viv State University, L'viv) pp. 1–46.

Pavlyuk, V.V., and O.I. Bodak, 1992a, Dopov. Akad. Nauk Ukr. RSR **3**, 104.

Pavlyuk, V.V., and O.I. Bodak, 1992b, Izv. Akad. Nauk SSSR, Neorg. Mater. **28**(5), 1119.

Pavlyuk, V.V., V.K. Pecharsky and O.I. Bodak, 1986, Dopov. Akad. Nauk Ukr. RSR, Ser. A **7**, 78.

Pavlyuk, V.V., V.K. Bel'sky, O.I. Bodak and V.K. Pecharsky, 1987a, Dopov. Akad. Nauk Ukr. RSR, Ser. B, 10, 45.

Pavlyuk, V.V., V.K. Pecharsky, O.I. Bodak and V.A. Bruskov, 1987b, Sov. Phys.-Crystallogr. **32**(1), 38.

Pavlyuk, V.V., V.K. Pecharsky and O.I. Bodak, 1988a, Sov. Phys.-Crystallogr. **33**(1), 22.

Pavlyuk, V.V., V.K. Pecharsky, O.I. Bodak and V.A. Bruskov, 1988b, Sov. Phys.-Crystallogr. **33**(1), 24.

Pavlyuk, V.V., V.K. Pecharsky and O.I. Bodak, 1989a, Dopov. Akad. Nauk URSR, B **2**, 51.

Pavlyuk, V.V., V.K. Pecharsky, O.I. Bodak and A.N. Sobolev, 1989b, Izv. Akad. Nauk SSSR, Met. **5**, 221.

Pavlyuk, V.V., O.I. Bodak and V.E. Zavodnik, 1990, Dopov. Akad. Nauk URSR, B **12**, 29.

Pavlyuk, V.V., O.I. Bodak and V.A. Bruskov, 1991a, Dopov. Akad. Nauk URSR, B **1**, 112.

Pavlyuk, V.V., O.I. Bodak and O.I. Sobolev, 1991b, Kristallografiya **36**(4), 880.

Pecharsky, V.K., and K.A. Gschneidner Jr, 1997, J. Alloys & Compounds **260**, 98.

Pecharsky, V.K., O.I. Bodak, V.K. Belsky, P.K. Starodub, I.R. Mokraya and E.I. Gladyshevsky, 1987, Kristallografiya **32**, 334.

Pecharsky, V.K., O.Ya. Mruz, M.B. Konyk, P.S. Salamakha, P.K. Starodub, M.F. Fedyna and O.I. Bodak, 1989, Zh. Strukt. Khim. **30**(5), 96.

Pecharsky, V.K., K.A. Gschneidner Jr, O.I. Bodak and A.S. Protsyk, 1991, J. Less-Common Met. **168**, 257.

Pecharsky, V.K., O.-B. Hyun and K.A. Gschneidner Jr, 1993, Phys. Rev. B **47**(18), 11839.

Pöttgen, R., 1995, J. Mater. Chem. **5**(3) 505.

Pöttgen, R., 1996, Z. Kristallogr. **210**, 925.

Pöttgen, R., H. Borrmann, C. Felser, O. Jepsen, R. Henn, R.K. Kremer and A. Simon, 1996a, J. Alloys & Compounds **235**, 170.

Pöttgen, R., R.K. Kremer, W. Schnelle, R. Mullmann and B.D. Mosel, 1996b, J. Mater. Chem. **6**(4), 635.

Protsyk, A.S., 1994, Ternary systems RE–Ag–(Si, Ge) (equilibrium phase diagram of the systems, crystal structures and some physical properties of compounds), Ph.D. Chemistry Thesis (L'viv State University, L'viv) pp. 1–17.

Raman, A., and H. Steinfink, 1967, Inorg. Chem. **6**, 1789.

Rieger, W., 1970, Monatsh. Chem. **101**, 449.

Rieger, W., and E. Parthé, 1969a, Monatsh. Chem. **100**, 439.

Rieger, W., and E. Parthé, 1969b, Monatsh. Chem. **100**, 444.

Rogl, P., B. Chevalier, M.J. Besnus and J. Etourneau, 1989, J. Magn. Magn. Mater. **80**, 305.

Rossi, D., and R. Ferro, 1996, J. Alloys & Compounds **236**, 212.

Rossi, D., R. Marazza and R. Ferro, 1978a, J. Less-Common Met. **58**(2), 203.

Rossi, D., R. Marazza, D. Mazzone and R. Ferro, 1978b, J. Less-Common Met. **59**, 79.

Rossi, D., R. Marazza and R. Ferro, 1979, J. Less-Common Met. **66**, 15.

Rossi, D., R. Marazza and R. Ferro, 1992, J. Alloys & Compounds **187**, 267.

Ryabokon', T.I., 1974, Vestn. Lvovs. Univ., Ser. Khim. **15**, 26.

Salamakha, P.S., 1986, Visn. L'viv Univers., Ser. Khim. **27**, 27.

Salamakha, P.S., 1988, Visn. L'viv State Univers., Ser. Khim. **29**, 62.

Salamakha, P.S., 1989, Phase equilibria and crystal structure of the compounds in the Nd–transition metal–germanium systems, Ph.D. Chemistry Thesis (Lv'iv State University, Lv'iv) pp. 1–17.

Salamakha, P.S., 1997, J. Alloys & Compounds **255**, 209.

Salamakha, P.S., and O.L. Sologub, 1997, unpublished data.

Salamakha, P.S., and O.L. Sologub, 1998, unpublished data.

Salamakha, P.S., and O.L. Sologub, 1999, unpublished data.

Salamakha, P.S., and P.K. Starodub, 1991, Visn. L'viv State Univers., Ser. Khim. **31**, 25.

Salamakha, P.S., V.K. Pecharsky, V.A. Bruskov and O.I. Bodak, 1986, Kristallografiya **31**, 587.

Salamakha, P.S., O.I. Bodak, V.K. Pecharsky and V.K. Belsky, 1989a, Izv. Akad. Nauk SSSR, Met. **1**, 206.

Salamakha, P.S., O.I. Bodak, V.K. Pecharsky and V.A. Bruskov, 1989b, Kristallografiya **34**, 122.

Salamakha, P.S., Yu.M. Prots', O.L. Sologub and O.I. Bodak, 1994, J. Alloys & Compounds **215**, 1994, 51.

Salamakha, P.S., M.B. Konyk, R. Dzynyi, O.L. Sologub and O.I. Bodak, 1996a, Pol. J. Chem. **70**, 270.

Salamakha, P.S., M.B. Konyk, O.L. Sologub and O.I. Bodak, 1996b, J. Alloys & Compounds **234**, 151.

Salamakha, P.S., M.B. Konyk, O.L. Sologub and O.I. Bodak, 1996c, J. Alloys & Compounds **236**, 206.

Salamakha, P.S., O.V. Zaplatynsky, O.L. Sologub and O.I. Bodak, 1996d, Pol. J. Chem. **70**, 158.

Salamakha, P.S., O.L. Sologub, O.I. Bodak and J. Stępień-Damm, 1996e, Pol. J. Chem. **70**, 708.

Salamakha, P.S., O.V. Zaplatynsky, O.L. Sologub and O.I. Bodak, 1996f, J. Alloys & Compounds **239**, 94.

Salamakha, P.S., O.L. Sologub, J. Stępień-Damm and A. Stash, 1996g, Kristallografiya **41**(6), 1135.

Savysyuk, I.A., and E.I. Gladyshevsky, 1995, Phase equilibria and crystal structure of compounds in Pr–Ag–Ge ternary system, in: Sixth Int. Conf. on Crystal Chemistry of Intermetallic Compounds, L'viv, 1995, Abstracts, p. 50.

Schuster, H.-U., and A. Czybulka, 1974, Z. Naturforsch. **29b**, 697.

Segre, C.U., H.F. Braun and K. Yvon, 1981a, Properties of $Y_3Ru_4Ge_{13}$ and isotypic compounds, in: Ternary Superconductors, Proc. Int. Conference, Lake Geneva, 1980, p. 243.

Segre, C.U., H.F. Braun, K. Yvon, C.K. Dunlap and E.Y. Fradin, 1981b, in: Ternary Superconductors (Elsevier North-Holland, New York) p. 239.

Seropegin, Yu.D., O.L. Borisenko, O.I. Bodak, V.N. Nikiforov, M.V. Kovachikova and Yu.V. Kochetkov, 1994, J. Alloys & Compounds **216**, 259.

Shapiev, B.I., 1993, Interaction of elements and properties of the compounds on their base in the system Ce–(Ru,Rh)–(Ge,Si), Ph.D. Thesis (Moscow State University, Moscow) p. 17.

Shapiev, B.I., O.L. Sologub, Yu.D. Seropegin, O.I. Bodak and P.S. Salamakha, 1991, J. Less-Common Met. **175**, L1.

Shpyrka, Z.M., 1988, Vesn. Lvov. Univers., Ser. Khim. **29**, 53.

Shpyrka, Z.M., 1990, Phase equilibria, Crystal structure and physical properties of compounds in the ternary Sc–(Y, Ce, Nd, Dy)–Ge and Ce–(Y, La, Gd, Lu)–Ge systems, Ph.D. Chemistry Thesis (L'viv State University, L'viv) pp. 1–17.

Shpyrka, Z.M., and I.R. Mokra, 1991, Visn. L'viv. Univers., Ser. Khim. **31**, 36.

Shpyrka, Z.M., O.M. Kokhan, O.I. Bodak and V.K. Pecharsky, 1986, Dokl. Akad. Nauk URSR, B **5**, 47.

Shpyrka, Z.M., V.A. Bruskov, I.R. Mokra, V.K. Pecharsky and O.I. Bodak, 1990, Izv. Akad. Nauk SSSR, Neorg. Mater. **26**(5), 969.

Sologub, O.L., 1995, Interaction of holmium and germanium with platinum metals, silver and gold (phase diagrams and crystal structure of ternary

compounds), Ph.D. Chemistry Thesis (Lv'iv State University, Lv'iv) pp. 1–22.

Sologub, O.L., and A.S. Protsyk, 1991, Visn. L'viv State Univers. **31**, 31.

Sologub, O.L., Yu.M. Prots', P.S. Salamakha, V.K. Pecharsky and O.I. Bodak, 1993, J. Alloys & Compounds **202**, 13.

Sologub, O.L., Yu.M. Prots', P.S. Salamakha and O.I. Bodak, 1994a, J. Alloys & Compounds **209**, 107.

Sologub, O.L., Yu.M. Prots', P.S. Salamakha, V.K. Pecharsky and O.I. Bodak, 1994b, J. Alloys & Compounds **216**, 231.

Sologub, O.L., K. Hiebl, P. Rogl and O.I. Bodak, 1995a, J. Alloys & Compounds **227**, 37.

Sologub, O.L., Yu.M. Prots', P.S. Salamakha, O.I. Bodak and J. Stępień-Damm, 1995b, Pol. J. Chem. **69**, 423.

Starodub, P.K., 1988, Phase equilibria, crystal structures and some physical properties of the ternary compounds in the systems Tb–Fe, Co, Ni, Cu–Ge, Ph.D. Chemistry Thesis (Lv'iv State University, Lvov) pp. 1–17.

Starodub, P.K., and O.Ya. Mruz, 1983, The new representatives of YCo_6Ge_6 structure type, in: Chetvertaya Vsesoyuzn. Konf. Kristallokhim. Intermetal Soed., Tezisy Dokl., Lv'iv, 1983 (Vyscha Shkola, Lvov) p. 91.

Starodub, P.K., I.R. Mokraya, O.I. Bodak, V.K. Pecharsky and V.A. Bruskov, 1986, Kristallografiya **31**, 394.

Starodub, P.K., L.M. Zapotots'ka and O.I. Bodak, 1996, Visn. L'viv Univers., Ser. Khim. **36**, 57.

Stetskiv, L.V., Z.M. Shpyrka and E.I. Gladyshevsky, 1995, Phase equilibria in La–Gd–Ge ternary system in the region 0.40–1.00 at. part of Ge at 870 K, in: Sixth Int. Conf. on Crystal Chemistry of Intermetallic Compounds, September 26–29, 1995, L'viv (Abstracts) p. 56.

Szytuła, A., J. Luciyevich and H. Bingzychka, 1980, Phys. Status Solidi A **58**, 67.

Thirion, F., J. Steinmetz and B. Malaman, 1983, Mater. Res. Bull. **23**(11), 1629.

Venturini, G., and B. Malaman, 1990, J. Less-Common Met. **167**, 45.

Venturini, G., and B. Malaman, 1996, J. Alloys & Compounds **235**, 201.

Venturini, G., and B. Malaman, 1997, J. Alloys & Compounds **261**, 19.

Venturini, G., M. Méot-Meyer, E. McRae, J.M. Mareche and B. Roques, 1984, Mater. Res. Bull. **19**, 1647.

Venturini, G., M. Méot-Meyer and B. Roques, 1985a, J. Less-Common Met. **107**, L5.

Venturini, G., M. Méot-Meyer, B. Malaman and B. Roques, 1985b, J. Less-Common Met. **113**, 197.

Venturini, G., M. Kamta, E. McRae, J.M. Mareche, B. Malaman and B. Roques, 1986a, Mater. Res. Bull. **21**, 1203.

Venturini, G., M. Méot-Meyer, J.F. Mareche, B. Malaman and B. Roques, 1986b, Mater. Res. Bull. **21**, 33.

Venturini, G., B. Malaman and B. Roques, 1989a, J. Less-Common Met. **146**, 271.

Venturini, G., B. Malaman and B. Roques, 1989b, J. Less-Common Met. **152**, 51.

Venturini, G., R. Welter and B. Malaman, 1992, J. Alloys & Compounds **185**, 99.

Verniere, A., P. Lejay, P. Bordet, J. Chenavas, J.L. Tholence, J.X. Boucherle and N. Keller, 1995, J. Alloys & Compounds **218**, 197.

Weitzer, F., H. Klesnar and P. Rogl, 1990, Phase equilibria and structural chemistry related to Al, Ga, In, Tl-substituted rare earth-base permanent magnet materials, in: Proc. Int. Conf. on Light Metals, Amsterdam, 1990, Abstracts, p. 577.

Welter, R., G. Venturini, B. Malaman and E. Ressouche, 1993a, J. Alloys & Compounds **201**, 191.

Welter, R., G. Venturini, B. Malaman and E. Ressouche, 1993b, J. Alloys & Compounds **202**, 165.

Welter, R., G. Venturini, E. Ressouche and B. Malaman, 1995, J. Alloys & Compounds **228**, 59.

Yanson, T.I., 1975, Crystal structures of the alumosilicides and alumogermanides of the rare earth elements, Ph.D. Chemistry Thesis (Lvov State University, Lvov) pp. 2-18.

Zanicchi, G., D. Mazzone, V. Contardi, R. Marazza, G. Rambaldi and D. Rossi, 1983, Gazz. Chim. Ital. **113**, 257.

Zaplatynsky, O.V., P.S. Salamakha, O.L. Sologub, A.S. Protsyk and O.I. Bodak, 1996, Pol. J. Chem. **70**, 267.

Zarechnyuk, O.S., A.A. Muravyeva and E.I. Gladyshevsky, 1970, Dopov. Akad. Nauk URSR, A, p. 753.

Zarechnyuk, O.S., T.I. Yanson and A.A. Muravyeva, 1981, Vestn. Lvovsk. Univ., Ser. Khim. **23**, 64.

Zaremba, V.I., J. Stępień-Damm, G.P. Nychyporuk, Yu.B. Tyvanchuk and Ya.M. Kalychak, 1997, Kristallografiya **42**(2), 354.

Zhao, J.T., and E. Parthé, 1990, Acta Crystallogr. C **46**, 2276.

Zhao, J.T., and E. Parthé, 1991a, Acta Crystallogr. C **47**, 1.

Zhao, J.T., and E. Parthé, 1991b, Acta Crystallogr. C **47**, 4.

Zhao, J.T., and E. Parthé, 1991c, Acta Crystallogr. C **47**, 1781.

Zhao, J.T., K. Cenzual and E. Parthé, 1991, Acta Crystallogr. C **47**, 1777.

Zmii, O.F., E.I. Gladyshevsky and V.S. Bulyo, 1973, Kristallografiya **18**(2), 277.

Handbook on the Physics and Chemistry of Rare Earths
Vol. 27
edited by K.A. Gschneidner, Jr. and L. Eyring

Chapter 174

CRYSTAL STRUCTURES AND CRYSTAL CHEMISTRY OF TERNARY RARE-EARTH GERMANIDES

Petro S. SALAMAKHA
Departamento de Química, Instituto Tecnológico e Nuclear, P-2686-953 Sacavém, Portugal

Contents

Symbols and abbreviations

a, *b*, *c*	Unit cell dimensions (in nm)	R, R′	Y, Sc, and the lanthanides
α, β, γ	Unit cell angles (in degrees)	*x*	indicate variable component contents, when it is used as index in compound compositional formula. Expressions like $N-x$ (where N is a number) mean N minus x, with the x value given in the text
x/a, *y/b*, *z/c*	Atomic coordinates		
SG	Space group		
Z	Number of formula units in a unit cell		
G (%)	Occupation of crystallographic position		
at.%	Composition in atomic percent		
M, M′	s-, p-, d-element		

1. Introduction

The ternary systems of rare-earth metals with metallic and semimetallic components have been studied intensively during the last 20 years. Among them, the systems containing germanium are most completely investigated.

The preceding chapter (173) of this volume (Salamakha et al. 1999) is a review of ternary R–M–Ge systems which have been studied over the entire concentration region and which have been only partly investigated. The character of interaction in these systems varies, and major differences are seen in the number of ternary germanides observed within the investigated concentration range. This chapter is devoted to the description of the structure types and the crystal chemistry of the ternary (quaternary) germanides of the rare-earth metals.

The known structures of the germanides belong to 135 structure types. For each structure type the following information is presented:

(i) chemical formula of the prototype;
(ii) space group symbol and the number of formula units in the unit cell;
(iii) lattice parameters (in nm) for the germanide (prototype or isotypic compound) on which the structure determination has been made and the appropriate reference;
(iv) atomic positions and refined atomic coordinates; for compounds where statistical occupations of structure sites are observed, the various atoms are expressed as X, X1 etc. and additional data are presented;
(v) projection of the structure and coordination polyhedra of the atoms;
(vi) list of isotypic germanides; the unit cell dimensions and references for the isostructural compounds are presented in the preceding chapter (173) of this volume (Salamakha et al. 1999).

2. Influence of a third component on the fields of formation of ternary germanides

As R and Ge are components with much different crystallochemical properties (atomic size, electronic structure, electronegativity, etc.), the deciding factor that affects the formation, composition and structure, is the nature of the third component in the systems.

The ternary systems with two rare-earth metals and germanium are characterized by the formation of compounds with compositions $(R,R')_5Ge_4$, $(R,R')_{11}Ge_{10}$, $(R,R')Ge$ and $(R,R')_2Ge$ which crystallize with the structure types of binary compounds and their superstructures. This is caused by the similarities in the electronic structure of R elements.

When the third component is a p element (Al, Ga, In, Si, Sn, Sb, Bi), the trends in formation of compounds are found to be maintained in the same R to Ge ratio as in the binary compounds. The compounds are characterized by a variable composition at constant R content, but in contrast to the R–R′–Ge systems, the compositions of compounds are more varied (fig. 1).

The main reason for the formation of a large number of ternary compounds in the R–M–Ge systems (M = s or d element) is the presence of components with significantly different crystallochemical properties (fig. 2).

Figures 1 and 2 presents only the compositions of compounds in which the crystal structure has been determined. In many cases, the substitution of a M component or a change in temperature leads to the formation of another structure (these compositions are marked with a square). In spite of the variety of compositions, one can see from fig. 2 that the predominant number of compounds are arranged on the lines connecting the elements with the binary phases of simple compositions (R–MGe, R–MGe_2 etc.).

The most favourable concentration for the formation of intermetallic compounds is 33 at.% of R (RM_2–RGe_2), particularly the composition RMGe. The compounds of equatomic composition crystallize in 20 structure types. The morphotropic transformation within the RMGe series occurs both if R is replaced by another R′, and when the M component is changed.

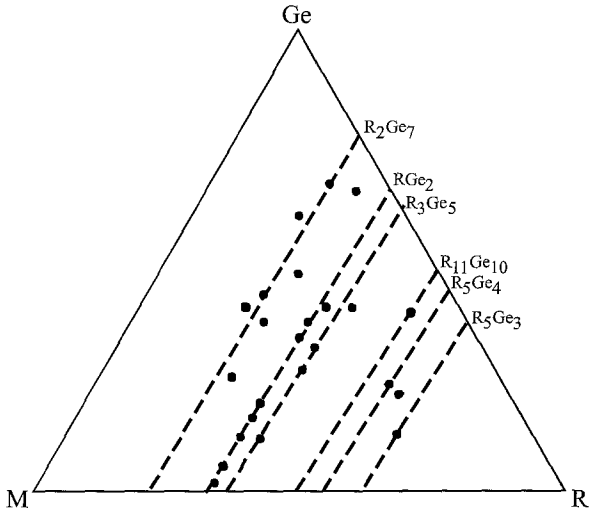

Fig. 1. Composition triangle showing the existence of ternary compounds in the R–M–Ge systems when M is p-element.

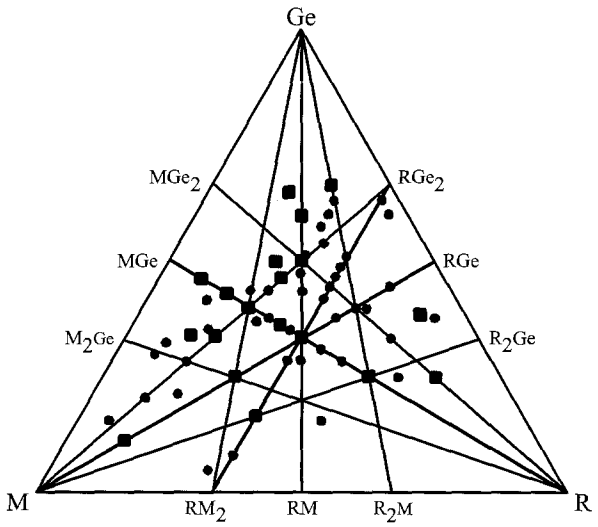

Fig. 2. Composition triangle showing the existence of ternary compounds in the R–M–Ge systems when M is s- and d-element.

For a better demonstration of the influence of the R component on the formation of ternary germanides and their crystal chemistry, and for the improvement and simplification of the presentation of the crystallographic data of the compounds, we have characterised the composition of a given phase according to its R/(M, Ge) ratio, and arranged the structure types according to increasing rare-earth content in the next section of this chapter.

The same approach is used for the description of the quaternary germanides (sect. 4 of the present review). However, the literature data on the crystal structures of quaternary germanides are quite sparse.

3. Structure types of ternary rare-earth germanides

3.1. *R(M,Ge)$_{13}$ compounds*

3.1.1. *NaZn$_{13}$ structure type*

SG Fm3c, $Z=8$, $a=1.1371$ for La(Ni$_{0.82}$Ge$_{0.18}$)$_{13}$ (Bruskov 1984)

Atom	Wyckoff notation	*x/a*	*y/b*	*z/c*	G (%)
La	8(a)	1/4	1/4	1/4	100
X1	8(b)	0	0	0	100
X2	96(i)	0	0.1782	0.1151	100

X = 0.82Ni+0.18Ge

No isotypic compounds are known.

3.1.2. *CeNi$_{8.5}$Si$_{4.5}$ structure type*

SG I4/mcm, $Z=4$, $a=0.7932$, $c=1.1817$ for Pr$_{1-x}$Co$_9$Ge$_4$ (Fedyna et al. 1987)

Atom	Wyckoff notation	*x/a*	*y/b*	*z/c*	G (%)
Pr	4(a)	0	0	1/4	69.3
Co1	16(l)	0.1815	0.6815	0.1284	100
Co2	16(l)	0.6273	0.1273	0.1668	100
Co3	4(d)	0	1/2	0	100
Ge	16(k)	0.0633	0.2002	0	100

Isotypic compounds:

RNi$_{8.5}$Ge$^*_{4.5}$: R = Ce, Pr, Nd, Sm, Eu

* In the RNi$_{8.5}$Ge$_{4.5}$ compounds the site in Wyckoff position 4(d) is occupied by a statistical mixture Ni$_{0.5}$Ge$_{0.5}$.

The praseodymium atoms have coordination number 24 (fig. 3a). Coordination polyhedra for cobalt and germanium are the icosahedra and their derivatives (fig. 3b–e).

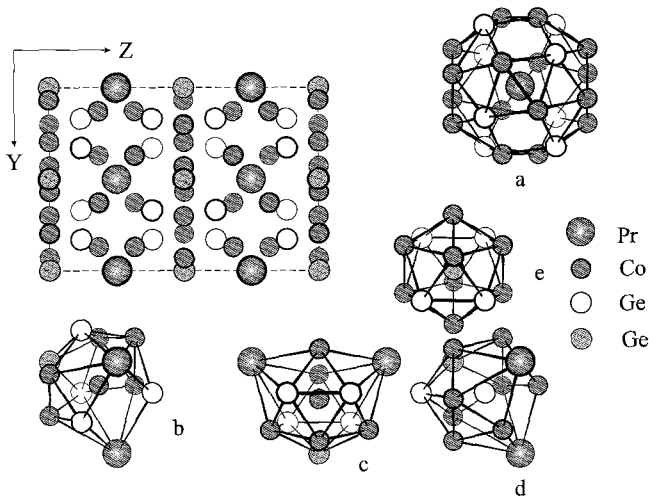

Fig. 3. Projection of the $Pr_{1-x}Co_9Ge_4$ unit cell and coordination polyhedra of the atoms: (a) Pr, (b–e) Co, Ge.

3.2. *R(M, Ge)$_{12}$ compounds*

3.2.1. *YCo_6Ge_6 structure type*

SG P6/mmm, $Z=1$, $a=0.5074$, $c=0.3908$ for YCo_6Ge_6 (Buchholz and Schuster 1981)

Atom	Wyckoff notation	*x/a*	*y/b*	*z/c*	G (%)
Y	1(a)	0	0	0	45
Co	3(g)	1/2	0	1/2	100
Ge1	2(e)	0	0	0.307	50
Ge2	2(c)	1/3	2/3	0	100

Isotypic compounds:
RMn_6Ge_6: R = Nd, Sm
RFe_6Ge_6: R = Y, Pr–Sm, Gd–Lu
RCo_6Ge_6: R = Y, Sc, Gd–Lu

For yttrium atoms, polyhedra with 20 apexes are typical (fig. 4a). Those for cobalt and germanium atoms are the icosahedra and their derivatives (fig. 4b–d).

3.2.2. *$MgFe_6Ge_6$ (or $HfFe_6Ge_6$) structure type*

SG P6/mmm, $Z=1$, $a=0.52262$, $c=0.81653$ for $DyMn_6Ge_6$ (Schöbinger-Papamantellos et al. 1994)

Atom	Wyckoff notation	*x/a*	*y/b*	*z/c*	G (%)
Dy	1(a)	0	0	0	100

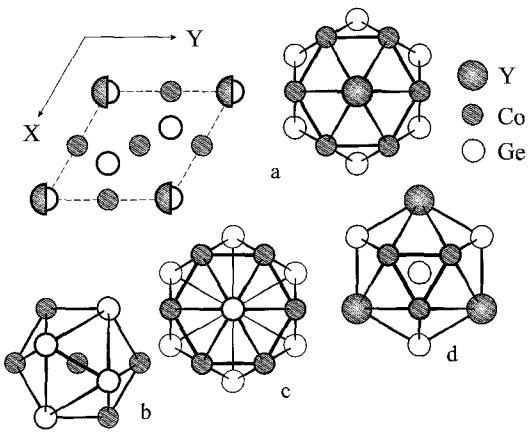

Fig. 4. Projection of the YCo_6Ge_6 unit cell and coordination polyhedra of the atoms: (a) Y, (b–d) Co and Ge.

Mn	6(i)	1/2	0	0.2504	100
Ge1	2(e)	0	0	0.3453	100
Ge2	2(d)	1/3	2/3	1/2	100
Ge3	2(c)	1/3	2/3	0	100

Isotypic compounds:
RCr_6Ge_6: R = Sc, Y, Tb–Er
RMn_6Ge_6: R = Sc, Y, Gd–Lu
RFe_6Ge_6: R = Sc, Yb, Lu

The coordination polyhedra for dysprosium atoms have 20 apexes (fig. 5a). For manganese and germanium atoms, icosahedra and their derivatives are typical (fig. 5b–e).

3.2.3. *$GdMn_6Ge_6$ structure type*

SG P6/mmm, $Z = 1$, $a = 0.52333$, $c = 0.81806$ (Belyavina et al. 1993)

Atom	Wyckoff notation	*x/a*	*y/b*	*z/c*	G (%)
Gd1	1(a)	0	0	0	70
Gd2	1(b)	0	0	1/2	30
Mn	6(i)	1/2	0	0.25	100
Ge1	2(e)	0	0	0.3465	100
Ge2	2(d)	1/3	2/3	1/2	100
Ge3	2(c)	1/3	2/3	0	100

No isotypic compounds are observed.

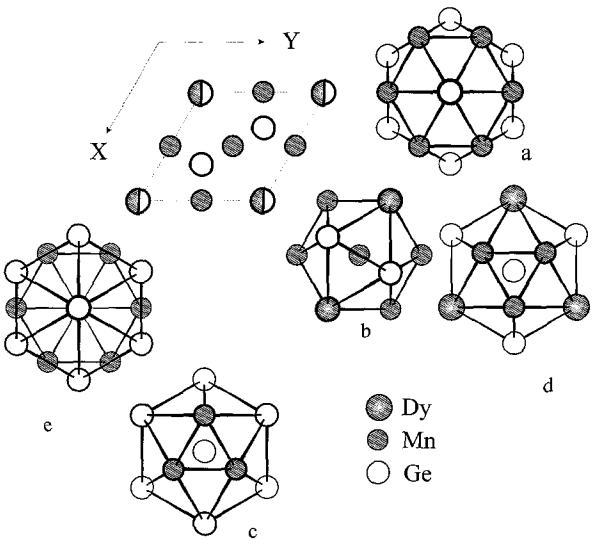

Fig. 5. Projection of the $DyMn_6Ge_6$ unit cell and coordination polyhedra of the atoms: (a) Dy, (b–e) Mn and Ge.

3.2.4. *$ScNi_6Ge_6$ structure type*

SG P6/mmm, $Z=4$, $a=1.0152$, $c=0.7813$ for $ScNi_6Ge_6$ (Buchholz and Schuster 1981)

Atom	Wyckoff notation	*x/a*	*y/b*	*z/c*	G (%)
Sc1	3(g)	1/2	0	1/2	100
Sc2	1(a)	0	0	0	100
Ni1	12(o)	0.247	0.494	0.250	100
Ni2	12(n)	0.238	0	0.258	100
Ge1	6(m)	0.162	0.324	1/2	100
Ge2	6(l)	0.160	0.320	0	100
Ge3	6(i)	1/2	0	0.158	100
Ge4	2(e)	0	0	0.340	100
Ge5	2(d)	1/3	2/3	1/2	100
Ge6	2(c)	1/3	2/3	0	100

No isotypic compounds are observed.

3.2.5. *$GdFe_6Ge_6$ structure type*

SG Pnma, $a=6.143$, $b=0.8137$, $c=7.979$ (Venturini et al. 1992)

Atomic coordinates have not been determined.

3.2.6. *$TbFe_6Sn_6$ structure type*

SG Cmcm, $Z=4$, $a=0.8116$, $b=1.7672$, $c=0.5120$ for YFe_6Ge_6 (Venturini et al. 1992)

Atomic coordinates for the germanides of this structure type have not been determined.

Isotypic compounds:

RFe_6Ge_6: R = Tb–Ho

3.2.7. *$HoFe_6Sn_6$ structure type*

SG Immm, $Z=6$, $a=0.8103$, $b=2.652$, $c=0.5108$ for $ErFe_6Ge_6$ (Venturini et al. 1992)

Atomic coordinates for the germanides of this structure type have not been determined.

Isotypic compound: RFe_6Ge_6: R = Tm

3.3. *$R_3(M, Ge)_{34}$ and $R_3(M, Ge)_{26}$ compounds*

3.3.1. *$Ce_3Pt_{23}Ge_{11}$ structure type*

SG $F\bar{4}3m$, $Z=8$, $a=1.71833$ for $Ce_3Pt_{23}Ge_{11}$ (Gribanov et al. 1993a). See fig. 6.

Atom	Wyckoff notation	x/a	y/b	z/c	G (%)
Ce	24(g)	0.0018	1/4	1/4	100
Pt1	48(h)	0.0841	0.0841	0.2479	100
Pt2	24(f)	0.1281	0	0	100
Pt3	16(e)	0.1927	0.1927	0.1927	100
Pt4	16(e)	0.4139	0.4139	0.4139	100
Pt5	16(e)	0.5787	0.5787	0.5787	100
Pt6	16(e)	0.8098	0.8098	0.8098	100
Ge1	24(f)	0.3285	0	0	100
Ge2	16(e)	0.1075	0.1075	0.1075	100
Ge3	16(e)	0.3357	0.3357	0.3357	100
Ge4	16(e)	0.6672	0.6672	0.6672	100
Xa	48(h)	0.0847	0.0847	0.7541	100
Xb	16(e)	0.8962	0.8962	0.8962	100

Xa = 0.78Pt+0.22Ge, Xb = 0.20Pt+0.80Ge

No isotypic compounds are observed.

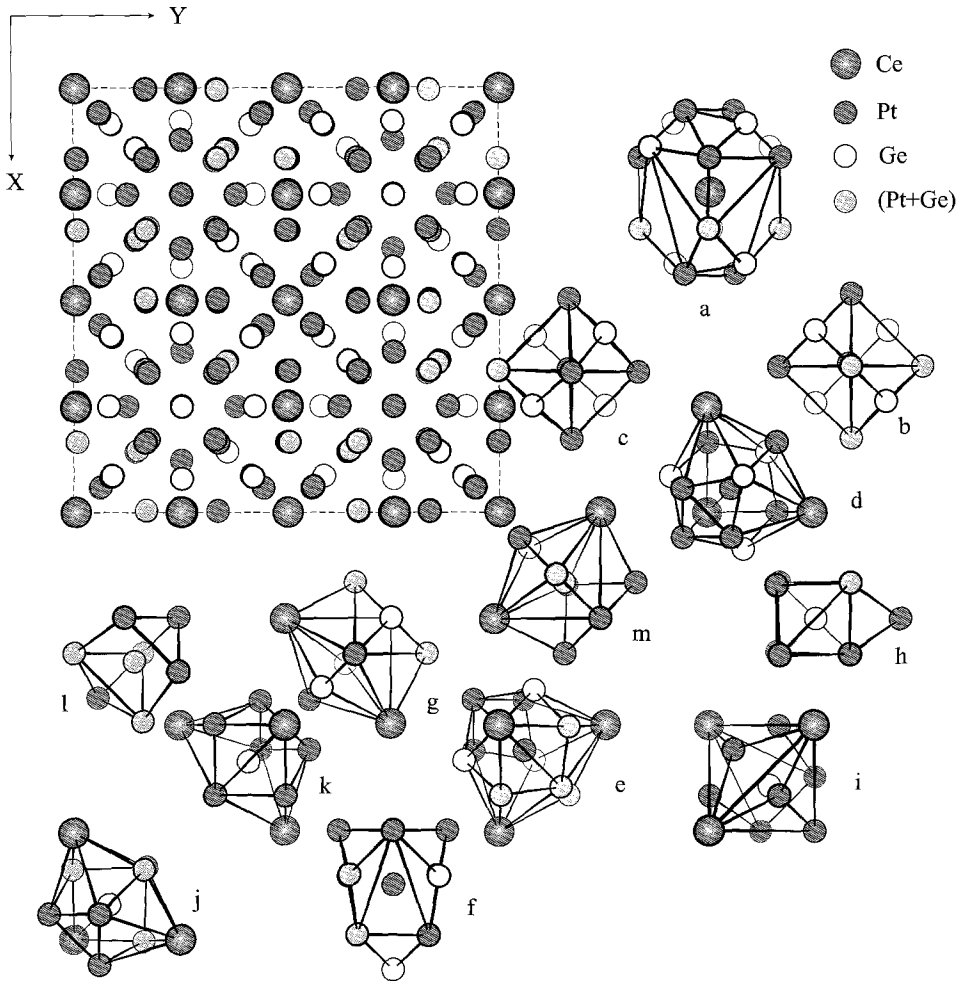

Fig. 6. Projection of the $Ce_3Pt_{23}Ge_{11}$ unit cell and coordination polyhedra of the atoms: (a) Ce, (b–g) Pt, (h–k) Ge, (l) Xa, (m) Xb.

3.3.2. *$Ce_3Pd_{20}Ge_6$ structure type*

SG Fm3m, $Z=4$, $a=1.24453$ for $Ce_3Pd_{20}Ge_6$ (Gribanov et al. 1994). See fig. 7.

Atom	Wyckoff notation	*x/a*	*y/b*	*z/c*	G (%)
Ce1	4(0)	0	0	0	100
Ce2	8(c)	1/4	1/4	1/4	100
Pd1	32(f)	0.38390	0.38390	0.38390	100

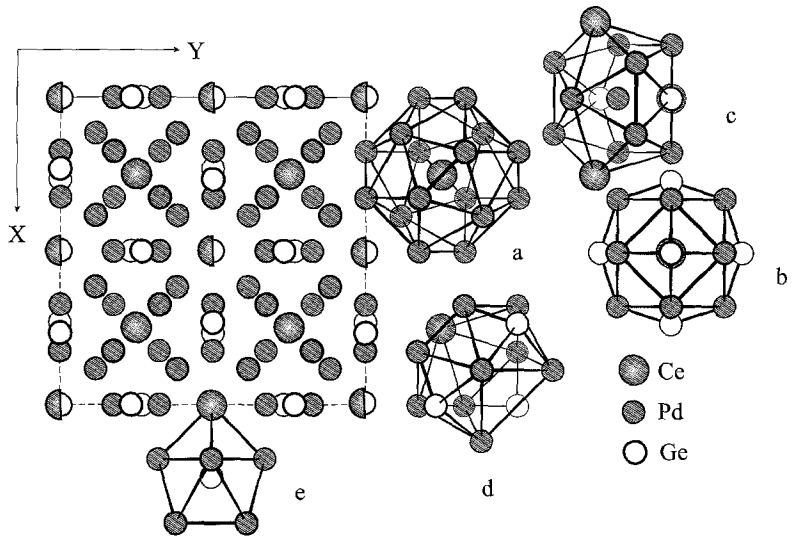

Fig. 7. Projection of the $Ce_3Pd_{20}Ge_6$ unit cell and coordination polyhedra of the atoms: (a, b) Ce, (c, d) Pd, (e) Ge.

Pd2	48(h)	0	0.17479	0.17479	100
Ge	24(e)	0.2325	0	0	100

Isotypic compounds:
$R_3Pd_{20}Ge_6$: R = Nd, Sm

3.4. *$R_2(M,Ge)_{17}$ compounds*

3.4.1. *Th_2Zn_{17} structure type*

SG $R\bar{3}m$, $Z = 3$, $a = 0.8425$–0.8433, $c = 1.2336$–1.2368 for $Sm_2Co_{15.1-14.1}Ge_{1.9-2.9}$ (Mruz 1988).

Atomic coordinates for this compound have not been determined.

3.4.2. *$Ce_2Al_2Co_{15}$ structure type*

SG $R\bar{3}m$, $Z = 3$, $a = 0.9021$, $c = 1.3787$ for $Ce_2Zn_{15}Ge_2$ (Opainych 1996)

Atomic coordinates for this compound have not been determined.

3.4.3. *$Nd_2Cr_9Ge_8$ structure type*

SG Pmma, $Z = 2$, $a = 0.9388$, $b = 0.4046$, $c = 0.8045$ (Bodak et al. 1989a)

Atom	Wyckoff notation	*x/a*	*y/b*	*z/c*	G (%)
Nd	2(e)	1/4	0	0.6680	100

Cr1	4(i)	0.1064	0	0.2973	100
Cr2	2(f)	1/4	1/2	0.0516	50
Cr3	2(d)	0	1/2	1/2	100
Cr4	2(a)	0	0	0	100
Ge1	4(k)	1/4	0.1587	0.0419	50
Ge2	4(j)	0.5387	1/2	0.1787	100
Ge3	2(f)	1/4	1/2	0.3780	100

No isotypic compounds are observed.

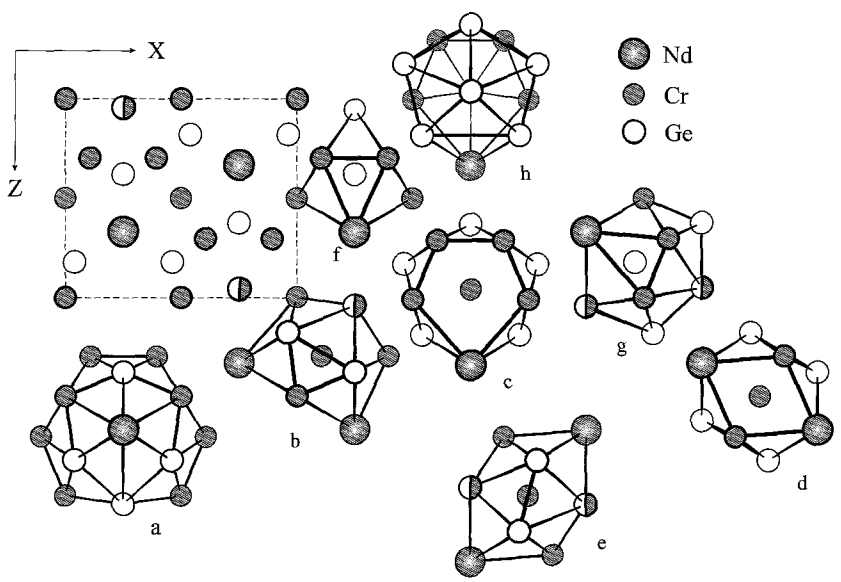

Fig. 8. Projection of the $Nd_2Cr_9Ge_8$ unit cell and coordination polyhedra of the atoms: (a) Nd, (b–e) Cr, (f–h) Ge.

For neodymium atoms, polyhedra with 18 apexes are typical (fig. 8a). The chromium atom polyhedra are distorted cubo-octahedra and pentagonal prisms with additional atoms (fig. 8b–e). Those for germanium atoms are polyhedra with 11 apexes and pentagonal prisms with additional atoms (fig. 8f–h).

3.5. *R(M, Ge)$_8$ compounds*

3.5.1. *YNi$_5$Si$_3$ structure type*

SG Pnma, $Z=4$, $a=1.90183$, $b=0.38398$, $c=0.67867$ for $TmNi_5Ge_3$ (Fedyna 1988)

Atom	Wyckoff notation	*x/a*	*y/b*	*z/c*	G (%)
Tm	4(c)	0.3542	1/4	0.878	100
Ni1	4(c)	0.0021	1/4	0.390	100
Ni2	4(c)	0.2070	1/4	0.067	100
Ni3	4(c)	0.2008	1/4	0.691	100
Ni4	4(c)	0.3854	1/4	0.365	100
Ni5	4(c)	0.4864	1/4	0.591	100
Ge1	4(c)	0.0765	1/4	0.645	100
Ge2	4(c)	0.0884	1/4	0.090	100
Ge3	4(c)	0.2598	1/4	0.380	100

Isotypic compounds:
RNi_5Ge_3: R = Y, Gd–Lu

The coordination polyhedra for thulium atoms have 20 apexes (fig. 9a). The nickel atoms are situated inside polyhedra with 12 and 15 apexes (fig. 9b–f). For germanium atoms, trigonal prisms with three additional atoms are typical (fig. 9g–i).

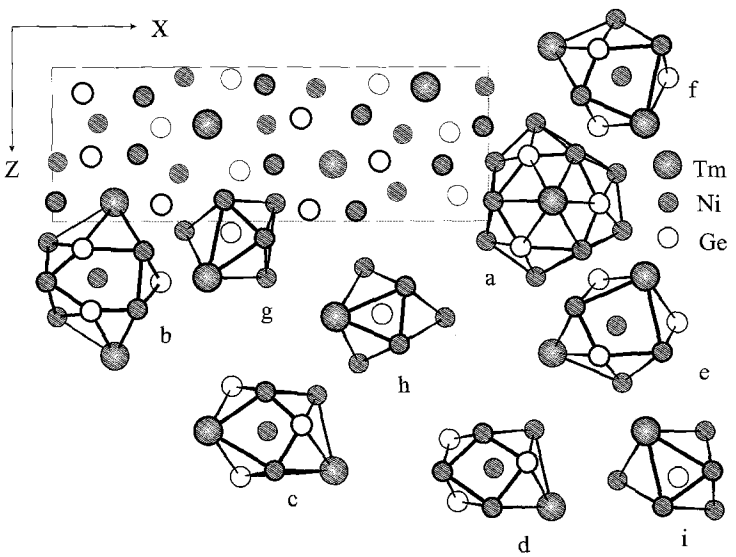

Fig. 9. Projection of the $TmNi_5Ge_3$ unit cell and coordination polyhedra of the atoms: (a) Tm, (b–f) Ni, (g–i) Ge.

3.5.2. *YCo_5P_3 structure type*

SG Pnma, $Z=4$, $a=1.3050$, $b=0.3904$, $c=1.1408$ for $TbMn_5Ge_3$ (Venturini and Malaman 1997)

Atom	Wyckoff notation	*x/a*	*y/b*	*z/c*	G (%)
Tb	4(c)	0.2068	1/4	0.9131	100
Mn1	4(c)	0.4807	1/4	0.7923	100
Mn2	4(c)	0.9986	1/4	0.0888	100
Mn3	4(c)	0.6852	1/4	0.2941	100
Mn4	4(c)	0.1879	1/4	0.6180	100
Mn5	4(c)	0.4366	1/4	0.0338	100
Ge1	4(c)	0.6211	1/4	0.0887	100
Ge2	4(c)	0.3766	1/4	0.2406	100
Ge3	4(c)	0.8796	1/4	0.9125	100

No isotypic compounds are observed.

3.6. *$R(M, Ge)_6$ compounds*

3.6.1. *$ZrFe_4Si_2$ structure type*

SG $P4_2/mnm$, $Z=2$, $a=0.72472$, $c=0.38705$ for $TmFe_4Ge_2$ (Fedyna 1988)

Atom	Wyckoff notation	*x/a*	*y/b*	*z/c*	G (%)
Tm	2(a)	0	0	0	100
Fe	8(i)	0.086	0.353	0	100
Ge	4(f)	0.215	0.215	1/2	100

Isotypic compounds:
RFe_4Ge_2: R = Y, Dy–Lu
RCo_4Ge_2: R = Er–Lu

Thulium atoms are situated inside the polyhedra with 20 apexes (fig. 10a). The coordination polyhedra of iron atoms are deformed cubo-octahedra (fig. 10b). The germanium atoms have an environment in a form of trigonal prism with three additional atoms (fig. 10c).

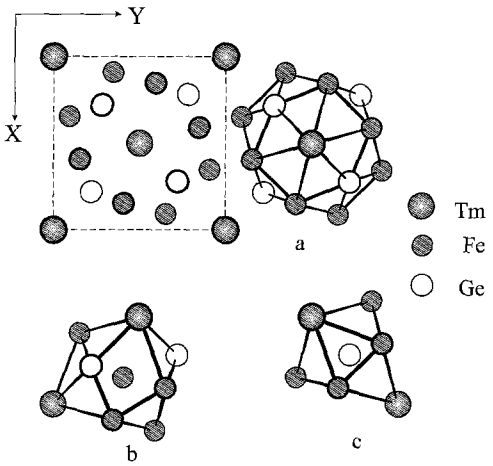

Fig. 10. Projection of the $TmFe_4Ge_2$ unit cell and coordination polyhedra of the atoms: (a) Tm, (b) Fe, (c) Ge.

3.6.2. *$SmNi_3Ge_3$ structure type*

SG I4/mmm, $Z=4$, $a=0.40659$, $c=2.5137$ (Mruz et al. 1990)

Atom	Wyckoff notation	*x/a*	*y/b*	*z/c*	G (%)
Sm	4(e)	0	0	0.3465	100
Ni1	8(g)	0	1/2	0.0553	100
Ni2	4(e)	0	0	0.1999	100
Ge1	4(e)	0	0	0.1063	100
Ge2	4(d)	0	1/2	1/4	100
Ge3	2(b)	0	0	1/2	100
Ge4	2(a)	0	0	0	100

No isotypic compounds are observed.

The coordination numbers for the Sm atoms are 22 (fig. 11a). The coordination polyhedra for the Ni atoms are tetragonal antiprisms with one additional atom and distorted cubo-octahedra with one additional apex (fig. 11b,c); those for Ge atoms are tetragonal antiprisms with two additional atoms and distorted cubo-octahedra with two additional apexes (fig. 11d–g).

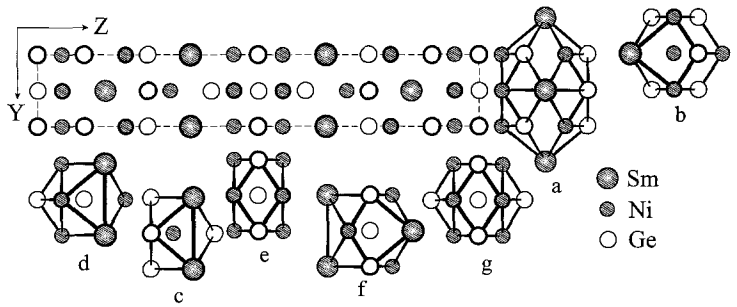

Fig. 11. Projection of the $SmNi_3Ge_3$ unit cell and coordination polyhedra of the atoms: (a) Sm, (b–c) Ni, (d–g) Ge.

3.6.3. *$EuMg_3Ge_3$ structure type*

SG Cmcm, $Z=4$, $a=0.4485$, $b=3.060$, $c=0.4485$ (Zmii et al. 1973)

Atom	Wyckoff notation	*x/a*	*y/b*	*z/c*	G (%)
Eu	4(c)	0	0.442	1/4	100
Mg1	4(c)	0	0.650	1/4	100
Mg2	4(c)	0	0.750	1/4	100
Mg3	4(c)	0	0.855	1/4	100
Ge1	4(c)	0	0.017	1/4	100
Ge2	4(c)	0	0.098	1/4	100
Ge3	4(c)	0	0.303	1/4	100

No isotypic compounds are observed.

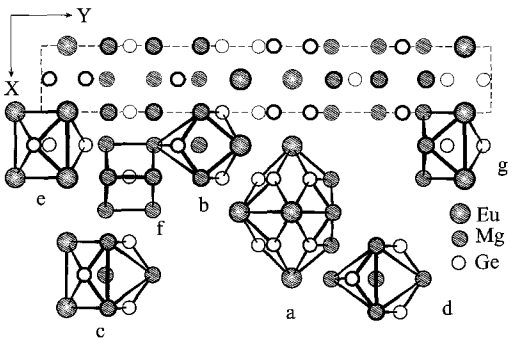

Fig. 12. Projection of the $EuMg_3Ge_3$ unit cell and coordination polyhedra of the atoms: (a) Eu, (b–d) Mg, (e–g) Ge.

The coordination polyhedra for europium atoms have 20 apexes (fig. 12a). Magnesium atoms are situated in the centre of the tetragonal prisms with additional atoms (fig. 12b, c)

and trigonal prisms with additional atoms (fig. 12d). Coordination polyhedra in the form of trigonal prism, tetragonal antiprism and cubo-octahedra are typical for the germanium atoms (fig. 12e–g).

3.7. *$R_3(M, Ge)_{17}$ compounds*

3.7.1. *$Yb_3Rh_4Sn_{13}$ structure type*

SG $Pm\bar{3}n$, $Z=2$, $a=0.8962$ for $Y_3Ru_4Ge_{13}$ (Segre et al. 1981). See fig. 13.

Atom	Wyckoff notation	*x/a*	*y/b*	*z/c*	G (%)
Y	6(c)	1/4	0	1/2	100
Ru	8(e)	1/4	1/4	1/4	100
Ge1	24(k)	0	0.15333	0.30570	100
Ge2	2(a)	0	0	0	100

Isotypic compounds:
$R_3Co_4Ge_{13}$: R = Y, Sm, Gd–Lu
$R_3Ru_4Ge_{13}$: R = Y, Ce–Sm, Gd–Lu
$R_3Rh_4Ge_{13}$: R = Y, Nd, Sm, Gd–Lu
$R_3Os_4Ge_{13}$: R = Y, Ce–Sm, Gd–Lu
$R_3Ir_4Ge_{13}$: R = Y, Ce–Sm, Gd–Lu

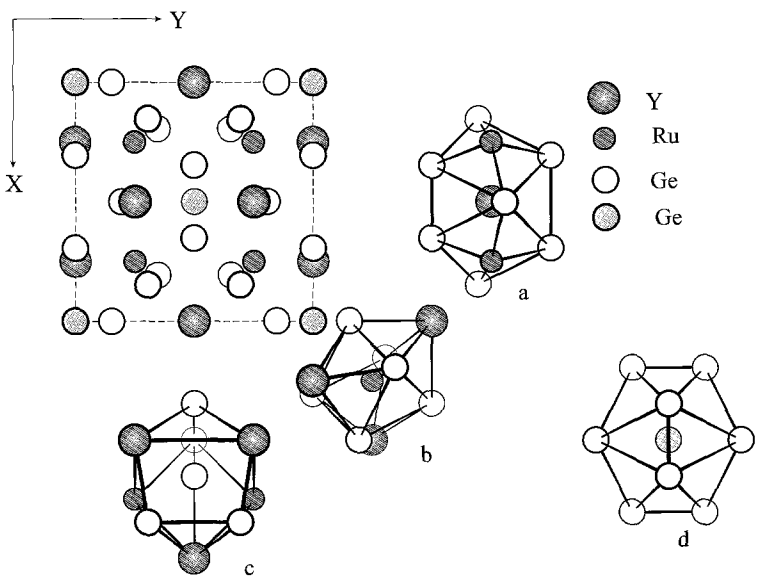

Fig. 13. Projection of the $Y_3Ru_4Ge_{13}$ unit cell and coordination polyhedra of the atoms: (a) Y, (b) Ru, (c, d) Ge.

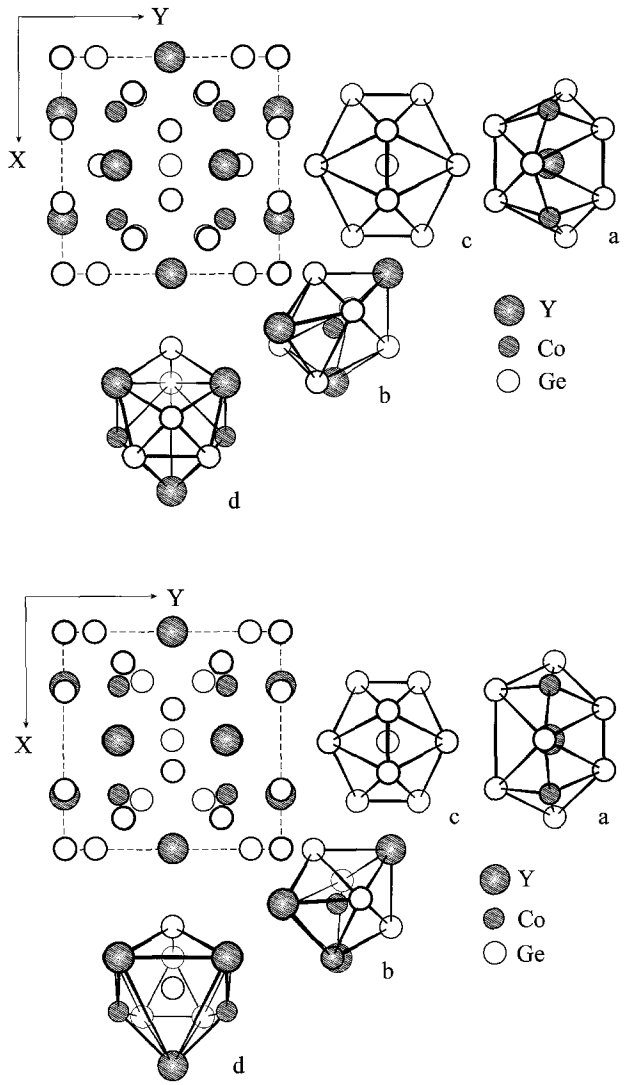

Fig. 14. Two types of unit cells in the $Y_3Co_4Ge_{13}$ structure and coordination polyhedra of the atoms.

3.7.2. *$Y_3Co_4Ge_{13}$ structure type*

SG $Pm\bar{3}n$, $Z=2$, $a=0.8769$ (Bruskov et al. 1986). See fig. 14.

Atom	Wyckoff notation	*x/a*	*y/b*	*z/c*	G (%)
Y	6(c)	1/4	0	1/2	100
Co	8(e)	1/4	1/4	1/4	100

Ge1	24(k)	0	0.142	0.273	42
Ge2	24(k)	0	0.161	0.327	58
Ge3	2(a)	0	0	0	100

This structure type differs from the $Yb_3Rh_4Sn_{13}$ type by the splitting of the site in Wyckoff position 24(k).
Isotypic compounds:
$R_3Co_4Ge_{13}$: R = Y, Gd–Lu
$R_3Ru_4Ge_{13}$: R = Ce, Nd
$R_3Os_4Ge_{13}$: R = Nd, Ho

3.8. *$R_2(M, Ge)_{11}$ compounds*

3.8.1. *$Ce_2Pt_7Ge_4$ structure type*

SG Pnma, $Z = 4$, $a = 1.9866$, $b = 0.4089$, $c = 1.1439$ (Gribanov et al. 1992a)

Atom	Wyckoff notation	*x/a*	*y/b*	*z/c*	G (%)
Ce1	4(c)	0.0281	1/4	0.7437	100
Ce2	4(c)	0.2199	1/4	0.5122	100
Pt1	4(c)	0.0351	1/4	0.0604	100
Pt2	4(c)	0.0412	1/4	0.4534	100
Pt3	4(c)	0.2139	1/4	0.1836	100
Pt4	4(c)	0.3465	1/4	0.2449	100
Pt5	4(c)	0.3664	1/4	0.8671	100
Pt6	4(c)	0.3707	1/4	0.6198	100
Pt7	4(c)	0.6610	1/4	0.5527	100
Ge1	4(c)	0.0942	1/4	0.2534	100
Ge2	4(c)	0.2440	1/4	0.7935	100
Ge3	4(c)	0.4123	1/4	0.0631	100
Ge4	4(c)	0.4144	1/4	0.4225	100

No isotypic compounds have been observed.

For cerium atoms, polyhedra with 22 and 21 apexes are typical (fig. 15a,b). The platinum atom polyhedra are distorted cubo-octahedra (fig. 15c–i). Trigonal prisms with additional atoms are typical for germanium atoms (fig. 15j–m).

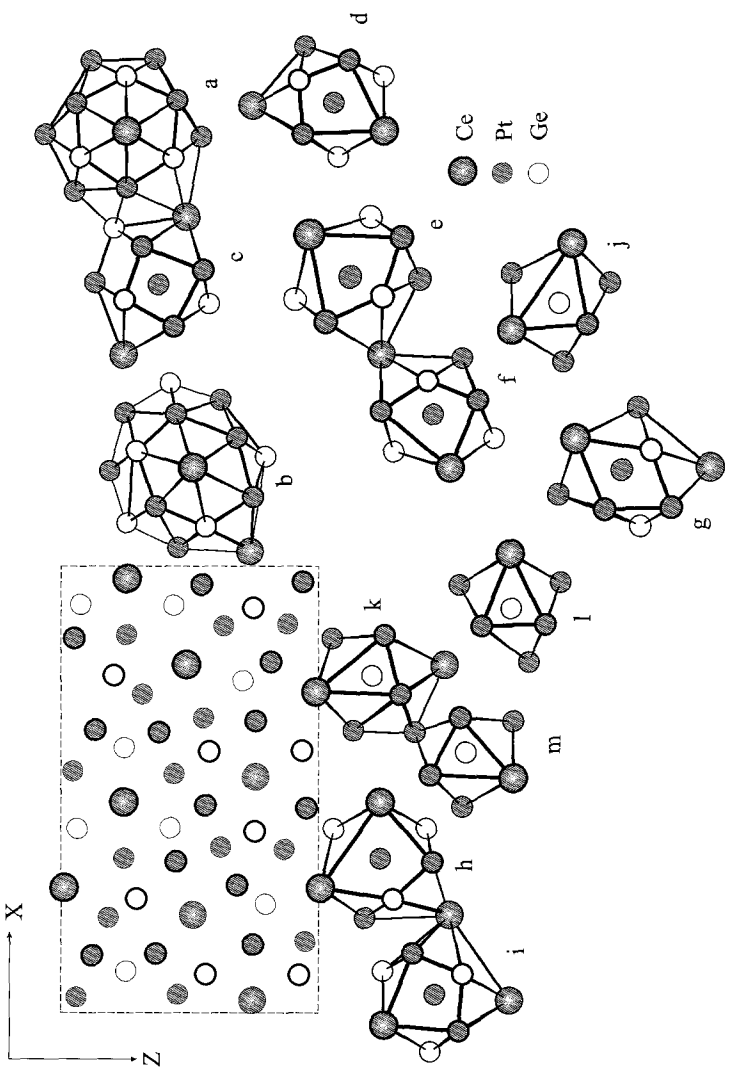

Fig. 15. Projection of the $Ce_2Pt_7Ge_4$ unit cell and coordination polyhedra of the atoms: (a–b) Ce, (c–i) Pt, (j–m) Ge.

3.8.2. *$Ho_4Ir_{13}Ge_9$ structure type*

SG Pmmn, $Z=2$, $a=0.3954$, $b=1.1186$, $c=1.9301$ (Sologub et al. 1993)

Atom	Wyckoff notation	x/a	y/b	z/c	G (%)
Ho1	4(e)	1/4	0.5591	0.70745	100
Ho2	2(b)	1/4	3/4	0.5216	100
Ho3	2(a)	1/4	1/4	0.0194	100
Ir1	4(e)	1/4	0.0497	0.54578	100
Ir2	4(e)	1/4	0.0673	0.16441	100
Ir3	4(e)	1/4	0.1227	0.85460	100
Ir4	4(e)	1/4	0.5589	0.04021	100
Ir5	4(e)	1/4	0.6265	0.35825	100
Ir6	2(b)	1/4	3/4	0.84250	100
Ir7	2(a)	1/4	1/4	0.3585	100
Ir8	2(a)	1/4	1/4	0.72724	100
Ge6	2(a)	1/4	1/4	0.5998	100
Ge1	4(e)	1/4	0.0646	0.4183	100
Ge2	4(e)	1/4	0.5705	0.9160	100
Ge3	4(e)	1/4	0.6195	0.2314	100
Ge4	2(b)	1/4	3/4	0.1012	100
Ge5	2(a)	1/4	1/4	0.2352	100

Isotypic compounds:

$R_4Rh_{13}Ge_9$:R=Y, La–Sm, Gd–Lu

$R_4Ir_{13}Ge_9$:R=Y, La–Sm, Gd–Lu

The coordination polyhedra of the holmium atoms have 20 apexes (fig. 16a–c). Those of iridium are tetragonal prisms with five additional atoms and distorted cubo-octahedra (fig. 16d–k). The coordination polyhedra of germanium atoms are trigonal prisms with three additional atoms (fig. 16l–q).

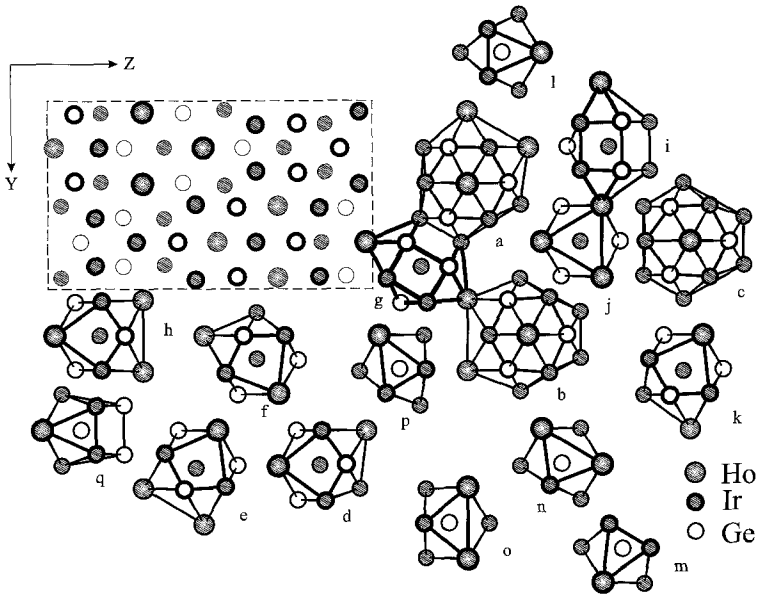

Fig. 16. Projection of the $Ho_4Ir_{13}Ge_9$ unit cell and coordination polyhedra of the atoms: (a–c) Ho, (d–k) Ir, (l–q) Ge.

3.9. *R(M, Ge)$_5$ compounds*

3.9.1. *$CaCu_5$ structure type*

SG P6/mmm, $Z=1$, $a=0.5296$, $c=0.4413$ for $SmPt_{4.4}Ge_{0.6}$ (Barakatova 1994)

Atomic coordinates for this compound have not been determined.

3.9.2. *$Sc_3Ni_{11}Si_4$ structure type*

SG $P6_3/mmc$, $Z=2$, $a=0.8321$, $c=0.8832$ for $Tm_3Ni_{11}Ge_4$ (Fedyna 1988). See fig. 17.

Atom	Wyckoff notation	*x/a*	*y/b*	*z/c*	G (%)
Tm	6(h)	0.1883	0.3766	1/4	100
Ni1	12(k)	0.1719	0.344	0.594	100
Ni2	6(h)	0.537	0.075	1/4	100
Ni3	4(f)	1/3	2/3	0.073	100
Ge1	6(g)	1/2	0	0	100
Ge2	2(b)	0	0	1/4	72

Isotypic compounds:

$R_3Ni_{11}Ge_4$: R = Tb–Lu, Y

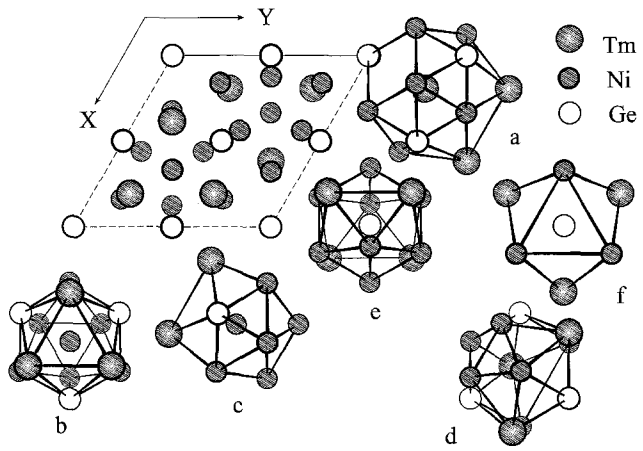

Fig. 17. Projection of the $Tm_3Ni_{11}Ge_4$ unit cell and coordination polyhedra of the atoms: (a) Tm, (b–d) Ni, (e, f) Ge.

3.9.3. *$Sc_3Ni_{11}Ge_4$ structure type*

SG $P6_3/mmc$, $Z=2$, $a=0.8130$, $c=0.8505$ (Andrusyak 1988)

Atom	Wyckoff notation	*x/a*	*y/b*	*z/c*	G (%)
Sc	6(h)	0.190	0.380	1/4	100
Ni1	12(k)	0.162	0.324	0.581	100
Ni2	6(h)	0.555	0.110	1/4	100
Ni3	4(f)	1/3	2/3	0.008	100
Ge1	6(g)	1/2	0	0	100
Ge2	2(b)	0	0	1/4	72
Ge3	2(a)	0	0	0	28

No isotypic compounds are observed.

The 2(a) atomic position, which is partly occupied in this structure, is vacant in the previous structure type.

3.9.4. *$ErNi_3Ge_2$ structure type*

SG $P\bar{6}$, $Z=12$, $a=1.79662$, $c=0.37941$ (Oleksyn and Bodak 1994). See fig. 18.

Atom	Wyckoff notation	*x/a*	*y/b*	*z/c*	G (%)
Er1	3(k)	0.0088	0.5756	1/2	100
Er2	3(k)	0.0969	0.3366	1/2	100
Er3	3(k)	0.3345	0.1678	1/2	100

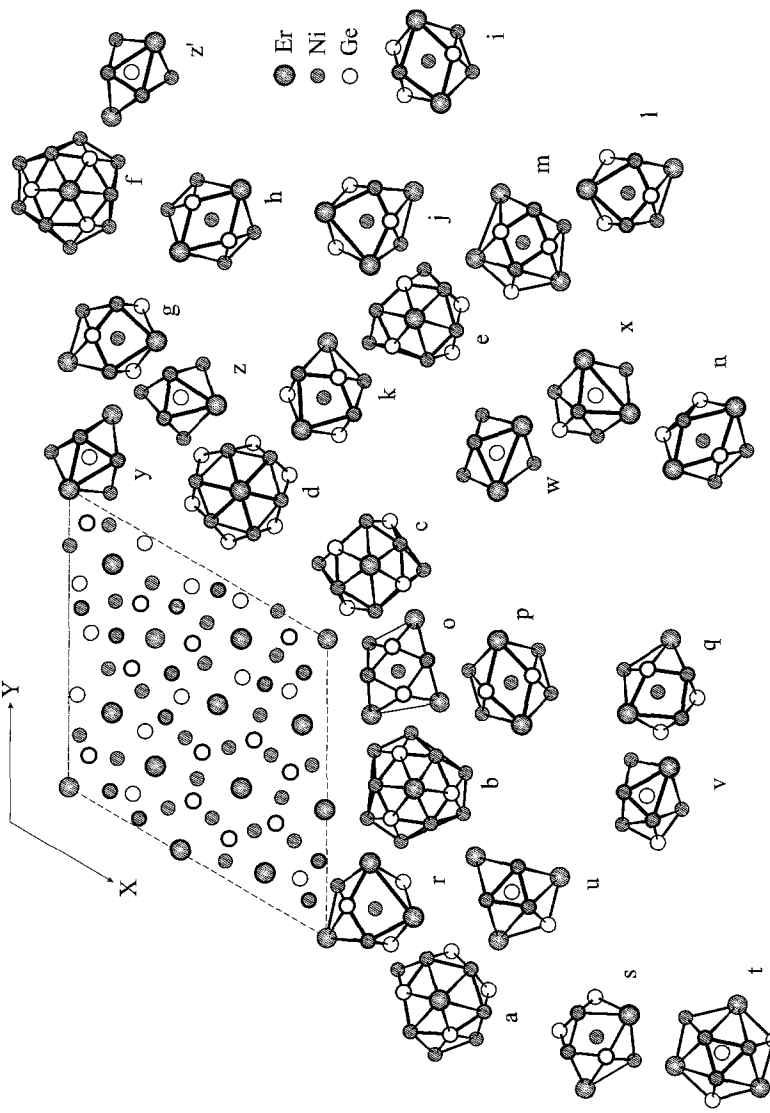

Fig. 18. Projection of the $ErNi_3Ge_2$ unit cell and coordination polyhedra of the atoms: (a–f) Er, (g–r) Ni, (s–z) Ge.

Er4	1(e)	2/3	1/3	0	100
Er5	1(d)	1/3	2/3	1/2	100
Er6	1(a)	0	0	0	100
Ni1	3(k)	0.0906	0.1590	1/2	100
Ni2	3(k)	0.2404	0.2725	1/2	100
Ni3	3(k)	0.4229	0.0487	1/2	100
Ni4	3(k)	0.5817	0.1831	1/2	100
Ni5	3(j)	0.0571	0.4509	0	100
Ni6	3(j)	0.1759	0.6205	0	100
Ni7	3(j)	0.1918	0.0037	0	100
Ni8	3(j)	0.1962	0.1541	0	100
Ni9	3(j)	0.2168	0.4970	0	100
Ni10	3(j)	0.2602	0.3850	0	100
Ni11	3(j)	0.4650	0.1803	0	100
Ni12	3(j)	0.4747	0.3216	0	100
Ge1	3(k)	0.1405	0.5176	1/2	100
Ge2	3(k)	0.1480	0.0690	1/2	100
Ge3	3(k)	0.2827	0.4804	1/2	100
Ge4	3(k)	0.5217	0.2772	1/2	100
Ge5	3(j)	0.1457	0.2482	0	100
Ge6	3(j)	0.3272	0.2933	0	100
Ge7	3(j)	0.3363	0.0410	0	100
Ge8	3(j)	0.5241	0.0859	0	100

No isotypic compounds are observed.

3.9.5. *$ErCo_3Ge_2$ structure type*

SG $P6_3/mcm$, $Z=2$, $a=0.5091$, $c=0.7861$ for $Er_{6-x}Co_6Ge_4$ ($x=3.94$) (Bodak et al. 1990)

Atom	Wyckoff notation	*x/a*	*y/b*	*z/c*	G (%)
Er1	4(e)	0	0	0.1533	27
Er2	2(b)	0	0	0	48
Co	6(g)	0.4813	0	1/4	100
Ge	4(d)	1/3	2/3	0	100

Isotypic compound: $Er_{6-x}Fe_6Ge_4$ ($x=4.17$)

3.10. *R(M, Ge)$_{\sim 4.5}$ compounds*

3.10.1. *$Sc_6Ni_{18}Si_{11}$ structure type*

SG Immm, $Z=4$, $a=1.8322$, $b=1.2461$, $c=0.8191$ for $Sc_6Ni_{18}Ge_{11}$ (Andrusyak and Kotur 1987)

Atom	Wyckoff notation	*x/a*	*y/b*	*z/c*	G (%)
Sc1	8(n)	0	0.1828	0.2036	100
Sc2	8(l)	0	0.1820	0.2804	100
Sc3	4(i)	0	1/2	0.1280	100
Sc4	4(i)	0	1/2	0.3079	100
Ni1	16(o)	0.1664	0.3471	0.21772	100
Ni2	16(o)	0.2169	0.1499	0.41399	100
Ni3	8(m)	0.8372	0	0.7916	100
Ni4	8(m)	0.7325	0	0.9237	100
Ni5	8(l)	0	0.3326	0.4230	100
Ni6	8(l)	0	0.0988	0.1139	100
Ni7	4(j)	0	0	0.4321	100
Ni8	4(h)	0	0.3798	0	100
Ge1	16(o)	0.2647	0.16866	0.15669	100
Ge2	8(m)	0.1810	0	0.33157	100
Ge3	8(l)	0	0.2864	0.11457	100
Ge4	4(g)	0	0.6772	1/2	100
Ge5	4(f)	0.7290	0	1/2	100
Ge6	2(b)	1/2	1/2	0	100
Ge7	2(a)	0	0	0	100

No isotypic compounds have been observed.

3.10.2. *$Nb_2Cr_4Si_5$ structure type*

SG Ibam, $Z=4$, $a=0.7821$, $b=1.6662$, $c=0.5146$ for the $Sc_2Cr_4Ge_5$ compound (Andrusyak 1988)

Atomic coordinates have not been determined.

3.11. *$R(M, Ge)_4$ compounds*

3.11.1. *$CeGa_2Al_2$ structure type*

SG I4/mmm, $Z=2$, $a=0.4042$, $c=1.0183$ for $NdCo_2Ge_2$ (Salamakha 1989)

Atom	Wyckoff notation	*x/a*	*y/b*	*z/c*	G (%)
Nd	2(a)	0	0	0	100
Co	4(d)	0	1/2	1/4	100
Ge	4(e)	0	0	0.387	100

Isotypic compounds:
RMn_2Ge_2: R = Y, La–Sm, Gd–Yb
RFe_2Ge_2: R = Y, La–Sm, Gd–Lu
RCo_2Ge_2: R = Y, La–Yb
RNi_2Ge_2: R = Y, La–Lu
RCu_2Ge_2: R = Y, La–Yb
RRu_2Ge_2: R = Y, La–Lu
RRh_2Ge_2: R = Y, La–Lu
RPd_2Ge_2: R = Y, La–Lu
RAg_2Ge_2: R = La–Gd
RPt_2Ge_2: R = Y, La–Dy, Er
RAu_2Ge_2: R = Ce, Nd

For neodymium atoms, polyhedra with 22 apexes are typical (fig. 19a). The cobalt atom polyhedra are distorted cubo-octahedra (fig. 19b). Tetragonal antiprisms with one additional atom are typical for germanium atoms (fig. 19c).

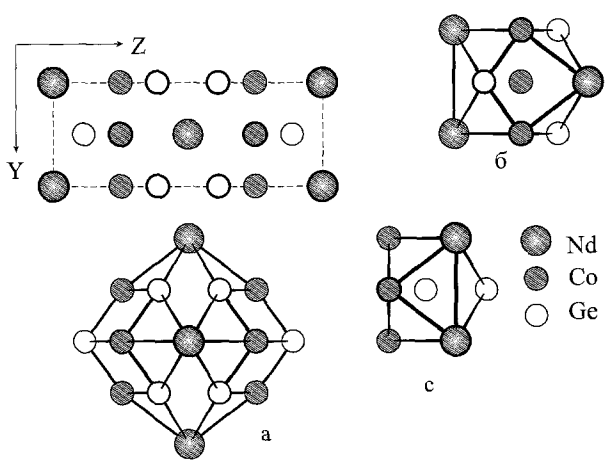

Fig. 19. Projection of the $NdCo_2Ge_2$ unit cell and coordination polyhedra of the atoms: (a) Nd, (b) Co, (c) Ge.

3.11.2. *$CaBe_2Ge_2$ structure type*

SG P4/nmm, $Z=2$, $a=0.4246$, $c=1.0098$ for $CeIr_2Ge_2$ (Mathur and Frost 1994)

Atom	Wyckoff notation	*x/a*	*y/b*	*z/c*	G (%)
Ce	2(c)	1/4	1/4	0.749	100
Ir1	2(c)	1/4	1/4	0.368	100
Ir2	2(a)	3/4	1/4	0	100
Ge1	2(c)	1/4	1/4	0.108	100
Ge2	2(b)	3/4	1/4	1/2	100

Isotypic compounds:
RIr_2Ge_2: R = La–Tb

For the cerium atoms, coordination polyhedra have 22 apexes (fig. 20a). Iridium and germanium atoms have an environment in the form of distorted cubo-octahedra and tetragonal antiprisms with one additional atom (fig. 20b–e).

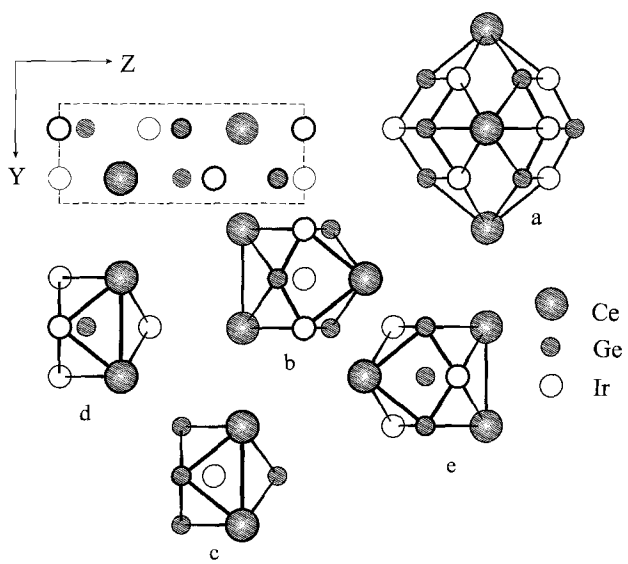

Fig. 20. Projection of the $CeIr_2Ge_2$ unit cell and coordination polyhedra of the atoms: (a) Ce, (b–e) Ir and Ge.

3.11.3. *$LaPt_2Ge_2$ structure type*

SG $P2_1$, $Z=2$, $a=0.4404$, $b=0.4421$, $c=0.9851$, $\beta=90.50°$ (Venturini et al. 1989a)

Atom	Wyckoff notation	*x/a*	*y/b*	*z/c*	G (%)
La	2(a)	0.2631	0.0151	0.7449	100
Pt1	2(a)	0..2559	0.0483	0.3790	100
Pt2	2(a)	0.2680	0.4650	0.0016	100
Ge1	2(a)	0.2647	0.0000	0.1267	100
Ge2	2(a)	0.2727	0.5687	0.5049	100

Isotypic compounds:

RPt_2Ge_2: R = La–Dy

The coordination polyhedra of the lanthanum atoms have 22 apexes (fig. 21a). Those of platinum and germanium are tetragonal antiprisms with one additional atom and distorted cubo-octahedra (fig. 21b–e).

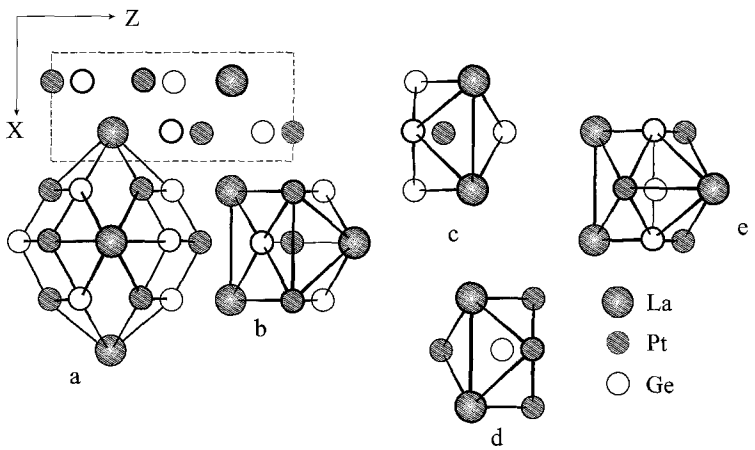

Fig. 21. Projection of the $LaPt_2Ge_2$ unit cell and coordination polyhedra of the atoms: (a) Ce, (b–e) Ir and Ge.

3.11.4. *$CaAl_2Si_2$ structure type*

SG P3m1, $Z=1$, $a=0.4271$, $c=0.6947$ for $CeAl_2Ge_2$ (Zarechnyuk et al. 1970). See fig. 22.

Atom	Wyckoff notation	*x/a*	*y/b*	*z/c*	G (%)
Ce	1(a)	0	0	0	100
Al	2(d)	1/3	2/3	0.63	100

Ge	2(d)	1/3	2/3	0.26	100

Isotypic compounds:
RAl_2Ge_2: R = Y, La–Lu

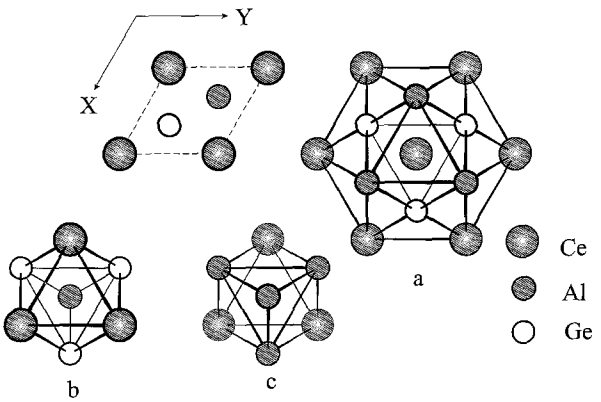

Fig. 22. Projection of the $CeAl_2Ge_2$ unit cell and coordination polyhedra of the atoms: (a) Ce, (b) Al, (c) Ge.

3.11.5. *$U_2Co_3Si_5$ structure type*

SG Ibam, $Z = 4$, $a = 0.9783$, $b = 1.1896$, $c = 0.5831$ for $Pr_2Co_3Ge_5$ (Fedyna et al. 1987). See fig. 23.

Atom	Wyckoff notation	*x/a*	*y/b*	*z/c*	G (%)
Pr	8(j)	0.2726	0.3602	0	100
Co1	8(j)	0.114	0.120	0	100
Co2	4(b)	1/2	0	1/4	100
Ge1	8(j)	0.3467	0.096	0	100
Ge2	8(g)	0	0.250	1/4	100
Ge3	4(a)	0	0	1/4	100

Isotypic compounds:
$R_2Co_3Ge_5$: R = Y, Ce–Nd, Tb
$R_2Ni_3Ge_5$: R = Ce, Pr
$R_2Ru_3Ge_5$: R = La–Sm, Gd–Tm
$R_2Rh_3Ge_5$: R = La–Pr
$R_2Ir_3Ge_5$: R = La–Sm, Gd–Dy

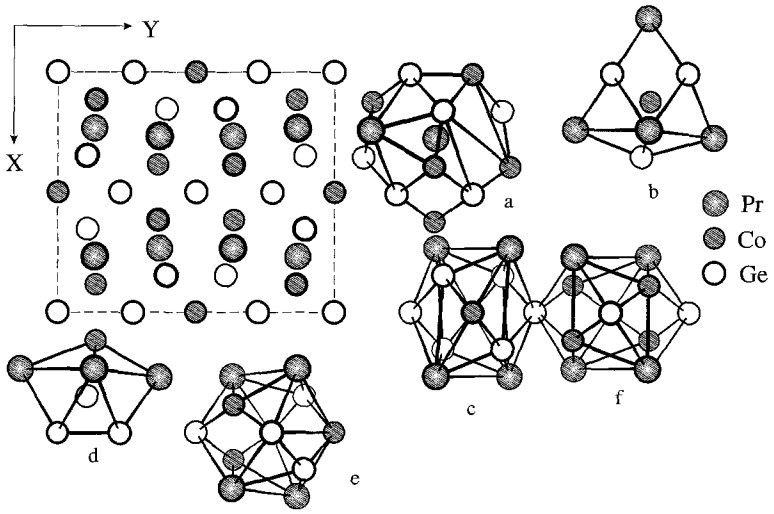

Fig. 23. Projection of the $Pr_2Co_3Ge_5$ unit cell and coordination polyhedra of the atoms: (a) Pr, (b,c) Co, (d–f) Ge.

3.11.6. *$Lu_2Co_3Si_5$ structure type*

SG C2/c, $Z=4$, $a=1.1353$, $b=1.1976$, $c=0.5813$ $\beta=119.05°$ for $Ho_2Rh_3Ge_5$ (Venturini et al. 1986). See fig. 24.

Atom	Wyckoff notation	*x/a*	*y/b*	*z/c*	G (%)
Ho	8(f)	0.2695	0.1370	0.2664	100
Rh1	8(f)	0.1001	0.3576	0.1172	100
Rh2	4(e)	0	0.0013	1/4	100
Ge1	8(f)	0.3313	0.4041	0.3319	100
Ge2	4(e)	0	0.2114	1/4	100
Ge3	4(e)	0	0.5071	1/4	100
Ge4	4(e)	0	0.7796	1/4	100

Isotypic compounds:
$R_2Co_3Ge_5$: R = Pr–Sm, Gd–Er
$R_2Rh_3Ge_5$: R = Nd–Sm, Gd–Tm

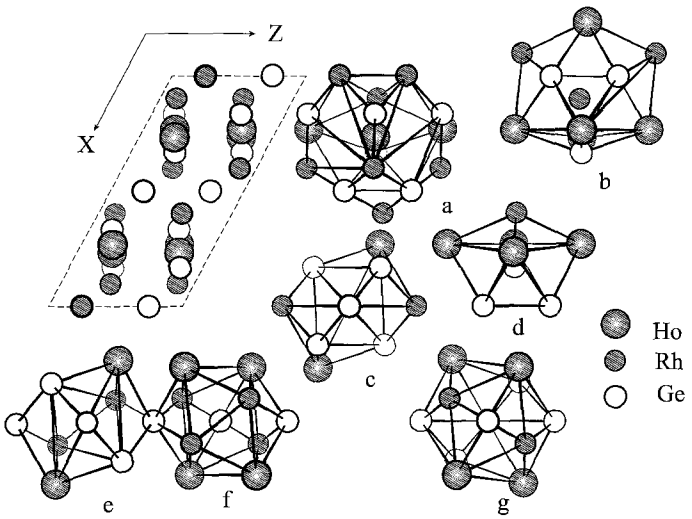

Fig. 24. Projection of the $Ho_2Rh_3Ge_5$ unit cell and coordination polyhedra of the atoms: (a) Ho, (b,c) Rh, (d–g) Ge.

3.11.7. *$SmNiGe_3$ structure type*

SG Cmmm, $Z=4$, $a=0.4102$, $b=2.1657$, $c=0.4092$ (Bodak et al. 1985)

Atom	Wyckoff notation	*x/a*	*y/b*	*z/c*	G (%)
Sm	4(j)	0	0.3318	1/2	100
Ni	4(i)	0	0.1092	0	100
Ge1	4(j)	0	0.0568	1/2	100
Ge2	4(i)	0	0.2164	0	100
Ge3	4(i)	0	0.4433	0	100

Isotypic compounds:

$RNiGe_3$: R = Y, Ce–Sm, Gd–Tm

$RGaGe_3$: R = Y, Gd

The coordination polyhedra with 20 apexes are typical for samarium atoms (fig. 25a). Those for nickel atoms are tetragonal antiprisms (fig. 25b). The germanium coordination polyhedra are trigonal prisms (fig. 25c–e).

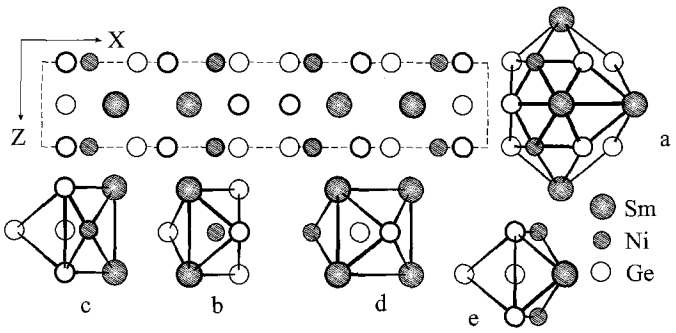

Fig. 25. Projection of the $SmNiGe_3$ unit cell and coordination polyhedra of the atoms: (a) Sm, (b) Ni, (c–e) Ge.

3.11.8. *$BaNiSn_3$ structure type*

SG I4mm, $Z=2$, $a=0.4350$, $c=0.9865$ for $LaCoGe_3$ (Venturini et al. 1985)

Atom	Wyckoff notation	*x/a*	*y/b*	*z/c*	G (%)
La	2(a)	0	0	0.5759	100
Co	2(a)	0	0	0.2313	100
Ge1	2(a)	0	0	0.0000	100
Ge2	4(b)	0	1/2	0.3253	100

Isotypic compounds:
$RCoGe_3$: R = Ce–Eu, Yb
$RRhGe_3$: R = La–Pr, Eu
$RIrGe_3$: R = La, Eu
$RRuGe_3$: R = La
$ROsGe_3$: R = La

The coordination number of lanthanum atoms is 21 (fig. 26a). Cobalt atoms have the coordination polyhedra in a form of tetragonal antiprisms (fig. 26b). Germanium atoms are situated inside the tetragonal antiprisms and distorted cubo-octahedra (fig. 26c, d).

3.12. *$R_2(M, Ge)_7$ compounds*

3.12.1. *$Ba_2Cd_3Bi_4$ structure type*

SG Cmca, $Z=4$, $a=0.6143$, $b=1.5193$, $c=0.8035$ for $La_2Al_3Ge_4$ (Zhao and Parthé 1991c). See fig. 27.

Atom	Wyckoff notation	*x/a*	*y/b*	*z/c*	G (%)
La	8(f)	0	0.11389	0.4170	100
Al1	8(e)	1/4	0.2842	1/4	100

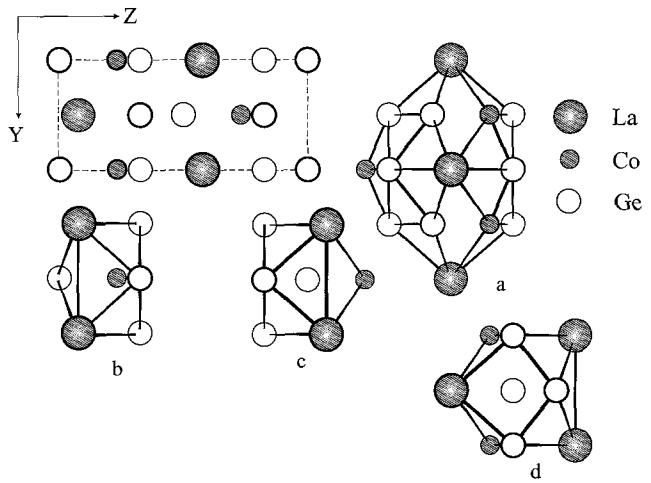

Fig. 26. Projection of the $LaCoGe_3$ unit cell and coordination polyhedra of the atoms: (a) La, (b) Co, (c–d) Ge.

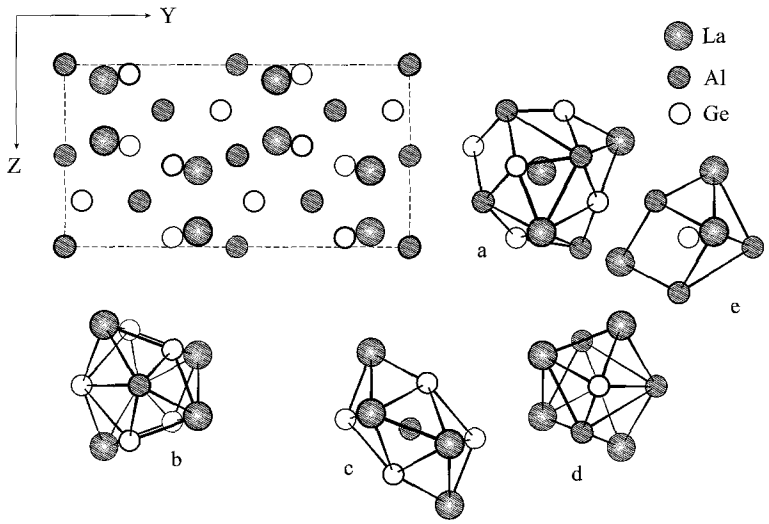

Fig. 27. Projection of the $La_2Al_3Ge_4$ unit cell and coordination polyhedra of the atoms: (a) La, (b,c) Al, (d,e) Ge.

Al2	4(a)	0	0	0	100
Ge1	8(f)	0	0.1873	0.0531	100
Ge2	8(e)	1/4	0.4512	1/4	100

Isotypic compounds:
$R_2Al_3Ge_4$: R = Ce–Sm, Gd–Er

3.12.2. *$Ce_2Sc_3Si_4$ structure type*
SG Pnma, $Z=4$, $a=0.7188$, $b=1.339$, $c=0.7416$ $Ce_{1.22}Sc_3Ge_4$ (Shpyrka 1990)

Atom	Wyckoff notation	*x/a*	*y/b*	*z/c*	G (%)
Ce	8(d)	0.0039	0.5949	0.1767	61
Sc1	8(d)	0.157	0.3757	0.333	100
Sc2	4(c)	0.183	3/4	0.499	100
Ge1	8(d)	0.3153	0.4593	0.0395	100
Ge2	4(c)	0.9556	3/4	0.8754	100
Ge3	4(c)	0.310	3/4	0.139	100

Isotypic compounds:
$R_{2-x}Sc_3Ge_4$: R = La–Sm
$R_2Nb_3Ge_4$: R = Sc, Y, Gd–Lu
$R_2Mo_3Ge_4$: R = Sc, Y, Tb–Tm, Lu
$Sc_2V_3Ge_4$

3.12.3. *Ce_2CuGe_6 structure type*
SG Amm2, $Z=2$, $a=0.40756$, $b=0.42152$, $c=2.15408$ (Konyk et al. 1988)

Atom	Wyckoff notation	*x/a*	*y/b*	*z/c*	G (%)
Ce1	2(b)	1/2	0	0.218	100
Ce2	2(b)	1/2	0	0.885	100
Cu	2(a)	0	0	0.451	100
Ge1	2(b)	1/2	0	0.498	100
Ge2	2(b)	1/2	0	0.610	100
Ge3	2(a)	0	0	0.000	100
Ge4	2(a)	0	0	0.115	100
Ge5	2(a)	0	0	0.344	100
Ge6	2(a)	0	0	0.772	100

Isotypic compounds:
R_2CoGe_6: R = Y, Gd–Tm, Lu
R_2NiGe_6: R = Y, Ce–Sm, Gd–Lu
R_2PdGe_6: R = Y, La–Sm, Gd–Yb
R_2PtGe_6: R = Y, La–Sm, Gd–Yb
R_2CuGe_6: R = Ce–Sm, Gd–Yb
R_2AgGe_6: R = La–Sm, Gd
R_2AuGe_6: R = Ce–Sm, Gd–Dy

Polyhedra with 16 and 20 apexes are typical for the cerium atoms (fig. 28a, b). Atoms of cooper are situated inside the tetragonal antiprisms, formed by the atoms of cerium and

germanium (fig. 28c). The germanium coordination polyhedra are trigonal prisms with two and three additional atoms, tetragonal antiprisms with additional atoms, distorted cubo-octahedra and polyhedra with 7 apexes (fig. 28d–i).

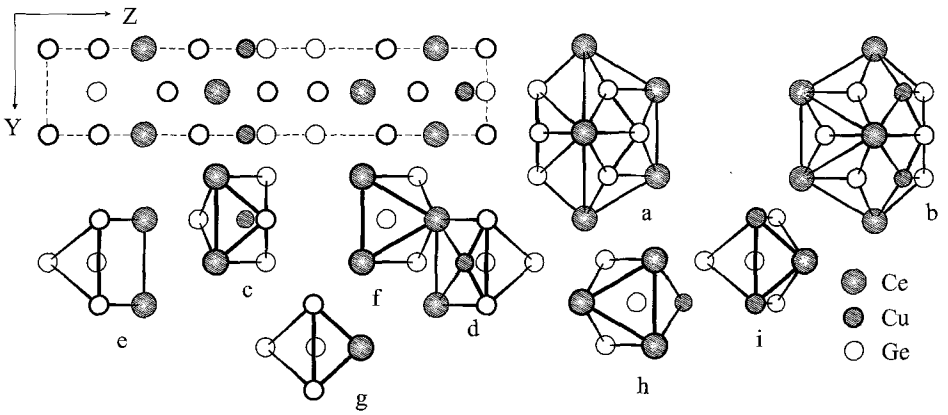

Fig. 28. Projection of the Ce_2CuGe_6 unit cell and coordination polyhedra of the atoms: (a,b) Ce, (c) Cu, (d–i) Ge.

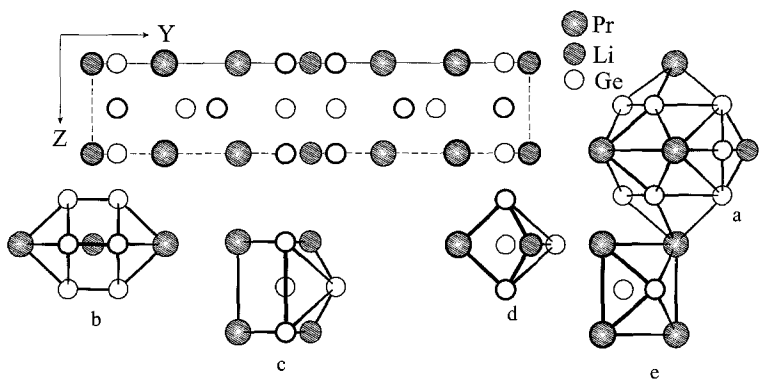

Fig. 29. Projection of the Pr_2LiGe_6 unit cell and coordination polyhedra of the atoms: (a) Pr, (b) Li, (c–e) Ge.

3.12.4. *Pr_2LiGe_6 structure type*

SG Cmmm, $Z=2$, $a=0.41268$, $b=2.10520$, $c=0.43455$ (Pavlyuk et al. 1988a). See fig. 29.

Atom	Wyckoff notation	*x/a*	*y/b*	*z/c*	G (%)
Pr	4(i)	0	0.1657	0	100
Li	2(a)	0	0	0	100

Ge1	4(j)	0	0.0579	1/2	100
Ge2	4(j)	0	0.2861	1/2	100
Ge3	4(i)	0	0.4431	0	100

Isotypic compounds:
Ce_2LiGe_6, $Y_{2.25}Ga_{0.67}Ge_{6.08}$

3.12.5. *$Ce_2(Ga, Ge)_7$ structure type*

SG Cmca, $Z=8$, $a=0.86373$, $b=0.82697$, $c=2.1451$ for $Ce_2Ga_{0.7}Ge_{6.3}$ (Yarmolyuk et al. 1989). See fig. 30.

Atom	Wyckoff notation	*x/a*	*y/b*	*z/c*	G (%)
Ce	16(g)	0.2511	0.3780	0.08185	100
X1	16(g)	0.2843	0.1240	0.19385	100
X2	8(f)	0	0.1186	0.4591	100
X3	8(f)	0	0.1231	0.1478	100
X4	8(f)	0	0.1309	0.0298	100
X5	8(f)	0	0.3357	0.3057	100
X6	8(f)	0	0.4123	0.1935	100

X=0.1Ga+0.9Ge
Isotypic compound: $Nd_2(Ga,Ge)_7$

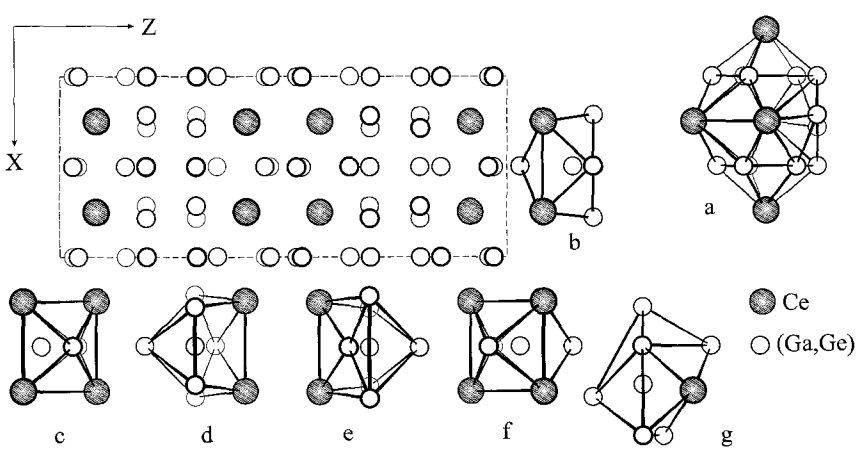

Fig. 30. Projection of the $Ce_2Ga_{0.7}Ge_{6.3}$ unit cell and coordination polyhedra of the atoms: (a) Ce, (b–g) X.

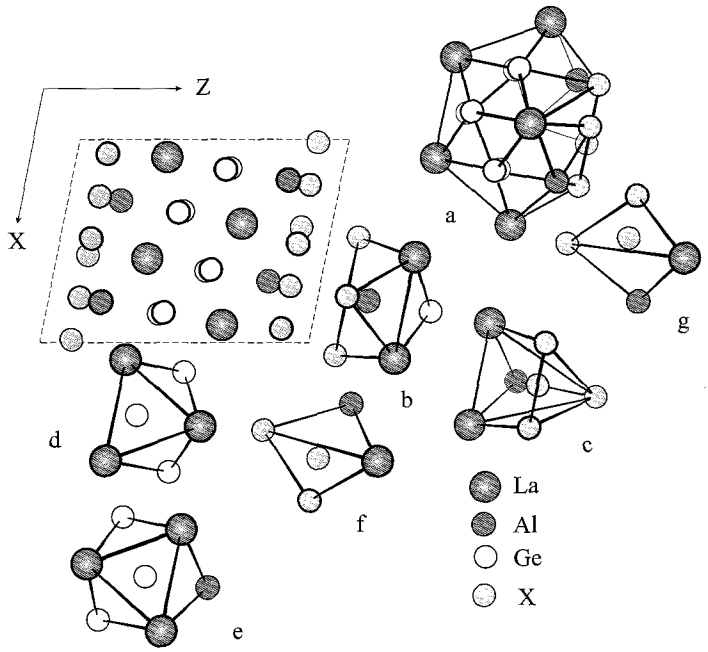

Fig. 31. Projection of the La_2AlGe_6 unit cell and coordination polyhedra of the atoms: (a) La, (b) Al, (c–g) X1, X2, X3, Ge1 and Ge2.

3.12.6. *La_2AlGe_6 structure type*

SG C2/m, $Z=4$, $a=0.8373$, $b=0.8833$, $c=1.0887$, $\beta=101.34°$ (Zhao et al. 1991). See fig. 31.

Atom	Wyckoff notation	*x/a*	*y/b*	*z/c*	G (%)
La	8(j)	0.08527	0.24828	0.33612	100
Al	4(i)	0.8006	0	0.1952	100
X1	4(i)	0.0694	0	0.1123	100
X2	8(j)	0.2783	0.2131	0.1125	100
X3	4(i)	0.4869	0	0.1133	100
Ge1	4(i)	0.1460	0	0.5640	100
Ge2	4(i)	0.3597	0	0.4195	100

X1 = 0.23Al+0.77Ge; X2 = 0.09Al+0.91Ge; X3 = 0.19Al+0.81Ge

Isotypic compounds:

R_2AlGe_6: R = Ce–Sm, Gd

$R_2(Ga,Ge)_7$: R = Y, Gd

3.13. *$R_3(M, Ge)_{10}$ and $R_4(M, Ge)_{13}$ compounds*

3.13.1. *$Ce_3Pt_4Ge_6$ structure type*

SG Cmcm, $Z=2$, $a=0.4419$, $b=2.6222$, $c=0.4422$ (Gribanov et al. 1992b)

Atom	Wyckoff notation	*x/a*	*y/b*	*z/c*	G (%)
Ce1	4(c)	0	0.1575	1/4	100
Ce2	4(c)	0	0.5292	1/4	50
Pt1	4(c)	0	0.29577	1/4	100
Pt2	4(c)	0	0.93714	1/4	100
Ge1	8(g)	0.201	0.0356	1/4	50
Ge2	4(c)	0	0.3898	1/4	100
Ge3	4(c)	0	0.7505	1/4	100

Isotypic compound: $Sm_3Pt_4Ge_6$

For the cerium atoms, polyhedra with 21 and 19 apexes are typical (fig. 32a, b). The polyhedra for platinum atoms are trigonal prisms with four additional atoms and tetragonal antiprisms with two additional atoms (fig. 32c, d). The germanium coordination polyhedra are deformed cubooctahedra and trigonal prisms with three additional atoms (fig. 32e–g).

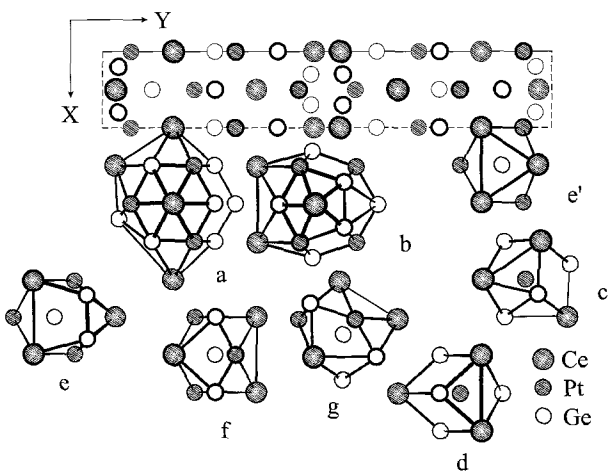

Fig. 32. Projection of the $Ce_3Pt_4Ge_6$ unit cell and coordination polyhedra of the atoms: (a, b) Ce, (c, d) Pt, (e–g) Ge.

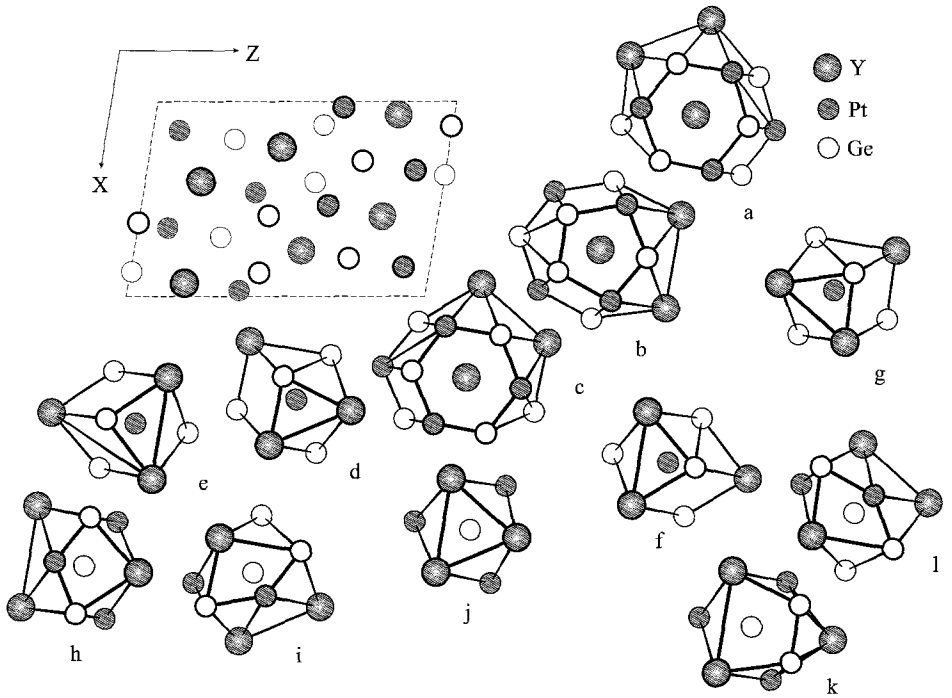

Fig. 33. Projection of the $Y_3Pt_4Ge_6$ unit cell and coordination polyhedra of the atoms: (a–c) Y, (d–g) Pt, (h–m) Ge.

3.13.2. *$Y_3Pt_4Ge_6$ stucture type*

SG $P2_1/m$, $Z=2$, $a=0.86922$, $b=0.43062$, $c=1.31615$, $\beta=99.45°$ (Venturini and Malaman 1990). See fig. 33.

Atom	Wyckoff notation	*x/a*	*y/b*	*z/c*	G (%)
Y1	2(e)	0.0673	1/4	0.8128	100
Y2	2(e)	0.5889	1/4	0.8135	100
Y3	2(e)	0.7653	1/4	0.5604	100
Pt1	2(e)	0.1496	1/4	0.0883	100
Pt2	2(e)	0.4672	1/4	0.3751	100
Pt3	2(e)	0.6473	1/4	0.1008	100
Pt4	2(e)	0.9703	1/4	0.3747	100
Ge1	2(e)	0.1191	1/4	0.5685	100
Ge2	2(e)	0.1945	1/4	0.2782	100
Ge3	2(e)	0.3777	1/4	0.9999	100

Ge4	2(e)	0.4145	1/4	0.5691	100
Ge5	2(e)	0.6957	1/4	0.2823	100
Ge6	2(e)	0.8738	1/4	0.0042	100

No isotypic compounds have been observed.

3.13.3. *$U_4Re_7Si_6$ structure type*

SG $Im\bar{3}m$, $Z=2$, $a=0.81255$ for $Sc_4Rh_7Ge_6$ (Engel et al. 1984). See fig. 34.

Atom	Wyckoff notation	*x/a*	*y/b*	*z/c*	G (%)
Sc	8(c)	1/4	1/4	1/4	100
Rh1	12(d)	1/4	0	1/2	100
Rh2	2(a)	0	0	0	100
Ge	12(e)	0.3128	0	0	100

Isotypic compounds:
$Sc_4M_7Ge_6$: M = Co, Ru, Ir, Os
$R_4Rh_7Ge_6$: R = Y, Dy–Lu
$R_4Ir_7Ge_6$: R = Y, Tb–Lu
$R_4Os_7Ge_6$: R = Y, Er–Lu

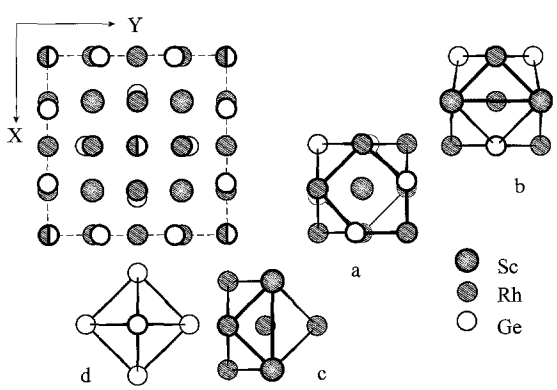

Fig. 34. Projection of the $Sc_4Rh_7Ge_6$ unit cell and coordination polyhedra of the atoms: (a) Sc, (b,c) Rh, (d) Ge.

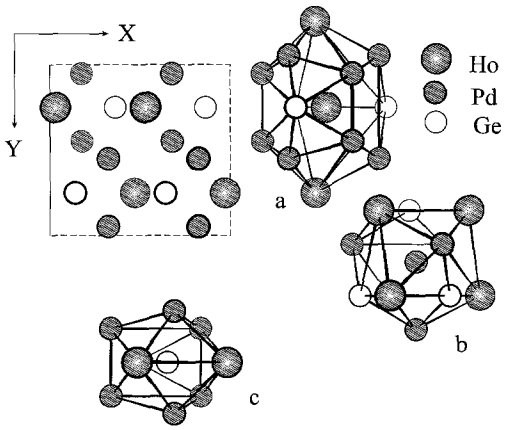

Fig. 35. Projection of the $HoPd_2Ge$ unit cell and coordination polyhedra of the atoms: (a) Ho, (b) Pd, (c) Ge.

3.14. *R(M, Ge)$_3$ compounds*

3.14.1. *YPd_2Si structure type*

SG Pnma, $Z=4$, $a=0.7321$, $b=0.7045$, $c=0.5563$ for $HoPd_2Ge$ (Sologub 1995). See fig. 35.

Atom	Wyckoff notation	*x/a*	*y/b*	*z/c*	G (%)
Ho	4(c)	0.6472	1/4	0.0324	100
Pd	8(d)	0.0948	0.0537	0.1789	100
Ge	4(c)	0.3560	1/4	0.3646	100

Isotypic compounds:
RPd_2Ge: R = Y, La–Sm, Gd–Tm, Lu

3.14.2. *$AlCr_2C$ structure type*

SG $P6_3/mmc$, $Z=2$, $a=0.4537$, $c=0.7568$ for $CeLi_2Ge$ (Pavlyuk 1993)

Atom	Wyckoff notation	*x/a*	*y/b*	*z/c*	G (%)
Ce	2(a)	0	0	0	100
Li	4(f)	1/3	2/3	0.625	100
Ge	2(c)	1/3	2/3	1/4	100

Isotypic compounds:
RLi_2Ge: R = La–Nd

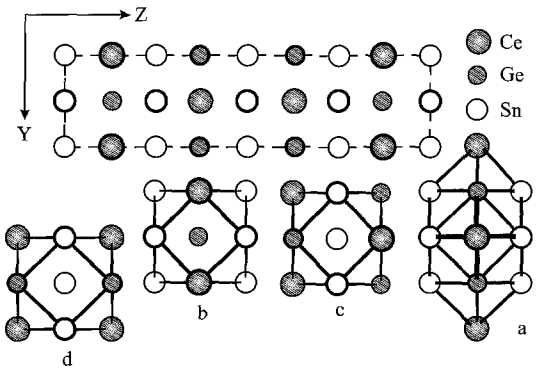

Fig. 36. Projection of the $CeSn_{3-x}Ge$ unit cell and coordination polyhedra of the atoms: (a) Ce, (b) Sn, (c) X, (d) Ge.

3.14.3. *$ZrAl_3$ structure type*

SG I4/mmm, $Z=4$, $a=0.4014$, $c=1.7320$ for $CeSn_{3-x}Ge_x$ (Stetskiv 1999). See fig. 36.

Atom	Wyckoff notation	*x/a*	*y/b*	*z/c*	G (%)
Ce	4(e)	0	0	0.1284	100
Sn	4(d)	0	1/2	1/2	100
X	4(c)	0	1/2	0	100
Ge	4(e)	0	0	0.3695	100

X = 0.90Sn+0.10Ge

Isotypic compounds:

$RSn_{3-x}Ge_x$: R = La, Pr, Sm

$CeBi_2Ge$

3.14.4. *$TiAl_3$ structure type*

SG I4/mmm, $Z=2$, $a=0.4619$, $c=0.9233$ for $PrSn_{3-x}Ge_x$ (HT modification) (Stetskiv 1999)

Atomic coordinates have not been determined for this germanide.

3.14.5. *$Ce_2Cu_3Ge_3$ structure type*

SG Cm2m, $Z=2$, $a=0.41680$, $b=1.7409$, $c=0.42108$ (Konyk 1988). See fig. 37.

Atom	Wyckoff notation	*x/a*	*y/b*	*z/c*	G (%)
Ce1	2(a)	0	0.000	0	100
Ce2	2(b)	0	0.779	1/2	100
Cu1	2(a)	0	0.618	0	100
Cu2	2(a)	0	0.212	0	100

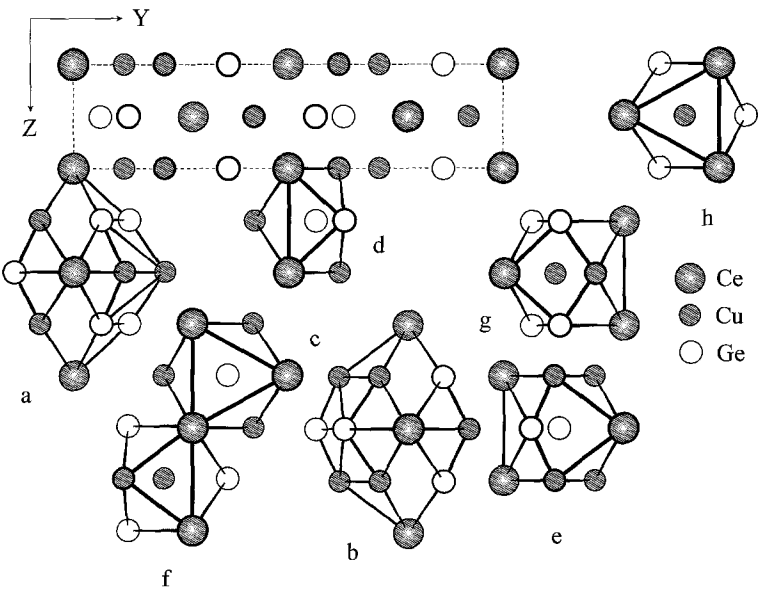

Fig. 37. Projection of the $Ce_2Cu_3Ge_3$ unit cell and coordination polyhedra of the atoms: (a, b) Ce, (c–e) Cu, (f–h) Ge.

Cu3	2(b)	0	0.420	1/2	100
Ge1	2(a)	0	0.361	0	100
Ge2	2(b)	0	0.129	1/2	100
Ge3	2(b)	0	0.563	1/2	100

Isotypic compounds:
$R_2Cu_3Ge_3$: R = Pr, Nd

3.14.6. *$CeNiSi_2$ structure type*

SG Cmcm, $Z = 4$, $a = 0.4199$, $b = 1.6765$, $c = 0.4174$ for $NdNiGe_2$ (Salamakha 1989)

Atom	Wyckoff notation	*x/a*	*y/b*	*z/c*	G (%)
Nd	4(c)	0	0.397	1/4	100
Ni	4(c)	0	0.100	1/4	100
Ge1	4(c)	0	0.034	1/4	100
Ge2	4(c)	0	0.751	1/4	100

Isotypic compounds:
$RMn_{1-x}Ge_2$: R = Nd, Sm, Gd–Tm, Lu
$RFe_{1-x}Ge_2$: R = Y, La–Sm, Gd–Lu

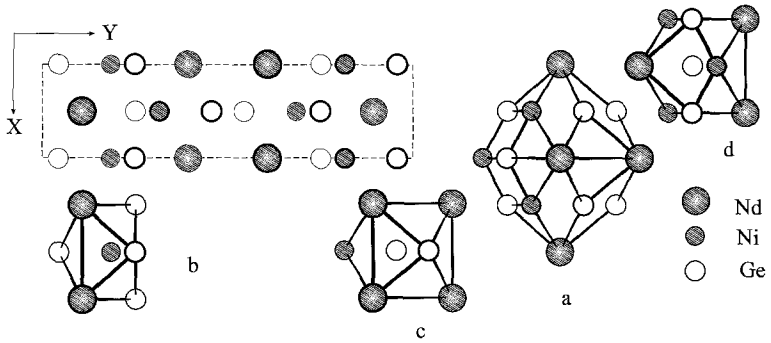

Fig. 38. Projection of the $NdNiGe_2$ unit cell and coordination polyhedra of the atoms: (a) Nd, (b) Ni, (c, d) Ge.

$RCo_{1-x}Ge_2$: R = Y, La–Sm, Gd–Lu
$RNi_{1-x}Ge_2$: R = Y, La–Lu
$RCu_{1-x}Ge_2$: R = La–Sm, Gd–Tm, Lu
$RRu_{1-x}Ge_2$: R = Gd, Ho, Lu
$RRh_{1-x}Ge_2$: R = Nd, Gd, Ho, Lu
$RPd_{1-x}Ge_2$: R = La–Nd, Gd, Ho, Lu
$RRe_{1-x}Ge_2$: R = Gd, Ho, Lu
$RIr_{1-x}Ge_2$: R = La, Ho
$RPt_{1-x}Ge_2$: R = La, Ho

The coordination number of neodymium atoms is 21 (fig. 38a). Nickel atoms have the coordination polyhedra in the form of tetragonal antiprisms with one additional atom (fig. 38b). Germanium atoms are situated inside the trigonal prisms and distorted cubo-octahedra (fig. 38c, d).

3.14.7. *$YIrGe_2$ structure type*

SG Immm, $Z = 8$, $a = 0.4358$, $b = 0.8909$, $c = 1.6153$ for $NdIrGe_2$ (Salamakha et al. 1989)

Atom	Wyckoff notation	*x/a*	*y/b*	*z/c*	G (%)
Nd1	4(i)	0	0	0.2057	100
Nd2	4(g)	0	0.2393	0	100
Ir	8(l)	0	0.2494	0.3541	100
Ge1	8(l)	0	0.3474	0.2002	100
Ge2	4(j)	1/2	0	0.0770	100
Ge3	4(i)	0	0	0.4215	100

Isotypic compounds:
$RIrGe_2$: R = Y, Pr–Sm, Gd–Er
$RPtGe_2$: R = Y, Ce–Sm, Gd–Yb
$RPdGe_2$: R = Y, Sm, Gd–Ho, Yb

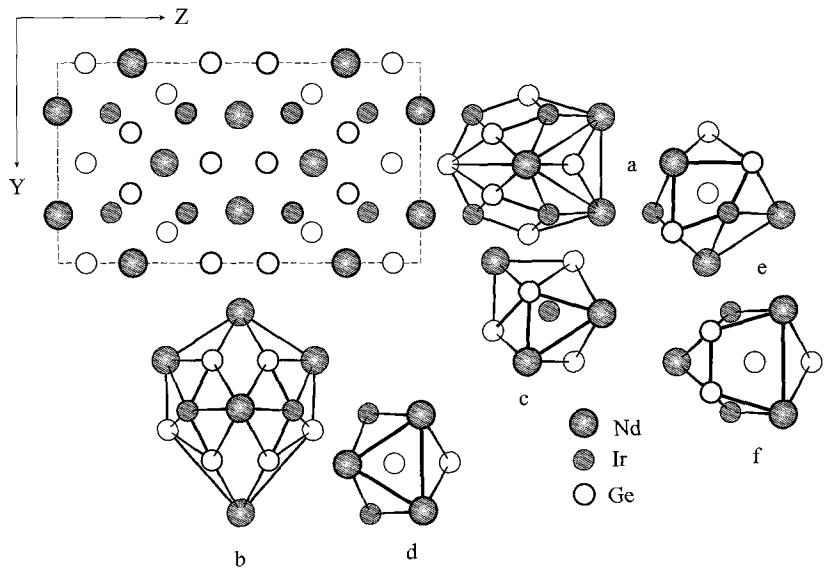

Fig. 39. Projection of the $NdIrGe_2$ unit cell and coordination polyhedra of the atoms: (a, b) Nd, (c) Ir, (d–f) Ge.

Polyhedra with 19 and 20 apexes are typical for the neodymium atoms (fig. 39a, b). Atoms of iridium are situated inside the trigonal prisms (fig. 39c). The germanium coordination polyhedra are trigonal prisms, distorted cubo-octahedra and distorted tetragonal prisms (fig. 39d–f).

3.14.8. *$LuMnGe_2$ structure type*

SG Cmmm, $Z = 12$, $a = 0.5466$, $c = 1.8519$, $c = 0.8173$ (Meyer et al. 1983)

Atom	Wyckoff notation	*x/a*	*y/b*	*z/c*	G (%)
Lu1	8(n)	0	0.40571	0.2481	100
Lu2	4(i)	0	0.1394	0	100
Mn1	8(m)	1/4	1/4	0.2476	100
Mn2	4(k)	0	0	0.2535	100
Ge1	8(n)	0	0.1383	0.3464	100
Ge2	4(j)	0	0.2905	1/2	100
Ge3	4(i)	0	0.2977	0	100
Ge4	4(h)	0.2624	0	1/2	100
Ge5	4(g)	0.2577	0	0	100

No isotypic compounds are observed.

3.14.9. *$ZrCrSi_2$ (or $TiMnSi_2$) structure type*

SG Pbam, $Z=12$, $a=1.0148$, $b=0.9355$, $c=0.8141$ for $ScCrGe_2$ (Andrusyak 1988). See fig. 40.

Atom	Wyckoff notation	x/a	y/b	z/c	G (%)
Sc1	8(i)	0.32742	0.04765	0.24668	100
Sc2	4(g)	0.33143	0.32009	0	100
Cr1	8(i)	0.08009	0.24822	0.24960	100
Cr2	4(e)	0	0	0.24469	100
Ge1	8(i)	0.32908	0.31885	0.35089	100
Ge2	4(h)	0.03891	0.37798	1/2	100
Ge3	4(h)	0.11388	0.09815	1/2	100
Ge4	4(g)	0.03886	0.38121	0	100
Ge5	4(g)	0.12715	0.10435	0	100

Isotypic compounds:
$ScMGe_2$: M = Mn, Fe, Co, Ru, Rh, Os
$ROsGe_2$: R = Er, Tm, Lu
$LuRuGe_2$

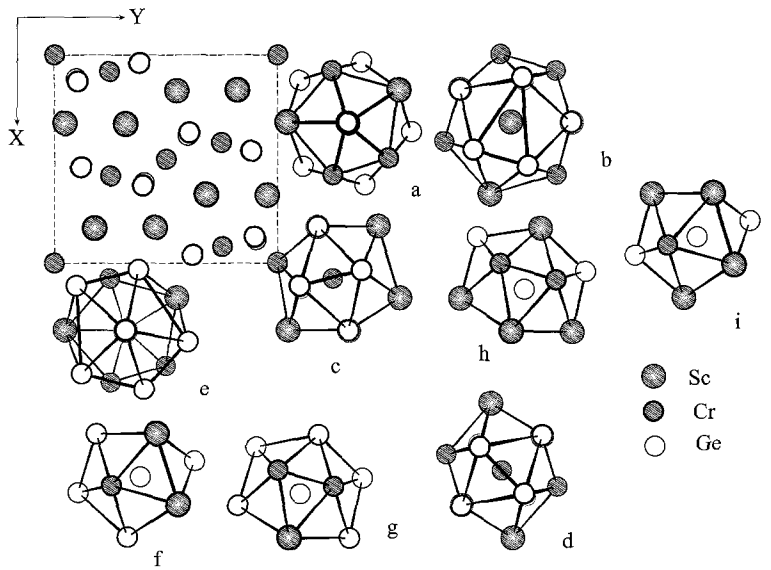

Fig. 40. Projection of the $ScCrGe_2$ unit cell and coordination polyhedra of the atoms: (a,b) Sc, (c,d) Cr, (e–i) Ge.

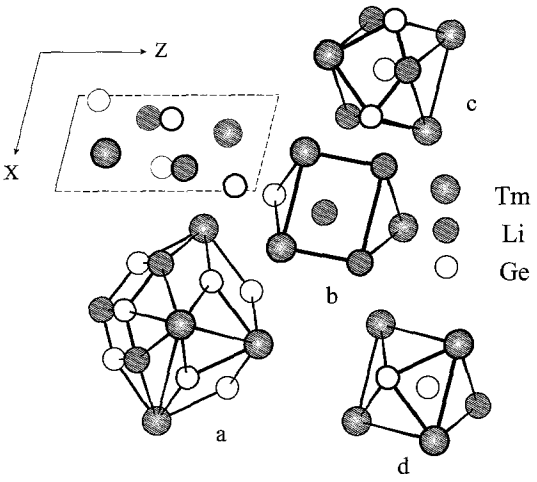

Fig. 41. Projection of the $TmLi_{1-x}Ge_2$ unit cell and coordination polyhedra of the atoms: (a) Tm, (b) Li, (c,d) Ge.

3.14.10. *$TmLi_{1-x}Ge_2$ structure type*

SG $P2_1/m$, $Z=2$, $a=0.4008$, $b=0.3875$, $c=0.8123$, $\beta=104.24°$ (Pavlyuk et al. 1991). See fig. 41.

Atom	Wyckoff notation	*x/a*	*y/b*	*z/c*	G (%)
Tm	2(e)	0.3967	1/4	0.7927	100
Li	2(e)	0.24	1/4	0.38	50
Ge1	2(e)	0.0526	1/4	0.1059	100
Ge2	2(e)	0.7531	1/4	0.5057	100

Isotypic compounds:
$RLi_{1-x}Ge_2$: R = Ho, Er, Lu

3.14.11. *$CaLiSi_2$ structure type*

SG Pnma, $Z=4$, $a=0.7815$, $b=0.3965$, $c=1.0748$ for $CeLiGe_2$ (Pavlyuk et al. 1986)

Atom	Wyckoff notation	*x/a*	*y/b*	*z/c*	G (%)
Ce	4(c)	0.142	1/4	0.364	100
Li	4(c)	0.498	1/4	0.613	100
Ge1	4(c)	0.160	1/4	0.683	100
Ge2	4(c)	0.217	1/4	0.072	100

Isotypic compounds:
$RLiGe_2$: R = La–Gd

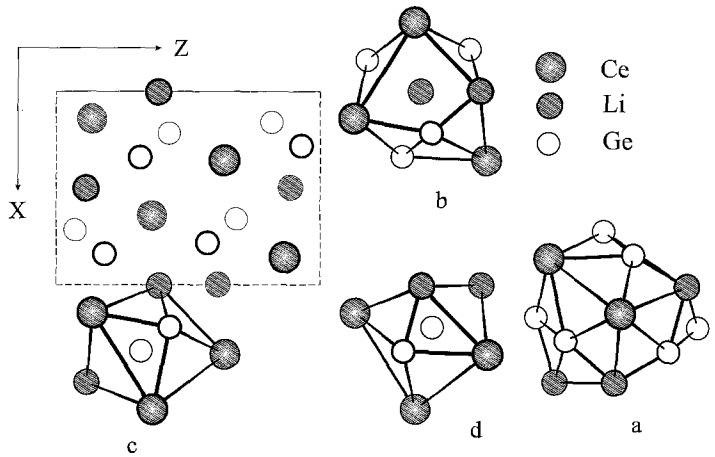

Fig. 42. Projection of the $CeLiGe_2$ unit cell and coordination polyhedra of the atoms: (a) Ce, (b) Li, (c,d) Ge.

The coordination number of cerium atoms is 18 (fig. 42a). Lithium atoms have the coordination polyhedra in the form of deformed cubo-octahedra (fig. 42b). Germanium atoms are situated inside the trigonal prisms with three additional atoms (fig. 42c,d).

3.14.12. *$CeRh_{1-x}Ge_{2+x}$ structure type*

SG Pmmn, $Z=2$, $a=0.4322$, $b=0.4339$, $c=1.7101$ (Shapiev et al. 1991)

Atom	Wyckoff notation	*x/a*	*y/b*	*z/c*	G (%)
Ce1	2(b)	1/4	3/4	0.3633	100
Ce2	2(a)	1/4	1/4	0.8514	100
Rh	2(b)	1/4	3/4	0.5753	100
Ge1	2(b)	1/4	3/4	0.0070	100
Ge2	2(b)	1/4	3/4	0.716	100
X	2(a)	1/4	1/4	0.0631	100
Ge3	2(a)	1/4	1/4	0.205	100
Ge4	2(a)	1/4	1/4	0.4937	100

X=0.35Rh+0.65Ge

Isotypic compound: $SmRh_{1-x}Ge_{2+x}$

The coordination polyhedra with 21 apexes are typical for the cerium atoms (fig. 43a,b). The atoms of rhodium, statistical mixture X (X=0.35Rh+0.65Ge) and germanium are placed inside of trigonal prisms with additional atoms and distorted cubo-octahedra (fig. 43c–h).

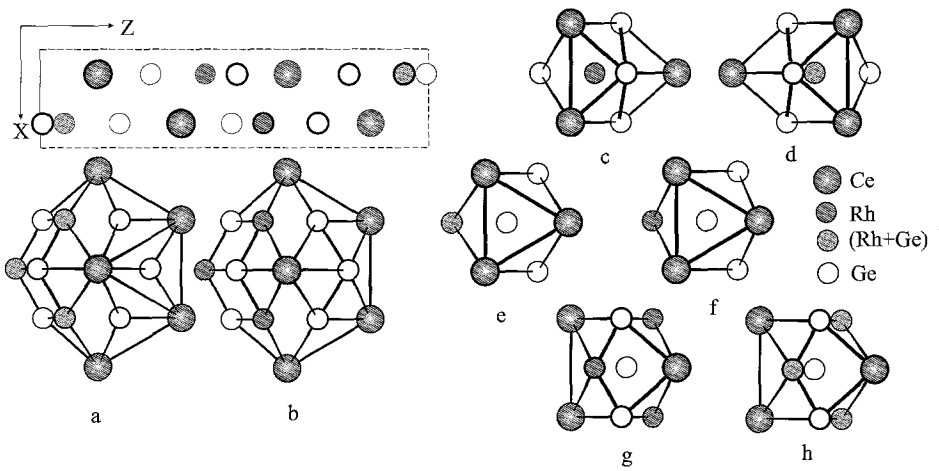

Fig. 43. Projection of the $CeRh_{1-x}Ge_{2+x}$ unit cell and coordination polyhedra of the atoms: (a) Ce, (c–h) Rh, X and Ge.

3.14.13. *$La_3Co_2Sn_7$ structure type*

SG Cmmm, $Z=2$, $a=0.4243$, $b=2.5758$, $c=0.4289$ for $Ce_3Ni_2Ge_7$ (Konyk 1986)

Atom	Wyckoff notation	*x/a*	*y/b*	*z/c*	G (%)
Ce1	4(j)	0	0.3151	1/2	100
Ce2	2(a)	0	0	0	100
Ni	4(i)	0	0.1272	0	100
Ge1	4(j)	0	0.090	1/2	100
Ge2	4(i)	0	0.222	0	100
Ge3	4(i)	0	0.4137	0	100
Ge4	2(c)	1/2	0	1/2	100

Isotypic compound: $Sm_3Co_2Ge_7$

For cerium atoms, polyhedra with 18 and 20 apexes are typical (fig. 44a, b). The nickel atom polyhedra are tetragonal antiprisms with one additional atom (fig. 44c). Those for germanium atoms are trigonal prisms, tetragonal antiprisms and distorted cubo-octahedra (fig. 44d–g).

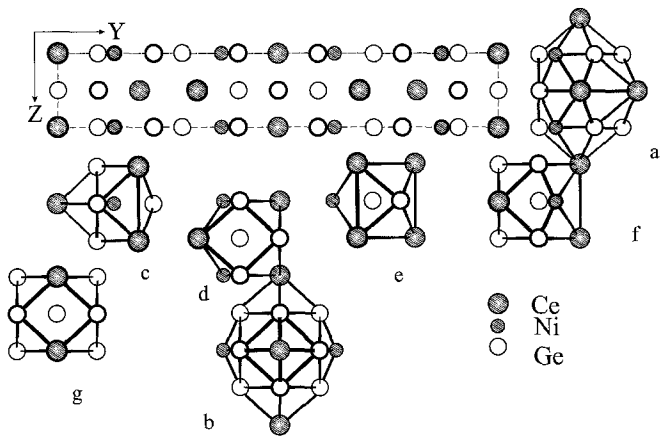

Fig. 44. Projection of the $Ce_3Ni_2Ge_7$ unit cell and coordination polyhedra of the atoms: (a, b) Ce, (c) Ni, (d–g) Ge.

3.14.14. *Ce_2MnGe_5 structure type*

SG Ammm, $Z=2$, $a=0.4308$, $b=0.4170$, $c=2.1134$ (Konyk 1989)

Atom	Wyckoff notation	*x/a*	*y/b*	*z/c*	G (%)
Ce	4(k)	0	1/2	0.1661	100
Ge1	4(l)	1/2	1/2	0.2898	100
Ge2	4(k)	0	1/2	0.4470	100
X	4(l)	1/2	1/2	0.0540	100

X = 0.5Mn+0.5Ge

Isotypic compounds:

R_2LiGe_5: R = Ce–Sm

The coordination polyhedra for the cerium atoms have 18 apexes (fig. 45a). For Ge1 atoms, the coordination polyhedra in the form of trigonal prisms with two additional atoms are typical (fig. 45b). Ge2 and the statistical mixture X (X = 0.5Mn+0.5Ge) are situated in the centres of trigonal prisms with one additional atoms (fig. 45c, d).

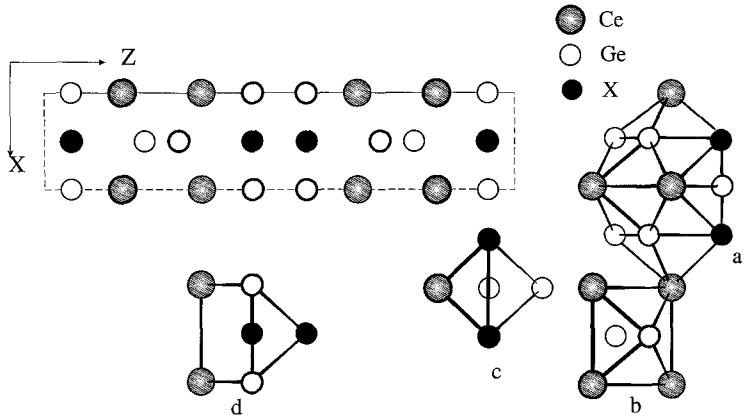

Fig. 45. Projection of the Ce_2MnGe_5 unit cell and coordination polyhedra of the atoms: (a) Ce, (b) Ge1, (c, d) Ge2 and X.

3.15. *$R_5(M, Ge)_{14}$ and $R_4(M, Ge)_{11}$ compounds*

3.15.1. *$Sc_5Co_4Si_{10}$ structure type*

SG P4/mbm, $Z=2$, $a=1.29336$, $c=0.42596$ for $Ho_5Rh_4Ge_{10}$ (Gladyshevsky et al. 1992a)

Atom	Wyckoff notation	*x/a*	*y/b*	*z/c*	G (%)
Ho1	4(h)	0.17458	0.67458	1/2	100
Ho2	4(h)	0.61279	0.11279	1/2	100
Ho3	2(a)	0	0	0	100
Rh	8(i)	0.2455	0.0210	0	100
Ge1	8(j)	0.1586	0.0027	1/2	100
Ge2	8(i)	0.1615	0.1997	0	100
Ge3	4(g)	0.0669	0.5669	0	100

Isotypic compounds:
$R_5Co_4Ge_{10}$: R = Tm–Lu
$R_5Rh_4Ge_{10}$: R = Y, Gd–Lu
$R_5Os_4Ge_{10}$: R = Y, Dy–Tm

The coordination numbers for holmium atoms are 17, 18 and 20 (fig. 46a–c). Rhodium atoms have coordination polyhedra in the form of trigonal prisms with four additional atoms (fig. 46d). Germanium atoms are situated inside the trigonal prisms with three additional atoms and deformed cubo-octahedra (fig. 46e–g).

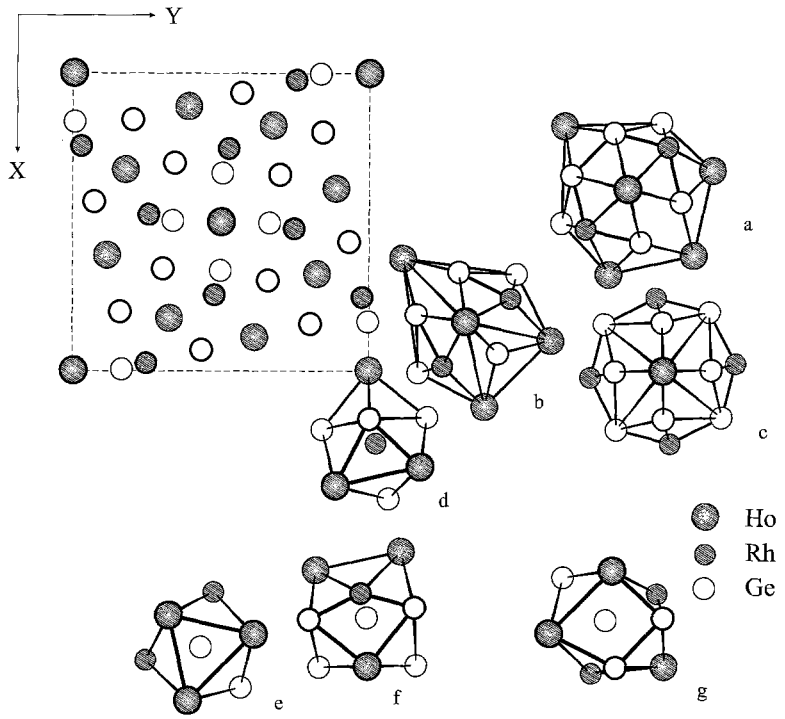

Fig. 46. Projection of the $Ho_5Rh_4Ge_{10}$ unit cell and coordination polyhedra of the atoms: (a–c) Ho, (d) Rh, (e–g) Ge.

3.15.2. *$Zr_4Co_4Ge_7$ structure type*

SG I4/mmm, $Z=4$, $a=1.3215$, $c=0.5229$ for $Sc_4Co_4Ge_{7-x}$ (Andrusyak 1988). See fig. 47.

Atom	Wyckoff notation	*x/a*	*y/b*	*z/c*	G (%)
Sc1	8(i)	0.1966	0	0	100
Sc2	8(h)	0.3608	0.3608	0	100
Co	16(k)	0.1483	0.6483	1/4	100
Ge1	8(j)	0.2080	1/2	0	100
Ge2	8(i)	0.4071	0	0	100
Ge3	8(h)	0.2069	0.2069	0	100
Ge4	4(e)	0	0	0.250	100

Isotypic compounds:
$Sc_4M_4Ge_{7-x}$: M=Fe, Ni

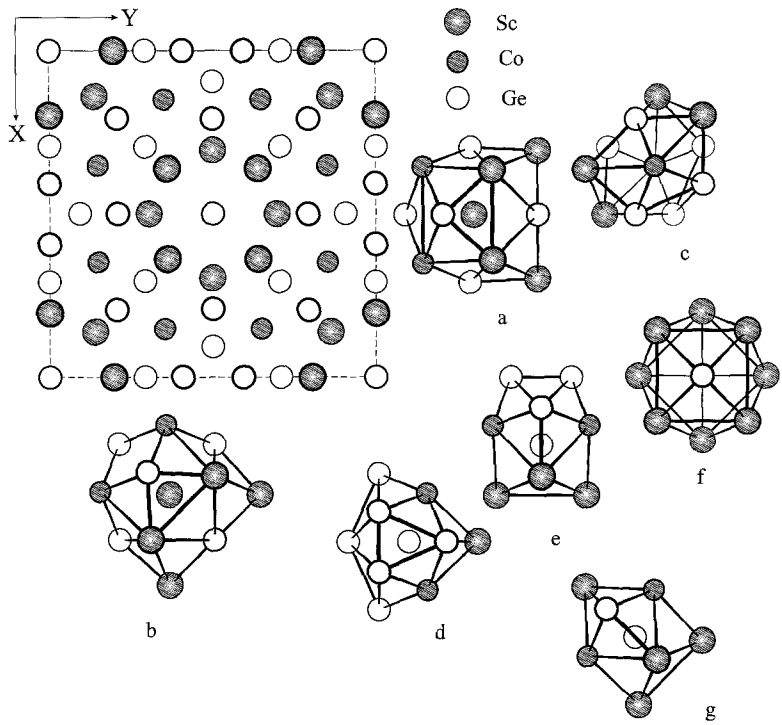

Fig. 47. Projection of the $Sc_4Co_4Ge_7$ unit cell and coordination polyhedra of the atoms: (a,b) Sc, (c) Co, (d–g) Ge.

3.15.3. *$La_4Ga_4Ge_7$ structure type*

SG Pmmm, $a=0.8414$, $b=0.8620$, $c=3.109$ for $Ce_4Ga_4Ge_7$ (Gryniv et al. 1989)

Atomic coordinates for the germanides of this structure type were not presented.

Isotypic compounds:

$R_4Ga_4Ge_7$: R = La, Nd

3.16. *$R_3(M, Ge)_8$ compounds*

3.16.1. *$Gd_3Cu_4Ge_4$ structure type*

SG Immm, $Z=2$, $a=0.4223$, $b=0.6655$, $c=1.4000$ (Rieger 1970)

Atom	Wyckoff notation	*x/a*	*y/b*	*z/c*	G (%)
Gd1	4(j)	1/2	0	0.36884	100
Gd2	2(a)	0	0	0	100
Cu	8(l)	0	0.31067	0.33048	100

Ge1	4(i)	0	0	0.21567	100
Ge2	4(h)	0	0.18902	1/2	100

Isotypic compounds:
$R_3Mn_4Ge_4$: R = Gd, Tb
$R_3Fe_4Ge_4$: R = Dy–Tm, Lu
$Sc_3Ni_4Ge_4$
$R_3Cu_4Ge_4$: R = Sc, Y, Pr–Sm, Gd–Lu
$R_3Ag_4Ge_4$: R = Pr–Sm, Gd
$R_3Pd_4Ge_4$: R = Y, Gd–Tm

The coordination numbers for the Gd atoms are 20 and 19 (fig. 48a, b). The coordination polyhedra for the Cu atoms are distorted cubo-octahedra (fig. 48c); those for Ge atoms are trigonal prisms with additional atoms (fig. 48d, e).

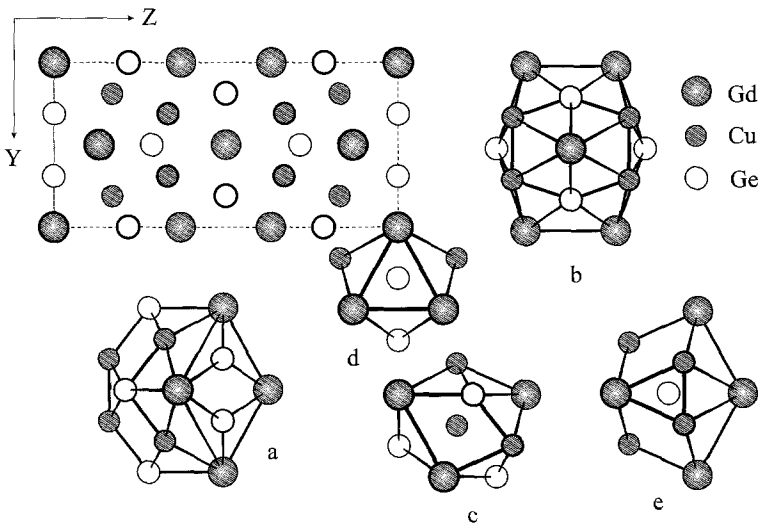

Fig. 48. Projection of the $Gd_3Cu_4Ge_4$ unit cell and coordination polyhedra of the atoms: (a, b) Gd, (c) Cu, (d, e) Ge.

3.16.2. *$U_3Ni_4Si_4$ structure type*
SG Immm, $Z = 2$, $a = 0.42234$, $b = 0.42295$, $c = 2.4156$ for $La_3Ni_4Ge_4$ (Bruskov 1984)

Atom	Wyckoff notation	*x/a*	*y/b*	*z/c*	G (%)
La1	4(j)	1/2	0	0.3494	100
La2	2(a)	0	0	0	100
Ni1	4(j)	1/2	0	0.0989	100

Ni2	4(i)	0	0	0.2490	100
Ge1	4(j)	1/2	0	0.2000	100
Ge2	4(i)	0	0	0.446	100

Isotypic compounds:
$R_3Ni_4Ge_4$: R = Ce, Pr
$R_3Rh_4Ge_4$: R = La

The coordination polyhedra for the lanthanum atoms have 20 and 21 apexes (fig. 49a, b). For nickel atoms, the coordination polyhedra are typically trigonal prisms and distorted cubo-octahedra (fig. 49c, d). Germanium atoms are situated in the centres of trigonal prisms and tetragonal antiprism (fig. 49e, f).

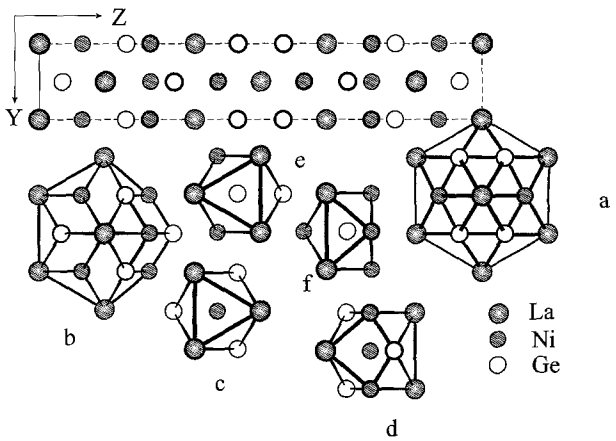

Fig. 49. Projection of the $La_3Ni_4Ge_4$ unit cell and coordination polyhedra of the atoms: (a, b) La, (c, d) Ni, (e, f) Ge.

3.17. *$R_2(M, Ge)_5$ compounds*

3.17.1. *$Ce_2Li_2Ge_3$ structure type*

SG Cmcm, $Z = 4$, $a = 0.44795$, $b = 1.8846$, $c = 0.69570$ (Pavlyuk et al. 1988b). See fig. 50.

Atom	Wyckoff notation	*x/a*	*y/b*	*z/c*	G (%)
Ce1	4(c)	0	0.4484	1/4	100
Ce2	4(c)	0	0.6583	1/4	100
Li	8(f)	0	0.1910	0.559	100

Ge1	8(f)	0	0.0611	0.0688	100
Ge2	4(c)	0	0.2801	1/4	100

Isotypic compounds:
$R_2Li_2Ge_3$: R = La–Sm

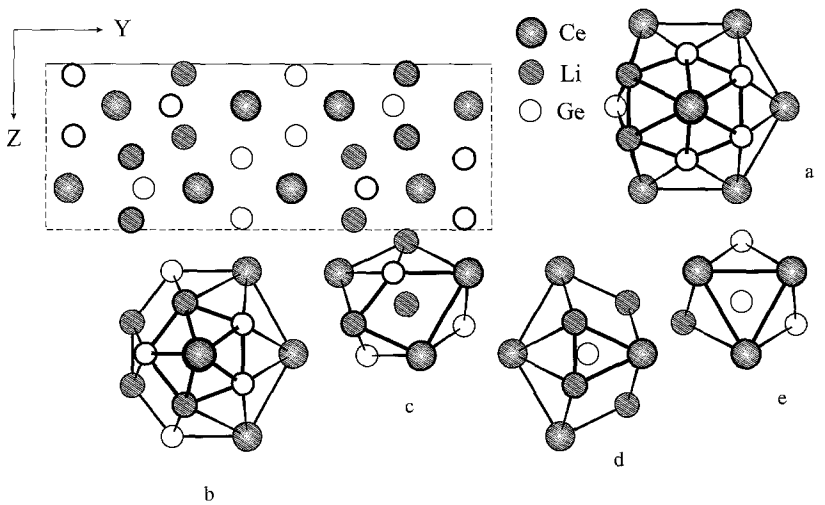

Fig. 50. Projection of the $Ce_2Li_2Ge_3$ unit cell and coordination polyhedra of the atoms: (a,b) Ce, (c) Li, (d,e) Ge.

3.17.2. *$Tm_2Ga_{0.5}Ge_{4.5}$ structure type*
SG Pmmm, $Z = 2$, $a = 0.3915$, $b = 0.4048$, $c = 1.8209$ (Gryniv and Myakush 1989)

Atom	Wyckoff notation	*x/a*	*y/b*	*z/c*	G (%)
Tm1	2(b)	1/4	3/4	0.6920	100
Tm2	2(a)	1/4	1/4	0.1275	100
X	2(b)	1/4	3/4	0.2626	100
X	2(b)	1/4	3/4	0.8000	100
X	2(a)	1/4	1/4	0.8381	100
X	2(a)	1/4	1/4	0.5675	100
X	2(a)	1/4	1/4	0.4287	100

X = 0.9Ge+0.1Ga
No isotypic compounds are observed.

3.18. *$R_3(M, Ge)_7$ and $R_9(M, Ge)_{20}$ compounds*

3.18.1. *$Nd_6Fe_{13}Si$ structure type*

SG I4/mcm, $Z=4$, $a=0.80710$, $c=2.3085$ for $Pr_6Fe_{13}Ge$ (Fedyna and Pecharsky 1989). See fig. 51.

Atom	Wyckoff notation	*x/a*	*y/b*	*z/c*	G (%)
Pr1	16(l)	0.1658	0.6658	0.1900	100
Pr2	8(f)	0	0	0.1094	100
Fe1	16(l)	0.1780	0.6780	0.0597	100
Fe2	16(l)	0.616	0.116	0.0955	100
Fe3	16(k)	0.065	0.212	0	100
Fe4	4(d)	0	1/2	0	100
Ge	4(a)	0	0	1/4	100

Isotypic compound: $Nd_6Fe_{13}Ge$

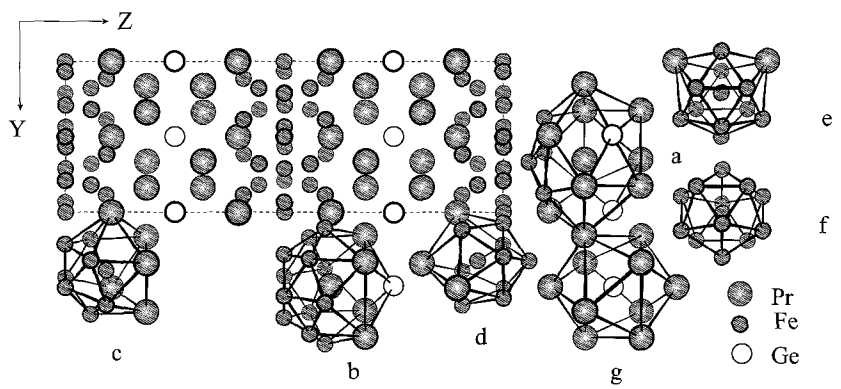

Fig. 51. Projection of the $Pr_6Fe_{13}Ge$ unit cell and coordination polyhedra of the atoms: (a, b) Pr, (c–f) Fe, (g) Ge.

3.18.2. *$Tm_9Fe_{10}Ge_{10}$ structure type*

SG Immm, $Z=2$, $a=0.5386$, $b=1.3306$, $c=1.3916$ (Pecharsky et al. 1987). See fig. 52.

Atom	Wyckoff notation	*x/a*	*y/b*	*z/c*	G (%)
Tm1	8(l)	0.1462	0.3644	0	100
Tm2	4(j)	0	0.3052	1/2	100
Tm3	4(g)	0.2836	0	0	100

Tm4	2(a)	0	0	0	100
Fe1	16(o)	0.1438	0.1541	0.2522	100
Fe2	4(j)	0	0.0904	1/2	100
Ge1	8(l)	0.2905	0.2049	0	100
Ge2	4(i)	0	0.2099	0	100
Ge3	4(h)	0.3252	1/2	0	100
Ge4	4(f)	1/2	0	0.249	100

Isotypic compounds:
$R_9Fe_{10}Ge_{10}$: R = Er, Yb

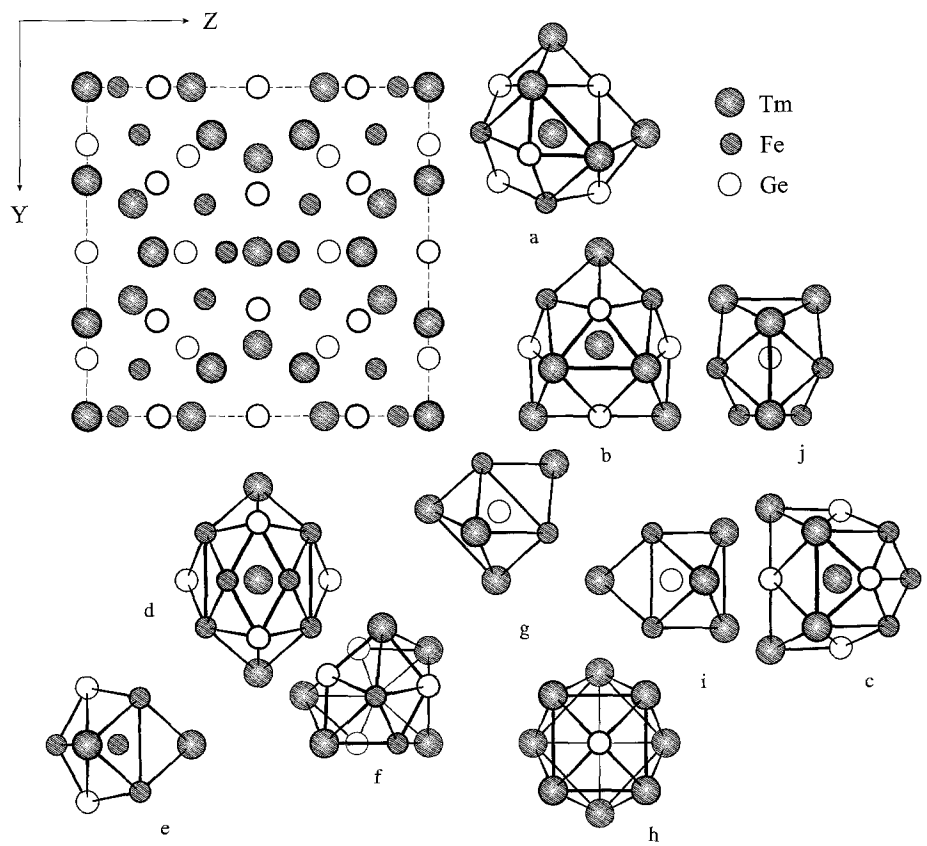

Fig. 52. Projection of the $Tm_9Fe_{10}Ge_{10}$ unit cell and coordination polyhedra of the atoms: (a–d) Tm, (e, f) Fe, (g–j) Ge.

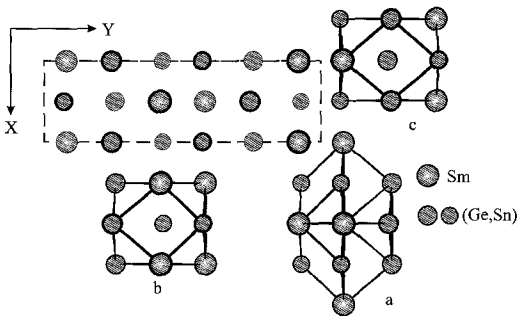

Fig. 53. Projection of the $SmSn_{1.5}Ge_{0.5}$ unit cell and coordination polyhedra of the atoms: (a) Sm, (b,c) X.

3.19. *R(M, Ge)$_2$ compounds*

3.19.1. *$ZrSi_2$ structure type*

SG Cmcm, $Z=4$, $a=0.4502$, $b=1.5367$, $c=0.4502$ for $SmSn_{1.5}Ge_{0.5}$ (Stetskiv 1999). See fig. 53.

Atom	Wyckoff notation	*x/a*	*y/b*	*z/c*	G (%)
Sm	4(c)	0	0.0811	1/4	100
X	4(c)	0	0.4280	1/4	100
X	4(c)	0	0.7579	1/4	100

X=0.25Ge+0.75Sn

Isotypic compounds:

$RSn_{1.5}Ge_{0.5}$: R=La–Pr

3.19.2. *$MgZn_2$ structure type*

SG $P6_3/mmc$, $Z=4$, $a=0.5006$, $c=0.8150$ for Sc_2Fe_3Ge (Andrusyak 1988)

Atomic coordinates have not been determined.

3.19.3. *$MgCu_2$ structure type*

SG Fd3m, $Z=8$, $a=0.7063$ for $Sc(Sc,Fe,Ge)_2$ (Andrusyak 1988)

Atomic coordinates have not been determined.

3.19.4. *Y_2Rh_3Ge structure type*

SG $R\bar{3}m$, $Z=3$, $a=0.5552$, $c=1.182$ for Y_2Rh_3Ge (Cenzual et al. 1987)

Atom	Wyckoff notation	*x/a*	*y/b*	*z/c*	G (%)
Y	6(c)	0	0	0.3718	100

Rh	9(d)	1/2	0	1/2	100
Ge	3(a)	0	0	0	100

Isotypic compounds:
R_2Rh_3Ge: R = Pr, Er

3.19.5. *PbFCl structure type*

SG P4/nmm, $Z = 2$, $a = 0.4170$, $c = 0.6865$ for CeCoGe (Welter et al. 1993)

Atom	Wyckoff notation	*x/a*	*y/b*	*z/c*	G (%)
Ce	2(c)	1/4	1/4	0.67	100
Co	2(a)	3/4	1/4	0	100
Ge	2(c)	1/4	1/4	0.19	100

Isotypic compounds:
RTiGe: R = Y, Gd–Tm
RMnGe: R = La–Sm
CeFeGe
RCoGe: R = La–Nd
RRuGe: R = La–Sm

For cerium atoms, polyhedra with 18 apexes are typical (fig. 54a). The cobalt atom polyhedra are distorted cubo-octahedra (fig. 54b). Those for germanium atoms are tetragonal antiprisms with one additional atom (fig. 54c).

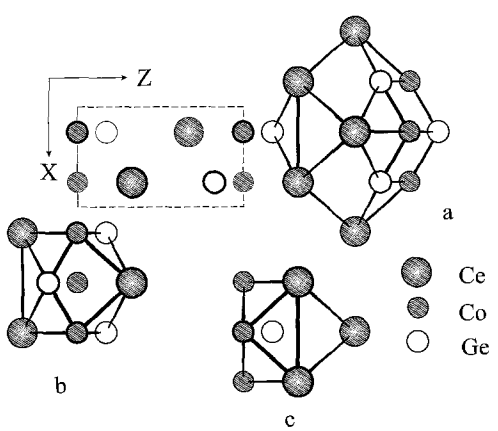

Fig. 54. Projection of the CeCoGe unit cell and coordination polyhedra of the atoms: (a) Ce, (b) Co, (c) Ge.

3.19.6. *CeScSi structure type*

SG I4/mmm, $Z=4$, $a=0.4314$, $c=1.5913$ for CeScGe (Shpyrka 1990)

Atom	Wyckoff notation	*x/a*	*y/b*	*z/c*	G (%)
Ce	4(e)	0	0	0.326	100
Sc	4(c)	0	1/2	0	100
Ge	2(e)	0	0	0.124	100

Isotypic compounds:
RScGe: R = La–Eu

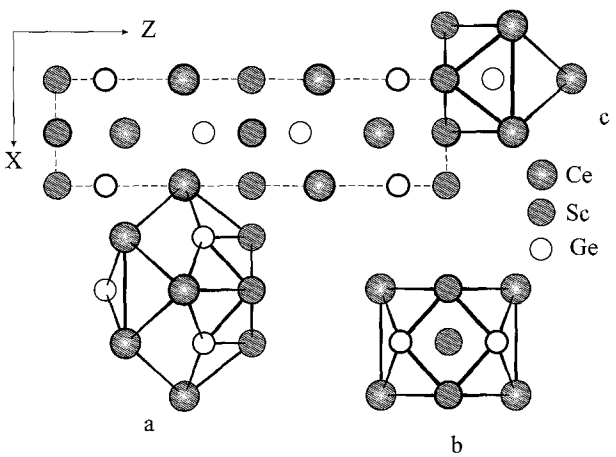

Fig. 55. Projection of the CeScGe unit cell and coordination polyhedra of the atoms: (a) Ce, (b) Sc, (c) Ge.

The coordination polyhedra for cerium atoms have 17 apexes (fig. 55a). Scandium atoms are situated in the centres of the cubo-octahedra (fig. 55b). The coordination polyhedra in the form of tetragonal antiprism with one additional atom are typical for the germanium atoms (fig. 55c).

3.19.7. *AlB_2 structure type*

SG P6/mmm, $Z=1$, $a=0.4277$, $c=0.3881$ for NdCuGe (Salamakha 1986)

Atom	Wyckoff notation	*x/a*	*y/b*	*z/c*	G (%)
Nd	1(a)	0	0	0	100
X	2(d)	1/3	2/3	1/2	100

X = 0.5Cu+0.5Ge

Isotypic compounds:
$RFe_{0.67}Ge_{1.33}$: R = La, Nd, Sm
$RCo_{0.5}Ge_{1.5}$: R = Ce–Nd
$RNi_{0.6}Ge_{1.4}$: R = La–Yb
$RCu_{0.7}Ge_{1.3}$: R = Y, La–Sm, Gd–Tm
RCuGe: R = La–Gd
$RZn_{1.5}Ge_{0.5}$: R = La–Sm
$RRh_{0.5}Ge_{1.5}$: R = Ce, Nd, Sm
$RPd_{0.6}Ge_{1.4}$: R = Ce, Nd, Sm, Ho, Yb
$RAg_{0.7}Ge_{1.3}$: R = Ce–Nd
$RIr_{0.5}Ge_{1.5}$: R = Nd
$RPt_{0.6}Ge_{1.4}$: R = Ce, Nd, Sm, Ho
$RAu_{0.7}Ge_{1.3}$, R = Ce, Nd, Yb

The coordination polyhedra of the neodymium atoms have 18 apexes (fig. 56a). Those of the statistical mixture X (X = 0.5Cu+0.5Ge) are trigonal prisms with three additional atoms (fig. 56b).

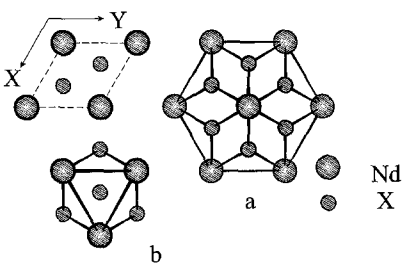

Fig. 56. Projection of the NdCuGe unit cell and coordination polyhedra of the atoms: (a) Nd, (b) X.

3.19.8. *$CaIn_2$ structure type*

SG $P6_3/mmc$, $Z = 2$, $a = 0.42491$, $c = 0.73111$ for TbCuGe (Baran et al. 1996)

Atom	Wyckoff notation	*x/a*	*y/b*	*z/c*	G (%)
Tb	2(b)	0	0	1/4	100
X	4(f)	1/3	2/3	0.0212	100

X = 0.5Cu+0.5Ge
Isotypic compounds:
RCuGe: R = Tb–Er

3.19.9. *LiGaGe (or NdPtSb) structure type*

SG $P6_3mc$, $Z=2$, $a=0.45587$, $c=0.78969$ for LaAgGe (Pecharsky et al. 1991)

Atom	Wyckoff notation	*x/a*	*y/b*	*z/c*	G (%)
La	2(a)	0	0	0.000	100
Ag	2(b)	1/3	2/3	0.2514	100
Ge	2(b)	1/3	2/3	0.7082	100

Isotypic compounds:
RAgGe: R = Ce, Pr
RAuGe: R = Sc, Y, La–Sm, Gd–Lu

The coordination polyhedra of the lanthanum atoms have 14 apexes (fig. 57a). Those for silver and germanium atoms are trigonal prisms with additional atoms (fig. 57b,c).

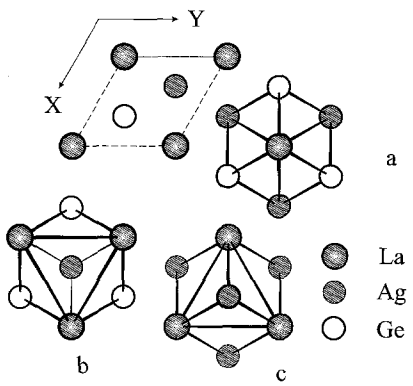

Fig. 57. Projection of the LaAgGe unit cell and coordination polyhedra of the atoms: (a) La, (b,c) Ag and Ge.

3.19.10. *KHg_2 structure type*

SG Imma, $Z=4$, $a=0.4366$, $b=0.6956$, $c=0.7596$ for HoPdGe (Sologub and Salamakha 1999)

Atom	Wyckoff notation	*x/a*	*y/b*	*z/c*	G (%)
Ho	4(e)	0	1/4	0.5402	100
X	8(h)	0	0.0473	0.1651	100

X = 0.5Pd+0.5Ge
Isotypic compounds:
RPdGe: R = Y, La–Sm, Gd–Tm
RPtGe: R = Ce–Nd

The coordination polyhedra for holmium atoms have 18 apexes (fig. 58a). The statistical mixture X (X = 0.5Pd+0.5Ge) occupies the centre of trigonal prism with four additional atoms (fig. 58b).

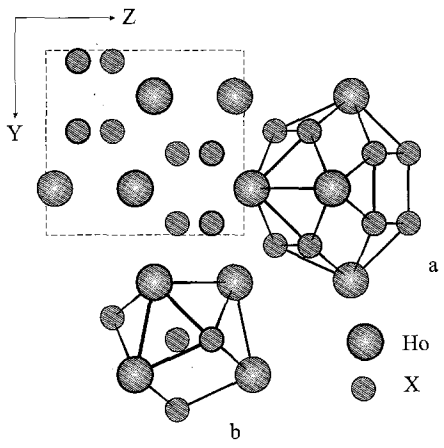

Fig. 58. Projection of the HoPdGe unit cell and coordination polyhedra of the atoms: (a) Ho, (b) X.

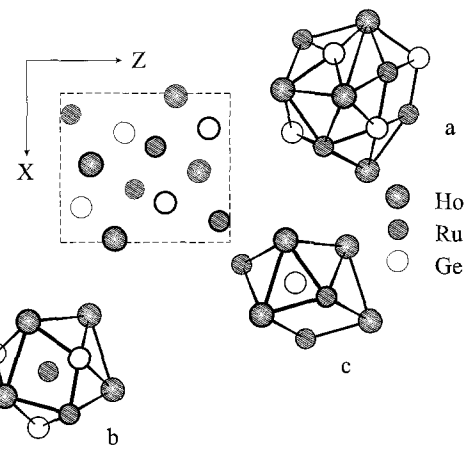

Fig. 59. Projection of the HoRuGe unit cell and coordination polyhedra of the atoms: (a) Ho, (b) Ru, (c) Ge.

3.19.11. *TiNiSi structure type*

SG Pnma, $Z = 4$, $a = 0.6980$, $b = 0.4351$, $c = 0.7281$ for HoRuGe (Sologub et al. 1993)

Atom	Wyckoff notation	*x/a*	*y/b*	*z/c*	G (%)
Ho	4(c)	0.00850	1/4	0.69089	100
Ru	4(c)	0.1562	1/4	0.0638	100
Ge	4(c)	0.2042	1/4	0.3771	100

Isotypic compounds:
RCoGe: R = Sc, Y, Sm, Gd–Lu
RNiGe: R = Sc, Y, Ce–Sm, Gd–Lu
RRuGe: R = Gd–Tm
RRhGe: R = Sc, Y, Ce–Sm, Gd–Tm
RIrGe: R = Sc, Y, Ce–Sm, Gd–Tm
RPtGe: R = Sc, Y, Sm, Gd–Tm

The polyhedra with 18 apexes are typical for the holmium atoms (fig. 59a). The polyhedra for ruthenium atoms are deformed cubo-octahedra (fig. 59b). The germanium coordination polyhedra are trigonal prisms with four additional atoms (fig. 59c).

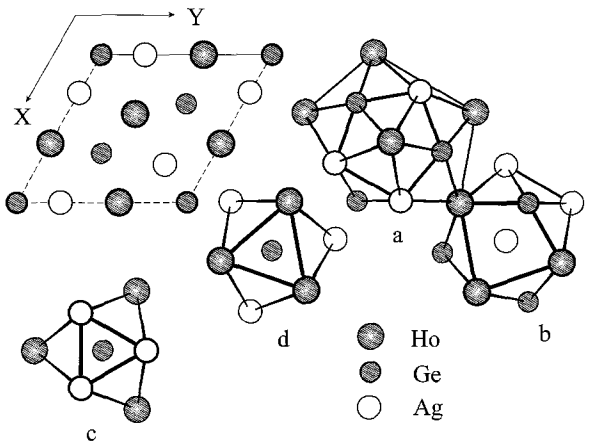

Fig. 60. Projection of the HoAgGe unit cell and coordination polyhedra of the atoms: (a) Ho, (b) Ag, (c, d) Ge.

3.19.12. *ZrNiAl structure type*

SG $P\bar{6}2m$, $Z=3$, $a=0.7084$, $c=0.4179$ for HoAgGe (Sologub and Protsyk 1991)

Atom	Wyckoff notation	*x/a*	*y/b*	*z/c*	G (%)
Ho	3(f)	0.5883	0	0	100
Ag	3(g)	0.255	0	1/2	100
Ge1	2(d)	1/3	2/3	1/2	100
Ge2	1(a)	0	0	0	100

Isotypic compounds:
RLiGe: R = Y, Pr–Sm, Gd–Lu
RAgGe: R = Sc, Y, Sm, Gd–Lu
$RAg_{1+x}Ge_{1-x}$: R = Pr, Nd
ScMGe: M = Cu, Ru, Rh, Pd, Os

For holmium atoms, polyhedra with 17 apexes are typical (fig. 60a). The silver atom polyhedra are distorted cubo-octahedra (fig. 60b). The trigonal prisms with three additional atoms are the polyhedra for germanium atoms (fig. 60c, d).

3.19.13. *LaPtSi structure type*

SG $I4_1md$, $Z=4$, $a=0.42663$, $c=1.4970$ for LaPtGe (Hovestreydt et al. 1982)

Atom	Wyckoff notation	*x/a*	*y/b*	*z/c*	G (%)
La	4(a)	0	0	0.581	100
Pt	4(a)	0	0	0.1660	100
Ge	4(a)	0	0	0.000	100

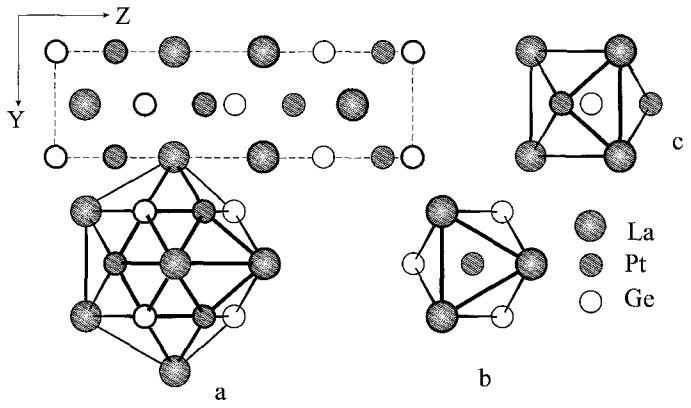

Fig. 61. Projection of the LaPtGe unit cell and coordination polyhedra of the atoms: (a) La, (b,c) Pt and Ge.

Isotypic compound: LaIrGe

The coordination polyhedra of lanthanum have 20 apexes (fig. 61a). The trigonal prisms with three additional atoms are the polyhedra for platinum and germanium atoms (fig. 61b,c).

3.19.14. *ZrOS (or LaIrSi) structure type*

SG $P2_13$, $Z=4$, $a=0.65463$ for EuPtGe (Pöttgen et al. 1996)

Atom	Wyckoff notation	*x/a*	*y/b*	*z/c*	G (%)
Eu	4(a)	0.13207	0.13207	0.13207	100
Pt	4(a)	0.41819	0.41819	0.41819	100
Ge	4(a)	0.83351	0.83351	0.83351	100

No isotypic compounds are observed.

For europium atoms, polyhedra with 20 apexes are typical (fig. 62a). The platinum and germanium atoms polyhedra have 10 apexes (fig. 62b,c).

3.19.15. *EuNiGe structure type*

SG $P2_1/c$, $Z=4$, $a=0.6158$, $b=0.6187$, $c=0.7581$, $\beta=119.83°$ (Oniskovetz et al. 1987). See fig. 63.

Atom	Wyckoff notation	*x/a*	*y/b*	*z/c*	G (%)
Eu	4(e)	0.3014	0.6394	0.1071	100
Ni	4(e)	0.1115	0.0957	0.1755	100
Ge	4(e)	0.2285	0.3564	0.4268	100

Isotypic compound: EuPdGe

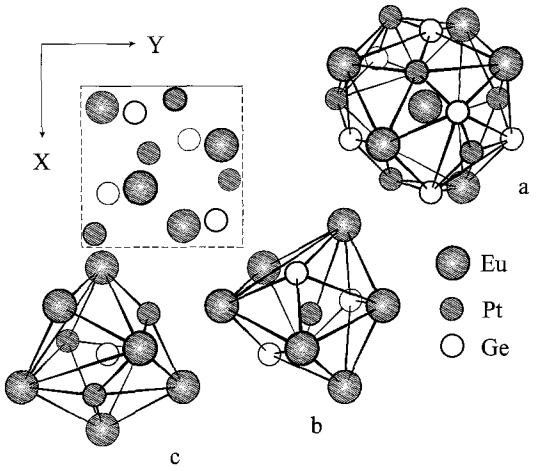

Fig. 62. Projection of the EuPtGe unit cell and coordination polyhedra of the atoms: (a) Eu, (b,c) Pt and Ge.

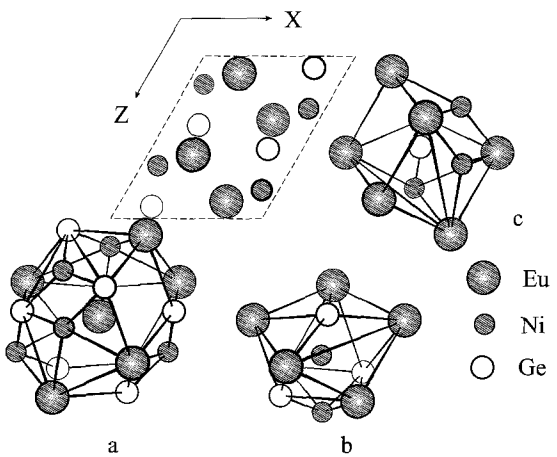

Fig. 63. Projection of the EuNiGe unit cell and coordination polyhedra of the atoms: (a) Eu, (b) Ni, (c) Ge.

3.19.16. *DyAlGe structure type*

SG $Cmc2_1$, $Z=4$, $a=0.4091$, $b=1.046$, $c=0.5874$ (Yanson 1975)

Atom	Wyckoff notation	*x/a*	*y/b*	*z/c*	G (%)
Dy	4(a)	0	0.0189	0.0000	100
Al	4(a)	0	0.4525	0.1470	100
Ge	4(a)	0	0.2524	0.4500	100

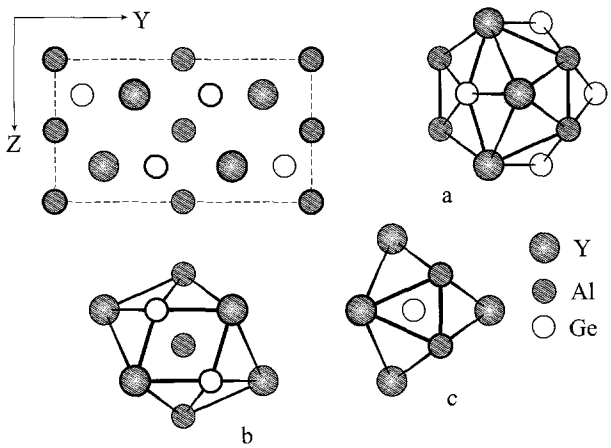

Fig. 64. Projection of the YAlGe unit cell and coordination polyhedra of the atoms: (a) Y, (b) Al, (c) Ge.

3.19.17. *YAlGe structure type*

SG Cmcm, $Z=4$, $a=0.40504$, $b=1.0440$, $c=0.57646$ (Zhao and Parthé 1990b)

Atom	Wyckoff notation	*x/a*	*y/b*	*z/c*	G (%)
Y	4(c)	0	0.3099	1/4	100
Al	4(a)	0	0	0	100
Ge	4(c)	0	0.6058	1/4	100

Isotypic compounds:

RAlGe: R = Gd–Tm

Polyhedra with 17 apexes are typical for the yttrium atoms (fig. 64a). Atoms of aluminium are situated inside the distorted cubo-octahedra (fig. 64b). The germanium atoms coordination polyhedra are trigonal prisms with three additional atoms (fig. 64c).

3.19.18. *EuAuGe structure type*

SG Imm2, $Z=4$, $a=0.4601$, $b=0.7371$, $c=0.7888$ (Pöttgen 1995a)

Atom	Wyckoff notation	*x/a*	*y/b*	*z/c*	G (%)
Eu1	2(a)	0	0	0.62735	100
Eu2	2(b)	0	1/2	0.70640	100
Au	4(d)	0	0.21432	0.00243	100
Ge	4(d)	0	0.31235	0.33353	100

Isotypic compound: $YbAu_{1.24}Ge_{0.76}$

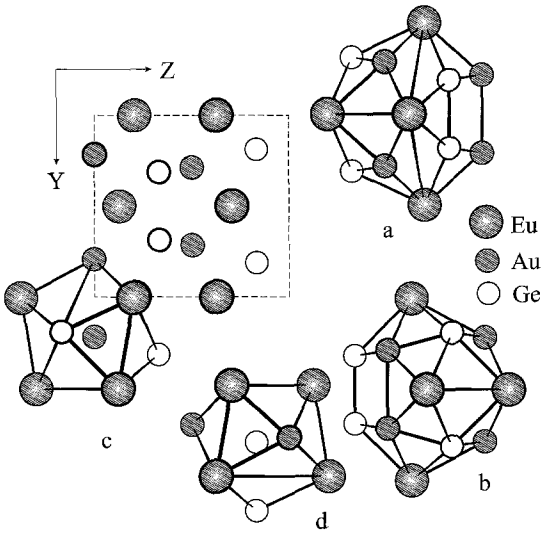

Fig. 65. Projection of the EuAuGe unit cell and coordination polyhedra of the atoms: (a, b) Eu, (c, d) Au and Ge.

For europium atoms, polyhedra with 18 apexes are typical (fig. 65a, b). The atoms of gold and germanium are situated inside the trigonal prisms with additional atoms (fig. 65c, d).

3.19.19. *CaCuGe structure type*

SG $Pna2_1$, $a=2.209$, $b=0.7543$, $c=0.4453$ for EuCuGe (Iandelli 1993)

Atomic coordinates for the rare-earth germanides of this structure type were not presented.

3.19.20. *α-YbAuGe structure type*

SG Pnma, $Z=12$, $a=2.1332$, $b=0.4485$, $c=0.7708$ (Merlo et al. 1998)

Atom	Wyckoff notation	*x/a*	*y/b*	*z/c*	G (%)
Yb1	4(c)	0.0005	1/4	0.7094	100
Yb2	4(c)	0.1663	1/4	0.7842	100
Yb3	4(c)	0.3331	1/4	0.7132	100
Au1	4(c)	0.0936	1/4	0.4153	100
Au2	4(c)	0.2380	1/4	0.4138	100
Au3	4(c)	0.4317	1/4	0.4186	100
Ge1	4(c)	0.0703	1/4	0.083	100
Ge2	4(c)	0.2714	1/4	0.082	100
Ge3	4(c)	0.3990	1/4	0.096	100

3.19.21. *β-YbAuGe structure type*

SG Pnma, $Z=12$, $a=2.1311$, $b=0.4481$, $c=0.7704$ for $YbAu_{1.03}Ge_{0.97}$ (Merlo et al. 1998)

Atom	Wyckoff notation	*x/a*	*y/b*	*z/c*	G (%)
Yb1	4(c)	0.0005	1/4	0.7127	100
Yb2	4(c)	0.1663	1/4	0.7864	100
Yb3	4(c)	0.3336	1/4	0.7126	100
Au	4(c)	0.2379	1/4	0.4172	100
Ge	4(c)	0.2701	1/4	0.083	100
X1	4(c)	0.0941	1/4	0.4162	100
X2	4(c)	0.4309	1/4	0.4123	100
X3	4(c)	0.0705	1/4	0.086	100
X4	4(c)	0.3983	1/4	0.0843	100

X1 = 0.69Au+0.31Ge; X2 = 0.56Au+0.44Ge; X3 = X4 = 0.43Au+0.57Ge

3.19.22. *LuNiGe structure type*

SG Cmcm, $Z=16$, $a=0.4116$, $b=2.2334$, $c=0.9194$ (Koterlyn et al. 1994)

Atom	Wyckoff notation	*x/a*	*y/b*	*z/c*	G (%)
Lu1	8(f)	0	0.58908	0.0645	100
Lu2	4(c)	0	0.72747	1/4	100
Lu3	4(c)	0	0.88557	1/4	100
Ni1	8(f)	0	0.1957	0.0184	100
Ni2	4(c)	0	0.0305	1/4	100
Ni3	4(a)	0	0	0	100
Ge1	8(f)	0	0.3020	0.1061	100
Ge2	4(c)	0	0.1399	1/4	100
Ge3	4(c)	0	0.4757	1/4	100

Isotypic compound: TmNiGe

For luthetium atoms, polyhedra with 18 and 19 apexes are typical (fig. 66a–c). Those for nickel and germanium atoms are trigonal prisms with additional atoms and distorted cubo-octahedra (fig. 66d–i).

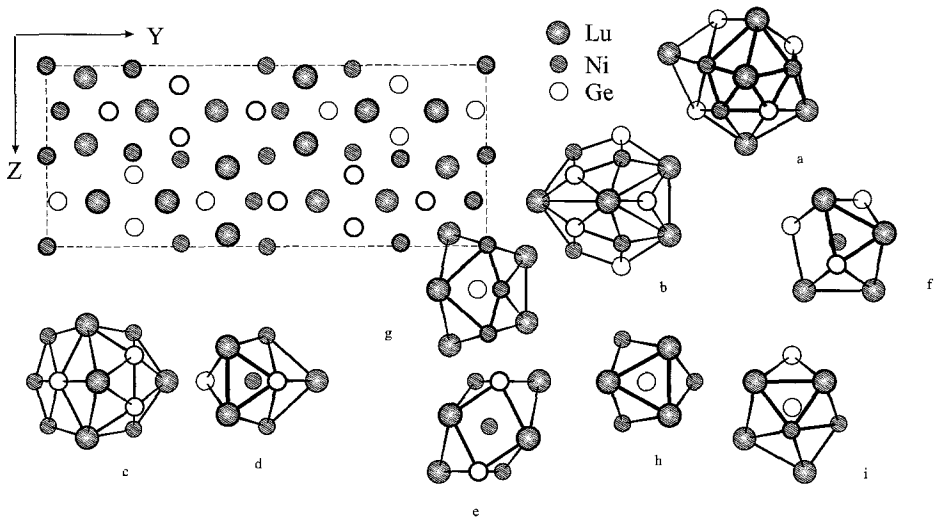

Fig. 66. Projection of the LuNiGe unit cell and coordination polyhedra of the atoms: (a–c) Lu, (d–i) Ni, Ge.

3.19.23. *ZrBeSi structure type*

SG $P6_3/mmc$, $Z=2$, $a=0.4372$, $c=0.8604$ for EuZnGe (Pöttgen 1995b)

Atom	Wyckoff notation	*x/a*	*y/b*	*z/c*	G (%)
Eu	2(a)	0	0	0	100
Zn	2(c)	1/3	2/3	1/4	100
Ge	2(d)	1/3	2/3	3/4	100

For europium atoms, polyhedra with 20 apexes are typical (fig. 67a). The atoms of zinc and germanium are situated inside the trigonal prisms with three additional atoms (fig. 67b, c).

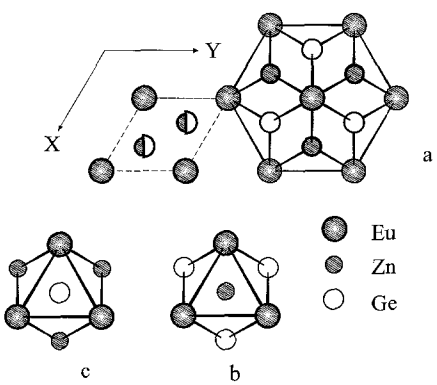

Fig. 67. Projection of the EuZnGe unit cell and coordination polyhedra of the atoms: (a) Eu, (b,c) Zn and Ge.

3.19.24. *α-$ThSi_2$ structure type*

SG $I4_1/amd$, $Z=4$, $a=0.4231$, $c=1.4219$ for $CeZn_{0.7}Ge_{1.3}$ (Opainych 1996)

Atom	Wyckoff notation	*x/a*	*y/b*	*z/c*	G (%)
Ce	4(a)	0	3/4	1/8	100
X	8(e)	0	1/4	0.4589	100

X = 0.35Zn+0.65Ge

Isotypic compounds:

RAlGe: R = La–Gd

3.19.25. *α-$GdSi_2$ structure type*

SG Imma, $Z=4$, $a=0.4044$, $b=0.3988$, $c=1.348$ for $YSi_{1.4}Ge_{0.6}$ (Muratova 1976)

Atomic coordinates were not determined for a germanide of this structure type.

3.19.26. *$CeSi_{1-y}Ge_{1-x}$ structure type*

SG $I\bar{4}m2$, $Z=4$, $a=0.4198$, $b=1.4004$ for $CeSi_{0.92}Ge_{0.66}$ (Boutarek et al. 1992)

Atom	Wyckoff notation	*x/a*	*y/b*	*z/c*	G (%)
Ce1	2(c)	0	1/2	1/4	100
Ce2	2(a)	0	0	0	100
Si	4(f)	0	1/2	0.6743	95
Ge	4(e)	0	0	0.4124	66

No isotypic compounds have been observed.

3.19.27. *Te_2Ag_3Tl structure type*

SG Cmmm, $Z=2$, $a=1.8894$, $b=0.4650$, $c=0.4299$ for Ce_2Sb_3Ge (Stetskiv et al. 1998). See fig. 68.

Atom	Wyckoff notation	*x/a*	*y/b*	*z/c*	G (%)
Ce	4(g)	0.1406	0	0	100
Sb1	2(b)	1/2	0	0	100
Sb2	4(h)	0.3047	0	1/2	100
Ge	2(d)	0	0	1/2	100

Isotypic compounds:

R_2Sb_3Ge: R = La, Pr, Sm

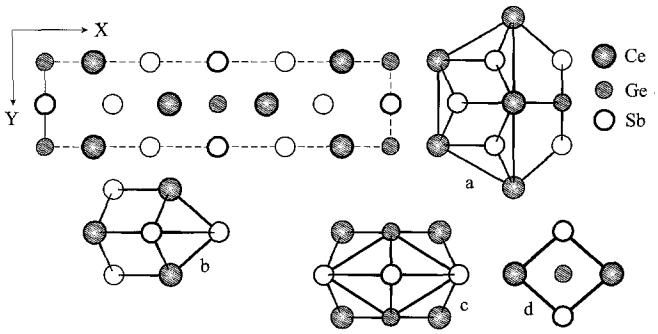

Fig. 68. Projection of the Ce_2Sb_3Ge unit cell and coordination polyhedra of the atoms: (a) Ce, (b,c) Sb, (d) Ge.

3.19.28. *$Tb_3Co_2Ge_4$ structure type*

SG C2/m, $Z=2$, $a=1.0692$, $b=0.4164$, $c=0.8067$, $\beta=107.72°$ (Starodub et al. 1986). See fig. 69.

Atom	Wyckoff notation	*x/a*	*y/b*	*z/c*	G (%)
Tb1	4(i)	0.3771	0	0.3076	100
Tb2	2(a)	0	0	0	100
Co	4(i)	0.3096	0	0.6312	100
Ge1	4(i)	0.0964	0	0.3998	100
Ge2	4(i)	0.7105	0	0.0796	100

Isotypic compounds:

$R_3Co_2Ge_4$: R = Y, Gd–Tm

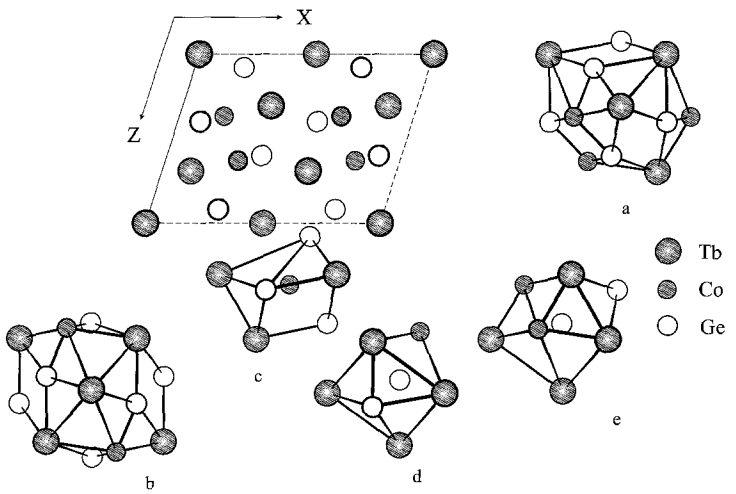

Fig. 69. Projection of the $Tb_3Co_2Ge_4$ unit cell and coordination polyhedra of the atoms: (a,b) Tb, (c) Co, (d,e) Ge.

3.19.29. *$Sc_7Cr_{4+x}Si_{10-x}$ structure type*

SG I4/mmm, $Z=4$, $a=0.9995$, $c=1.4168$ for $Sc_7Mn_{4+x}Ge_{10-x}$, x = 1.3 (Kotur et al. 1988)

Atom	Wyckoff notation	*x/a*	*y/b*	*z/c*	G (%)
Sc1	16(n)	0	0.2520	0.3119	100
Sc2	8(h)	0.3253	0.3253	0	100
Sc3	4(e)	0	0	0.1621	100
Mn	16(n)	0	0.3283	0.1014	100
Ge4	16(m)	0.2055	0.2055	0.1670	100
Ge3	8(j)	0.8714	1/2	0	100
Ge2	4(e)	0	0	0.3891	100
Ge1	4(d)	0	1/2	1/4	100
X	8(h)	0.1238	0.1238	0	25

X = 0.64Mn+0.36Ge

Isotypic compound: $Sc_7Cr_{4+x}Ge_{10-x}$, $x=1.3$

3.19.30. *$Sm_4Co_{1-x}Ge_7$ structure type*

SG Amm2, $Z=2$, $a=0.4166$, $b=0.4083$, $c=3.018$ (Mruz et al. 1987)

Atom	Wyckoff notation	*x/a*	*y/b*	*z/c*	G (%)
Sm1	2(b)	1/2	0	0.5284	100
Sm2	2(b)	1/2	0	0.9165	100
Sm3	2(a)	0	0	0.1832	100
Sm4	2(a)	0	0	0.7966	100
Co	2(a)	0	0	0.0745	64
Ge1	2(b)	1/2	0	0.1048	100
Ge2	2(b)	1/2	0	0.2665	100
Ge3	2(b)	1/2	0	0.7130	100
Ge4	2(a)	0	0	0.0000	100
Ge5	2(a)	0	0	0.3680	100
Ge6	2(a)	0	0	0.4521	100
Ge7	2(a)	0	0	0.6038	100

Isotypic compounds:

$R_4Fe_{1-x}Ge_7$: R = Pr, Nd, Sm

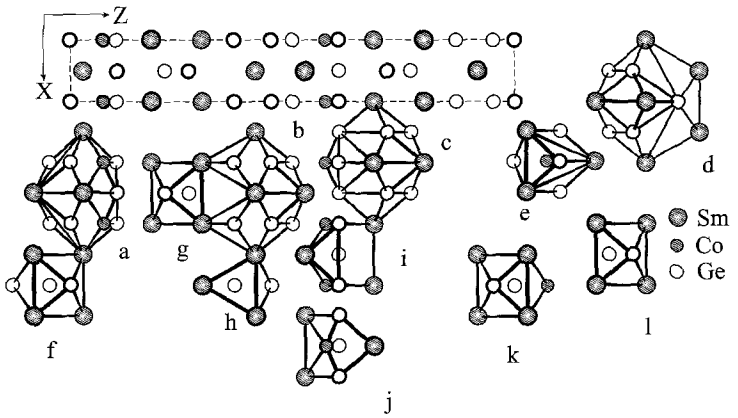

Fig. 70. Projection of the $Sm_4Co_{1-x}Ge_7$ unit cell and coordination polyhedra of the atoms: (a–d) Sm, (e) Co, (f–l) Ge.

For samarium atoms, polyhedra with 16, 17, 18 and 20 apexes are typical (fig. 70a–d). The cobalt atoms polyhedra are tetragonal antiprisms with two additional atoms (fig. 70e). The trigonal prisms and distorted cubo-octahedra are the polyhedra for germanium atoms (fig. 70f–l).

3.20. *$R_7(M, Ge)_{13}$ and $R_4(M, Ge)_7$ compounds*

3.20.1. *$Yb_7Al_5Ge_8$ structure type*

SG C2/m, $Z=2$, $a=1.5958$, $b=0.42871$, $c=1.2611$, $\beta=95.78°$ (Zhao and Parthé 1991a). See fig. 71.

Atom	Wyckoff notation	*x/a*	*y/b*	*z/c*	G (%)
Yb1	4(i)	0.01782	0	0.2983	100
Yb2	4(i)	0.15884	0	0.54329	100
Yb3	4(i)	0.81087	0	0.1358	100
Yb4	2(a)	0	0	0	100
Al1	4(i)	0.2242	0	0.3052	100
Al2	4(i)	0.6087	0	0.1671	100
Al3	2(d)	0	1/2	1/2	100
Ge1	4(i)	0.1751	0	0.1050	100
Ge2	4(i)	0.3484	0	0.6203	100
Ge3	4(i)	0.3877	0	0.3150	100
Ge4	4(i)	0.4468	0	0.1345	100

No isotypic compounds have been observed.

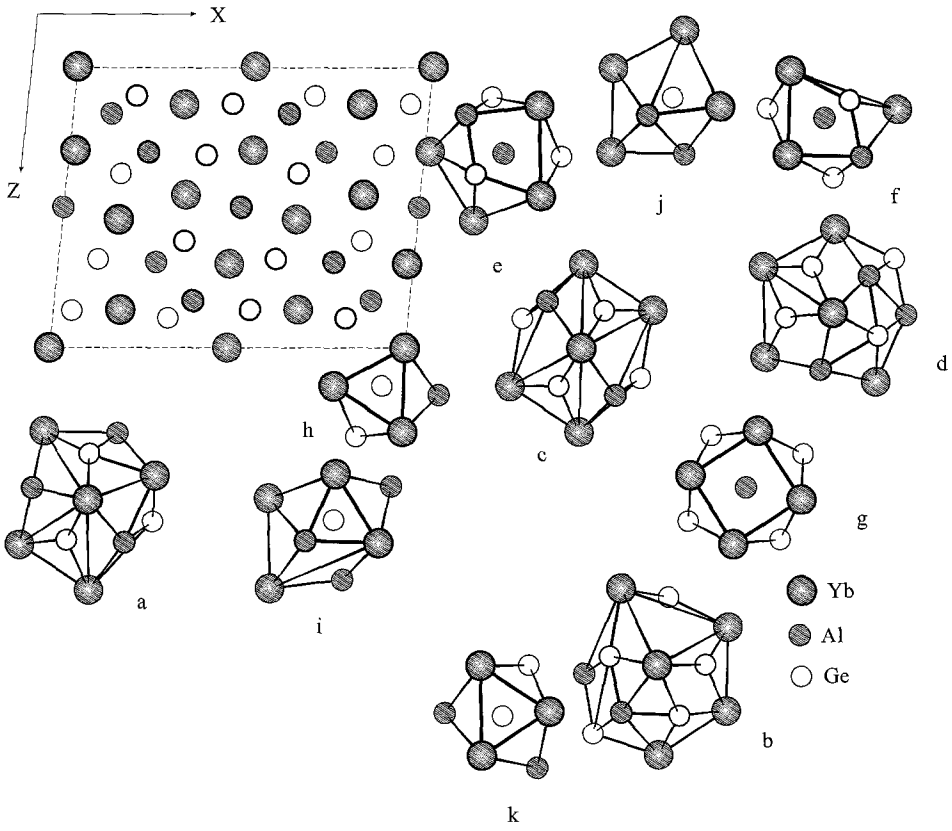

Fig. 71. Projection of the $Yb_7Al_5Ge_8$ unit cell and coordination polyhedra of the atoms: (a–d) Yb, (e–g) Al, (h–k) Ge.

3.20.2. *$Nd_4Rh_4Ge_3$ structure type*

SG C2/c, $Z=4$, $a=2.1021$, $b=0.5652$, $c=0.7941$, $\beta=110.08°$ (Salamakha 1989). See fig. 72.

Atom	Wyckoff notation	*x/a*	*y/b*	*z/c*	G (%)
Nd1	8(f)	0.17058	0.1154	0.3993	100
Nd2	8(f)	0.43350	0.1479	0.3317	100
Rh1	8(f)	0.06212	0.1340	0.01774	100
Rh2	8(f)	0.27848	0.1509	0.1849	100
Ge1	8(f)	0.17147	0.3813	0.0582	100
Ge2	4(e)	0	0.1493	1/4	100

No isotypic compounds have been observed.

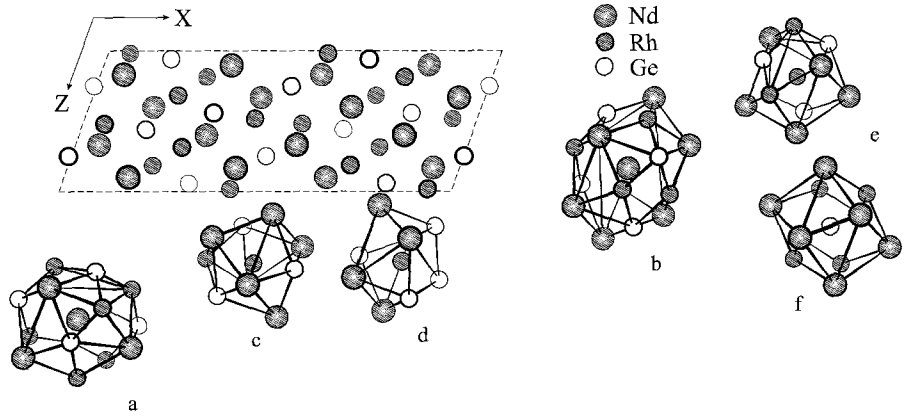

Fig. 72. Projection of the $Nd_4Rh_4Ge_3$ unit cell and coordination polyhedra of the atoms: (a, b) Nd, (c–f) Rh and Ge.

3.20.3. *Yb_8LiGe_{13} structure type*

SG $P2_1/c$, $Z=4$, $a=1.1317$, $b=1.0817$, $c=1.5577$, $\beta=106.40°$ (Pavlyuk et al. 1987a)

Atom	Wyckoff notation	*x/a*	*y/b*	*z/c*	G (%)
Yb1	4(e)	0.0946	0.7707	0.0684	100
Yb2	4(e)	0.1199	0.3541	0.3026	100
Yb3	4(e)	0.1285	0.0178	0.4334	100
Yb4	4(e)	0.1421	0.0634	0.1732	100
Yb5	4(e)	0.3548	0.5124	0.5419	100
Yb6	4(e)	0.3814	0.3122	0.1812	100
Yb7	4(e)	0.5947	0.1431	0.3996	100
Yb8	4(e)	0.6667	0.1094	0.1958	100
Li	4(e)	0.16	0.425	0.129	100
Ge1	4(e)	0.0507	0.6229	0.2303	100
Ge2	4(e)	0.0704	0.3144	0.1029	100
Ge3	4(e)	0.0863	0.4928	0.4615	100
Ge4	4(e)	0.1540	0.8291	0.2786	100
Ge5	4(e)	0.1773	0.5207	0.1364	100
Ge6	4(e)	0.1946	0.2165	0.0060	100
Ge7	4(e)	0.3115	0.1519	0.3381	100
Ge8	4(e)	0.4018	0.3691	0.3801	100

Ge9	4(e)	0.4064	0.4221	0.0007	100
Ge10	4(e)	0.4361	0.0435	0.2393	100
Ge11	4(e)	0.5108	0.2117	0.0386	100
Ge12	4(e)	0.6685	0.3362	0.2992	100
Ge13	4(e)	0.7530	0.2474	0.0586	100

No isotypic compounds have been observed.

3.21. *$R_3(M, Ge)_5$ and $R_5(M, Ge)_8$ compounds*

3.21.1. *La_3In_4Ge structure type*

SG I4/mcm, $Z=4$, $a=0.8516$, $c=1.1902$ (Guloy and Corbett 1996)

Atom	Wyckoff notation	*x/a*	*y/b*	*z/c*	G (%)
La1	4(a)	0	0	0.25	100
La2	8(h)	0.3354	0.8354	0	100
In	16(l)	0.1428	0.6428	0.1863	100
Ge	4(c)	0	0	0	100

No isotypic compounds have been observed.

3.21.2. *$Hf_3Ni_2Si_3$ structure type*

SG Cmcm, $Z=4$, $a=0.42730$, $b=1.0403$, $c=1.4128$ for $Ho_3Ir_2Ge_3$ (Salamakha et al. 1996)

Atom	Wyckoff notation	*x/a*	*y/b*	*z/c*	G (%)
Ho1	4(c)	0	0.6407	1/4	100
Ho2	8(f)	1/2	0.5839	0.1107	100
Ir	8(f)	1/2	0.7016	0.1008	100
Ge1	8(f)	0	0.6224	0.0357	100
Ge2	4(c)	0	0.3431	1/4	100

Isotypic compounds:
$R_3Li_2Ge_3$: R = Y, Tb–Tm, Lu
$R_3Fe_2Ge_3$: R = Er, Lu
$Sc_3Co_2Ge_3$
$Er_3Ni_2Ge_3$

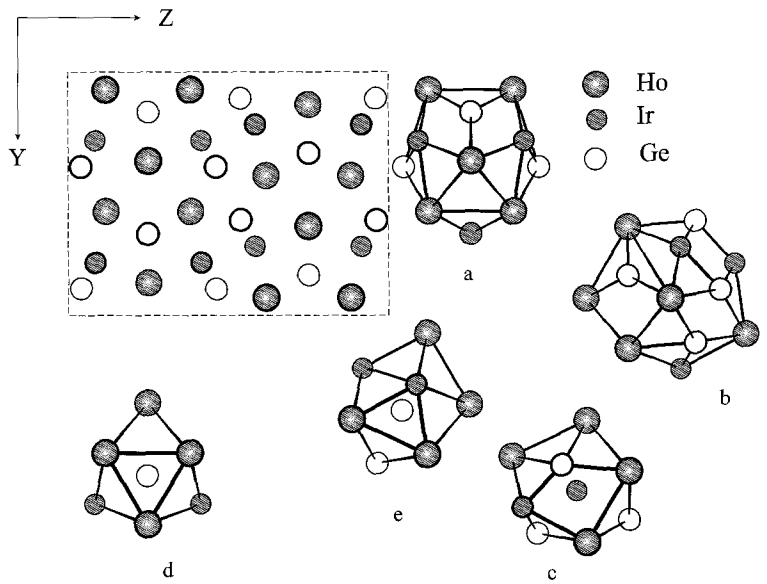

Fig. 73. Projection of the $Ho_3Ir_2Ge_3$ unit cell and coordination polyhedra of the atoms: (a, b) Ho, (c–e) Ir and Ge.

The coordination numbers of holmium are 17 and 18 (fig. 73a, b). The iridium and germanium atoms are situated in the centres of trigonal prisms with additional atoms (fig. 73c–e).

3.21.3. *$Tm_3(Ga_{0.5}Ge_{0.5})_5$ structure type*

SG I4/mcm, $Z=4$, $a=0.7748$, $c=1.0836$ (Gryniv and Myakush 1989)

Atomic coordinates were not presented.

3.21.4. *$U_3Sb_3Cu_2$ structure type*

SG $P6_3/mmc$, $Z=2$, $a=0.4142$, $c=2.2315$ for $Ce_3Sn_3Ge_2$ (Stetskiv 1999). See fig. 74.

Atom	Wyckoff notation	*x/a*	*y/b*	*z/c*	G (%)
Ce1	4(f)	1/3	2/3	0.0788	100
Ce2	2(c)	1/3	2/3	1/4	100
Sn1	4(f)	1/3	2/3	0.6580	100
Sn2	2(a)	0	0	0	100
Ge	4(e)	0	0	1/6	100

Isotypic compounds:

$R_3Sn_3Ge_2$: R = La, Pr, Sm

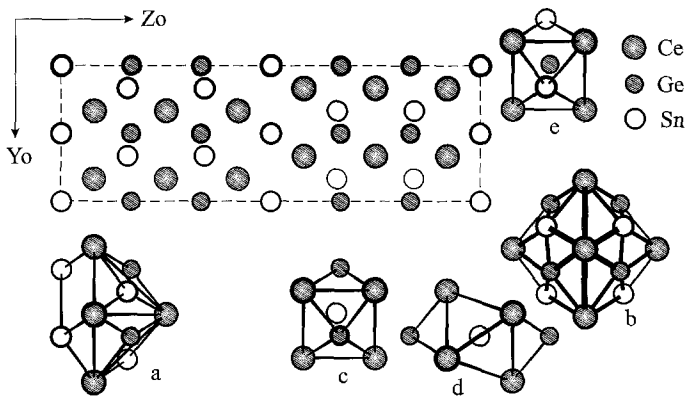

Fig. 74. Projection of the $Ce_3Sn_3Ge_2$ unit cell and coordination polyhedra of the atoms: (a,b) Ce, (c,d) Sn, (e) Ge.

3.21.5. *$Nb_5Cu_4Si_4$ structure type*

SG I4/m, $Z=2$, $a=1.1210$, $c=0.43698$ for $Yb_5Li_4Ge_4$ (Pavlyuk et al. 1989)

Atom	Wyckoff notation	*x/a*	*y/b*	*z/c*	G (%)
Yb1	2(a)	0	0	0	100
Yb2	8(h)	0.1957	0.1188	0	100
Li	8(h)	0.079	0.400	0	100
Ge	8(h)	0.4307	0.2456	0	100

No isotypic compounds have been observed.

3.22. *$R_2(M,Ge)_3$ compounds*

3.22.1. *$Nd_6Co_5Ge_4$ structure type*

SG $P\bar{6}m2$, $Z=1$, $a=0.9272$, $c=0.4188$ for $Nd_6Co_5Ge_{2.2}$ (Salamakha et al. 1986)

Atom	Wyckoff notation	*x/a*	*y/b*	*z/c*	G (%)
Nd1	3(k)	0.8696	0.1304	1/2	100
Nd2	3(j)	0.5179	0.4821	0	100
Co1	3(j)	0.1519	0.8481	0	100
Co2	1(c)	1/3	2/3	0	100
Co3	1(a)	0	0	0	100

Ge1	3(k)	0.2359	0.7641	1/2	40
Ge2	1(f)	2/3	1/3	1/2	100

No isotypic compounds have been observed.

For the neodymium atoms, polyhedra with 17 and 15 apexes are typical (fig. 75a, b). The polyhedra for cobalt atoms are trigonal prisms and icosahedra (fig. 75c–e). The germanium coordination polyhedra are trigonal prisms and deformed cubo-octahedra (fig. 75f, g).

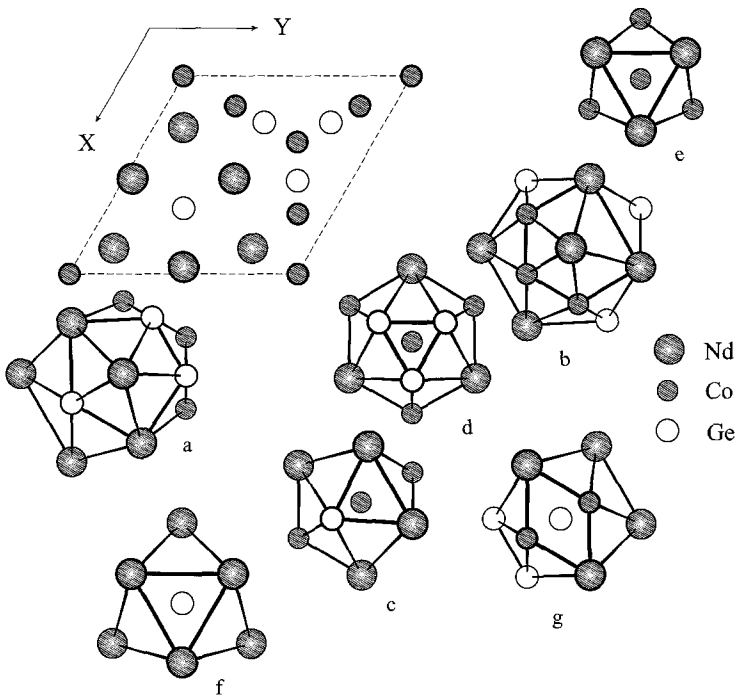

Fig. 75. Projection of the $Nd_6Co_5Ge_{2.2}$ unit cell and coordination polyhedra of the atoms: (a, b) Nd, (c–e) Co, (f, g) Ge.

3.22.2. *Sc_2CoSi_2 structure type*

SG C2/m, $Z=4$, $a=1.0691$, $b=0.42618$, $c=1.0050$, $\beta=118.07°$ for Ho_2OsGe_2 (Gladyshevsky et al. 1991b)

Atom	Wyckoff notation	*x/a*	*y/b*	*z/c*	G (%)
Ho1	4(i)	0.9968	0	0.3253	100
Ho2	4(i)	0.1848	0	0.1130	100

Os	4(i)	0.2710	0	0.6320	100
Ge1	4(i)	0.3585	0	0.4386	100
Ge2	4(i)	0.4876	0	0.1251	100

Isotypic compounds:
R_2CoGe_2: R = Sc, Y, Nd–Tm
R_2RuGe_2: R = Nd, Sm, Ho
R_2RhGe_2: R = Nd, Sm, Ho
R_2IrGe_2: R = Nd, Ho

For holmium atoms, polyhedra with 17 and 18 apexes are typical (fig. 76a,b). The atoms of osmium are situated inside the distorted cubo-octahedra (fig. 76c). The coordination polyhedra for the germanium atoms are trigonal prisms with additional atoms (fig. 76d,e).

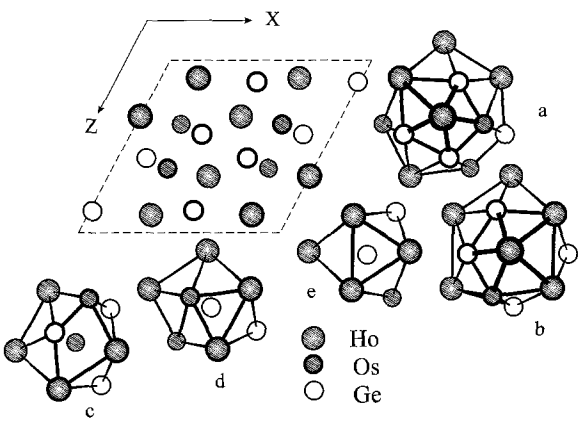

Fig. 76. Projection of the Ho_2OsGe_2 unit cell and coordination polyhedra of the atoms: (a,b) Ho, (c) Os, (d,e) Ge.

3.22.3. *Mo_2FeB_2 structure type*

SG P4/mbm, $Z = 2$, $a = 0.7205$, $c = 0.4294$ for Yb_2InGe_2 (Zaremba et al. 1997)

Atom	Wyckoff notation	*x/a*	*y/b*	*z/c*	G (%)
Yb	4(g)	0.32492	0.82492	0	100
In	2(b)	0	0	1/2	100
Ge	4(h)	0.1229	0.6229	1/2	100

Isotypic compounds:
R_2InGe_2: R = Y, La–Sm, Gd–Ho

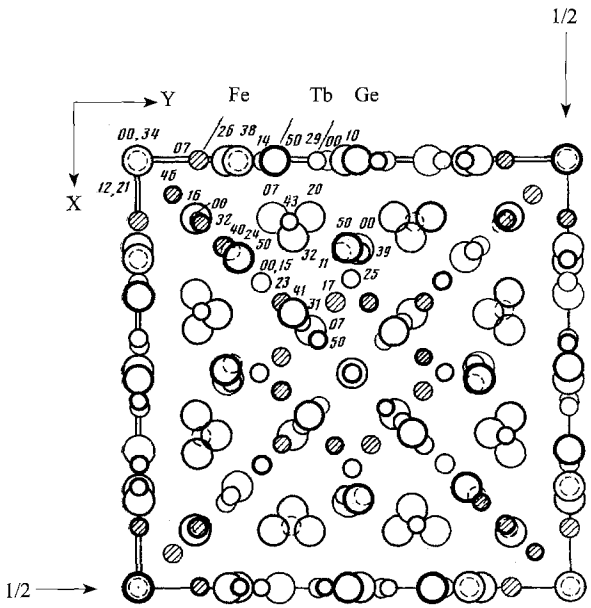

Fig. 77. Projection of the 1/8 of the $Tb_{117}Fe_{52}Ge_{112}$ unit cell.

3.23. *$R_9(M, Ge)_{13-11}$ compounds*

3.23.1. *$Tb_{117}Fe_{52}Ge_{112}$ structure type*

SG Fm-3m, $Z=4$, $a=2.8580$ (Pecharsky et al. 1987). See figs. 77 and 78.

Atom	Wyckoff notation	*x/a*	*y/b*	*z/c*	G (%)
Tb1	96(k)	0.0681	0.0681	0.1557	100
Tb2	96(k)	0.1793	0.1793	0.4084	100
Tb3	96(k)	0.1995	0.1995	0.0663	100
Tb4	96(j)	0	0.1036	0.2550	100
Tb5	48(i)	1/2	0.1158	0.1158	100
Tb6	24(e)	0.3384	0	0	100
Tb7	8(c)	1/4	1/4	1/4	100
Tb8	4(a)	0	0	0	100
Fe1	96(k)	0.1676	0.1676	0.2302	100
Fe2	48(h)	0	0.0723	0.0723	100
Fe3	32(f)	0.3983	0.3983	0.3983	100
Fe4	32(f)	0.4503	0.4503	0.4503	100
Ge1	96(k)	0.0738	0.0738	0.3228	100

Ge2	96(k)	0.1071	0.1071	0.2423	100
Ge3	48(i)	1/2	0.2094	0.2094	100
Ge4	48(h)	0	0.1447	0.1447	100
Ge5	48(g)	0.1395	1/4	1/4	100
Ge6	32(f)	0.1464	0.1464	0.1464	100
Ge7	32(f)	0.3088	0.3088	0.3088	100
Ge8	24(e)	0.1152	0	0	100
Ge9	24(e)	0.2150	0	0	100

Isotypic compounds:
$Nd_{117}Cr_{52}Ge_{112}$
$R_{117}Fe_{52}Ge_{112}$: R = Y, Pr, Sm, Dy–Tm, Lu
$R_{117}Co_{52}Ge_{112}$: R = Pr, Sm

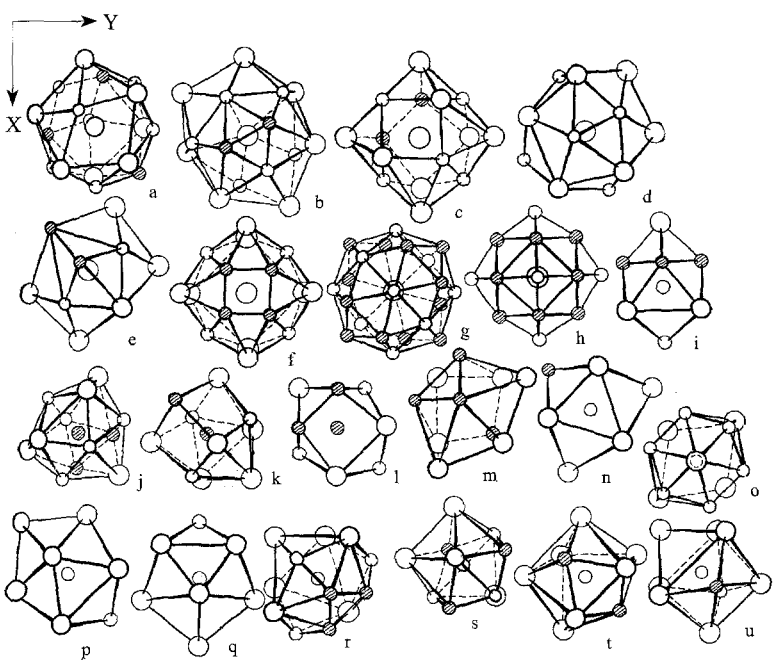

Fig. 78. Coordination polyhedra of the atoms in the $Tb_{117}Fe_{52}Ge_{112}$ structure: (a–h) Tb, (i–l) Fe, (m–u) Ge.

3.23.2. *Tm_4LiGe_4 structure type*

SG Pnma, $Z=4$, $a=0.7013$, $b=1.4429$, $c=0.7573$ (Pavlyuk et al. 1990)

Atom	Wyckoff notation	*x/a*	*y/b*	*z/c*	G (%)
Tm1	8(d)	0.828	0.127	0.676	100
Tm2	8(d)	0.476	0.096	0.317	100
Li	4(c)	0.158	1/4	0.479	100
Ge1	8(d)	0.165	0.037	0.533	100
Ge2	4(c)	0.784	1/4	0.363	100
Ge3	4(c)	0.517	1/4	0.588	100

Isotypic compounds:
R_4LiGe_4: R = Y, Gd–Lu

3.23.3. *$La_3Ni_2Ga_2$ structure type*

SG Pbcm, $Z=4$, $a=0.5658$, $b=0.7863$, $c=1.3581$ for $Nd_3Ru_2Ge_2$ (Bodak et al. 1989b). See fig. 79.

Atom	Wyckoff notation	*x/a*	*y/b*	*z/c*	G (%)
Nd1	8(e)	0.1509	0.4021	0.0981	100
Nd2	4(d)	0.6282	0.2379	1/4	100
Ru	8(e)	0.3572	0.0318	0.0902	100
Ge1	4(d)	0.1353	0.1102	1/4	100
Ge2	4(c)	0.6223	1/4	0	100

Isotypic compounds:
$R_3Ru_2Ge_2$: R = La–Sm
$R_3Rh_2Ge_2$: R = Y, La–Sm, Gd–Tm, Lu

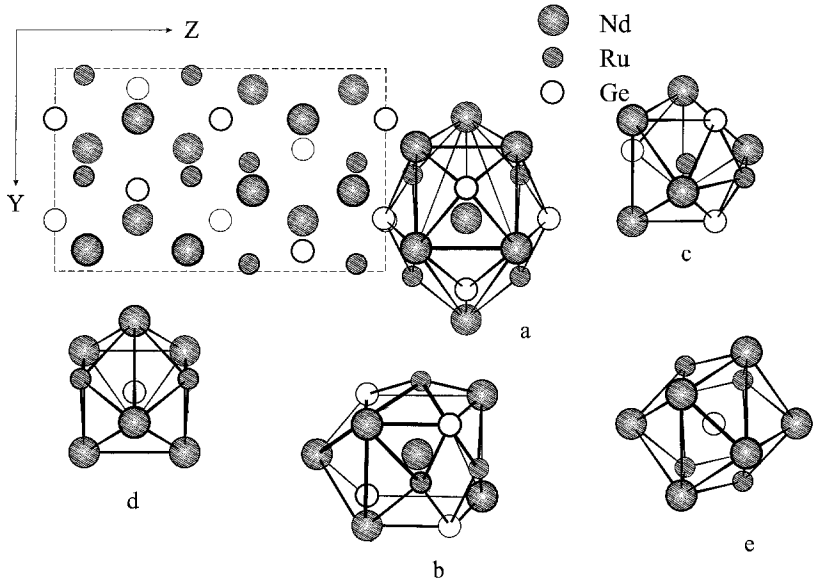

Fig. 79. Projection of the $Nd_3Ru_2Ge_2$ unit cell and coordination polyhedra of the atoms: (a, b) Nd, (c) Ru, (d, e) Ge.

3.23.4. *$Sc_9Ni_5Ge_8$ structure type*

SG Immm, $Z=2$, $a=0.39822$, $b=0.9129$, $c=2.0426$ (Kotur et al. 1989)

Atom	Wyckoff notation	*x/a*	*y/b*	*z/c*	G (%)
Sc1	8(l)	0	0.31373	0.08338	100
Sc2	4(j)	1/2	0	0.10743	100
Sc3	4(j)	1/2	0	0.27270	100
Sc4	2(c)	1/2	1/2	0	100
Ni1	8(l)	0	0.22699	0.30457	100
Ni2	2(a)	0	0	0	100
Ge1	8(l)	0	0.13854	0.19132	100
Ge2	4(i)	0	0	0.36590	100
Ge3	4(g)	0	0.20724	0	100

No isotypic compounds have been observed.

3.24. *R(M, Ge) compounds*

3.24.1. *CrB structure type*

SG Cmcm, $Z=4$, $a=0.4033$, $b=1.0884$, $c=0.4287$ for Sm_2PtGe (Barakatova 1994)

Atom	Wyckoff notation	*x/a*	*y/b*	*z/c*	G (%)
Sm	4(c)	0	0.1392	1/4	100
X	4(c)	0	0.4200	1/4	100

X = 0.5Pt+0.5Ge

Isotypic compounds:

$Ce_{0.8}R_{0.2}Ge$: R = Y, Dy–Tm

3.24.2. *FeB structure type*

SG Pnma, $Z=4$, $a=0.8453$, $b=0.3732$, $c=0.5582$ for Sm_2PdGe (Barakatova 1994)

Atomic coordinates have not been determined.

3.24.3. *La_2NiGe structure type*

SG I4/mcm, $Z=8$, $a=0.7947$, $c=1.4262$ (Bruskov et al. 1983). See fig. 80.

Atom	Wyckoff notation	*x/a*	*y/b*	*z/c*	G (%)
La	16(l)	0.1678	0.6678	0.1457	100
Ni	8(h)	0.6151	0.1151	0	100
Ge1	4(c)	0	0	0	100
Ge2	4(a)	0	0	1/4	100

No isotypic compounds have been found.

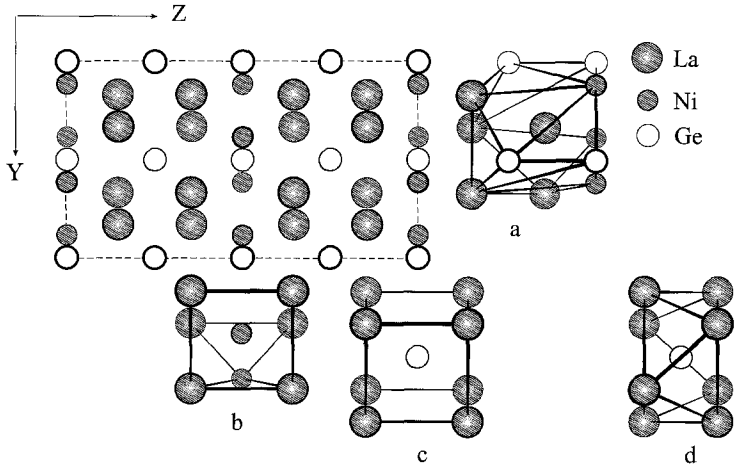

Fig. 80. Projection of the La_2NiGe unit cell and coordination polyhedra of the atoms: (a) La, (b) Ni, (c, d) Ge.

3.24.4. *Gd_3NiSi_2 structure type*

SG Pnma, $Z=4$, $a=1.20401$, $b=0.4358$, $c=1.1871$ for La_3NiGe_2 (Bodak et al. 1982). See fig. 81.

Atom	Wyckoff notation	x/a	y/b	z/c	G (%)
La1	4(c)	0.0576	1/4	0.12471	100
La2	4(c)	0.21649	1/4	0.80142	100
La3	4(c)	0.38309	1/4	0.05697	100
Ni	4(c)	0.12757	1/4	0.36719	100
Ge1	4(c)	0.30183	1/4	0.49409	100
Ge2	4(c)	0.47464	1/4	0.81216	100

Isotypic compounds:
R_3CoGe_2: R = Ce–Sm
R_3NiGe_2: R = Y, Ce–Sm, Gd–Er

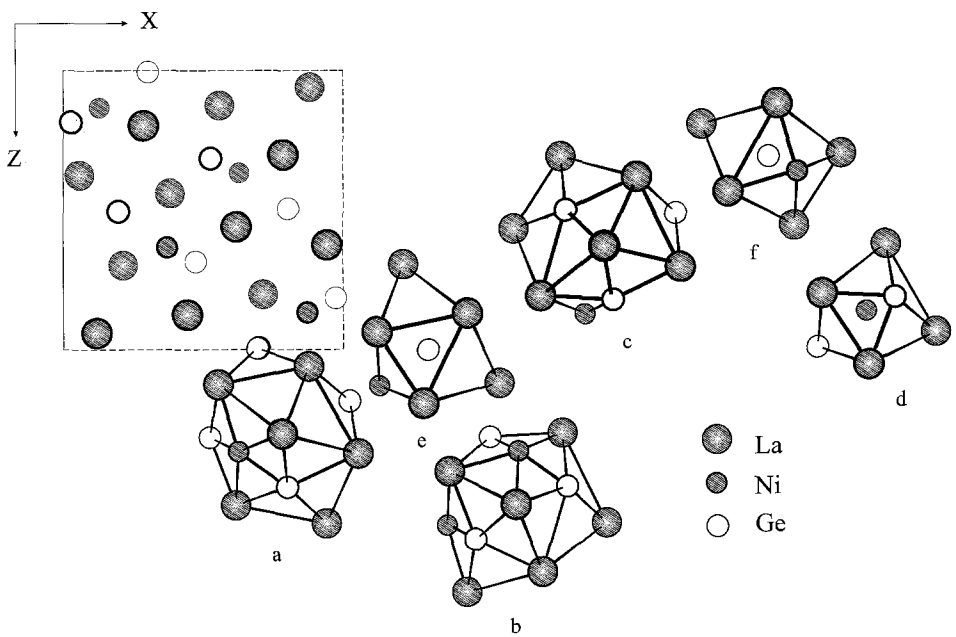

Fig. 81. Projection of the La_3NiGe_2 unit cell and coordination polyhedra of the atoms: (a–c) La, (d) Ni, (e, f) Ge.

3.25. $R_{11}(M, Ge)_{10}$ compounds

3.25.1. $Sc_{11}Al_2Ge_8$ structure type

SG I4/mmm, $Z=4$, $a=1.0419$, $c=1.4974$ (Zhao and Parthé 1991b). See fig. 82.

Atom	Wyckoff notation	x/a	y/b	z/c	G (%)
Sc1	16(n)	0	0.2507	0.3102	100
Sc2	16(n)	0	0.3356	0.1024	100
Sc3	8(h)	0.3272	0.3272	0	100
Sc4	4(e)	0	0	0.1688	100
Al	8(h)	0.1270	0.1270	0	100
Ge1	16(m)	0.2047	0.2047	0.1711	100
Ge2	8(j)	0.1470	1/2	0	100
Ge3	4(e)	0	0	0.3815	100
Ge4	4(d)	0	1/2	1/4	100

No isotypic compounds have been observed.

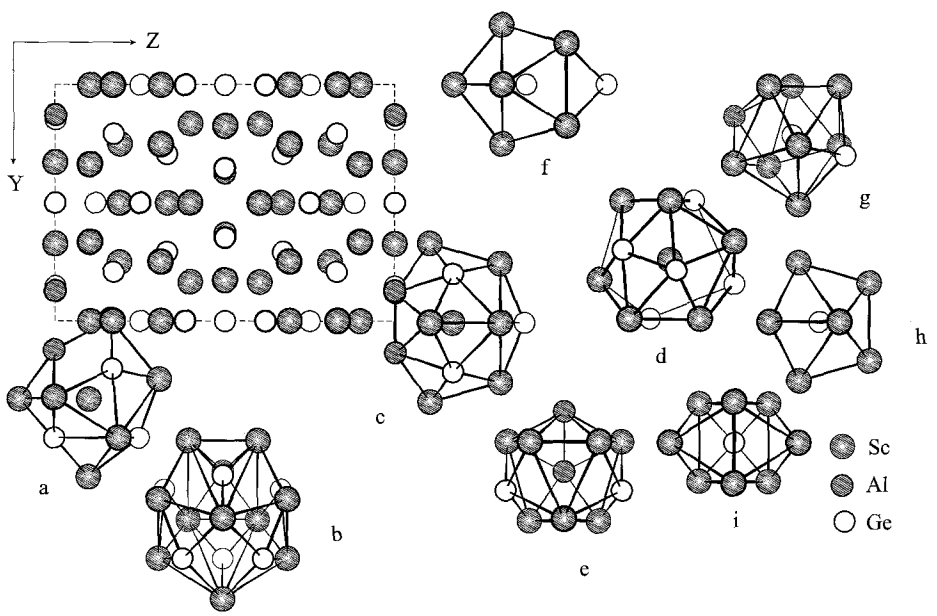

Fig. 82. Projection of the $Sc_{11}Al_2Ge_8$ unit cell and coordination polyhedra of the atoms: (a–d) Sc, (e) Al, (f–i) Ge.

3.25.2. *$La_{11}Ni_4Ge_6$ structure type*

SG C2/m, $Z=2$, $a=1.8637$, $b=0.4384$, $c=1.4191$, $\beta=106.13°$ (Pecharsky et al. 1986)

Atom	Wyckoff notation	*x/a*	*y/b*	*z/c*	G (%)
La1	4(i)	0.0957	0	0.2840	100
La2	4(i)	0.1422	0	0.8494	100
La3	4(i)	0.2160	0	0.5999	100
La4	4(i)	0.4515	0	0.3738	100
La5	4(i)	0.6601	0	0.0935	100
La6	2(a)	0	0	0	100
Ni1	4(i)	0.0594	0	0.4752	100
Ni2	4(i)	0.2477	0	0.0503	100
Ge1	4(i)	0.2614	0	0.2345	100

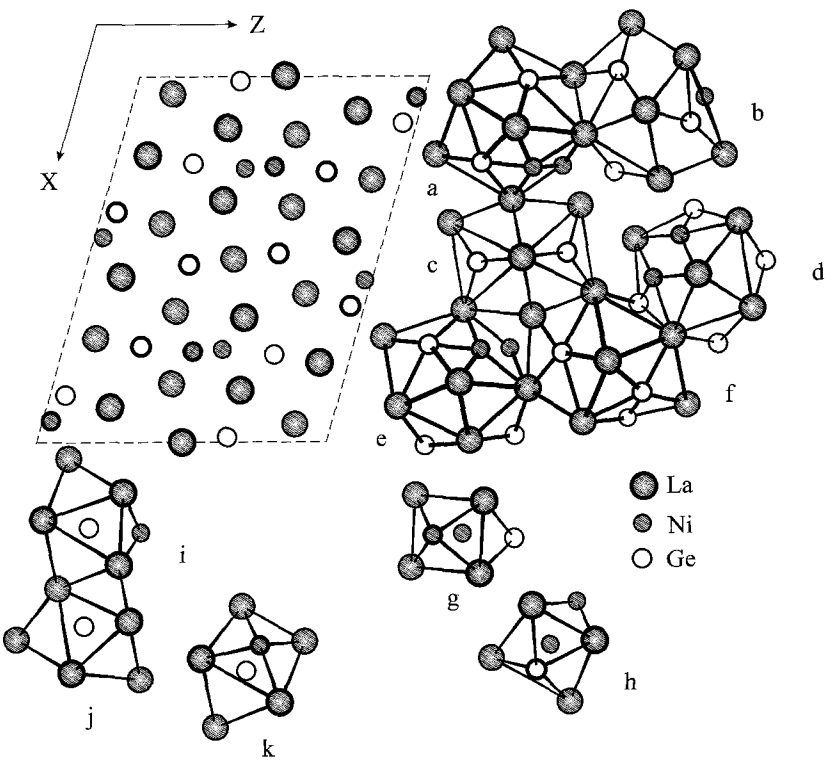

Fig. 83. Projection of the $La_{11}Ni_4Ge_6$ unit cell and coordination polyhedra of the atoms: (a–f) La, (g–k) Ni and Ge.

Ge2	4(i)	0.3713	0	0.5490	100
Ge3	4(i)	0.4864	0	0.1512	100

No isotypic compounds have been found.

The coordination polyhedra for the lanthanum atoms have 17 and 18 apexes (fig. 83a–f). For nickel and germanium atoms, the coordination polyhedra as trigonal prisms with additional atoms are typical (fig. 83g–k).

3.26. *$R_{26}(M, Ge)_{23}$ compounds*

3.26.1. *$Ho_{26}Pd_4(Pd, Ge)_{19}$ structure type*

SG P4/nmm, $Z=2$, $a=1.4523$, $c=1.0318$ (Sologub et al. 1994)

Atom	Wyckoff notation	*x/a*	*y/b*	*z/c*	G (%)
Ho1	4(f)	3/4	1/4	0.2690	100
Ho2	8(h)	0.3688	0.6312	1/2	100
Ho3	8(i)	1/4	0.0709	0.9446	100
Ho4	8(i)	1/4	0.0665	0.3844	100
Ho5	8(j)	0.3922	0.3922	0.6647	100
Ho6	16(k)	0.3805	0.57087	0.1745	100
Pd1	2(c)	1/4	1/4	0.184	50
Pd2	8(j)	0.3682	0.3682	0.1729	100
Ge1	2(c)	1/4	1/4	0.7904	100
Ge2	8(i)	1/4	0.5379	0.6926	100
Ge3	8(j)	0.4538	0.4538	0.3880	100
Ge4	8(j)	0.4420	0.4420	0.9597	100
X1	2(c)	1/4	1/4	0.5396	100
X2	8(i)	1/4	0.6300	0.9716	100

X1 = 0.21Pd+0.79Ge; X2 = 0.27Pd+0.73Ge

No isotypic compounds have been observed.

The coordination polyhedra of the holmium atoms have 14–17 apexes (fig. 84a–f). Those of the palladium atoms are cubes with four additional atoms (fig. 84g) and distorted trigonal prisms with additional atoms (fig. 84h). The germanium and X atoms occupy the centres of tetragonal antiprisms with additional atoms and distorted trigonal prisms with additional atoms (fig. 84i–m).

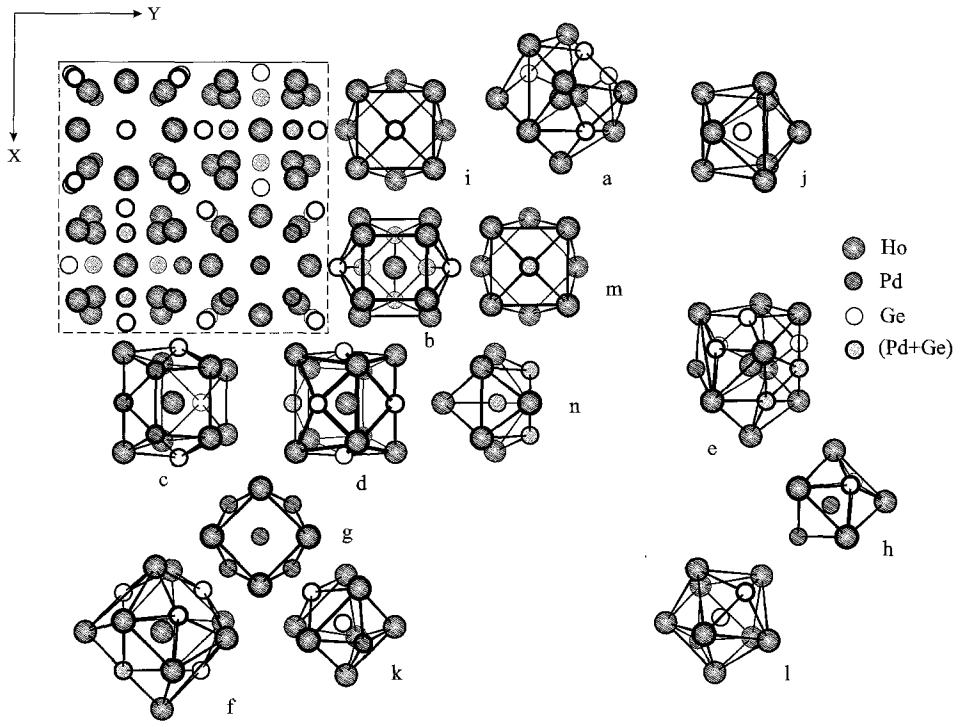

Fig. 84. Projection of the $Ho_{26}Pd_4(Pd,Ge)_{19}$ unit cell and coordination polyhedra of the atoms: (a–f) Ho, (g,h) Pd, (i–m) Ge.

3.26.2. *$Ce_{26}Li_5Ge_{23-y}$ structure type*

SG P4/nmm, $Z=2$, $a=1.5402$, $c=1.0900$ (Pavlyuk et al. 1987b)

Atom	Wyckoff notation	*x/a*	*y/b*	*z/c*	G (%)
Ce1	16(k)	0.0786	0.6170	0.1796	100
Ce2	8(j)	0.1115	0.1115	0.3409	100
Ce3	8(i)	1/4	0.0634	0.6321	100
Ce4	8(i)	1/4	0.0651	0.0929	100
Ce5	8(h)	0.3674	0.6326	1/2	100
Ce6	4(f)	3/4	1/4	0.2652	100
Li1	8(i)	1/4	0.600	0.649	100
Li2	2(b)	3/4	1/4	1/2	100
Ge1	8(j)	0.0382	0.0382	0.5998	100

Ge2	8(j)	0.0550	0.0550	0.0353	100
Ge3	8(j)	0.1239	0.1239	0.8456	100
Ge4	8(i)	1/4	0.5322	0.3170	100
Ge5	8(i)	1/4	0.6325	0.0149	100
Ge6	2(c)	1/4	1/4	0.204	100
Ge7	2(c)	1/4	1/4	0.470	100
Ge8	2(c)	1/4	1/4	0.853	37

No isotypic compounds have been observed.

3.27. *$R_7(M, Ge)_6$ and $R_5(M, Ge)_4$ compounds*

3.27.1. *$Ce_7Pd_4Ge_2$ structure type*

SG $P2_1/c$, $Z=4$, $a=0.9315$, $b=1.2277$, $c=1.2273$, $\beta=109.46°$ (Gribanov et al. 1993b). See fig. 85.

Atom	Wyckoff notation	*x/a*	*y/b*	*z/c*	G (%)
Ce1	4(e)	0.0003	0.6613	0.3803	100
Ce2	4(e)	0.0017	0.5898	0.0992	100
Ce3	4(e)	0.0021	0.3799	0.3395	100
Ce4	4(e)	0.3535	0.0014	0.3363	100
Ce5	4(e)	0.3624	0.2482	0.0895	100
Ce6	4(e)	0.6321	0.0011	0.1545	100
Ce7	4(e)	0.6374	0.2532	0.4076	100
Pd1	4(e)	0.2508	0.0007	0.0605	100
Pd2	4(e)	0.2759	0.2489	0.3204	100
Pd3	4(e)	0.2989	0.4997	0.0749	100
Pd4	4(e)	0.7276	0.2464	0.1861	100
Ge1	4(e)	0.1441	0.3801	0.1574	100
Ge2	4(e)	0.8561	0.3772	0.0826	100

No isotypic compounds have been found.

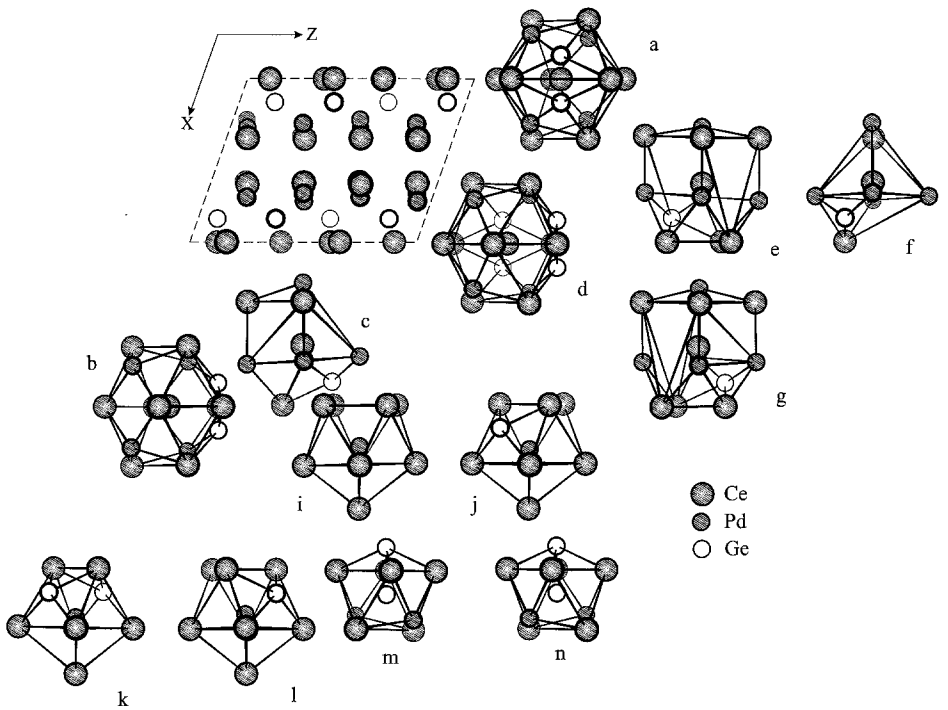

Fig. 85. Projection of the $Ce_7Pd_4Ge_2$ unit cell and coordination polyhedra of the atoms: (a–g) Ce, (i–l) Pd, (m,n) Ge.

3.27.2. *Sm_5Ge_4 structure type*

SG Pnma, $Z=4$, $a=0.7666$, $b=1.4925$, $c=0.7649$ for $Ce_{3.25}Lu_{1.75}Ge_4$ (Shpyrka 1990)

Atom	Wyckoff notation	*x/a*	*y/b*	*z/c*	G (%)
X1	8(d)	0.0253	0.1004	0.6781	100
X2	8(d)	0.3795	0.1157	0.3388	100
X3	4(c)	0.2120	1/4	0.0024	100
Ge1	8(d)	0.2206	0.0449	0.0312	100
Ge2	4(c)	0.0868	1/4	0.3885	100
Ge3	4(c)	0.3239	1/4	0.6333	100

X1 = X2 = X3 = 0.65Ce+0.35Lu

Isotypic compounds:

$Sc_{2.7}Y_{2.3}Ge_4$, $Sc_{1.35}Y_{3.65}Ge_4$, $Sc_{2.7}Dy_{2.3}Ge_4$, $Sc_{1.8}Dy_{3.2}Ge_4$

$Ce_{1.8}Y_{3.2}Ge_4$, $Ce_{0.45-1.35}Lu_{4.55-3.65}Ge_4$

Rare-earth atoms are surrounded by 14–17 neighbours (fig. 86a–c). Trigonal prisms with additional atoms are typical as coordination polyhedra for germanium atoms (fig. 86d–f).

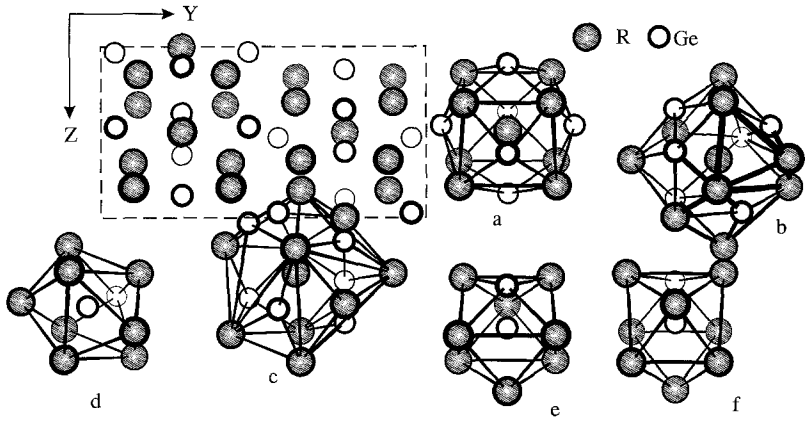

Fig. 86. Projection of the $Ce_{3.25}Lu_{1.75}Ge_4$ unit cell and coordination polyhedra of the atoms: (a–c) R, (d–f) Ge.

3.27.3. *$Gd_5Si_2Ge_2$ structure type*

SG $P112_1/a$, $Z=4$, $a=0.75808$, $b=1.4802$, $c=0.77799$, $\gamma=93.190°$ (Pecharsky and Gschneidner 1997)

Atom	Wyckoff notation	*x/a*	*y/b*	*z/c*	G (%)
Gd1	4(e)	0.325	0.2509	0.003	100
Gd2	4(e)	–0.008	0.1010	0.180	100
Gd3	4(e)	0.016	0.4012	0.188	100
Gd4	4(e)	0.360	0.8817	0.161	100
Gd5	4(e)	0.333	0.6209	0.176	100
X1	4(e)	0.189	0.245	0.360	100
X2	4(e)	0.945	0.254	0.898	100
X3	4(e)	0.201	0.959	0.460	100
X4	4(e)	0.152	0.547	0.467	100

X = 0.5Si+0.5Ge

No isotypic compounds have been observed.

3.28. $R_4(M, Ge)_3$ and $R_3(M, Ge)_2$ compounds

3.28.1. La_8NiGe_5 structure type

SG Pmmn, $Z = 8$, $a = 1.5586$, $b = 1.8384$, $c = 1.1351$ (Bruskov et al. 1984)

Atom	Wyckoff notation	x/a	y/b	z/c	G (%)
La1	8(g)	0.1111	0.1439	0.3842	100
La2	8(g)	0.1198	0.5753	0.2274	100
La3	8(g)	0.6003	0.5510	0.1028	100
La4	8(g)	0.6042	0.0641	0.4219	100
La5	8(g)	0.6186	0.1570	0.1031	100
La6	4(f)	0.1039	1/4	0.0799	100
La7	4(f)	0.1155	1/4	0.7273	100
La8	4(f)	0.5804	1/4	0.5926	100
La9	4(e)	1/4	0.0883	0.1425	100
La10	4(e)	1/4	0.0928	0.6394	100
La11	2(b)	1/4	3/4	0.1419	100
La12	2(b)	1/4	3/4	0.6598	100
Ni1	4(f)	0.5515	1/4	0.8855	100
Ni2	4(e)	1/4	0.5585	0.0105	100
Ge1	8(g)	0.0435	0.0742	0.1547	100
Ge2	8(g)	0.0445	0.1007	0.6233	100
Ge3	4(f)	0.5494	1/4	0.3207	100
Ge4	4(e)	1/4	0.0079	0.3914	100
Ge5	4(e)	1/4	0.1736	0.9011	100
Ge6	4(e)	1/4	0.5543	0.7714	100
Ge7	4(e)	1/4	0.6537	0.4091	100
Ge8	2(a)	1/4	1/4	0.2678	100
Ge9	2(a)	1/4	1/4	0.5124	100

No isotypic compounds have been observed.

3.28.2. *La_3InGe structure type*

SG I4/mcm, $Z=16$, $a=1.2423$, $c=1.5662$ for Ce_3SnGe (Stetskiv 1999). See fig. 87.

Atom	Wyckoff notation	*x/a*	*y/b*	*z/c*	G (%)
Ce1	32(m)	0.1999	0.0668	0.1357	100
Ce2	8(g)	1/2	0	0.1439	100
Ce3	8(h)	0.1674	0.6674	1/2	100
Sn1	4(c)	0	0	0	100
Ge1	8(h)	0.1199	0.6199	0	100
Ge2	4(a)	0	0	1/4	100
X	16(l)	0.1752	0.6752	0.2976	100

X = 0.75Sn+0.25Ge
Isotypic compounds:
R_3SnGe: R = La–Sm
Ce_3MGe: M = Sb, Bi

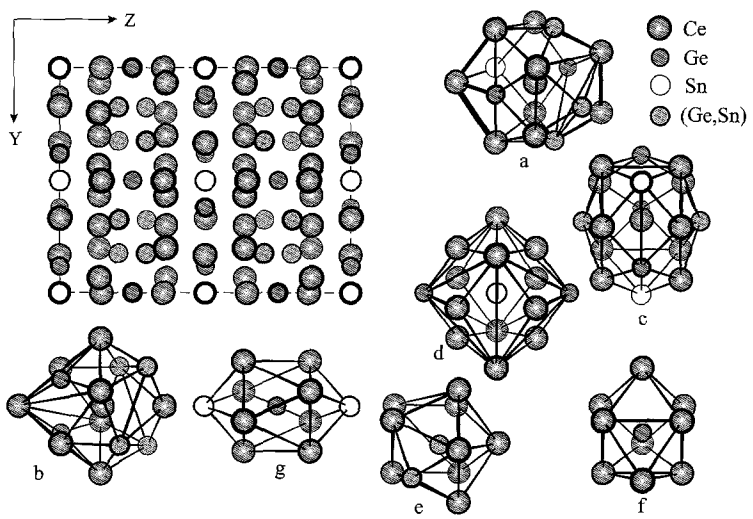

Fig. 87. Projection of the Ce_3SnGe unit cell and coordination polyhedra of the atoms: (a–c) Ce, (d) Sn, (e, f) Ge, (g) X.

3.29. $R_5(M,Ge)_3$ compounds

3.29.1. Y_2HfS_5 structure type

SG Pnma, $Z=4$, $a=1.2255$, $b=0.8898$, $c=0.8008$ Ce_5RuGe_2 (Gladyshevsky et al. 1992b). See fig. 88.

Atom	Wyckoff notation	x/a	y/b	z/c	G (%)
Ce1	8(d)	0.0703	0.5309	0.3156	100
Ce2	4(c)	0.0016	1/4	0.0343	100
Ce3	4(c)	0.2051	1/4	0.6420	100
Ce4	4(c)	0.2866	1/4	0.1630	100
Ru	4(c)	0.0188	1/4	0.4234	100
Ge	8(d)	0.3287	0.5050	0.4331	100

No isotypic compounds have been found.

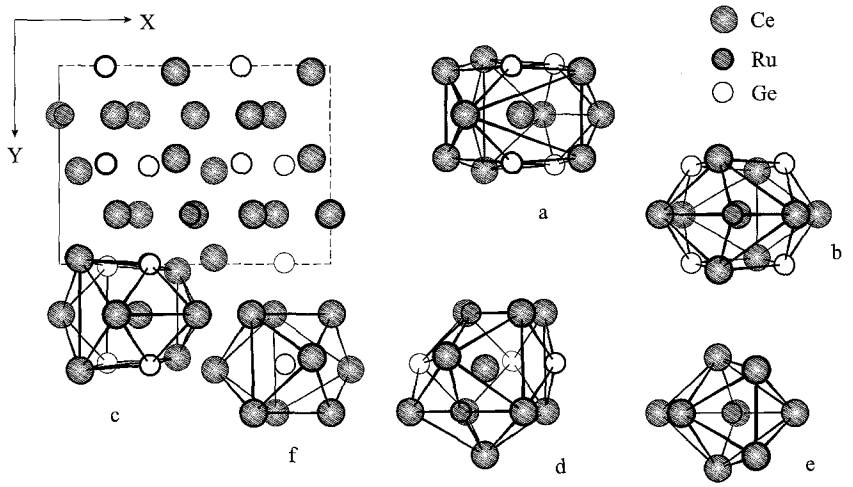

Fig. 88. Projection of the Ce_5RuGe_2 unit cell and coordination polyhedra of the atoms: (a–d) Ce, (e) Ru, (f) Ge.

3.29.2. Ce_5NiGe_2 structure type

SG P4/ncc, $Z=4$, $a=1.1760$, $c=0.6429$ (Belsky et al. 1987). See fig. 89.

Atom	Wyckoff notation	x/a	y/b	z/c	G (%)
Ce1	16(g)	0.0358	0.1636	0.3372	100
Ce2	4(b)	3/4	1/4	0	100

Ni	4(c)	1/4	1/4	0.082	100
Ge	8(f)	0.4095	0.5905	1/4	100

No isotypic compounds have been observed.

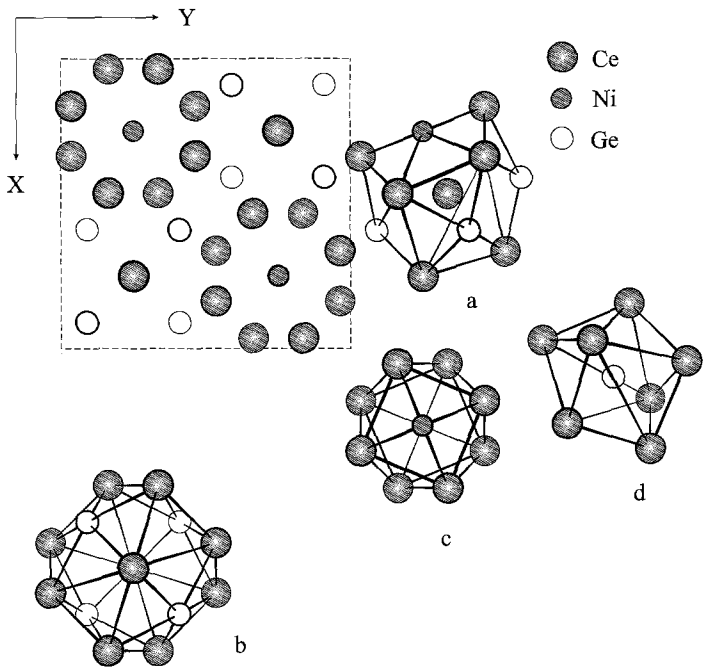

Fig. 89. Projection of the Ce_5NiGe_2 unit cell and coordination polyhedra of the atoms: (a, b) Ce, (c) Ni, (d) Ge.

3.29.3. *Cr_5B_3 structure type*

SG I4/mcm, $Z=4$, $a=0.7939$, $c=1.3908$ for $Nd_5(Ga, Ge)_3$ (Opainych et al. 1992)
Atomic coordinates have not been determined.
Isotypic compound: Ce_5Ga_2Ge

4. Structure types of quaternary rare-earth germanides

4.1. *$R(M, M'Ge)_4$ compounds*

Investigation of the quaternary alloys has been carried out mainly between two isotypic compounds, gradually substituting one of the components in the initial compounds. Thus, as typical for the ternary phases, the $CeGa_2Al_2$ structure type also occurs in the quaternary compounds $Y_xR_{1-x}Mn_2Ge_2$ (R = La, Lu) (Venturini 1996), $Sm_xR_{1-x}Mn_2Ge_2$ (R = Y, Gd)

(Duraj et al. 1989), $Nd_xU_{1-x}M_2Ge_2$ (M=Mn, Co, Ni, Cu) (Sologub and Salamakha 1998), $LaMn_{2-x}M_xGe_2$ (M=Fe, Cu) (Venturini and Malaman 1996), $LaRu_xRh_{2-x}Ge_2$ (Venturini et al. 1989b). The same authors show, that when the LaM_2Ge_2 ternary compounds crystallize with the structure types of $CeGa_2Al_2$ (for M=Ru, Rh, Pd) and of $CaBe_2Ge_2$ (for M=Ir), solid solutions originating from the ternary compounds are found to exist.

The formation of compounds with four individual components with the $CaBe_2Ge_2$ structure becomes possible when the initial ternary compounds crystallize with the $ClGa_2Al_2$ (SG I4/mmm) and $LaPt_2Ge_2$ (SG $P2_1$) types of structure: $LaPt_{1.2}Ru_{0.8}Ge_2$, $LaPt_{1.1}Rh_{0.9}Ge_2$, and $LaPt_{0.7-1.4}Pd_{1.3-0.6}Ge_2$. The compound $LaPt_{1.42}Pd_{0.58}Ge_2$, however, forms a unique structure type which is a superstructure to the $CaBe_2Ge_2$ type. Atomic coordinates for this type are presented below.

4.1.1. *$LaPt_{1.42}Pd_{0.58}Ge_2$ structure type*

SG P4/nmm, $Z=2$, $a=0.4373$, $c=0.9914$ for La $Pt_{1.48}Pd_{0.52}Ge_2$ (Venturini et al. 1989b)

Atom	Wyckoff notation	*x/a*	*y/b*	*z/c*	G (%)
La	2(c)	1/4	1/4	0.7539	100
Pt	2(c)	1/4	1/4	0.1218	100
Ge1	2(c)	1/4	1/4	0.3713	100
Ge2	2(a)	3/4	1/4	0	100
X	2(b)	3/4	1/4	1/2	100

X=0.48Pt+0.52Pd

4.2. *$R(M, M', Ge)_3$ compounds*

4.2.1. *$TbFeSi_2$ structure type*

SG Cmcm, $Z=4$, $a=0.4203$, $b=1.8266$, $c=0.4229$ for $LaMnCu_{0.5}Ge_{1.5}$ (Norlidah et al. 1998)

Atom	Wyckoff notation	*x/a*	*y/b*	*z/c*	G (%)
La	4(c)	0	0.1015	1/4	100
Mn	4(c)	0	0.7494	1/4	100
Ge	4(c)	0	0.3306	1/4	100
X	4(c)	0	0.4680	1/4	100

X=0.5Cu+0.5Ge

Isotypic compounds:

$RMnCu_{0.5}Ge_{1.5}$: R=Ce–Sm

$RMnNi_{0.5}Ge_{1.5}$: R = La–Nd
$RMnPd_{0.5}Ge_{1.5}$: R = La–Nd
$RRhCu_{0.5}Ge_{1.5}$: R = La–Nd
$LaMnPt_{0.5}Ge_{1.5}$

4.2.2. *$LaTmIr_2Ge_4$ structure type*
SG Immm, $Z = 4$, $a = 0.43230$, $b = 0.8825$, $c = 1.6101$ (Malaman et al. 1989)

Atom	Wyckoff notation	*x/a*	*y/b*	*z/c*	G (%)
La	4(g)	0	0.2399	0	100
Tm	4(i)	0	0	0.2067	100
Ir	8(l)	0	0.2486	0.3513	100
Ge1	8(l)	0	0.3484	0.2002	100
Ge2	4(j)	1/2	0	0.0796	100
Ge3	4(i)	0	0	0.4206	100

4.3. *$R(M, M'Ge)_2$ compounds*

4.3.1. *$Y_3NiAl_3Ge_2$ structure type*
SG $P\bar{6}2m$, $Z = 1$, $a = 0.69481$, $c = 0.41565$ (Zhao and Parthé 1990a)

Atom	Wyckoff notation	*x/a*	*y/b*	*z/c*	G (%)
Y	3(f)	0.5963	0	0	100
Ni	1(a)	0	0	0	100
Al	3(g)	0.2261	0	1/2	100
Ge	2(d)	1/3	2/3	1/2	100

5. Discussion

In many cases, ternary germanides of rare-earth metals crystallize with the structure types characteristic for the compounds with silicon which have been discussed extensively in the reviews of Gladyshevsky and Bodak (1982) and Parthé and Chabot (1984). The analysis of many structure types of germanium containing compounds was presented by Gladyshevsky et al. (1990). Our discussion will not be concerned with those types that have been considered in these three surveys.

5.1. *Classification of the ternary structure types of the germanides*

The rare-earth atoms in the above described compounds are generally the largest atoms in the unit cells. Therefore their structure types can be categorized as definite classes in the classification scheme of Kripyakevich (1977), by the coordination number and coordination polyhedra of the atoms of other components with the smaller radii.

Among the R–M–Ge compounds, the most important three classes of structure types are: (1) class 5 with a coordination number equal to 12, and the icosahedron coordination polyhedron; (2) class 9 with coordination numbers of 8–10 and a tetragonal antiprism coordination polyhedron; (3) class 10 with coordination numbers of $6+n$ ($n=1$, 2, 3 or 5) and a trigonal prism coordination polyhedron and its derivatives.

5.1.1. *Structure types with icosahedral coordination of the smallest atoms*

The compound $Nd_2Cr_9Ge_8$ is the first representative of a novel structure type. The coordination polyhedra for the smallest atoms (Cr and Ge) have the form of an icosahedron and its derivatives. The $Nd_2Cr_9Ge_8$ structure can be considered as a linear stacking of the $CaCu_5$ segments and hypothetical RX_{12} slabs (fig. 90).

The $ErCo_3Ge_2$ (or $Er_{6-x}Co_6Ge_4$) structure is a defected derivative from $CaCu_5$ and differs from the present structure by a slight shift of the x coordinate of Co atoms from the site 3(g), $\frac{1}{2}\,0\,\frac{1}{2}$. As result, the symmetry is changed, and the c lattice parameter is doubled.

A part of the same atomic positions from the $CaCu_5$ structure are retained in YCo_6Ge_6, which is formed by the substitution of R atoms by pairs of M atoms. The RM_6Ge_6 compounds crystallize with different structure types, and in most cases polymorphism is observed in these compounds. All of these structure types are related with the YCo_6Ge_6 type. The lattice parameters for the RM_6Ge_6 structures expressed as the lattice parameters of YCo_6Ge_6 (a_1, c_1) are presented in table 1.

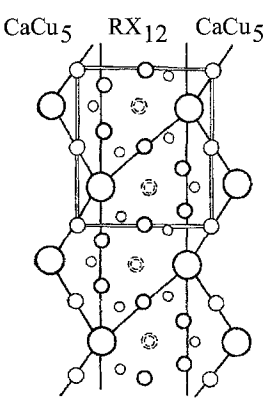

Fig. 90. Structure type $Nd_2Cr_9Ge_8$ as a linear hybrid of $CaCu_5$ and hypothetical RX_{12} structure.

Table 1
Structure types of germanides, related with YCo_6Ge_6 type

Structure type	Space group	Representatives	Lattice parameters		
			a	*b*	*c*
YCo_6Ge_6	P6/mmm	RCo_6Ge_6 (R = Gd–Lu)	a_1	a_1	c_1
$MgFe_6Ge_6$	P6/mmm	RCr_6Ge_6(R = Y, Tb–Er)	a_1	a_1	$2c_1$
$GdMn_6Ge_6$	P6/mmm	$GdMn_6Ge_6$	a_1	a_1	$2c_1$
$ScNi_6Ge_6$	P6/mmm	$ScNi_6Ge_6$	$2a_1$	$2a_1$	$2c_1$
$TbFe_6Sn_6$	Cmcm	RFe_6Ge_6(R = Tb–Ho)	$2c_1$	$2\sqrt{3}a_1$	a_1
$HoFe_6Sn_6$	Immm	$TmFe_6Ge_6$	$2c_1$	$3\sqrt{3}a_1$	a_1
$GdFe_6Ge_6$	Pnma	$GdFe_6Ge_6$	$12a_1$	c_1	$9\sqrt{3}a_1$

5.1.2. *Structure types with tetragonal antiprismatic coordination of the smallest atoms*

An example of the tetragonal antiprism polyhedron (R_4M_4) is a fragment typical for the $BaAl_4$ structure. The structure types with tetragonal antiprismatic coordination generally occur at a rare-earth concentration of R ≈ 20%. The structures which are built from $BaAl_4$ fragments are presented in table 2.

Table 2
Distorted and substited derivatives of $BaAl_4$ in ternary rare-earth germanides

Structure type	Space group	Representatives
$CeAl_2Ga_2$	I4/mmm	RMn(Fe, Co, Ni, Cu, Ru, Rh, Pd, Ag, Pt, Au)$_2Ge_2$
$CaBe_2Ge_2$	P4/nmm	RIr_2Ge_2, R = La–Tb
$LaPt_2Ge_2$	$P2_1$	RPt_2Ge_2, R = La–Dy
$BaNiSn_3$	I4mm	$RCoGe_3$, R = Ce–Eu
$U_2Co_3Si_5$	Ibam	$R_2Ru_3Ge_5$, R = La–Sm, Gd–Tm; $R_2Rh_3Ge_5$, R = La–Pr; $R_2Ir_3Ge_5$, R = La–Sm, Gd–Dy
$Lu_2Co_3Si_5$	C2/c	$R_2Co_3Ge_5$, R = Pr–Sm, Gd–Er; $R_2Rh_3Ge_5$, R = Nd–Sm, Gd–Tm
$LaPt_{1.42}Pd_{0.58}Ge_2$	P4/nmm	$LaPt_{1.42}Pd_{0.58}Ge_2$

5.1.3. *Structure types with trigonal prismatic coordination of the smallest atoms*

Among ternary germanides of rare earths, the most widespread are the structure types which belong to the trigonal prismatic category. In these structures, the trigonal prisms can completely occupy the space without gaps to form columns, walls and stacks, or to connect the peaks (edges). This fragment which is formed by the six large (R) atoms at the corners, and the small seventh one (M or X) inside it gives the AlB_2 type. The

Table 3
Distorted, substituted and vacancy derivatives of AlB_2 in ternary rare-earth germanides

Structure type	Space group	Representatives
AlB_2	P6/mmm	RCuGe, R = La–Sm
$CaIn_2$	$P6_3/mmc$	RCuGe, R = Gd–Yb
KHg_2	Imma	$R(Pd,Ge)_2$, R = Gd–Yb; YbAuGe
ZrBeSi	$P6_3/mmc$	EuZnGe
LiGaGe	$P6_3mc$	RAgGe, R = La–Pr; RAuGe, R = Sc, Y, La–Sm, Gd–Yb
DyAlGe	$Cmc2_1$	DyAlGe
YAlGe	Cmcm	RAlGe, R = Y, Gd–Tm
TiNiSi	Pnma	RCoGe, R = Sc, Y, Sm, Gd–Yb; RNi(Pt)Ge, R = Sc, Y, Ce–Sm, Gd–Yb
$Tb_3Co_2Ge_4$	C2/m	$R_3Co_2Ge_4$, R = Sm, Gd–Tm
CaCuGe	$Pna2_1$	EuCuGe
α-YbAuGe	Pnma	YbAuGe
β-YbAuGe	Pnma	YbAuGe
EuAuGe	Imm2	EuAuGe, $YbAu_{1.24}Ge_{0.76}$

structure types related with the farther structure type AlB_2 by various deformations are presented in table 3.

The new structural types YAlGe, and α-YbAuGe and β-YbAuGe are the centrosymmetric variants of the earlier observed DyAlGe type and CaCuGe type, respectively. EuAuGe is a superstructure to the KHg_2 type.

Mutual rotation of plane segments by 90° in the AlB_2 structure leads to the formation of α-$ThSi_2$, α-$GdSi_2$, LaPtSi and $CeGe_{0.66}Si_{0.92}$ types.

5.2. *Formation of superstructures*

Structure types may have the same positions of atoms, but differ by the number of components substituting at these positions. Simultaneously, the symmetry and outline of the unit cell may be changed. An ordered substitution of the atom positions by different atoms leads to the formation of superstructures. An increase of the number of components in a compound enhances the number of possible variants of their distribution over the atom positions of the parent structure.

Table 4 demonstrates the superstructures which are formed as a result of an ordered substitution of the smallest atoms in the initial binary structure type by the other small atoms.

The structure type $Y_3NiAl_3Ge_2$ is an example of a quaternary substitution variant of a binary structure type: $Fe_2P \rightarrow ZrNiAl \rightarrow Y_3NiAl_3Ge_2$ (SG $P\bar{6}2m$). The partly ordered occupation of the atomic positions of Be in the $CaBe_2Ge_2$ structure by the transition metal atoms leads to the formation of the $LaPt_{1.42}Pd_{0.58}Ge_2$ superstructure.

Table 4
Formation of superstructures by ordered substitution of smaller atoms

Structure type	Space group	Structure type	Space group
Yb_5Sb_3	Pnma	Ce_5RuGe_2	Pnma
Nd_5Ir_3	P4/ncc	Ce_5NiGe_2	P4/ncc
$EuMg_5$	$P6_3/mmc$	$Sc_3Ni_{11}Si_4$	$P6_3/mmc$
$ZrGa_2$	Cmmm	Te_2Ag_3Al	Cmmm
$BaAl_4$	I4/mmm	$CeGa_2Al_2$	I4/mmm
UPt_2	Cmcm	YAlGa	Cmcm
α-$ThSi_2$	$I4_1/amd$	LaPtSi	$I4_1md$
$CaIn_2$	$P6_3/mmc$	LiGaGe	$P6_3mc$
Fe_2P	$P\bar{6}2m$	ZrNiAl	$P\bar{6}2m$
Eu_3Ga_8	Immm	$U_3Ni_4Si_4$	Immm
Ni_2In	$P6_3/mmc$	ZrBeSi	$P6_3/mmc$
$PbCl_2$	Pnma	TiNiSi	Pnma
$SrSi_2$	$P2_13$	ZrOS	$P2_13$

The $LaTmIrGe_2$ structure is a superstructure of $YIrGe_2$ and is formed as a consequence of an ordered occupation of large atoms in the initial structure by rare-earth atoms with different sizes.

The occupation of the atomic positions of Cr in the $Cr_{23}C_6$ structure by the large Ce atoms and the small Pd atoms gives the new $Ce_3Pd_{20}Ge_6$ structure type, i.e. a superstructure of the $Cr_{23}C_6$ type.

A new structure type EuAuGe was derived from the binary KHg_2 structure by an ordered arrangement of the Eu(1) and Eu(2) atoms substituting on the K positions, and the Au and Ge atoms on the Hg positions of KHg_2. Thus, EuAuGe is a superstructure of the binary intermetallic KHg_2.

5.2.1. *Formation of superstructures of the binary rare-earth germanides*

The crystal structure of $Ho_{26}Pd_4(Pd,Ge)_{19-x}$ represents a substitutional variant of the $Er_{26}Ge_{23-x}$ structure type. The difference between the two structures lies only in the replacement of germanium atoms by palladium atoms in positions 2(c) and 8(j) and the presence of a statistical distribution of Ce and Pd atoms in positions 2(c) and 8(i). Other isotypical ternary phases are not known. Only the compound $Ce_{26}Li_5Ge_{23-y}$, where the Li atoms occupy the 2(b) and 8(i) positions which are vacant in the previous phases, has a similar structure (table 5).

The formation of superstructures from the Sm_5Ge_4 type originates from an ordered occupation of the Sm atomic positions by other atoms (table 6). The symmetry of the structures remains unchanged.

Table 5
Site occupancies in $Er_{26}Ge_{23-x}$, $Ho_{26}Pd_4(Pd,Ge)_{19-x}$ and $Ce_{26}Li_5Ge_{23-y}$ (SG P4/nmm)

Site	$Er_{26}Ge_{23-x}$	$Ho_{26}Pd_4(Pd,Ge)_{19-x}$	$Ce_{26}Li_5Ge_{23-y}$
4(f)	Er	Ho	Ce
8(h)	Er	Ho	Ce
8(I)	Er	Ho	Ce
8(I)	Er	Ho	Ce
8(j)	Er	Ho	Ce
16(k)	Er	Ho	Ce
2(c)	Ge	Pd	Ge
2(c)	Ge	Ge	Ge
2(c)	Ge	$Pd_{0.21}Ge_{0.79}$	Ge
8(I)	Ge	Ge	Ge
8(I)	Ge	$Pd_{0.27}Ge_{0.73}$	Ge
8(j)	Ge	Pd	Ge
8(j)	Ge	Ge	Ge
8(j)	Ge	Ge	Ge
2(b)			Li
8(I)			Li

Table 6
Site occupancies in Sm_5Ge_4, $Ce_2Sc_3Ge_4$, $Sc_2V_3Ge_4$ and Tm_4LiGe_4 (SG Pnma)

Site	Sm_5Ge_4	$Ce_2Sc_3Ge_4$	$Sc_2V_3Ge_4$	Tm_4LiGe_4
4(c)	Sm	Sc	V	Li
8(d)	Sm	Sc	V	Tm
8(d)	Sm	Ce	Sc	Tm
4(c)	Ge	Ge	Ge	Ge
4(c)	Ge	Ge	Ge	Ge
8(d)	Ge	Ge	Ge	Ge

The compound $Gd_5Si_2Ge_2$ occurs between two isotypic binary compounds, Gd_5Si_4 and Gd_5Ge_4 (structure type Sm_5Ge_4). An internal deformation in the structure leads to the exterior one. The initial orthorhombic structure transforms to a monoclinic structure.

In contrast to the previously described examples, the formation of three types of superstructures of the $Ho_{11}Ge_{10}$ type is possible (table 7):

(i) an ordered substitution of the site originally occupied by the large atom 16(n) – $Sc_{11-x}Yb_xGe_{10}$;
(ii) an ordered substitution of the site originally occupied by the small atom 8(h) – $Sc_{11}Al_2Ge_8$.
(iii) an $Sc_7Mn_{4-x}Ge_{10-x}$ structure: the Mn atom occupies the 16(n) position, and the statistical mixture (Mn, Ge) fills the 8(h) position.

Table 7
Site occupancies in $Ho_{11}Ge_{10}$, $Sc_{11}Al_2Ge_8$, $Sc_7Mn_{4+x}Ge_{10-x}$ ($x = 1.3$) and $Sc_{11-x}Yb_xGe_{10}$ ($x \approx 5$) (SG I4/mmm)

Site	$Ho_{11}Ge_{10}$	$Sc_{11}Al_2Ge_8$	$Sc_7Mn_{4+x}Ge_{10-x}$	$Sc_{11-x}Yb_xGe_{10}$
4(e)	Ho	Sc	Sc	$Sc_{0.22}Yb_{0.78}$
8(h)	Ho	Sc	Sc	$Sc_{0.29}Yb_{0.71}$
16(n)	Ho	Sc	Sc	$Sc_{0.32}Yb_{0.68}$
16(n)	Ho	Sc	Mn	Sc
4(d)	Ge	Ge	Ge	Ge
4(e)	Ge	Ge	Ge	Ge
8(h)	Ge	Al	$Mn_{0.64}Ge_{0.36}$	Ge
8(I)	Ge	Ge	Ge	Ge
16(m)	Ge	Ge	Ge	Ge

5.3. *Analysis of some new structure types*

The atoms in the $Ho_4Ir_{13}Ge_9$ structure are located in two planes with $x = \frac{1}{4}$ and $x = \frac{3}{4}$. The metal atoms form trigonal prisms with their axes parallel to one another. The prisms centered by germanium atoms form two types of blocks: $HoIr_6Ge_3$ and $Ho_3Ir_{10}Ge_6$ which are mutually connected through empty trigonal prisms formed by iridium atoms. The blocks are shifted with respect to each other by a half translation along the shortest (a) axis (fig. 91). A survey of the literature of known structure types revealed that these blocks are typical for compounds such as YNi_5Si_3 (fig. 91, a) and $Y_6Ni_{20}P_{13}$ (fig. 91, b).

The unit cell dimensions of the $Ce_2Pt_7Ge_4$ structure correspond to the lattice parameters of the previous one. The atoms of cerium and platinum produce trigonal prisms in which the germanium atoms are located. Three trigonal prisms combine with each other owing to a common edge to give a typical "star". The fourth prism has a common edge with one of these prisms. This fragment corresponds to the composition $Ce_2Pt_7Ge_4$. The packing arrangement of the prisms in the $Ce_2Pt_7Ge_4$ structure are shown in fig. 92. The distance between two similarly oriented "star" fragments in terms of the lattice parameter a is $1/2a$. The crystal structure of $Ce_2Pt_7Ge_4$ (I) is similar to that of the compound $Nd_2Ni_7P_4$ (II) (space group $Pmn2_1$) ($a_I \approx 2b_{II}$, $b_I \approx a_{II}$, $c_I \approx c_{II}$) in which the packing of the same "stars" is observed.

In the ternary cross section of the Ce–Pt–Ge system the compound $Ce_3Pt_4Ge_6$ is located between $CePt_2Ge_2$ and $CePtGe_2$. Analysis of the crystal structures shows $Ce_3Pt_4Ge_6$ to be a combination of the two structures. The relationship between the $CePt_2Ge_2$, $Ce_3Pt_4Ge_6$ and $CePtGe_2$ structures is shown in fig. 93. The marked fragment in $CePtGe_2$ (structural type $NdIrGe_2$) has the composition $Ce_2Pt_2Ge_4$. The composition $2Ce_3Pt_4Ge_6$ is the result of the following fragment packing: $\frac{1}{2}Ce_2Pt_2Ge_4 + CePt_2Ge_2 + Ce_2Pt_2Ge_4 + CePt_2Ge_2 + \frac{1}{2}Ce_2Pt_2Ge_4$.

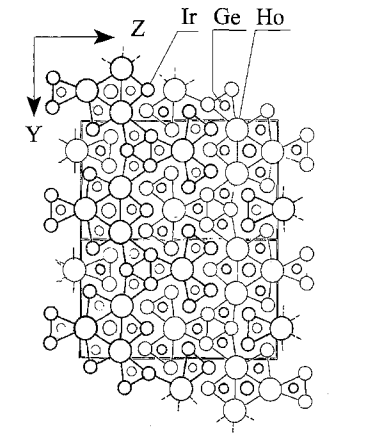

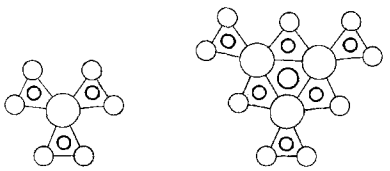

Fig. 91. Blocks of atoms, typical for the structures related to the $Ho_4Ir_{13}Ge_9$ type: (a) YNi_5Si_3 and (b) $Y_6Ni_{20}P_{13}$.

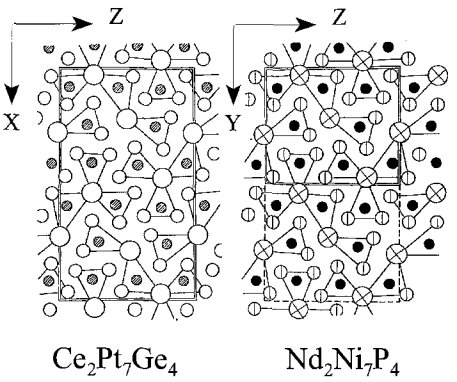

Fig. 92. The interrelation between $Ce_2Pt_7Ge_4$ and $Nd_2Ni_7P_4$ structures.

The structural type $Y_3Pt_4Ge_6$ is monoclinically deformed $Ce_3Pt_4Ge_6$ with $a \approx 2a$, $b \approx b$ and $c \approx \frac{1}{2}c$. The structure of $Y_3Pt_4Ge_6$ is a stacking variant of the monoclinic structures $LaPt_2Ge_2$ and $NdIrGe_2$.

The $Nd_4Rh_4Ge_3$ structure type can be described as a stacking of fragments typical for the YPd_2Si and $La_3Ni_2Ga_2$ structures (fig. 94). In turn, the $La_3Ni_2Ga_2$ structure consists of YAlGe and CrB fragments.

The structure types $Ce_2(Ga_{0.9}Ge_{0.1})_7$ and $La_2Al_{1+x}Ge_{6-x}$ are the vacancy variant of the orthorhombic $SmNiGe_3$ and can be considered as an intergrowth of AlB_2-, deformed Po- and partially vacant $BaAl_4$-type slabs.

The $Yb_7Al_5Ge_8$ structure type can be considered as an intergrowth of TiNiSi-, AlB_2- and CsCl-type columns.

The new structure types $CeRh_{1-x}Ge_{2+x}$ and $Ce_2Cu_3Ge_3$ are formed as a result of an internal deformation of the $CeNiSi_2$ structure; the unit cell dimensions, however, remain unchanged. The $TmLi_{1-x}Ge_2$ structure is a monoclinically deformed derivative of the $CeNiSi_2$ structure and it can be described as a result of an inclusion of Li atoms into the empty tetragonal prisms which are typical for the $CaSb_2$ structure.

The $TmLi_{1-x}Ge_2$, $CeRh_{1-x}Ge_{2+x}$ and $Ce_2Cu_3Ge_3$ structures together with $CeNiSi_2$, $TbFeSi_2$ and $U_3Ni_4Si_4$ are the members of the homological series of compounds with the common formulae $R_{m+0.5n}M_{2m}X_{2n}$ where m is the number of AlB_2 fragments and n is the number of $BaAl_4$ fragments. For $TmLi_{1-x}Ge_2$, $m=1$ and $n=2$; for the $CeRh_{1-x}Ge_{2+x}$, $Ce_2Cu_3Ge_3$, $CeNiSi_2$ and $TbFeSi_2$ structures $m=2$ and $n=4$; and for $U_3Ni_4Si_4$, $m=n=4$.

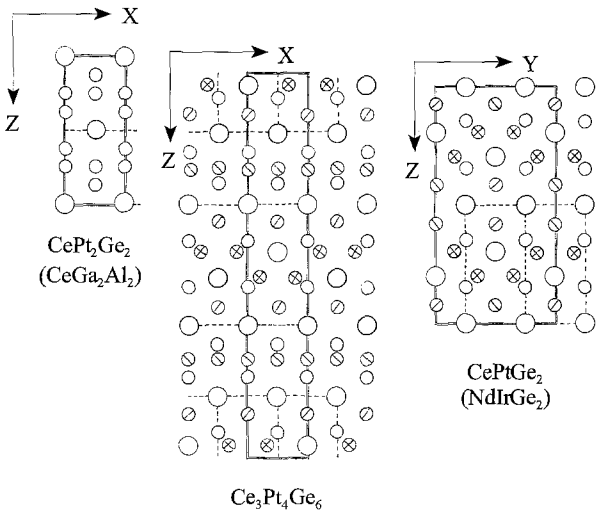

Fig. 93. The interrelation between $CePt_2Ge_2$, $Ce_3Pt_4Ge_6$ and $CePtGe_2$ structures.

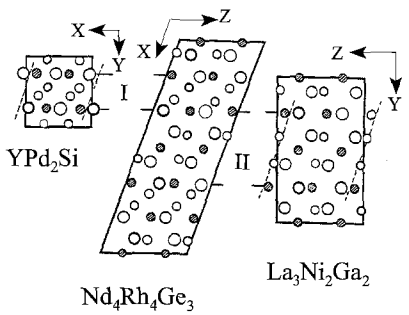

Fig. 94. The $Nd_4Rh_4Ge_3$ as a stacking of (I) YPd_2Si and (II) $La_3Ni_2Ga_2$ fragments.

Acknowledgement

This work was partially supported by NATO Research Fellowship in Portugal.

References

Andrusyak, R.I., 1988, Interaction of scandium with transition metals of IVth period and germanium (equilibrium phase diagrams, crystal structures and physical properties of compounds) Ph.D. Chemistry Thesis (Lvov State University, Lvov) pp. 1–235.

Andrusyak, R.I., and B.Ya. Kotur, 1987, Kristallografiya **32**, 1018.

Barakatova, J.M., 1994, Physical chemistry interaction of palladium, platinum, silicon and germanium with samarium, Ph.D. Chemistry Thesis (Moscow State University, Moscow) pp. 1–21.

Baran, S., A. Szytuła, J. Leciejewicz, N. Stusser, A. Zygmunt, Z. Tomkowicz and M. Guillot, 1996, J. Alloys & Compounds **243**, 112.

Belsky, V.K., M.B. Konyk, V.K. Pecharsky and O.I. Bodak, 1987, Kristallografiya **32**, 241.

Belyavina, N.M., O.Ya. Beloborodova, V.Ya. Markiv and N.V. Alekseeva, 1993, Dopov. Akad. Nauk URSR **9**, 84.

Bodak, O.I., V.A. Bruskov and V.K. Pecharsky, 1982, Kristallografiya **27**, 896.

Bodak, O.I., V.K. Pecharsky, O.Ya. Mruz, V.E. Zavodnik, G.M. Vytvitska and P.S. Salamakha, 1985, Dopov. Akad Nauk URSR, Ser. B **2**, 36.

Bodak, O.I., E.I. Gladyshevsky, P.S. Salamakha, V.K. Pecharsky and V.A. Bruskov, 1989a, Kristallografiya **34**, 1285.

Bodak, O.I., V.K. Pecharsky, O.L. Sologub and V.B. Rybakov, 1989b, Izv. Akad. Nauk SSSR, Met. **2**, 34.

Bodak, O.I., O.Ya. Oleksyn and V.K. Pecharsky, 1990, Dopov. Akad Nauk URSR, Ser. B **2**, 30.

Boutarek, N., R. Madar, B. Lambert-Andron, S. Auffret and J. Pierre, 1992, J. Alloys & Compounds **189**, 9.

Bruskov, V.A., 1984, New structure types of rare earth germanides, Ph.D. Chemistry Thesis (Lvov State University, Lvov) pp. 1–17.

Bruskov, V.A., V.K. Pecharsky and E.I. Gladyshevsky, 1983, New ternary germanides of lanthanum and nickel, in: Tezisy dokl. IV Vsesoyuzn. Konf. Po Kristalloch. Intermetall. Soed., Lvov, 1983, p. 95.

Bruskov, V.A., V.K. Pecharsky, O.I. Bodak and E.I. Gladyshevsky, 1984, Kristallografiya **29**, 1071.

Bruskov, V.A., V.K. Pecharsky and O.I. Bodak, 1986, Izv. Akad. Nauk SSSR, Neorg. Mater. **22**, 1471.

Buchholz, W., and H.-U. Schuster, 1981, Z. Anorg. Allg. Chem. **482**, 40.

Cenzual, K., B. Chabot and E. Parthé, 1987, J. Solid State Chem. **70**, 229.

Duraj, M., R. Duraj and A. Szytuła, 1989, J. Magn. Magn. Mater. **82**, 319.

Engel, N., B. Chabot and E. Parthé, 1984, J. Less-Common Met. **96**, 291.

Fedyna, M.F., 1988, Phase equilibria, crystal structures and physical properties of compounds in the (Pr, Tm)–(Fe, Co, Ni)–Ge systems, Ph.D. Chemistry Thesis (Lvov State University, Lvov) pp. 1–17.

Fedyna, M.F., and V.K. Pecharsky, 1989, Crystal structure of compound $Pr_6Fe_{13}Ge$, in: V Vsesoyuzn. Konf. Kristallokh. Intermet. Soed., Lvov, 1989, p. 36.

Fedyna, M.F., V.K. Pecharsky and O.I. Bodak, 1987, Izv. Akad. Nauk SSSR, Neorg. Mater. **23**, 570.

Gladyshevsky, E.I., and O.I. Bodak, 1982, Crystal Chemistry of Rare Earth Intermetallic Compounds (Vyscha Shkola, Lvov) pp. 1–253.

Gladyshevsky, E.I., O.I. Bodak and V.K. Pecharsky, 1990, Phase equilibria and crystal chemistry in ternary rare earth systems with metallic elements, in: Handbook on the Physics and Chemistry of Rare Earths, Vol. 13, eds K.A. Gschneidner Jr and L. Eyring (North-Holland, Amsterdam) pp. 1–191.

Gladyshevsky, R.E., O.L. Sologub and E. Parthé, 1991b, J. Alloys & Compounds **176**, 329.

Gladyshevsky, R.E., E. Parthé, O.L. Sologub and P.S. Salamakha, 1992a, Z. Kristallogr. **232**, 161.

Gladyshevsky, R.E., K. Cenzual, J.T. Zhao and E. Parthé, 1992b, Acta Crystallogr. C **48**, 221.

Gribanov, A.V., O.L. Sologub, P.S. Salamakha, O.I. Bodak, Yu.D. Seropegin, V.V. Pavlyuk and V.K. Pecharsky, 1992a, J. Alloys & Compounds **189**, L11.

Gribanov, A.V., O.L. Sologub, P.S. Salamakha, O.I. Bodak, Yu.D. Seropegin and V.K. Pecharsky, 1992b, J. Alloys & Compounds **179**, L7.

Gribanov, A.V., Yu.D. Seropegin, O.I. Bodak, V.V. Pavlyuk, L.G. Akselrud, V.N. Nikiforov and A.A. Velikhovskii, 1993a, J. Alloys & Compounds **202**, 133.

Gribanov, A.V., Yu.D. Seropegin, O.I. Bodak, V.V. Pavlyuk, V.K. Pecharsky, O.L. Sologub and P.S. Salamakha, 1993b, J. Alloys & Compounds **198**, 39.

Gribanov, A.V., Yu.D. Seropegin and O.I. Bodak, 1994, J. Alloys & Compounds **204**, L9.

Gryniv, I.O., and O.R. Myakush, 1989, System Tm–Ga–Ge, in: V Vsesoyuzn. Konf. Kristallokh. Intermet. Soed., Lvov, 1989, p. 80.

Gryniv, I.O., A.S. Noga and Yu.N. Grin', 1989, Ternary systems of gallium and germanium with rare earth (Ce) and transition (Mn) metals, in: V Vsesoyuzn. Soveshch. Diagr. Sost. Metal. system., Tezisy Dokl., Zvenigorod, 1989, p. 154.

Guloy, A.M., and J.D. Corbett, 1996, J. Inorg. Chem. **35**, 2616.

Hovestreydt, E., N. Engel, K. Klepp, B. Chabot and E. Parthé, 1982, J. Less-Common Met. **85**, 247.

Iandelli, A., 1993, J. Alloys & Compounds **198**, 141.

Konyk, M.B., 1986, Visn. L'viv Univers. **27**, 35.

Konyk, M.B., 1988, Visn. L'viv Univers., Ser. Khim. **29**, 25.

Konyk, M.B., 1989, Phase equilibria, crystal structure and physical properties of compounds in the

Ce–(Mn, Fe, Co, Ni, Cu)–Ge systems, Ph.D. Thesis (Lvov State University, Lvov) pp. 1–17.

Konyk, M.B., P.S. Salamakha, O.I. Bodak and V.K. Pecharsky, 1988, Kristallografiya **33**, 838.

Koterlyn, G.M., M.F. Fedyna and V.M. Baranyak, 1994, Visn. L'viv Univers., Ser. Khim. **33**, 37.

Kotur, B.Ya., R.I. Andrusyak and V.E. Zavodnik, 1988, Kristallografiya **1**, 240.

Kotur, B.Ya., O.M. Vozniak and O.I. Bodak, 1989, Izv. Akad. Nauk, Neorg. Mater. **25**(3), 399.

Kripyakevich, P.I., 1977, Structure Types of Intermetallic Compounds (Nauka, Moscow) pp. 1–288.

Malaman, B., G. Venturini, M. Francois and B. Roques, 1989, J. Alloys & Compounds **192**, 203.

Mathur, N.D., and C.D. Frost, 1994, J. Alloys & Compounds **215**, 325.

Merlo, F., M. Pani, F. Canepa and M.L. Fornasini, 1998, J. Alloys & Compounds **264**, 82.

Meyer, M., G. Venturini, B. Malaman, J. Steinmetz and B. Roques, 1983, Mater. Res. Bull. **18**, 1983.

Mruz, O.Ya., 1988, Ternary systems Sm–(Fe, Co, Ni)–Ge, Ph.D. Chemistry Thesis (Lvov State University, Lvov) pp. 1–17.

Mruz, O.Ya., V.K. Pecharsky, O.I. Bodak and V.A. Bruskov, 1987, Dopov. Akad. Nauk URSR, Ser. B **6**, 51.

Mruz, O.Ya., V.K. Pecharsky, A.N. Sobolev and O.I. Bodak, 1990, Sov. Phys.-Crystallogr. **35**, 122.

Muratova, L.A., 1976, Ternary systems (yttrium, lanthanum, cerium, praseodymium, gadolinium)–germanium–silicon, Ph.D. Chemistry Thesis (Lvov University, Lvov) pp. 1–17.

Norlidah, M.N., G. Venturini and B. Malaman, 1998, J. Alloys & Compounds **267**, 182.

Oleksyn, O.Ya., and O.I. Bodak, 1994, J. Alloys & Compounds **215**, 45.

Oniskovetz, B.D., V.K. Belsky, V.K. Pecharsky and O.I. Bodak, 1987, Kristallografiya **32**, 888.

Opainych, I.M., 1996, Phase equilibria and crystal structure of compounds in the Ce–(Fe, Ni)–(Mg, Zn) and Ce–Zn–Ge systems, Ph.D. Chemistry Thesis (L'viv State University, L'viv) pp. 1–21.

Opainych, I.M., O.M. Sichevich and Yu.N. Grin', 1992, Crystal structure and magnetic properties of compounds in the system Nd–Ga–Ge, in: VI Sov. Kristallokh. Neorg. Koord. Soedin., Tezisy dokl., Lvov, 1992, p. 205.

Parthé, E., and B. Chabot, 1984, Crystal structures and crystal chemistry of ternary rare earth–transition metal borides, silicides and homologues, in: Handbook on the Physics and Chemistry of Rare Earths, Vol. 6, eds. K.A. Gschneidner Jr and L. Eyring (North-Holland, Amsterdam) pp. 113–334.

Pavlyuk, V.V., 1993, Synthesis and crystal chemistry of the intermetallic compounds of lithium, Dr.Sc. Chemistry Thesis, Abstracts (L'viv State University, L'viv) pp. 1–46.

Pavlyuk, V.V., V.K. Pecharsky and O.I. Bodak, 1986, Dopov. Akad. Nauk URSR, Ser. A **7**, 78.

Pavlyuk, V.V., V.K. Bel'sky, O.I. Bodak and V.K. Pecharsky, 1987a, Dopov. Akad. Nauk URSR, Ser. B **10**, 45.

Pavlyuk, V.V., V.K. Pecharsky, O.I. Bodak and V.A. Bruskov, 1987b, Sov. Phys.-Crystallogr. **32**(1), 38.

Pavlyuk, V.V., V.K. Pecharsky and O.I. Bodak, 1988a, Sov. Phys.-Crystallogr. **33**(1), 22

Pavlyuk, V.V., V.K. Pecharsky, O.I. Bodak and V.A. Bruskov, 1988b, Sov. Phys.-Crystallogr. **33**(1), 24.

Pavlyuk, V.V., V.K. Pecharsky, O.I. Bodak and A.N. Sobolev, 1989, Izv. Akad. Nauk SSSR, Met. **5**, 221.

Pavlyuk, V.V., O.I. Bodak and V.E. Zavodnik, 1990, Dopov. Akad. Nauk URSR, Ser. B **12**, 29.

Pavlyuk, V.V., O.I. Bodak and O.I. Sobolev, 1991, Kristallografiya **36**(4), 880.

Pecharsky, V.K., and K.A. Gschneidner Jr, 1997, J. Alloys & Compounds **260**, 131.

Pecharsky, V.K., O.I. Bodak and V.A. Bruskov, 1986, Sov. Phys.-Crystallogr. **31**, 184.

Pecharsky, V.K., O.I. Bodak, V.K. Belsky, P.K. Starodub, I.R. Mokraya and E.I. Gladyshevsky, 1987, Kristallografiya **32**, 334.

Pecharsky, V.K., K.A. Gschneidner Jr, O.I. Bodak and A.S. Protsyk, 1991, J. Less-Common Met. **168**, 257.

Pöttgen, R., 1995a, J. Mater. Chem. **5**(3) 505.

Pöttgen, R., 1995b, Z. Kristallogr. **210**, 924.

Pöttgen, R., R.K. Kremer, W. Schnelle, R. Mullmann and B.D. Mosel, 1996, J. Mater. Chem. **6**(4), 635.

Rieger, W., 1970, Monatsh. Chem. **101**, 449.

Salamakha, P.S., 1986, Visn. L'viv Univers., Ser. Khim. **27**, 27.

Salamakha, P.S., 1989, Phase equilibria and crystal structure of the compounds in the Nd–transition metal–germanium systems, Ph.D. Chemistry Thesis (Lvov State University, Lvov) pp. 1–184.

Salamakha, P.S., V.K. Pecharsky, V.A. Bruskov and O.I. Bodak, 1986, Kristallografiya **31**, 587.

Salamakha, P.S., O.I. Bodak, V.K. Pecharsky and V.A. Bruskov, 1989, Kristallografiya **34**, 122.

Salamakha, P.S., O.L. Sologub, J. Stępień-Damm and A. Stash, 1996, Kristallografiya **41**(6), 1135.

Salamakha, P.S., O.L. Sologub and O.I. Bodak, 1999, Ternary rare-earth–germanium systems, this volume, ch. 173.

Schöbinger-Papamantellos, P., E.B. Altofer, J.H.V.J. Brabers, F.R. de Boer and K.H.J. Buschow, 1994, J. Alloys & Compounds **203**, 243.

Segre, C.U., H.F. Braun and K. Yvon, 1981, Properties of $Y_3Ru_4Ge_{13}$ and isotypic compounds, in: Ternary Superconductors, Proc. Int. Conf., Lake Geneva, 1980, p. 243.

Shapiev, B.I., O.L. Sologub, Yu.D. Seropegin, O.I. Bodak and P.S. Salamakha, 1991, J. Less-Common Met. **175**, L1.

Shpyrka, Z.M., 1990, Phase equilibria, crystal structure and physical properties of compounds in the ternary Sc–(Y, Ce, Nd, Dy)–Ge and Ce–(Y, La, Gd, Lu)–Ge systems, Ph.D. Chemistry Thesis (Lvov State University, Lvov) pp. 1–17.

Sologub, O.L., 1995, Interaction of holmium and germanium with platinum metals, silver and gold (phase equilibria and crystal structures of ternary germanides) Ph.D. Chemistry Thesis (L'viv State University, L'viv) pp. 1–145.

Sologub, O.L., and A.S. Protsyk, 1991, Visn. L'viv State Univers. **31**, 31.

Sologub, O.L., and P.S. Salamakha, 1998, Structural chemistry of new quaternary germanides of uranium, in: Actinides and the Environment, NATO ASI Series 2 (Kluwer Academic Publishers, Dordrecht) p. 125.

Sologub, O.L., and P.S. Salamakha, 1999, J. Alloys & Compounds **291**, 181.

Sologub, O.L., Yu.M. Prots', P.S. Salamakha, V.K. Pecharsky and O.I. Bodak, 1993, J. Alloys & Compounds **202**, 13.

Sologub, O.L., Yu.M. Prots', P.S. Salamakha, V.K. Pecharsky and O.I. Bodak, 1994, J. Alloys & Compounds **216**, 231.

Starodub, P.K., I.R. Mokraya, O.I. Bodak, V.K. Pecharsky and V.A. Bruskov, 1986, Kristallografiya **31**, 394.

Stetskiv, A.O., 1999, Interaction of the component in the ternary systems Ce–(Si, Ge)–(C, Sn, Sb, Bi) (phase equilibria and crystal structures of ternary compounds) Ph.D. Chemistry Thesis (L'viv State University, L'viv) pp. 1–150.

Stetskiv, A.O., V.V. Pavlyuk and O.I. Bodak, 1998, Pol. J. Chem. **72**, 956.

Venturini, G., 1996, J. Alloys & Compounds **232**, 133.

Venturini, G., and B. Malaman, 1990, J. Less-Common Met. **167**, 45.

Venturini, G., and B. Malaman, 1996, J. Alloys & Compounds **235**, 201.

Venturini, G., and B. Malaman, 1997, J. Alloys & Compounds **261**, 19.

Venturini, G., M. Méot-Meyer, B. Malaman and B. Roques, 1985, J. Less-Common Met. **113**, 197.

Venturini, G., M. Méot-Meyer, J.M. Mareche, B. Malaman and B. Roques, 1986, Mater. Res. Bull. **21**, 33.

Venturini, G., B. Malaman and B. Roques, 1989a, J. Less-Common Met. **146**, 271.

Venturini, G., B. Malaman and B. Roques, 1989b, J. Solid State Chem. **79**, 229.

Venturini, G., R. Welter and B. Malaman, 1992, J. Alloys & Compounds **185**, 99.

Welter, R., G. Venturini, B. Malaman and E. Ressouche, 1993, J. Alloys & Compounds **202**, 165.

Yanson, T.I., 1975, Crystal structures of the alumosilicides and alumogermanides of the rare earth elements, Ph.D. Chemistry Thesis (Lvov State University, Lvov) pp. 1–17.

Yarmolyuk, Ya.P., V.K. Pecharsky, I.A. Gryniv, O.I. Bodak and V.E. Zavodnik, 1989, Sov. Phys.-Crystallogr. **34**, 174.

Zarechnyuk, O.S., A.A. Muravyeva and E.I. Gladyshevsky, 1970, Dopov. Akad. Nauk URSR, Ser. A, p. 753.

Zaremba, V.I., J. Stępień-Damm, G.P. Nychyporuk, Yu.B. Tyvanchuk and Ya.M. Kalychak, 1997, Kristallografiya **42**(2), 354.

Zhao, J.T., and E. Parthé, 1990a, Acta Crystallogr. C **46**, 2273.

Zhao, J.T., and E. Parthé, 1990b, Acta Crystallogr. C **46**, 2276.

Zhao, J.T., and E. Parthé, 1991a, Acta Crystallogr. C **47**, 1.

Zhao, J.T., and E. Parthé, 1991b, Acta Crystallogr. C **47**, 4.

Zhao, J.T., and E. Parthé, 1991c, Acta Crystallogr. C **47**, 1781.

Zhao, J.T., K. Cenzual and E. Parthé, 1991, Acta Crystallogr. C **47**, 1777.

Zmii, O.F., E.I. Gladyshevsky and V.S. Bulyo, 1973, Kristallografiya **18**(2), 277.

Handbook on the Physics and Chemistry of Rare Earths
Vol. 27
edited by K.A. Gschneidner, Jr. and L. Eyring

Chapter 175

SCANDIUM ALLOY SYSTEMS AND INTERMETALLICS

Bogdan Ya. KOTUR
Department of Inorganic Chemistry, Ivan Franko Lviv National University, Kyryla & Mefodiya Str. 6, 79005 Lviv, Ukraine

Ernst GRATZ
Institute for Experimental Physics, Technical University Vienna, Wiedner Hauptstrasse 8–10, A-1040 Wien, Austria

---

Contents

List of symbols

A	Coefficient of resistivity ($\rho_{mag}=AT^2$)	bcc	Body centered cubic
A_4, A_6	Crystal field parameters	C	Curie constant
a, b, c	Lattice parameters	c	Total heat capacity
B	Magnetic induction	CF	Crystal field

CN	Coordination number
CP	Coordination polyhedron
c_m	Magnetic heat capacity
Δc	Difference in the heat capacity at T_S
cub	Cubic symmetry
dhcp	Double hexagonal close packed
DOS	Density of states
E	Eutectic transition
Ed	Eutectoid transition
fcc	Face centered cubic
hcp	Hexagonal close packed
hex	Hexagonal symmetry
HT	High temperature
iL	Immiscibility gap in liquid
L	Congruently melting compound; liquid
LT	Low temperature
M	Magnetization
M, M′	Metallic element (s-, d-, f-element)
Mt	Metatectic transition
$N(\varepsilon_F)$	Density of states at the Fermi level
orthorh	Orthorhombic symmetry
P	Peritectic transition
Pd	Peritectoid transition
p_S	Saturation moment
S	Polymorphic transition
S, S_{tot}	Total thermopower
S_{diff}	Diffusion thermopower
S_{drag}	Thermopower due to drag effects
SG	Space group
ST	Structure type
s,p,d,f	Band index
tetr	Tetragonal symmetry
T_{sf}	Spin fluctuation temperature
T_C	Curie temperature
T_N	Néel temperature
T_S	Superconducting transition temperature
W	Total thermal resistivity
$W_{e.0}$	Residual thermal resistivity
$W_{e.ph}$	Thermal resistivity due to phonon scattering
$W_{e.sf}$	Thermal resistivity due to spin fluctuation scattering
x, W	Crystal field parameters of cubic systems
X, X′	p-element
α	Thermal expansion coefficient
α, β, γ	Lattice parameters
$\alpha_n, \beta_n, \gamma_n$	Specific heat coefficients in the normal state
$\alpha_s, \beta_s, \gamma_s$	Specific heat coefficients in superconducting state
β	Lattice specific heat coefficient
χ	Magnetic susceptibility
χ_0	Temperature independent magnetic susceptibility
γ	Electronic specific heat coefficient
ε_F	Fermi energy
λ	Total thermal conductivity
λ_l	Lattice thermal conductivity
λ_e	Electronic thermal conductivity
μ_B	Bohr magneton
μ_{Fe}	Bohr magneton per Fe atom
μ_{eff}	Effective magnetic moment
ρ, ρ_{ges}	Total electrical resistivity
ρ_0	Residual electrical resistivity
ρ_{sf}	Electrical resistivity due to spin fluctuation scattering
ρ_{mag}	Electrical resistivity due to magnetic scattering
ρ_{ph}	Electrical resistivity due to phonon scattering
$\Delta\rho/\rho$	Magnetoresistance
~	Precedes the composition formula of a compound to indicate that the composition is given tentatively

1. Introduction

The last comprehensive treatment of scandium as an element and of its alloys and compounds was given in the book *Scandium. Its occurrence, chemistry, physics, metallurgy, biology and technology* in 1975 (Gschneidner 1975). Meanwhile numerous

structural investigations have been published in the literature mainly concerning structural properties. It seems that the time is ready to summarise the new results with the aim to give an overview over the last most significant and relevant results. Since one of us (B.K.) has been working for more than twenty years in the field of structural and chemical investigations of scandium-based alloys and compounds, it is obvious that problems such as phase stability and the phase diagrams represent the main part of the chapter. Many investigations of ternary scandium-based phase diagrams have been investigated and published since 1975. However, there are also numerous new investigations of binary compounds and their phase diagrams are now known, and these are included in this chapter. The aim is to give an overview of the newly published data up to the beginning of 1997. In sections 2 and 3 the binary and ternary scandium containing systems are treated, whereas sect. 4 is dedicated to multicomponent systems.

At the beginning of each section an explanation is given of how the information is subdivided in the subsequent text. Each phase diagram is accompanied by a brief statement about what seems to be necessary for understanding the phase relationships and where the data have been published. Also included are the crystal structure data of binary, ternary and multinary phases as far as they are given in the literature.

Since in some cases the published data are controversial, we have tried to make objective and critical comments to the best of our abilities.

Section 5 presents general trends among the binary and ternary Sc-based intermetallics, since this information may be interesting for the syntheses of new Sc compounds for both basic research as well as for technical applications.

In the last section the physical properties of several selected intermetallic compounds containing scandium are discussed and some of their physical properties are depicted in diagrams. In most of the cases the physical properties of the Sc-containing compounds and those of the isostructural Y, La or Lu compounds are compared.

2. Binary systems containing scandium

The phase diagrams of the Sc–E (E = element) binary systems have been investigated in the entire or partial concentration region for majority of elements. These data are presented in summarised form in table 1. The data have been obtained primarily from the original papers, supplemented by data from the 2nd edition of *Binary Alloy Phase Diagrams* by Massalski (1990) and from the 2nd edition of *Pearson's Handbook of Crystallographic Data for Intermetallic Phases* by Villars and Calvert (1991).

There are no data for about 24 Sc–E binary systems out of 89 possible. Among them there are 10 systems with the transuranium elements with atomic numbers higher than 95. The phase diagrams of 54 Sc–E binary systems have been investigated for the entire or partial concentration region up to the beginning of 1997. The figures of the phase diagrams of binary systems presented and discussed by Gschneidner (1975) are not shown in this section if no additional controversial literature data appeared in the meantime. In these cases a brief summary and references are given. 23 binary phase diagrams have been

Table 1
Summary of information known about the Sc–E binary phase diagrams[a]

	1A	2A	3A	4A	5A	6A	7A	8A			1B	2B	3B	4B	5B	6B
2	Li	Be 3											B ■2 →	C ■3 ←		
3	Na	Mg ▨1 →←											Al ■4 ←	Si ■3	P 4	
4	K	Ca ■0 *iL* ←	Sc	Ti ■0 ∞	V ■0 *E*	Cr ■0 *E*	Mn □1 →	Fe ■3 →←	Co ■4	Ni ■5	Cu ■3	Zn ▨5	Ga ■8	Ge ■5 ←	As 4	Se 2
5	Rb	Sr ■0 *iL* ←	Y ■0 ∞	Zr ■0 ∞	Nb ■0 *E*	Mo ■0 *E*	Tc 5	Ru ■4	Rh ■5 →←	Pd ■5 →	Ag ■3 →	Cd ▨3	In ■6 ←	Sn ▨4	Sb 3	Te 2
6	Cs	Ba ■0 *iL* ←	La ■0 ∞	Hf ■0 ∞	Ta □0 *E*	W ■0 *E*	Re ■2 →	Os 3	Ir ■7 →←	Pt ▨4	Au □4 →	Hg 2	Tl ■7 ←	Pb ▨2	Bi 1	Po 1
7	Fr	Ra	Ac	Ku	Ns											

6	Ce ■0 ∞	Pr	Nd ■0 ∞	Pm	Sm □0	Eu □0 *iL*	Gd ■0 ∞	Tb □0 ∞	Dy □0 ∞	Ho □0 ∞	Er ■0 ∞	Tm	Yb □0 *iL*	Lu □0 ∞
7	Th ■0 ∞	Pa	U ■0 *iL* →←	Np	Pu ■1 ∞	Am	Cm	Bk	Cf	Es	Fm	Md	No	Lr

[a] The squares indicate the concentration range in which the phase diagram of the Sc–E binary system was investigated: black square, 75–100%; grey square, 25–75%; open square, less than 25%; no square, not investigated.
The number of binary compounds found is listed next to the square.
The character of the mutual solubility of Sc and E is indicated as follows:
iL, miscibility gap in the liquid state;
E, mutual solubility in the solid state <1 at.% (simple eutectic, no binary compound occurs);
→ , solubility of Sc in solid E >1 at.%;
← , solubility of E in solid Sc >1 at.%;
∞, at least one continuous solid solution of Sc and E occurs.

published after Gschneidner's review article in 1975. These diagrams will be discussed in more detail. All controversial data about the systems will be analysed and discussed. In some cases necessary corrections are made and the revised phase diagrams are presented, whereas in other cases diverging results in the literature are only mentioned. The data in the section are arranged according to the stretched form of the periodic table of elements. Within one group of elements the systems are given according to increasing atomic number of the elements. The data about all scandium binary intermetallics including

their composition, melting temperature (in °C) and crystallographic data (structure type (ST) or symmetry and lattice parameters) are presented. The reference source of the crystallographic data is presented first followed by the references in which these data appeared. The reference source with data of the melting temperature of compound is printed in italics. The following abbreviations are used for compounds' formation and decomposition:

L, congruently melting compound;
P, peritectically melting compound;
Pd, compound is formed according to peritectoid reaction;
S, polymorphic transition;
Ed, compound decomposes according to eutectoid reaction;
Mt, metatectic transition.

2.1. *Sc–M (M = 1A element) systems*

There are no data about the interaction of scandium with the alkaline metals. Taking into consideration the large differences in the melting temperatures of Sc and 1A elements the occurrence of immiscibility gaps in liquid and solid binary alloys are possible as they occur in the Sc–E (E = alkaline-earth element) alloys (see sect. 2.2). The absence of binary compounds in these systems is very likely.

2.2. *Sc–M (M = 2A element) systems*

Occurrence of three scandium–beryllium intermetallic compounds and their crystal structures are the only data existing about the Sc–Be binary system. Their characteristics are presented in table 2. Gschneidner and Calderwood (1987) reviewed all available papers on scandium–beryllium binary alloys.

Beaudry and Daane (1969) established the Sc–Mg phase diagram in the range of 0–60 at.% Sc. βSc dissolves up to 80 at.% Mg and magnesium dissolves up to 15 at.% Sc. The latter data was refined by Sviderskaya and Nikitina (1972), who established the

Table 2
Intermetallic compounds in the Sc–M (M = Be, Mg) binary systems[a]

Compound	Melting temperature (°C)	Structure type or symmetry	Lattice parameters		Reference
			a (Å)	*c* (Å)	
$ScBe_{13}$	?	$NaZn_{13}$	10.102		Laube and Nowotny (1962)
Sc_2Be_{17}	?	*hex*	7.61	7.50	Gladyshevsky et al. (1964)
$ScBe_5$	?	$CaCu_5$	4.55	3.50	Protasov and Gladyshevsky (1964)
ScMg(β′)	*Pd*, 520	CsCl	3.597		Schob and Parthé (1965), *Beaudry and Daane (1969)*

[a] References in italics contain data about a compound's melting temperature.

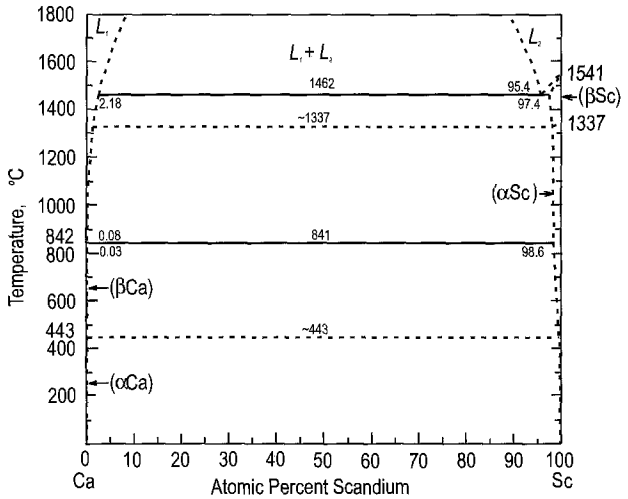

Fig. 1. The Sc–Ca phase diagram.

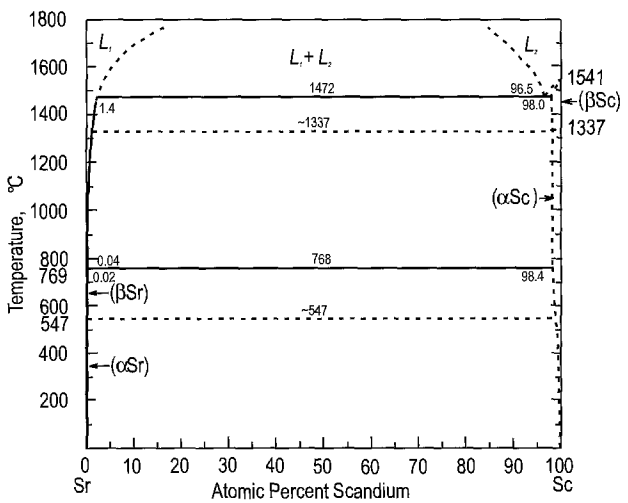

Fig. 2. The Sc–Sr phase diagram.

temperature dependence of the solubility of Sc in Mg. One binary compound ScMg with a broad homogeneity range, isotypic with CsCl, occurs in the system (table 2). Reviews of the papers on Sc–Mg alloys have been given by Gschneidner (1975) and by Nayeb-Hashemi and Clark (1986). The latter authors presented the assessed phase diagram of the system with only few small corrections of the earlier data of Beaudry and Daane (1969). New data concerning the phase diagram are not known.

Dzuraev and Altynbaev (1986) determined the solubility of Sc in βCa, βSr and Ca and Sr in βSc and αSc as well as the temperatures of the monotectic and eutectic reactions

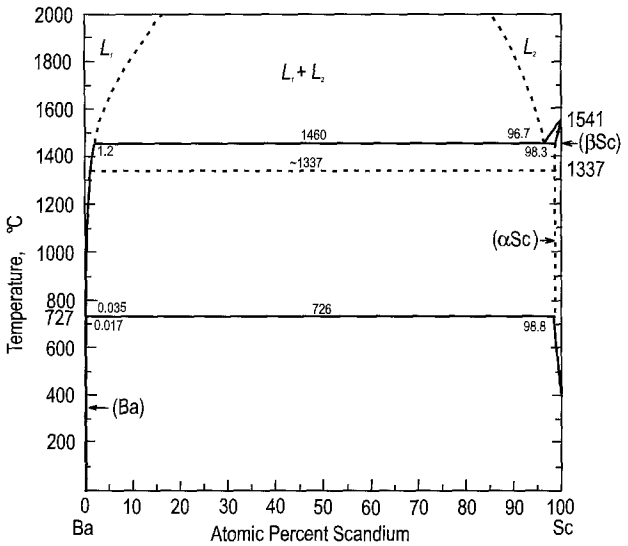

Fig. 3. The Sc–Ba phase diagram.

in the Sc–Ca and Sc–Sr systems. The Sc–Ca and Sc–Sr phase diagrams constructed on the base of these data are presented in figs. 1 and 2, respectively.

The phase diagram of Sc–Ba system has been reported by Altynbaev et al. (1988). The allotropic transition βSc ↔ αSc, which was not shown by these authors, has been added to the phase diagram presented in fig. 3. The melting temperature for Sc has been corrected for the now accepted value.

The interaction of scandium with the earth alkaline elements is similar. An immiscibility gap occurs in the liquid alloys and no binary compound exists in any of these systems.

2.3. *Sc–M (M = RE) systems*

The majority of the data concerning binary Sc–RE systems have been obtained between 1960 and 1970. Since that time practically no new information has been published on the Sc–RE phase diagrams.

The Sc–Y phase diagram was investigated by Beaudry and Daane (1963). The HT and LT modifications of scandium and yttrium are completely miscible in each other. The list of references concerning this system and the phase diagram with the corrected temperatures of phase transitions can be found in the reviews of Gschneidner (1975) and Gschneidner and Calderwood (1983e, 1986a).

Naumkin et al. (1970) investigated the Sc–La phase diagram. γLa and βSc form continuous series of solid solutions, while βLa, αLa and αSc dissolve from 12 to 16 at.% of the second component. The phase diagram and the reference list are given by Gschneidner (1975) and Gschneidner and Calderwood (1982a, 1986a).

The Sc–Ce phase diagram has been determined by Naumkin et al. (1964). Gschneidner (1975) and Gschneidner and Calderwood (1982b, 1986a) corrected only the values of the melting and allotropic transition temperatures of the pure components to conform with the accepted values. The bcc phases of Sc and Ce are completely miscible in each other. The LT modifications of Sc and Ce dissolve about 12 and about 17 at.% of Ce and Sc, respectively.

There are no available data about the phase diagram of the Sc–Pr system. Taking into consideration the data on the Sc–Ce system it is possible to predict a complete mutual miscibility of the components in each other in liquid and in bcc solid phases. αSc and αPr have different crystal structures (hcp and dhcp respectively), therefore, they probably form limited solid solutions.

Beaudry et al. (1965) investigated the Sc–Nd phase diagram. Pairs of HT and LT phases of these components are completely miscible in each other. The attempts of the authors to find two phase region between the hcp phase of Sc and double hcp phase of Nd failed. This continuous solid solution decomposes beginning at 700°C by forming an immiscibility gap. The phase diagram has been analysed earlier by Gschneidner (1975) and Gschneidner and Calderwood (1982c, 1986a).

There are no data known about investigations of Sc–Pm system.

The only data about interaction between Sc and Sm are those published by Kotur et al. (1991). It was found that at 600°C samarium dissolves about 18 at.% Sc. From a comparison of the phase diagrams of other light RE (La, Ce and Nd) it is possible to predict a complete miscibility of the components in each other in the liquid and solid bcc phases.

Massalski (1990) presented the hypothetical Sc–Eu phase diagram based on thermodynamic calculations of Miedema (1976). They predict the occurrence of a broad immiscibility gap in liquid and solid alloys and the absence of binary compounds in this system.

The phase diagram of Sc–Gd system has been established by Beaudry and Daane (1964). The figure of the phase diagram is also presented in the reviews of Gschneidner (1975) and Gschneidner and Calderwood (1983c, 1986a) who corrected only the values of melting and the bcc $\leftrightarrow$ hcp transitions temperatures of the components with their new values. One liquid and two solid continuous solutions exist in this system.

The lattice parameters of several Sc–Tb alloys have been measured indicating a complete solubility of αTb and αSc. These data were reviewed and analysed by Gschneidner (1975) and Gschneidner and Calderwood (1983d, 1986a).

The phase diagram of the Sc–Dy binary system has not been investigated. Kotur et al. (1991) reported about a complete solubility of the components at 600°C. The *a* and *c* lattice spacing of the hcp solid solution appear to follow Vegard's rule within the experimental error.

Considering the above presented data it is possible to predict the existence of one liquid and two solid rows of continuous solutions in the Sc–Tb and Sc–Dy systems like in the Sc–Gd system. The occurrence of two of these solid solutions (αSc, αTb) and (αSc, αDy) has been already confirmed experimentally.

Cavin et al. (1967) reported the lattice spacings of five binary Sc–Ho alloys. Their data were also presented and analysed by Gschneidner (1975) and Gschneidner and Calderwood (1983b, 1986a). βSc forms a continuous series of solid solutions with holmium.

The Sc–Er phase diagram has been investigated by Naumkin et al. (1964). Gschneidner (1975) and Gschneidner and Calderwood (1983a, 1986a) critically revised and corrected the values of temperatures of all phase transitions presented in the original paper. Er and αSc are completely soluble in each other. βSc dissolves about 24 at.% Er.

There are no known data about the Sc–Tm system in the literature.

Since Ho, Er and Tm have only one solid phase (hcp); it appears that these three binary systems will have similar phase diagrams, i.e. occurrence of one liquid and one solid continuous solutions and a limited solubility in bcc Sc phase. One of such solutions, namely (αSc, Ho), has already been determined experimentally.

The hypothetical Sc–Yb phase diagram has been constructed by Massalski (1990) on the basis of thermodynamic calculations of de Boer et al. (1979). Immiscibility gaps in liquid and solid alloys and the absence of binary compounds are predicted for that system. This is in agreement with the data of Kotur (1995) who prepared several binary alloys and observed immiscibility of liquid components and two separate layers in solid alloys.

Kotur and Mokra (1994) reported the complete solubility of scandium and lutetium at 800°C. These are the only available experimental data about the Sc–Lu system. It is possible to predict the complete miscibility of the components in the liquid and a limited solubility of lutetium in βSc.

2.4. *Sc–M (M = actinide element) systems*

Among the family of the actinide elements data concerning binary systems with scandium only exists for the three elements thorium, uranium and plutonium.

Terekhov and Sinyakova (1990) reported on the Sc–Th phase diagram (fig. 4). Their results are an improvement on the data of Badaeva and Kuznetsova (1969) who were the first to investigate the phase diagram on the basis of thermal analysis of 8 alloys. A continuous series of solid solutions occur between the HT phases of the components. αTh dissolves up to 66 at.% Sc and αSc dissolves up to 20 at.% Th. With decreasing temperature the mutual solubility of the components also decreases. The authors presented a plot of lattice spacing a vs. Sc content of the fcc $Th_{1-x}Sc_x$ solid solution at 950°C. As estimated from the plot $a = 5.095$ Å for pure αTh; a does not change out to about 7–8 at.% Sc content. In the concentration range $0.08 < x \leqslant 0.61$, a follows Vegard's rule with $a = 4.937$ Å at $x = 0.61$. There is a considerable discrepancy between the values of the melting point of Sc (1530°C) and the αSc ↔ βSc transition temperature (1415°C) as obtained by Terekhov and Sinyakova (1990) and the now accepted values. For that reason we present in fig. 4 the corrected values for the temperatures of the phase transitions of the pure components.

Figure 5 displays the Sc–U phase diagram established by Terekhov and Sinyakova (1992). No binary compounds and an immiscibility gap in the liquid alloys occur in

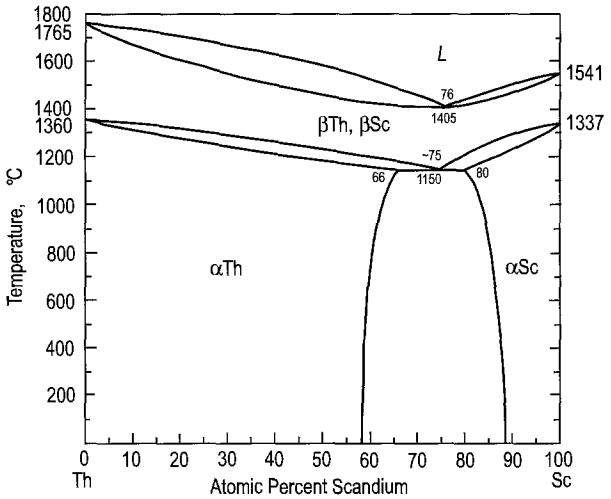

Fig. 4. The Sc–Th phase diagram.

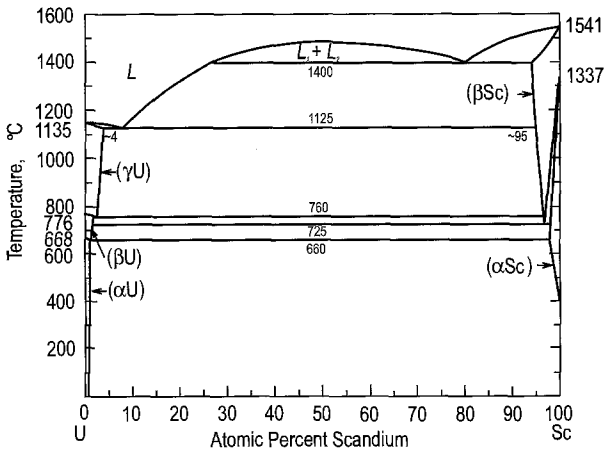

Fig. 5. The Sc–U phase diagram.

the system. Okamoto (1993) indicated the necessity of further confirmation of the (βSc)/(βSc)+(αSc) boundary since it is too steep and does not follow the van't Hoff relation.

The Sc–Pu phase diagram has been investigated by Kutaitsev et al. (1967), Ellinger et al. (1968, 1972) and Ballagny et al. (1970). These and other papers concerning this system have been analysed in the review of Gschneidner (1975). The diagrams reported by Ellinger et al. (1968, 1972) and Ballagny et al. (1970) are very similar and are the accepted version. HT bcc phases of the components (βSc, εPu) are completely miscible in each other. The other phases of Sc (β) and Pu (δ, δ′, γ, β, α) form limited solid solutions. One

Table 3
The intermetallic compound in the Sc–Pu binary system

Compound	Melting temperature (°C)	Structure type or symmetry	Lattice parameters		Reference
			a (Å)	c (Å)	
~Sc_2Pu_3	*Pd*, 753	αLa	3.308–3.310[a]	10.709–10.717	*Ellinger et al. (1968)*

[a] The first and second values of lattice spacings are for the Sc-rich and Pu-rich side of the homogeneity range, respectively.

binary compound of the approximate composition Sc_2Pu_3 occurs in the system (table 3). Different authors, however, give different values for the homogeneity limits of Sc_2Pu_3, and additional investigations are necessary. Massalski (1990) indicated that the diagram cannot be modelled with a reasonable set of thermodynamic functions and therefore some phase boundaries need further refinement.

2.5. *Sc–M (M = 4A element) systems*

Two variants of the Sc–Ti phase diagram have been reported by Savitskii and Burkhanov (1961) and Beaudry and Daane (1962). Gschneidner (1975) and Murray (1987) analysed them and showed that the Beaudry and Daane one is probably more correct. In these reviews one can find the figure of the phase diagram and the list of references concerning the properties of the Sc–Ti alloys. There are no binary compounds in the system. The bcc HT phases of these components form a continuous series of solid solutions. The hcp LT phases of Sc and Ti dissolve up to 6.9 and 12.8 at.% of the other component, respectively.

Beaudry and Daane (1963) investigated the phase diagram of the Sc–Zr system. The two solid phases of the components are completely miscible in each other. The components also form a continuous liquid solution. These data and the data of other publications on Sc–Zr alloys are presented and reviewed by Gschneidner (1975) and Palenzona and Cirafici (1993).

The Sc–Hf phase diagram is similar to that of Sc–Zr. It was established by Naumkin et al. (1967). Gschneidner (1975) presented the figure of the phase diagram. He corrected only the values of phase transition temperatures of the pure components to the now accepted values. In the review one can find also the list of references concerning the physical properties of Sc–Hf alloys.

2.6. *Sc–M (M = 5A, 6A element) systems*

The character of interaction of scandium with 5A elements, vanadium, niobium and tantalum and the 6A elements, chromium, molybdenum and tungsten is similar. No binary

compounds occur in any of these systems. The components are completely miscible in each other in the liquid state and form simple eutectics.

Savitskii et al. (1970, 1971a) reported on the Sc–V phase diagram. The figure of the phase diagram is also presented in the review of Gschneidner (1975) who corrected the temperatures of phase transitions of pure components to the now accepted values. βSc and αSc dissolve <2 and <0.5 at.% V, respectively. The solubility of Sc in V is <2 at.%. Smith and Lee (1989) noticed an inconsistency of the original phase diagram with van't Hoff's thermodynamic functions. They presented the calculated phase diagram and predicted the occurrence of an immiscibility gap in liquid state in the temperature range from 1593°C to 1459°C and a monotectic reaction occurring at 1459°C. The validity of this theoretical phase diagram needs to be experimentally examined.

The phase diagram of the Sc–Nb system has been reported by Savitskii et al. (1970) and Savitskii and Efimov (1972). The figure of the phase diagram is also presented by Gschneidner (1975). The mutual solubility of the components is as follows: <0.4 at.% Nb in βSc, <0.3 at.% Nb in αSc, and <0.1 at.% Sc in Nb.

Dennison et al. (1966a) established part of the Sc–Ta phase diagram in the high Sc concentration range (0 to 6 at.% Ta). The solubility of Ta in liquid Sc is very low (about 0.2 to 0.5 at.%) but was not determined accurately. According to the data of Taylor et al. (1965) solid Ta dissolves <0.0001 at.% Sc at 1625°C.

Two variants of the Sc–Cr phase diagram have been reported, by Savitskii et al. (1970) and Svechnikov et al. (1972). As was stated by Gschneidner (1975), who preferred the data of Savitskii et al. (1970), the major difference between the two diagrams is that Savitskii et al. found that chromium has insignificant effect on the $\beta Sc \leftrightarrow \alpha Sc$ transformation, while Svechnikov et al. (1972) established the transformation to be lowered from 1340 to 990°C by means of an eutectoid reaction. Contrary to Gschneidner (1975), Venkatraman and Neumann (1985) preferred the diagram of Svechnikov et al. and presented the phase diagram based on these data correcting only the phase transition temperatures of the components. Thus, additional experimental investigation of the system is necessary to clarify the situation. Taylor et al. (1965) determined the solubility of Sc in solid Cr to be <0.1 at.%. The value of solubility of Cr in solid Sc is <1 at.% according to the data of Savitskii et al. and <2 at.% according to the data of Svechnikov et al. and needs, perhaps, to be refined too.

Brewer and Lamoreaux (1980) reported on the calculated Sc–Mo phase diagram based on the assumed thermodynamic functions. They predicted an eutectic $L \leftrightarrow \beta Sc + Mo$ reaction at 1370±50°C and an eutectoid $\beta Sc \leftrightarrow \alpha Sc + Mo$ reaction at ~1337°C in this system. The mutual solubility of the components in the solid phases is very low according to their calculation. These data have been partially confirmed by Kotur and Bodak (1988) who investigated several Sc–Mo alloys at 800°C and observed the immiscibility of the components and no binary compounds.

The solubility of tungsten in liquid scandium in the temperature range 1647–2045°C has been determined by Dennison et al. (1966b). They established it to be 2.4–7.9 at.%. The extrapolation of these data towards the melting temperature of Sc, 1541°C, revealed a 1.3 at.% solubility of W. Taylor et al. (1965) determined the solubility of scandium in

solid tungsten as <0.004 at.% at 1625°C. Pandian et al. (1988) used these data to evaluate the hypothetical Sc–W phase diagram. They assumed a temperature of 1510°C for the eutectic reaction $L \leftrightarrow \beta Sc + W$. The immiscibility of the components in the solid state and absence of binary compounds at 800°C have been confirmed by Kotur et al. (1989a).

2.7. *Sc–M (M = Mn, Tc, Re) systems*

The Mn-rich part of the Sc–Mn phase diagram in the range 0–5 at.% Sc has been established by Hellawell (1962). This phase diagram is shown in the review of Gschneidner (1975). The limit of solubility of scandium in βMn and δMn is about 1 at.%, in γMn it is only 0.4 at.%. Dwight (1961a) reported the existence of one binary compound in the system, namely $ScMn_2$ (table 4). His data were confirmed by Kripyakevich et al. (1964). From that time no new data concerning the phase diagram appeared in the literature.

The Sc–Tc phase diagram is still unknown. Darby et al. (1962) synthesised five binary compounds and determined the crystal structure of two of them (table 4). $ScTc_7$ was observed in the cast alloy and $ScTc_2$ in an alloy annealed at 700°C. Gschneidner (1975) doubted the composition of the $ScTc_7$ phase. His reason is that binary compounds isotypic with αMn have in general the 5:24 stoichiometry, i.e. the true composition of the phase must be Sc_5Tc_{24}. This statement needs experimental verification. During the last two decades no new data concerning Sc–Tc phase diagram appeared in the literature.

Savitskii et al. (1966) reported on the Sc–Re phase diagram. It follows from the figure in their paper that the liquidus curve in the phase diagram and the boundaries of some phase fields need additional refinement. Two binary compounds occur in this system (table 4). βSc dissolves <1 at.% Re, and the solubility of scandium in solid rhenium does not exceed ~5–6 at.%. Gschneidner (1975) presented the data of Savitskii et al., however he corrected in the figure of the phase diagram the temperatures of some phase transitions with the accepted values.

Table 4
Intermetallic compounds in the Sc–M (M = Mn, Tc, Re) binary systems

Compound	Melting temperature (°C)	Structure type or symmetry	Lattice parameters		Reference
			a (Å)	*c* (Å)	
$ScMn_2$	?	$MgZn_2$	5.033	8.278	Dwight (1961a)
$ScTc_7$	?	αMn	9.509		Darby et al. (1962)
~$ScTc_3$	?	?			Darby et al. (1962)
$ScTc_2$	?	$MgZn_2$	5.223	8.571	Darby et al. (1962)
~Sc_3Tc_2	?	?			Darby et al. (1962)
~Sc_4Tc	?	?			Darby et al. (1962)
Sc_5Re_{24}	*P*, 2570	αMn	9.6448		*Savitskii et al. (1966)*
$ScRe_2$	*P*, 2030	$MgZn_2$	5.270	8.590	*Savitskii et al. (1966)*

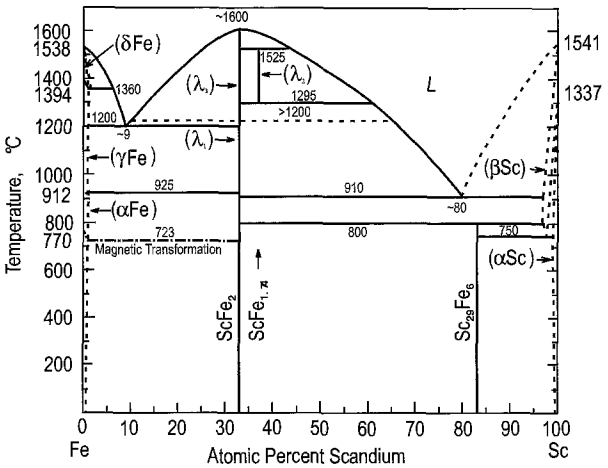

Fig. 6. The Sc–Fe phase diagram.

2.8. *Sc–M (M = Fe, Co, Ni) systems*

Naumkin et al. (1969) reported on the Sc–Fe phase diagram. They established the occurrence of two binary compounds $ScFe_2$ (*L*, 1600°C) and Sc_3Fe (*Pd*, 800°C) but did not investigate their crystal structures. The existence of $ScFe_2$ is consistent with the earlier data of Dwight (1961a) and Gladyshevsky et al. (1964). Dwight synthesised the $ScFe_2$ compound and established it to be isotypic with $MgNi_2$,SG $P6_3/mmc$, with the lattice spacings $a = 4.972$, $c = 16.278$ Å. Gladyshevsky et al. obtained an $ScFe_2$ sample which was isotypic with $MgZn_2$, SG $P6_3/mmc$, with the lattice spacings $a = 4.92$, $c = 7.90$ Å, and in cast alloys with the content of iron less than 50 at.% they observed the occurrence of the cubic $MgCu_2$-type structure, SG $Fd3m$, with the lattice spacing $a = 7.09$ Å.

Taking these data into consideration Bodak et al. (1978) reinvestigated the Sc–Fe phase diagram in the concentration range 0–90 at.% Sc. They confirmed the polymorphism of $ScFe_2$ (HT phase of $MgNi_2$ type [given as λ_3 in fig. 6] and LT phase of $MgZn_2$ type [λ_1]) and discovered a new binary phase $ScFe_{1.74}$ (λ_2) with the $MgCu_2$ type structure. Their lattice spacings are given in table 5. The stoichiometry of the scandium richest binary phase was shown to be about 7:1, not in agreement with the 3:1 stoichiometry found by Naumkin et al. Consequently Kotur et al. (1986a) established the structure and the composition of that phase being $Sc_{29}Fe_6$ in their single-crystal investigation (table 5).

Kubashewski (1982) presented a revised phase diagram of this system. The only changes which were introduced to the phase diagram of Naumkin et al. were a schematical indication of three polymorphic modifications for $ScFe_2$.

The revised phase diagram is shown in fig. 6. The temperatures of the majority of phase transitions are the data of Naumkin et al. since they investigated a larger number of samples, 39 vs. 24 by Bodak et al. The compositions of binary phases, temperatures of phase transitions of the $ScFe_{1.74}$ and $ScFe_2$ compounds are the data taken from Bodak

Table 5
Intermetallic compounds in the Sc–M (M = Fe, Co, Ni) binary systems

Compound	Melting temperature (°C)	Structure type or symmetry	Lattice parameters			Reference
			a (Å)	b (Å)	c (Å)	
$ScFe_2(\lambda_3)$	L, ~1600–S, >1200	$MgNi_2$	4.974		16.29	*Bodak et al. (1978)*
$ScFe_2(\lambda_1)$	S, >1200	$MgZn_2$	4.977		8.146	*Bodak et al. (1978)*
$ScFe_{1.74}(\lambda_2)$	P, 1525–Mt, 1295	$MgCu_2$	7.039			*Bodak et al. (1978)*
$Sc_{29}Fe_6$	Pd, 800	$Sc_{29}Fe_6$	14.361			Kotur et al. (1986a), *Naumkin et al. (1969)*
$ScCo_2$	L, 1520	$MgCu_2$	6.921			Dwight (1961a), *Markiv et al. (1978)*
ScCo	P, 1050	CsCl	3.145			Aldred (1962), *Markiv et al. (1978)*
Sc_2Co	L, 840	Al_2Cu	6.370		5.618	Kotur et al. (1977a), *Markiv et al. (1978)*
Sc_3Co	P, 870	Sc_3Co	13.102	8.624	5.829	Chabot and Parthé (1978), *Markiv et al. (1978)*
$ScNi_5$(HT)	P, 1180–	$CaCu_5$	4.69		3.887	*Braslavskaya and Maslenkov (1987)*
	S, 800		4.74		3.76	Goebel and Rosen (1968)
$ScNi_5$(LT)	S, 800	?				*Braslavskaya and Maslenkov (1987)*
Sc_2Ni_7	L, ~1295	Ce_2Ni_7	4.761		22.395	*Braslavskaya and Maslenkov (1987)*
			4.98		24.52	Goebel and Rosen (1968)
$ScNi_2$	L, 1310	$MgCu_2$	6.921			Dwight (1961a), *Markiv et al. (1978)*
ScNi	L, 1270	CsCl	3.171			Aldred (1962), *Markiv et al. (1978)*
Sc_2Ni	L, 1000	Ti_2Ni	12.120			Aldred (1962), *Markiv et al. (1978)*

et al. The now accepted temperatures of the phase transitions of the pure components are indicated in the phase diagram shown in fig. 6.

The Sc–Co phase diagram, which is shown in fig. 7 is based primarily on the results reported by Markiv et al. (1978). The authors confirmed the occurrence of the compounds $ScCo_2$, ScCo, Sc_2Co (table 5) and discovered a new one, Sc_3Co with an orthorhombic unit cell. Chabot and Parthé (1978) established its crystal structure (table 5). There were controversial data about the crystal structure of the Sc_2Co compound. Gladyshevsky et al. (1964) reported it to be of Ti_2Ni type, however, these data were not confirmed by Aldred

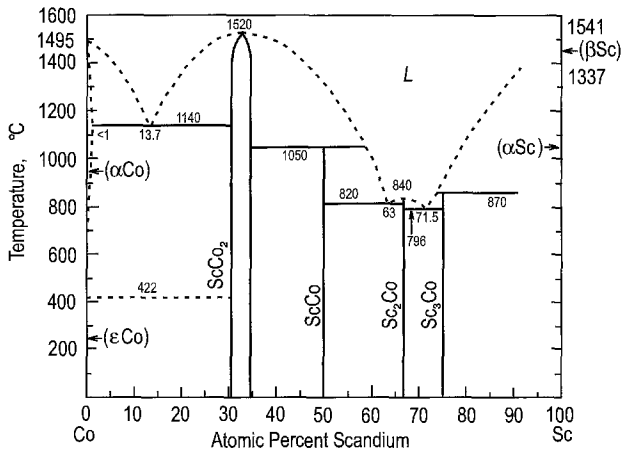

Fig. 7. The Sc–Co phase diagram in the range 0–90 at.% Sc.

(1962), Kotur et al. (1977a) and Markiv et al. (1978) (table 5). Kotur (1977a) determined the homogeneity range of $ScCo_2$ phase at 800°C. The lattice spacing increases linearly from $a = 6.892$ to $a = 6.921$ Å within its homogeneity range from 30 to 34.5 at.% Sc. These data are in agreement with the data of Markiv et al.

Markiv et al. (1978) published also the Sc–Ni phase diagram in the range 0–80 at.% Sc. These authors confirmed the five binary compounds $ScNi_5$, Sc_2Ni_7, $ScNi_2$, ScNi and Sc_2Ni, which were earlier synthesised and structurally determined (table 5). There was a disagreement between the data of Goebel and Rosen (1968) and Markiv et al. concerning the homogeneity range of the $ScNi_2$ phase. Goebel and Rosen reported it from 27.2 to 33.4 at.% Sc at 1000°C, while Markiv et al. fixed the lower and upper limits at 30 and 36 at.% Sc ($a = 6.866$–6.938 Å), respectively.

Maslenkov and Braslavskaya (1984) reinvestigated part of the Sc–Ni phase diagram in the range 0–36 at.% Sc. Their data are in excellent agreement with the data of Markiv et al. The temperatures of the phase transitions differ no more than 5–10°C at temperatures >1000°C, which is within the experimental error limits. $ScNi_2$ forms a homogeneous solid solution in the range of 31–35 at.% Sc as reported by Maslenkov and Braslavskaya. The lattice spacing displays a positive deviation from Vegard's rule and changes from $a = 6.871$ to $a = 6.920$ Å as determined from a plot of a vs. concentration. Finally, the same authors, Braslavskaya and Maslenkov (1987), established the occurrence of polymorphism for $ScNi_5$and reinvestigated the crystal structure of $ScNi_5$ and Sc_2Ni_7 phases (table 5). The data of Braslavskaya and Maslenkov for lattice spacings of $ScNi_5$ (HT) and especially of Sc_2Ni_7 differ remarkably from the data of Goebel and Rosen (table 5). The reason for that is unknown.

The revised Sc–Ni phase diagram is presented in fig. 8. This figure includes the data of Markiv et al. in the range >36 at.% Sc and the data of Maslenkov and Braslavskaya, and Braslavskaya and Maslenkov in the range 0–36 at.% Sc. The temperatures of phase transitions of pure components are in agreement with the accepted values.

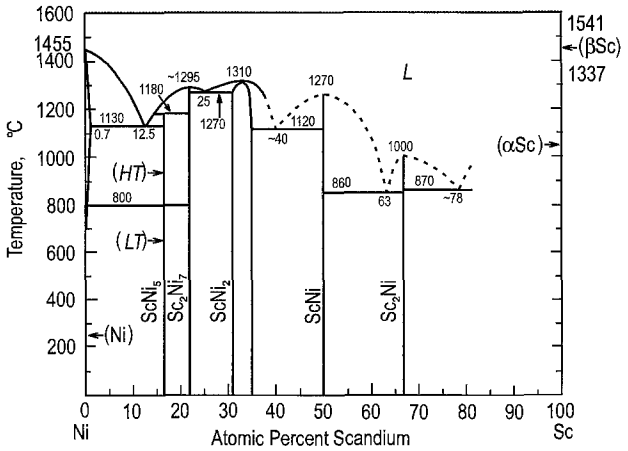

Fig. 8. The Sc–Ni phase diagram in the range 0–80 at.% Sc.

2.9. *Sc–M (M = platinum group element) systems*

The Sc–Ru phase diagram has been investigated by Savitskii et al. (1971b). They confirmed the existence of the two binary compounds $ScRu_2$ and ScRu (table 6) and synthesised a third one with an unknown structure. Chabot et al. (1980a) determined the composition of the latter phase as $Sc_{11}Ru_4$ as well as its structure (table 6). The same group of authors, Chabot et al. (1980b), synthesised a fourth binary compound in the system with an approximate composition Sc_6Ru and a cubic structure. Finally five years later Cenzual et al. (1985) established its real composition, $Sc_{57}Ru_{13}$, and the crystal structure (table 6). Other data, which also support the reinvestigation of this phase diagram, are the two reported sets of values for the lattice spacings of the $ScRu_2$ compound (table 6). They indicate that $ScRu_2$ has, perhaps, a homogeneity range.

Khorujaya et al. (1995) reported on the Sc–Rh phase diagram which is presented in fig. 9. These authors found extended homogeneity ranges for ScRh and $ScRh_3$ compounds which explained the different values of the lattice spacings for these phases reported earlier by different authors (table 6). However, it is unknown to which composition these published values belong. Three other binary compounds Sc_2Rh, Sc_3Rh and $Sc_{57}Rh_{13}$ exist in this system (table 6).

The Sc–Pd phase diagram was established by Savitskii et al. (1971c,d). Gschneidner (1975) presented a revised phase diagram, based primarily on these data. He corrected the composition of earlier known Sc_2Pd phase, which was shown in the original diagram at the composition "Sc_3Pd_2" and changed the temperatures of phase transitions for pure components to the presently accepted values. Gschneidner presented also the arguments in favour of occurrence of the broad homogeneity range for $ScPd_3$ (see values of lattice spacing in table 6) and the much higher solubility of scandium in solid palladium. The different values of the lattice spacing reported for Sc_2Pd (see table 6) may also indicate the existence of a homogeneity range of that phase too. Finally, Savitskii et al. established very

Table 6
Intermetallic compounds in the Sc–M (M = Ru, Rh, Pd, Os, Ir, Pt) binary systems

Compound	Melting temperature (°C)	Structure type or symmetry	Lattice parameters			Reference
			a (Å)	*b* (Å)	*c* (Å)	
$ScRu_2$	*P*, 1840	$MgZn_2$	5.119		8.542	Compton and Matthias (1959), *Savitskii et al. (1971b)*
			5.135		8.525	Dwight (1961a)
ScRu	*L*, 2210	CsCl	3.203			Aldred (1962), *Savitskii et al. (1971b)*
$Sc_{11}Ru_4$	*P*, 1510	$Sc_{11}Ir_4$	13.367			Chabot et al. (1980a), *Savitskii et al. (1971b)*
$Sc_{57}Ru_{13}$	?	$Sc_{57}Rh_{13}$	14.394			Cenzual et al. (1985)
$ScRh_3$	*P*, 1650	$AuCu_3$	3.900			Dwight et al. (1961), *Khorujaya et al. (1995)*
			3.898			Geballe et al. (1965)
			3.909			Erdmann and Keller (1973)
ScRh	*L*, 1990	CsCl	3.206			Gschneidner (1961), *Khorujaya et al. (1995)*
			3.204			Dwight et al. (1965)
Sc_2Rh	*P*, 1080 - *Ed*, 980	?				*Khorujaya et al. (1995)*
Sc_3Rh	*L*, 1110 - *Ed*, 930	?				*Khorujaya et al. (1995)*
$Sc_{57}Rh_{13}$	*L*, 1150	$Sc_{57}Rh_{13}$	14.4051			Cenzual et al. (1985), *Khorujaya et al. (1995)*
$ScPd_3$	*P*, 1450	$AuCu_3$	3.981			Dwight et al. (1961), *Savitskii et al. (1971c)*
			3.969			Erdmann and Keller (1973), Norman and Harris (1969)
$ScPd_2$	*P*, 1430	$MgCu_2$(?)				*Savitskii et al. (1971c)*
ScPd	*L*, 1570	CsCl	3.283			Aldred (1962), *Savitskii et al. (1971c)*
Sc_2Pd	*L*, 1200	Ti_2Ni	12.427			Aldred (1962), *Savitskii et al. (1971c)*
			12.441			Geballe et al. (1965)
~Sc_4Pd	*P*, 1040	?				*Savitskii et al. (1971c)*
$ScOs_2$	?	$MgZn_2$	5.179		8.484	Compton and Matthias (1959), Gschneidner (1961)
			5.188		8.505	Dwight et al. (1966)
$Sc_{11}Os_4$	?	$Sc_{11}Ir_4$	13.344			Chabot et al. (1980a)
$Sc_{44}Os_7$	?	$Mg_{44}Rh_7$	20.771			Chabot et al. (1980b)
$ScIr_3$	*P*, 1980	$AuCu_3$	3.900			*Eremenko et al. (1994)*

continued on next page

Table 6, *continued*

Compound	Melting temperature (°C)	Structure type or symmetry	Lattice parameters			Reference
			a (Å)	*b* (Å)	*c* (Å)	
$ScIr_2$	*L*, 2150	$MgCu_2$	7.345			*Eremenko et al. (1994)*
			7.348			Compton and Matthias (1959)
ScIr	*L*, 2100	CsCl	3.205			*Eremenko et al. (1994)*
			3.206			Aldred (1962)
Sc_2Ir	*P*, 1420	Ti_2Ni	12.290			*Eremenko et al. (1994)*
$Sc_{11}Ir_4$	*L*, 1410	$Sc_{11}Ir_4$	13.430			*Eremenko et al. (1994)*
			13.350			Chabot et al. (1980a)
$Sc_{57}Ir_{13}$	*L*, 1480	$Sc_{57}Rh_{13}$	14.350			*Eremenko et al. (1994)*
			14.364			Cenzual et al. (1985)
$Sc_{44}Ir_7$	*P*, 1420	$Mg_{44}Rh_7$	20.750			*Eremenko et al. (1994)*
			20.755			Chabot et al. (1980b)
$ScPt_3$	*P*, 1850(?)	$AuCu_3$	3.958			Dwight et al. (1961), *Savitskii et al. (1978a)*
			3.954			Bronger (1967)
			3.953			Erdmann and Keller (1973)
ScPt	*L*, 2200(?)	CsCl	3.270			Aldred (1962), *Savitskii et al. (1978a)*
Sc_2Pt	?	Co_2Si	6.592	4.491	8.206	Chabot and Parthé (1979)
$Sc_{57}Pt_{13}$	?	$Sc_{57}Rh_{13}$	14.350			Cenzual et al. (1985)

approximately the whole liquidus curve except in the concentration range 90–100 at.% Sc. Thus, a reinvestigation of phase diagram would be necessary. Altogether there exist five binary compounds in this system. Their characteristics are presented in table 6.

As yet no phase diagram is known for the Sc–Os system. However there are data for three binary compounds; these data are presented in table 6. Various values reported for the lattice spacings of $ScOs_2$ suggest a homogeneity range for that phase.

The Sc–Ir phase diagram, which is shown in fig. 10, is based on the results reported by Eremenko et al. (1994). Five of seven binary compounds have been confirmed, and two new compounds Sc_2Ir and $ScIr_3$ have been synthesised by the authors. The crystal structures of all of them are known and given in table 6. The lattice spacings of several of these compounds reported by Eremenko et al. are in excellent agreement with the earlier reported data (see table 6). However in the case of the compound $Sc_{11}Ir_4$ with a constant composition there is remarkably large difference in the values of lattice spacing, which is not understood.

Four intermetallic scandium–platinum compounds have been prepared and their crystal structures were determined (table 6). Only a few of the phase equilibria in the Sc–Pt phase diagram up to 50 at.% Sc were determined by Savitskii et al. (1978a). The solubility of

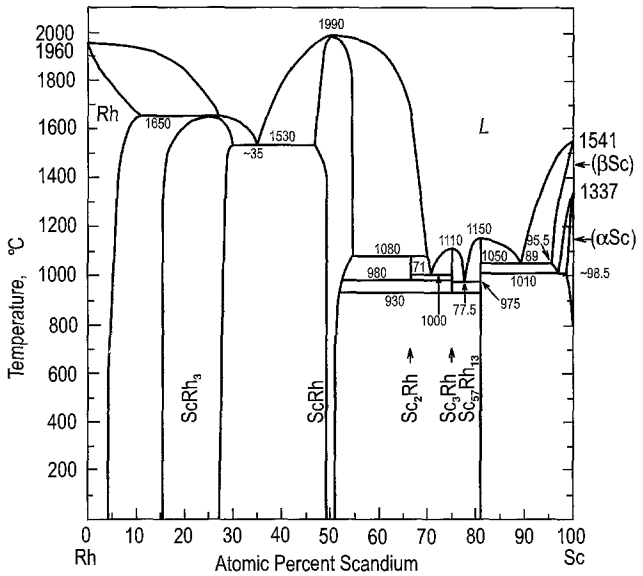

Fig. 9. The Sc–Rh phase diagram.

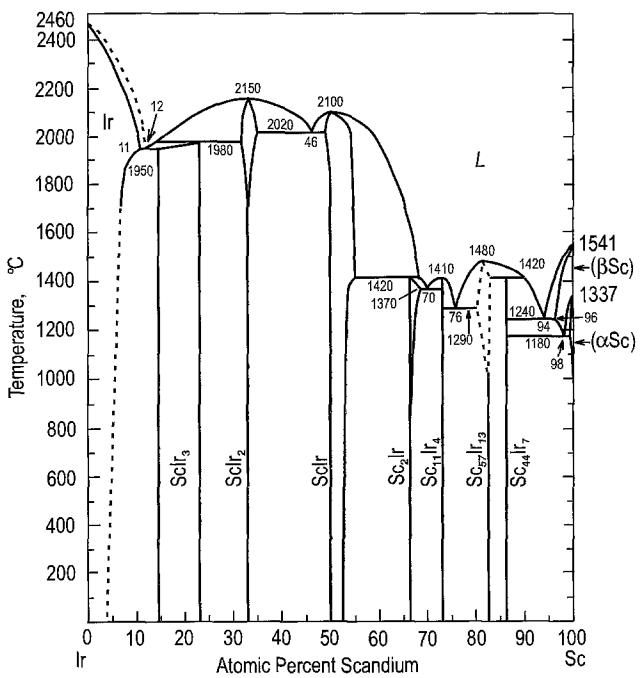

Fig. 10. The Sc–Ir phase diagram.

scandium in solid platinum is about 10 at.%. In the single invariant phase transformation shown in the original diagram at 1850±25°C, four phases, namely *L*, Pt(Sc), $ScPt_3$ and ScPt, are involved, which is in contradiction with the Gibbs phase rule. The slight variations of lattice spacing for $ScPt_3$ (see table 6) may be due to the result of a homogeneity range similar to that in the cases of $ScRh_3$ and $ScIr_3$. However, in the figure of the phase diagram presented by Savitsky et al. $ScPt_3$ has a constant composition. Thus, the Sc–Pt phase diagram is too tentative and needs additional investigation.

2.10. *Sc–M (M = 1B element) systems*

Savitskii et al. (1970) and Naumkin et al. (1971) were the first to study the Sc–Cu phase diagram. Two binary compounds ScCu and $ScCu_2$ which were known earlier were confirmed, and a third one, $ScCu_4$, was reported for the first time. Markiv et al. (1978) reinvestigated the phase diagram in the range 0–80 at.% Sc. In general the data presented in these three papers are in good agreement with each other except for the way of formation of the $ScCu_2$ compound and its melting temperature, and the homogeneity range of the $ScCu_4$ phase. Savitskii et al. and Naumkin et al. established the peritectic formation of $ScCu_2$ at 890°C, while Markiv et al. reported that it is congruently melting at 990°C. The RCu_2 compounds with the heavy rare earths Gd, Dy or Y are also congruently melting phases (Massalski 1990). It is known that scandium resembles the alloying behaviour of these rare earths. For that reason we prefer the data of Markiv et al. concerning the way and temperature of formation of the $ScCu_2$ compound. We think that the data of Markiv et al. who reported the homogeneity range for $ScCu_4$ compound from 19 to 23 at.% Sc are more correct. The Cu-rich side of the $ScCu_4$ phase was determined by microprobe analysis as 18.6 at.% Sc (see Kotur et al. 1996a). Its crystal structure is unknown (table 7). All attempts to solve its structure using powder or single-crystal methods were unsuccessful since the phase is terribly sensitive to mechanical grinding (see Kotur et al. 1996a). The Sc–Cu phase diagram is presented in fig. 11. It is based primarily on the data of Savitskii et al. and Naumkin et al., and in some regions, as mentioned above, on the data of Markiv et al. However, there are also indications that the melting temperature of $ScCu_4$ is higher than 1000°C (Kotur et al. 1996a). Thus, the phase diagram needs an additional investigation in the range 15–35 at.% Sc as well as in the Sc-rich region (>80 at.% Sc). An extended list of references on this system can be found in the paper by Subramanian et al. (1988).

The solubility of scandium in silver was investigated by Gschneidner et al. (1970) who presented the part of Sc–Ag phase diagram in the range 0–12 at.% Sc. The phase diagram in the concentration region 0–85 at.% Sc has been established by Stapf et al. (1975). Three earlier known binary compounds have been confirmed. Their characteristics are presented in table 7. Stapf et al. reported the eutectic temperature of 910°C between the Ag solid solution and $ScAg_4$,and the composition of the melt at that temperature containing 10 at.% Sc. These data do not agree with the data of Gschneidner et al. who reported a maximum solubility of 10.5 at.% Sc in solid Ag at the eutectic temperature of 926°C. We prefer these latter data since they were obtained from a larger number of samples.

Table 7
Intermetallic compounds in the Sc–M (M = Cu, Ag, Au) binary systems

Compound	Melting temperature (°C)	Structure type or symmetry	Lattice parameters		Reference
			a (Å)	c (Å)	
$ScCu_4$	L, 925	?			*Savitskii et al. (1970)*
$ScCu_2$	L, 990	$MoSi_2$	3.290	8.388	Dwight et al. (1967), *Markiv et al. (1978)*
ScCu	L, 1125	CsCl	3.256		Aldred (1962), *Savitskii et al. (1970)*
$ScAg_4$	P, ~936	$MoNi_4$	6.5740	4.0686	McMasters et al. (1970), *Stapf et al. (1975)*
			6.575	4.067	Reule et al. (1971)
$ScAg_2$	L, 1155	$MoSi_2$	3.519	8.922	Dwight et al. (1967), *Stapf et al. (1975)*
			3.517	8.923	Reule et al. (1971)
ScAg	L, 1230	CsCl	3.412		Aldred (1962), *Stapf et al. (1975)*
$ScAu_4$	?	$MoNi_4$	6.536	4.031	Reule et al. (1971)
$ScAu_2$	?	$MoSi_2$	3.508	8.725	Dwight et al. (1967)
			3.504	8.720	Reule et al. (1971)
ScAu	?	CsCl	3.370		Aldred (1962)
Sc_2Au	?	?			Aldred (1962)

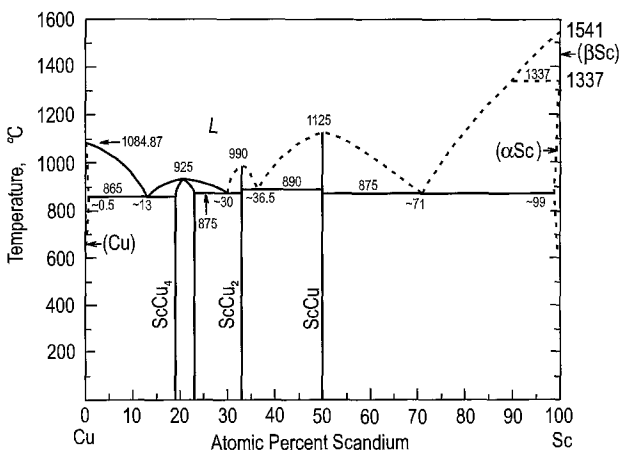

Fig. 11. The Sc–Cu phase diagram.

This assumption required the shifting of the $L + ScAg_2 \leftrightarrow ScAg_4$ peritectic temperature by 16°C of the data of Stapf et al. as well as the shifting of the composition of the eutectic.

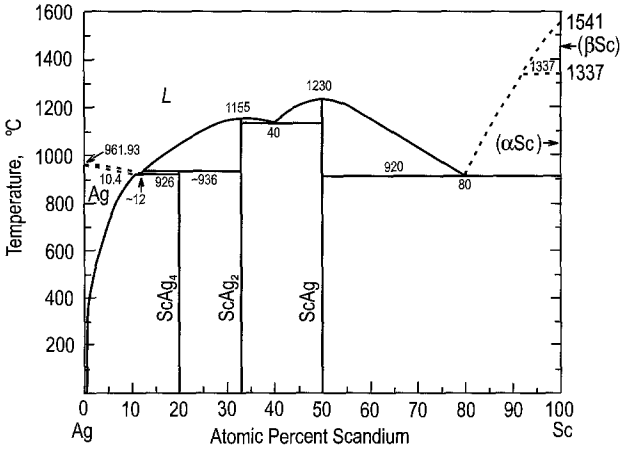

Fig. 12. The Sc–Ag phase diagram.

The Sc–Ag phase diagram presented in fig. 12 is based primarily on the data of Stapf et al. and the above mentioned modification based on the data of Gschneidner et al. The temperatures of the Sc phase transitions are indicated too, although the Sc-rich part of the phase diagram needs to be determined.

The 0–14 at.% Sc part of the Sc–Au phase diagram was reported over three decades ago (Rider et al. 1965). The figure is also presented by Gschneidner (1975). The maximum solubility of scandium (8.8 at.%) in solid gold occurs at the eutectic temperature of 1040°C. Four binary compounds have been synthesised in the system. Their crystal structure data are presented in table 7.

2.11. *Sc–M (M = 2B element) systems*

The Sc–Zn phase diagram in the range 0–60 at.% Sc has been recently reported by Palenzona and Manfrinetti (1997); it is presented in fig. 13. Four of the earlier known binary compounds have been confirmed by them and a new one, $Sc_{13}Zn_{58}$ has been added. The crystal structure data are given in table 8. Earlier, Kripyakevich et al. (1966) reported the existence of a cubic compound with the lattice spacing 13.79 Å and the approximate composition Sc_2Zn_7. The authors identified the structure to be closely related to the Ru_3Be_{17} type. Andrusyak et al. (1989) using single-crystal structure investigation corrected its composition to Sc_3Zn_{17} and established that it belongs to the Ru_3Be_{17} structure type (table 8).

Palenzona and Manfrinetti (1996) investigated the Sc–Cd phase diagram in the range 0–70 at.% Sc, which is shown in fig. 14. The Sc-rich part of the phase diagram is drawn schematically since it has not been investigated experimentally and further investigations are necessary. Scandium is practically insoluble in solid cadmium. The solubility of cadmium in βSc is comparatively high, as can be established from the change of the variation of the lattice parameter which varies from 3.73 Å for pure Sc to 3.58 Å in

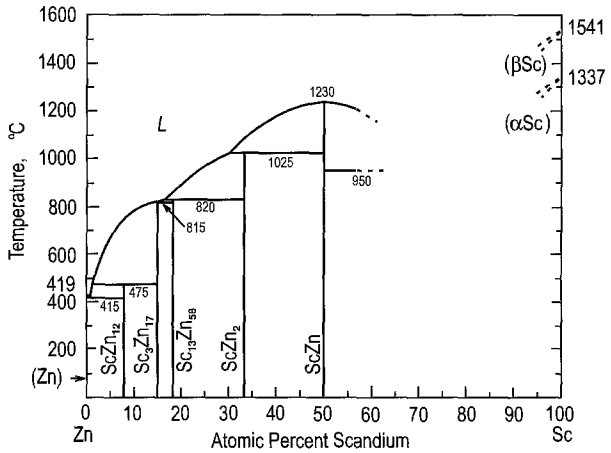

Fig. 13. The Sc–Zn phase diagram in the range 0–60 at.% Sc.

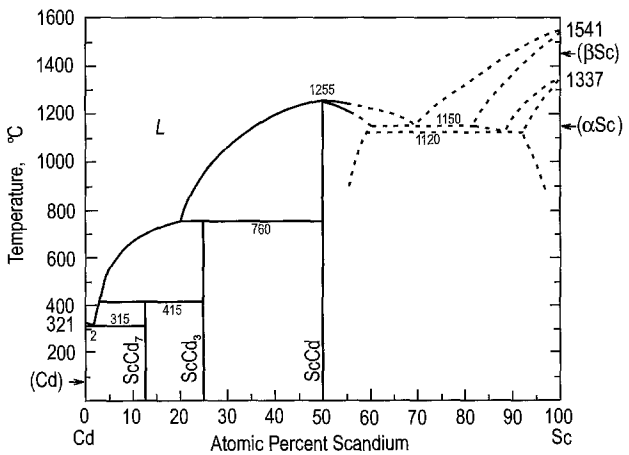

Fig. 14. The Sc–Cd phase diagram in the range 0–70 at.% Sc.

a quenched two-phase alloy containing 30 at.% Cd (Palenzona and Manfrinetti). These authors confirmed the existence of two known binary compounds, namely ScCd and $ScCd_2$, and synthesised a third one, $ScCd_7$. The crystal structures of all these compounds have been determined and are given in table 8. The data given by the different authors for the lattice spacings of these compounds are in good agreement (see table 8). The ScCd phase is characterised by the homogeneity region ranging from 50 to about 62 at.% Sc. The lattice spacing changes from $a = 3.510$ Å for the equiatomic composition to $a = 3.524$ Å for the Sc-rich composition (Palenzona and Manfrinetti).

Only two binary compounds, ScHg and $ScHg_3$, are known in the Sc–Hg phase diagram. Their crystal structures have been determined by Laube and Nowotny (1963b) (table 8).

Table 8
Intermetallic compounds in the Sc–M (M = Zn, Cd, Hg) binary systems

Compound	Melting temperature (°C)	Structure type or symmetry	Lattice parameters			Reference
			a (Å)	b (Å)	c (Å)	
$ScZn_{12}$	*P*, 475	$ThMn_{12}$	8.814		5.140	Kripyakevich et al. (1966), *Palenzona and Manfrinetti (1997)*
Sc_3Zn_{17}	*P*, 815	Ru_3Be_{17}	13.852			Andrusyak et al. (1989), *Palenzona and Manfrinetti (1997)*
$Sc_{13}Zn_{58}$	*P*, 820	$Gd_{13}Zn_{58}$	13.741		13.632	*Palenzona and Manfrinetti (1997)*
$ScZn_2$	*P*, 1025	AlB_2	4.363		3.196	Kripyakevich et al. (1965), *Palenzona and Manfrinetti (1997)*
ScZn	*L*, 1230	CsCl	3.350			*Laube and Nowotny (1963a), Palenzona and Manfrinetti (1997)*
$ScCd_7$	*P*, 415	$ScCd_7$	7.306	9.998	9.318	*Palenzona and Manfrinetti (1996)*, Pani et al. (1995)
$ScCd_3$	*P*, 760	Ni_3Sn	6.332		4.854	*Palenzona and Manfrinetti (1996)*
			6.330		4.853	Schablaske et al. (1964)
ScCd	*L*, 1255	CsCl	3.513			Schablaske et al. (1964), *Palenzona and Manfrinetti (1996)*
			3.507			Laube and Nowotny (1963a)
$ScHg_3$	?	Ni_3Sn	6.369		4.762	Laube and Nowotny (1963b)
ScHg	?	CsCl	3.480			Laube and Nowotny (1963b)

2.12. *Sc–X (X = 3B element) systems*

The Sc–B phase diagram has been published by Spear (1976, 1977). Figure 15 presents the Sc–B phase diagram based on these papers. Two binary compounds occur in this system, namely ScB_{12} and ScB_2. Earlier it was claimed that there exist two other B-rich compounds ScB_4 and ScB_6, however already Peshev et al. (1970) could not confirm the existence of these two phases. The published data for the crystal structure of ScB_2 phase and its lattice spacings are in good agreement with each other (see table 9). However, two different crystal structures have been reported for the ScB_{12} compound. Przybylska et al. (1963) found its structure to be isotypic with the cubic UB_{12}. A single-crystal investigation by Matkovich et al. (1965) revealed however that the ScB_{12} structure is tetragonal, isotypic with $ThMn_{12}$ (SG *I4/mmm*, $a = 5.22$, $c = 7.35$ Å). Its pseudocubic

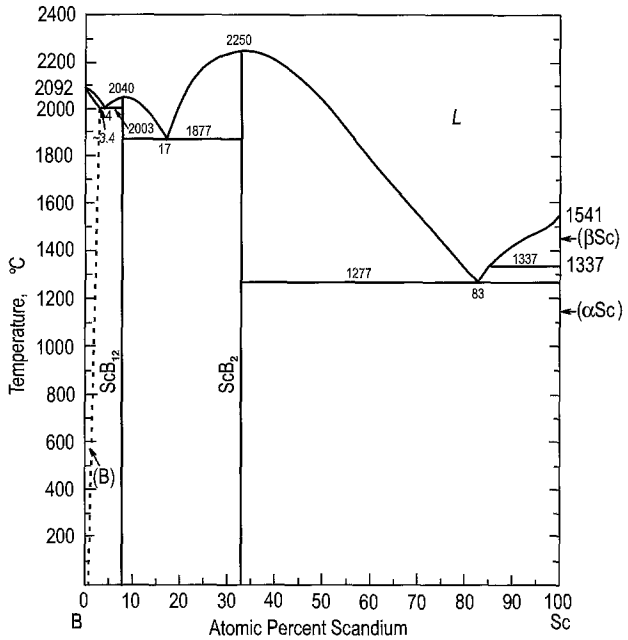

Fig. 15. The Sc–B phase diagram.

tetragonal structure was confirmed also by Peshev et al. (1970) and by Callmer (1978) ($a = 5.2347$, $c = 7.3583$ Å). However a recent single-crystal investigation of ScB_{12} by Bruskov et al. (1988) confirmed the cubic UB_{12}-type structure (table 9). It seems that this question needs additional investigation. Perhaps ScB_{12} occurs in two polymorphic modifications, but this does not agree with the presented phase diagram.

A detailed reference list on the scandium–boron alloys and their properties can be found in the reviews of Gschneidner (1975) and Spear and Liao (1990).

The Sc–Al phase diagram has been established by Naumkin et al. (1965). The Al-rich region was later refined by Drits et al. (1973). A phase diagram based on these papers is presented in the review of Gschneidner and Calderwood (1989a). In this paper and in the review of Gschneidner (1975) an extended list of references has been given. The solubility of scandium in solid aluminium does not exceed 0.22 at.% (Drits et al.), whereas Sc dissolves about 4 at.% Al (Naumkin et al.). Four binary compounds of constant composition occur in the system. Their compositions and characteristics are given in table 9. Schob and Parthé (1965) reported the CsCl structure type (SG *Pm3m*) for ScAl ($a = 3.450$ Å) and noticed several extra lines in its X-ray patterns. Schuster and Bauer (1985) during an investigation of the Sc–Al–N ternary system determined that pure ScAl had the CrB-type structure. These authors claimed that either oxygen or nitrogen (or both) can stabilize the CsCl structure in the Sc–Al alloys.

There exist two variants of the Sc–Ga phase diagram in the literature. The first one was reported by Markiv et al. (1977) who investigated only 13 binary alloys within

Table 9
Intermetallic compounds in the Sc–X (X = B, Al, Ga, In, Tl) binary systems

Compound	Melting temperature (°C)	Structure type or symmetry	Lattice parameters			Reference
			a (Å)	*b* (Å)	*c* (Å)	
ScB_{12}	*L*, 2040	UB_{12}	7.402			Bruskov et al. (1988), *Spear (1976)*
ScB_2	*L*, 2250	AlB_2	3.148		3.516	Peshev et al. (1970), *Spear (1976)*
			3.146		3.517	Zhuravlev and Stepanova (1958)
$ScAl_3$	*P*, 1320	$AuCu_3$	4.101			Schuster and Bauer (1985), *Naumkin et al. (1965)*
			4.105			Zalutskii and Kripyakevich (1967)
$ScAl_2$	*L*, 1420	$MgCu_2$	7.5748			Schuster and Bauer (1985), *Naumkin et al. (1965)*
			7.580			Rechkin et al. (1965)
ScAl	*L*, ~1300	CrB	5.0299	9.8945	3.1263	Schuster and Bauer (1985), *Naumkin et al. (1965)*
Sc_2Al	*P*, 1195	Ni_2In	4.8813		6.167	Schuster and Bauer (1985), *Naumkin et al. (1965)*
			4.888		6.166	Eymond and Parthé (1969)
$ScGa_3$	*P*, 1030	$AuCu_3$	4.095			*Yatsenko et al. (1979)*
			4.096			Markiv et al. (1977)
$ScGa_2$	*L*, 1140	KHg_2	4.140	6.614	7.914	Belyavina and Markiv (1980a), *Yatsenko et al. (1979)*
Sc_3Ga_5	*L*, 1130(?)	Tm_3Ga_5	10.910	9.231	5.695	Markiv et al. (1981), *Markiv et al. (1977)*
ScGa	*P*, 1090	CrB	4.023	10.212	3.894	*Yatsenko et al. (1979)*
			4.022	10.205	3.895	Schob and Parthé (1965)
Sc_5Ga_4	*P*, 1230	$Ho_{11}Ge_{10}$	10.366		15.305	Markiv et al. (1989), *Yatsenko et al. (1979)*
Sc_3Ga_2	?	Gd_3Ga_2	10.767		14.045	Markiv et al. (1987)
Sc_5Ga_3	*L*, 1430	Mn_5Si_3	8.067		6.036	*Yatsenko et al. (1979)*
			8.074		5.951	Schob and Parthé (1964a)
Sc_2Ga	*P*, 1065(?)	Sc_2Ga	8.085	5.933	14.014	Belyavina and Markiv (1992), *Markiv et al. (1977)*
			$\gamma = 90.95°$			
$ScIn_3$	*P*, 930	$AuCu_3$	4.479			*Palenzona and Manfrinetti (1996)*, Yatsenko et al. (1983)
			4.477			Parthé et al. (1965)
$ScIn_2$	*P*, 970	$ZrGa_2$	4.440	13.571	4.459	*Palenzona and Manfrinetti (1996)*

continued on next page

Table 9, *continued*

Compound	Melting temperature (°C)	Structure type or symmetry	Lattice parameters			Reference
			a (Å)	*b* (Å)	*c* (Å)	
ScIn	*P*, 1125	AuCu	4.539		4.326	*Palenzona and Manfrinetti (1996)*
$ScIn_{1-x}$	*P*, 1280	CsCl	3.564			*Palenzona and Manfrinetti (1996)*
Sc_2In	*L*, 1400	Ni_2In	5.024		6.276	*Palenzona and Manfrinetti (1996)*, Yatsenko et al. (1983)
			5.0260		6.2771	Hines and Harris (1971)
Sc_3In	*P*, 1340	Ni_3Sn	6.43		5.17	*Yatsenko et al. (1983)*, *Palenzona and Manfrinetti (1996)*
			6.421		5.183	Compton and Matthias (1962)
~$ScTl_2$	*P*, 967	?				*Sabirzyanov (1988)*
Sc_3Tl_5	*P*, 987–*Ed*, 477	Pu_3Pd_5	9.970	7.948	10.235	*Sabirzyanov (1988)*
ScTl	*P*, 1152–*Ed*, 367	*cub*	13.382			*Sabirzyanov (1988)*
Sc_5Tl_4	*P*, 1262	Ti_5Ga_4	8.590		6.356	*Sabirzyanov (1988)*
$Sc_5Tl_{3-3.85}$	*L*, 1372	Mn_5Si_3	8.396–8.432		6.160–6.465	*Sabirzyanov (1988)*
Sc_2Tl	*P*, 1287	Ni_2In	4.984		6.255	*Sabirzyanov (1988)*
~Sc_3Tl	*P*, 1262–*Ed*, 1117	?				*Sabirzyanov (1988)*

the concentration range of 35–68 at.% Ga, which is only half of the number of alloys investigated by Yatsenko et al. (1979) (see below). From this investigation Markiv et al. (1977) concluded that there exist seven binary compounds. Three of them, Sc_5Ga_3, Sc_2Ga_3 and $ScGa_3$, were reported to melt congruently at temperatures 1380, 1130 and 1090°C, respectively. The others, Sc_2Ga, Sc_5Ga_4, ScGa and $ScGa_2$, are formed by peritectic reactions at 1065, 1240, 1080 and 1070°C, respectively. In this paper and in the following papers (Belyavina and Markiv 1980a, 1992, Markiv et al. 1981, 1987, 1989), the same group of scientists presented results of crystal structure investigations of the above mentioned gallides and also reported about the synthesis of an extra binary compound Sc_3Ga_2. Markiv et al. (1981) corrected the composition of the earlier reported "Sc_2Ga_3" compound which they subsequently found to be Sc_3Ga_5. The crystal structure data are given in table 9. Belyavina and Markiv (1992) reinvestigated the structure of the Sc–Ga alloys in the range 30–38.5 at.% Ga. The Sc_2Ga compound has a narrow homogeneity range from 33 to 35 at.% Ga. Its monoclinic crystal structure is related to Mn_5Si_3 type.

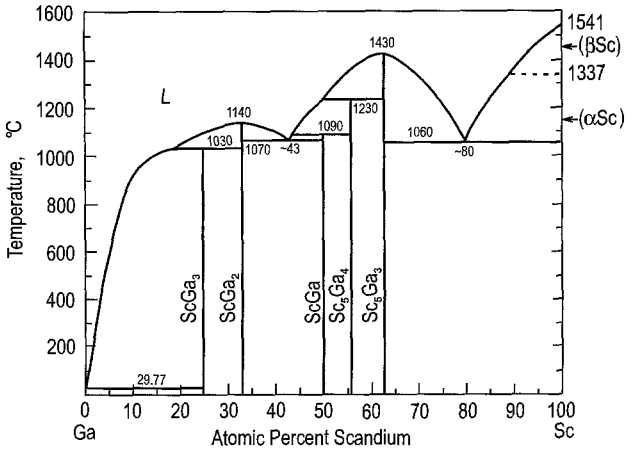

Fig. 16. The Sc–Ga phase diagram.

In the alloys with the content 36–8.5 at.% Ga they observed two hexagonal phases which they presented as h-Sc_5Ga_3 and r-Sc_5Ga_3 with the lattice spacings $a = 8.048$–8.062 and $c = 6.112$–6.073 Å, and $a = 8.084$ and $c = 5.958$ Å respectively. The pure r-Sc_5Ga_3 was observed in a specimen with 36 at.% Ga and heat treated at 800°C. Thus, the composition of the phase is shifted from stoichiometry 5:3 (37.5 at.% Ga). This compound appears at temperatures lower than 1000°C, and its structure was determined to be of the Mn_5Si_3 type. The crystal structure of the h-Sc_5Si_3 phase, which is observed at high temperatures with the content of about 38 at.% Ga, has not been established and needs additional investigation. The structure of another compound isotypic with h-R_5Ga_3 (R = Y, Tm, Lu) reported by Markiv and Belyavina (1992) is also unknown, however, as stated by Markiv and Belyavina the structure of these compounds should closely be related to the Mn_5Si_3 type structure.

A second variant of the Sc–Ga phase diagram was presented by Yatsenko et al. (1979). These authors investigated 28 alloys over the whole concentration region of the system. Figure 16 presents the Sc–Ga phase diagram based on the data of Yatsenko et al. The two variants of the Sc–Ga phase diagram considerably differ from each other. Yatsenko et al. observed only five binary compounds in the system (see fig. 16). For three of them, $ScGa_3$, Sc_5Ga_3 and ScGa, they determined the crystal structure. These data perfectly agree with the data of Markiv et al. But in general the disagreement between the two reported versions is drastic. Such disagreement is hard to explain as the two groups of scientist used practically the same experimental methods: differential thermal, X-ray and microscopic analyses. Markiv et al. used also the microprobe analysis and Yatsenko et al. performed also microhardness measurements on their samples. These diverging results strongly suggest that the Sc–Ga phase diagram needs to be reinvestigated.

The Sc–In phase diagram was determined by Yatsenko et al. (1983). Earlier the part of the phase diagram in the range 0–40 at.% In was proposed by Gardner et al. (1968), but their data were tentative. Yatsenko et al. confirmed the compositions and crystal structures

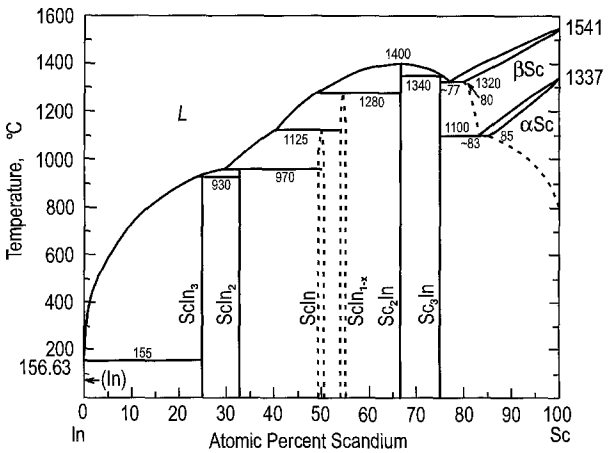

Fig. 17. The Sc–In phase diagram.

of three binary scandium indides, $ScIn_3$, Sc_2In and Sc_3In, which had been synthesised earlier, and observed three new compounds of the tentative compositions Sc_3In_5, ScIn and Sc_5In_3 with unknown structures.

Recently Palenzona et al. (1996) reinvestigated the Sc–In phase diagram in the range 30–100 at.% In. The compounds Sc_3In_5 and Sc_5In_3 could not be confirmed and were replaced by $ScIn_2$ and $ScIn_{1-x}$, respectively. In addition four other binary phases have been confirmed. Their characteristics are given in table 9. The temperatures of the phases transitions reported by Palenzona et al. are in average 5 to 20°C higher than those reported by Yatsenko et al. with the exception of the temperature for the peritectic formation of $ScIn_{1-x}$ which is 50°C lower than that of the corresponding "Sc_5In_3" phase reported by Yatsenko et al. Figure 17 presents the phase diagram based on the data of Palenzona et al. (1996) (in the range 0–70 at%. Sc) and those of Yatsenko et al. (1983) (in the range 70–100 at.% Sc). Gschneidner (1975) reviewed the physical properties of Sc–In compounds. Sc_3In is a well known weak ferromagnetic compound with a Curie temperature near 6 K. Since it has been considered as a prototype of an intermetallic compound where spin fluctuations play an important role its physical properties are discussed in sect. 6.

Sabirzyanov (1988) was the only scientist who investigated the interaction of scandium with thallium. He established the phase diagram shown in fig. 18. The investigation was carried out by means of thermal, X-ray and microscopic analyses. He also measured the magnetic susceptibility of the alloys. Seven binary compounds occur in the system. Sabirzyanov determined the crystal structure of five of them (table 9). For two phases with unknown structures the compositions of Sc_3Tl and $ScTl_2$ are given as the most likely ones. The homogeneity range for $Sc_5Tl_{3-3.85}$ reaches 6 at.% at 1262°C. The limits of solubility of thallium in βSc and αSc are 18±1 at.% and 11±1 at.%, respectively. The data concerning the temperatures of the phase transitions, the compositions and crystal structures of the compounds (except lattice spacings) were also presented by Sabirzyanov (1989); however, the phase diagram was not shown.

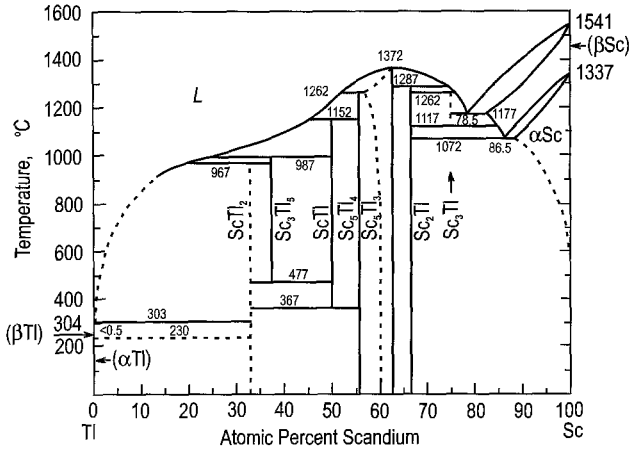

Fig. 18. The Sc–Tl phase diagram.

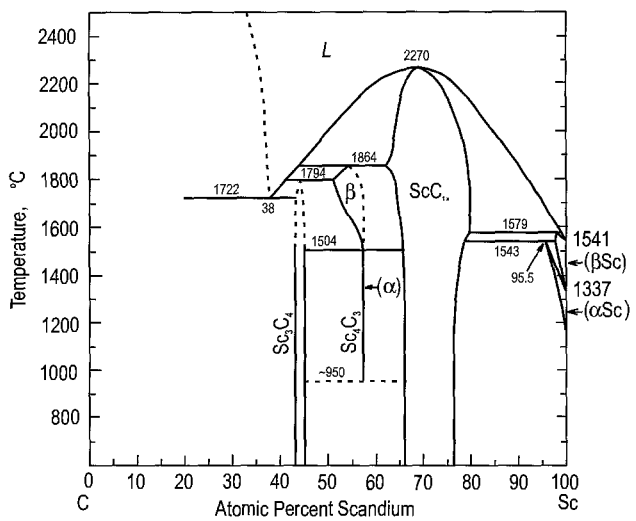

Fig. 19. The Sc–C phase diagram in the range 20–100 at.% Sc.

2.13. *Sc–X (X = 4B element) systems*

Many papers have been dedicated to the investigation of interaction of scandium with carbon. The early papers which appeared before 1973 have been reviewed by Gschneidner (1975) and Gschneidner and Calderwood (1986c). In total seven compounds have been reported to occur in this system, however, the majority of them were not confirmed. Gordijchuk et al. (1981) first reported on the Sc–C phase diagram in the range 20–100 at.% Sc and refined it afterwards (Gordijchuk 1987). The phase diagram presented in fig. 19 is based mainly on the latter data; there are only three binary compounds. Their

crystal structure data are presented in table 10. One of the phases, Sc_4C_3, exists in two polymorphic modifications. The data of Gorgijchuk agree with the results of Krikorian et al. (1969a) who also observed that Sc_4C_3 (ST anti-Th_3P_4, SG $I43d$, $a = 7.207$ Å) remained stable when heated to 1500°C. Its X-ray pattern changed when heating the sample up to 1600°C. Krikorian et al. (1969b) reported also about a bcc phase with the approximate composition $Sc_{13}C_{10}$ (~56.5 at.% Sc, $a = 8.5268$ Å). It was synthesised after annealing the Sc_4C_3 sample with an addition of germanium. However the Ge atoms are not involved into the structure of this scandium carbide. Possibly Krikorian et al. obtained the high temperature phase of Sc_4C_3 (β) reported by Gordijchuk. Jedlichka et al. (1971) were the first to determine the composition and the crystal structure of the scandium carbide with the highest Sc content, which was earlier reported by Krikorian et al. (1969a) as "$ScC_{1.2-1.3}$". Jedlichka et al. (1971) determined its composition as $Sc_{15}C_{19}$ (ST $Sc_{15}C_{19}$, SG $P42_1c$, $a = 7.50$, $c = 15.00$ Å). Recently Pöttgen and Jeitschko (1991) reinvestigated the structure of $Sc_{15}C_{19}$ using a single crystal and reported its composition as Sc_3C_4. The tetragonal unit cell of Sc_3C_4 contains two additional carbon atoms in comparison to the $Sc_{15}C_{19}$ structure. Its lattice spacings are given in table 10. Maybe that these two investigated single crystals Sc_3C_4 (42.9 at.% Sc) and $Sc_{15}C_{19}$ (44.1 at.% Sc) can be treated in favour of occurrence of homogeneity range of this compound reported by Gordijchuk (see fig. 19). Gordijchuk determined its homogeneity range from 43.5 to 45.7 at.% Sc and the lattice spacings changing from $a = 7.53$, $c = 15.04$ Å to $a = 7.51$, $c = 15.51$ Å. Thus, to clarify the conflicting data additional investigations of the system, particularly in the range 40–80 at.% Sc, have to be carried out.

Although three binary scandium silicides, Sc_5Si_3, ScSi and Sc_3Si_5, were obtained and structurally investigated already in the early 1960s (table 10), a Sc–Si phase diagram was only presented in 1988. It is shown in fig. 20. The data are taken from Eremenko et al. (1988) with corrections for the phase transition temperatures of pure components to the presently accepted values. For scandium the difference between the reported melting temperature (1615°C) and the $\beta Sc \leftrightarrow \alpha Sc$ transition temperature (1430°C) and the corresponding present temperatures 1541 and 1337°C is rather large. In the case of silicon the difference in the melting temperature (1412°C reported and 1414°C accepted) was within the experimental error. Eremenko et al. confirmed the data of Bodak et al. (1976) and Kotur (1977a) that the binary phase with the highest Si content exists only at high temperature (see fig. 20). Bodak et al. and Kotur observed that phase only in the as cast alloys. After heat treatment at 800°C for 340 h this phase totally decomposed to Si and ScSi. There is a disagreement between the data about the composition of the highest silicon-containing scandium silicide. Gladyshevsky and Emes-Misenko (1963) reported it as Sc_3Si_5 (62.5 at.% Si), Schob and Parthé (1964b) found it to have the homogeneity range from 60 (composition Sc_2Si_3 or $ScSi_{1.5}$) to 62.5 at.% Si (composition Sc_3Si_5 or $ScSi_{1.67}$), whereas Eremenko et al. claimed a constant composition $ScSi_{1.5}$. For the reported lattice spacings for this phase, it is given as $ScSi_{2-x}$ in table 10.

Recently Kotroczo and McColm (1994) established the phase equilibria for rapidly cooled Sc–Si alloys (cooling rate 150–200°C/s). Their phase diagram shows many similarities with that of Eremenko et al. But in general the liquid boundaries and

Table 10
Intermetallic compounds in the Sc–X (X = C, Si, Ge, Sn, Pb) binary systems

Compound	Melting temperature (°C)	Structure type or symmetry	Lattice parameters			Reference
			a (Å)	*b* (Å)	*c* (Å)	
Sc_3C_4	*P*, 1794	Sc_3C_4	7.5138		14.704	Pöttgen and Jeitschko (1991), *Gordijchuk (1987)*
$Sc_{15}C_{19}$		$Sc_{15}C_{19}$	7.50		15.00	*Jedlichka et al. (1971)*
Sc_4C_3 (β)	*P*, 1864 – *S*, 1504	?				*Gordijchuk (1987)*
Sc_4C_3 (α)	*S*, 1504 – *Ed*, ~950	anti-Th_3P_4	7.2078			*Gordijchuk (1987)*
ScC_{1-x}	*L*, 2270	NaCl	4.67–4.72			*Gordijchuk (1987)*
			4.509			Nowotny and Auer-Welsbach (1961), Auer-Welsbach and Nowotny (1961)
$ScSi_{2-x}$(β)	*P*, 1260 – *S*, 1070	AlB_2	3.66 3.664– 3.646		3.87 3.877– 3.881	Gladyshevsky and Emes-Misenko (1963), *Eremenko et al. (1988)*, Schob and Parthé (1964b)
$ScSi_{2-x}$(α)	*S*, 1070– *Ed*, 925	?				*Eremenko et al. (1988)*
ScSi	*P*, 1785	CrB	3.988	9.882	3.659	Schob and Parthé (1965), *Eremenko et al. (1988)*
Sc_5Si_3	*L*, 2060	Mn_5Si_3	7.861		5.812	Arbuckle and Parthé (1962), *Eremenko et al. (1988)*
$ScGe_2$	*P*, 1116	$ZrSi_2$	3.889	14.866	3.796	*Eremenko et al. (1981)*
			3.888	14.873	3.793	Schob and Parthé (1964b)
ScGe	*P*, 1192	CrB	3.98	10.08	3.763	*Eremenko et al. (1981)*
			4.007	10.06	3.762	Schob and Parthé (1965)
$Sc_{11}Ge_{10}$	*P*, 1675	$Ho_{11}Ge_{10}$	10.12		15.54	*Eremenko et al. (1981)*
			10.285		15.54	Kotur (1991)
Sc_5Ge_4	*P*, 1870	Sm_5Ge_4	7.269	13.980	7.152	*Eremenko et al. (1981)*
			7.118	13.79	7.140	Kotur (1991)
Sc_5Ge_3	*L*, 2065	Mn_5Si_3	7.921		5.881	*Eremenko et al. (1981)*
			7.939		5.883	Arbuckle and Parthé (1962)
$ScSn_2$	*P*, 895	$ScSn_2$	4.238		31.073	*Palenzona and Manfrinetti (1995)*
ScSn	*P*, 945	CsCl	3.666			Kotur and Derkach (1994), *Palenzona and Manfrinetti (1995)*
Sc_6Sn_5	*P*, 1455	Ti_6Ge_5	8.830	19.045	6.057	*Palenzona and Manfrinetti (1995)*

continued on next page

Table 10, *continued*

Compound	Melting temperature (°C)	Structure type or symmetry	Lattice parameters			Reference
			a (Å)	*b* (Å)	*c* (Å)	
Sc_5Sn_3	*L*, ~1800	Mn_5Sn_3	8.401		6.073	*Palenzona and Manfrinetti (1995)*
			8.408		6.081	Jeitschko and Parthé (1965)
Sc_6Pb_5	*P*, 1290	Ti_6Ge_5	8.889	19.274	6.177	*Palenzona and Manfrinetti (1995)*
Sc_5Pb_3	*L*, ~1700	Mn_5Si_3	8.473		6.162	*Palenzona and Manfrinetti (1995)*
			8.467		6.158	Jeitschko and Parthé (1965)

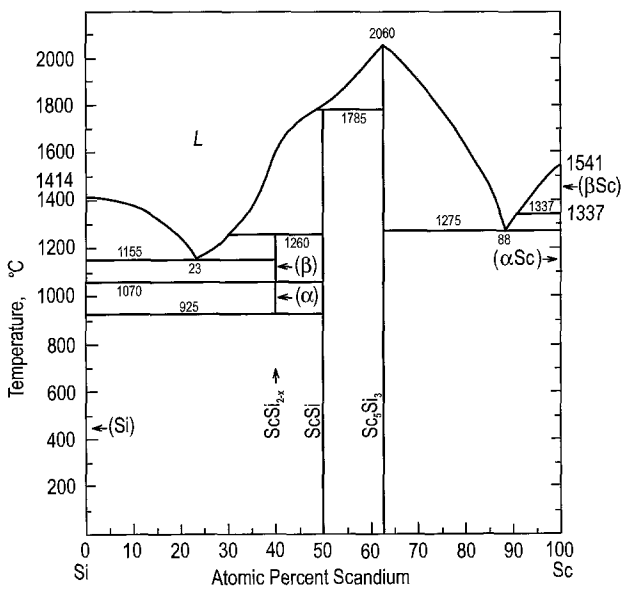

Fig. 20. The Sc–Si phase diagram.

the nonvariant reactions were 10 to 110°C and in one case (for peritectic reaction $L + ScSi \leftrightarrow \beta ScSi_{2-x}$) even 525°C higher than those reported by Eremenko et al. Kotroczo and McColm reported the highest silicon-containing silicide as having the homogeneity range $ScSi_{1.22-1.67}$ (55–62.5 at.% Si), a polymorphic transition in the temperature range 1325–1350°C, and being stable down to the room temperature. Neither Kotroczo and McColm nor Eremenko et al. obtained pure AlB_2-type structure specimens of this silicide. They observed in the X-ray patterns the presence of a nonstoichiometric AlB_2-type

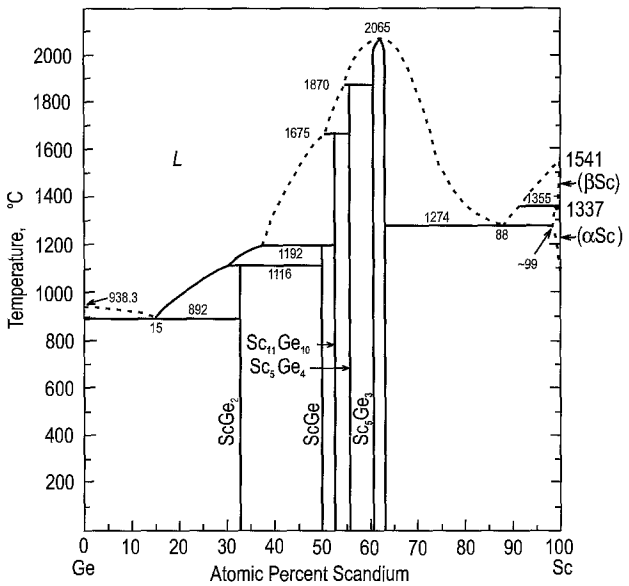

Fig. 21. The Sc–Ge phase diagram.

structure, however, together with extra weak lines. Eremenko et al. determined the lattice spacings of this AlB_2-type phase as $a = 3.654$, $c = 3.87$ Å. Kotroczo and McColm observed an increase of the lattice parameters from $a = 3.656$, $c = 3.872$ Å to $a = 3.665$, $c = 3.880$ Å as the silicon content increases. An indexing of almost all lines of the patterns was possible assuming an orthorhombic unit cell with $a = 8.27(9)$, $b = 8.69(7)$, $c = 9.98(9)$ Å. The fourth binary silicide Sc_5Si_4 (P, 1920°C) was observed by Kotroczo and McColm in rapidly cooled alloys. Its X-ray pattern was indexed as an orthorhombic cell with $a = 6.78(2)$, $b = 13.11(4)$, $c = 7.03(1)$ Å. In our opinion these data indicate that the Sm_5Ge_4 structure type as a possible structure for Sc_5Si_4, which is structure for the corresponding scandium germanide Sc_5Ge_4 (see table 10).

Okamoto (1992) mentioned the thermodynamical inconsistency of the liquidus curve in the Sc–Si phase diagram of Eremenko et al. (see fig. 20, between 30 and 45 at.% Si). Therefore a new investigation of the Sc–Si phase diagram in the range 40–65 at.% Si is advisable.

The Sc–Ge system was experimentally investigated by Eremenko et al. (1981). Figure 21 displays the Sc–Ge phase diagram based on these data. The solubility of germanium in βSc is less than 0.5 at.% whereas in solid αSc it is more than 1 at.% but this value is not yet exactly determined. The solubility of scandium in germanium is less than 1 at.%. Three germanides, namely Sc_5Ge_3, ScGe and $ScGe_2$ were known before Eremenko et al. synthesised two others, Sc_5Ge_4 and $Sc_{11}Ge_{10}$. The data from different authors about the crystal structure of scandium germanides are in general agreement (see table 10). Only in

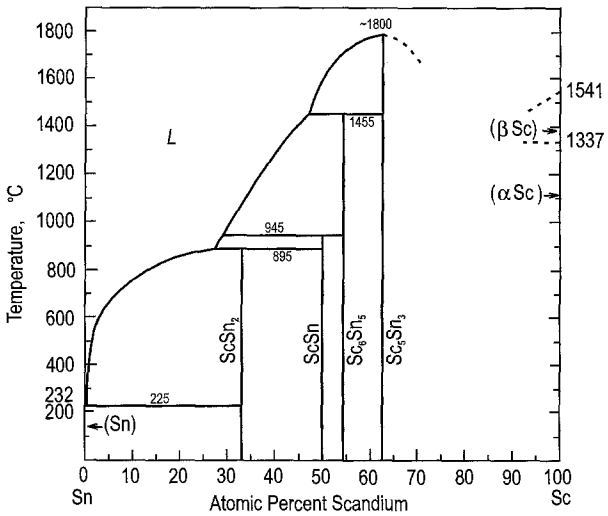

Fig. 22. The Sc–Sn phase diagram in the range 0–70 at.% Sc.

the case of $Sc_{11}Ge_{10}$ is there a considerable difference in the reported *a* lattice spacings, while the *c* values are identical.

Palenzona and Manfrinetti (1995) published the Sc–Sn phase diagram in the range 0–70 at.% Sc which is presented in fig. 22. Earlier only the experimental data by Eremenko et al. (1990) existed, and they reported that Sc_5Sn_3 melts congruently at 1775°C. These data were confirmed by Palenzona and Manfrinetti (1995). Four binary stannides occur in the system. Two of them, $ScSn_2$ and Sc_6Sn_5 have been prepared and structurally investigated by Palenzona and Manfrinetti for the first time. These authors did not mention the data of Kotur and Derkach (1994) who reported that ScSn has the CsCl structure type. Since scandium–tin alloys are extremely oxidizable the ScSn phase could not be obtained in pure state. Palenzona and Manfrinetti did not determine the crystal structure of ScSn, however they mentioned the rather simple character of its powder X-ray pattern. The crystal structure characteristics of scandium stannides are presented in table 10.

The Sc–Pb phase diagram has been determined by Palenzona and Manfrinetti (1995) in the range 0–70 at.% Sc (see fig. 23). The Sc-rich part of this system (as well as the Sc–Sn system, discussed above) has not been investigated because of the high melting temperatures of the corresponding alloys and contamination of them by molybdenum which was used as container material during preparation of the samples. Two binary compounds occur in the system (table 10), one of them, Sc_5Pb_3 was known before the investigation of Palenzona and Manfrinetti.

2.14. *Sc–X (X = P, As, Sb, Bi) systems*

There is no information in the literature about the binary phase diagrams of scandium with the 5B elements (P, As, Sb, Bi). Although in each of the systems from one to four binary

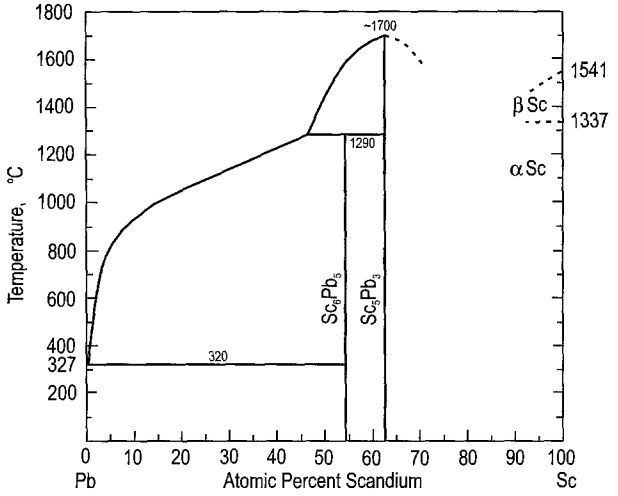

Fig. 23. The Sc–Pb phase diagram in the range 0–70 at.% Sc.

compounds have been synthesised and their crystal structures have been determined, there is no information about their melting temperatures and the way of formation (see table 11). The only exception are the data of Komissarova et al. (1965) who found that ScP has a melting temperature higher than 2000°C. Evidently some phases occur in two (Sc_3P_2) or three (Sc_3As_2) polymorphic modifications, but nothing is known about the temperatures of their phases transitions. Different values of lattice spacings observed for NaCl-type compounds (see table 11) may be originating from the homogeneity ranges of these phases or from scandium of different purity used by different groups of scientists. Additional investigations are necessary to clarify these data. Additional literature can be found in Gschneidner (1975), and Gschneidner and Calderwood (1986b, 1989b).

2.15. *Sc–X (X = Se, Te, Po) systems*

Only a little information exists about the interaction of scandium with the elements of selenium subgroup (Se, Te and Po). No phase diagrams are available for any of these binary systems.

Two binary compounds have been synthesised in the Sc–Se system by different groups of scientists. The results presented in table 12 indicate the possibility of homogeneity ranges of these phases.

Men'kov et al. (1959, 1961) synthesised two scandium tellurides and determined their crystal structures. The data of Men'kov et al. (1959) about the cubic γ'-Al_2O_3-type structure for the compound Sc_2Te_3 had not been confirmed by a single-crystal structure investigation of that phase performed by White and Dismukes (1965) (see table 12). The latter authors obtained also a specimen of $Sc_{2.3}Te_3$ composition isotypic with Sc_2Te_3 with the lattice parameters $a = 4.113$, $c = 4.051$ Å. This result seems to indicate the occurrence

Table 11
Intermetallic compounds in the Sc–X (X=P, As, Sb, Bi) binary systems

Compound	Melting temperature (°C)	Structure type or symmetry	Lattice parameters			Reference
			a (Å)	*b* (Å)	*c* (Å)	
ScP	?	NaCl	5.312			Parthé and Parthé (1963)
			5.3088			Yim et al. (1972)
Sc_3P_2 (I)	?	Cr_3C_2	6.9781	3.7570	14.3655	Berger (1980a)
Sc_3P_2 (II)	?	S_3Sb_2	10.1075	3.6944	10.1793	Berger (1980a)
Sc_7P_3	?	Th_7Fe_3	8.9340		5.7349	Berger (1981)
Sc_3P	?	Fe_3C	6.7540	8.4449	5.7662	Berger (1981)
ScAs	?	NaCl	5.4638			Yim et al. (1972)
			5.4687			Brixner (1960)
Sc_3As_2 (I)	?	Cr_3C_2	7.1423	3.8698	14.7073	Berger (1980a)
Sc_3As_2 (II)	?	S_3Sb_2	10.3754	3.8063	10.3754	Berger (1980a,b)
Sc_3As_2(III)	?	V_3As_2	10.3755		3.8064	Berger (1977)
Sc_5As_3	?	βYb_5Sb_3	10.7038	8.1418	7.2272	Berger (1980a)
Sc_7As_3	?	Sc_7As_3	14.3751		8.0281	Berger et al. (1981), Berger (1977)
ScSb	?	NaCl	5.8517			Berger (1977)
			5.859			Brixner (1960)
Sc_5Sb_3	?	βYb_5Sb_3	11.0792	8.7126	7.6272	Berger (1977)
Sc_2Sb	?	Cu_2Sb	4.2049		7.7902	Berger (1977)
ScBi	?	NaCl	5.954			Zhuravlev and Smirnova (1962)

Table 12
Intermetallic compounds in the Sc–X (X=Se, Te, Po) binary systems

Compound	Melting temperature (°C)	Structure type or symmetry	Lattice parameters			Reference
			a (Å)	*b* (Å)	*c* (Å)	
Sc_2Se_3	?	Sc_2S_3	10.836	7.673	22.95	Dismukes and White (1965)
			10.846	7.668	23.004	Brozek et al. (1974)
ScSe	?	NaCl	5.398			Hulliger and Hull (1970)
			5.434			Brozek et al. (1974)
Sc_2Te_3	?	Ti_7S_{12}	4.109		4.059	White and Dismukes (1965)
ScTe	?	NiAs	4.120		6.749	Men'kov et al. (1961)
ScPo	?	NiAs	4.206		6.92	Prokin et al. (1977)

of a homogeneity range of this phase. There is a disagreement between the data reported about the crystal structure of another phase, namely ScTe. Brixner (1960) determined it as

hexagonal with the lattice spacings $a = 6.728$, $c = 8.360$ Å, however, Men'kov et al. (1961) reported it as isotypic with NiAs (see table 12). We consider the data of Men'kov et al. to be more reliable since the neighbouring scandium telluride, Sc_2Te_3, contains NiAs-type fragments in its structure.

In the literature there is information only about one binary compound occurring in the Sc–Po system. Its crystal structure data are given in table 12.

3. Ternary systems containing scandium

At the beginning of 1997 there was information on about 110 scandium ternary systems. Of these systems the phase equilibria have been investigated either for the entire concentration region of an isothermal section (or sometimes several sections), or for only in part of it. Selected alloys have been investigated in 85 of these ternary systems. A compilation of these data are given in table 13. As can be seen from that table, there is a considerable amount of data concerning the Sc–M–X ternaries, where M is a metal and X stands for a p-element. In this section we have arranged the data in the following subsections: Sc–M–B, Sc–M–Al, Sc–M–Ga, Sc–M–In, Sc–M–C, Sc–M–Si, Sc–M–Ge, Sc–M–Sn, and Sc–M–X with X = P, As, Sb, Bi and with X = Se, Te, Po. Since there is only a small amount of data available for the latter two cases, these subsections have not been subdivided. The last two subsections of the ternary systems include either two p-elements (Sc–X–X′), or two s-, d-, or f-metals (Sc–M–M′). If the isothermal section of a system is known from the literature it is shown in a figure together with a brief comment. If these isothermals have already been treated in one of the previous chapters of the *Handbook on the Physics and Chemistry of Rare Earths* then they are omitted. As in the previous section controversial data are mentioned separately and are critically evaluated as best we are able to do so.

Since there is only a small amount of data concerning the melting temperatures and the way of formation of ternary scandium intermetallics given in the literature, these data are not included in the tables which list the compositions and lattice parameters of ternary compounds. The reference from which the lattice parameters have been taken is listed first, and is followed by other references. The reference where the corresponding atomic coordinates of the structure have been published (if it is available) is italicized.

3.1. *Sc–M–B ternary systems*

3.1.1. *Sc–La–B*

The phase diagram of the Sc–La–B system is unknown. The solubility of scandium in LaB_6 has been investigated by Tsolovski and Peshev (1972). It has been reported that the solubility reaches 0.5 mole fraction Sc, but according to the data of Kondrashov (1978) and Samsonov et al. (1979) the solubility is considerably lower. The limiting composition of the solid solution is $La_{0.9}Sc_{0.1}B_6$, and there is practically no change of the lattice parameter within this homogeneity range ($La_{0.9}Sc_{0.1}B_6$ to LaB_6).

3.1.2. *Sc–Cr–B*

Zavalii and Mikhalenko (1989) reported about an investigation of the phase equilibria in the Sc–Cr–B system at 800°C (0–33.3 at.% Sc) and at 600°C (33.3–100 at.% Sc) but

Table 13
Summary of information known about the Sc–M–X, Sc–M–M′ and Sc–X–X′ ternary phase diagrams

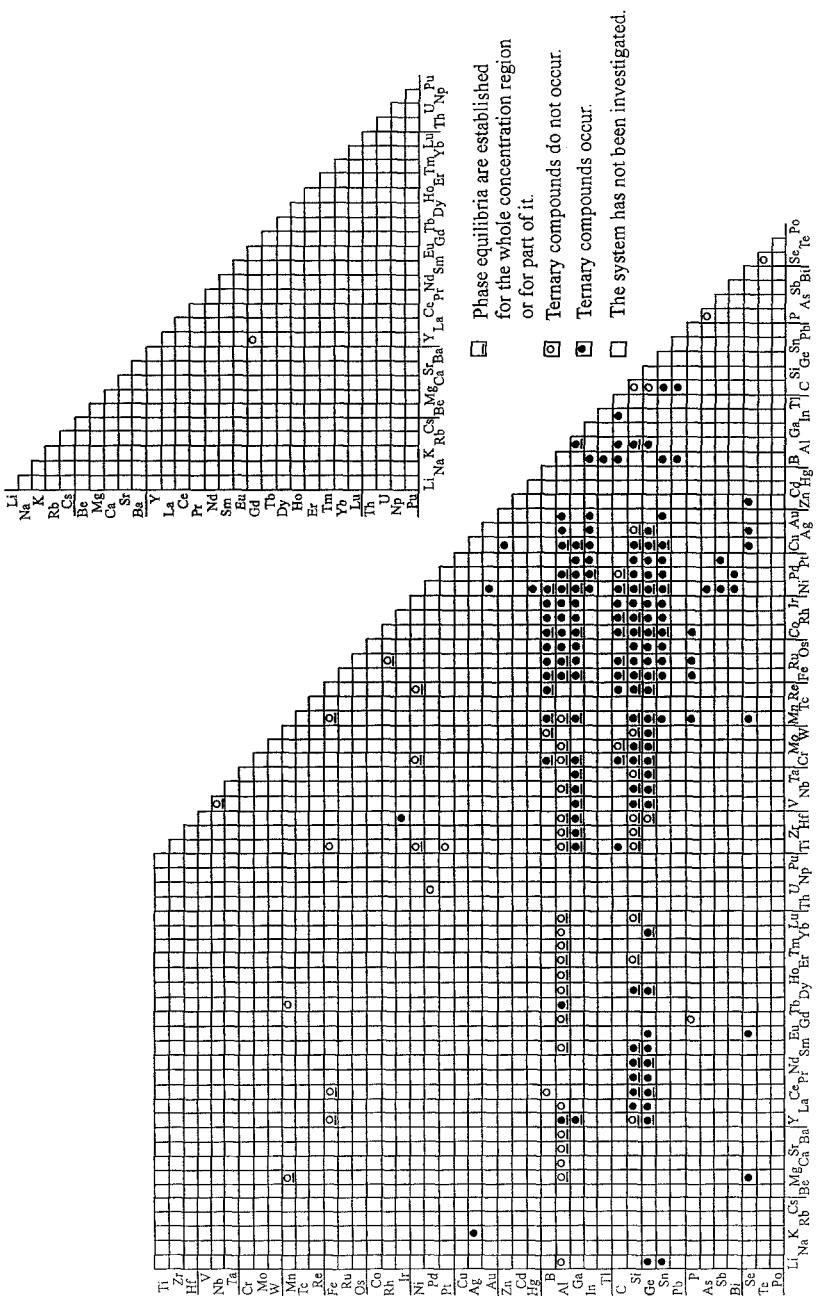

these authors did not present figures of these isothermal sections. CrB_2 dissolves up to 7 at.% Sc. One ternary compound $ScCrB_4$, which is isotypic with $YCrB_4$, occurs in the system, but the lattice spacings have not been reported (table 14).

Table 14
Ternary intermetallic compounds in the Sc–M–B systems

Compound	Structure type or symmetry	Lattice parameters			Reference
		a (Å)	*b* (Å)	*c* (Å)	
$ScCrB_4$	$YCrB_4$	?	?	?	Zavalii and Mikhalenko (1989)
$ScMnB_4$	$YCrB_4$	?	?	?	Zavalii and Mikhalenko (1989)
Sc_2ReB_6	Y_2ReB_6	8.856	11.169	3.4937	Mikhalenko et al. (1991)
$ScFeB_4$	$YCrB_4$	5.884	11.318	3.3424	Zavalii et al. (1988), Stepanchikova and Kuz'ma (1981)
$Sc_2Co_{21}B_6$	$W_2Cr_{21}C_6$	10.546			Gangleberger et al. (1966), Stepanchikova (1979)
		10.537			Kuz'ma and Voroshilov (1967)
$ScCo_4B_4$	$CeCo_4B_4$	4.902		6.961	Stepanchikova (1979)
$ScCo_3B_2$	$CeCo_3B_2$	4.889		2.977	Kuz'ma et al. (1969), Stepanchikova (1979)
$ScCoB_4$	$YCrB_4$	5.762	11.172	3.250	Zavalii et al. (1988), Stepanchikova (1979)
$Sc_{3-4}Ni_{20-19}B_6$	$W_2Cr_{21}C_6$	10.585			Kuz'ma and Voroshilov (1967), Stepanchikova and Kuz'ma (1981)
$Sc_4Ni_{29}B_{10}$	$Sc_4Ni_{29}B_{10}$	7.680		15.380	*Kuz'ma et al. (1988)*, Stepanchikova and Kuz'ma (1981)
$\sim Sc_4Ni_{15}B_6$	?	5.7853	11.208	3.2737	Stepanchikova and Kuz'ma (1981)
$ScNiB_4$	$YCrB_4$	5.7853	11.208	3.2737	Zavalii et al. (1988), Stepanchikova and Kuz'ma (1981)
$ScNi_3B$	$CaTiO_3$	3.776			Stepanchikova and Kuz'ma (1981)
$ScRu_4B_4$	$LuRu_4B_4$	7.346		14.895	Ku et al. (1979)
$Sc_2Ru_5B_4$	$Sc_5Ru_2B_4$	9.9833	8.4859 $\beta = 90.01°$	3.0001	*Rogl (1984a)*
$ScRuB_4$	?				Ku et al. (1979)
$Sc_2Os_5B_4$	$Sc_2Ru_5B_4$	10.0477	8.5499 $\beta = 90.03°$	3.0216	Rogl (1984a)
$ScOsB_2$	$LuRuB_2$	5.647	5.178	6.184	Shelton and Ku (1980)
$ScIr_3B_4$	$ZrIr_3B_4$	7.576		3.442	Rogl and Nowotny (1979)
$ScIr_3B_2$	$ErIr_3B_2$	5.344	9.307 $\beta = 92.1°$	3.062	Ku and Meissner (1981)
$ScIr_3B_{1-x}$	$CaTiO_3$	3.999			Holleck (1977)

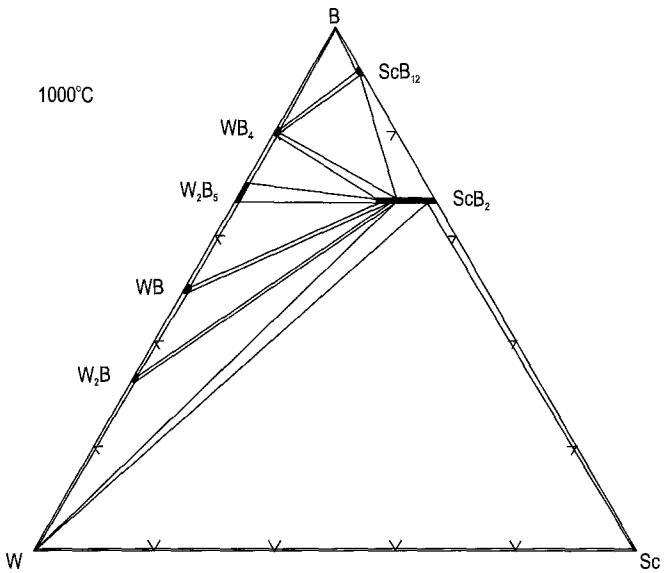

Fig. 24. Sc–W–B, isothermal section at 1000°C.

3.1.3. *Sc–W–B*

Zavalii and Mikhalenko (1989) briefly reported about an investigation of the phase equilibria in the Sc–W–B system at 1000°C (0–33.3 at.% Sc) and at 600°C (33.3–100 at.% Sc) without presenting the illustrations. The isothermal section at 1000°C, which is shown in fig. 24, is based on the data of Mikhalenko et al. (1991). Binary compound ScB_2 dissolves up to 10 at.% W. No ternary compounds were found.

3.1.4. *Sc–Mn–B*

The phase equilibria in the Sc–Mn–B system at 800°C (0–33.3 at.% Sc) and at 500°C (33.3–100 at.% Sc) have been investigated by Zavalii and Mikhalenko (1989). Figures of these isothermal sections were not presented in the original paper. Scandium stabilises the high temperature binary phase MnB_2 at 800°C (ST AlB_2). In the binary system it is stable in the temperature range 1827–1100°C. This solid solution has the homogeneity range of about 4–8 at.% Sc. One ternary compound, namely $ScMnB_4$ occurs in the system, but its lattice spacings have not been reported (table 14).

3.1.5. *Sc–Re–B*

Zavalii and Mikhalenko (1989) have investigated the phase equilibria in the Sc–Re–B system at 1000°C (0–33.3 at.% Sc) and at 600°C (33.3–100 at.% Sc), but they did not show figures in their publication. The isothermal section of the phase diagram at 1000°C for the whole concentration region, which is shown in fig. 25, is based on the data of Mikhalenko et al. (1991). Scandium diboride dissolves up to 7 at.% Re. One ternary compound, Sc_2ReB_6, occurs in the system. Its characteristics are shown in table 14.

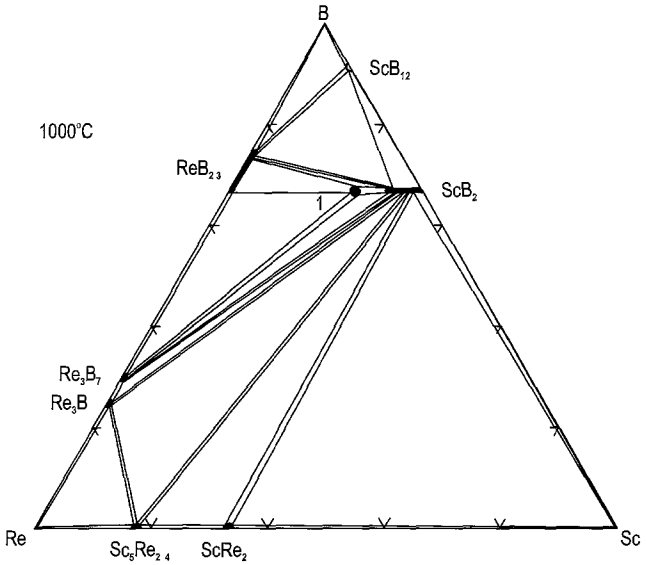

Fig. 25. Sc–Re–B, isothermal section at 1000°C. Ternary compound: (1) Sc_2ReB_6.

3.1.6. *Sc–Fe–B*

Stepanchikova and Kuz'ma (1981) studied isothermal sections of the Sc–Fe–B phase diagram at 700°C (0–50 at.% B) and at 1000°C (50–100 at.% B). In fig. 26 we corrected

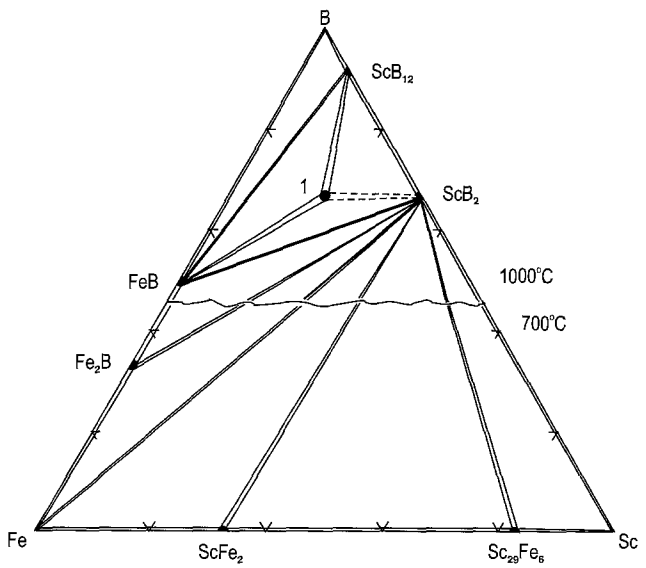

Fig. 26. Sc–Fe–B, isothermal sections at 700°C (0–50 at.% B) and at 1000°C (50–100 at.% B). Ternary compound: (1) $ScFeB_4$.

the composition of the binary compound, earlier known as ~Sc_7Fe, to $Sc_{29}Fe_6$ (see sect. 2.8). One ternary compound was observed in this system, the data are given in table 14.

3.1.7. *Sc–Co–B*

The phase equilibria at 800 and 600°C in the Sc–Co–B system have been investigated by Stepanchikova (1979). The isothermal sections (depicted in fig. 27) are corrected for the homogeneity range of the binary compound $ScCo_2$, which was found to exist from 30 to 34.5 at.% Sc at 800°C (see sect. 2.8). Stepanchikova confirmed two ternary compounds which were known earlier and synthesized two new ternaries, namely $ScCo_4B_4$ and $ScCoB_4$ (table 14).

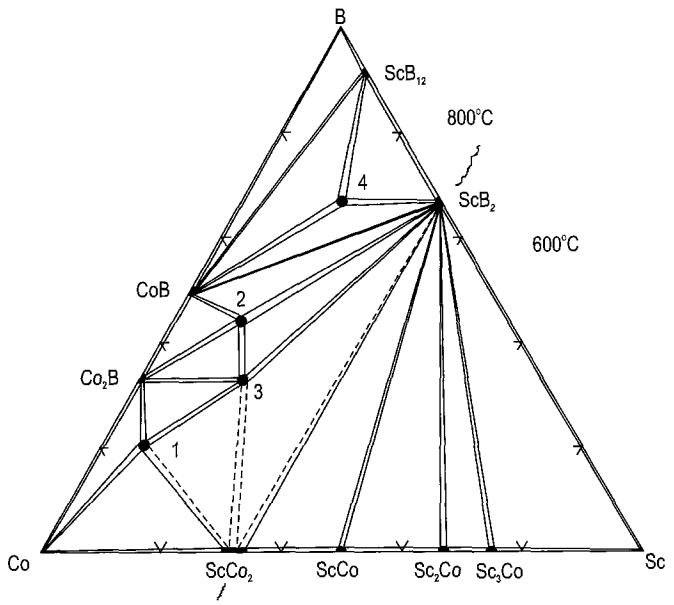

Fig. 27. Sc–Co–B, isothermal sections at 800°C (0–33.3 at.% Sc) and at 600°C (33.3–100 at.% Sc). Ternary compounds: (1) $Sc_2Co_{21}B_6$; (2) $ScCo_4B_4$; (3) $ScCo_3B_2$; (4) $ScCoB_4$.

3.1.8. *Sc–Ni–B*

The isothermal section of Sc–Ni–B at 800°C has been established by Stepanchikova and Kuz'ma (1981). The occurrence of an earlier known ternary compound, $Sc_3Ni_{20}B_6$ has been confirmed and four new ternary borides have been added (table 14). Zavalii et al. (1988) used a single crystal investigation for the refinement of the composition of the ~$ScNi_4B_4$ compound reported by Stepanchikova and Kuz'ma. According to the results of

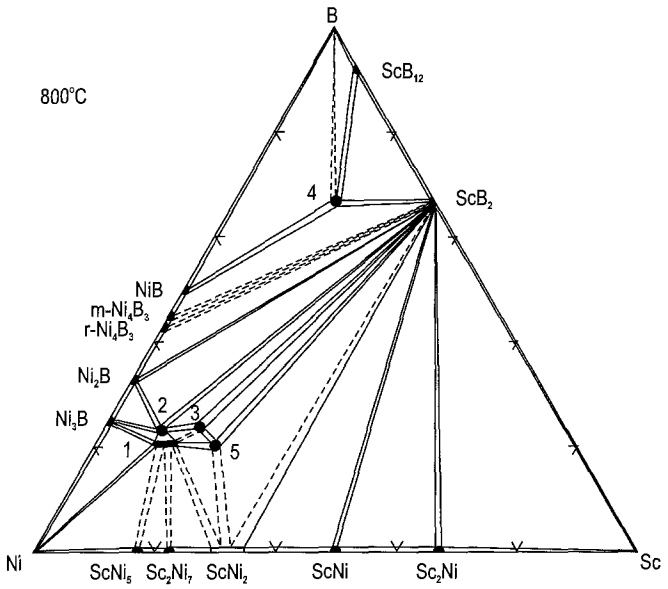

Fig. 28. Sc–Ni–B, isothermal section at 800°C. Ternary compounds: (1) $Sc_{3-4}Ni_{20-19}B_6$; (2) $Sc_4Ni_{29}B_{10}$; (3) ~$Sc_4Ni_{15}B_6$; (4) $ScNiB_4$; (5) $ScNi_3B$.

Zavalii et al. it is $Sc_4Ni_{29}B_{10}$. Figure 28 displays the isothermal section of the Sc–Ni–B phase diagram, based on the data of Stepanchikova and Kuz'ma with corrected data of Zavalii et al. and the recently observed homogeneity range for $ScNi_2$ at 800°C (see sect. 2.8).

3.1.9. *Sc–Ru–B*

Ku et al. (1979) investigated part of the Sc–Ru–B phase diagram. Based on an X-ray analysis of the as-cast alloys, these authors observed the occurrence of the following two-phase equilibria: RuB–$ScRuB_4$, "$ScRu_2B_2$"–$ScRuB_4$ and "$ScRu_2B_2$"–Ru_7B_3, as well as the metastable equilibria of $ScRu_4B_4$ with $ScRuB_4$, "$ScRu_2B_2$", Ru_7B_3 and RuB. The metastable $ScRu_4B_4$ ternary phase decays during the homogenisation of alloys at temperatures between 800 and 1300°C. Later Rogl (1984a) refined the composition of "$ScRu_2B_2$" and showed that the actual composition is $Sc_2Ru_5B_4$. The crystal structure data for all these ternary compounds are given in table 14.

3.1.10. *Sc–Rh–B*

In the study of the Rh-rich end of the Sc–Rh–B system Holleck (1977) established the existence of the solid solution of boron in the binary compound $ScRh_3$ at 1300°C: $ScRh_3B_{0-0.8}$(ST $AuCu_3$, $a = 3.900$–4.075 Å). Evidently that solid solution can reach the composition $ScRh_3B$ (ST $CaTiO_3$).

3.1.11. *Sc–M–B (M = Os, Ir)*

There are no data yet available concerning the phase equilibria in the Sc–Os–B and Sc–Ir–B systems. Two ternary compounds in the Os system and three ternary compounds with Ir have been synthesized and their crystal structures determined (see table 14). The boron content in the compound $ScIr_3B_{1-x}$ was not accurately determined because of the loss of some of the components during arc melting.

3.2. *Sc–M–Al ternary systems*

3.2.1. *Sc–Li–Al*

Berezina et al. (1986) investigated binary Al–(2.75–3) wt.% Li specimens alloyed with 0.1 to 0.7 wt.% Sc, which have been quenched from 580°C and subsequently homogenized at 175°C for 16 h. Their data indicate that a three-phase region $Al + Al_3Li + Al_3Sc$ exists in the ternary system at 175°C.

3.2.2. *Sc–Mg–Al*

The part of the Sc–Mg–Al isothermal section (0–33.3 at.% Sc) at 400°C reported by Odinaev et al. (1989) is presented in fig. 29. No ternary compounds were observed. Turkina and Kuzmina (1976) investigated also the phase equilibria at 430°C and two polythermal sections in the Al-rich part of the phase diagram (alloys containing up to 26 wt.% Mg and up to 3 wt.% Sc). Three other quasibinary polythermal sections $ScAl_2$–Mg, $ScAl_2$–Mg_2Al_3 and $ScAl_2$–$Mg_{17}Al_{12}$ of the eutectic type, have been reported by Odinaev et al. (1991). All of the data are in good agreement with each other.

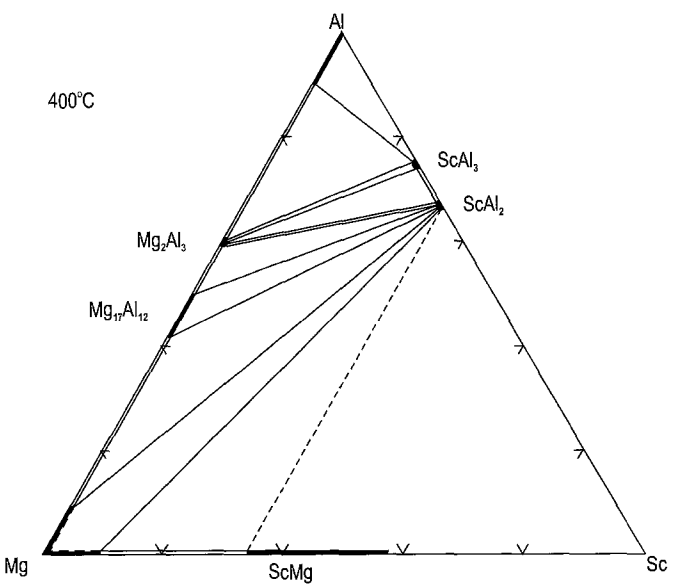

Fig. 29. Sc–Mg–Al, part of the isothermal section at 400°C (0–33.3 at.% Sc).

3.2.3. *Sc–Ca–Al*

Iandelli and Olcese (1985) investigated the alloys of the $ScAl_2$–$CaAl_2$ section in the Sc–Ca–Al ternary system. Between 800 and 900°C $CaAl_2$ (ST $MgCu_2$) dissolves 0.14 mole fraction of $ScAl_2$, whereas $ScAl_2$ (ST $MgCu_2$) dissolves 0.08 mole fraction of $CaAl_2$. These limited solid solutions are in two phase equilibria with each other. No ternary compounds were observed.

3.2.4. *Sc–Sr–Al*

The isothermal section of the Al corner of the Sc–Sr–Al phase diagram at 500°C (fig. 30) has been published by Trubniakova et al. (1987). The same group of scientists (Trubniakova and Ganiev 1989) reported on the polythermal section $SrAl_4$–$ScAl_3$. The section is of eutectic type with a limited mutual solubility of the components. No ternary compounds occur in the investigated part of the system.

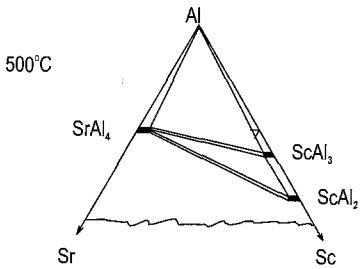

Fig. 30. Sc–Sr–Al, part of the isothermal section at 500°C (66.7–100 at.% Al).

3.2.5. *Sc–Ba–Al*

The isothermal section of Sc–Ba–Al at 500°C, which is based on the data of Altynbaev et al. (1987), is presented in fig. 31. The immiscibility gap observed in the binary Sc–Ba system spreads deeply into the ternary system up to 56 at.% Al (dashed line in fig. 31). Six additional polythermal sections of the Sc–Ba–Al phase diagram, namely $ScAl_2$–$BaAl_4$, $ScAl_2$–Ba, ScAl–Ba, $ScAl_3$–$BaAl_4$, $ScAl_2$–$BaAl_2$, $ScAl_2$–BaAl have been investigated by the same group (Altynbaev et al., 1990). No ternary compounds were observed.

3.2.6. *Sc–R–Al (R = La, Ce, Yb)*

Iandelli and Olcese (1985) ivestigated the alloys of the sections $ScAl_2$–RAl_2. No ternary compounds were found in any of the three systems. At 800–900°C the mutual solubility of scandium in $LaAl_2$ and lanthanum in $ScAl_2$ is low. The boundary compositions of these solid solutions are: $Sc_{0.04}La_{0.96}Al_2$ and $La_{0.96}Sc_{0.04}Al_2$.

In as-cast alloys $ScAl_2$ and $CeAl_2$ (ST $MgCu_2$) are completely miscible in each other. The miscibility at 800°C decreases to about 0.15 mole fraction of $ScAl_2$ in $CeAl_2$ and about 0.19 mole fraction of $CeAl_2$ in $ScAl_2$.

A continuous series of solid solutions have been observed in the as-cast alloys between isotypic $ScAl_2$ and $YbAl_2$.

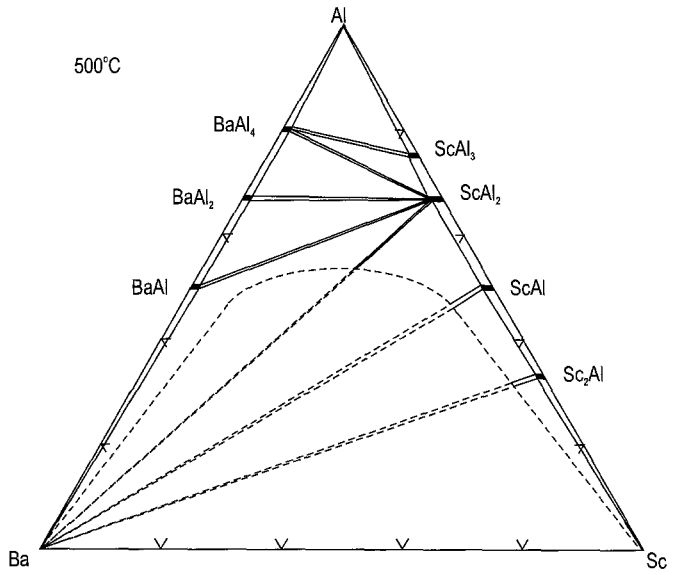

Fig. 31. Sc–Ba–Al, isothermal section at 500°C. The dashed line shows the extent of the Sc–Ba liquid immiscibility region.

3.2.7. *Sc–R–Al (R = Y, Sm, Gd, Tb, Dy, Ho, Er, Tm, Lu)*

The phase equilibria at 500°C and 800°C between $ScAl_3$ and RAl_3 been investigated by Zalutska et al. (1969) (systems with R = Y, Tb, Dy, Ho and Er), Zalutska et al. (1970) (the system with R = Gd), and Zalutska et al. (1974) (systems with R = Sm, Tm and Lu). The terminal binary compounds have different stacking variants of cubic and hexagonal atomic layers: hexagonal, γ_2 (ST Ni_3Sn or Mg_3Cd, 100% hexagonal stacking, for the compound $GdAl_3$), cubic, γ_3 (ST $AuCu_3$, 0% hexagonal stacking, for the compounds $ScAl_3$, $ErAl_3$, $TmAl_3$, $LuAl_3$) and mixed variants γ_9 (ST $BaPb_3$, 66.7% hexagonal stacking, for the compounds YAl_3, $TbAl_3$), γ_4 (ST $TiNi_3$, 50% hexagonal stacking, for the compound $DyAl_3$) and γ_{15} (ST $HoAl_3$, 40% hexagonal stacking, for the compounds $HoAl_3$ and $DyAl_3$). Isotypic trialuminides are completely miscible in each other: Sc–Er–Al, Sc–Tm–Al and Sc–Lu–Al. In other ternary systems trialuminides form limited solid solutions. $ScAl_3$ dissolves 10, 3, 3.75, 10.75, 15 and 18 at.% of Y, Sm, Gd, Tb, Dy and Ho, respectively. The solubility of Sc is 3.25, 2.5, 0.5, 2.5, 7.5 and 5.5 at.% in YAl_3, $SmAl_3$, $GdAl_3$, $TbAl_3$, $DyAl_3$ (in both polymorphic modifications γ_4 and γ_{15}) and $HoAl_3$, respectively. The values of the lattice spacings of these solid solutions and figures of parts of the isothermal sections of the phase diagrams of these systems are available in the original papers and (except for the systems with Sm, Tm and Lu) in the review by Gschneidner (1975). Ternary compounds isotypic with $TiNi_3$ (γ_4) occur only in the Sc–Y–Al and Sc–Tb–Al systems. Their lattice spacings are presented in table 15. Visible differences between the phase equilibria occurring at 500 and 800°C have not been observed.

Table 15
Ternary intermetallic compounds in the Sc–M–Al systems

Compound	Structure type or symmetry	Lattice parameters			Reference
		a (Å)	*b* (Å)	*c* (Å)	
$Sc_{0.18-0.50}Y_{0.82-0.50}Al_3$	$TiNi_3$	6.077–6.053		9.508–9.480	Zalutska et al. (1969)
$Sc_{0.15-0.45}Tb_{0.85-0.55}Al_3$	$TiNi_3$	6.084–6.060		9.526–9.480	Zalutska et al. (1969)
$ScFe_{4.0-7.1}Al_{8.0-4.9}$	$ThMn_{12}$	8.70–8.68		4.81–4.77	Zarechnyuk et al. (1970)
$ScFe_{0.30-1.35}Al_{1.70-0.65}$	$MgZn_2$	5.301–5.108		8.587–8.319	Zarechnyuk et al. (1970)
~$Sc_6Co_8Al_{15}$	$Mg_6Cu_{16}Si_7$	12.09			Markiv and Burnashova (1969), Markiv and Storozhenko (1973)
ScCoAl	$MgZn_2$	5.12		8.20	Teslyuk and Protasov (1965a)
$Sc_2Co_3Al_9$	$Y_2Co_3Ga_9$	12.57	7.337	9.216	*Markiv and Belyavina (1987a)*
~$ScNiAl_4$	?				Zarechnyuk and Rykhal (1977)
~$Sc_6Ni_7Al_{16}$	$Mg_6Cu_{16}Si_7$	12.16			Markiv and Burnashova (1969), Markiv and Storozhenko (1973)
~$ScNiAl_2$	?				Zarechnyuk and Rykhal (1977)
$ScNi_{1-0.6}Al_{1-1.4}$	$MgZn_2$	5.12[a]		8.20	Teslyuk and Protasov (1965a), Zarechnyuk and Rykhal (1977)
$ScNi_2Al$	$MnCu_2Al$	5.990			Dwight and Kimball (1987), Goebel and Rosen (1968)
~$ScRu_{2.3}Al_{3.9}$	?				Raevskaya and Sokolovskaya (1979)
~$ScRu_{0.8}Al_{3.7}$	?				Raevskaya and Sokolovskaya (1979)
$Sc_6Ru_7Al_{16}$	$Mg_6Cu_{16}Si_7$	12.38			Markiv and Storozhenko (1973)
~$ScRuAl_2$	$MnCuAl_2$	6.175			Raevskaya and Sokolovskaya (1979)
~$ScRu_{1.1-1.04}Al_{0.9-0.96}$	?				Raevskaya and Sokolovskaya (1979)
~$ScRu_{0.9-0.8}Al_{1.1-1.2}$	?				Raevskaya and Sokolovskaya (1979)
$ScRu_{0.68-0.26}Al_{1.32-1.74}$	$MgZn_2$	5.25–5.33		8.46–8.58	Raevskaya and Sokolovskaya (1979), Karatygina et al. (1974b)
$Sc_6Rh_7Al_{16}$	$Mg_6Cu_{16}Si_7$	12.34			Markiv and Storozhenko (1973)
~$ScPd_{1.73}Al_{6.36}$	?				Karatygina et al. (1974b)
~$ScPdAl_3$	?				Karatygina et al. (1974b)
$ScPd_{0.30-0.57}Al_{1.70-1.43}$	$MgZn_2$	5.51[b]		8.62	Karatygina et al. (1974b)
$Sc_6Pd_7Al_{16}$	$Mg_6Cu_{16}Si_7$	12.34			Markiv and Storozhenko (1973)
$ScPd_2Al$	$MnCu_2Al$	6.327			Dwight and Kimball (1987)

continued on next page

Table 15, *continued*

Compound	Structure type or symmetry	Lattice parameters			Reference
		a (Å)	*b* (Å)	*c* (Å)	
$Sc_6Os_7Al_{16}$	$Mg_6Cu_{16}Si_7$	12.41			Markiv and Storozhenko (1973)
$Sc_6Ir_7Al_{16}$	$Mg_6Cu_{16}Si_7$	12.31			Markiv and Storozhenko (1973)
$ScCu_{4.0-6.15}Al_{8.0-5.85}$	$ThMn_{12}$	8.656–8.570		5.000–4.947	Kotur (1989), Prevarskii et al. (1976)
~$ScCu_4Al_3$	?				Prevarskii et al. (1976)
$Sc_2Cu_{7.5}Al_{3.5}$	*hex*	4.913		8.420	Gladyshevsky et al. (1992)
$Sc_3Cu_9Al_7$	*orthorh*	21.88	8.292	8.344	Gladyshevsky et al. (1992)
$Sc_6Cu_{16.4}Al_{13.9}$	*hex*	8.493		8.870	Gladyshevsky et al. (1992)
$ScCu_2Al_2$	*orthorh*	8.46	8.88	14.65	Gladyshevsky et al. (1992)
$ScCu_2Al$	$MnCu_2Al$	6.199			Dwight and Kimball (1987)
		6.203			Nakonechna and Shpyrka (1996)
~$ScCu_{1.4}Al_{0.6}$	?				Prevarskii et al. (1976)
ScCuAl	$MgZn_2$	5.04		8.24	Teslyuk and Protasov (1965b)
$ScCu_{0.6}Al_{1.4}$	$MgNi_2$	5.252		17.113	Gladyshevsky et al. (1992), Nakonechna and Shpyrka (1996)
$ScAg_2Al$	$MnCu_2Al$	6.564			Dwight and Kimball (1987)
$ScAu_2Al$	$MnCu_2Al$	6.536			Dwight and Kimball (1987)

[a] For the composition ScNiAl. [b] For an unknown composition.

3.2.8. *Sc–M–Al (M = Ti, Zr, Hf)*

Parts of the isothermal sections at 500°C of the Sc–M–Al (M = Ti, Zr, Hf) phase diagrams (66.7–100 at.% Al) reported by Kotur et al. (1989b) are presented in fig. 32. No ternary compounds were found. Binary scandium aluminides dissolve different quantities (in at.%) of the third element: $ScAl_3$ – 6 Ti, 10 Zr, 15 Hf; $ScAl_2$ – 5 Ti, 8 Zr, 13 Hf. The solubility of Sc in the aluminides of the 4A-elements does not exceed 5 at.%. These data are in good agreement with the data of Toropova et al. (1990) who reported on the phase equilibria in the Sc–Zr–Al system at 600°C. $ScAl_3$ and $ZrAl_3$ dissolve 10 at.% Zr and

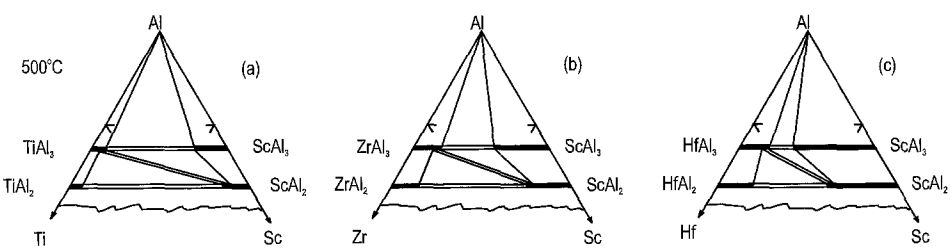

Fig. 32. (a) Sc–Ti–Al, (b) Sc–Zr–Al, and (c) Sc–Hf–Al parts of the isothermal sections at 500°C (66.7–100 at.% Al).

5 at.% Sc, respectively. A two-phase region ($Sc_{1-x}Zr_xAl_3 + Zr_{1-y}Sc_yAl_3$) and a three-phase region ($Al + Sc_{1-x}Zr_xAl_3 + Zr_{1-y}Sc_yAl_3$) have been confirmed too.

3.2.9. *Sc–Nb–Al*

Shamrai et al. (1988) reported on the phase equilibria in the Sc–Nb–Al system at 200–800°C (fig. 33). Their data, which indicate a solubility of about 1 at.% Al in αSc, are in disagreement with the data of Naumkin et al. (1965) who report a solubility of about 4 at.% Al. There are no ternary compounds in the system. Binary aluminides dissolve less than 1 at.% of the third component.

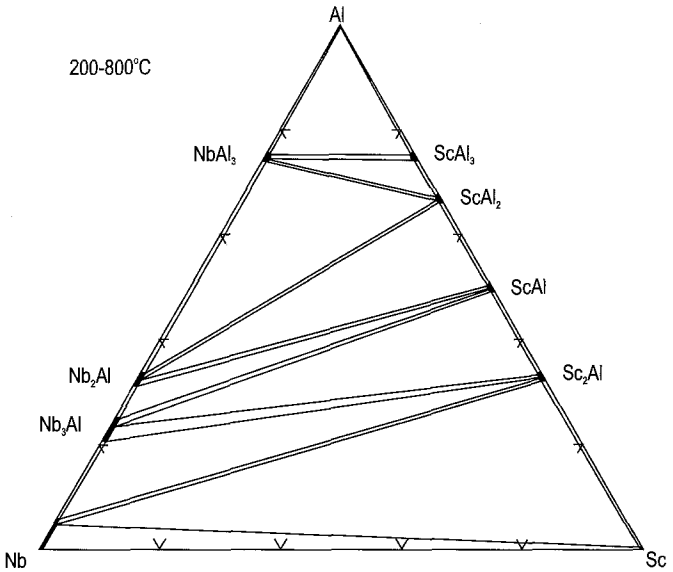

Fig. 33. Sc–Nb–Al, phase equilibria at 200–800°C.

3.2.10. *Sc–Cr–Al*

Part of the Sc–Cr–Al isothermal section at 500°C (30–100 at.% Al), which is shown in fig. 34, has been investigated by Sokolovskaya et al. (1989). No ternary compounds were found. $ScAl_3$ dissolves up to 11 at.% Cr. Other binary aluminides also dissolve large amounts of the third element, but there are no data available about lattice parameters of these solid solutions.

3.2.11. *Sc–Mo–Al*

Only a little information concerning the Sc–Mo–Al system is available. Cheldieva et al. (1989) investigated an isothermal section of the Al-rich part of the phase diagram at 500°C, and the polythermal sections between aluminides $ScAl_3$ and $MoAl_{12}$ and from the Al corner along the atomic ratio Mo:Sc = 2:1 line, however no figure was given.

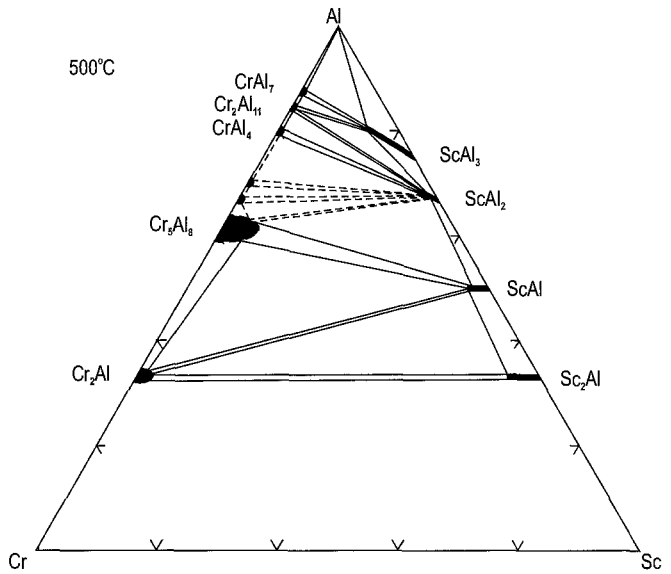

Fig. 34. Sc–Cr–Al, part of the isothermal section at 500°C (30–100 at.% Al).

They found that the binary scandium and molybdenum aluminides dissolve very small quantities of a third component. Ternary compounds have not been observed.

3.2.12. *Sc–Mn–Al*

Drits et al. (1984) reported about investigations of the Al-rich parts (96–100 at.% Al) of the Sc–Mn–Al isothermal sections at 500 and 600°C, and on the polythermal sections (Al + 0.8 wt.% Sc)–Mn and Sc–(Al + 0.8 wt.% Mn) in the regions 0–2.8 wt.% Mn and Sc, respectively. A three-phase area (α solid solution (Al) + $ScAl_3$ + $MnAl_6$) was found; however, no ternary compounds have been observed. Al dissolves less than 0.2 at.% Sc and 0.3 at.% Mn. Scandium appreciably decreases the solubility of manganese in aluminium.

3.2.13. *Sc–Fe–Al*

Part of the Sc–Fe–Al isothermal section (0–33.3 at.% Sc) at 500°C has been investigated by Zarechnyuk et al. (1970). This isothermal section is included in the review of Gladyshevsky et al. (1990). There are two ternary compounds with wide homogeneity ranges observed in the investigated part of the system (table 15). It is interesting to note that two isostructural compounds, $ScFe_2$ and $ScFe_{1.35-0.30}Al_{0.65-1.70}$ (ST $MgZn_2$), are in two-phase equilibrium with each other. Alloys of the $ScAl_2$–$ScFe_2$ section at 800°C were also examined by Dwight et al. (1975). From the figure shown there it follows that $ScAl_2$ dissolves up to 6 at.% Fe whereas $ScFe_2$ dissolves only about 1 at.% Al. Dwight et al. also observed two ternary compounds $ScFe_{1.96-1.4}Al_{0.04-0.6}$ (ST $MgCu_2$) and $ScFe_{1.37-0.2}Al_{0.63-1.8}$ (ST $MgZn_2$) along the $ScFe_2$–$ScAl_2$ pseudo-binary line. These

data are in agreement with the results of Sankar and Wallace (1976) who investigated the alloys of this section too. In addition Sankar and Wallace reported the composition ranges for these two ternary compounds at 1000°C: $ScFe_{1.87-1.42}Al_{0.13-0.88}$ (ST $MgCu_2$) and $ScFe_{1.31-0.15}Al_{0.69-1.85}$ (ST $MgZn_2$). However, no lattice spacings of these compounds are given in the papers of Dwight et al. (1975) and Sankar and Wallace (1976).

3.2.14. *Sc–Co–Al*

Three ternary compounds have been synthesized and their crystal structures were determined (see table 15). Phase equilibria in this system have not been completely investigated.

3.2.15. *Sc–Ni–Al*

Parts of two isothermal sections of the Sc–Ni–Al system have been studied by Goebel and Rosen (1968) (Ni corner at 1000°C) and Zarechnyuk and Rykhal (1977) (0–33.3 at.% Sc at 600°C). Their figures are presented in the review of Gladyshevsky et al. (1990). The data of Goebel and Rosen need to be completed in the region close to Sc_2Ni_7 compound. Goebel and Rosen confirmed the ScNiAl ternary compound known from an earlier investigation by Teslyuk and Protasov (1965a) (ST $MgZn_2$, $a = 5.12$, $c = 8.12$ Å), and they observed a new one, $ScNi_2Al$ (ST $MnCu_2Al$, $a = 6.02$ Å). Zarechnyuk and Rykhal synthesized the two ternary compounds ~ $ScNiAl_4$, ~ $ScNiAl_2$ and confirmed an extended homogeneity range for ScNiAl (see table 15). There are also the data of Markiv and Burnashova (1969) and Markiv and Storozhenko (1973) who reported an aluminide with the following composition ~ $Sc_6Ni_7Al_{16}$ (ST Th_6Mn_{23} or $Mg_6Cu_{16}Si_7$, $a = 12.16$ Å). Maybe this compound and the compound ~ $ScNiAl_2$ identified by Zarechnyuk and Rykhal are the same.

3.2.16. *Sc–Ru–Al*

Karatygina et al. (1974a) investigated part of the Sc–Ru–Al isothermal section at 600°C. One ternary compound $ScRu_{0.92-0.32}Al_{1.08-1.68}$ with the $MgZn_2$ structure type was found ($a = 5.27$, $c = 8.57$ Å for the composition $ScRu_{0.5}Al_{1.5}$). A continuous series of solid solutions occur between the isotypic binary compounds ScRu and ScAl (ST CsCl) whereas a two-phase region exists between ScRu and RuAl (ST CsCl). In our opinion these data need additional verification if one takes into account the later data of Schuster and Bauer (1985) who observed the CrB structure type for pure ScAl (see sect. 2.12).

Karatygina et al. (1974b) reported the phase equilibria at 800°C in the region 0–85 at.% Al; later the same scientific group (Raevskaya and Sokolovskaya 1979) refined their earlier data. In addition to the earlier reported ternary compound, five other compounds were observed (see table 15). Of these, the crystal structure of ~$ScRuAl_2$ was determined to be of the $MnCu_2Al$ type. Markiv and Storozhenko (1973) also synthesized a cubic ternary compound with a similar composition, namely $Sc_6Ru_7Al_{16}$ crystallising in the $Mg_6Cu_{16}Si_7$ structure type. To clarify these contradictory data additional work needs to be done. In our opinion, the data of Markiv and Storozhenko seem to be more reliable,

which is based on analysis of the data of related systems. Figures of the two isothermal sections mentioned above can be found in the review of Gladyshevsky et al. (1990).

3.2.17. *Sc–M–Al (M = Rh, Os, Ir, Pt)*

There is information in the literature about a ternary compound of the composition $Sc_6M_7Al_{16}$ in each of the Sc–M–Al (M = Rh, Os, Ir) ternary systems. Their lattice parameters are presented in table 15. Phase equilibria were not investigated. According to the investigation of Markiv and Storozhenko (1973) the compound of the 6:7:16 stoichiometry does not occur in the Sc–Pt–Al ternary system.

3.2.18. *Sc–Pd–Al*

Part of the Sc–Pd–Al isothermal section at 800°C shown in fig. 35 is based mainly on the data of Karatygina et al. (1974b). An extended solid solution is formed on the basis of the ScPd binary compound where the atoms of the initial components can substitute by each other in the structure. The binary compounds Sc_2Pd and Sc_4Pd dissolve about 13 and 8 at.% Al, whereas $ScAl_2$ dissolves about 7 at.% Pd. Karatygina et al. synthesized three ternary compounds (see fig. 35); the existence of two other ternary compounds, namely $Sc_6Pd_7Al_{16}$ and $ScPd_2Al$ was reported by other authors (see table 15). The composition of the latter one occurs within the homogeneity range of the (Sc, Al)Pd solid solution observed by Karatygina et al. These conflicting data need additional refinement.

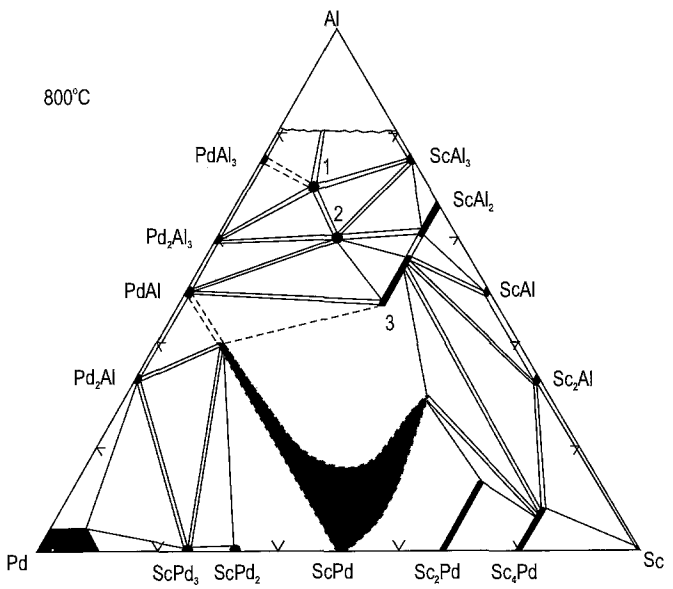

Fig. 35. Sc–Pd–Al, part of the isothermal section at 800°C (0–80 at.% Al). Ternary compounds: (1) ~$ScPd_{1.73}Al_{6.36}$; (2) ~$ScPdAl_3$; (3) $ScPd_{0.30-0.57}Al_{1.70-1.43}$.

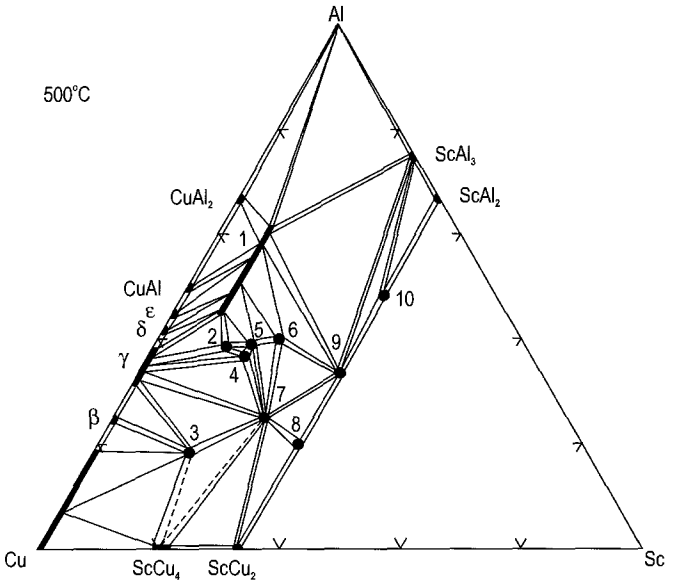

Fig. 36. Sc–Cu–Al, part of the isothermal section at 500°C (0–33.3 at.% Sc). Ternary compounds: (1) $ScCu_{4.0-6.15}Al_{8.0-5.85}$; (2) ~$ScCu_4Al_3$; (3) $Sc_2Cu_{7.7}Al_{3.5}$; (4) $Sc_3Cu_9Al_{17}$; (5) $Sc_6Cu_{16.4}Al_{13.9}$; (6) $ScCu_2Al_2$; (7) $ScCu_2Al$; (8) ~$ScCu_{1.4}Al_{0.6}$; (9) ScCuAl; (10) $ScCu_{0.6}Al_{1.4}$.

3.2.19. *Sc–Cu–Al*

Many investigations of the Sc–Cu–Al system have been reported. The phase equilibria in the range 0–33.3 at.% Sc at 500°C were first reported in the paper of Prevarskii et al. (1976). Nine ternary compounds were obtained: (1) $ScCu_{4-6.6}Al_{8-5.4}$ (ST $ThMn_{12}$, $a = 8.66–8.63$, $c = 4.43–5.10$ Å), (2) ~$ScCu_4Al_3$, (3) ~$ScCu_{4.3}Al_{1.3}$, (4) ~$ScCu_{2.6}Al_{2.3}$, (5) ~$ScCu_3Al_2$, (6) ~$ScCu_2Al_2$, (7) $ScCu_2Al$ (8) ~$ScCu_{1.4}Al_{0.6}$and (9) ScCuAl. Two of them, (9) ScCuAl (ST $MgZn_2$) and (7) $ScCu_2Al$ (ST CsCl), were synthesized earlier (Teslyuk and Protasov 1965b). Toropova et al. (1989) and Kharakterova (1991) reinvestigated the Al corner of the system at 450 and 500°C. They did not confirm the two phase equilibria between $CuAl_2$ and $ScAl_3$, however they established the two phase equilibrium between Al and ternary compound (1). Kotur (1989) refined the homogeneity range and the lattice parameters of compound (1) (see table 15). Kharakterova determined the solubility of Sc and Cu in solid Al (about 1.5 at.% Cu and about 0.1 at.% Sc at 500°C). Gladyshevsky et al. (1992), who conducted a crystal structure investigation of four of the ternary compounds reported earlier by Prevarskii et al., refined their compositions to (3) $Sc_2Cu_{7.5}Al_{3.5}$, (4) $Sc_3Cu_9Al_7$, (5) $Sc_6Cu_{16.4}Al_{13.9}$, (6) $ScCu_2Al_2$, discovered an additional ternary compound (10) $ScCu_{0.6}Al_{1.4}$, and determined the crystal structures of all five compositions. These data are presented in table 15. The revised isothermal section at 500°C based on the above mentioned papers is shown in fig. 36. There is some controversy concerning the published data for the crystal structure of the $ScCu_2Al$ compound. Teslyuk and Protasov (1965b) investigated an as-cast sample and a sample

homogenized at 800°C of the $ScCu_2Al$ composition, and they obtained identical X-ray patterns for both samples. Between the two possible structure types ($MnCu_2Al$ and CsCl) they preferred the latter one ($a = 3.10$ Å), however, there were two weak extra lines which could be indexed assuming $MnCu_2Al$ type. The $MnCu_2Al$ structure for this phase was reported by Dwight and Kimball (1987). Recently Nakonechna and Shpyrka (1996) confirmed the $MnCu_2Al$ type structure by single-crystal investigation (see table 15).

3.2.20. *Sc–M–Al (M = Ag, Au)*

Dwight and Kimball (1987) prepared the Heusler phases $ScAg_2Al$ and $ScAu_2Al$ and determined their lattice parameters (see table 15). Data about phase equilibria in these systems are not available in the literature.

3.3. *Sc–M–Ga ternary systems*

3.3.1. *Sc–Y–Ga*

Markiv et al. (1981) reported on the isothermal section of the Sc–Y–Ga system at 800°C in the range 0–75 at.% Sc (fig. 37). The gallides $ScGa_2$ and $ScGa_3$ dissolve about 9 at.% Y, Sc_3Ga_5 (in the original paper "Sc_2Ga_3") dissolves about 36 at.% Y. One ternary compound with an extended homogeneity range along 44.5 at.% Ga isoconcentrate occurs in the system, however its crystal structure is unknown (table 16). Markiv et al. found the solubility of gallium in solid scandium at 800°C to be about 1 at.%. This value differs from those (between about 4 and 6 at.% Ga) reported in other papers on the Sc–M–Ga

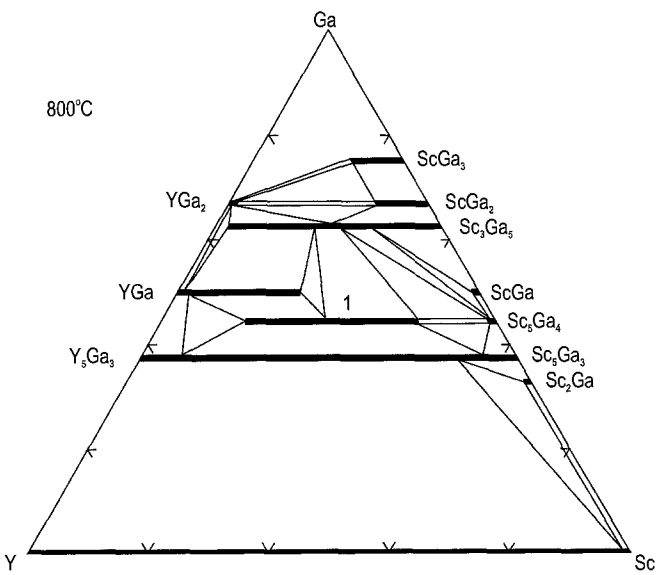

Fig. 37. Sc–Y–Ga, part of the isothermal section at 800°C (0–75 at.% Sc). Ternary compound: (1) $Sc_{1.26-3.82}Y_{3.74-1.18}Ga_4$.

Table 16
Ternary intermetallic compounds in the Sc–M–Ga systems

Compound	Structure type or symmetry	Lattice parameters			Reference
		a (Å)	*b* (Å)	*c* (Å)	
$Sc_{1.26-3.82}Y_{3.74-1.18}Ga_4$	?				Markiv et al. (1981)
$Sc_{1-4}Ti_{4-1}Ga_3$	?				Gavrilenko and Markiv (1978a)
$ScTi_2Ga_4$	$YbMo_2Al_4$	6.578		5.475	Grin' et al. (1980), Gavrilenko and Markiv (1978a)
$Sc_{6.8-9.4}Ti_{4.2-1.8}Ga_{10}$	$Ho_{11}Ge_{10}$	10.23–10.343		14.68–14.98	Markiv et al. (1989), Gavrilenko and Markiv (1978a)
$Sc_{3.2-4.7}Zr_{7.8-6.3}Ga_{10}$	$Ho_{11}Ge_{10}$	10.401–10.399		14.98–15.01	Markiv et al. (1989), Markiv et al. (1979)
$Sc_{0.2}Hf_{0.8}Ga_3$	$ZrAl_3$	3.948		17.35	*Markiv and Belyavina (1981)*
$Sc_{0.2-0.9}Hf_{0.8-0.1}Ga$	αMoB	3.851[a]		20.27	*Markiv and Belyavina (1981)*
ScV_2Ga_4	$YbMo_2Al_4$	6.482		5.216	Grin' et al. (1980)
~$ScNbGa_4$	?				Savitskii et al. (1980a)
$Sc_{8.4-9.4}Nb_{2.6-1.6}Ga_{10}$	$Ho_{11}Ge_{10}$	10.378–10.385		15.07–15.24	Markiv et al. (1989)
~$Sc_4Cr_4Ga_3$	?				Gavrilenko and Markiv (1978a)
$Sc_3Mn_2Ga_6$	$Sc_3Mn_2Ga_6$	8.051	8.533	10.607	*Markiv and Belyavina (1987b)*, Gavrilenko and Markiv (1978b)
$ScMn_{0.33}Ga_{1.67}$	$CaIn_2$	4.354		6.418	*Kuzmenko et al. (1983)*, Gavrilenko and Markiv (1978b)
$Sc_{8.5}Mn_{1.2}Ga$	$Sc_{8.5}Mn_{1.2}Ga$	14.284	14.284	14.840	*Markiv and Belyavina (1989a)*, Gavrilenko and Markiv (1978b)
$ScFe_{6-4.73}Ga_{6-7.27}$	$ScFe_6Ga_6$	8.431–8.507	8.613–8.585	5.009–5.040	*Belyavina and Markiv (1982a)*
$Sc_2Fe_{8.83}Ga_{8.17}$	Th_2Zn_{17}	8.695		12.641	Belyavina and Markiv (1982a)
$ScFeGa_5$	$HoCoGa_5$	4.145		6.623	Belyavina and Markiv (1980b), Gavrilenko and Markiv (1978b)
$Sc_3Fe_2Ga_6$	$Sc_3Mn_2Ga_6$	8.081	8.425	10.457	*Markiv and Belyavina (1987b)*, Gavrilenko and Markiv (1978b)
$ScFe_{1.82-1.44}Ga_{0.18-0.56}$	$MgCu_2$	7.03–7.15			Gavrilenko and Markiv (1978b)
$ScFe_{1.37-0.71}Ga_{0.63-1.29}$	$MgZn_2$	5.053–5.156		8.287–8.386	Gavrilenko and Markiv (1978b)
$ScFe_{0.33}Ga_{1.67}$	KHg_2	4.304	6.498	7.433	*Kuzmenko et al. (1983)*
$ScFe_{0.14}Ga_{1.86}$	$CaIn_2$	4.294		6.578	*Kuzmenko et al. (1983)*, Gavrilenko and Markiv (1978b)
$Sc_{8.5}Fe_{1.2}Ga$	$Sc_{8.5}Mn_{1.2}Ga$	14.213	14.213	14.785	*Markiv and Belyavina (1989a)*, Gavrilenko and Markiv (1978b)
$ScFe_{4.73}Ga_{7.27}$	$ThMn_{12}$	8.567		5.060	Belyavina and Markiv (1982a)
$ScCo_{5.8}Ga_{6.2}$	$ThMn_{12}$	8.345		5.048	Belyavina and Markiv (1982a), Gavrilenko and Markiv (1979)

continued on next page

Table 16, *continued*

Compound	Structure type or symmetry	Lattice parameters			Reference
		a (Å)	*b* (Å)	*c* (Å)	
$ScCo_{4.5}Ga_{4.1}$	$TbCu_7$	5.007		4.044	*Markiv and Belyavina (1987a)*, Gavrilenko and Markiv (1979)
$Sc_2Co_3Ga_9$	$Y_2Co_3Ga_9$	12.58	7.272	9.216	*Markiv and Belyavina (1987a)*, Gavrilenko and Markiv (1979)
$ScCoGa_5$	$HoCoGa_5$	4.135		6.642	*Belyavina and Markiv (1980b)*, Gavrilenko and Markiv (1979)
$\sim Sc_{17}Co_{64-62}Ga_{19-21}$	?				Gavrilenko and Markiv (1979)
$Sc_2Co_7Ga_4$	Mg_2Zn_{11}	8.074			*Markiv and Belyavina (1987a)*, Gavrilenko and Markiv (1979)
Sc_2CoGa_8	Ho_2CoGa_8	4.126		10.68	*Belyavina and Markiv (1980b)*, Gavrilenko and Markiv (1979)
$Sc_6Co_{7.2-6.3}Ga_{15.8-16.7}$	Th_6Mn_{23}	12.14[b]			Markiv and Burnashova (1969), Gavrilenko and Markiv (1979)
$\sim Sc_{22}Co_{63-60}Ga_{15-18}$	?				Gavrilenko and Markiv (1979)
$\sim Sc_{22}Co_{53-49}Ga_{25-29}$	?				Gavrilenko and Markiv (1979)
$ScCo_{1.2}Ga_{1.8}$	$ScCo_{1.2}Ga_{1.8}$	12.255		8.223	*Belyavina and Markiv (1989)*, Gavrilenko and Markiv (1979)
$Sc_{29-34}Co_{48-24}Ga_{29-42}$	$MgZn_2$	5.021[c] 5.170		8.137– 8.175	Gavrilenko and Markiv (1979)
$ScCo_{0.35}Ga_{1.65}$	TiFeSi	8.070	11.46	6.618	Belyavina and Markiv (1982b), Gavrilenko and Markiv (1979)
$\sim Sc_{37}Co_{14}Ga_{49}$	?				Gavrilenko and Markiv (1979)
$Sc_5Co_{0.925}Ga_{0.925}$	$Sc_5Ni_{1-x}Ga_{1-x}$	8.769		8.639	Markiv and Belyavina (1989b), Gavrilenko and Markiv (1979)
$ScCo_{0.5}Ga_{1.5}$	KHg_2	4.267	6.419	7.400	*Kuzmenko et al. (1983)*
$ScCo_{0.14}Ga_{1.86}$	$CaIn_2$	4.283		6.594	*Kuzmenko et al. (1983)*
$ScNiGa_5$	$HoCoGa_5$	4.140		6.477	Belyavina and Markiv (1980b), Gavrilenko and Markiv (1979)
$ScNi_{2.36}Ga_{3.64}$	Ru_3Be_{17}	13.440			Markiv and Belyavina (1990b), Gavrilenko and Markiv (1979)
$Sc_2Ni_{7-5.5}Ga_{4-5.5}$	$Hf_2Ni_{6.5}Ga_{4.5}$	17.800– 17.997		8.197– 8.288	Markiv and Belyavina (1990a), Gavrilenko and Markiv (1979)
$\sim Sc_{17}Ni_{64-59}Ga_{19-24}$	?				Gavrilenko and Markiv (1979)
$\sim Sc_{22}Ni_{58}Ga_{20}$	?				Gavrilenko and Markiv (1979)
$\sim Sc_{23}Ni_{61}Ga_{16}$	?				Gavrilenko and Markiv (1979)
Sc_2NiGa_8	Ho_2CoGa_8	4.127		10.56	Belyavina and Markiv (1980b), Gavrilenko and Markiv (1979)
$ScNi_2Ga$	$MnCu_2Al$	6.001			Gavrilenko and Markiv (1979)
$ScNi_{1.2}Ga_{1.8}$	$ScCo_{1.2}Ga_{1.8}$	12.217		8.155	Belyavina and Markiv (1989), Gavrilenko and Markiv (1979)

continued on next page

Table 16, *continued*

Compound	Structure type or symmetry	Lattice parameters			Reference
		a (Å)	*b* (Å)	*c* (Å)	
$ScNiGa_2$	$MgCuAl_2$	4.037	9.552	6.467	*Markiv and Belyavina (1983)*, Gavrilenko and Markiv (1979)
$Sc_{30-36}Ni_{55-39}Ga_{15-25}$	$MgZn_2$	5.054[d]		8.002	Gavrilenko and Markiv (1979)
$ScNi_{0.35}Ga_{1.65}$	TiFeSi	8.042	11.44	6.602	Belyavina and Markiv (1982b), Gavrilenko and Markiv (1979)
$ScNi_{1-0.67}Ga_{1-1.33}$	KHg_2	4.166–4.210	6.309–6.419	7.216–7.291	*Kuzmenko et al. (1983)*
ScNiGa	TiNiSi	6.309	4.166	7.216	*Kuzmenko et al. (1983)*
$ScNi_{0.14}Ga_{1.86}$	$CaIn_2$	4.283		6.587	*Kuzmenko et al. (1983)*
$Sc_5Ni_{0.963}Ga_{0.963}$	$Sc_5Ni_{1-x}Ga_{1-x}$	8.819		8.600	*Markiv and Belyavina (1989b)*, Gavrilenko and Markiv (1979)
$Sc_6Ru_7Ga_{16}$	$Mg_6Cu_{16}Si_7$	12.44			Markiv and Storozhenko (1973)
$Sc_6Rh_7Ga_{16}$	$Mg_6Cu_{16}Si_7$	12.38			Markiv and Storozhenko (1973)
$ScPd_2Ga$	$MnCu_2Al$	6.346			Dwight and Kimball (1987)
ScPdGa	TiNiSi	6.281	4.3582	7.5520	Hovestreydt et al. (1982)
$Sc_6Os_7Ga_{16}$	$Mg_6Cu_{16}Si_7$	12.49			Markiv and Storozhenko (1973)
$Sc_6Ir_7Ga_{16}$	$Mg_6Cu_{16}Si_7$	12.43			Markiv and Storozhenko (1973)
ScPtGa	TiNiSi	6.454	4.342	7.479	Hovestreydt et al. (1982)
$ScCu_{5.49-4.85}Ga_{6.51-7.15}$	$ThMn_{12}$	8.62[e]		4.78	Gavrilenko and Markiv (1979)
$ScCu_{3.7}Ga_{2.3}$	Ru_3Be_{17}	13.545			Markiv and Belyavina (1990b), Gavrilenko and Markiv (1979)
~$ScCu_{3.6}Ga_{1.4}$	?				Gavrilenko and Markiv (1979)
~$ScCu_{3.2}Ga_{1.6}$	?				Gavrilenko and Markiv (1979)
$Sc_{14}Cu_{37}Ga_{14}$	$Gd_{14}Ag_{51}$	11.438		8.352	*Markiv et al. (1984)*, Gavrilenko and Markiv (1979)
$ScCu_2Ga$	$MnCu_2Al$	6.158			Gavrilenko and Markiv (1979)
$ScCu_{0.77-0.26}Ga_{1.23-1.74}$	$CaIn_2$	4.248[f]		6.588	Gavrilenko and Markiv (1979), Markiv et al. (1984)
$ScCu_{1.40-0.86}Ga_{0.60-1.14}$	KHg_2	4.229[g]	6.450	7.325	Markiv et al. (1984)

[a] For the composition $Sc_{0.34}Hf_{0.66}Ga$.
[b] For the composition $Sc_6Co_7Ga_{16}$.
[c] For the composition $Sc_{33}Co_{38-25}Ga_{29-42}$.
[d] For the composition $Sc_{33.3}Ni_{43.7}Ga_{23}$.
[e] for the composition $ScCu_{5.5}Ga_{6.5}$.
[f] For the composition $ScCu_{0.26}Ga_{1.74}$.
[g] For the composition $ScCu_{0.95}Ga_{1.05}$.

system (see figs. 38–46). This is an additional reason for a reinvestigation of the Sc–Ga binary system which we mentioned in sect. 2.12. Complete miscibility between Sc_5Ga_3 and Y_5Ga_3 is observed (fig. 37).

3.3.2. *Sc–Ti–Ga*

The Sc–Ti–Ga isothermal section at 800°C (0–75 at.% Ga) has been investigated by Gavrilenko and Markiv (1978a); three ternary compounds were observed. Markiv et al. (1989) determined the solubility of titanium in Sc_5Ga_4 (5 at.%) together with the composition and the crystal structure of another ternary compound, reported in the original paper as "$Sc_{2-2.37}TiGa_{3-2.63}$" [compound (3) in the modified isothermal section presented in fig. 38]. The characteristic data of the ternary compounds are given in table 16.

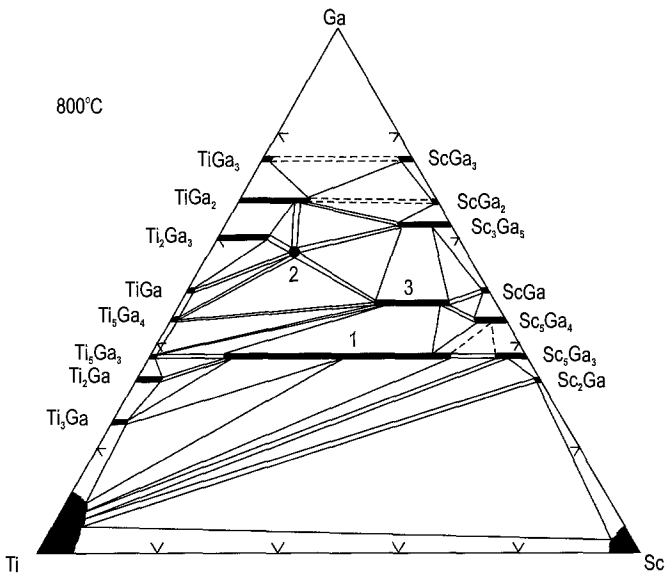

Fig. 38. Sc–Ti–Ga, part of the isothermal section at 800°C (0–75 at.% Sc). Ternary compounds: (1) $Sc_{1-4}Ti_{4-1}Ga_3$; (2) $ScTi_2Ga_4$; (3) $Sc_{6.8-9.4}Ti_{4.2-1.6}Ga_{10}$.

3.3.3. *Sc–Zr–Ga*

The revised isothermal section of the Sc–Zr–Ga system at 800°C (0–75 at.% Ga) presented in fig. 39 is based mainly on the data of Markiv et al. (1979). They observed one ternary compound "$Sc_{1.8-2.7}Zr_{3.2-2.3}Ga_4$". Its composition and crystal structure, as well as the solubility of zirconium in Sc_5Ga_4 (10 at.%), were determined by Markiv et al. (1989) (see table 16). The other binary gallides Sc_3Ga_5, Zr_3Ga_2 and ZrGa dissolve about 15 at.% Zr, about 12 and 46 at.% Sc, respectively (see fig. 39). Zr_5Ga_3–Sc_5Ga_3 form a continuous series of solid solutions between the two binary end members.

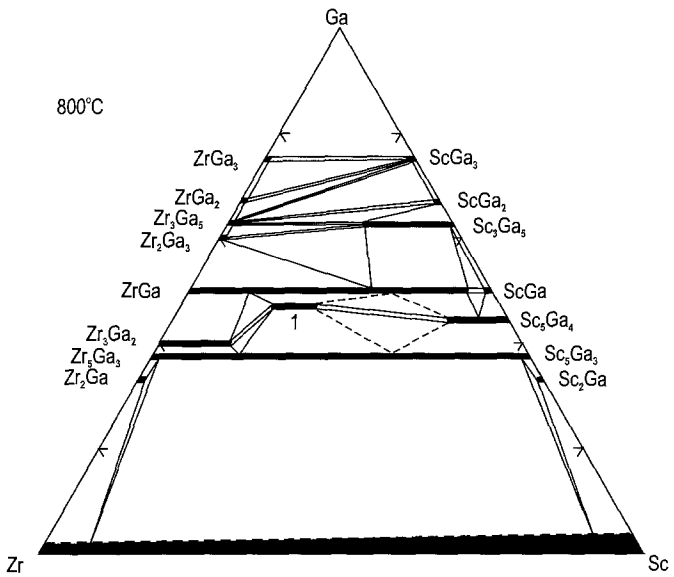

Fig. 39. Sc–Zr–Ga, part of the isothermal section at 800°C (0–75 at.% Sc). Ternary compound: (1) $Sc_{3.2-4.7}Zr_{7.8-6.3}Ga_{10}$.

3.3.4. *Sc–Hf–Ga*

Investigations of the Sc–Hf–Ga phase equilibria at 800°C in the range 0–63 at.% Ga have been reported by Belyavina et al. (1981), and by Markiv and Belyavina (1981) in the range 0–75 at.% Ga. The data of both papers are identical in the concentration range 0–50 at.% Ga. Sc_5Ga_4 dissolves up to 15 at.% Hf. The hafnium gallide "Hf_5Ga_4" dissolves up to 20 at.% Sc. Later the same scientific group (Markiv et al., 1989) refined the composition of this compound to $Hf_{11}Ga_{10}$ and found its solubility of Sc to be 30 at.%. Other binary gallides, such as Sc_5Ga_3 (in the original paper "Sc_2Ga_3") and $HfGa_2$ also dissolve rather large amounts of the third component: 30 at.% Hf and 10 at.% Sc, respectively. Two ternary compounds have been synthesized by Markiv and Belyavina who also established their crystal structure (see table 16). Sc_5Ga_3 and Hf_5Ga_3 mutually dissolve 100% of each other. The revised isothermal section at 800°C is shown in fig. 40.

3.3.5. *Sc–V–Ga*

Savitskii et al. (1978b) studied the Sc–V–Ga phase equilibria at 800°C. The figure of the isothermal section is available in the review of Gladyshevsky et al. (1990). One ternary compound ScV_2Ga_4 occurs in this system, its crystal structure was determined by Grin' et al. (1980) (see table 16). The solubility of V in Sc(Ga) solid solution slightly increases with increase temperature, but it does not exceed 2 at.%. In as-cast alloys the solid solution based on vanadium spreads up to about 20 at.% Sc with increasing gallium content. The solubility of V in Sc_5Ga_3 also increases with the increasing temperature and reaches about 10–12 at.% V.

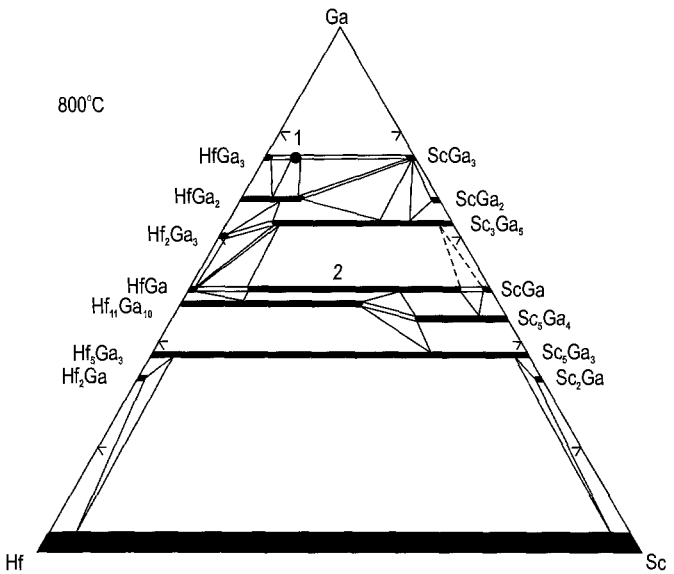

Fig. 40. Sc–Hf–Ga, part of the isothermal section at 800°C (0–75 at.% Sc). Ternary compounds: (1) $Sc_{0.2}Hf_{0.8}Ga_3$; (2) $Sc_{0.2-0.9}Hf_{0.8-0.1}Ga$.

3.3.6. *Sc–Nb–Ga*

During the investigation of the Sc–Nb–Ga alloys by Savitskii et al. (1980a) part of the phase equilibria at 800°C were established (0–75 at.% Sc) and two ternary compounds were observed (see fig. 41). One of the compounds, ~$ScNbGa_2$, is formed after long-term homogenization of the alloys at 800°C. The composition of the second reported compound, "$Sc_{3.8-4.2}Nb_{1.2-0.4}Ga_4$", was refined to $Sc_{8.4-9.4}Nb_{2.6-1.6}Ga_{10}$ by Markiv et al. (1989) who also determined its crystal structure (see table 16).

3.3.7. *Sc–Cr–Ga*

Gavrilenko and Markiv (1978a) investigated part of the Sc–Cr–Ga isothermal section at 800°C, and its figure is presented in the review of Gladyshevsky et al. (1990). One ternary compound ~$Sc_4Cr_2Ga_3$ occurs in this system, but its crystal structure is unknown (table 16).

3.3.8. *Sc–Mn–Ga*

Gavrilenko and Markiv (1978b) investigated part of the Sc–Mn–Ga isothermal section at 500°C (0–80 at.% Ga). Among the binary compounds of the Sc–Mn, Sc–Ga and Mn–Ga binary systems only $ScMn_2$ (ST $MgZn_2$) dissolves a large amount of the third component: up to 40 at.% Ga. The lattice parameters increase from $a = 5.03$, $c = 8.19$ (for $ScMn_2$) to $a = 5.22$, $c = 8.52$ Å for $ScMn_{0.8}Ga_{1.2}$. Three ternary compounds were synthesized in the system and their compositions and the crystal structures were published in subsequent papers of the same scientific group: compound (1) "$Sc_{25}Mn_{25}Ga_{50}$" by Markiv and Belyavina (1987b), compound (2) "$Sc_{36}Mn_{10}Ga_{54}$" by Belyavina (1983), compound (3)

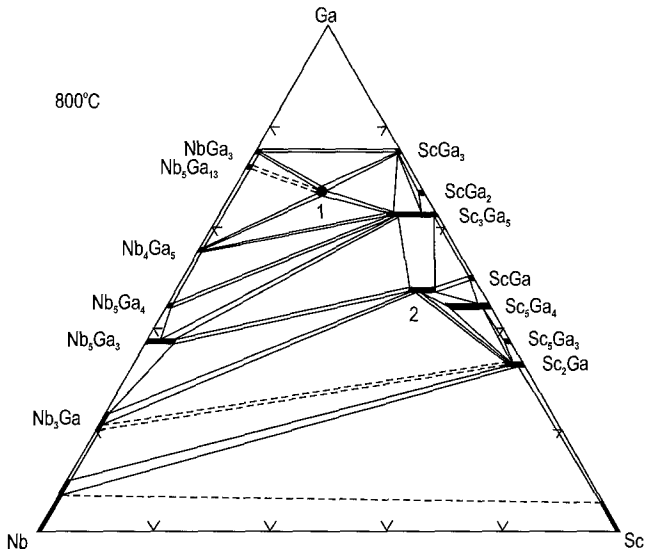

Fig. 41. Sc–Nb–Ga, part of the isothermal section at 800°C (0–75 at.% Sc). Ternary compounds: (1) ~$ScNbGa_4$; (2) $Sc_{8.4-9.4}Nb_{2.6-1.6}Ga_{10}$.

"$Sc_{77}Mn_{13}Ga_{10}$" by Markiv and Belyavina (1989a). The refined compositions of these compounds are presented in a modified isothermal section, which is shown in fig. 42.

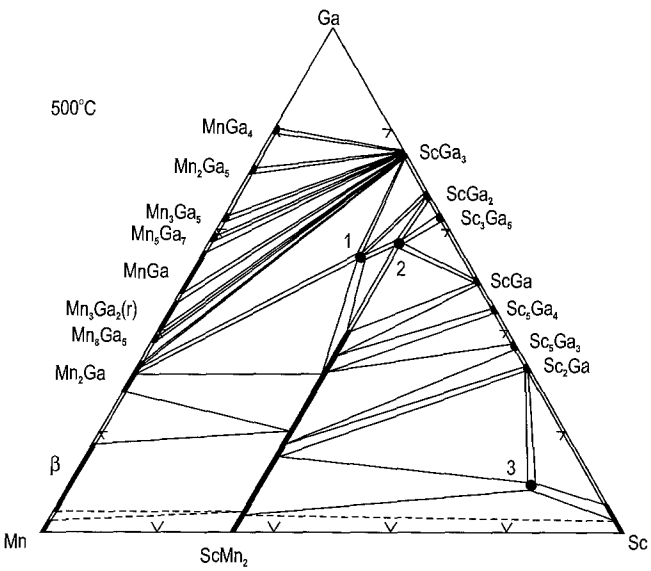

Fig. 42. Sc–Mn–Ga, part of the isothermal section at 500°C (0–80 at.% Sc). Ternary compounds: (1) $Sc_3Mn_2Ga_6$; (2) $ScMn_{0.33}Ga_{1.67}$; (3) $Sc_{8.5}Mn_{1.2}Ga$.

The characteristics of their crystal structures are summarised in table 16.

3.3.9. *Sc–Fe–Ga*

The Sc–Fe–Ga isothermal section at 800°C in the range 0–75 at.% Ga had been reported by Gavrilenko and Markiv (1978b). They established seven ternary compounds, for four of them a complete or partially investigated crystal structure was given. Belyavina and Markiv (1982a) reinvestigated the alloys of 7.7 at.% Sc isoconcentrate with the Ga content from 38 to 62 at.%. They did not confirm the data of Gavrilenko and Markiv about the crystal structure of "$ScFe_{6.75-4.96}Ga_{5.25-7.04}$" at 800°C (ST $ThMn_{12}$). A phase isotypic with $ThMn_{12}$ was found to occur at 600°C in an alloy with the composition $ScFe_{4.73}Ga_{7.27}$ (its lattice spacings are given in table 16). At 800°C an orthorhombic phase occurs closely related to $ThMn_{12}$ type structure (see table 16). At 800°C a new compound, namely $Sc_2Fe_{8.83}Ga_{8.17}$ was found; it is in equilibrium with the above-mentioned ternary phase and the α(Fe, Ga) solid solution. Kuzmenko et al. (1983) reported about another ternary compound: $ScFe_{0.14}Ga_{1.86}$ (ST $CaIn_2$) which was found in an as-cast alloy as well as in alloys annealed at 800°C. In other publications the compositions and the crystal structures of four other ternary compounds observed by Gavrilenko and Markiv were determined: (3) "$ScFe_{1-0.8}Ga_{5-5.2}$" (Belyavina and Markiv 1980b), (7) "$Sc_{36}Fe_9Ga_{55}$" (Kuzmenko et al., 1983), (4) "$Sc_{28}Fe_{26.5-22.5}Ga_{45.4-49.4}$" (Markiv and Belyavina 1987b), (9) "$Sc_{80}Fe_{12}Ga_8$" (Markiv and Belyavina 1989a). The modified isothermal section at 800°C based on these papers is presented in fig. 43. The composition of the " Sc_7Fe"

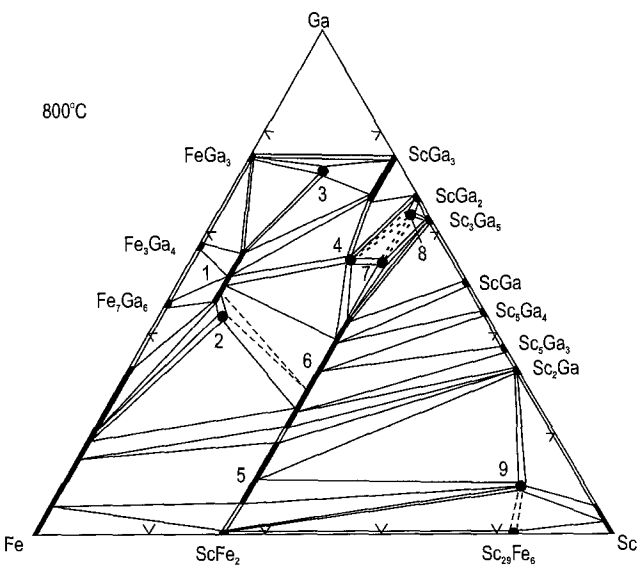

Fig. 43. Sc–Fe–Ga, part of the isothermal section at 800°C (0–75 at.% Sc). Ternary compounds: (1) $ScFe_{6-4.73}Ga_{6-7.27}$; (2) $ScFe_{8.83}Ga_{8.17}$; (3) $ScFeGa_5$; (4) $Sc_3Fe_2Ga_6$; (5) $ScFe_{1.82-1.44}Ga_{0.18-0.56}$; (6) $ScFe_{1.37-0.71}Ga_{0.63-1.29}$; (7) $ScFe_{0.33}Ga_{1.67}$; (8) $ScFe_{0.14}Ga_{0.86}$; (9) $Sc_{8.5}Fe_{1.2}Ga$.

binary compound has been corrected in this figure too (see also sect. 2.8). The crystal structure characteristics of all observed Sc–Fe–Ga ternary compounds are presented in table 16.

3.3.10. *Sc–Co–Ga*

A number of papers dealing with investigations of Sc–Co–Ga alloys and compounds have been published. Figure 44 presents a revised isothermal section at 800°C. Gavrilenko and Markiv (1979) reported on the isothermal section at 800°C in the range 0–75 at.% Ga. Sc–Co binary compounds dissolve large quantities of Ga: from 8 at.% (Sc_3Co) to 37 at.% (ScCo). The solubility of Co in Sc_5Ga_3 is about 11 at.%. Fifteen ternary compounds were reported to occur in the system at 800°C. Gavrilenko and Markiv confirmed the data of Markiv and Burnashova (1969) concerning $Sc_6Co_7Ga_{16}$ and determined its homogeneity range at 800°C: (8) $Sc_6Co_{7.2-6.3}Ga_{15.8-16.7}$. They also established the crystal structure of the phase (12) $Sc_{29-34}Co_{40-24}Ga_{29-42}$ (see table 16). In later publications of Markiv and co-workers data about the crystal structure and proper compositions of other nine ternary compounds are given: (4) "$ScCo_{1-0.75}Ga_{4-4.25}$" and (7) "$Sc_{19}Co_{12}Ga_{69}$" by Belyavina and Markiv (1980b), (1) "$Sc_9Co_{45}Ga_{46}$" by Belyavina and Markiv (1982a), (13) "$ScCo_{0.35-0.20}Ga_{1.65-1.80}$" by Belyavina and Markiv (1982b), (2) "$ScCo_{3.96-3.72}Ga_{3.04-3.28}$", (3) "$ScCo_2Ga_5$" and (6) "$ScCo_3Ga_2$" by Markiv and Belyavina (1987a), (15) "$Sc_{74}Co_{13}Ga_{13}$" by Markiv and Belyavina (1989b), and

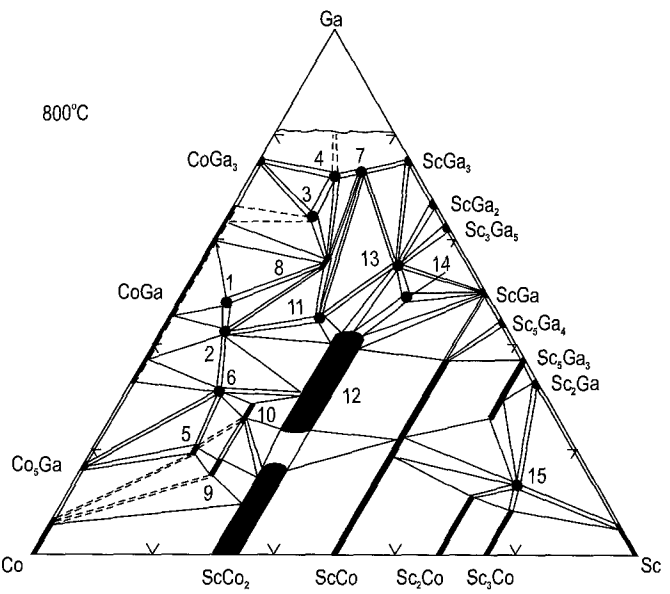

Fig. 44. Sc–Co–Ga, part of the isothermal section at 800°C (0–75 at.% Sc). Ternary compounds: (1) $ScCo_{5.8}Ga_{6.2}$; (2) $ScCo_{4.5}Ga_{4.1}$; (3) $Sc_2Co_3Ga_9$; (4) $ScCoGa_5$; (5) ~$Sc_{17}Co_{64-62}Ga_{19-21}$; (6) $Sc_2Co_7Ga_4$; (7) Sc_2CoGa_8; (8) $Sc_6Co_{7.2-6.3}Ga_{15.8-16.7}$; (9) ~$Sc_{22}Co_{63-60}Ga_{15-18}$; (10) ~$Sc_{22}Co_{53-49}Ga_{25-29}$; (11) $ScCo_{1.2}Ga_{1.8}$; (12) $Sc_{29-34}Co_{48-24}Ga_{29-42}$; (13) $ScCo_{0.35}Ga_{1.65}$; (14) ~$Sc_{37}Co_{14}Ga_{49}$; (15) $Sc_5Co_{0.925}Ga_{0.925}$.

(11) "$Sc_{27}Co_{26}Ga_{47}$" by Belyavina and Markiv (1989). The refined compositions and the crystal structure data of these compounds are presented in fig. 44 and in table 16. The crystal structures of four Sc–Co–Ga ternary compounds are still unknown (see table 16). Kuzmenko et al. (1983) reinvestigated the alloys of the $ScCu_2$–$ScGa_2$ section and identified two other ternary compounds, namely $ScCo_{0.14}Ga_{1.86}$ (ST $CaIn_2$) and $ScCo_{0.5}Ga_{1.5}$ (ST KHg_2), which were observed only in the as-cast alloys (for their lattice spacings see table 16). The latter compound disintegrates into the ternary phases (12) and (13) during homogenization at 800°C.

3.3.11. *Sc–Ni–Ga*

Gavrilenko and Markiv (1979) presented data about the phase equilibria in the Sc–Ni–Ga system at 800°C in the range 0–75at.% Ga. They synthesized fourteen ternary compounds, but for only three of them [$ScNi_2Ga$ (ST $MnCu_2Al$), $Sc_{30-36}Ni_{55-39}Ga_{15-25}$(ST $MgZn_2$), $Sc_{33-38}Ni_{35-18}Ga_{32-44}$ (ST $CaIn_2$)] has the crystal structure data been given. The compositions of the other eleven compounds were determined tentatively. For eight of them the crystal structure investigations were performed afterwards, this also led to a refinement of their compositions: (1) "$ScNi_{1-0.85}Ga_{4-4.15}$" and (7) "$Sc_{20}Ni_{12}Ga_{68}$" by Belyavina and Markiv (1980b), (12) "$ScNi_{0.50.26}Ga_{1.5-1.74}$" by Belyavina and Markiv (1982b), (10) $ScNiGa_2$ by Markiv and Belyavina (1983), (9) "$Sc_{27}Ni_{26}Ga_{47}$" by Belyavina and Markiv (1989), (14) "$Sc_{70-73}Ni_{20-12}Ga_{10-15}$" by Markiv and Belyavina (1989b), (3) "$Sc_{17}Ni_{54-41}Ga_{29-42}$" by Markiv and Belyavina (1990a), and (2) "$ScNi_{2.60}Ga_{4.03}$" by Markiv and Belyavina (1990b). The refined compositions, the structure data of these compounds and the compositions of three other ternary compounds with unknown structures are given in table 16. Figure 45 shows the corrected isothermal section at 800°C based on all these publications. The solubility of Ga in $ScNi_5$, Sc_2Ni_7, $ScNi_2$ and ScNi is 11.5, 8.0, 12.2 and 30 at.%, respectively. Kuzmenko et al. (1983) reinvestigated the alloys of the $ScNi_2$–$ScGa_2$ section. They rejected the data of Gavrilenko and Markiv (1979) concerning the crystal structure of the $Sc_{33-38}Ni_{35-18}Ga_{32-44}$ compound (ST $CaIn_2$, $a = 4.184$–4.240, $c = 6.387$–6.584 Å). Kuzmenko et al. observed the ternary compound of $CaIn_2$ type only in the as-cast alloy at the composition of $ScNi_{0.14}Ga_{1.86}$ (see table 16). For a compound of composition $ScNi_{1-0.67}Ga_{1-1.33}$ at 800°C they found a structure of KHg_2 type. For the alloy of the equiatomic composition, ScNiGa, the ordered structure of the TiNiSi type was preferred by Kuzmenko et al. (see table 16). Earlier, Dwight (1968) reported about the ScNiGa compound crystallising in the KHg_2 type structure; the lattice parameters reported by Dwight for that phase, $a = 4.164$, $b = 6.306$, $c = 7.230$ Å are in good agreement with the parameters found by Kuzmenko et al. (see table 16). There are no further data in the paper of Kuzmenko et al. whether the $ScNi_{1-0.67}Ga_{1-1.33}$ compound has variable content of scandium or not. For that reason we have drawn a broad homogeneity range for that compound (13) in fig. 45 according to the earlier data of Gavrilenko and Markiv (1979).

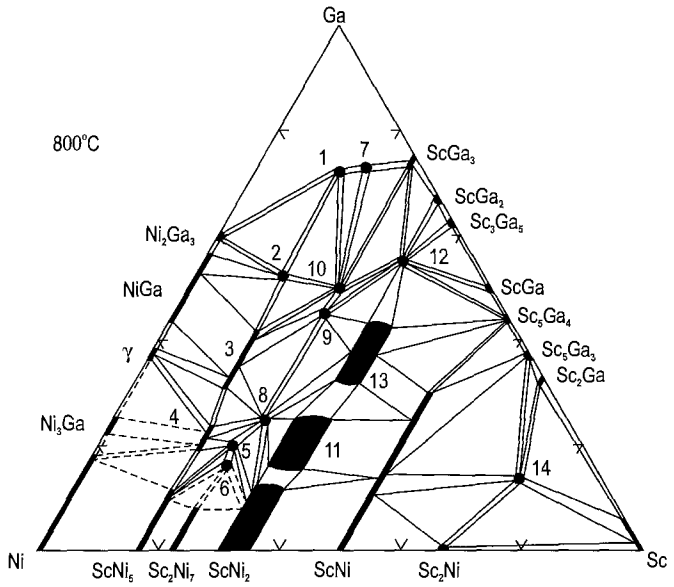

Fig. 45. Sc–Ni–Ga, part of the isothermal section at 800°C (0–75 at.% Sc). Ternary compounds: (1) $ScNiGa_5$; (2) $ScNi_{2.36}Ga_{3.64}$; (3) $Sc_2Ni_{7-5.5}Ga_{4-5.5}$; (4) $\sim Sc_{17}Ni_{64-59}Ga_{19-24}$; (5) $\sim Sc_{22}Ni_{58}Ga_{20}$; (6) $\sim Sc_{23}Ni_{61}Ga_{16}$; (7) Sc_2NiGa_8; (8) $ScNi_2Ga$; (9) $ScNi_{1.2}Ga_{1.8}$; (10) $ScNiGa_2$; (11) $Sc_{30-36}Ni_{55-39}Ga_{15-25}$; (12) $ScNi_{0.35}Ga_{1.65}$; (13) $Sc_{33-38}Ni_{35-18}Ga_{32-44}$; (14) $Sc_5Ni_{0.963}Ga_{0.963}$.

3.3.12. *Sc–M–Ga (M = Ru, Rh, Pd, Os, Ir, Pt)*

No data are available about phase equilibria in the six Sc–M–Ge (M = Ru, Rh, Pd, Os, Ir, Pt) ternary systems. Only occasional alloys were examined in each of these systems. As a result, in the Sc–Pd–Ga system two ternary compounds were synthesized and structurally characterised: $ScPd_2Ga$ and ScPdGa (see table 16). In each of the remaining five systems one ternary compound was observed: their compositions are $Sc_6M_7Ga_{16}$ (M = Ru, Rh, Os, Ir) and ScPtGa. The crystal structure data are given in table 16. According to the data of Markiv and Storozhenko (1973) $Sc_6M_7Ga_{16}$ (M = Pd, Pt) ternary compounds do not occur in either the as-cast alloys or the alloys homogenised at 800°C.

3.3.13. *Sc–Cu–Ga*

Gavrilenko and Markiv (1979) investigated a part of the Sc–Cu–Ga isothermal section at 800°C (0–75 at.% Ga), however without showing a figure. The isothermal section shown in fig. 46 is mainly based on the figure presented by Gavrilenko (1982). Eight ternary compounds occur in the investigated part of the system. The crystal structure was determined for six of them (see table 16). The compositions of two of these compounds, (2) "$Sc_{15}Cu_{52}Ga_{33}$" and (5) "$Sc_{22}Cu_{55}Ga_{23}$", were refined as part of the crystal structure investigations by Markiv and Belyavina (1990b, 1989a). The compound (1) $ScCu_{5.49-4.85}Ga_{6.51-7.15}$ was observed by Gavrilenko and Markiv in the as-cast alloy and in a sample homogenised at 600°C. At 800°C the alloys of this concentration region of the

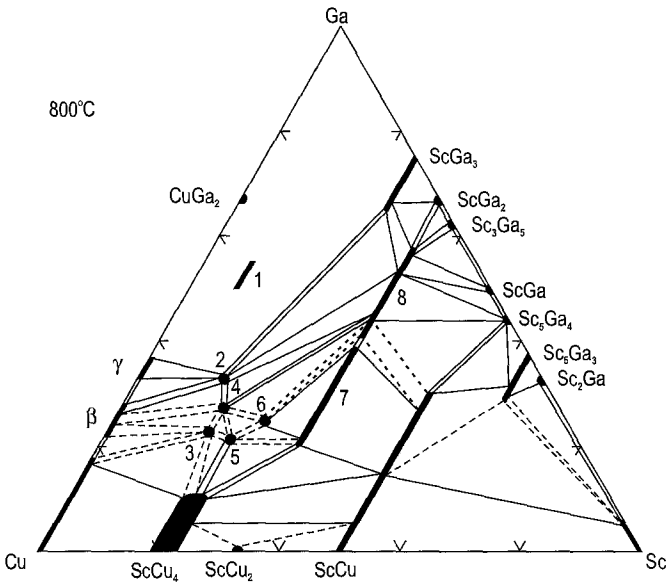

Fig. 46. Sc–Cu–Ga, part of the isothermal section at 800°C (0–75 at.% Sc). Ternary compounds: (1) $ScCu_{5.49-4.85}Ga_{6.51-7.15}$ (at 600°C); (2) $ScCu_{3.7}Ga_{2.3}$; (3) ~$ScCu_{3.6}Ga_{1.4}$; (4) ~$ScCu_{3.2}Ga_{1.6}$; (5) $Sc_{14}Cu_{37}Ga_{14}$; (6) $ScCu_2Ga$; (7) $ScCu_{1.40-0.86}Ga_{0..60-1.14}$; (8) $ScCu_{0.77-0.26}Ga_{1.23-1.74}$.

system are in the liquid state. Gavrilenko and Markiv (1979) reported about one ternary compound in the $ScCu_2$–$ScGa_2$ section: $ScCu_{1.4-0.26}Ga_{0.6-1.74}$ (ST $CaIn_2$, $a = 4.211$–4.248, $c = 6.459$–6.588 Å). In a later paper Markiv et al. (1984) examined again the alloys of that section and reported the existence of two ternary phases within that composition region, namely (7) $ScCu_{1.40-0.86}Ga_{0.60-1.14}$ (ST KHg_2) and (8) $ScCu_{0.77-0.26}Ga_{1.23-1.74}$ (ST $CaIn_2$) (for their lattice parameters see table 16). Dwight (1968) also reported about the existence of a hexagonal compound $ScCu_{0.5}Ga_{1.5}$ (ST Ni_2In, $a = 4.254$, $c = 6.612$), with a composition within the homogeneity range of the hexagonal compound (8) observed by Markiv et al. (1984), however, the values of the lattice spacings of the Dwight phase are higher than those reported by Gavrilenko and Markiv (1979) and Markiv et al. (1984).

3.4. *Sc–M–In ternary systems*

3.4.1. *Sc–Ni–In*

There are no data about the phase equilibria in the Sc–Ni–In system. Three ternary compounds $ScNi_4In$, $ScNi_2In$ and Sc_2Ni_2In have been synthesized and their crystal structure determined (see table 17).

3.4.2. *Sc–Pd–In*

Savitskii et al. (1980b) investigated the polythermal PdIn–PdSc section of the Sc–Pd–In ternary system. They observed a complete miscibility between the isotypic binary

Table 17
Intermetallic compounds in the Sc–M–In ternary systems

Compound	Structure type or symmetry	Lattice parameters		Reference
		a (Å)	c (Å)	
$ScNi_4In$	$MgCu_4Sn$	6.872		Zaremba et al. (1984)
$ScNi_2In$	$MnCu_2Al$	6.256		Zaremba et al. (1984)
Sc_2Ni_2In	Mo_2FeB_2	7.1679	3.33154	Pöttgen and Dronskowski (1996)
$Sc_{0.76-1.44}Pd_2In_{1.24-0.56}$	$MnCu_2Al$	6.496[a]		Dwight and Kimball (1987), Urvachev et al. (1983)
$ScPt_2In$	$MnCu_2Al$	6.512		Dwight and Kimball (1987)
$ScCu_2In$	$MnCu_2Al$	6.378		Dwight and Kimball (1987)
$ScAg_2In$	$MnCu_2Al$	6.720		Dwight and Kimball (1987)
$ScAu_2In$	$MnCu_2Al$	6.692		Dwight and Kimball (1987)

[a] For the $ScPd_2In$ composition.

compounds PdIn and PdSc (ST CsCl). After a reinvestigation of the same section Urvachev et al. (1983) established the occurrence of one ternary compound with an extended homogeneity range: $Sc_{0.76-1.44}Pd_2In_{1.24-0.56}$, which is formed as the result of an atomic ordering of the observed earlier $Pd(In_xSc_{1-x})$ solid solution. Dwight and Kimball (1987) reported about a $ScPd_2In$ compound crystallizing in the $MnCu_2Al$ type structure (see table 17) which is, obviously, the ordered type for the compound observed by Urvachev et al. (1983).

3.4.3. *Sc–Pt–In*

Dwight and Kimball (1987) identified a ternary compound of $MnCu_2Al$ type structure in the Sc–Pt–In alloy with the $ScPt_2In$ composition, homogenized at 700°C (see table 17). No information is available about other compounds or alloys of this system.

3.4.4. *Sc–M–In (M = Cu, Ag, Au)*

The occurrence of a Heusler type ternary compound, ScM_2In, in each of the three Sc–M–In (M = Cu, Ag, Au) ternary systems has been reported by Dwight and Kimball (1987). Their lattice spacings are given in table 17. The alloys were homogenized at 700°C. No phase equilibria in these systems were investigated.

3.5. *Sc–M–C ternary systems*

3.5.1. *Sc–Th–C*

Krupka et al. (1973) observed the occurrence of a solid solution of scandium in the cubic thorium carbide, Th_2C_3 (ST Pu_2C_3). The lattice parameter changes within the homogeneity range of $Th_{2-0.6}Sc_{0-1.4}C_3$ from $a = 8.556$ to $a = 8.563$ Å, the value for $Th_{1.4}Sc_{0.6}C_3$ is $a = 8.530$ Å.

3.5.2. *Sc–Ti–C*

Nowotny and Auer-Welsbach (1961) synthesized the ternary compound $ScTi_3C_4$ isotypic with NaCl ($a = 4.5$ Å). Velikanova et al. (1989) evaluated the hypothetical projection of the solidus surfaces of the phase diagram. A wide range of continuous solid solutions between the isotypic binary carbides ScC_{1-x} and TiC_{1-x} (ST NaCl) was predicted by them. It might be that the ternary phase observed by Nowotny and Auer-Welsbach is a part of this solid solution, and possibly not an individual ternary compound. Recently this prediction was confirmed experimentally by Ilyenko et al. (1996) who confirmed a complete mutual solubility of ScC_{1-x} and TiC_{1-x}. These authors reported also that the ScC_{1-x} phase is in equilibrium with all the phases of the solidus surface. However, the paper by Ilyenko et al. does not contain a figure of the phase equilibria.

3.5.3. *Sc–M–C (M = Zr, Hf, V, Nb, Ta)*

Hypothetical projections of the solidus surfaces of the Sc–M–C (M = Zr, Hf, V, Nb, Ta) phase diagrams are proposed in a paper of Velikanova et al. (1989). A complete miscibility of the binary carbides ScC_{1-x} and MC_{1-x} (M = Zr, Hf, V, Nb, Ta) crystallizing in the NaCl type structure, and the absence of ternary compounds in each of these ternary systems is predicted. However, these data need to be confirmed experimentally. Recently Ilyenko et al. (1996) reported the existence of continuous solid solutions between ScC_{1-x} and MC_{1-x} (M = Zr, Hf), and accordingly these solid solutions are in equilibria with all the phases of the solidus surface. The same authors reported that the VC_{1-x} binary carbidedissolves at least 15 at.% Sc while the V solubility in ScC_{1-x} is at least 17 at.%. These data reject the earlier prediction of a complete miscibility of the NaCl-type binary carbides in the system Sc–V–C. However, no figures of the phase equilibria are presented in the brief communication of Ilyenko et al.

3.5.4. *Sc–Cr–C*

A hypothetical projection of the solidus surfaces of the Sc–Cr–C phase diagram has been proposed and experimentally confirmed in the range 0–30 at.% C by Velikanova et al. (1989) and Artyukh et al. (1989) (see fig. 47a). At high carbon content one ternary compound Sc_2CrC_3 occurs in the system (Artyukh et al.). Its melting temperature does not exceed 1600°C. Pecharskaya et al. (1990) established its crystal structure (see table 18). A second ternary compound $ScCrC_2$, occurring in two very closely related modifications β (HT) and α (LT), has been reported by Pöttgen et al. (1995) (see table 18). Recently Artyukh et al. (1997) presented the phase equilibria over the whole concentration region of the system. In the carbon-rich range ScC_{1-x}–C–Cr_3C_2 all the phases are in equilibria with the ternary compound Sc_2CrC_3. Scandium and chromium binary carbides dissolve no more than 1 to 1.5 at.% of the third component. However, the $ScCrC_2$ ternary compound was not mentioned. Thus, an additional investigation of the system in the >40 at.% C region is necessary.

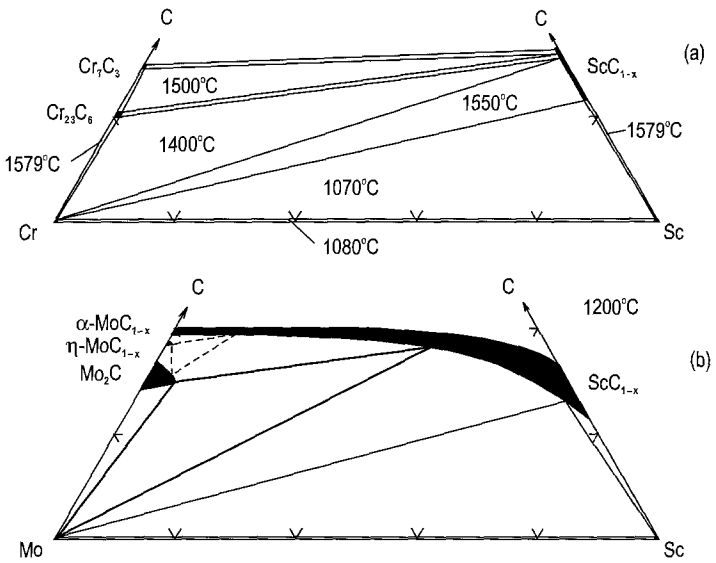

Fig. 47. (a) Sc–Cr–C, and (b) Sc–Mo–C parts of the projections of solidus surfaces (a, 0–30 at.% C; b, 0–42 at.% C).

3.5.5. *Sc–Mo–C*

Velikanova et al. (1989) evaluated hypothetical projection of solidus surfaces of the Sc–Mo–C phase diagram and confirmed it, at least partially, by experiment in 0–42 at.% C concentration region (see fig. 47b). The forecasted and the experimental data are in good agreement. No ternary compounds were observed. In the diagram presented by Velikanova et al. it is shown that about 8 at.% Sc is soluble in Mo at 1200°C. These data are in disagreement with the prediction of Brewer and Lamoreaux (1980) and the experimentally determined Sc–M (M = 5A, 6A element) binary phase diagrams (see sect. 2.6). The solubility of scandium in these elements is very low (<0.1 at.%). The diagram presented in fig. 47b has been modified by taking this into account.

3.5.6. *Sc–M–C (M = W, Re, Tc)*

Hypothetical projections of solidus surfaces of the Sc–M–C (M = W, Re, Tc) phase diagrams have been proposed: Sc–W–C by Velikanova et al. (1989), Sc–Re–C by Velikanova et al. and by Eremenko et al. (1989a), and Sc–Tc–C by Eremenko et al. (1989b). However, all these results need an experimental verification. No ternary compounds were predicted. Pöttgen and Jeitschko (1992) synthesized a ternary carbide $Sc_5Re_2C_7$ and investigated its crystal structure (see table 18); these data do not confirm the predictions mentioned above.

Table 18
Intermetallic compounds in the Sc–M–C ternary systems

Compound	Structure type or symmetry	Lattice parameters			Reference
		a (Å)	*b* (Å)	*c* (Å)	
Sc_2CrC_3	Sc_2CrC_3	14.110	5.809	3.271	*Pecharskaya et al. (1990)*, Artyukh et al. (1989)
$ScCrC_2$ (β)	$ScCrC_2$ (β)	3.237		9.149	*Pöttgen et al. (1995)*
$ScCrC_2$ (α)	$ScCrC_2$ (α)	3.2434	9.1502	5.6148	*Pöttgen et al. (1995)*
$Sc_5Re_2C_7$	$Sc_5Re_2C_7$	7.7926	13.620	3.2062	*Pöttgen and Jeitschko (1992)*
$ScFeC_2$	$ScCoC_2$	3.293		7.487	Marusin et al. (1985), Pecharskaya (1989)
Sc_3FeC_4	Sc_3CoC_4	3.3636	4.3748	12.087	Tsokol' et al. (1986a), Pecharskaya (1989)
$ScCo_3C$	$CaTiO_3$	3.8291			Pecharskaya (1989)
		3.827			Holleck (1977)
$ScCoC_2$	$ScCoC_2$	3.3344		7.292	*Marusin et al. (1985)*, Pecharskaya (1989)
Sc_3CoC_4	Sc_3CoC_4	3.3933	4.3727	11.989	*Tsokol' et al. (1986a)*, Pecharskaya (1989)
$ScNiC_2$	$ScCoC_2$	3.325		7.368	Marusin et al. (1985), Pecharskaya (1989)
Sc_3NiC_4	Sc_3CoC_4	3.4118	4.3772	11.916	Tsokol' et al. (1986a), Pecharskaya (1989)
$ScRu_3C$	$CaTiO_3$	4.031			Holleck (1977)
$ScIr_3C_{1-x}$	$CaTiO_3$	3.994			Holleck (1977)

3.5.7. *Sc–Fe–C*

The isothermal section of the Sc–Fe–C system at 600°C has been investigated by Pecharskaya (1989). The phase diagram presented in fig. 48 is mainly based on these data. The data concerning the binary Sc–C system are not in agreement with the Sc–C phase diagram presented by Gordijchuk (1987) (see sect. 2.14). Two ternary compounds $ScFeC_2$ and Sc_3FeC_4 occur in this system. Their crystal structures were studied earlier by Marusin et al. (1985) and Tsokol' et al. (1986a) (see table 18).

3.5.8. *Sc–Co–C*

The Sc–Co–C phase equilibria at 600°C have been established by Pecharskaya (1989) and are shown in fig. 49. The data about the existence at 600°C of Sc_4C_3 binary carbide are not in agreement with the other literature sources (see sect. 2.14). Earlier the existence of three ternary compounds were reported in the system. Their compositions and the crystal structure data are given in table 18.

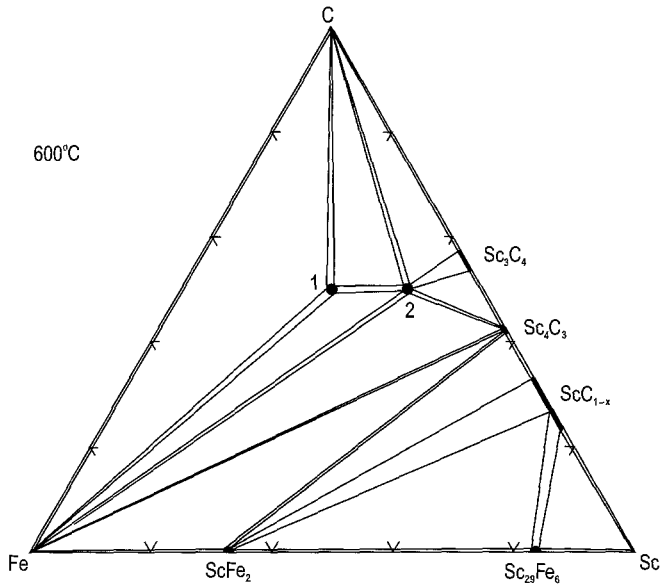

Fig. 48. Sc–Fe–C, isothermal section at 600°C. Ternary compounds: (1) $ScFeC_2$; (2) Sc_3FeC_4.

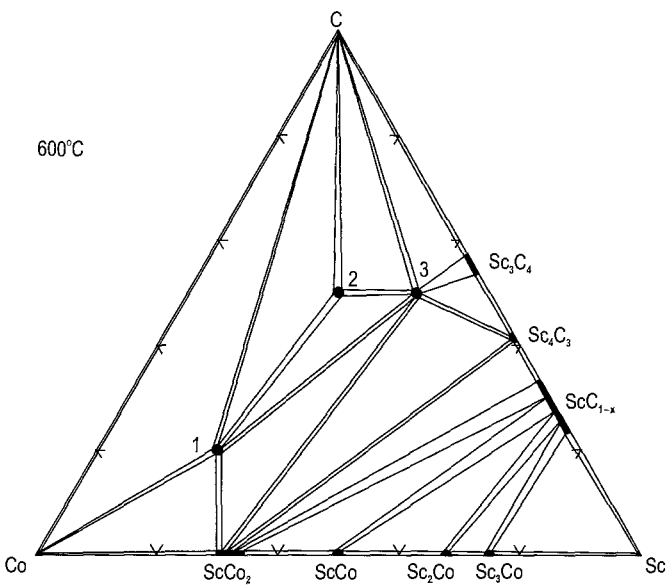

Fig. 49. Sc–Co–C, isothermal section at 600°C. Ternary compounds: (1) $ScCo_3C$; (2) $ScCoC_2$; (3) Sc_3CoC_4.

3.5.9. *Sc–Ni–C*

Two ternary compounds $ScNiC_2$ and Sc_3NiC_4 were synthesized and their crystal structure determined (see table 18). Later, Pecharskaya (1989) presented isothermal section at 600°C (see fig. 50). However, the existence of a Sc_4C_3 binary compound at 600°C does not agree with the Sc–C phase diagram published by Gordijchuk (1987) (see sect. 2.13); this discrepancy needs to be cleared-up by a new investigation.

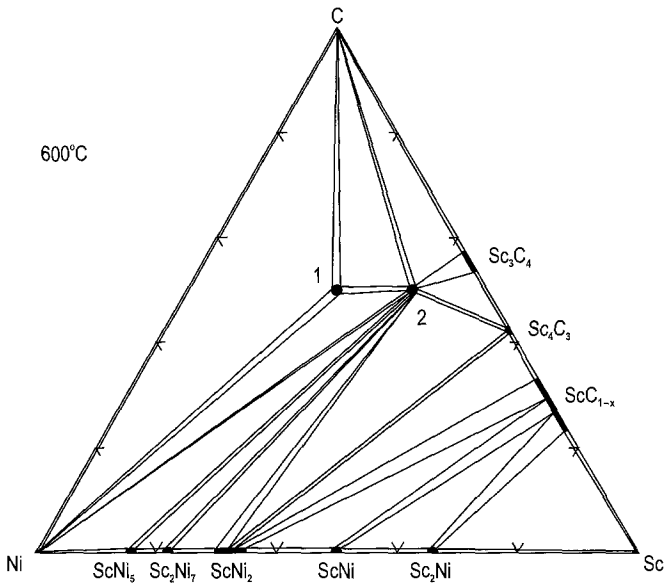

Fig. 50. Sc–Ni–C, isothermal section at 600°C. Ternary compounds: (1) $ScNiC_2$; (2) Sc_3NiC_4.

3.5.10. *Sc–M–C (M = Ru, Rh, Pd)*

Holleck (1977) investigated the phase equilibria of the Sc–M–C (M = Ru, Rh, Pd) systems at 1300°C in the ranges 0–40 (for M = Ru), 0–50 (for M = Rh) and 0–25 (for M = Pd) at.% Sc. The isothermal sections presented in fig. 51 are modified by taking into account the newest data concerning the Sc–M (M = Ru, Rh, Pd) phase diagrams. The compositions and their homogeneity ranges of the binary compounds at 1300°C were corrected (see sect. 2.9). One ternary compound occurs in the Sc–Ru–C system (see table 18). In the Sc–Rh–C system the solid solution due to the inclusion of carbon atoms into the lattice of the $ScRh_3$ compound (ST $AuCu_3$) was observed: $ScRh_3C_{0-0.75}$. Its lattice parameter varies from $a = 3.900$ up to $a = 4.025$ Å. Possibly this solid solution may reach the $ScRh_3C$ composition.

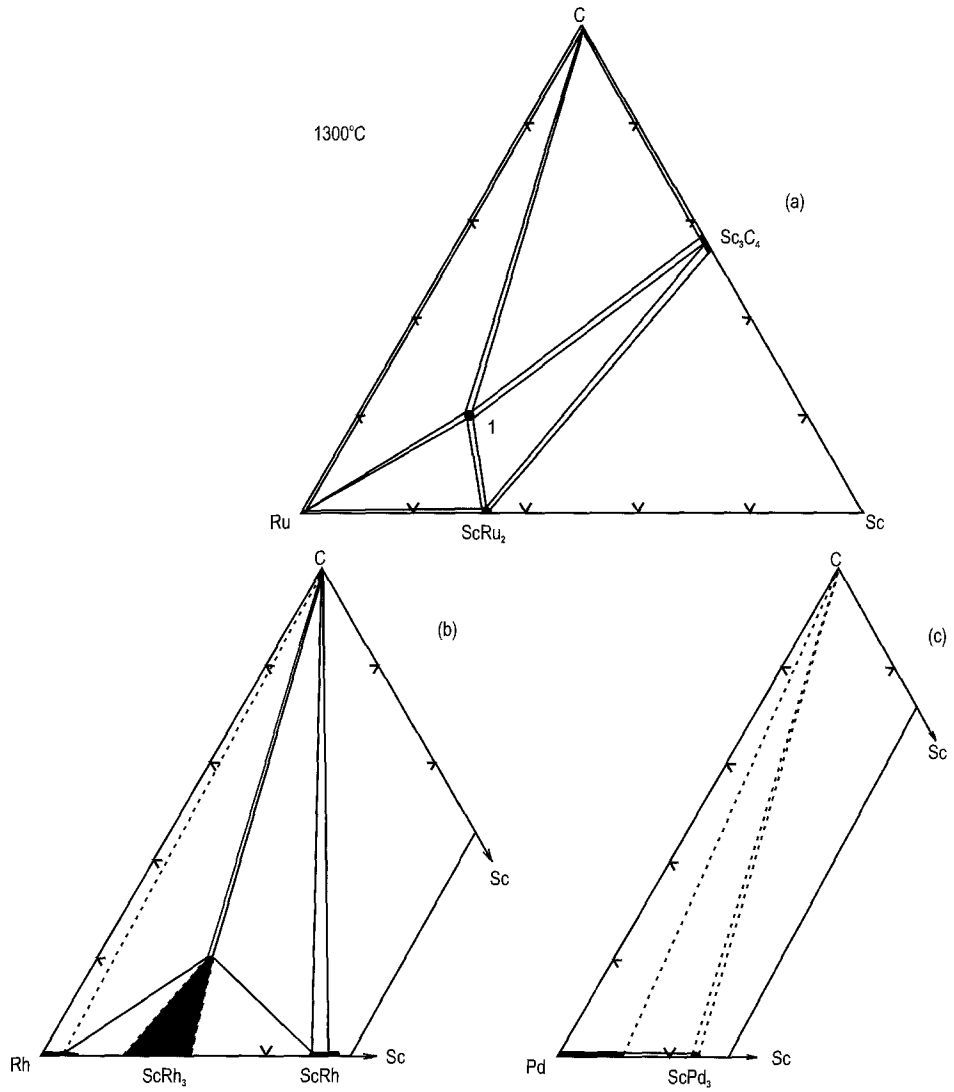

Fig. 51. (a) Sc–Ru–C, (b) Sc–Rh–C, and (c) Sc–Pd–C parts of the isothermal sections at 1300°C (a, 0–40; b, 0–50; c, 0–25 at.% Sc). Ternary compound: (1) $ScRu_3C$.

3.5.11. *Sc–Ir–C*

One ternary compound $ScIr_3C_{1-x}$ of the perovskite type structure has been synthesized by Holleck (1977) (see table 18), however the proper carbon content is unknown because of the loss of some of the component during its preparation. The compound is in the two phase equilibria with $ScIr_2$ and C.

3.6. *Sc–M–Si ternary systems*

3.6.1. *Sc–Y–Si*

Kotroczo and McColm (1987) investigated the quasibinary section Sc_5Si_3–Y_5Si_3 of the Sc–Y–Si ternary system and found a limited solid solutions $Y_{5-x}Sc_xSi_3$ ($0 \leqslant x \leqslant 0.75$) and $Sc_{5-y}Y_ySi_3$ ($0 \leqslant y \leqslant 1$) during an examination of as-cast alloys. Later Kotur and Mokra (1994) during an investigation of the isothermal section of the ternary system at 800°C observed a complete miscibility of these isotypic binary silicides (see fig. 52). Another continuous solid solution occurs between the isotypic monosilicides of scandium and yttrium. The highest yttrium silicide, YSi_2, dissolves 20 at.% Sc. One ternary compound with a variable composition occurs in this system (see table 19).

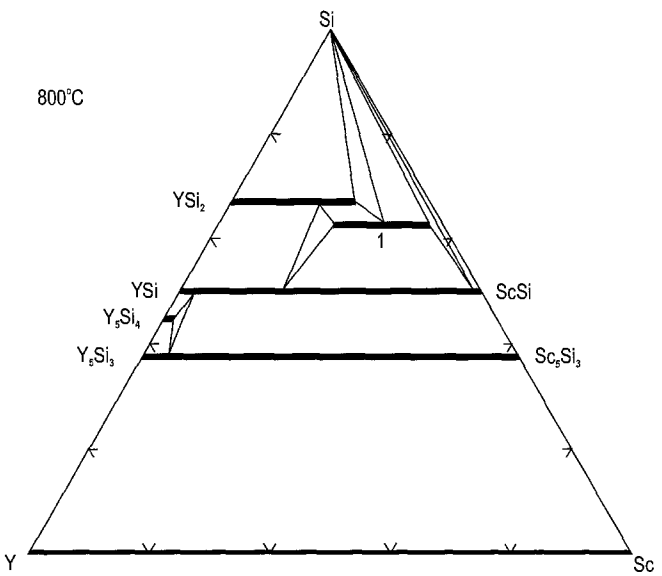

Fig. 52. Sc–Y–Si, isothermal section at 800°C. Ternary compound: (1) $Sc_{0.95-0.52}Y_{0.05-0.48}Si_{1.67}$.

3.6.2. *Sc–La–Si*

There are two ternary compounds known in the Sc–La–Si system: ScLaSi (Mokra and Bodak 1979) and ~$ScLa_2Si_2$ (Mokra 1979), however, the lattice parameters have been reported only for the first compound (see table 19).

3.6.3. *Sc–Ce–Si*

An isothermal section of the Sc–Ce–Si phase diagram at 600°C has been investigated by Mokra (1979) and Bodak et al. (1981). Its figure was presented in the review of Rogl (1984b). Binary silicides of cerium and scandium do not dissolve more than 5 at.% of Sc and Ce respectively. All eight ternary compounds known in this system have variable

Table 19
Intermetallic compounds in the Sc–M–Si ternary systems

Compound	Structure type or symmetry	Lattice parameters			Reference
		a (Å)	*b* (Å)	*c* (Å)	
$Sc_{0.95-0.52}Y_{0.05-0.48}Si_{1.67}$	AlB_2	3.687–3.735		3.935–4.033	Kotur and Mokra (1994)
$ScLa_2Si_2$	Mo_2FeB_2				Mokra (1979)
ScLaSi	ScCeSi	4.344		15.98	Mokra and Bodak (1979)
~$Sc_3Ce_{11}Si_6$	?				Mokra (1979)
~$Sc_3Ce_8Si_9$	?				Mokra (1979)
$ScCe_2Si_2$	Mo_2FeB_2	7.61		4.402	*Mokra (1979)*
		7.518		4.393	Kotur et al. (1989c)
~$Sc_4Ce_7Si_9$	?				Mokra (1979)
~$Sc_5Ce_6Si_9$	?				Mokra (1979)
ScCeSi	ScCeSi	4.300		15.80	*Mokra and Bodak (1979)*, Mokra (1979)
		4.302		15.768	Kotur et al. (1989c)
$Sc_3Ce_2Si_4$	$Ce_2Sc_3Si_4$	7.248	14.255	7.551	*Mokra et al. (1979)*, Mokra (1979)
~$Sc_7Ce_3Si_{10}$	?				Mokra (1979)
~$ScPr_4Si_3$	?				Banakh and Kotur (1997)
$Sc_{1.26}Pr_{3.74}Si_4$	Sm_5Ge_4	7.453	14.842	7.825	*Kotur et al. (1997a)*, Banakh and Kotur (1997)
~$Sc_2Pr_5Si_3$	?				Banakh and Kotur (1997)
$ScPr_2Si_2$	Mo_2FeB_2	7.585		4.328	Banakh and Kotur (1997), Mokra (1979)
~$Sc_2Pr_3Si_4$	?				Banakh and Kotur (1997)
ScPrSi	ScCeSi	4.292		15.78	Mokra and Bodak (1979)
		4.301		15.810	Banakh and Kotur (1997)
$Sc_3Pr_2Si_4$	$Ce_2Sc_3Si_4$	7.196	14.150	7.495	*Kotur et al. (1997a)*, Banakh and Kotur (1997)
$Sc_{0.89}Pr_{0.11}Si_{1.53}$	AlB_2	3.6648		3.8876	Banakh and Kotur (1997)
~$ScNd_4Si_3$	?				Banakh and Kotur (1998)
$ScNd_2Si_2$	Mo_2FeB_2	7.307		4.323	Banakh and Kotur (1998), Mokra (1979)
ScNdSi	ScCeSi	4.224		15.567	Kotur et al. (1992), Banakh and Kotur (1998)
		4.248		15.73	Mokra and Bodak (1979)
$Sc_{0.85-0.95}Nd_{0.15-0.05}Si_{1.67}$	AlB_2	3.6644–3.6596		3.8896–3.8860	Kotur et al. (1992), Banakh and Kotur (1998)
Sc_4NdSi_4	Sm_5Ge_4	7.058	13.912	7.361	Kotur et al. (1997a), *Kotur et al. (1992)*
$Sc_{0.2-0.4}Sm_{0.8-0.6}Si$	CrB	4.193–4.200	10.51–10.50	3.846–3.817	*Kotur et al. (1991)*

continued on next page

Table 19, *continued*

Compound	Structure type or symmetry	Lattice parameters			Reference
		a (Å)	*b* (Å)	*c* (Å)	
$Sc_{0.3}Sm_{0.7}Si_2$	$\alpha ThSi_2$	4.049		13.388	*Kotur et al. (1991)*
$ScSm_2Si_2$	Mo_2FeB_2	7.420		4.350	*Kotur et al. (1991)*
ScSmSi	ScCeSi	4.255		15.56	*Kotur et al. (1991)*, Mokra and Bodak (1979)
$Sc_3Sm_2Si_4$	$Ce_2Sc_3Si_4$	7.42	14.21	7.51	Kotur et al. (1991)
$Sc_{0.3}Dy_{0.7}Si_2$	$\alpha ThSi_2$	3.943		13.188	*Kotur et al. (1991)*
$Sc_{0.4-0.7}Dy_{0.6-0.3}Si_{1.67}$	AlB_2	3.762–3.688		4.048–3.929	Kotur et al. (1991)
ScV_5Si_5	Ti_6Ge_5	7.644	16.223	4.971	Kotur (1987)
$Sc_2V_3Si_4$	$Sc_2Re_3Si_4$	6.644		12.270	*Kotur et al. (1986b)*, Kotur (1987)
$Sc_2V_3Si_3$	Mn_5Si_3	7.360		4.997	Kotur et al. (1983a), Kotur (1987)
$Sc_{0.4}Nb_{4.6}Si_3$	W_5Si_3	10.046		5.076	Kotur (1986)
$Sc_2Nb_3Si_4$	$Ce_2Sc_3Si_4$	6.684	13.11	7.010	Kotur (1986)
$Sc_2Cr_4Si_5$	$Nb_2Cr_4Si_5$	7.585	16.138	4.932	*Kotur and Sikirica (1982a)*, Kotur and Bodak (1987)
$Sc_2Cr_3Si_4$	$Sc_2Re_3Si_4$	6.559		12.150	Kotur et al. (1986b), Kotur and Bodak (1987)
$Sc_7Cr_{4.8}Si_{9.2}$	$Sc_7Cr_{4+x}Si_{10-x}$	9.757		13.884	*Kotur et al. (1985a)*, Kotur and Bodak (1987)
$Sc_2Mo_3Si_4$	$Ce_2Sc_3Si_4$	6.536	12.641	6.784	Kotur et al. (1986c), Kotur and Bodak (1988)
$Sc_{2-3}W_{3-2}Si_4$	Sm_5Ge_4	6.537–6.568	12.645–12.734	6.786–6.793	Kotur et al. (1989a)
$ScMnSi_2$	$ZrCrSi_2$	9.077	9.854	7.928	Kotur et al. (1977b, 1980)
$Sc_4Mn_4Si_7$	$Zr_4Co_4Ge_7$	13.06		5.227	Kotur et al. (1977b), *Kotur et al. (1980)*
ScMnSi	ZrNiAl	6.551		3.861	*Kotur et al. (1980)*, Kotur et al. (1977b)
$ScMn_{0.25}Si_{1.75}$	$ZrSi_2$	3.878	14.46	3.776	*Kotur and Bodak (1977)*, Kotur et al. (1980)
$Sc_5Re_8Si_{12}$	$Sc_5Re_8Si_{12}$	14.475	19.66	5.237	*Chabot and Parthé (1987)*
$Sc_2Re_3Si_4$	$Sc_2Re_3Si_4$	6.619		12.36	*Pecharsky et al. (1978)*, Pecharsky (1979)
~$ScReSi_2$	?				Pecharsky (1979)
$Sc_3Re_2Si_4$	$Sc_3Re_2Si_4$	19.567	15.336 $\beta = 125.768°$	13.705	*Chabot and Parthé (1985)*
$Sc_7Re_{3.35}Si_{10.65}$	$Sc_7Re_{4-x}Si_{10+x}$	9.8123		14.274	*Zhao et al. (1988)*
$Sc_{0.35}Fe_{4.65}Si_3$	Mn_5Si_3	6.763		4.718	Gladyshevsky et al. (1977)

continued on next page

Table 19, *continued*

Compound	Structure type or symmetry	Lattice parameters			Reference
		a (Å)	*b* (Å)	*c* (Å)	
$ScFe_{10}Si_2$	$ThMn_{12}$	8.280		4.706	*Bodak et al. (1995)*, Gladyshevsky et al. (1977)
$Sc_{1.2}Fe_4Si_{9.8}$	$Sc_{1.2}Fe_4Si_{9.8}$	3.897		15.160	*Kotur and Bruvo (1991)*, Gladyshevsky et al. (1977)
~$ScFe_5Si_3$	?				Gladyshevsky et al. (1977)
$ScFe_4Si_2$	$ZrFe_4Si_2$	6.947		3.796	Gladyshevsky et al. (1977)
$ScFe_2Si_2$	$HfFe_2Si_2$	7.5002	7.1375	5.0224	*Kotur et al. (1997b)*, Gladyshevsky et al. (1977)
$Sc_2Fe_3Si_5$	$Sc_2Fe_3Si_5$	10.05		5.313	*Bodak et al. (1977)*, Gladyshevsky et al. (1977)
		10.225		5.275	Braun (1980)
$ScFeSi_2$ (I)	$ZrCrSi_2$	8.984	9.739	7.795	Gladyshevsky et al. (1977)
$ScFeSi_2$ (II)	$ScFeSi_2$	5.115	18.929	14.298	*Yarmolyuk et al. (1980)*, Gladyshevsky et al. (1977)
$Sc_4Fe_4Si_7$	$Zr_4Co_4Ge_7$	13.099		5.075	*Chabot et al. (1984)*, Kotur (1983)
$Sc_{1-1.09}Fe_{1.97-1.82}Si_{0.06-0.12}$	$MgCu_2$	7.038[a]			Gladyshevsky et al. (1977)
$ScFe_{1.5-1.42}Si_{0.5-0.58}$	$MgZn_2$	4.962 -		8.079-	Kotur (1977b), Gladyshevsky et al. (1977)
		4.974		8.060	*Kotur et al. (1998)*
$ScFe_{0.25}Si_{1.75}$	$ZrSi_2$	3.861	14.48	3.762	Kotur and Bodak (1977), Gladyshevsky et al. (1977)
Sc_2FeSi_2	Sc_2CoSi_2	9.917	3.984 $\beta = 123.48°$	9.944	Kotur and Sikirica (1983), Gladyshevsky et al. (1977)
ScFeSi	TiNiSi	6.512	3.8391	7.298	*Chabot et al. (1984)*
$Sc_3Fe_2Si_3$	$Hf_3Ni_2Si_3$	3.959	9.960	12.941	*Chabot et al. (1984)*
$Sc_6Co_{30}Si_{19}$	$Sc_6Co_{30}Si_{19}$	14.776		3.613	*Kotur and Sikirica (1991)*, Kotur et al. (1977a)
~$Sc_4Co_{14}Si_9$	*hex*	10.16		3.614	Kotur et al. (1977a)
$Sc_6Co_{16}Si_7$	$Mg_6Cu_{16}Si_7$	11.438			Dwight et al. (1963a), Kotur et al. (1977a)
$ScCo_2Si_2$	$CeGa_2Al_2$	3.7756		9.598	Kotur et al. (1977a, 1989c)
		3.72		9.51	Voroshilov et al. (1967)
$Sc_2Co_3Si_5$	$U_2Co_3Si_5$	9.206	11.26	5.320	Kotur et al. (1977a), *Kotur (1977a)*
$Sc_5Co_4Si_{10}$	$Sc_5Co_4Si_{10}$	12.01		3.936	Kotur et al. (1977a)
		12.041		3.936	*Braun et al. (1980)*

continued on next page

Table 19, *continued*

Compound	Structure type or symmetry	Lattice parameters			Reference
		a (Å)	*b* (Å)	*c* (Å)	
$ScCo_{1.52-1.46}Si_{0.48-0.54}$	$MgZn_2$	4.934–		7.918–	Kotur (1977b), Kotur et al. (1977a)
		4.973		7.830	*Kotur et al. (1998)*
ScCoSi	TiNiSi	6.419	3.953	6.896	Kotur and Bodak (1977), Kotur et al. (1977a)
$ScCo_{0.25}Si_{1.75}$	$ZrSi_2$	3.856	14.54	3.744	*Kotur and Bodak (1977)*, Kotur et al. (1977a)
$Sc_3Co_2Si_3$	$Hf_3Ni_2Si_3$	3.996	9.815	12.67	*Gladyshevsky and Kotur (1978)*, Kotur et al. (1977a)
Sc_2CoSi_2	Sc_2CoSi_2	9.74	3.954 $\beta = 122.6°$	9.82	*Gladyshevsky and Kotur (1978)*, Kotur et al. (1977a)
$Sc_2Co_{0.85}Si_{0.15}$	Ti_2Ni	12.099			Kotur et al. (1977a)
$\sim Sc_2Ni_9Si_9$	?				Bodak et al. (1976)
$Sc_3Ni_{11}Si_4$	$Sc_3Ni_{11}Si_4$	8.024		8.429	*Kotur et al. (1983b)*, Bodak et al. (1976)
$ScNi_2Si_3$	$ScNi_2Si_3$	3.830		23.50	Kotur et al. (1978), Bodak et al. (1976)
$Sc_6Ni_{18}Si_{11}$	$Sc_6Ni_{18}Si_{11}$	17.945	12.223	8.029	*Kotur et al. (1986d)*, Bodak et al. (1976)
$Sc_6Ni_{16}Si_{7-x}$	$Mg_6Cu_{16}Si_7$	11.46			Gladyshevsky et al. (1962), Bodak et al. (1976)
		11.429			Dwight et al. (1963a)
$\sim Sc_2Ni_5Si_3$	?				Bodak et al. (1976)
$ScNi_2Si_2$	$CeGa_2Al_2$	3.8018		9.567	Kotur et al. (1989c), Bodak et al. (1976)
		3.72		9.50	Voroshilov et al. (1967)
$ScNiSi_3$	$ScNiSi_3$	3.815	3.825	20.62	*Kotur et al. (1977c)*, Bodak et al. (1976)
$Sc_3Ni_4Si_4$	$Gd_6Cu_8Ge_8$	12.68	6.38	3.89	Bodak et al. (1976)
$ScNi_{1.52-1.49}Si_{0.48-0.51}$	$MgZn_2$	4.989–		7.730–	Kotur (1977b), Bodak et al. (1976)
		5.000		7.719	Kotur et al. (1998)
ScNiSi	TiNiSi	6.383	4.011	6.868	*Kotur and Bodak (1977)*, Bodak et al. (1976)
$Sc_3Ni_2Si_4$	$Sc_3Ni_2Si_4$	11.678	3.976	11.940	*Zhao and Parthé (1989a)*, Bodak et al. (1976)
$ScNi_{0.25}Si_{1.75}$	$ZrSi_2$	3.843	14.68	3.727	Kotur and Bodak (1977), Bodak et al. (1976)
$Sc_3Ni_2Si_3$	$Hf_3Ni_2Si_3$	3.9812	9.688	13.111	Zhao and Parthé (1989b), Bodak et al. (1976)

continued on next page

Table 19, *continued*

Compound	Structure type or symmetry	Lattice parameters			Reference
		a (Å)	*b* (Å)	*c* (Å)	
Sc_3NiSi_3	Sc_3NiSi_3	9.801	3.974 $\beta = 114.16°$	13.193	*Kotur and Gladyshevsky (1983)*, Bodak et al. (1976)
~$Sc_3Ru_2Si_6$	*orthorh*	8.939	9.061	4.175	Braun and Segre (1980)
ScRuSi	ZrNiAl	6.851		3.423	Hovestreydt et al. (1982)
$ScRh_3Si_7$	$ScRh_3Si_7$	7.5056		19.691	*Chabot et al. (1981b)*, Braun et al. (1979)
~$Sc_3Rh_2Si_9$	?				Braun et al. (1979)
~$Sc_2Rh_3Si_4$	?				Braun et al. (1979)
$ScRhSi_2$	$ScRhSi_2$	6.292	4.025	9.517	*Chabot et al. (1981a)*, Braun et al. (1979)
$Sc_5Rh_4Si_{10}$	$Sc_5Co_4Si_{10}$	12.325		4.032	Braun et al. (1980), Braun et al. (1979)
~$Sc_3Rh_3Si_5$	?				Braun et al. (1979)
~Sc_4RhSi_8	?				Braun et al. (1979)
~$Sc_6Rh_4Si_9$	?				Braun et al. (1979)
ScRhSi	TiNiSi	6.4736	4.0500	7.2483	Hovestreydt et al. (1982)
~$Sc_3Rh_2Si_4$	?	6.543	4.069	7.396	Braun et al. (1979)
ScPdSi	TiNiSi	6.543	4.069	7.396	Hovestreydt et al. (1982)
~$Sc_3Os_2Si_6$	*orthorh*	8.963	9.044	4.195	Braun and Segre (1980)
$ScIr_3Si_7$	$ScRh_3Si_7$	7.5010		19.909	Chabot et al. (1981b)
$Sc_5Ir_4Si_{10}$	$Sc_5Co_4Si_{10}$	12.316		4.076	Braun et al. (1980)
ScIrSi	TiNiSi	6.418	4.036	7.299	Hovestreydt et al. (1982)
$Sc_4Ir_7Si_6$	$U_4Re_7Si_6$	8.003			Engel et al. (1984)
ScPtSi	TiNiSi	6.566	4.130	7.275	Hovestreydt et al. (1982)
$ScCu_2Si_2$	$CeGa_2Al_2$	3.810		10.091	*Kotur (1984)*, Kotur et al. (1985b)
$Sc_3Cu_4Si_4$	$Gd_6Cu_8Ge_8$	13.096	6.411	3.945	Kotur and Bodak (1980), Kotur et al. (1985b)
		13.09	6.42	3.94	Hanel and Nowotny (1970)
ScCuSi (h)	ZrNiAl	6.426		3.922	*Kotur et al. (1981)*, Kotur et al. (1985b)
		6.44		3.92	Dwight et al. (1973)
ScCuSi (r)	TiNiSi	6.566	3.976	7.224	*Kotur et al. (1981)*, Kotur et al. (1985b)
$Sc_2Cu_{0.8}Si_{0.2}$	Ti_2Ni	12.290			Kotur et al. (1985b)
ScAuSi	ScAuSi	4.212		6.803	*Fornasini et al. (1992)*

[a] For the composition $Sc_{1.05}Fe_{1.89}Si_{0.06}$.

content of Ce and Sc within 2 to 4 at.%. These results were partially confirmed by Kotur et al. (1989c) who reported slightly different values for the lattice spacings for two of the ternary compounds, $ScCe_2Si_2$ and ScCeSi (see table 19). The crystal structures of five ternary compounds are still unknown.

3.6.4. *Sc–Pr–Si*

Banakh and Kotur (1997) reported about the Sc–Pr–Si isothermal section at 600°C. However, a figure of the section was not presented in that short communication. Eight ternary compounds occur in the system. Two of them, ScPrSi and ~$ScPr_2Si_2$, had been synthesized earlier by Mokra and Bodak (1979) and Mokra (1979). The crystal structure has been determined for five of these compounds (see table 19).

3.6.5. *Sc–Nd–Si*

Figure 53 shows the isothermal section of the Sc–Nd–Si system at 600°C which was determined by Banakh and Kotur (1998). The binary silicides $NdSi_{2-x}$ and NdSi dissolve 15 and 7 at.% Sc, respectively. The solubility of the third component in other neodymium and scandium binary silicides does not exceed 2 at.%. Five ternary compounds exist in this system (see table 19). One of them, (4) in fig. 53, has variable composition of Sc and Nd. Four other have practically constant composition.

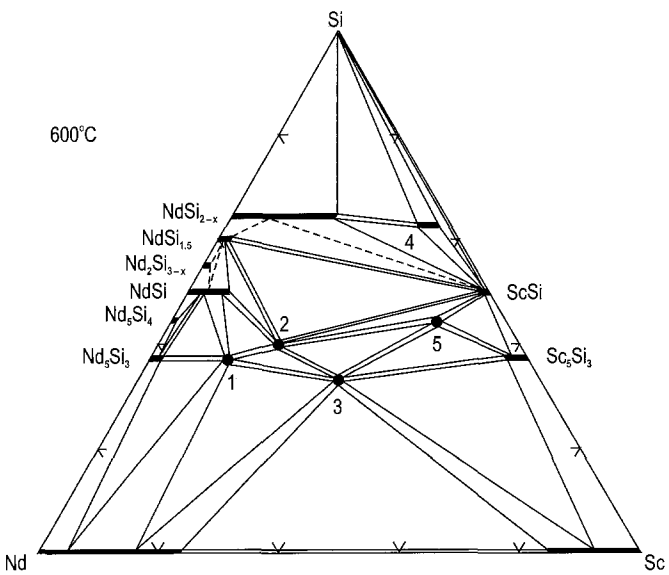

Fig. 53. Sc–Nd–Si, isothermal section at 600°C. Ternary compounds: (1) ~$ScNd_4Si_3$; (2) $ScNd_2Si_2$; (3) ScNdSi; (4) $Sc_{0.85-0.95}Nd_{0.15-0.05}Si_{1.67}$; (5) Sc_4NdSi_4.

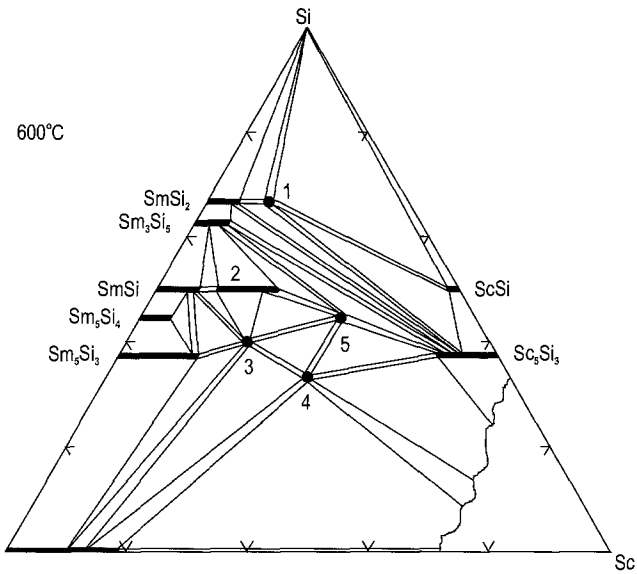

Fig. 54. Sc–Sm–Si, part of the isothermal section at 600°C (0–80 at.% Sc). Ternary compounds: (1) $Sc_{0.3}Sm_{0.7}Si_2$; (2) $Sc_{0.2-0.4}Sm_{0.8-0.6}Si$; (3) $ScSm_2Si_2$; (4) ScSmSi; (5) $Sc_3Sm_2Si_4$.

3.6.6. *Sc–Sm–Si*

Kotur et al. (1991) reported on part of the Sc–Sm–Si isothermal section at 600°C which is shown in fig. 54. All the samarium and scandium binary silicides dissolve different amounts of the third component, from 2 at.% Sm (ScSi compound) up to 13 at.% Sc (Sm_5Si_3 compound). Five ternary compounds exist in the system, and the crystal structure is known for all of them (see table 19).

3.6.7. *Sc–Dy–Si*

The Sc–Dy–Si phase equilibria at 600°C have been investigated by Kotur et al. (1991) (fig. 55). Solid solutions of substitution of Sc and Dy of different extent on the basis of binary silicides occur in the system. DySi dissolve only 1 at.% Sc while the isotypic silicides Sc_5Si_3 and Dy_5Si_3 are completely miscible. The variations of the lattice spacings vs. composition of solid solutions obey Vegard's rule in case of $Sc_{1-x}Dy_xSi$, or show slight deviations from this rule ($Dy_{5-x}Sc_xSi_3$, $Dy_{5-x}Sc_xSi_4$). Two ternary compounds occur in this system (see table 19). One of them also has a variable composition of Sc and Dy.

3.6.8. *Sc–Er–Si*

Kotur and Parasiuk (1994) investigated the Sc–Er–Si isothermal section at 600°C which is depicted in fig. 56. Ternary compounds do not exist in this system. Pairs of isotypic binary silicides, namely ScSi and ErSi, Sc_5Si_3 and Er_5Si_3, form continuous series of solid solutions. $ErSi_{1.67}$ dissolves 32 at.% Sc.

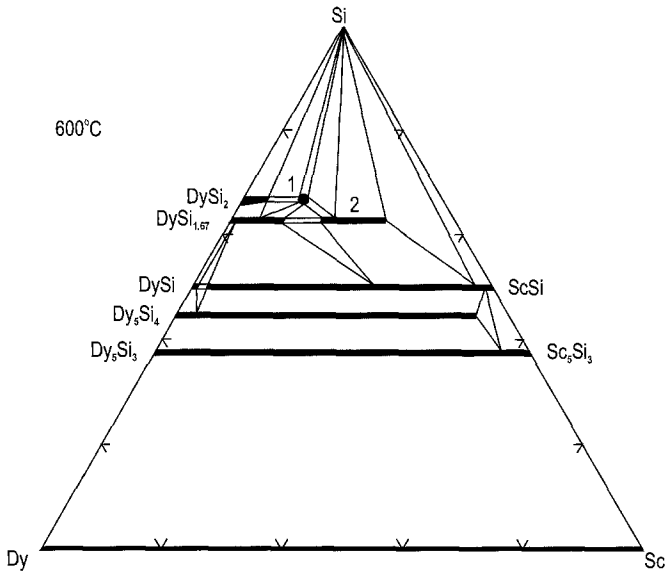

Fig. 55. Sc–Dy–Si, isothermal section at 600°C. Ternary compounds: (1) $Sc_{0.3}Dy_{0.7}Si_2$; (2) $Sc_{0.4-0.7}Dy_{0.6-0.3}Si_{1.67}$.

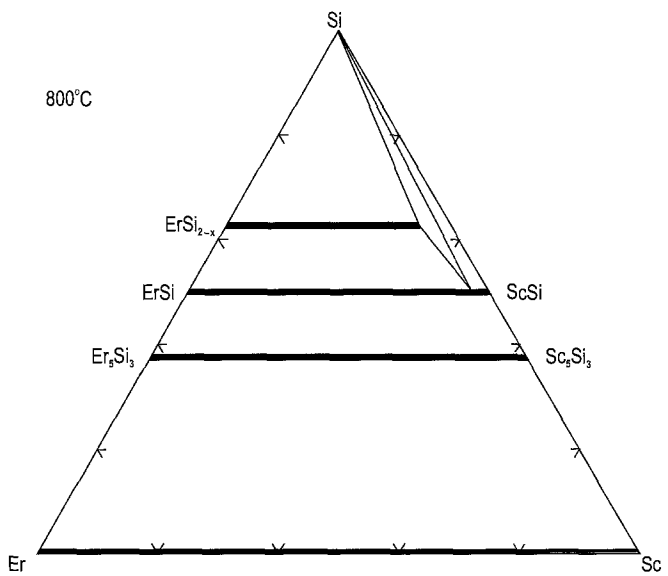

Fig. 56. Sc–Er–Si, isothermal section at 600°C.

3.6.9. *Sc–Lu–Si*

The Sc–Lu–Si isothermal section at 800°C, published by Kotur and Mokra (1994) (see fig. 57), is similar to that of the Sc–Er–Si system. $LuSi_{2-x}$ dissolves 35 at.% Sc.

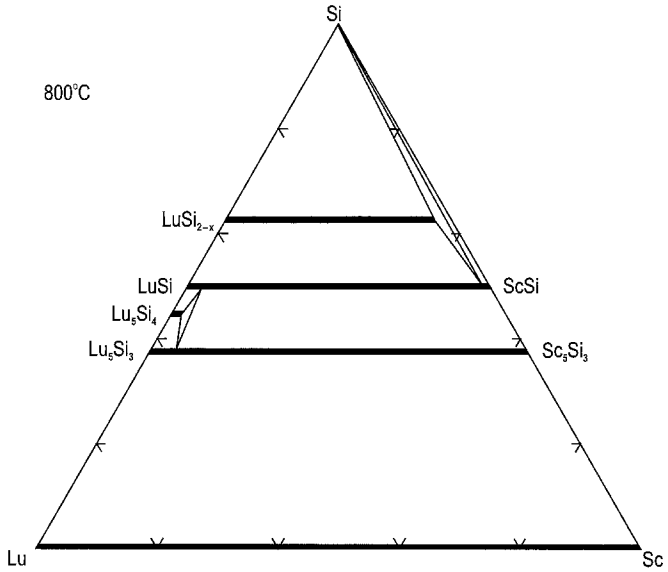

Fig. 57. Sc–Lu–Si, isothermal section at 800°C.

3.6.10. *Sc–Ti–Si, Sc–Zr–Si*

Parts of the isothermal sections of the Sc–Ti–Si and Sc–Zr–Si systems at 800°C were investigated by Kotur et al. (1989b) and are displayed in fig. 58. The phase equilibria are quite similar in both systems; no ternary compounds were observed. The binary silicides TiSi, $TiSi_2$, ZrSi and $ZrSi_2$ dissolve 12, 10, 22 and 11 at.% Sc, respectively. Scandium monosilicide dissolves 9 at.% Ti or 15 at.% Zr.

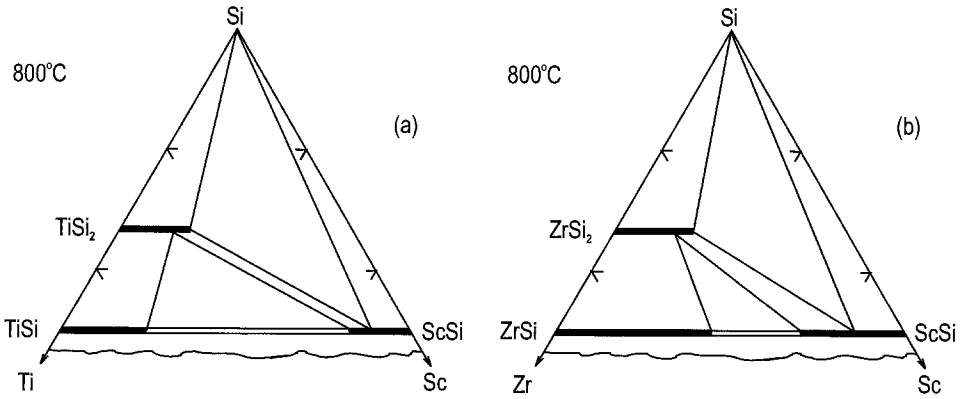

Fig. 58. (a) Sc–Ti–Si, and (b) Sc–Zr–Si parts of the isothermal sections at 800°C (50–100 at.% Si).

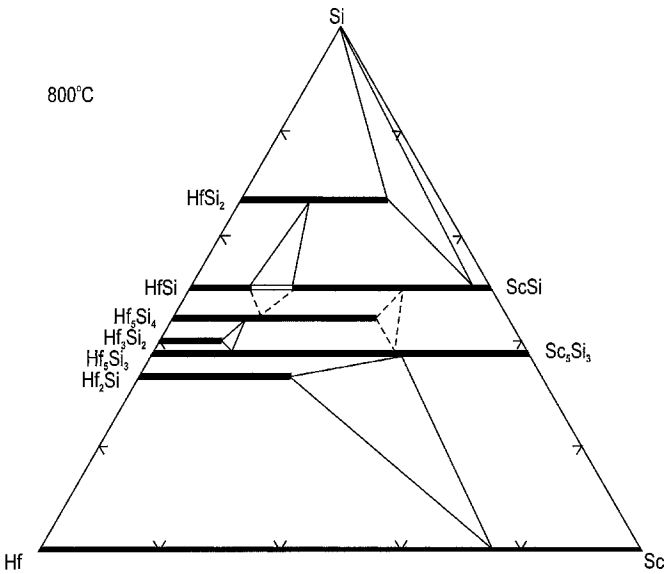

Fig. 59. Sc–Hf–Si, isothermal section at 800°C.

3.6.11. *Sc–Hf–Si*

Kotur et al. (1989b) reported on a part of the Sc–Hf–Si isothermal section at 800°C (50–100 at.% Si). Later Kotur and Ratush (1991) investigated the isothermal section over the whole concentration region (see fig. 59). No ternary compounds exist in this system. The hafnium silicides Hf_2Si, Hf_3Si_2, Hf_5Si_4, HfSi and $HfSi_2$ dissolve 25, 10, 33, 10 and 24 at.% Sc, respectively. ScSi dissolves 33 at.% Hf. Continuous series of solid solutions occur between the isotypic silicides Hf_5Si_3 and Sc_5Si_3. The variations of the lattice spacings of these solid solutions were measured by Kotur and Ratush.

3.6.12. *Sc–V–Si*

Kotur et al. (1983a) investigated alloys of the section Sc_5Si_3–V_5Si_3, and later Kotur (1987) published the phase equilibria at 800°C for the whole concentration range (fig. 60). Three ternary compounds were synthesized and their crystal structures determined (see table 19). One of the compounds, namely ScV_5Si_5, has variable content of Sc and V within 2 at.%.

3.6.13. *Sc–Nb–Si*

The Sc–Nb–Si isothermal section at 800°C presented in fig. 61 has been reported by Kotur (1986). Solid solution of substitution $Sc_{5-1.5}Nb_{0-3.5}Si_3$ occurs in the system. The variation of the lattice parameters show negative deviation from Vegard's rule. Other binary scandium and niobium silicides do not dissolve the third component. Two ternary compounds exist in the system. Probably $Sc_{0.4}Nb_{4.6}Si_3$ is a solid solution of the binary

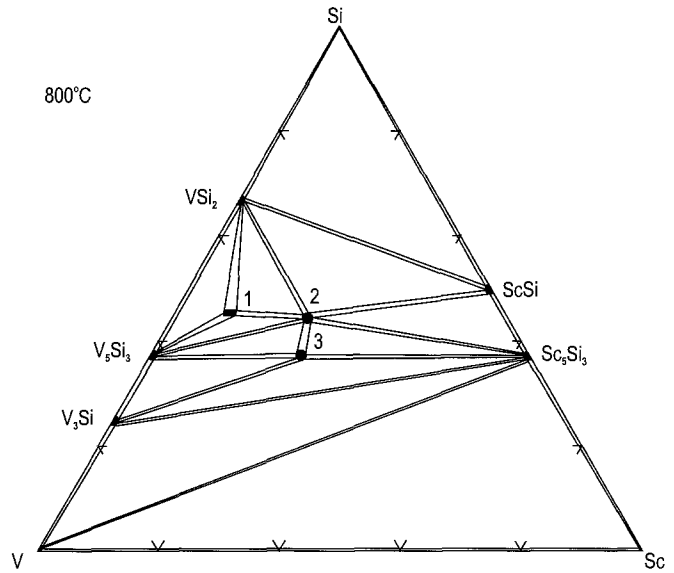

Fig. 60. Sc–V–Si, isothermal section at 800°C. Ternary compounds: (1) ScV_5Si_5; (2) $Sc_2V_3Si_4$; (3) $Sc_2V_3Si_3$.

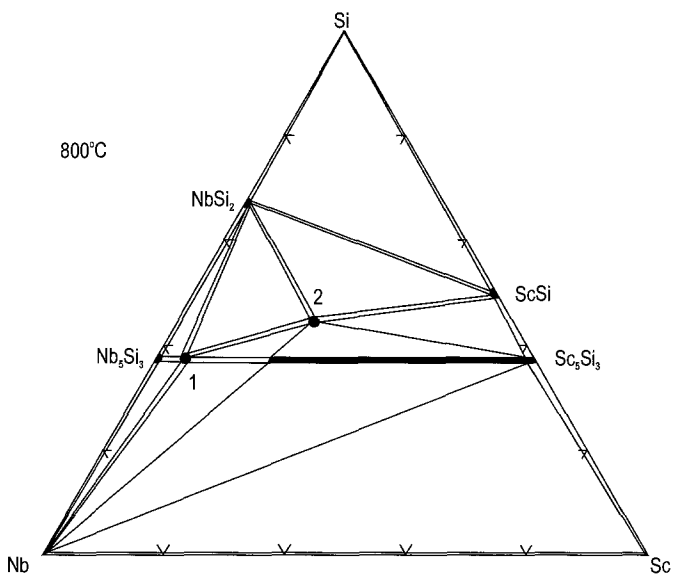

Fig. 61. Sc–Nb–Si, isothermal section at 800°C. Ternary compounds: (1) $Sc_{0.4}Nb_{4.6}Si_3$; (2) $Sc_2Nb_3Si_4$.

βNb_5Si_3 compound (which occurs in the Nb–Si system in the temperature range 2480–2000°C) stabilized by scandium.

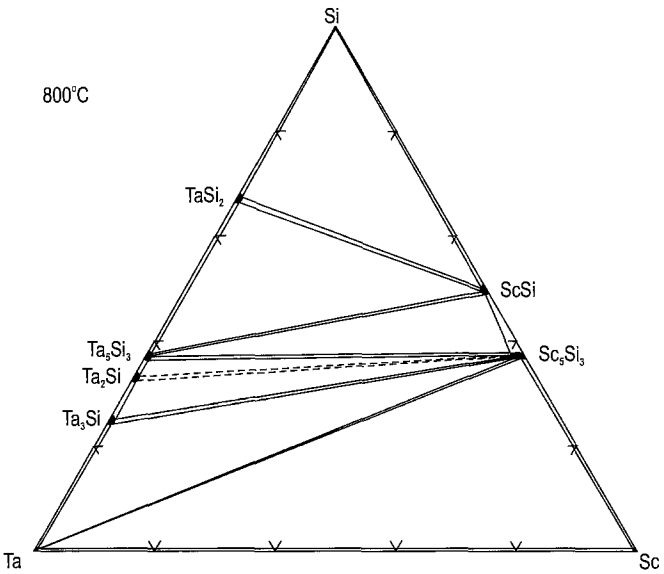

Fig. 62. Sc–Ta–Si, isothermal section at 800°C.

3.6.14. *Sc–Ta–Si*

Figure 62 displays the isothermal section of the Sc–Ta–Si system at 800°C reported by Kotur and Bodak (1990). Binary tantalum and scandium silicides (except Sc_5Si_3) practically do not dissolve the third component. Sc_5Si_3dissolves less than 2 at.% Ta. No ternary compounds were observed.

3.6.15. *Sc–Cr–Si*

Kotur and Bodak (1987) investigated the Sc–Cr–Si isothermal section at 800°C (see fig. 63). The scandium silicide Sc_5Si_3 dissolves up to 2 at.% Cr. Three ternary compounds were synthesized and their crystal structures determined, the data are given in table 19.

3.6.16. *Sc–Mo–Si*

The Sc–Mo–Si isothermal section at 800°C, which is based on the data of Kotur and Bodak (1988), is displayed in fig. 64. Only one binary compound, namely Sc_5Si_3, dissolves the third component: 25 at.% Mo. The lattice spacings change linearly within the homogeneity range of the solid solution. One ternary compound exists in this system, its crystal structure data are given in table 19.

3.6.17. *Sc–W–Si*

The phase equilibria of the Sc–W–Si system at 800°C presented in fig. 65 are similar to those of Sc–Mo–Si system (Kotur et al., 1989a). The solubility of W in Sc_5Si_3 is about

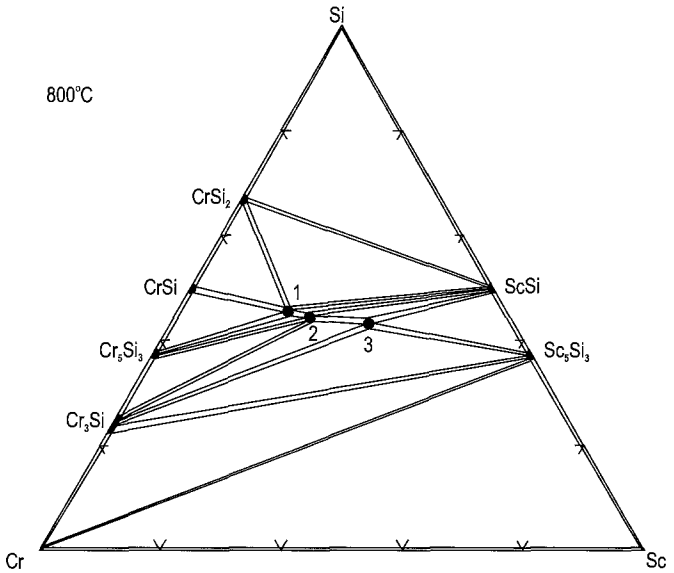

Fig. 63. Sc–Cr–Si, isothermal section at 800°C. Ternary compounds: (1) $ScCr_4Si_5$; (2) $Sc_2Cr_3Si_4$; (3) $Sc_7Cr_{4.8}Si_{9.2}$.

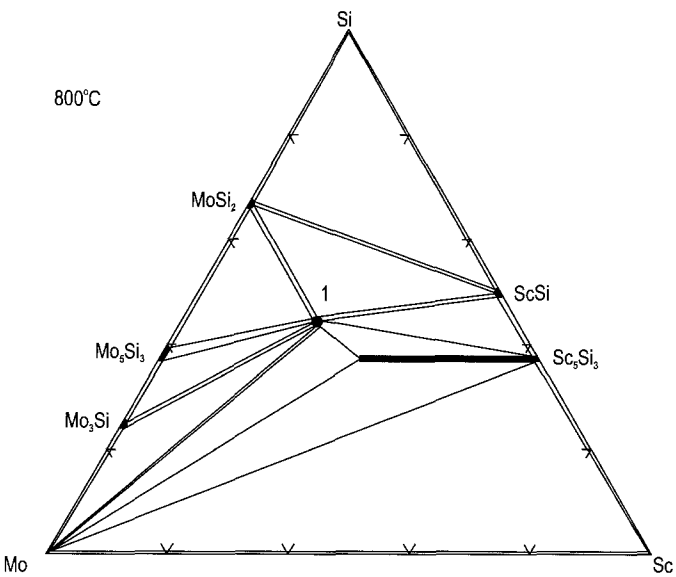

Fig. 64. Sc–Mo–Si, isothermal section at 800°C. Ternary compound: (1) $Sc_2Mo_3Si_4$.

4 at.%. The single ternary compound has variable content of Sc and W; it is isotypic with Sm_5Ge_4 (table 19).

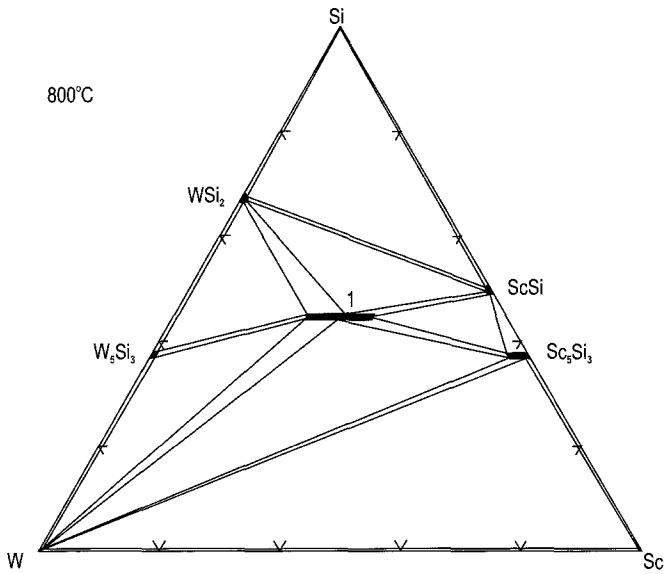

Fig. 65. Sc–W–Si, isothermal section at 800°C. Ternary compound: (1) $Sc_{2-3}W_{3-2}Si_4$.

3.6.18. *Sc–Mn–Si*

Kotur et al. (1977b, 1980) reported on a part of the Sc–Mn–Si isothermal section at 800°C. A figure of this section is available in the review of Rogl (1984b). Among the binary compounds only $ScMn_2$ dissolves up to 20 at.% Si; the lattice parameters of this solid solution obey Vegard's rule within the homogeneity range. Four ternary compounds of constant compositions occur in this system, the crystal structures of all of them are known (see table 19).

3.6.19. *Sc–Re–Si*

Pecharsky (1979) and Bodak et al. (1981) each reported about parts of the phase equilibria of the Sc–Re–Si system at 800°C namely in the ranges 0–66.7 at.% Sc and 0–33.3 at.% Sc, respectively. $ScRe_2$ dissolves about 21 at.% Si. The lattice parameters of the solid solution decrease linearly (from $a = 5.28$, $c = 8.58$ to $a = 5.17$, $c = 8.39$ Å) within the homogeneity range. Five ternary compounds were synthesized and the crystal structures of three of them: $Sc_2Re_3Si_4$, $ScRe_2Si_3$ and $Sc_3Re_2Si_3$ were determined by Pecharsky et al. (1978, 1979). The structures of the two other $ScReSi_2$ and ~$Sc_8Re_3Si_9$ were not reported. The single crystal investigation of Chabot and Parthé (1985) did not confirm the existence of compound "$Sc_3Re_2Si_3$" at 800°C, it revealed a composition of $Sc_3Re_2Si_4$. As a result of precised single crystal investigations the compositions and crystal structures of two other compounds were refined: "$ScRe_2Si_3$" to $Sc_5Re_8Si_{12}$ (Chabot and Parthé, 1987) and "$Sc_8Re_3Si_9$" to $Sc_7Re_{3.35}Si_{10.65}$ (Zhao et al., 1988). The crystal structure data of these compounds are presented in table 19. A modified isothermal section at 800°C with the

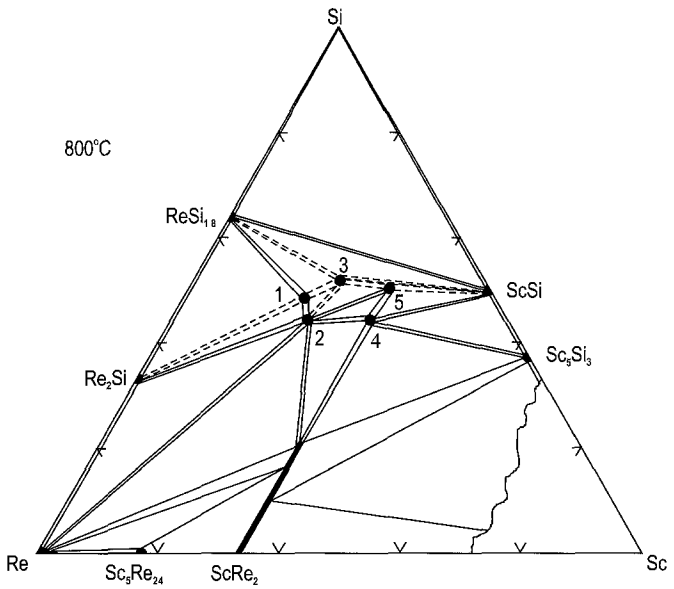

Fig. 66. Sc–Re–Si, part of the isothermal section at 800°C (0–66.7 at.% Sc). Ternary compounds: (1) $Sc_5Re_8Si_{12}$; (2) $Sc_2Re_3Si_4$; (3) ~$ScReSi_2$; (4) $Sc_3Re_2Si_4$; (5) $Sc_7Re_{3.35}Si_{10.65}$.

corrected compositions of the ternary compounds and corrections concerning the binary Re–Si system (according to the data of Massalski 1990) is shown in fig. 66.

3.6.20. *Sc–Fe–Si*

The isothermal section at 800°C presented in fig. 67 has been investigated by Gladyshevsky et al. (1977). Fourteen ternary compounds occur at that temperature in the system. Twelve of them have a constant composition. The composition of three compounds were refined afterwards: "$Sc_3Fe_2Si_6$" to $ScFeSi_2$(II) (Yarmolyuk et al., 1980), "$Sc_3Fe_3Si_4$" to $Sc_4Fe_4Si_7$ (Chabot et al. (1984) and Kotur (1983) independently), and "$ScFe_3Si_6$" to $Sc_{1.2}Fe_4Si_{9.8}$ (Kotur and Bruvo 1991). It is interesting to mention the existence of the ternary compound $ScFeSi_2$(I), which is in two-phase equilibria at 800°C with the ternary compounds $ScFeSi_2$(II), $Sc_2Fe_3Si_5$ and $Sc_4Fe_4Si_7$. Possibly the composition of the silicide $ScFeSi_2$(I) is slightly shifted from the ideal stoichiometry; additional investigations are necessary to clarify this. Chabot et al. (1984) also found two other ternary compounds $Sc_3Fe_2Si_3$ and ScFeSi in the as-cast alloys and confirmed the results published by Kotur and Sikirica (1983) concerning the Sc_2FeSi_2 compound. The phase equilibria presented in fig. 67 include all the corrections mentioned above. The crystal structure data of the ternary compounds are summarized in table 19. A recently performed X-ray structure analysis of compound 12 in fig. 67 conducted by Kotur et al. (1998) revealed that this compound does not crystallize in a superstructure of the Mg_2Cu_3Si-type as reported earlier by Gladyshevsky et al. (1977) and Kotur (1977b), but shows a random distribution

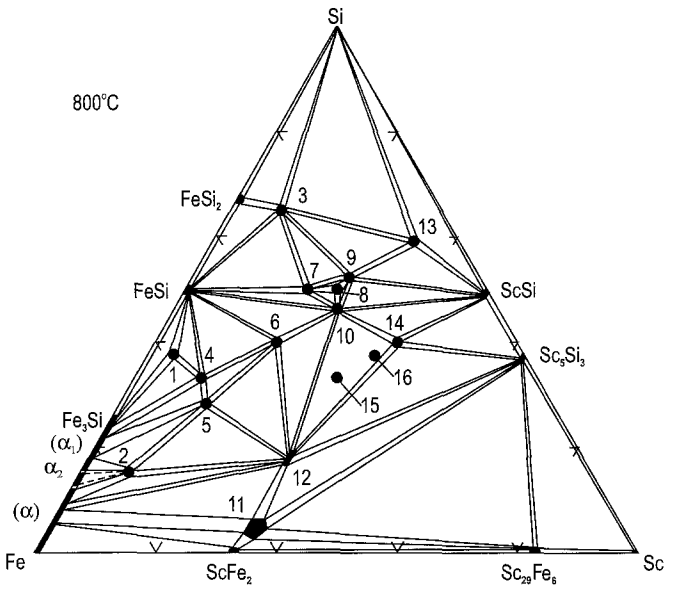

Fig. 67. Sc–Fe–Si, isothermal section at 800°C. Ternary compounds: (1) $Sc_{0.35}Fe_{4.65}Si_3$; (2) $ScFe_{10}Si_2$; (3) $Sc_{1.2}Fe_4Si_{9.8}$; (4) ~$ScFe_5Si_3$; (5) $ScFe_4Si_2$; (6) $ScFe_2Si_2$; (7) $Sc_2Fe_3Si_5$; (8) $ScFeSi_2$(I); (9) $ScFeSi_2$(II); (10) $Sc_4Fe_4Si_7$; (11) $Sc_{1-1.09}Fe_{1.97-1.82}Si_{0.06-0.12}$; (12) $ScFe_{1.5-1.42}Si_{0.5-0.58}$; (13) $ScFe_{0.25}Si_{1.75}$; (14) Sc_2FeSi_2; (15) ScFeSi; (16) $Sc_3Fe_2Si_3$.

of Fe and Si atoms on the two crystallographic sites in the $MgZn_2$-type structure. For that reason the composition is $ScFe_{1.5}Si_{0.5}$, and not Sc_2Fe_3Si as in the earlier publications.

3.6.21. *Sc–Co–Si*

Figure 68 presents the Sc–Co–Si isothermal section at 800°C (and a part of it at 700°C) investigated by Kotur et al. (1977a). $ScCo_2$ dissolves 6 at.% Si. The lattice parameter a of this solid solution increases linearly from 6.911 to 6.920 Å within the alloys on the isoconcentrate of 33.3 at.% Sc (Kotur 1977a). Kotur et al. confirmed the occurrence of two ternary compounds $ScCo_2Si_2$ and $Sc_6Co_{16}Si_7$ and synthesized ten new ternary silicides (see table 19). In the later papers the compositions of two ternary compounds have been refined: "$ScCo_7Si_4$" to $Sc_6Co_{30}Si_{19}$ (Kotur and Sikirica 1991), and "$Sc_3Co_2Si_5$" to $Sc_5Co_4Si_{10}$ (Braun et al. 1980). The phase equilibria shown in fig. 68 include all these refinements. Kotur et al. (1998) corrected the crystal structure of compound 7 in fig. 68 to the $MgZn_2$-type instead of the superstructure Mg_2Cu_3Si-type as reported earlier (see Kotur 1977b). The compound $Sc_2Co_{0.85}Si_{0.15}$ exists only in alloys annealed at 800°C; perhaps it is formed by a solid-state phase reaction.

3.6.22. *Sc–Ni–Si*

In a systematic investigation of the Sc–Ni–Si phase equilibria at 800°C in the range 0–70 at.% Sc performed by Bodak et al. (1976) fifteen ternary compounds have been

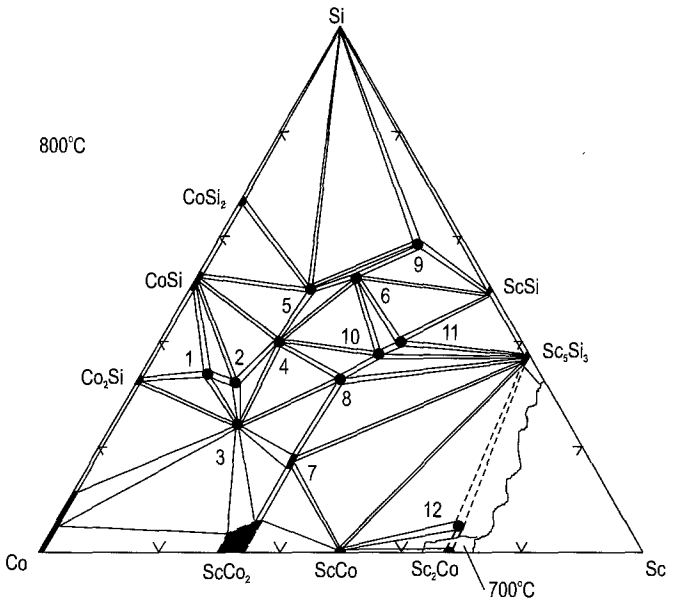

Fig. 68. Sc–Co–Si, part of the isothermal sections at 800°C and at 700°C (0–70 at.% Sc). Ternary compounds: (1) $Sc_6Co_{30}Si_{19}$; (2) ~$Sc_4Co_{14}Si_9$; (3) $Sc_6Co_{16}Si_7$; (4) $ScCo_2Si_2$; (5) $Sc_2Co_3Si_5$; (6) $Sc_5Co_4Si_{10}$; (7) $ScCo_{1.52-1.46}Si_{0.48-0.54}$; (8) ScCoSi; (9) $ScCo_{0.25}Si_{1.75}$; (10) $Sc_3Co_2Si_3$; (11) Sc_2CoSi_2; (12) $Sc_2Co_{0.85}Si_{0.15}$.

synthesized (fig. 69); two of these ternary compounds, namely $ScNi_2Si_2$ and $Sc_6Ni_{16}Si_7$ had been known earlier (see table 19). Further investigations revealed a change of the compositions of six ternary compounds observed by Bodak et al.: (2) "$Sc_{15}Ni_{62.5}Si_{22.5}$" (Kotur et al. 1983b), (3) "$Sc_{17.5}Ni_{30}Si_{52.5}$" (Kotur et al. 1978), (4) "$Sc_{15}Ni_{50}Si_{35}$" (Kotur et al. 1986d), (12) "$Sc_{35}Ni_{20}Si_{45}$" (Zhao and Parthé 1989a,b), (13) "$Sc_{32}Ni_8Si_{60}$" (Kotur and Bodak 1977), (15) "$Sc_{44}Ni_{12}Si_{44}$" (Kotur and Gladyshevsky 1983). Their crystal structure data can be found in table 19. The phase equilibria at 800°C are presented in fig. 69 assuming these refinements. The binary $ScNi_2$ compound dissolves a large amount of the third component: about 7 at.% Si. The lattice spacing of the solid solution increases linearly from $a = 6.901$ to 6.909 Å (Kotur 1977a). Other Sc–Ni binary compounds dissolve less than 2 to 3 at.% Si.

3.6.23. *Sc–Ru–Si*

No data are known about the phase equilibria occurring in the Sc–Ru–Si system. Only two ternary compounds have been synthesized and their crystal structures investigated (see table 19).

3.6.24. *Sc–Rh–Si*

Braun et al. (1979) investigated a part of the Sc–Rh–Si isothermal section at 1000°C (44–100 at.% Si); the figure can be found in Rogl (1984b). Nine ternary compounds

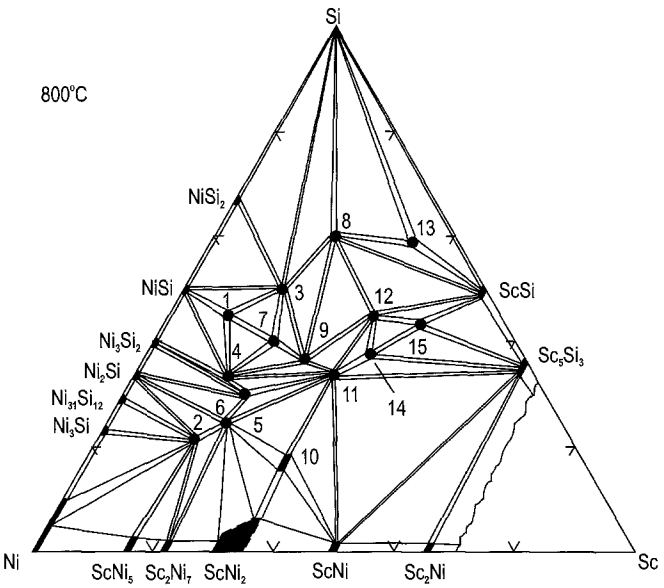

Fig. 69. Sc–Ni–Si, part of the isothermal section at 800°C (0–70 at.% Sc). Ternary compounds: (1) ~$Sc_2Ni_9Si_9$; (2) $Sc_3Ni_{11}Si_4$; (3) $ScNi_2Si_3$; (4) $Sc_6Ni_{18}Si_{11}$; (5) $Sc_6Ni_{16}Si_7$; (6) ~$Sc_2Ni_5Si_3$; (7) $ScNi_2Si_2$; (8) $ScNiSi_3$; (9) $Sc_3Ni_4Si_4$; (10) $ScNi_{1.52-1.49}Si_{0.48-0.51}$; (11) ScNiSi; (12) $Sc_3Ni_2Si_4$; (13) $ScNi_{0.25}Si_{1.75}$; (14) $Sc_3Ni_2Si_3$; (15) Sc_3NiSi_3.

were observed. Hovestreydt et al. (1982) reported about the existence of another one, ScRhSi. Chabot et al. (1981b) refined the composition of the "$ScRh_3Si_6$" compound to $ScRh_3Si_7$ and determined its crystal structure. But the proper compositions and the crystal structures of six other ternary compounds remain still unknown (see table 19). Braun et al. also investigated a part of the phase equilibria at 800 and 1150°C. These investigations revealed that $ScRhSi_2$ is not in equilibrium with Si at 1150°C, and the ternary compound $Sc_5Rh_4Si_{10}$ does not exist at 800°C; furthermore it is shown that the silicides Sc_4RhSi_8 and $ScRhSi_2$ are in equilibrium.

3.6.25. *Sc–Pd(Os, Ir, Pt)–Si*

There are no literature data about the phase equilibria of the Sc–Pd(Os, Ir, Pt)–Si systems. Only one ternary compound within each system (except Sc–Ir–Si) were observed by the examination of separate alloys for isotypic compounds existing in related ternary systems. In the Sc–Ir–Si system four ternary compounds were obtained. Their compositions and the crystal structure data are collected in table 19.

3.6.26. *Sc–Cu–Si*

According to the investigation of Kotur et al. (1985b) there are insignificant differences in the phase equilibria at 600 and 800°C of the Sc–Cu–Si system (see fig. 70). Five ternary compounds occur in the system. Two of them, $Sc_3Cu_4Si_4$ and ScCuSi(h), had been known

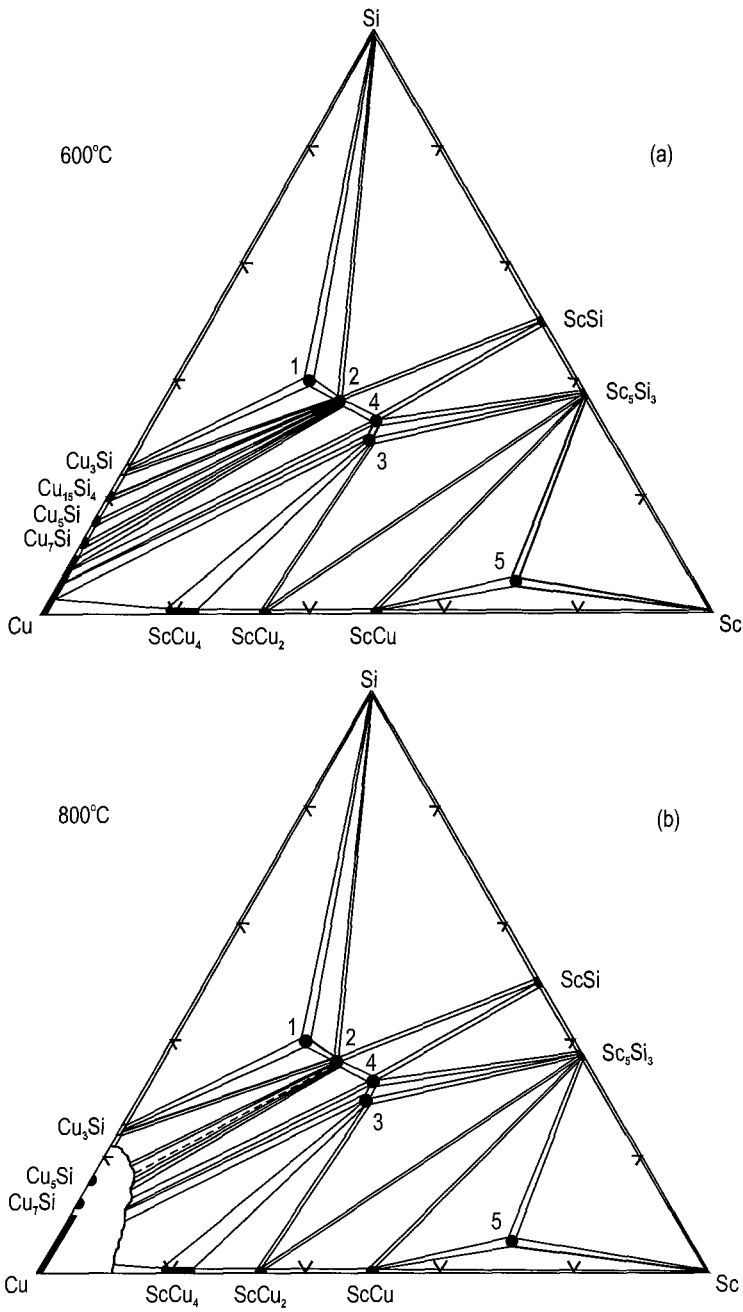

Fig. 70. Sc–Cu–Si, isothermal sections at (a) 600°C and (b) 800°C. Ternary compounds: (1) $ScCu_2Si_2$; (2) $Sc_3Cu_4Si_4$; (3) ScCuSi(h); (4) ScCuSi(r); (5) $Sc_2Cu_{0.8}Si_{0.2}$.

earlier. The crystal structures are established for all compounds (see table 19). Two ternary phases ScCuSi(h) and $Sc_2Cu_{0.8}Si_{0.2}$ appear only after a long-term homogenization of alloys, whereas three other ternary silicides were observed also in the as-cast alloys. Two ternary compounds with compositions close to equiatomic coexist in the system (Kotur et al. 1981). They are separated by a narrow two-phase region, thus a detailed investigation is necessary to find out their proper compositions.

3.6.27. *Sc–Ag–Si*

No ternary compound was observed by Kotur and Boichuk (1988) in the Sc–Ag–Si isothermal section at 600°C, which is shown in fig. 71. These results agree with those of Iandelli (1985), who investigated the alloy of equiatomic composition and established the existence of two phases.

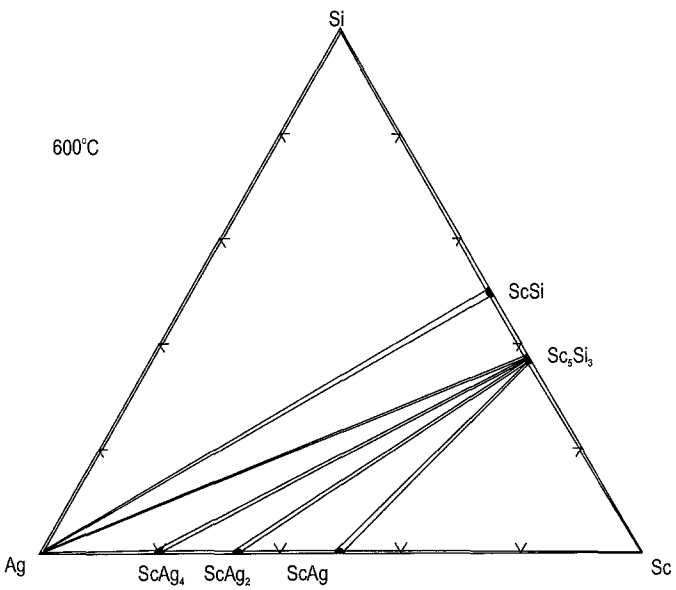

Fig. 71. Sc–Ag–Si, isothermal section at 600°C.

3.6.28. *Sc–Au–Si*

One ternary compound ScAuSi has been synthesized and its crystal structure was determined by Fornasini et al. (1992) (see table 19). There are no data about the phase equilibria in this system.

3.7. *Sc–M–Ge ternary systems*

3.7.1. *Sc–Li–Ge*

The only data about the Sc–Li–Ge system concerns the ScLiGe ternary compound. Its crystal structure is presented in table 20 (overleaf). The phase diagram is unknown.

3.7.2. *Sc–Y–Ge*

Shpyrka and Mokra (1991) published the isothermal section of the Sc–Y–Ge system at 600°C, which is shown in fig. 72. A continuous series of solid solutions occur between the isotypic binary compounds Sc_5Si_3 and Y_5Si_3. Other binary germanides $ScGe_2$, $Sc_{11}Ge_{10}$, Y_2Ge_3 dissolve 18, 8, and 10 at.% Y or Sc, respectively. Three ternary compounds have been found. The crystal structures were determined for two compounds (see table 20).

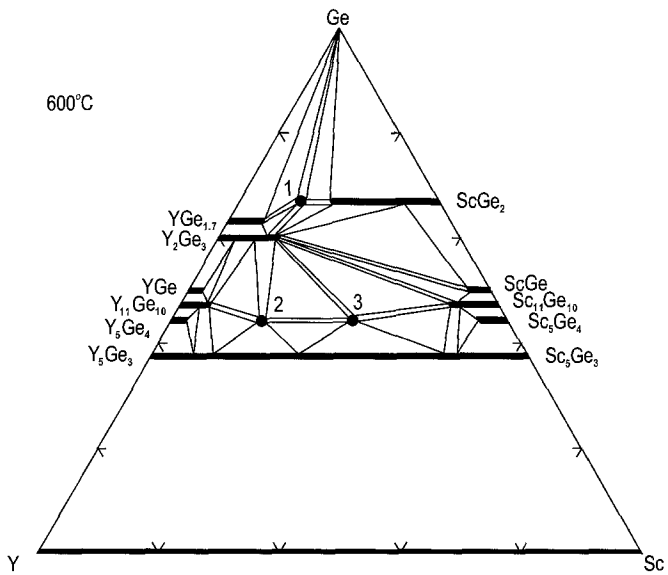

Fig. 72. Sc–Y–Ge, isothermal section at 600°C. Ternary compounds: (1) $Sc_{0.3}Y_{0.7}Ge_2$; (2) $Sc_{1.35}Y_{3.65}Ge_4$; (3) $Sc_{2.7}Y_{2.3}Ge_4$.

3.7.3. *Sc–La–Ge*

Two Sc–La–Ge ternary compounds were synthesized, and their crystal structure data are given in table 20. There are no published data concerning the phase equilibria in this system.

3.7.4. *Sc–Ce–Ge*

Bodak and Kokhan (1983) investigated the Sc–Ce–Ge isothermal section at 600°C; fig. 73 is based on these data. Four ternary compounds exist in this system; the crystal structures

Table 20
Intermetallic compounds in the Sc–M–Ge ternary systems

Compound	Structure type or symmetry	Lattice parameters			Reference
		a (Å)	*b* (Å)	*c* (Å)	
ScLiGe	MgAgAs	6.407			Grund (1985)
~$Sc_{0.3}Y_{0.7}Ge_2$	?				Shpyrka and Mokra (1991)
$Sc_{1.35}Y_{3.65}Ge_4$	Sm_5Ge_4	7.440	14.31	7.578	Shpyrka and Mokra (1991)
$Sc_{2.7}Y_{2.3}Ge_4$	Sm_5Ge_4	7.283	14.18	7.461	Shpyrka and Mokra (1991)
ScLaGe	ScCeSi	4.351		16.067	Bodak and Kokhan (1983)
$Sc_3La_{1.22}Ge_4$	$Ce_2Sc_3Si_4$	7.252	14.350	7.652	Shpyrka (1990)
~$Sc_2Ce_5Ge_6$	?				Bodak and Kokhan (1983)
ScCeGe	ScCeSi	4.314		15.91	Bodak and Kokhan (1983)
$Sc_3Ce_{1.22}Ge_4$	$Ce_2Sc_3Si_4$	7.188	13.99	7.416	Shpyrka (1990), Bodak and Kokhan (1983)
~$Sc_{4.5}Ce_{0.5}Ge_4$	?				Bodak and Kokhan (1983)
ScPrGe	ScCeSi	4.325		15.874	Bodak and Kokhan (1983)
$Sc_3Pr_{1.22}Ge_4$	$Ce_2Sc_3Si_3$	7.116	14.059	7.576	Shpyrka (1990)
~$Sc_2Nd_5Ge_6$	?				Shpyrka (1990)
ScNdGe	ScCeSi	4.3106		15.823	Bodak and Kokhan (1983), Shpyrka (1990)
		4.3022		15.788	Bodak et al. (1997)
$Sc_3Nd_{1.22}Ge_4$	$Ce_2Sc_3Si_4$	7.119	14.065	7.574	Shpyrka (1990)
		7.204	13.925	7.474	Bodak et al. (1997)
ScSmGe	ScCeSi	4.264		15.623	Bodak and Kokhan (1983)
$Sc_3Sm_{1.22}Ge_4$	$Ce_2Sc_3Si_4$	7.102	14.020	7.546	Shpyrka (1990)
ScEuGe	ScCeSi	4.270		15.636	Shpyrka (1990)
~$Sc_{0.3}Dy_{0.7}Ge_2$	?				Shpyrka and Mokra (1991)
$Sc_{1.8}Dy_{3.2}Ge_4$	Sm_5Ge_4	7.346	14.295	7.555	Shpyrka and Mokra (1991)
$Sc_{2.7}Dy_{2.3}Ge_4$	Sm_5Ge_4	7.260	14.151	7.477	Shpyrka and Mokra (1991)
~$Sc_{0.3}Yb_{0.7}Ge_2$	?				Kotur and Mokra (1995)
$Sc_6Yb_5Ge_{10}$	$Ho_{11}Ge_{10}$	10.505		15.87	Kotur et al. (1996b)b*; Kotur and Mokra (1995)
$Sc_{1-1.8}V_{5-4.2}Ge_5$	Ti_6Ge_5	7.782–7.890	16.59–16.73	5.091–5.157	Kotur (1987)
$Sc_2V_3Ge_4$	$Ce_2Sc_3Si_4$	6.614	12.774	6.776	*Kotur et al. (1986c)*, Kotur (1987)
$Sc_2Nb_3Ge_4$	$Ce_2Sc_3Si_4$	6.860	13.39	7.160	Kotur (1986)
$Sc_{2-3}Ta_{3-2}Ge_4$	Sm_5Ge_4	6.823–6.855	13.177–13.230	6.977–6.993	Kotur and Bodak (1990)
$ScCr_6Ge_6$	$HfFe_6Ge_6$	5.101		8.229	*Andrusyak (1986)*, Kotur et al. (1988b)
$Sc_2Cr_4Ge_5$	$Nb_2Cr_4Si_5$	7.821	16.662	5.146	Kotur et al. (1988b)

continued on next page

Table 20, *continued*

Compound	Structure type or symmetry	Lattice parameters			Reference
		a (Å)	*b* (Å)	*c* (Å)	
$ScCrGe_2$	$ZrCrSi_2$	9.390	10.142	8.135	Kotur et al. (1988b)
		9.37	10.09	8.13	Venturini et al. (1985)
$Sc_7Cr_{5.2}Ge_{8.8}$	$Sc_7Cr_{4+x}Si_{10-x}$	10.150		14.352	Kotur et al. (1988a,b)
$Sc_{2-4}Mo_{3-1}Ge_4$	Sm_5Ge_4	6.691–6.813	12.872–13.285	6.905–7.027	Kotur and Bodak (1988)
$ScMn_6Ge_6$	$HfFe_6Ge_6$	5.176		8.099	Andrusyak (1986), Andrusyak and Kotur (1991)
$ScMn_6Ge_4$	$ZrFe_6Ge_4$	5.066		20.013	Kotur (1995), Andrusyak and Kotur (1991)
~$Sc_5Mn_7Ge_8$	?				Andrusyak and Kotur (1991)
$ScMnGe_2$	$ZrCrSi_2$	9.342	10.191	8.083	Andrusyak and Kotur (1991)
		9.30	10.13	8.06	Meyer et al. (1983)
ScMnGe	ZrNiAl	6.677		3.946	Kotur and Andrusyak (1984a), Andrusyak and Kotur (1991)
$Sc_7Mn_{5.3}Ge_{8.7}$	$Sc_7Cr_{4+x}Si_{10-x}$	9.951		14.168	*Kotur et al. (1988a),* Andrusyak and Kotur (1991)
$ScReGe_2$	$ZrCrSi_2$	9.385	10.173	8.323	Kotur (1995)
		9.39	10.17	8.32	Venturini et al. (1985)
$ScFe_6Ge_6$	$HfFe_6Ge_6$	5.062		8.056	Andrusyak (1986)
		5.069		8.077	Andrusyak and Kotur (1991)
$ScFe_6Ge_5$	$ScFe_6Ge_5$	5.0631		44.11	*Kotur (1995),* Andrusyak and Kotur (1991)
$ScFe_6Ge_4$	$ZrFe_6Ge_4$	5.066		20.013	Kotur (1995), Andrusyak and Kotur (1991)
$ScFeGe_2$	$ZrCrSi_2$	9.227	10.098	8.263	Andrusyak and Kotur (1991)
		9.22	10.09	8.00	Venturini et al. (1985)
$Sc_4Fe_4Ge_{6.6}$	$Zr_4Co_4Ge_7$	13.296		5.235	*Andrusyak and Kotur (1989),* Andrusyak and Kotur (1991)
$Sc_{1-1.17}Fe_{1.94-1.70}Ge_{0.06-0.30}$	$MgCu_2$	7.060[a]			Andrusyak and Kotur (1991)
$ScFe_{1.5}Ge_{0.5}$	$MgZn_2$	5.006		8.147	Andrusyak and Kotur (1991)
ScFeGe	ZrNiAl	6.547		3.895	Kotur and Andrusyak (1984a), Andrusyak and Kotur (1991)
$ScCo_6Ge_6$	$HfFe_6Ge_6$	5.064		7.778	Andrusyak (1986), Kotur and Andrusyak (1991)
		5.056		7.799	Buchholz and Schuster (1981)
~$Sc_4Co_{11}Ge_5$	?				Kotur and Andrusyak (1991)
$Sc_4Co_7Ge_6$	$U_4Re_7Si_6$	7.850			Kotur and Andrusyak (1991)

continued on next page

Table 20, *continued*

Compound	Structure type or symmetry	Lattice parameters			Reference
		a (Å)	*b* (Å)	*c* (Å)	
$ScCoGe_2$	$ZrCrSi_2$	9.186	10.102	7.958	Kotur and Andrusyak (1991)
		9.19	10.09	7.96	Venturini et al. (1985)
$Sc_4Co_4Ge_6$	$Zr_4Co_4Ge_7$	13.215		5.229	*Andrusyak and Kotur (1989)*, Kotur and Andrusyak (1991)
ScCoGe	TiNiSi	6.495	4.000	7.072	Kotur and Andrusyak (1984a), Kotur and Andrusyak (1991)
Sc_2CoGe_2	Sc_2CoSi_2	9.595	9.828 $\gamma = 123.2°$	3.914	Kotur and Andrusyak (1991)
$Sc_3Co_2Ge_3$	$Hf_3Ni_2Si_3$	4.078	9.930	13.243	Kotur and Andrusyak (1991)
$ScNi_6Ge_6$	$ScNi_6Ge_6$	10.158		7.816	Andrusyak (1986), Kotur and Andrusyak (1991)
		10.152		7.813	*Buchholz and Schuster (1981)*
$Sc_{12.3}Ni_{40.7}Ge_{31}$	$Sc_{12.3}Ni_{40.7}Ge_{31}$	17.865		8.220	*Bodak et al. (1990)*, Kotur and Andrusyak (1991)
$Sc_3Ni_{11}Ge_4$	$Sc_3Ni_{11}Ge_4$	8.130		8.505	*Andrusyak (1988)*, Kotur and Andrusyak (1991)
$Sc_6Ni_{18}Ge_{11}$	$Sc_6Ni_{18}Si_{11}$	18.322	12.461	8.191	*Andrusyak and Kotur (1987)*, Kotur and Andrusyak (1991)
$Sc_6Ni_{16}Ge_7$	$Mg_6Cu_{16}Si_7$	11.654			GlMK, 62; Kotur and Andrusyak (1991)
		11.663			Dwight et al. (1963a)
$Sc_3Ni_4Ge_4$	$Gd_6Cu_8Ge_8$	12.910	6.598	3.908	Kotur and Sikirica (1982b), Kotur and Andrusyak (1991)
ScNiGe	TiNiSi	6.454	4.071	7.068	Kotur and Andrusyak (1984a), Kotur and Andrusyak (1991)
$\sim Sc_{13}Ni_6Ge_{15}$	?				Kotur and Andrusyak (1991)
$Sc_4Ni_4Ge_{6.2}$	$Zr_4Co_4Ge_7$	13.276		5.225	*Andrusyak and Kotur (1989)*
$Sc_9Ni_5Ge_8$	$Sc_9Ni_5Ge_8$	20.426	9.129	3.9822	*Kotur et al. (1989d)*
$Sc_4Ru_7Ge_6$	$U_4Re_7Si_6$	8.129			Engel et al. (1984)
$ScRuGe_2$	$ZrCrSi_2$	9.28	10.32	8.12	Venturini et al. (1985)
ScRuGe	ZrNiAl	6.962		3.4683	Hovestreydt et al. (1982)
$Sc_4Rh_7Ge_6$	$U_4Re_7Si_6$	8.1255			Engel et al. (1984)
$ScRhGe_2$	$ZrCrSi_2$	9.302	10.359	8.146	Parthé and Chabot (1984)
ScRhGe (I)	TiNiSi	6.497	4.112	7.385	Hovestreydt et al. (1982)
ScRhGe (II)	ZrNiAl	6.672		3.794	Hovestreydt et al. (1982)
ScPdGe	ZrNiAl	6.7153		3.9250	Hovestreydt et al. (1982)
$Sc_4Os_7Ge_6$	$U_4Re_7Si_6$	8.146			Engel et al. (1984)
$ScOsGe_2$	$ZrCrSi_2$	9.29	10.33	8.17	Venturini et al. (1985)
ScOsGe	ZrNiAl	6.928		3.467	Hovestreydt et al. (1982)

continued on next page

Table 20, *continued*

Compound	Structure type or symmetry	Lattice parameters			Reference
		a (Å)	*b* (Å)	*c* (Å)	
$Sc_4Ir_7Ge_6$	$U_4Re_7Si_6$	8.136			Engel et al. (1984)
ScIrGe	TiNiSi	6.446	4.107	7.482	Hovestreydt et al. (1982)
$Sc_3Cu_4Ge_4$	$Gd_6Cu_8Ge_8$	13.32	6.523	4.004	*Kotur and Andrusyak (1984b)*
		13.30	6.516	3.996	Thirion et al. (1983)
ScCuGe	ZrNiAl	6.510		3.998	Kotur and Andrusyak (1984b)
		6.514		3.972	Dwight (1968)
ScAgGe	ZrNiAl	6.882		4.026	Kotur and Bodak (1988)

[a] For the composition $ScFe_{1.79}Ge_{0.21}$.

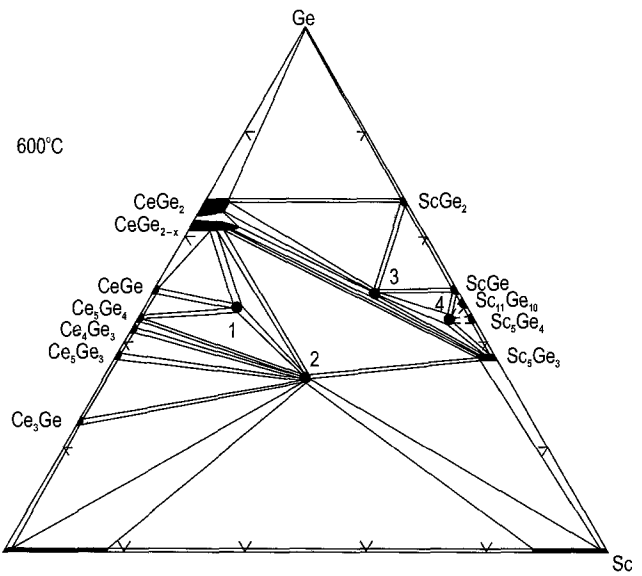

Fig. 73. Sc–Ce–Ge, isothermal section at 600°C. Ternary compounds: (1) ~$Sc_2Ce_5Ge_6$; (2) ScCeGe; (3) $Sc_3Ce_{1.22}Ge_4$; (4) ~$Sc_{4.5}Ce_{0.5}Ge_4$.

are known for two of them (see table 20). Shpyrka (1990) refined the composition of compound "Sc_2CeGe_3" to $Sc_3Ce_{1.22}Ge_4$. This correction has been taken into account in fig. 73.

3.7.5. *Sc–Pr(Sm)–Ge*

In both the Sc–Pr–Ge and Sc–Sm–Ge ternary systems two ternary compounds of the same compositions and crystal structures occur (table 20). The phase equilibria have not been investigated.

3.7.6. *Sc–Nd–Ge*

The Sc–Nd–Ge phase equilibria at 600°C investigated by Bodak and Kokhan (1983) (presented in fig. 74), are similar to those of the system with cerium. However, the mutual solubility of Sc and Nd in the binary germanides reaches 10 at.% which is considerably higher than the solubility of Sc and Ce in binary germanides. Three ternary compounds are known in this system. The crystal structure data for two of them are given in table 20. However, the same group of authors reported different values for the lattice parameters for these compounds in different papers (see table 20).

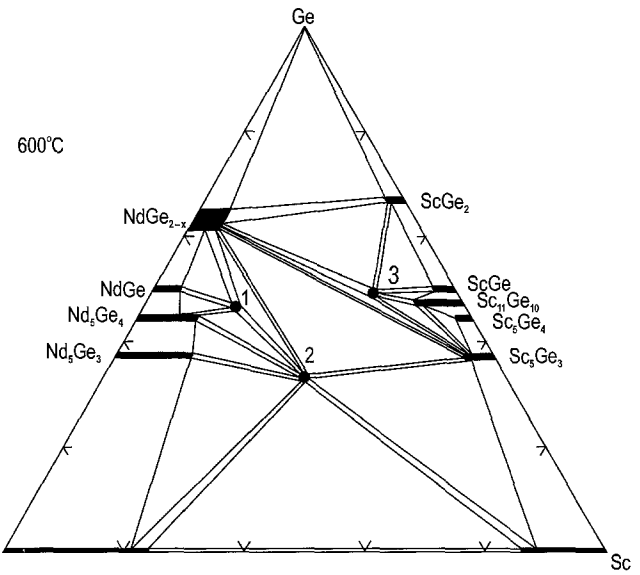

Fig. 74. Sc–Nd–Ge, isothermal section at 600°C. Ternary compounds: (1) ~$Sc_2Nd_5Ge_6$; (2) ScNdGe; (3) $Sc_3Nd_{1.22}Ge_4$.

3.7.7. *Sc–Eu–Ge*

The only ternary compound synthesized in the system, ScEuGe, belongs to the ScCeSi structure type (Shpyrka 1990) (see table 20). The phase diagram is still unknown.

3.7.8. *Sc–Dy–Ge*

As can be seen from fig. 75 which shows the phase equilibria in the Sc–Dy–Ge system at 600°C, there are many similarities with the Sc–Y–Ge system. Three ternary compounds of similar compositions and crystal structures occur in both systems (see table 20); these data were taken from Shpyrka and Mokra (1991).

3.7.9. *Sc–Yb–Ge*

The Sc–Yb–Ge isothermal section at 400°C investigated by Kotur and Mokra (1995) is presented in fig. 76. The immiscibility gap occurring in the Sc–Yb binary system spreads

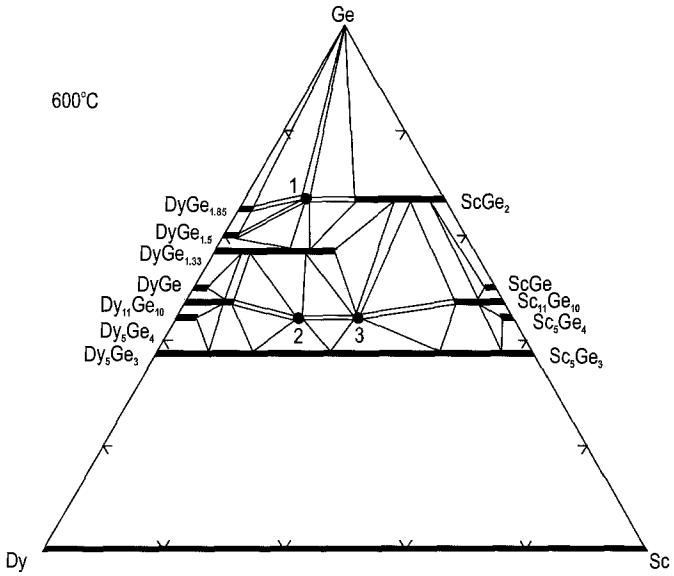

Fig. 75. Sc–Dy–Ge, isothermal section at 600°C. Ternary compounds: (1) $Sc_{0.3}Dy_{0.7}Ge_2$; (2) $Sc_{1.8}Dy_{3.2}Ge_4$; (3) $Sc_{2.7}Dy_{2.3}Ge_4$.

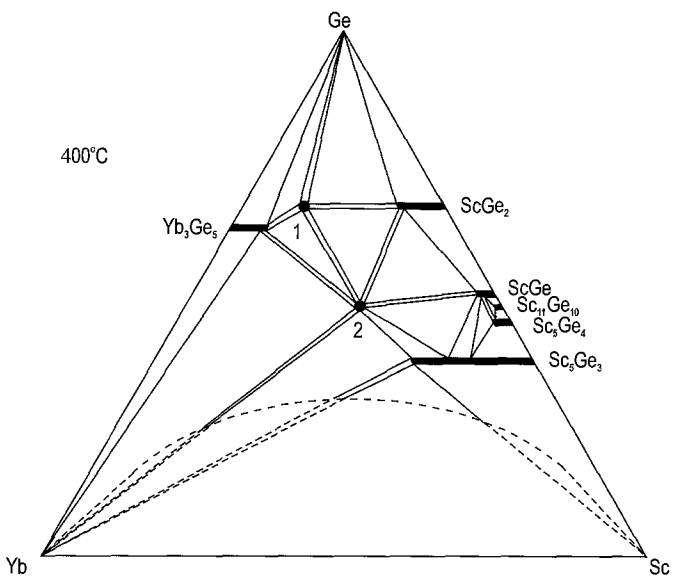

Fig. 76. Sc–Yb–Ge, isothermal section at 400°C. Ternary compounds: (1) ~$Sc_{0.3}Yb_{0.7}Ge_2$; (2) $Sc_6Yb_5Ge_{10}$.

into the ternary system up to about 30 at.% Ge. The Yb_3Ge_5 (Th_3Pd_5 type) germanide dissolves about 6 at.% Sc. Large amounts of Yb (8 and 20 at.%) dissolve in the $ScGe_2$

and the Sc_5Ge_3 compounds, respectively. Two ternary compounds were observed in this system (table 20). For one of them, $Sc_6Yb_5Ge_{10}$ the crystal structure has been determined by Kotur et al. (1996b), it crystallizes in the $Ho_{11}Ge_{10}$ type of structure, the same as $Sc_{11}Ge_{10}$, however with a partial disorder of the Sc and the Yb atoms on the rare-earth sites.

3.7.10. *Sc–Hf–Ge*

Kotur (1991) studied the Sc–Hf–Ge isothermal section at 800°C, which is shown in fig. 77. Ternary compounds do not occur. Isotypic pairs of binary germanides $ScGe_2$–$HfGe_2$, Sc_5Ge_4–Hf_5Ge_4 and Sc_5Ge_3–Hf_5Ge_3 are completely miscible. Other Sc and Hf binary germanides dissolve appreciable quantities of the third component.

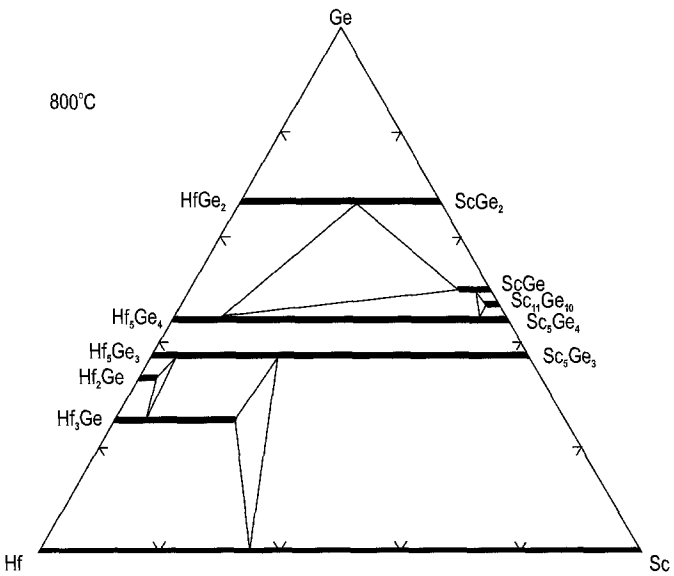

Fig. 77. Sc–Hf–Ge, isothermal section at 800°C.

3.7.11. *Sc–V–Ge*

The isothermal section at 800°C, which was determined by Kotur (1987), can be found in the review of Gladyshevsky et al. (1990). In contrast to the previous system the mutual solubility of Sc and V in the binary germanides is low and does not exceed 1 to 3 at.%. Kotur et al. (1983a) found a single crystal isotypic with Sc_5Ge_3 in one of the ternary as-cast alloys. Its lattice spacings are $a = 7.43$, $c = 5.02$ Å, but the proper composition is unknown. These data (Kotur 1987, Kotur et al. 1983a) indicate the large solubility of Sc in V_5Ge_3 and V in Sc_5Ge_3 at elevated temperatures. Two ternary compounds occur in the system. Their crystal structure data are in table 20.

3.7.12. *Sc–Nb–Ge*

The isothermal section at 800°C of the Sc–Nb–Ge system has been studied by Kotur (1986). The figure is presented also in Gladyshevsky et al. (1990). A solid solution of Nb in Sc_5Ge_3 has been observed, $Sc_{5-1.2}Nb_{0-3.8}Ge_3$. The lattice parameters vary nonlinearly within the homogeneity range reaching the values of $a = 7.752$, $c = 5.365$ Å at $Sc_{1.2}Nb_{3.8}Ge_3$. One ternary compound, $Sc_2Nb_3Ge_4$, which is isotypic with $Sc_3Ce_2Si_4$, exists in this system (table 20).

3.7.13. *Sc–Ta–Ge*

Kotur and Bodak (1990) investigated the Sc–Ta–Ge isothermal section at 800°C which is displayed in fig. 78. The system is similar to the Nb-based one, however the solubility of Ta in Sc_5Ge_3 is lower. The variation of the lattice parameters vs. composition of the solid solution $Sc_{5-3.25}Ta_{0-1.75}Ge_3$ does not obey Vegard's rule, exhibiting a negative deviation. The only ternary compound, isotypic with Sm_5Ge_4 has a variable Sc and Ta content. Its lattice spacings display a positive deviation from Vegard's rule. The limiting values of the lattice parameters are given in table 20.

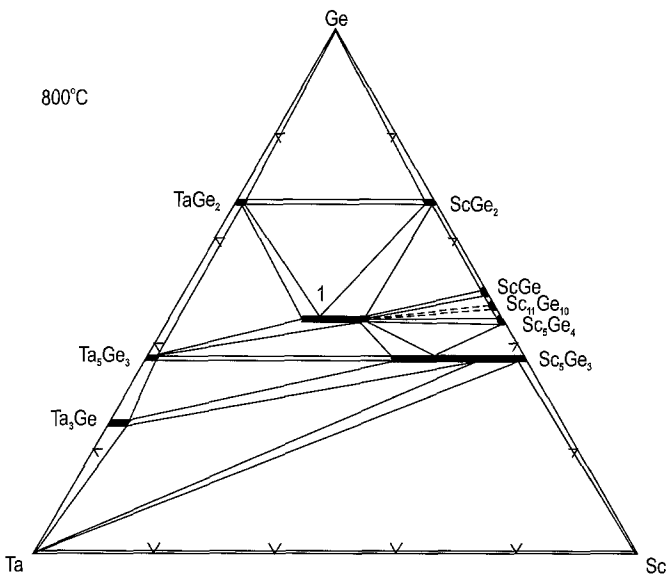

Fig. 78. Sc–Ta–Ge, isothermal section at 800°C. Ternary compound: (1) $Sc_{2-3}Ta_{3-2}Ge_4$.

3.7.14. *Sc–Cr–Ge*

The isothermal section at 800°C of the Sc–Cr–Ge system has been studied by Kotur et al. (1988b) (fig. 79). The binary Sc_5Ge_3 germanide dissolves 7.5 at.% Cr. A positive deviation from Vegard's rule is observed for the lattice parameters of this solid solution. Four ternary compounds exist in this system, their crystal structure data are shown in table 20. The compound $ScCrGe_2$ (3) has been synthesized independently by Kotur et al. (1988b) and Venturini et al. (1985).

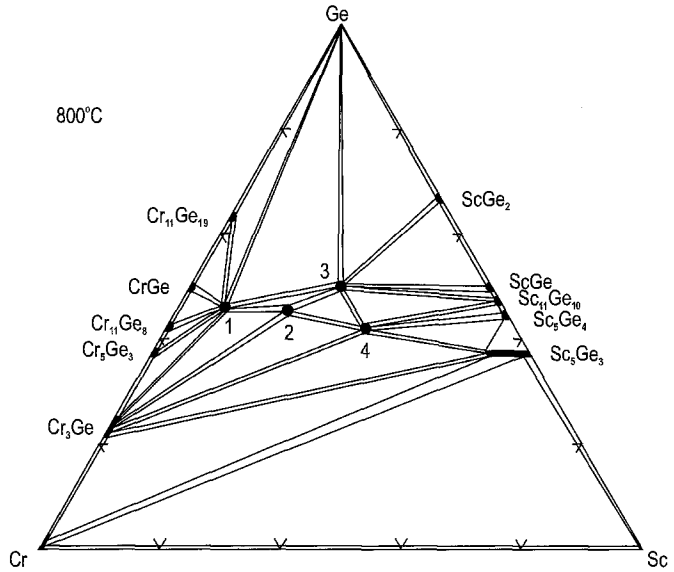

Fig. 79. Sc–Cr–Ge, isothermal section at 800°C. Ternary compounds: (1) $ScCr_6Ge_6$; (2) $Sc_2Cr_4Ge_5$; (3) $ScCrGe_2$; (4) $Sc_7Cr_{5.2}Ge_{8.8}$.

3.7.15. *Sc–Mo–Ge*

Figure 80 displays the Sc–Mo–Ge isothermal section at 800°C according to the

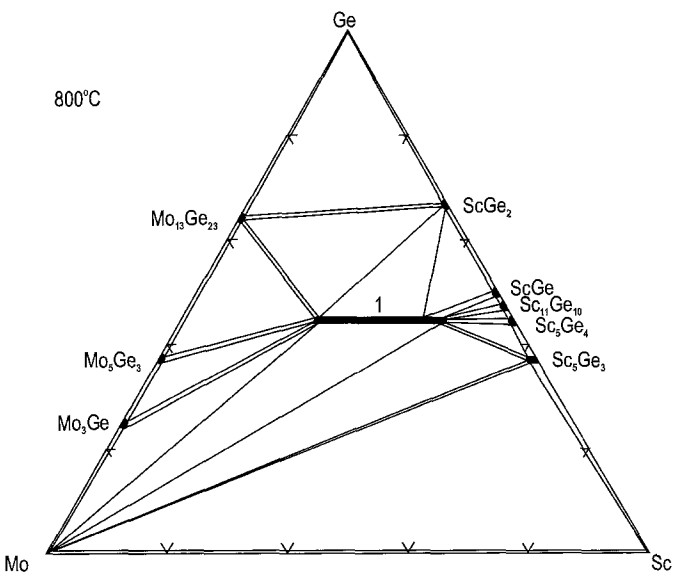

Fig. 80. Sc–Mo–Ge, isothermal section at 800°C. Ternary compound: (1) $Sc_{2-4}Mo_{3-1}Ge_4$.

data of Kotur and Bodak (1988). The binary scandium and molybdenum germanides practically do not dissolve the third component at 800°C. Only Sc_5Ge_3 forms a solid solution, $Sc_{5-4.92}Mo_{0-0.08}Ge_3$. One ternary compound isotypic with Sm_5Ge_4 occurs: $Sc_{2-4}Mo_{3-1}Ge_4$ with a variable content of Sc and Mo (table 20). It is separated by a two-phase region from the binary Sc_5Ge_4 compound which crystallizes in the same structure.

3.7.16. *Sc–W–Ge*

The solubility of W in binary scandium germanides is not worth mentioning, except for Sc_5Ge_3, where a solid solution of up to 3 at.% W exists: $Sc_{5-4.76}W_{0-0.24}Ge_3$. No ternary compounds were observed in the ternary Sc–W–Ge system (fig. 81, Kotur et al. 1989a).

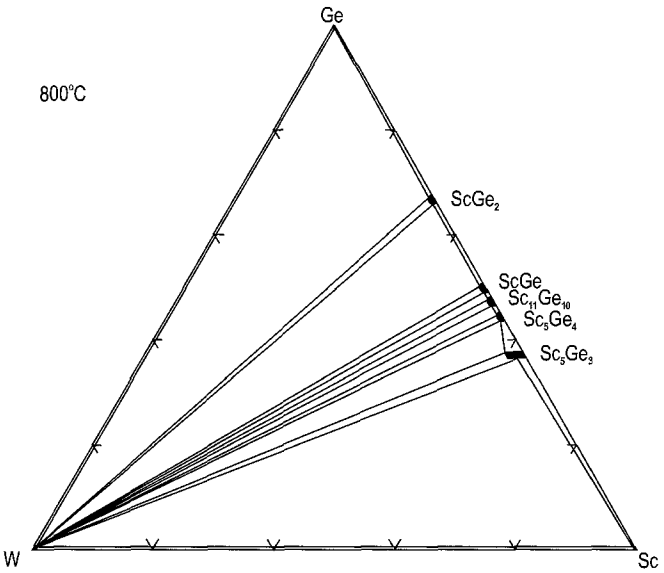

Fig. 81. Sc–W–Ge, isothermal section at 800°C.

3.7.17. *Sc–Mn–Ge*

Andrusyak and Kotur (1991) investigated a part of the Sc–Mn–Ge isothermal section at 600°C, which is presented in fig. 82. One ternary compound known earlier, $ScMnGe_2$ (Meyer et al. 1983), has been confirmed, and five new ternary compounds have been obtained by Andrusyak and Kotur (see table 20). Later Kotur (1995) refined the composition of one compound, "$ScMn_5Ge_3$" to $ScMn_6Ge_4$. This refinement was taken into account in fig. 82. The binary scandium germanides $ScGe_2$, $Sc_{11}Ge_{10}$ and Sc_5Ge_4 dissolve 4, 2 and 3 at.% Mn, respectively. The other binary germanides do not dissolve appreciable quantities of the third component.

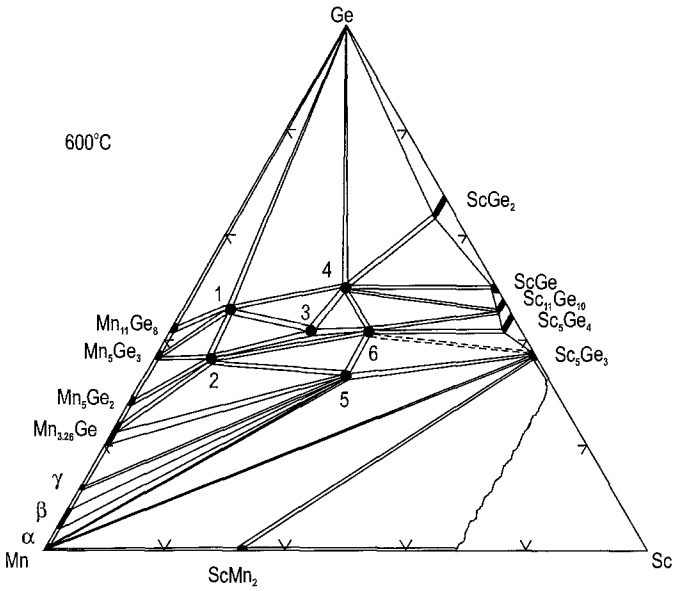

Fig. 82. Sc–Mn–Ge, isothermal section at 600°C. Ternary compounds: (1) $ScMn_6Ge_6$; (2) $ScMn_6Ge_4$; (3) ~$Sc_5Mn_7Ge_8$; (4) $ScMnGe_2$; (5) ScMnGe; (6) $Sc_7Mn_{5.3}Ge_{8.7}$.

3.7.18. *Sc–Re–Ge*

Venturini et al. (1985) reported about the ternary compound $ScReGe_2$ isotypic with $ZrCrSi_2$. These data were confirmed by Kotur (1995). The lattice parameters reported in the two publications are in good agreement (table 20).

3.7.19. *Sc–Fe–Ge*

The Sc–Fe–Ge isothermal section at 600°C has been published by Andrusyak and Kotur (1991). All together eight ternary compounds were observed. Two of them, $ScFe_6Ge_6$ and $ScFeGe_2$ were synthesized earlier by Olenych et al. (1981) and Venturini et al. (1985), respectively. Using X-ray diffraction Kotur (1995) refined the compositions of two ternary compounds reported by Andrusyak and Kotur: "$ScFe_5Ge_3$" to $ScFe_6Ge_4$ and "$ScFe_5Ge_4$" to $ScFe_6Ge_5$. The crystal structure data of the ternary compounds are given in table 20. Figure 83 shows an isothermal section at 600°C with the refined compositions of the ternary phases. Among binary scandium germanides only $ScGe_2$ and Sc_5Ge_3 dissolve a somewhat large amount of Fe: 6 at.%.

3.7.20. *Sc–Co–Ge*

The first data about this system were reported by Buchholz and Schuster (1981) and later by Venturini et al. (1985) who synthesized the following ternary compounds, $ScCo_6Ge_6$ and $ScCoGe_2$, respectively. Kotur and Andrusyak (1991) investigated the isothermal section at 600°C which is shown in fig. 84. Seven ternary compounds were observed,

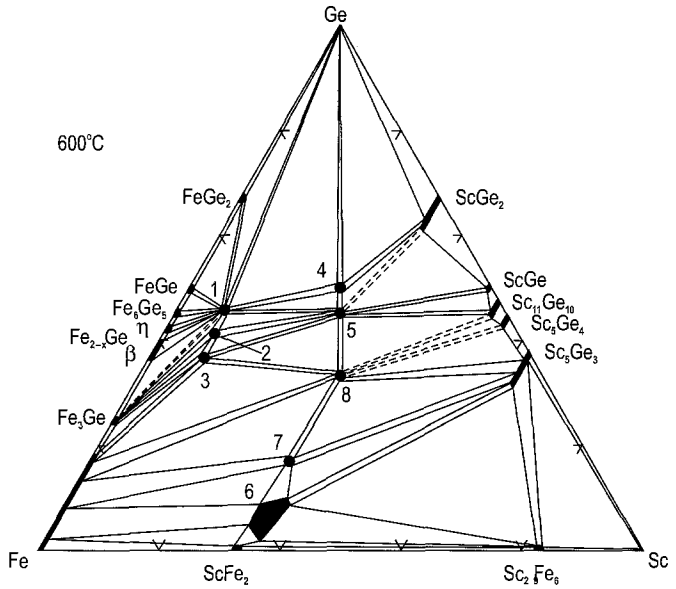

Fig. 83. Sc–Fe–Ge, isothermal section at 600°C. Ternary compounds: (1) $ScFe_6Ge_6$; (2) $ScFe_6Ge_5$; (3) $ScFe_6Ge_4$; (4) $ScFeGe_2$; (5) $Sc_4Fe_4Ge_{6.6}$; (6) $Sc_{1-1.17}Fe_{1.94-1.70}Ge_{0.06-0.30}$; (7) $ScFe_{1.5}Ge_{0.5}$; (8) ScFeGe.

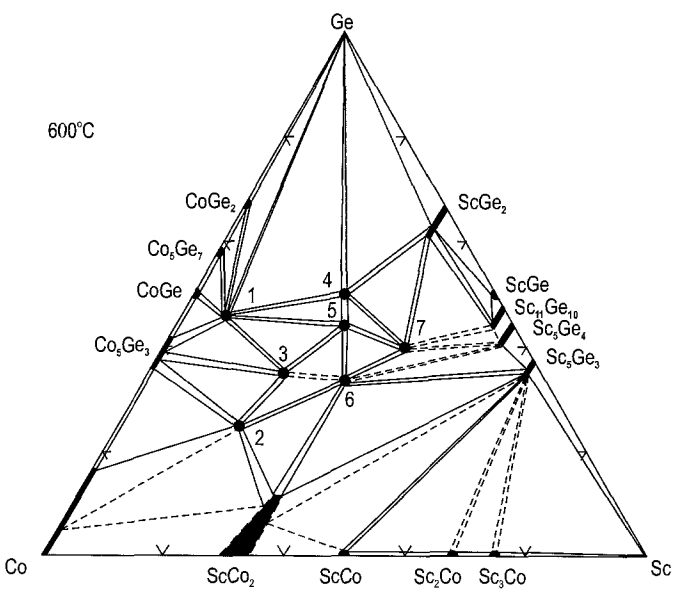

Fig. 84. Sc–Co–Ge, isothermal section at 600°C. Ternary compounds: (1) $ScCo_6Ge_6$; (2) ~$Sc_4Co_{11}Ge_5$; (3) $Sc_4Co_7Ge_6$; (4) $ScCoGe_2$; (5) $Sc_4Co_4Ge_6$; (6) ScCoGe; (7) Sc_2CoGe_2.

five of them for the first time (table 20). Single crystals of a new ternary compound, $Sc_3Co_2Ge_3$ were extracted from the alloy cooled at a rate of 10–20°C/min (Kotur and Andrusyak). Maybe this germanide exists over a narrow temperature range, which was not determined. The binary compounds $ScCo_2$, $ScGe_2$, $Sc_{11}Ge_{10}$, Sc_5Ge_4, Sc_5Ge_3 dissolve 11.5 at.% Ge, and 6, 4, 4, and 3 at.% Co, respectively. The lattice parameter a of the solid solution $ScCo_{2-1.65}Ge_{0-0.35}$ varies linearly from 6.902 to 6.984 Å (Kotur and Andrusyak 1991). The lattice spacings of the $ScCo_{0-0.18}Ge_{2-1.82}$ solid solution also obey Vegard's rule.

3.7.21. *Sc–Ni–Ge*

The phase equilibria in the Sc–Ni–Ge system at 600°C have been investigated by Kotur and Andrusyak (1991) (see fig. 85). Eight ternary compounds occur at that temperature (table 20). From the as-cast samples single crystals of two other ternary compounds $Sc_4Ni_4Ge_{6.2}$ and $Sc_9Ni_5Ge_8$ have been extracted and their crystal structures have been determined by Andrusyak and Kotur (1989) and Kotur et al. (1989d), respectively (table 20). The binary scandium germanides dissolve from 2 to 8 at.% Ni, $ScNi_2$ dissolves about 3.5 at.% Ge.

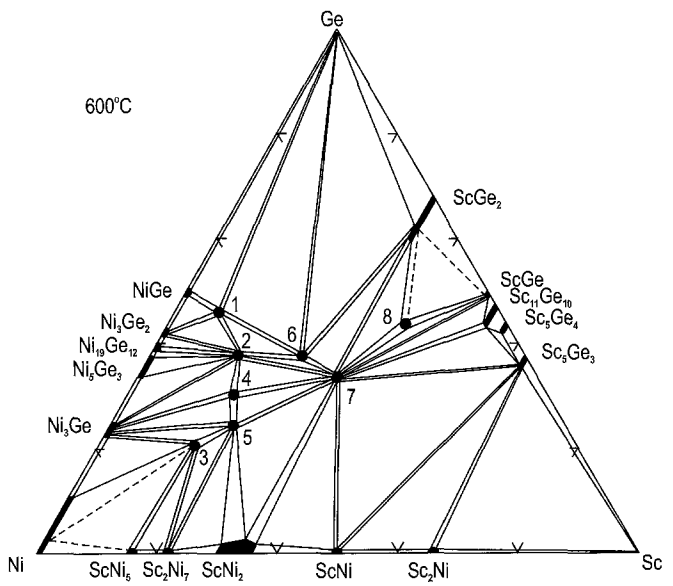

Fig. 85. Sc–Ni–Ge, isothermal section at 600°C. Ternary compounds: (1) $ScNi_6Ge_6$; (2) $Sc_{12.3}Ni_{40.7}Ge_{31}$; (3) $Sc_3Ni_{11}Ge_4$; (4) $Sc_6Ni_{18}Ge_{11}$; (5) $Sc_6Ni_{16}Ge_7$; (6) $Sc_3Ni_4Ge_4$; (7) ScNiGe; (8) ~$Sc_{13}Ni_6Ge_{15}$.

3.7.22. *Sc–Ru(Rh, Pd, Os, Ir)–Ge*

There are no literature data concerning the phase diagrams of Sc–M–Ge for M = Ru, Rh, Pd, Os, or Ir. From one to three ternary compounds have been synthesized in each of these

systems. Their crystal structure data are presented in table 20. The ScRhGe compound, possibly, occurs in two polymorphic modifications. The temperature of the phase transition is unknown.

3.7.23. *Sc–Cu–Ge*

Kotur and Andrusyak (1984b) investigated the Sc–Cu–Ge isothermal section at 600°C; the figure is also shown in the review of Gladyshevsky et al. (1990). Two ternary compounds have been found (table 20). Dwight (1968) was the first to report on the ScCuGe compound. Another germanide, $Sc_3Cu_4Ge_4$ was synthesized independently by Thirion et al. (1983) and Kotur and Andrusyak (1984b). The data on the lattice spacings of these ternaries obtained by different authors are in good agreement (table 20).

3.7.24. *Sc–Ag–Ge*

One ternary compound, ScAgGe, exists at 600°C according to the data of Kotur and Boichuk (1988) (fig. 86, table 20). The mutual solubility of the components in Sc–Ag and Sc–Ge binary compounds is practically zero.

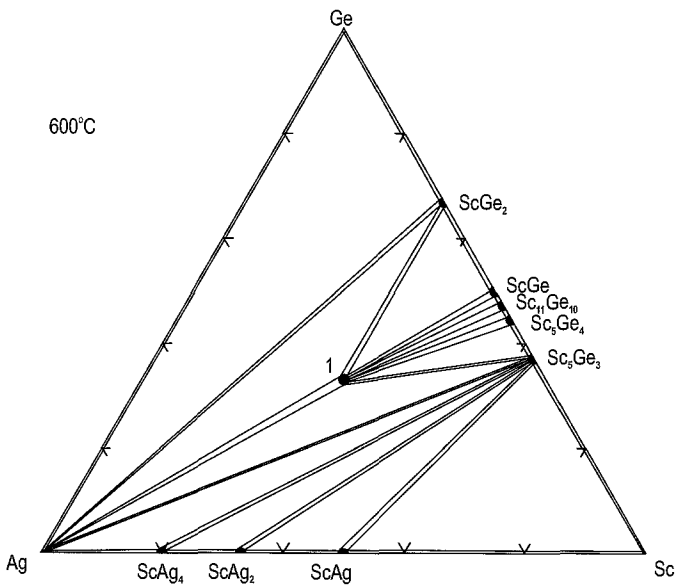

Fig. 86. Sc–Ag–Ge, isothermal section at 600°C. Ternary compound: (1) ScAgGe.

3.8. *Sc–M–Sn ternary systems*

3.8.1. *Sc–Li–Sn*

The data published by Grund (1985) about the ternary compound, ScLiSn, which is isotypic with MgAgAs (table 21) are the only data known for the Sc–Li–Sn system.

Table 21
Intermetallic compounds in the Sc–M–Sn ternary systems

Compound	Structure type or symmetry	Lattice parameters			Reference
		a (Å)	*b* (Å)	*c* (Å)	
ScLiSn	MgAgAs	6.748			Grund (1985)
$ScMn_6Sn_6$	$HfFe_6Ge_6$	5.474		8.973	Malaman et al. (1988)
$ScFe_6Sn_6$	$HfFe_6Ge_6$	5.330		8.845	Malaman et al. (1988)
$ScCo_6Sn_6$	YCo_6Ge_6	5.3048		4.2734	*Derkach and Kotur (1996)*
$ScCo_{1.1}Sn_{3.6}$	*tetr* (?)	13.324[a]			Espinosa et al. (1982)
$ScCo_2Sn$	$MnCu_2Al$	6.188			Kotur and Klyuchka (1989)
		6.187			Dwight and Kimball (1987)
ScCoSn	TiNiSi	6.773	4.402	7.339	Kotur and Klyuchka (1989)
$ScNi_4Sn$	$MgCu_4Sn$	6.897			*Kotur and Klyuchka (1989)*
$ScNi_2Sn$	$MnCu_2Al$	6.228			*Kotur and Klyuchka (1989)*
		6.214			Dwight and Kimball (1987)
ScNiSn	TiNiSi	6.625	4.333	7.536	*Kotur and Klyuchka (1989)*
Sc_2Ni_2Sn	Mo_2FeB_2	7.0928		3.3800	*Derkach and Kotur (1994)*
$ScRu_{1.1}Sn_{3.6}$	*tetr* (?)	13.567[a]			Espinosa et al. (1982)
$ScRh_{1.1}Sn_{3.6}$	*tetr* (?)	13.567[a]			Espinosa et al. (1982), Cooper (1980)
$ScPd_2Sn$	$MnCu_2Al$	6.509			Johnson and Shelton (1984)
		6.503			Malik et al. (1985)
ScPdSn (I)	ZrNiAl	7.471		3.537	Dwight et al. (1973)
ScPdSn (II)	TiNiSi	6.543	4.069	7.396	Hovestreydt et al. (1982)
$ScOs_{1.1}Sn_{3.6}$	*cub*	13.606			Espinosa et al. (1982)
$ScIr_{1.1}Sn_{3.6}$	*tetr* (?)	13.575[a]			Espinosa et al. (1982), Cooper (1980)
$ScPt_2Sn$	$MnCu_2Al$	6.514			Dwight and Kimball (1987)
ScPtSn (I)	ZrNiAl	7.41		3.62	Dwight et al. (1973)
ScPtSn (II)	AlLiSi	6.352			Eberz et al. (1980)
ScPtSn (III)	TiNiSi	6.566	4.130	7.275	Hovestreydt et al. (1982)
$ScCu_4Sn$	$MgCu_4Sn$	6.997			Kotur and Klyuchka (1989), Kotur and Derkach (1994)
ScCuSn	$CaIn_2$	4.384		6.827	Kotur and Klyuchka (1989), Kotur and Derkach (1994)
		4.39		6.82	Dwight (1976)
~Sc_6CuSn_2	?				Kotur and Derkach (1994)
ScAuSn (I)	MgAgAs	6.422			Dwight (1976)
ScAuSn (II)	AlLiSi	6.422			Eberz et al. (1980)

[a] lattice parameter of pseudocubic cell.

3.8.2. *Sc–Mn–Sn*

The Sc–Mn–Sn phase diagram is unknown, but one ternary compound, $ScMn_6Sn_6$ has been synthesized and its crystal structure determined (Malaman et al. 1988) (table 21).

3.8.3. *Sc–Fe–Sn*

Kotur and Klyuchka (1989) investigated alloys of the compositions ScFeSn, $ScFe_2Sn$ and $ScFe_4Sn$, but no ternary compounds of such stoichiometries were found. Malaman et al. (1988) reported the existence and the crystal structure of the ternary compound $ScFe_6Sn_6$ (table 21). There are no data in the literature about the phase equilibria in this system.

3.8.4. *Sc–Co–Sn*

There are data in the literature about four ternary Sc–Co–Sn compounds (see table 21). Espinosa et al. (1982) reported the lattice parameter of a pseudocubic unit cell for a compound with the tentative composition $ScCo_{1.1}Sn_{3.6}$. Rare earths form numerous groups of closely related ternary compounds of such a stoichiometry which crystallize in different cubic and tetragonal structure types. A single-crystal investigation is necessary to determine the actual crystal structure of $ScCo_{1.1}Sn_{3.6}$. The data of Kotur and Klyuchka (1989) and Dwight and Kimball (1987) concerning $ScCo_2Sn$ are in good agreement with each other (table 21). According to the data of Kotur and Klyuchka this ternary compound is in equilibrium with Co at 400°C.

3.8.5. *Sc–Ni–Sn*

Four ternary compounds in the Sc–Ni–Sn system have been synthesized and structurally investigated (table 21). However, there are only few data known about the phase equilibria. Kotur and Klyuchka (1989) reported that at 400°C the $ScNi_4Sn$ stannide is in equilibria with Ni and $ScNi_2Sn$. The latter compound is also in equilibrium with ScNiSn. Derkach and Kotur (1994) also found that at 400°C the Sc_2Ni_2Sn ternary compound is in equilibria with the ternary phase ScNiSn and also with the binary phases $ScNi_2$, ScNi and Sc_5Sn_3.

3.8.6. *Sc–Ru(Rh, Pd, Os, Ir, Pt)–Sn*

The phase equilibria of the Sc–M–Sn (where M = Ru, Rh, Pd, Os, Ir, or Pt) systems are not known. One or two ternary compounds have been synthesized in each of the systems. These data are shown in table 21. Espinosa et al. (1982) reported on the tetragonal ternary compounds of a tentative composition $ScM_{1.1}Sn_{3.6}$ (M = Ru, Rh, Ir) giving their pseudocubic cell parameters (table 21). Probably, these compounds are isotypic with $Er_{5-x}Rh_6Sn_{18+x}$ found by Hodeau and Marezio (1984), however, additional investigations are necessary to determine the proper composition and structure of these stannides. Two and three different crystal structure types have been reported for ScPdSn and ScPtSn, respectively (see table 21). This might be an indication for a polymophism of these compounds.

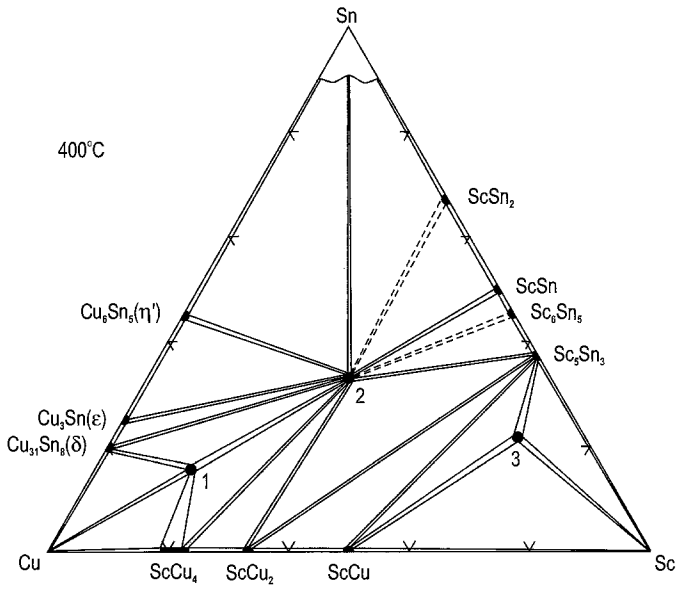

Fig. 87. Sc–Cu–Sn, isothermal section at 400°C. Ternary compounds: (1) $ScCu_4Sn$; (2) ScCuSn; (3) ~Sc_6CuSn_2.

3.8.7. *Sc–Cu–Sn*

The Sc–Cu–Sn system is the only one of the Sc–M–Sn series for which an isothermal section at 400°C has been reported (fig. 87, Kotur and Derkach 1994). Three ternary compounds occur, and for two of the compounds the crystal structure is known (table 21).

3.8.8. *Sc–Au–Sn*

The existence of a cubic ternary compound of equiatomic composition (ScAuSn) has been reported by Dwight (1976) and by Eberz et al. (1980). In both publications the same lattice parameter $a = 6.422$ Å is mentioned, however for different structure types, MgAgAs (Dwight) and AlLiSi (Eberz et al.) (table 21).

3.9. *Sc–M–P(As, Sb, Bi) ternary systems*

3.9.1. *Sc–Gd–P*

Jansen and Sperlich (1975) reported about a continuous series of solid solutions between isotypic binary phosphides ScP and GdP, these are the only data known about this system.

3.9.2. *Sc–Mn(Fe, Co)–P*

No data exist for the Sc–M–P (M = Mn, Fe and Co) phase equilibria. Jeitschko et al. (1993, 1990), Reinbold and Jeitschko (1987) and Jeitschko and Reinbold (1985) reported

Table 22
Intermetallic compounds in the Sc–M–P(As, Sb, Bi) ternary systems

Compound	Structure type or symmetry	Lattice parameters			Reference
		a (Å)	*b* (Å)	*c* (Å)	
$Sc_2Mn_{12}P_7$	$Zr_2Fe_{12}P_7$	9.392		3.562	Jeitschko et al. (1993)
$ScFe_4P_2$	$ZrFe_4Si_2$	6.962		3.622	*Jeitschko et al. (1990)*
$Sc_2Fe_{12}P_7$	$Zr_2Fe_{12}P_7$	?		?	Reinbold and Jeitschko (1987)
$ScFe_5P_3$	YCo_5P_3	?	?	?	Reinbold and Jeitschko (1987)
$Sc_2Co_{12}P_7$	$Zr_2Fe_{12}P_7$	8.973		3.531	Jeitschko and Reinbold (1985)
$ScCo_5P_3$	YCo_5P_3	11.691	3.583	10.206	Jeitschko and Reinbold (1985)
$Sc_5Co_{19}P_{12}$	$Sc_5Co_{19}P_{12}$	12.124		3.633	Jeitschko and Reinbold (1985)
ScCoP	TiNiSi	6.268	3.750	7.050	Jeitschko and Reinbold (1985)
$Sc_2Ru_{12}P_7$	$Zr_2Fe_{12}P_7$	9.318		3.87	*Ghetta et al. (1986)*
ScRuP	ZrNiAl	6.524		3.610	*Ghetta et al. (1986)*
$ScNi_4As_2$	$ZrFe_4Si_2$	7.077		3.738	Jeitschko et al. (1990)
ScNiSb	MgAgAs	6.062			Dwight (1974)
		6.055			Pecharsky et al. (1983)
ScPtSb	MgAgAs	6.312			Dwight (1974)
ScNiBi	MgAgAs	6.191			Dwight (1974)
ScPdBi	MgAgAs	6.4353			Block et al. (1990)

on one, three and four ternary compounds and their crystal structures in the Mn, Fe and Co systems, respectively. These data are shown in table 22.

3.9.3. *Sc–Ru–P*

Ghetta et al. (1986) synthesized two ternary compounds, $Sc_2Ru_{12}P_7$ and ScRuP, and established their crystal structure (table 22). The phase equilibria for Sc–Ru–P alloys are unknown.

3.9.4. *Sc–Ni–As*

One ternary compound $ScNi_4As_2$ has been synthesized by Jeitschko et al. (1990) (table 22). This paper is the only one about ternary alloys with scandium and arsenic.

3.9.5. *Sc–Ni(Pt, Au)–Sb*

Isothermal sections of the Sc–M–Sb (M = Ni, Pt and Au) systems have not been investigated. Only a few alloys were examined, among them the compounds ScNiSb and ScPtSb have been synthesized by Dwight (1974) and Pecharsky et al. (1983) (table 22). Later Dwight (1977) reported that no compound of $Sc_3Au_3Sb_4$ composition exists.

3.9.6. *Sc–Ni(Pd)–Bi*

In both the Sc–Ni–Bi and Sc–Pd–Bi systems the compounds with the equiatomic composition have been obtained by Dwight (1974) and Block et al. (1990). Their crystal structure data are given in table 22. There are no literature data for the phase equilibria in any of the Sc–M–Bi ternary system.

3.10. *Sc–M–Se ternary systems*

3.10.1. *Sc–Mg(Eu, Mn, Cu, Ag, Cd)–Se*

None of the Sc–M–Se (M = Mg, Eu, Mn, Cu, Ag and Cd) ternary systems was investigated systematically. Only separate alloys have been examined with respect to the occurrence of ternary compounds known to exist in other related ternary systems. As a result one ternary compound in the six systems has been reported. These data are given in table 23.

Table 23
Intermetallic compounds in the Sc–M–Se ternary systems

Compound	Structure type or symmetry	Lattice parameters			Reference
		a (Å)	*b* (Å)	*c* (Å)	
Sc_2MgSe_4	Al_2MgO_4	11.12			Guittard et al. (1964)
Sc_2EuSe_4	Fe_2CaO_4	12.128	14.243	3.932	Hulliger and Vogt (1966)
Sc_2MnSe_4	Al_2MgO_4	11.11			Guittard et al. (1964)
$Sc_{1-0.67}Cu_{1-2}Se_2$	$ErCuSe_2$	3.889–3.898		6.265–6.267	Julien-Pouzol et al. (1968)
$ScAgSe_2$	$ErAgSe_2$	4.25	6.73	13.52	Julien-Pouzol and Guittard (1969)
Sc_2CdSe_2	Al_2MgO_4	11.208			Pawlak et al. (1981)

3.11. *Sc–X–X′ ternary systems*

3.11.1. *Sc–Ga–Al*

Markiv et al. (1987) reported about a part of the Sc–Ga–Al isothermal section at 900°C (25–100 at.% Sc), which is depicted in fig. 88. Four ternary compounds were observed and for two of them (Nos. 1 and 4 in fig. 88) the crystal structure has been determined (table 24). The binary compound $ScGa_2$ (ST KHg_2) dissolves 22 at.% Al. The lattice spacings of the solid solution $ScGa_{2-x}Al_x$ increase from $a = 4.140$, $b = 6.614$, $c = 7.914$ to $a = 4.143$, $b = 6.618$, $c = 7.922$ Å. Another binary gallide, Sc_5Ga_4 (ST $Ho_{11}Ge_{10}$) dissolves about 12 at.% Al. The lattice parameters a and c vary within the limits 10.366–10.395 and 15.305–15.305 Å. Sc_5Ga_3 (ST Mn_5Si_3) dissolves about 20 at.% Al: $a = 8.07$–8.162, $c = 5.951$–5.923 Å, respectively. The solubility of Al in Sc_3Ga_2 (ST Gd_3Ga_2) is about 13 at.%, the lattice parameters of the solid solution vary from $a = 10.767$, $c = 14.045$ to $a = 10.781$, $c = 14.131$ Å. A large amount of Ga (about 15 at.%) can be dissolved by $ScAl_2$

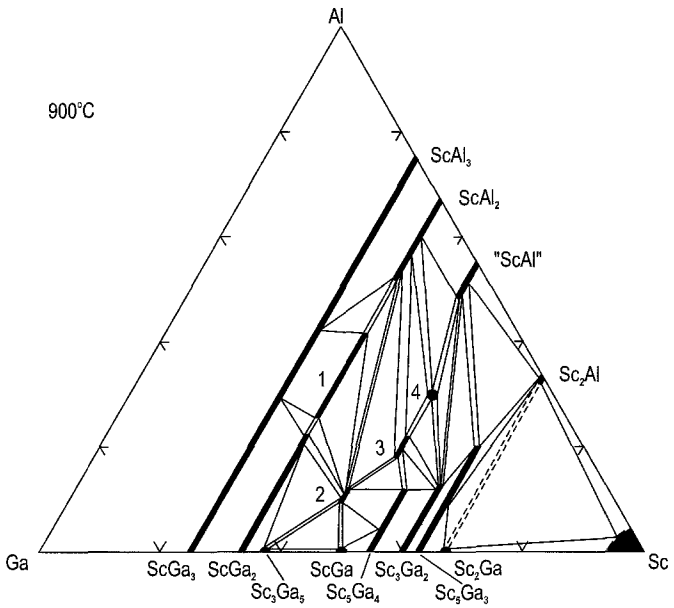

Fig. 88. Sc–Ga–Al, part of the isothermal section at 900°C (25–100 at.% Si). Ternary compounds: (1) $ScGa_{0.75-1.23}Al_{1.25-0.77}$; (2) ~$Sc_4Ga_4Al$; (3) ~$ScGa_{0.56-0.64}Al_{0.44-0.36}$; (4) $ScGa_{0.4}Al_{0.6}$.

(ST $MgCu_2$): $a = 7.580$–7.552 Å. A compound of the approximate ScAl composition (55 at.% Al) dissolves up to 7 at.% Ga. The isotypic binary compounds $ScGa_3$ and $ScAl_3$ (ST $AuCu_3$) are completely miscible.

3.11.2. *Sc–C–B(Al)*

No data are known about phase equilibria in the Sc–C–B and Sc–C–Al systems. However, three and two ternary compounds have been synthesized and structurally investigated in the boron and aluminium systems, respectively. These data are presented in table 24. Bauer (1982) observed also a solid solution of C in ScB_2: $ScB_{2-1.9}C_{0-0.1}$.

3.11.3. *Sc–In(Tl, Sn, Pb)–B*

Holleck (1977) reported the existence of a ternary compound of the tentative composition Sc_3XB_{1-x} of the perovskite type structure in the Sc–X–B (X = In, Tl, Sn and Pb) systems (table 24). The actual composition, however, is unknown due to the evaporation of the components during the synthesis procedure. The alloys were homogenized at 800°C.

3.11.4. *Sc–In(Tl, Sn, Pb)–C*

Holleck (1977) synthesized the ternary Sc_3XC_x (X = In, Tl, Sn and Pb) compounds which are isotypic with $CaTiO_3$ (table 24). However, the exact content of carbon in these compounds is unknown.

Table 24
Intermetallic compounds in the Sc–X–X′ ternary systems

Compound	Structure type or symmetry	Lattice parameters			Reference
		a (Å)	*b* (Å)	*c* (Å)	
$ScGa_{0.75-1.23}Al_{1.25-0.77}$	AlB_2	4.362–4.396		3.230–3.256	Markiv et al. (1987)
~Sc_4Ga_4Al	?				Markiv et al. (1987)
~$ScGa_{0.56-0.64}Al_{0.44-0.36}$	?				Markiv et al. (1987)
$ScGa_{0.4}Al_{0.6}$	DyAl	5.494	10.674	5.343	Markiv et al. (1987)
ScB_2C_2	ScB_2C_2	5.175	10.075	3.440	*Smith et al. (1965)*
ScB_2C	YB_2C	6.651		6.673	Bauer (1982)
Sc_2BC_2	Sc_2BC_2	3.300		10.691	*Halet et al. (1990)*
$ScAl_3C_3$	$ScAl_3C_3$	3.355		16.766	*Tsokol' et al. (1986b)*
Sc_3AlC	$CaTiO_3$	4.48			Rosen and Sprang (1965)
Sc_3InB_{1-x}	$CaTiO_3$	4.560			Holleck (1977)
Sc_3TlB_{1-x}	$CaTiO_3$	4.520			Holleck (1977)
Sc_3SnB_{1-x}	$CaTiO_3$	4.571			Holleck (1977)
Sc_3PbB_{1-x}	$CaTiO_3$	4.528			Holleck (1977)
Sc_3InC_x	$CaTiO_3$	4.533			Holleck (1977)
Sc_3TlC_x	$CaTiO_3$	4.517			Holleck (1977)
Sc_3SnC_x	$CaTiO_3$	4.516			Holleck (1977)
Sc_3PbC_x	$CaTiO_3$	4.528			Holleck (1977)
Sc_2AlSi_2	Mo_2FeB_2	6.597		3.994	Tyvanchuk et al. (1988)
$Sc_{11}Al_2Ge_8$	$Sc_{11}Al_2Ge_8$	10.419		14.974	Zhao and Parthé (1991)

3.11.5. *Sc–Si–C*

Kotroczo and McColm (1987) investigated solubility of carbon in Sc_5Si_3 (ST Mn_5Si_3) and observed a solid solution, $Sc_5Si_3C_{0-0.8}$. The lattice parameters vary nonlinearly within the homogeneity range: $a = 7.876–7.877$, $c = 5.821–5.902$ Å.

3.11.6. *Sc–Al–Si*

Toropova et al. (1985) established part of the polythermal section of the Sc–Al–Si system at a constant content of 2 at.% Al. They observed a ternary phase of unknown composition. Its crystal structure was determined in a detailed structural investigation which showed that it had the Sc_2AlSi_2 composition (Tyvanchuk et al. 1988) (table 24). These authors published also the isothermal section at 500°C, which is shown in fig. 89.

3.11.7. *Sc–Ge–Si*

Muratova (1978) studied the Sc–Ge–Si isothermal section at 600°C, however, no figure was presented in her paper. A continuous series of solid solutions exist between pairs of isotypic binary compounds Sc_5Ge_3 and Sc_5Si_3, ScGe and ScSi. The scandium germanide

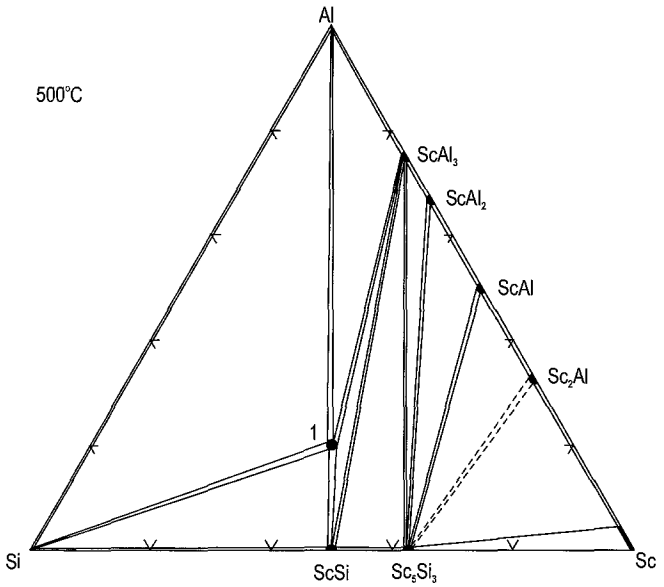

Fig. 89. Sc–Al–Si, isothermal section at 500°C. Ternary compound: (1) Sc_2AlSi_2.

with the highest Ge content, $ScGe_2$, dissolves 35 at.% Si. The lattice spacings of these solid solutions vary linearly within their homogeneity ranges. Ternary compounds have not been observed.

3.11.8. *Sc–Al–Ge*

The ternary compound $Sc_{11}Al_2Ge_8$ with one of the superstructures of the $Ho_{11}Ge_{10}$ type has been synthesized and investigated by Zhao and Parthé (1991). The lattice parameters are given in table 24. Phase equilibria are unknown.

3.11.9. *Sc–As–P*

Yim et al. (1972) found a continuous series of solid solutions between the isotypic binary compounds ScP and AsP. These are the only data known about this system.

3.11.10. *Sc–Te–Se*

Dismukes and White (1965) obtained the alloy $Sc_2Te_{0.33}Se_{2.67}$ at 950–1000°C with the structure of Sc_2Se_3 and the lattice parameters $a = 10.915$, $b = 7.729$ and $c = 23.12$ Å. These data indicate the occurrence of a solid solution $Sc_2Te_xSe_{2-x}$ ($0 \leqslant x \leqslant 0.33$). A substitution of Te for Se leads to an increase of the lattice constants.

3.12. *Sc–M–M' ternary systems*

3.12.1. *Sc–Mg–Mn*

Drits et al. (1977) reported on the isothermal sections at 500 and 300°C in the magnesium corner of this system. The solubility of Sc and Mn decrease as a result of their alloying with Mg. Four phases in a peritectic nonvariant equilibrium $L+\beta \leftrightarrow \alpha+Mn$ (β: solid solution of Mg in βSc) at 700°C have been detected.

3.12.2. *Sc–Y–Gd*

A single crystal with the composition $Sc_{0.075}Y_{0.175}Gd_{0.75}$ with the hcp structure has been prepared and its magnetic properties investigated by Ito et al. (1988), however, no data about the lattice parameters were presented in this paper. These data indicate a complete miscibility of the components in the ternary system, similar to what occurs in the binary Sc–Y and Sc–Gd systems (see sect. 2.3).

3.12.3. *Sc–Tb–Mn*

Lelievre-Berna et al. (1993) prepared two alloys of the solid solution $Tb_{1-x}Sc_xMn_2$ ($x=0.00$, 0.01 and 0.03) (ST $MgCu_2$) and investigated their magnetic structures. The alloys, annealed at 730°C, were essentially single phase according to the X-ray powder diffraction analysis, however, a small amount of pure Tb metal was detected by neutron scattering. These data indicate the occurrence of a limited solid solution of Sc in $TbMn_2$. No data about variation of lattice parameter are available.

3.12.4. *Sc–Y–Fe*

The isothermal section of the Sc–Y–Fe system at 600°C, which is presented in fig. 90, has been established by Koshel' et al. (1984). The phase equilibria at 800°C are the same. Ternary compounds were not observed. The highest solubility of Sc, 30 at.%, occurs in the binary YFe_2 (ST $MgCu_2$) compound. The lattice parameter a changes within the limits 7.358–7.037 Å. Other Y–Fe binary compounds do not dissolve more than 5 at.% Sc.

3.12.5. *Sc–Ce–Fe*

Figure 91 displays the Sc–Ce–Fe isothermal section at 600°C, which was investigated by Koshel' et al. (1984). This system is similar to the previous Y-based one. $CeFe_2$ (ST $MgCu_2$) dissolves about 22 at.% Sc. The lattice parameter a of the solid solution $Ce_{1-0.33}Sc_{0-0.67}Fe_2$ changes within the limits 7.272–7.159 Å. $ScFe_2$ dissolves less than 5 at.% Ce. Ternary compounds have not been reported. The same phase equilibria were observed at 800°C.

3.12.6. *Sc–U–Pd*

Maple et al. (1996) reported about a solid solution of Sc in the binary compound UPd_3 (ST $AuCu_3$), $U_{1-x}Sc_xPd_3$ ($0 \leqslant x \leqslant 0.5$). Data concerning the variation of the lattice parameter with the composition were not presented. Dhar et al. (1996) reported about an alloy

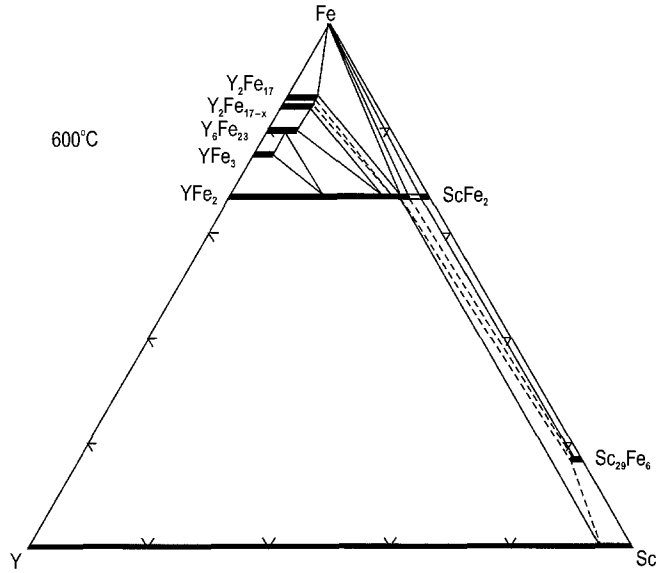

Fig. 90. Sc–Y–Fe, isothermal section at 600°C.

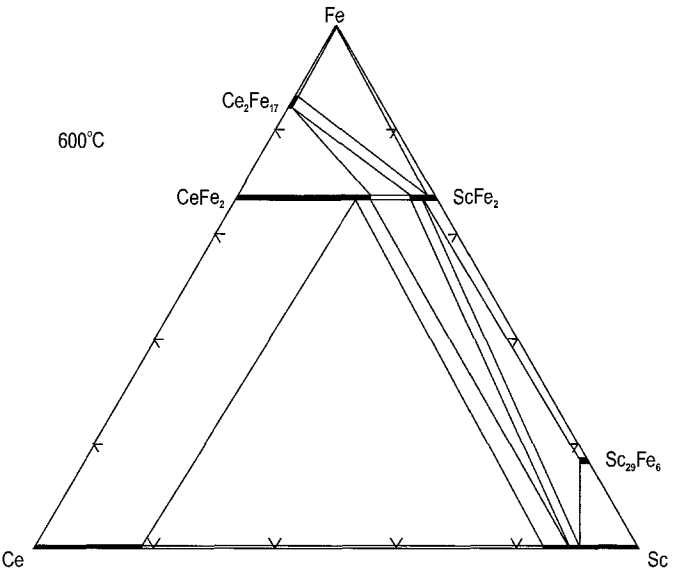

Fig. 91. Sc–Ce–Fe, isothermal section at 600°C.

with the composition $Sc_{0.8}U_{0.2}Pd_3$ crystallizing in the cubic $AuCu_3$ type structure with the lattice parameter $a = 3.980$ Å. These data support the occurrence of the $Sc_{1-x}U_xPd_3$ ($0 \leqslant x \leqslant ?$) solid solution.

3.12.7. *Sc–Ti–Fe*

Nishihara and Yamaguchi (1985, 1986) reported the occurrence of the complete miscibility of the isotypic binary compounds $ScFe_2$ and $TiFe_2$ (ST $MgZn_2$). However, no data about lattice parameters of the solid solution were presented. The $ScFe_2$–$TiFe_2$ magnetic phase diagram has been studied in detail, see sect. 6.

3.12.8. *Sc–Ti–Ni*

The melting diagram of the Sc–Ti–Ni system in the range of 50–100 at.% Ni has been investigated by Semenova et al. (1996b). Two ternary eutectics and two ternary peritectics occur at 1110 and 980°C, and 1210 and 1130°C, respectively. Semenova et al. (1996a) investigated the system for the same concentration range at the subsolidus temperatures. No ternary compounds were observed. The solid solubility limits of the phases based on the binary compounds were determined. The polythermal section TiNi–ScNi was shown to be quasibinary.

3.12.9. *Sc–Ti–Pt*

Dwight (1961b) investigated the alloys of the section $ScPt_3$–$TiPt_3$ at 900°C. The isotypic binary compounds of the $AuCu_3$ structure type are completely miscible. Other regions of the diagram were not investigated.

3.12.10. *Sc–Hf–Ir*

Dwight et al. (1963b) synthesized one ternary compound, $Sc_{0.2}Hf_{0.8}Ir$ and showed that it crystallizes in the γTiCu type structure (table 25). These are the only data known about this system.

Table 25
Intermetallic compounds in the Sc–M–M′ ternary systems

Compound	Structure type or symmetry	Lattice parameters		Reference
		a (Å)	*c* (Å)	
$Sc_{0.2}Hf_{0.8}Ir$	γTiCu	3.32	6.22	Dwight et al. (1963b)
$ScNi_4Au$	$MgCu_4Sn$	6.828		Dwight (1975)
ScCuZn (I)	$MgZn_2$	5.164	8.364	Dwight (1968)
ScCuZn (II)	$CaIn_2$	4.39	6.82	Dwight (1968)

3.12.11. *Sc–V–Nb*

According to the investigations of Savitskii et al. (1975) ternary compounds do not exist in this system. A narrow region of continuous series of solid solutions adjoining the V–Nb binary system was observed in the ternary system. The solubility of scandium in V(Nb) solid solution decrease from 2 at.% in binary Sc–V alloys to 0.1 at.% in binary Sc–Nb alloys. The lowest solubility of scandium occurs in the $V_{20}Nb_{80}$ alloy.

3.12.12. *Sc–Cr–Ni*

Maslenkov and Braslavskaya (1986a) reported on the Sc–Cr–Ni phase diagram in the temperature range 1100–1860°C. The quasibinary sections Cr–$ScNi_2$ and Cr–Sc_2Ni_7 are of eutectic type. The isothermal section at 1300°C and the projection of a part of the liquidus surface (Ni–Cr–$ScNi_2$) are presented in the paper too. The lowest ternary eutectic $L \leftrightarrow \gamma_{Ni} + \langle ScNi_5 \rangle + \langle Sc_2Ni_7 \rangle$ occurs at 1125°C. The same authors (Maslenkov and Braslavskaya 1986b) presented parts (Ni–Cr–$ScNi_2$) of isothermal sections at 800 and 1050°C. The figure of the latter is shown in the review of Gladyshevsky et al. (1990). These isothermal sections differ from one another due to the rapid decrease of the solubility of scandium in the Ni(Cr) solid solution (γ_{Ni} phase), which is 0.27 and 0.1 at.% at 1050 and 800°C, respectively. Ternary compounds were not observed. Part of the alloys of the three-phase region $ScNi_5$–Ni–Cr were inhomogeneous.

3.12.13. *Sc–Mn–Fe*

Kyrchiv (1983) reported about an investigation of part of the Sc–Mn–Fe isothermal section at 600°C (0–33.3 at.% Sc), however, no figure was presented. Isotypic binary compounds $ScMn_2$ and $ScFe_2$ (ST $MgZn_2$) are completely miscible. No ternary compounds were observed.

3.12.14. *Sc–Re–Ni*

Part of the Sc–Re–Ni isothermal section at 1000°C (Ni corner) has been studied by Arskaya et al. (1970) and Savitskii et al. (1972). Ternary compounds do not occur. The solubility of Sc in Ni is about 0.2 wt.%, and it decreases rapidly with increasing rhenium content. Nickel dissolves up to 40 wt.% Re.

3.12.15. *Sc–Ru–Rh*

Khorujaya and Korniyenko (1996, 1997) reported on part of the projection of the liquidus surface (0–50 at.% Sc). The projection of the solidus surfaces in the same concentration region has been determined by Eremenko et al. (1996). Ternary compounds do not exist. The liquidus surface consists of five surfaces of primary crystallization of Ru and Rh solid solutions as well as of the phases based on $ScRu_2$, $ScRh_3$ and on a continuous series of solid solutions between the isotypic compounds ScRu and ScRh (δ phase). The highest temperature on the surface is 2334°C (Ru melting point) and the lowest one is 1520°C (ternary eutectic $L(E_1) \leftrightarrow \delta + \langle ScRh_3 \rangle + \langle Ru \rangle$).

3.12.16. *Sc–Ni–Au*

One ternary compound $ScNi_4Au$ has been synthesized and structurally investigated by Dwight (1975) (table 25). These are the only data reported about this system.

3.12.17. *Sc–Cu–Zn*

Dwight (1968) reported that the ternary compound ScCuZn exists in two polymorphic modifications. Their crystal structure data are presented in table 25. Phase equilibria have not been investigated.

4. Multicomponent systems containing scandium

Little information has been published in the literature concerning four-component systems containing scandium. The starting material for the preparation of multicomponent (four-component) alloys is normally a pair of ternary compounds. Multicomponent systems are frequently prepared if one (or both) ternary system show outstanding physical properties, such as superconductivity with high transition temperatures, a possible coexistence of superconductivity and magnetism, or if the multicomponent system can be used for hard magnetic materials. In that cases the effect of alloying on the properties of ternary compound is examined in a four-component system. Data about five-component systems containing scandium are even more rare.

4.1. *Sc–Mg–Mn–Li(Ca, Y, Ce, Nd, Zr, Ni, Cd, Zn, Al, In, Si, Ge, Sn)*

Drits et al. (1971) investigated the effect of alloying on the properties (tensile and yield strengths, elongation and hardness) at ambient and elevated (300–350°C) temperatures of multiphase Mg-based ternary alloys Mg + 11%Sc + 1.0%Mn and Mg + 11%Sc + 0.6%Mn (composition in wt.%). The quantities of the alloyed elements did not exceed 2 wt.%. Additions of 0.5–1.0% Ca, Cd, Si, Y and Zn increase the strength of Mg + 11%Sc + 0.6%Mn alloy at ambient temperature. Additions of 0.5–1.0% rare earths, Zn and Sn had the same effect on the strength at 350°C. Additions of Li, Al and Sn (in larger amounts) have a negative influence. This improvement in the mechanical properties is attributed to the appearance of noticeable amounts of second phase intermetallic compounds, especially in the case of Al. Additions of Zr, Ni, In and Ge practically do not have an effect on the strength of these ternary Mg–Sc–Mn alloys.

4.2. *Sc–Ca–Rh–B*

Matthias et al. (1978) obtained the compound $Sc_{0.3}Ca_{0.7}Rh_4B_4$ occurring in two polymophic modifications. However, their structures and lattice spacings were not reported. One of the phases, probably HT, is of $CeCo_4B_4$ type structure (Vandenberg and Matthias 1977).

4.3. *Sc–Ce(Pr, Nd, Sm, Gd, Tb, Dy, Ho, Er, Tm)–Rh–B*

Matthias et al. (1978) prepared the alloys with the compositions $Sc_xR_{1-x}Rh_4B_4$ (x = 0.2, 0.3, 0.4). Compositions of single phases alloys for different R are presented in

Table 26
Compositions of single phase alloys prepared in the Sc–R–Rh–B systems (R = Ce, Pr, Nd, Sm, Gd, Tb, Dy, Ho, Er, Tm)[a]

Composition of alloy	Modification	Composition of alloy	Modification
$Sc_{0.3}Ce_{0.7}Rh_4B_4$	HT	$Sc_{0.3}Dy_{0.7}Rh_4B_4$	HT
$Sc_{0.3}Pr_{0.7}Rh_4B_4$	HT	$Sc_{0.3}Ho_{0.7}Rh_4B_4$	LT
$Sc_{0.3}Nd_{0.7}Rh_4B_4$	HT	$Sc_{0.4}Ho_{0.6}Rh_4B_4$	HT
$Sc_{0.3}Sm_{0.7}Rh_4B_4$	HT+LT	$Sc_{0.2}Er_{0.8}Rh_4B_4$	HT
$Sc_{0.3}Gd_{0.7}Rh_4B_4$	LT	$Sc_{0.3}Er_{0.7}Rh_4B_4$	?
$Sc_{0.3}Tb_{0.7}Rh_4B_4$	HT	$Sc_{0.3}Tm_{0.7}Rh_4B_4$	HT

[a] Source: Matthias et al. (1978).

table 26. One of the two modifications of compounds is tetragonal. However, the original paper does not indicate which of them, and neither gives the data about their lattice spacings. Taking into account the data of Vandenberg and Matthias (1977) about the occurrence of ternary compounds RRh_4B_4 (R = Nd, Sm, Gd, Tb, Dy, Ho, Er, Tm) with the tetragonal structure of the $CeCo_4B_4$ type (SG $P4_2/nmc$), it is possible to state that the formation of solid solutions occur when R is substituted for Sc in these ternary compounds, $Sc_xR_{1-x}Rh_4B_4$. These solutions are metastable (Matthias et al. 1978). Additional investigation is necessary to establish their homogeneity regions. Possibly, $Sc_{0.3}Ce_{0.7}Rh_4B_4$ and $Sc_{0.3}Pr_{0.7}Rh_4B_4$ are individual quaternary compounds; however there is no data about the occurrence of ternary compounds $CeRh_4B_4$ and $PrRh_4B_4$.

4.4. *Sc–Y(Nd, Dy, Er, Lu)–Fe–B*

Chen and Duh (1988) reported the occurrence of the solid solution $(Sc_{0-0.2}R_{1-0.8})_2Fe_{14}B$ at 1000°C and variations of the lattice spacings within its homogeneity range (see table 27). The alloys are ferromagnetic. The Curie temperature of the alloys monotonically decrease with the increasing scandium content (see table 27).

Table 27
Variations of lattice parameters and Curie temperature (T_C) within the homogeneity ranges of the solid solutions $(Sc_{0-0.2}R_{1-0.8})_2Fe_{14}B$ (R = Y, Nd, Dy, Er, Lu) which are isotypic with $Nd_2Fe_{14}B$

Solid solution	Lattice parameters (Å)		T_C
	a	*c*	
$(Sc_{0-0.2}Y_{1-0.8})_2Fe_{14}B$	8.767–8.750	12.037–11.988	564–557
$(Sc_{0-0.2}Nd_{1-0.8})_2Fe_{14}B$	8.792–8.769	12.190–12.186	589–585
$(Sc_{0-0.2}Dy_{1-0.8})_2Fe_{14}B$	8.762–8.756	12.022–11.977	592–583
$(Sc_{0-0.2}Er_{1-0.8})_2Fe_{14}B$	8.738–8.730	11.964–11.917	553–544
$(Sc_{0-0.2}Lu_{1-0.8})_2Fe_{14}B$	8.703–8.656	11.876–11.893	535–528

4.5. *Sc–Lu–Ru–B*

The as-cast and homogenized at 1150°C Sc–Lu–Ru–B alloys of the section "$ScRu_4B_4$"–$LuRu_4B_4$ have been examined by Ku et al. (1979). The boundary ternary compound $LuRu_4B_4$ (ST $LuRu_4B_4$, SG $I4_1/acd$) is thermodynamically stable while the compound "$ScRu_4B_4$" is metastable and decomposes after homogenization at 800–1300°C. A metastable continuous series of solid solutions $Sc_{0-1}Lu_{1-0}Ru_4B_4$ occur. The lattice parameters vary within the limits $a = 7.419$–7.346 and $c = 14.955$–14.895 Å. All the alloys are superconducting. More details are given in sect. 6.

4.6. *Sc–U–Pd–B*

Five alloys $Sc_{0.8}U_{0.2}Pd_3B_x$ ($x = 0$, 0.1, 0.2, 0.3, 0.5) have been prepared by Dhar et al. (1996). An X-ray phase examination shows the occurrence of the $Sc_{0.8}U_{0.2}Pd_3B_x$ ($0 \leqslant x \leqslant 0.3$) solid solution of $AuCu_3$ type structure with the lattice constants 3.980, 3.999 and 4.017 Å for $x = 0$, 0.1 and 0.3, respectively. The non-Fermi liquid behaviour reported in the literature for $x = 0$ alloy (Gajewski et al. 1994) persists in $x = 0.1$, but is absent in $x = 0.2$ and 0.3 alloys at least down to 1.4 K.

4.7. *Sc–Th–Rh–B*

Vandenberg and Matthias (1977) presented the crystal structure data of two alloys: $Sc_{0.5}Th_{0.5}Rh_4B_4$ (ST $CeCo_4B_4$, SG $P4_2/nmc$), lattice parameters $a = 5.322$, $c = 7.453$ Å, and $Sc_{0.65}Th_{0.35}Rh_4B_4$ (ST $CeCo_4B_4$), $a = 5.317$, $c = 7.422$ Å. These data indicate the existence of the limited solid solution of substitution of Sc for Th in the ternary compound $ThRh_4B_4$.

4.8. *Sc–Y(Lu)–Ir–Si*

Venturini et al. (1989) reported about the occurrence of continuous series of solid solutions between the isotypic ternary compounds $Sc_5Ir_4Si_{10}$-$Lu_5Ir_4Si_{10}$ (ST $Sc_5Co_4Si_{10}$) at 900°C. They investigated the variation of the lattice parameters with composition and the distribution of Sc and Lu atoms in the structure using four single crystals obtained from the solid solution region. The tetragonal lattice spacings of the solid solution $Sc_{5-0}Lu_{0-5}Ir_4Si_{10}$ change within the limits $a = 12.314$–12.475 and $c = 4.076$–4.171 Å. A negative deviation from Vegard's rule is observed. An isotypic single crystal $Sc_{2.5}Y_{2.5}Ir_4Si_{10}$ with the lattice parameters $a = 12.3926$, $c = 4.1292$ Å has been investigated too. These data indicate the formation of a solid solution $Sc_{5-x}Y_xIr_4Si_{10}$ ($0 \leqslant x \leqslant ?$). The alloys of the both four component systems are superconducting.

4.9. *Sc–Dy–Ir–Si*

Another pseudobinary section $Sc_5Ir_4Si_{10}$–$Dy_5Ir_4Si_{10}$ has been investigated by Ramakrishnan et al. (1992). These isotypic ternaries form a solid solution $Sc_{5-x}Dy_xIr_4Si_{10}$

($0 \leqslant x \leqslant 5$) with the linear dependence of both tetragonal lattice parameters a and c with x. Within this series superconductivity has been found for $0 \leqslant x < 1.5$ and antiferromagnetic ordering for $x > 1.5$. The coexistence of superconductivity and magnetism is reported for $x = 1.5$. The superconducting transition temperature decreases rapidly with increasing x from $T_c = 8.45$ K for $x = 0$ down to about 4 K for the $x = 1.5$ sample where the coexistence of superconductivity and magnetic order is observed. The magnetic ordering temperature T_N increases linearly from 3.5 to 5.0 K in the concentration range $2 \leqslant x \leqslant 5$. The temperature dependence of the resistivity of alloys is typical for a metal in the investigated temperature range up to 300 K.

4.10. *Sc–Ni–C–B, Sc–Lu–Ni–C–B*

A superconducting transition was reported for metastable as-cast alloy of composition $ScNi_2B_2C$ by Ku et al. (1994). The major phase has been indexed as the tetragonal $LuNi_2B_2C$-type structure (SG *I4/mmm*) with the lattice parameters $a = 3.34$, $c = 10.2$ Å. Annealing of the alloy at 1050°C for 24 h led to the disappearance of the tetragonal phase and superconductivity.

The same authors reported on the pseudoquaternary system $(Lu_{1-x}Sc_x)Ni_2B_2C$. The unstable boundary is near the Sc-rich region ($x > 0.5$). All the alloys are superconducting.

4.11. *Sc–Y–Ge–Si*

Three alloys with the compositions $Sc_{0.48}Y_{4.52}Ge_{0.29}Si_{2.71}$, $Sc_{0.72}Y_{4.28}Ge_{0.43}Si_{2.57}$ and $Sc_{4.25}Y_{0.75}Ge_{0.45}Si_{2.55}$ with the Mn_5Si_3 type structure (SG $P6_3/mcm$) have been prepared and examined by McColm and Kotroczo (1987). Taking into account the existence of isotypic binary compounds Sc_5Si_3, Sc_5Ge_3, Y_5Si_3 and Y_5Ge_3 it is possible to forecast the occurrence of continuous series of solid solutions between these binary phases with complete mutual substitution of Sc and Y and Si and Ge as well. Hydrogenation of the above mentioned alloys has been investigated.

4.12. *Sc–Rh–Os–Si*

Braun and Segre (1980) investigated the phase composition at 1000°C of alloys within the section $Sc_3Os_2Si_6$–"$Sc_3Rh_2Si_6$". One of the components of this section, the compound of the tentative composition, $Sc_3Os_2Si_6$, is orthorhombic (see table 19, above). The second component, "$Sc_3Rh_2Si_6$", is a two-phase alloy containing the ternary compounds $Sc_5Rh_4Si_{10}$ (ST $Sc_5Co_4Si_{10}$, see table 19) and ~Sc_4RhSi_8 (structure unknown, see table 19). The silicide $Sc_3Os_2Si_6$ dissolves about 5.5 at.% Rh as deducted from the data presented in the table of the original paper. However, this value is not in agreement with the value given in the text, where a solubility of about 30 at.% Rh is mentioned. Variation of the lattice parameters vs. composition of the solid solution is not presented. Judging from the phase composition of the section, the $Sc_3Rh_xOs_{2-x}Si_6$ solid solution is

in two-phase equilibrium with $Sc_5Rh_4Si_6$ and in three-phase equilibrium with the phases $Sc_5Rh_4Si_{10}$ and ~Sc_4RhSi_8. The alloys of the section are superconducting.

4.13. *Sc–Re–Ni–Si*

Zhao and Parthé (1989a) obtained a single crystal $Sc_3(Ni_{0.96}Re_{0.04})_2Si_4$ and investigated its crystal structure: ST $Sc_3Ni_2Si_4$, SG *Pnma*, $a = 11.679$, $b = 3.985$, $c = 11.991$ Å. These data are indicative of the formation of a limited solid solution of the substitution of Re for Ni in the ternary compound $Sc_3Ni_2Si_4$. However, these data are not complete and an additional investigation is necessary to define the limits of the solid solution.

4.14. *Sc–Ca–Pt–P*

The only data about the Sc–Ca–Pt–P system concerns the $ScCa_2Pt_7P_{\sim 3}$ quaternary compound, which has been reported by Lux et al. (1991). It is isotypic with $Eu_2Pt_7AlP_{\sim 3}$, SG *I4/mmm*, $a = 4.038$, $c = 27.027$.

4.15. *Sc–Y–Ti–Co*

The alloy with the composition $Sc_{0.4}Y_{0.4}Ti_{0.2}Co_2$ is a single phase. It crystallizes in the cubic $MgCu_2$-type structure, $a = 6.962$ Å. It was established by Burnashova et al. (1981) who also investigated the hydrogenation of the alloy. These data and the data about the binary compounds $ScCo_2$, YCo_2 and $TiCo_2$ which also crystallize with the same structure indicate that there is possibly a complete solubility of these binary compounds, or a limited solubility of Ti in $(Y_{1-x}Sc_x)Co_2$.

5. Generalisation of the data on scandium metal systems and intermetallics

Phase diagrams give a fundamental insight into how two or more elements behave when they are combined in a system. An understanding of the interaction mechanism between the elements which results in different types of phase diagrams is one of the aims of physical and chemical investigations. The responsible physical parameters (factors) which determine this interaction are: the size, electrochemical, valence-electron, cohesive-energy and atomic number factors (Villars 1995). A review of the methods (usually semiempirical) proposed for the explanation and prediction of the constitution of phase diagrams, and the occurrence and crystal structure of intermediate compounds in the systems has been written by Villars (1995). The best semiempirical method for the calculation of the enthalpy of binary alloys based on the first three of the above-mentioned factors has been deducted by Miedema (1976). The prediction based on Miedema's model is in agreement with many experimental data. However, the attempts to apply this model to ternary systems failed. Villars (1995) introduced a new model using two additional factors (cohesive energy and atomic number) in order to explain the stability of ternary

compounds of proper structure types. Of course, each of these five factors used in Villars's model is related to the position of the corresponding element in the periodic table; however, it is impossible to replace them by only one.

Besides these semiempirical models, successful attempts have recently been undertaken in order to calculate the stability of binary, and in some cases ternary, compounds from first-principle band-structure calculations. As an example we want to mention the Vienna ab-initio simulation package VASP (see Kresse and Hafner 1993, 1994a and Kresse and Furthmueller 1996a,b). It performs an iterative solution of the Kohn–Sham equations of the local-density-functional (LDF) theory and allows one to use generalised gradient corrections. The electronic states are expanded in terms of plane waves, the electron–ion interaction is described in terms of ultrasoft pseudopotentials (see Vanderbilt 1990 and Kresse and Hafner 1994b). VASP allows for the calculations of the Hellmann–Feynman forces acting on the atoms and of the stresses on the unit cell. Hence the total energy may be optimised with respect to the volume and shape of the unit cell and of the positions of the atoms within the cell, with no other restrictions than those imposed by space-group symmetry. If such calculations are performed for several structure types it is possible to predict that structure which has the lowest equilibrium total energy, i.e. which is the stable one. Furthermore, it is possible to calculate the structural parameters (lattice parameters, atomic positions within the unit cell) from first principles, i.e. with no fitted parameters.

In any case a systematic analysis and generalisation of the available experimental data on the phase diagrams and compounds can contribute to improve the existing empirical or theoretical concepts. These regularities can also be used to predict the structure type and the properties of system not yet investigated. Below, some regularities and peculiarities of scandium metal systems and intermetallics found as a result of an analysis of the experimental data presented in sects. 2–4 are summarised.

5.1. *Regularities found in binary scandium phase diagrams*

All 65 investigated Sc–E binary phase diagrams can be divided into four types:

(1) Systems with complete mutual solubility of components in liquid and solid (in at least one phase). Binary compounds do not occur. (E = 3A (except Eu, Yb, U), or 4A element).
(2) Systems with immiscibility gap in liquid (monotectic). Binary compounds do not occur (E = 2A element or 3A element Eu, Yb, or U).
(3) Systems with low or no mutual solubility of the components in solid (eutectic). Binary compounds do not occur (E = 5A, 6A element).
(4) Systems with one or more binary compounds. Limited mutual solubility of the components in solid. (E = 2A, 7A–8A, 1B–6B element).

There are only two exceptions: the systems with U and Pu. Pu forms one binary compound with Sc, and in the Sc–U system appreciable limited mutual solubility of components in solid occurs. All rare earths (except Eu and Yb) and the 4A elements (Ti, Zr and Hf) are completely miscible with Sc in liquid and solid. It is necessary to indicate that Sc is the only element among the rare earths which forms continuous series

of solid solutions with other rare earths and with 4A elements. Zr and Hf, which have nearly the same atomic radius as Sc (1.602, 1.580 and 1.641 Å, respectively), usually form binary systems of the eutectic type with other rare earths, e.g. Zr–Y, Zr–Gd, Zr–Dy, Zr–Er, Hf–Y, Hf–Er (Massalski 1990).

Only Eu and Yb, among the rare earths, form immiscibility gaps with Sc in the liquid and solid. The difference in valence of these two rare earths and Sc is, perhaps, the main reason of this difference of interaction. The divalent state is more typical for Eu and Yb, whereas the other rare earths are usually trivalent. The same divalent state is characteristic for alkaline earths which are immiscible with Sc in the liquid and solid too. Therefore, it is possible to predict the same type of binary phase diagrams of Sc with alkaline metals. These elements are even more different from Sc in the valence state and other characteristics (melting temperature, electronegativity, etc.) than are the alkaline-earth metals.

All 5A–6A elements form eutectic-type binary systems with Sc with a low mutual solid solubility. With increasing melting temperature of the transition element the eutectic point shifts towards scandium.

The elements of all other groups form binary compounds with scandium. The number of binary compounds in each system is indicated in table 1 (above). Within each large period Sc forms the largest number of binary compounds with 8A and 3B elements. In the rows of the p-elements the number of binary compounds decreases with the increase of the group number of the element. The number of binary compounds changes inconsiderably with the increase of the period's number.

In the Sc–M (M = d element) binary systems, binary compounds of equiatomic composition ScM usually have the highest absolute values of enthalpy (Colinet and Pasturel 1994) and the highest melting temperature in the system. In the systems of scandium with p-elements the richest in scandium compound usually is the most thermodynamically stable one. Its composition is Sc_5E_3 (E = Ga, Si, Ge, Sn, Pb), or ScE_2 (E = B), or ScE_{1-x} (E = C). As was stated by Lukashenko et al. (1990a,b, 1991) scandium silicides and germanides are much more thermodynamically stable in comparison to silicides and germanides of other 3d elements. The thermodynamic properties are closer to those of the silicides and germanides of the lanthanides, than the 3d elements.

114 binary intermetallic compounds of scandium with definite crystal structure crystallize in 29 different compositions and belong to 56 structure types (table 28). The majority of them occur at constant compositions. In the cases when compounds have a variable composition their homogeneity ranges usually do not exceed 1 to 5 at.%. The compounds ScMg(β') and ScC_{1-x} are the only two exceptions. The most common compositions of the scandium intermetallics occur at the stoichiometries ScE (30 compounds), ScE_2 (20 compounds), ScE_3 (9 compounds), Sc_2E (8 compounds) and Sc_5E_3 (8 compounds). Thus, more than 55% of binary scandium intermetallics (75 compounds among 134 known today) occur only at five simple stoichiometries out of 29 known to date. At these stoichiometries the compounds crystallize in different structure types depending on the position of element in the periodic table, as seen in table 28.

Table 28
Stoichiometries and structure types of binary scandium intermetallics

Formula	Sc content (at.%)	Structure type	Pearson's symbol	Element (E) which forms the compound
ScE_{13}	7.14	$NaZn_{13}$	cF112	Be
ScE_{12}	7.69	$ThMn_{12}$	tI26	Zn
		UB_{12}	cF52	B
ScE_7	12.50	αMn	cI58	Tc
		$ScCd_7$	oS32	Cd
Sc_3E_{17}	15.00	Ru_3Be_{17}	cI160	Zn
ScE_5	16.67	$CaCu_5$	hP6	Be, Ni
Sc_5E_{24}	17.24	αMn	cI56	Re
$Sc_{13}E_{58}$	18.31	$Gd_{13}Cd_{58}$	hP142	Zn
ScE_4	20.00	$MoNi_4$	tI10	Ag, Au
Sc_2E_7	22.22	Ce_2Ni_7	hP36	Ni
ScE_3	25.00	$AuCu_3$	cP4	Rh, Pd, Ir, Pt, Al, Ga, In
		$SnNi_3$	hP8	Cd, Hg
ScE_2	33.33	$MgZn_2$	hP12	Mn, Tc, Re, Fe, Ru, Os
		$MgCu_2$	cF24	Co, Ni, Ir, Al
		$MgNi_2$	hP24	Fe
		$MoSi_2$	tI6	Cu, Ag, Au
		AlB_2	hP3	Zn, B
		KHg_2	oI12	Ga
		$ZrGa_2$	oS12	In
		$ZrSi_2$	oS12	Ge
		$ScSn_2$	tI24	Sn
$ScE_{1.74}$	36.50	$MgCu_2$	cF24	Fe
Sc_3E_5	37.50	Tm_3Ga_5	oP32	Ga
		Pu_3Pd_5	oS32	Tl
Sc_2E_3	40.00	AlB_2	hP3	Si
		Sc_2S_3	oF80	Se
		Ti_7S_{12}	hR8	Te
Sc_3E_4	42.86	Sc_3C_4	tP70	C
ScE	50.00	CsCl	cP2	Mg, Co, Ni, Ru, Rh, Pd, Ir, Pt, Cu, Ag, Au, Zn, Cd, Hg, Sn
		CrB	oS8	Al, Ga, Si, Ge
		AuCu	tP4	In
		NaCl	cF8	C, P, As, Sb, Bi, Se
		NiAs	hP4	Te, Po
$Sc_{11}E_{10}$	52.38	$Ho_{11}Ge_{10}$	tI84	Ge
Sc_6E_5	54.55	Ti_6Ge_5	oI44	Sn, Pb

continued on next page

Table 28, *continued*

Formula	Sc content (at.%)	Structure type	Pearson's symbol	Element (E) which forms the compound
Sc_5E_4	55.56	$Ho_{11}Ge_{10}$	tI84	Ga
		CsCl	cP2	In
		Ti_5Ga_4	hP18	Tl
		Sm_5Ge_4	oP36	Ge
Sc_4E_3	57.14	Th_3P_4	cI28	C
Sc_3E_2	60.00	Gd_3Ga_2	tI80	Ga
		Cr_3C_2	oP20	P, As
		S_3Sb_2	oP20	P, As
		V_3As_2	tP32	As
Sc_5E_3	62.50	Mn_5Si_3	hP16	Ga, Tl, Si, Ge, Sn, Pb
		βYb_5Sb_3	oP32	As, Sb
Sc_2E	66.67	Al_2Cu	tI12	Co
		Ti_2Ni	cF96	Ni, Pd, Ir
		Co_2Si	oP12	Pt
		Ni_2In	hP6	In, Tl
		Cu_2Sb	tP6	Sb
Sc_7E_3	70.00	Th_7Fe_3	hP10	P
		Sc_7As_3	tI80	As
$Sc_{11}E_4$	73.33	$Sc_{11}Ir_4$	cF120	Ru, Os, Ir
Sc_3E	75.00	Sc_3Co	oP32	Co
		Ni_3Sn	hP8	In
		Fe_3C	oP16	P
$Sc_{57}E_{13}$	81.43	$Sc_{57}Rh_{13}$	cP140	Ru, Rh, Ir, Pt
$Sc_{29}E_6$	82.86	$Sc_{29}Fe_6$	cP140	Fe
$Sc_{44}E_7$	86.27	$Mg_{44}Rh_7$	cF408	Os, Ir

Some binary compounds occur in two ($ScFe_2$, $ScNi_5$, Sc_4C_3, $ScSi_{1.5}$, Sc_3P_2) or in three (Sc_3As_2) polymorphic modifications. The crystal structures of polymorphic forms are structurally related.

There is also a relation between the interval of stoichiometries (i.e. the composition range where the intermetallic phases are formed in the binary Sc–E system, see fig. 92) of binary compounds and the position of element in the periodic table. The widest intervals of compositions of the binary compounds with Sc display 8A and 3B elements (fig. 92). These are the elements which form the largest number of binary compounds with scandium. In the rows of d elements the least scandium content in compounds increases from 7A to 1B element and then sharply decreases for the 2B elements. A similar relation

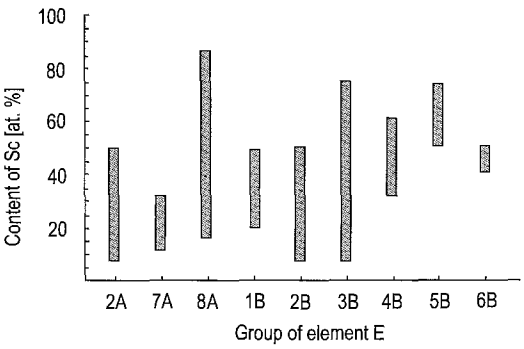

Fig. 92. Intervals of stoichiometries of Sc–E binary compounds depending on the position of the E element in the periodic table.

is observed in the rows of p elements. The least scandium content sharply increases from 3B to 5B element and then decreases.

5.2. *Regularities found in ternary scandium phase diagrams*

Assuming that the data concerning a certain ternary system are complete if at least one isothermal section of the system has been investigated for $\frac{3}{4}$ of the concentration region. There are about 70 such Sc–M–X ternary systems preferably with M = d, f element and X = B, Al, Ga, C, Si, Ge (table 13, above). The corresponding data are summarised in the tables 29 and 30. However, in such ternary systems additional ternary compounds which are stable over a limited temperature range may also exist. They, of course, will not be observed in investigation of the system at one temperature only, or if only a part of the system has been studied. In total, 420 ternary scandium intermetallic compounds have been synthesized. For 348 compounds (82.9%) the crystal structure was defined, and these compounds belong to 111 structure types.

The crystal structures have been investigated most completely for ternary compounds of the Sc–M–X systems with M = 3d, 4d, 5d, 4f element: with X = B, Al, Ga 102 compounds are known and with X = C, Si, Ge 178 compounds are known. Their compositions are given in figs. 93 and 94. Similarly as in the case of the binary systems, within the sequence of these ternary systems Sc–M–B, Sc–M–Al and Sc–M–Ga etc., within each period of the periodic table the number of ternary compounds usually increases with increasing atomic number of component M. The 8A-group elements therefore form the largest number of ternary compounds. Among the systems with 3B and 4B elements the ternary systems with boron differ considerably from those with aluminium and gallium. Also, the carbon systems behave different when compared with the Si and Ge systems. These systems differ by the number of ternary compounds occurring and by their compositions (tables 29 and 30, figs. 93 and 94). The ternary compounds $ScMB_2$ and $ScMC_2$ are exceptions in this sense. However, even in these cases the crystal structures of the $ScMB_2$ and $ScMC_2$ compounds are different from those of the $ScMAl_2$, $ScMSi_2$ or $ScMGe_2$ compounds. In all other cases the stoichiometries of the ternary borides and carbides are different from

Table 29
Summary of information known about the Sc–M–B(Al, Ga) and Sc–X–B(Al, Ga) ternary systems

	1A	2A	3A	4A	5A	6A	7A	8A			1B	2B	3B	4B	5B	6B
2	Li □ 0	Be											B	C		
3	Na	Mg ■ 0											Al	Si	P	
4	K	Ca □ 0	Sc	Ti ■ 0 ■ 3	V ■ 1	Cr ■ 1 ■ 0 ■ 1	Mn ■ 1 ■ 0 ■ 3	Fe ■ 1 ■ 3 ■ 8	Co ■ 4 □ 3 ■ 17	Ni ■ 5 ■ 4 ■ 14	Cu ■ 10 ■ 9	Zn	Ga	Ge	As	Se
5	Rb	Sr ■ 0	Y ■ 1 ■ 1	Zr ■ 0 ■ 1	Nb ■ 0 ■ 2	Mo ■ 0	Tc	Ru □ 3 ■ 6 □ 1	Rh □ 1 □ 1	Pd ■ 5	Ag □ 1	Cd	In □ 1	Sn □ 1	Sb	Te
6	Cs	Ba ■ 0	La □ 0 □ 0	Hf ■ 0 ■ 2	Ta	W □ 2 □ 1 □ 1	Re □ 2 □ 1 □ 1	Os □ 2 □ 1 □ 1	Ir □ 3 □ 1 □ 1	Pt □ 1	Au □ 1	Hg	Tl □ 1	Pb □ 1	Bi	Po
7	Fr	Ra	Ac	Ku	Ns											

	Ce	Pr	Nd	Pm	Sm	Eu	Gd	Tb	Dy	Ho	Er	Tm	Yb	Lu
6	□ 0				■ 0		■ 0	■ 1	■ 0	■ 0	■ 0	■ 0	□ 0	■ 0
7	Th	Pa	U	Np	Pu	Am	Cm	Bk	Cf	Es	Fm	Md	No	Lr

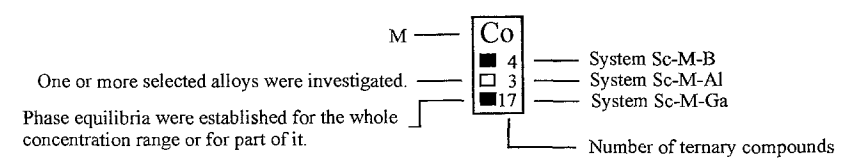

Lack of the symbol means the system has not been investigated.

the stoichiometries of ternary compounds of their neighbours among 3B and 4B elements, respectively.

In inorganic chemistry it is known that within each group of the periodic table the elements of the second period differ considerably in their properties from those

Table 30
Summary of information known about the Sc–M–C(Si, Ge) and Sc–X–C(Si, Ge) ternary systems

	1A	2A	3A	4A	5A	6A	7A	8A			1B	2B	3B	4B	5B	6B
2	Li	Be											B □ 3	C		
3	Na	Mg											Al □ 2 ■ 1 □ 1	Si □ 0	P	
4	K	Ca	Sc	Ti □ 0 ■ 0	V ■ 3 ■ 2	Cr ■ 2 ■ 3 ■ 4	Mn ■ 4 ■ 6	Fe ■ 2 ■ 16 ■ 8	Co ■ 3 ■ 12 ■ 8	Ni ■ 2 ■ 15 ■ 10	Cu ■ 5 ■ 2	Zn	Ga	Ge ■ 0	As	Se
5	Rb	Sr	Y ■ 1 ■ 3	Zr ■ 0	Nb ■ 2 ■ 1	Mo ■ 0 ■ 1 ■ 1	Tc	Ru ■ 1 □ 2 □ 3	Rh ■ 0 ■ 10 □ 3	Pd ■ 0 □ 1 □ 1	Ag ■ 0 ■ 1	Cd	In	Sn □ 1	Sb	Te
6	Cs	Ba	La □ 2 □ 2	Hf ■ 0 ■ 0	Ta ■ 0 ■ 1	W ■ 1 ■ 0	Re □ 1 ■ 5 □ 1	Os □ 1 □ 3	Ir □ 1 □ 4 □ 2	Pt □ 1	Au □ 1	Hg	Tl	Pb □ 1	Bi	Po
7	Fr	Ra	Ac	Ku	Ns											

	Ce	Pr	Nd	Pm	Sm	Eu	Gd	Tb	Dy	Ho	Er	Tm	Yb	Lu
6	■ 8 ■ 4	■ 8 □ 2	■ 5 ■ 3		■ 5 □ 2	□ 1			■ 2 ■ 3		■ 0		■ 2	■ 0
7	Th □ 0	Pa	U	Np	Pu	Am	Cm	Bk	Cf	Es	Fm	Md	No	Lr

M — Re
One or more selected alloys were investigated. — □ 1 — System Sc-M-C
Phase equilibria were established for the whole concentration range or for part of it. — ■ 5 — System Sc-M-Si
□ 1 — System Sc-M-Ge
Lack of the symbol means the system has not been investigated. — Number of ternary compounds

of their neighbours in the group. This difference exists also among their intermetallic compounds.

Intermetallic compounds of scandium with the 6B elements Se, Te and Po are different compared to all of the previously described scandium compounds. They crystallize in structures typical for oxides, sulphides and other ionic compounds (Al_2MgO_4, Fe_2CaO_4, $ErCuS_2$, ErAgAs, NaCl structure types). In these structure types each atom is coordinated

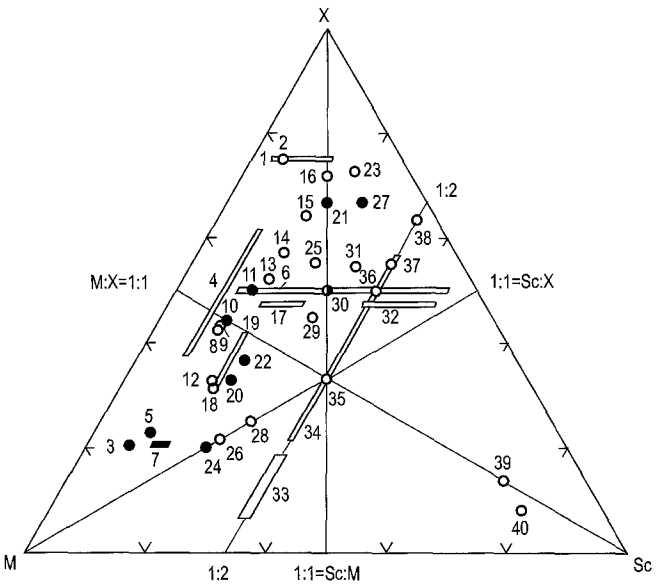

Fig. 93. Compositions of ternary compounds with established crystal structure in the systems Sc–M–X (M = 3d, 4d, 5d, 4f element; solid circles: X = B; open circles: X = Al, Ga). (1) $Sc_{0.15-0.55}M_{0.85-0.45}Al_3$ (2 compounds); (2) $Sc_{0.2}Hf_{0.8}Ga_3$; (3) $Sc_2Co_{21}B_6$; (4) $ScM_{7.1-4.0}X_{4.9-8.0}$ (6 compounds); (5) $Sc_4Ni_{29}B_{10}$; (6) $Sc_{0.2-0.9}Hf_{0.8-0.1}Ga$; (7) $Sc_{3-4}Ni_{20-19}B_6$; (8) $ScCo_{4.5}Ga_{4.1}$; (9) $Sc_2Fe_{8.83}Ga_{8.17}$; (10) ScM_4B_4 (2 compounds); (11) $ScIr_3B_4$; (12) $ScCu_{3.7}Ga_{2.3}$; (13) $ScNi_{2.36}Ga_{3.64}$; (14) ScM_2Ga_4 (2 compounds); (15) $Sc_2Co_3Ga_9$; (16) $ScMGa_5$ (3 compounds); (17) $Sc_{3.2-4.7}Zr_{7.8-6.3}Ga_{10}$; (18) $Sc_2Co_7Ga_4$; (19) $Sc_2Ni_{7-5.5}Ga_{4-5.5}$; (20) ScM_3B_2 (2 compounds); (21) $ScMB_4$ (5 compounds); (22) $Sc_2M_5B_4$ (2 compounds); (23) Sc_2MGa_8 (2 compounds); (24) ScM_3B (2 compounds); (25) $Sc_6M_7X_{16}$ (12 compounds); (26) $Sc_{14}Cu_{37}Ga_{14}$; (27) Sc_2ReB_6; (28) ScM_2X (8 compounds); (29) $ScM_{1.2}Ga_{1.8}$ (2 compounds); (30) $ScMX_2$ (2 compounds); (31) $Sc_3M_2Ga_6$ (2 compounds); (32) $Sc_{6.8-9.4}M_{4.2-1.6}Ga_{10}$ (2 compounds); (33) $ScFe_{1.82-1.44}X_{0.18-0.56}$ (2 compounds); (34) $ScM_{1.37-0.30}X_{0.63-1.70}$ (15 compounds); (35) ScMGa (2 compounds); (36) $ScM_{0.5}Ga_{1.5}$ (2 compounds); (37) $ScM_{0.35}Ga_{1.65}$ (2 compounds); (38) $ScM_{0.1}Ga_{1.9}$ (2 compounds); (39) $Sc_5M_{1-x}Ga_{1-x}$ (2 compounds); (40) $Sc_{8.5}M_{1.2}Ga$ (2 compounds).

by the atoms of the other elements, e.g. Sc atoms are surrounded by 6B atoms and vice versa. The coordination about a given atom is preferably octahedral and/or tetrahedral. At the same time these compounds show a metallic glide and a semimetal type of electrical conductivity (White and Dismukes 1965, Guittard et al. 1964, Hulliger and Vogt 1966, Julien-Pouzol et al. 1968, Julien-Pouzol and Guittard 1969). These compounds represent borderline cases between metallic and semimetal behaviours. On the other hand the atoms in the structures of typical intermetallic compounds are surrounded by both different atoms and identical atoms. The coordination number of atoms in intermetallics is rather high, from 6 to 20. The majority of scandium-containing phosphides and arsenides belong to the structure types which are typical for intermetallics, e.g. TiNiSi, $ZrFe_4Si_2$, $Zr_2Fe_{12}P_7$, etc.

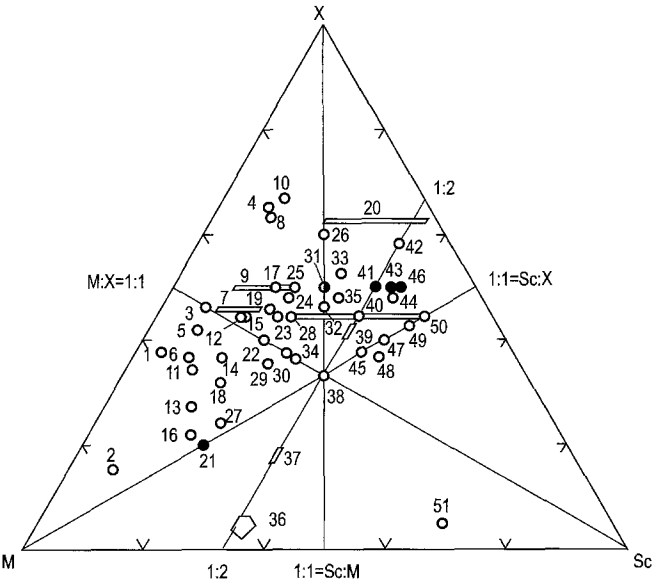

Fig. 94. Compositions of ternary compounds with established crystal structure in the systems Sc–M–X (M = 3d, 4d, 5d, 4f element; solid circles: X = C; open circles: X = Si, Ge). (1) $Sc_{0.35}M_{4.65}Si_3$ (2 compounds); (2) $ScFe_{10}Si_2$; (3) ScM_6Ge_6 (5 compounds); (4) $Sc_{1.2}Fe_4Si_{9.8}$; (5) $ScFe_6Ge_5$; (6) ScM_6Ge_4 (2 compounds); (7) $Sc_{1-1.8}V_{5-4.2}X_5$ (2 compounds); (8) ScM_3Si_7 (2 compounds); (9) $Sc_{0.2-0.4}Sm_{0.8-0.6}Si$; (10) $Sc_{0.3}M_{0.7}Si_2$ (2 compounds); (11) $Sc_6Co_{30}Si_{19}$; (12) $Sc_{1.26}Pr_{3.74}Si_4$; (13) $ScFe_4Si_2$; (14) $Sc_{12.3}Ni_{40.7}Ge_{31}$; (15) $Sc_{1.35}Y_{3.65}Ge_4$; (16) $Sc_3Ni_{11}X_4$ (2 compounds); (17) $ScNi_2Si_3$; (18) $Sc_6Ni_{18}X_{11}$ (2 compounds); (19) $Sc_2Cr_4X_5$ (2 compounds); (20) $Sc_{0.52+x}M_{0.48-x}Si_{1.67}$ (4 compounds); (21) ScM_3C (3 compounds); (22) ScM_2X_2 (9 compounds); (23) $Sc_{1.8}Dy_{3.2}Ge_4$; (24) $Sc_5Re_8Si_{12}$; (25) $Sc_2M_3Si_5$ (2 compounds); (26) $ScNiSi_3$; (27) $Sc_6M_{16}X_7$ (3 compounds); (28) $Sc_{2+x}M_{3-x}X_4$ (11 compounds); (29) $Sc_4M_7X_6$ (6 compounds); (30) $Sc_2V_3Si_3$; (31) $ScMX_2$ (16 compounds); (32) $Sc_4M_4X_7$ (5 compounds); (33) $Sc_5M_4Si_{10}$ (3 compounds); (34) $Sc_3M_4X_4$ (4 compounds); (35) $Sc_6Yb_5Ge_{10}$; (36) $Sc(Fe, X)_2$ (2 compounds); (37) $ScM_{1.5}X_{0.5}$ (4 compounds); (38) ScMX (34 compounds); (39) $Sc_7M_{4+x}X_{10-x}$ (4 compounds); (40) $Sc_3M_2Si_4$ (6 compounds); (41) Sc_2CrC_3; (42) $ScM_{0.25}Si_{1.75}$ (4 compounds); (43) $Sc_5Re_2C_7$; (44) $Sc_3M_{1.22}Ge_4$ (5 compounds); (45) $Sc_3M_2X_3$ (4 compounds); (46) Sc_3MC_4 (3 compounds); (47) Sc_2MX_2 (3 compounds); (48) $Sc_9Ni_5Ge_8$; (49) Sc_3NiSi_3; (50) Sc_4NdSi_4; (51) $Sc_2M_{0.85}Si_{0.15}$ (2 compounds).

A large number of ternary Sc–M–X compounds occur at stoichiometries which lie on three cross sections of a ternary phase diagram with the atomic ratios Sc : X = 1 : 1, Sc–M = 1 : 1, and M : X = 1 : 1, and on the section with Sc content of 33.3 at.% (see figs. 93 and 94). 55 ternary compounds with X = B, Al, Ga and 111 compounds with X = C, Si, Ge occur on these sections. Thus, more than half of the ternary compounds of 3B and 4B elements with known crystal structures lies on these four characteristic cross sections.

The analysis of the stoichiometries of 68 ternary scandium intermetallics determined in other systems (Sc–M–X, X = 5B, 6B element; Sc–X–X′; Sc–M–M′) shows that 48 of them (~71%) also belong to these four sections. This means that about $\frac{2}{3}$ of all scandium ternary intermetallics known today crystallize only on four appointed sections of phase diagrams and generally have simple stoichiometries.

This regularity had been discovered by Kotur and Bodak (1981) in a limited series of Sc–M–Si (M = 3d element) systems. However, it seems to be characteristic for all ternary systems of scandium. As was mentioned by Villars (1995), simple stoichiometric ratios are in general preferred by intermetallic compounds.

A summary of the crystal structure data of the 463 (114 binary, 348 ternary and 1 quaternary) intermetallic compounds of scandium reviewed in this chapter are presented in Appendix A. They belong to 155 structure types, which are arranged in decreasing order according to the number of existing compounds. Structure types with the same number of representatives are arranged according to increasing number of atoms per unit cell. The number of the binary and ternary compounds representing each structure type is also given. Generalised data about the occurrence of ternary compounds of the various structure types in each group of systems is indicated too. The corresponding data for the binary systems are shown in table 28.

The largest number of ternary compounds are those with the simplest compositions: ScMX (a total of 61 compounds); $ScMX_2$ (19), ScM_2X (18), ScM_2X_2 (10), Sc_3MX (9). A similar regularity has been found for binary scandium intermetallics (see sect. 5.1).

As one can see from figs. 93 and 94 more than 90% of all the intermetallic Sc compounds occur in the region of ternary system where the scandium content is less than ~50 at.% and which is limited by the sections Sc : M = 1 : 1 with X content from 0 to 33.3 at.% and Sc : X = 1 : 1 with the M content from 0 to 33.3 at.%.

A comparison of the investigated ternary systems of scandium with the related ternary systems of other rare-earth elements, which was presented in a Handbook by Bodak and Gladyshevsky (1985), reveals that especially for the light rare earths the ternary compounds often occur at larger RE content ($\geqslant$50 at.%). In this regard the scandium systems are closer to the systems of the d elements, especially those of the 4A group, Ti, Zr and Hf.

The majority of the scandium intermetallic structure types can also be found among intermetallic compounds of other rare earths as well as among intermetallics of the 4A elements (Villars and Calvert 1991). However, taking into consideration all 155 structure types of scandium intermetallics, from a crystal-chemical point of view, scandium appears to be closer to 4A elements, especially to Zr and Hf, rather than to the other rare earths.

The compounds of equiatomic composition ScMX, which occur frequently in ternary systems, belong to TiNiSi structure type and rarely to the ZrNiAl type structure. These two structure types are characteristic for intermetallics of d transition elements. The compounds of the other rare-earth elements prefer FClPb, ZrNiAl and AlB_2 structure types (Villars and Calvert 1991). The RM_2X_2 compounds belong to one of the most frequently occurring structure types, namely $CeGa_2Al_2$ (or $ThCr_2Si_2$) and La_2O_2S. We note that among ScM_2X_2 compounds only three representatives are known with the $CeGa_2Al_2$ type structure, but none with the La_2O_2S type structure. The $ScFe_2Si_2$ compound is isotypic with $HfFe_2Si_2$, which does not occur among other rare-earth intermetallics. Another typical stoichiometric ratio of the rare-earth compounds is RMX_2, however, scandium is the only rare-earth element which does not form phases with $CeNiSi_2$ structure type, but instead forms compounds of the

$ZrCrSi_2$ (or $TiMnSi_2$) type. Scandium is the only rare earth which forms compounds with $ZrSi_2$, $Zr_4Co_4Ge_7$, $Zr_2Cr_4Si_5$ structure types, which are frequently observed among intermetallics of d elements. There are no d-element compounds of the $ScNiSi_3$, $Sc_2Fe_3Si_5$, $Sc_2Co_3Si_5$, $Sc_3Ni_{11}Si_4$ structure types, however, a lot of them are found among rare-earth intermetallics. These are examples confirming the unique position of scandium within the family of rare-earth elements. To some extent Sc is the linking element between the rare earths and the d elements.

5.3. *Atomic size factor and its influence on the nature of scandium intermetallics*

The constant compositions of ternary compounds and the absence of solid solutions on the basis of binary compounds are other characteristic features of scandium systems (with the exception of the systems Sc–M–Ga with M = rare earth or 4A element). However, in some systems solid solutions of phases with narrow homogeneity regions occur. Sometimes a substitution of Sc and M atoms occurs and sometimes the M and the X atoms are mutually substituted. There is no doubt that the atomic size factor has a dominating influence on the formation of solid solutions and their nature (solid solutions of substitution, of inclusion or of subtraction of atoms). Examples of solid solutions of substitution are presented in table 31. It is interesting to note that all ternary compounds which form such solid solutions crystallize in structures characteristic for binary compounds.

Julien-Pouzol et al. (1968) found that in the Sc–Cu–Se ternary system a solid solution with the limit compositions $ScCuSe_2$–$Sc_{0.67}Cu_2Se_2$ exists due to the subtraction of a

Table 31
Mutually substituted atoms in the structures of ternary compounds of the Sc–M–X systems

Mutually substituted atoms			Ratio of atomic radii		Structure type of ternary compound
Sc–M	X–M		r_{Sc}/r_M	r_X/r_M	
	X	M			
Y, Nd, Sm, Dy			0.91–0.93		$\alpha ThSi_2$, AlB_2
Y, Tb			0.91; 0.92		$TiNi_3$
V			1.22		Ti_6Ge_5
Nb, Mo			1.13; 1.18		Mn_5Si_3; $Ho_{11}Ge_{10}$
Y, Ta, Mo, W			0.91–1.18		Sm_5Ge_4
Ti, Zr			1.12; 1.03		$Ho_{11}Ge_{10}$
	Al–	Ni, Fe, Ru, Pd		1.12–1.04	$MgZn_2$
		Fe, Cu		1.10; 1.09	$MgZn_2$, $MgCu_2$
	Ga–	Fe, Co, Ni		1.10–1.12	$MgZn_2$, $MgCu_2$
		Ni, Cu		1.12; 1.09	$CaIn_2$
	Si–	Mn, Fe, Co, Ni		1.03–1.08	$MgZn_2$
	Ge–	Cr, Mn		1.03; 1.06	$Ho_{11}Ge_{10}$

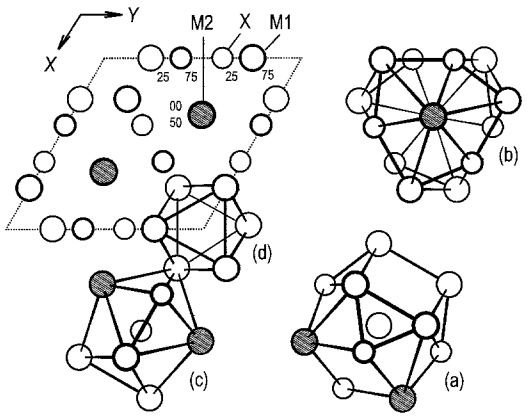

Fig. 95. Projection of the structure Mn_5Si_3 along 001. CP of atoms: (a) M1 occupying 6(g) site with CN = 15; (b) M2 occupying 4(f) site with CN = 14; (c) Si occupying another 6(g) site with CN = 11. Empty octahedra [$M1_6$] are labelled (d).

fraction of Sc atoms and the addition of Cu atoms in different atomic sites. Other examples of solid solutions of addition or subtraction are observed in other ternary systems, such as Sc–M–X and Sc–X′–X (X = B, C) where small boron or carbon atoms are added into the octahedral cavities of the $AuCu_3$ type structure, revealing the formation of perovskite-type ternary compounds ScM_3B_{1-x}, $Sc_3X'B_{1-x}$, ScM_3C_x and $Sc_3X'C_x$ (Holleck 1977).

The binary compounds Sc_5Si_3 and Sc_5Ge_3 can be distinguished among other binary scandium intermetallics. Both crystallize in the Mn_5Si_3 structure type (hP16; SG $P6_3/mcm$), which is a common structure type of intermetallics. Its projection along the 001 direction is presented in fig. 95. The A_5B_3 compounds with the Mn_5Si_3 structure type are formed by 3A–8A elements as the A constituent with the 3B–5B elements as the B constituent (Villars and Calvert 1991). The ratios of atomic radii (r_A/r_B) for these compounds are observed over a wide interval, from 0.83 for Ti_5Pb_3 to 1.35 for Y_5Si_3. This is, perhaps, the main reason for the existence of substitutional solid solutions of Sc and the majority of d and f elements in Sc_5Si_3 and Sc_5Ge_3 over wide compositional intervals up to formation of continuous series of solid solutions.

Usually the lattice parameters of these solid solutions display a nonlinear dependence on the composition. These data are available in numerous papers, see e.g. Kotur and Parasiuk (1994), Kotur (1986, 1991), Kotur and Mokra (1994). The nature of mutual substitution of Sc and other atoms has been investigated by Kotur and Parasiuk (1994) for the $Sc_2Er_3Si_3$ and $Sc_3Er_2Si_3$ continuous series of solid solutions, i.e. $Sc_xEr_{5-x}Si_3$. Scandium and erbium atoms substitute for each other statistically in two crystallographic sites 6(g) and 4(f) of the structure within the solid solution. Contrary to these data the investigation of the ScV_4Si_3 single crystal revealed a partial ordering of Sc and V atoms in the structure (Kotur et al. 1983a). V atoms occupy the 4(f) site with CN = 14, and the rest of the V atoms together with Sc atoms occupy the 6(g) site with the higher CN = 15. The solubility of V in Sc_5Si_3 at 800°C does not exceed 1 at.%. The ternary compound $Sc_2V_3Si_3$ with practically a constant composition at 800°C isotypic with Mn_5Si_3 has been found in the system. The reason seems to be the considerably large difference in the atomic sizes of Sc and V in comparison to the sizes of Sc and Er atoms.

The Mn_5Si_3 structure type can be also stabilized in systems by the inclusion of small C, N, O or B atoms into the empty octahedra [$\square M1_6$]. Columns of these octahedra are stretched along 6_3 axes in the structure (fig. 95). Kotroczo and McColm (1987) and McColm and Kotroczo (1987) investigated hydrogen sorption into the [$\square R_6$] octahedra of Sc_5Si_3, Sc_5Ge_3 binary compounds and of three- and four-component alloys of solid solutions based on these binary phases. As a result the hydrides of the $Y_{5-a}Sc_aSi_3H_{2.5}$, $Y_{5-a}Sc_aSi_3H_{1.5}$, $Y_{5-a}Sc_aSi_{3-b}Ge_bH_{2.5}$ and $Y_{5-a}Sc_aSi_{3-b}Ge_bH_{1.5}$ compositions have been obtained.

Venturini et al. (1989) investigated the nature of solid solutions $(Lu_{1-x}Sc_x)_5Ir_4Si_{10}$ and $(Y_{1-x}Sc_x)_5Ir_4Si_{10}$ which occur between isotypic ternary compounds $R_5Ir_4Si_{10}$ (ST $Sc_5Co_4Si_{10}$). The lattice parameters of the $(Lu_{1-x}Sc_x)_5Ir_4Si_{10}$ solution exhibit a negative deviation from Vegard's rule within its homogeneity range. Single-crystal investigations reveal that the Lu and Sc atoms statistically occupy three R atomic sites in this structure. A statistical substitution of Sc by the heavy R atoms is commonly observed in the systems, however, such admixture is rare in ternaries with light R elements. As a result, ternary compounds with ordered or partially ordered structures in the rare-earth sites occur. This is also the result of the influence of the atomic size factor. The number of compounds in the Sc–R–Si systems decreases remarkably when passing from systems with light rare earths (Sc–Ce–Si, eight ternary compounds; Sc–Nd–Si, five compounds) towards heavy rare-earth systems (Sc–Dy–Si, two compounds; Sc–Lu–Si, no compounds known) (Kotur 1995), however, simultaneously the possibility for a mutual substitution of Sc and R atoms increases. For example, the highest solubility of Sc and R at 600°C in the binary phases in the Sc–R–Si systems is as follows: 6 at.% (R = Ce), 13 at.% (R = Sm), continuous solid solution (R = Dy, Lu). The main reason for this is the decrease of the R atomic radius from Ce towards Lu due to the lanthanide contraction.

Among the d elements only Ti, Zr and Hf can form solid solutions of substitution with Sc up to continuous series of solid solutions. Such solid solutions are observed in binary as well as in ternary systems. The atomic size factor is the main reason for these phenomena.

However, the influence of other factors (beside the atomic size factor) on the interaction of the elements is obvious when comparing the ternary systems R–Sc–Si and R–Zr(Hf)–Si. These data are presented in table 32. Although the atomic sizes of Sc, Zr and Hf are nearly the same the interaction of 4A elements with the rare earths in binary and ternary systems is different from that in the corresponding systems of scandium with the rare earths. It does not depend on whether R is a light or heavy rare earth. Sc is completely miscible with Ce and Y in binary systems while Y–Zr and Y–Hf systems are of eutectic type with low mutual solubility of the components in the solid. In the Ce–Hf system an immiscibility gap in the liquid and solid occurs (Massalski 1990). The same type of behaviour is predicted for the Ce–Zr binary system.

Thus, the position of scandium among the family of rare earths is to some extent unique. Sometimes it behaves as a typical R element (e.g. showing a complete miscibility, except with Eu and Yb), however in other cases it exhibits a behaviour more similar to the d elements (e.g. displaying complete miscibility with them too, namely with Zr and Hf).

Table 32
Comparison of characteristics of R–M–Si (M = Sc, Zr, Hf) ternary systems

Characteristic	Systems					
	Y–M–Si			Ce–M–Si		
	Sc	Zr	Hf	Sc	Zr	Hf
Number of ternary compounds	1	1	0	8	3	0
Occurrence of continuous series of solid solutions	+	–	–	–	–	–
Average mutual solubility of R and M in solid solutions at 600°C (at.%)	30	10	<5	<5	<2	<2
Maximum mutual solubility of R and M in solid in binary R–M systems (Massalski 1990)	100	3	1	100	5	1
References	1	2	2	2	2	2

References
1. Kotur and Mokra (1994)
2. Bodak and Gladyshevsky (1985)

This peculiarity of scandium is also observed in ternary systems. It is a linking element between the rare earth and the d transition elements. Zr, Hf and the heavy rare earths are the elements with which scandium forms statistical mixtures of atoms, up to a complete mutual substitution in the structures. With other elements scandium occupies regular atomic positions in the structures and forms, as usual, ternary compounds of constant composition.

5.4. *Relations between compositions and crystal structures of scandium intermetallics*

There are 155 known structure types of scandium intermetallics having a different number of representatives from only 1 up to 20 (see Appendix A). More than half of the ternary compounds studied up to now (207, ~60%) belong to only 25 structure types with representatives from 5 to 20. Of these 25, 21 structure types also occur in binary compounds or are superstructures to corresponding binary prototypes. In the group of 27 most frequently occurring structure types of scandium intermetallics there are 9 structure types, namely $MgZn_2$, CsCl, AlB_2, $MgCu_2$, Mn_5Si_3, $AuCu_3$, CrB, $ZrSi_2$, Ti_2Ni, observed for 52 binary scandium intermetallics (46%) of 5 stoichiometric compositions (see sect. 5.1). As is seen from Pearson's symbol, the compounds with simple structures and small numbers of atoms in the unit cell (from 2 up to 20) and with high symmetry (not lower than orthorhombic) occur most frequently. Only 5 structure types among 155 types are monoclinic. 28 and 77 structure types have, respectively, only two or one representatives among scandium intermetallics. Their compositions and crystal structures usually are not simple. The highest number of atoms (408) in a unit cell has $Mg_{44}Rh_7$ type structure.

The formation of comparatively simple, highly symmetrical crystal structures is not only characteristic for scandium intermetallics, but is typical for intermetallics in general,

Table 33
Types of relations between structure types of scandium intermetallics

Type of relation	Operation of transition from initial to resulting type	Examples of structure types	
		Initial	Resulting
I. Positions of all atoms are the same	I. Ordered substitution of atomic positions by different atoms (→ superstructure)	Sm_5Ge_4 La_2Sb $CaIn_2$	$Ce_2Sc_3Si_4$ Mo_2FeB_2 ScAuSi
II. Positions of all atoms are roughly the same	II. Distortion (internal and/or external)	$CaIn_2$ $CeCo_3B_2$	KHg_2 $ErIr_3B_2$
III. Positions of part of atoms are the same	IIIa. Multiple substitution of atoms (1 → 2)	FClPb $CaCu_5$	$ScCoC_2$ $ThMn_{12}$
	IIIb. Addition (subtraction) of atoms	$AuCu_3$ NaCl	$CaTiO_3$ Sc_2S_3
	IIIc. Redistribution of part of atoms and cavities	MgAgAs	MgLiAl
	IIId. Redistribution of atoms	Th_2Zn_{17}	Th_2Ni_{17}
IV. Fragments of both structures are the same	IV. Different stacking types of fragments (homeotypic rows or structures)	$MgZn_2$ AlB_2 TiNiSi	$MgCu_2$ $\alpha ThSi_2$ ZrNiAl
V. Roughly the same fragments, but different ratios of them	Va. One-dimensional stacking of fragments	($CaCu_5$, Zr_4Al_3) ($CeGa_2Al_2$, αPo)	$HfFe_6Ge_6$ $ScNi_2Si_3$
	Vb. Two-dimensional stacking of fragments	(CrB, TiNiSi)	Sc_2CoSi_2, Sc_3NiSi_3
	Vc. Three-dimensional stacking of fragments	(αFe, AlB_2, FeB) (αFe, AlB_2)	$Ce_2Sc_3Si_4$ Th_7Fe_3

as was stated by Villars (1995). This is due to the metallic bonding prevailing in intermetallics. Structures of higher complexity appear frequently in compounds with covalent-type bonding.

Different relations within the various structure types are known to exist in intermetallic compounds in general, and this is also valid in the case of scandium intermetallics. These relations are summarised in table 33 and illustrated using examples of scandium structure types. The relations between structure types of intermetallic compounds were treated in more details by Kripyakevich (1977). He proposed systematics of the structure types of intermetallic and other related compounds, which is based on the analysis of the coordination surroundings (CN and shape of CP) of the smallest atoms in the structure.

As already mentioned, ternary scandium intermetallics often crystallize in structure types which are superstructures to binary prototypes (table 33, Appendix A). It seems convenient to us to select structure types among them which occur in large groups of elements and their combinations, see table 34. These structure types as well as their binary prototypes are frequently observed among all intermetallics having up to hundreds of known representatives. The atomic size factor has a dominant influence on distribution of atoms in ternary phases. The largest atoms in the structure normally occupy atomic

Table 34
Occurrence of some structure types of ternary compounds and their binary prototypes

Composition	$M_2M'X_2$ (M_3X_2)	$M_2M'_3X_4$ $(M,M')_5X_4$ (M_5X_4)	MM′X (M_2X)	MM′X (M_2X)	$M_6M'_{16}X_7$ $M_6M'_7X_{16}$ (M_6X_{23})	MM'_3X (M_4X)
Structure type (binary prototype)	Mo_2FeB_2 (U_3Si_2)	$Ce_2Sc_3Si_4$ (Sm_5Ge_4)	TiNiSi (anti-$PbCl_2$)	ZrNiAl (Fe_2P)	$Mg_6Cu_{16}Si_7$ (Th_6Mn_{23})	$CaTiO_3$ (γFe_4N)
Nature of M and M′ elements	3A, 4A, 3B, 4B	3A–6A	3A–8A, 1B	3A, 7A, 8A, 1B	2A–8A, 3B–4B	3A–8A, 3B–4B
Nature of X element	3B, 4B, 8A	8A, 1B, 4B	3B–5B	3B, 4B	8A, 3B, 4B	3B–6B

Table 35
Atomic distribution in the structure of U_3Si_2 and in ternary compounds with a superstructure to U_3Si_2 (SG *P4/mbm*)

Atomic position	Site	CN	U_3Si_2	Mo_2FeB_2	Sc_2AlSi_2	Sc_2Ni_2Sn	$ScCe_2Si_2$
M1	2(*a*)	14	U	Fe	Al	Sn	Sc
M2	4(*h*)	17	U	Mo	Sc	Sc	Ce
X	4(*g*)	9	Si	B	Si	Ni	Si
Reference			1	2	3	4	5

References
(1) Gladyshevsky (1971);
(2) Kuz'ma (1983);
(3) Tyvanchuk et al. (1988);
(4) Derkach and Kotur (1994)
(5) Mokra (1979)

sites with the largest CN and the smallest atoms occupy positions with the smallest CN. Scandium atoms are often the largest ones in the structures, with the exception of other R elements. In those cases scandium atoms occupy atomic sites with a medium value of CN. Ternary aluminides, gallides, silicides and germanides sometimes form isotypic compounds which belong to the same superstructure types, for e.g. ZrNiAl, $Mg_6Cu_{16}Si_7$ (see Appendix A). The Al and Ga atoms in these structures are usually larger than transition element atoms. Therefore they occupy opposite sites in comparison with the isotypic ternary scandium transition element silicides and germanides in which Si and Ge atoms are usually the smallest ones. Some examples are presented in table 35. Sometimes it causes the change of stoichiometry of compounds: $Sc_6Co_{16}Si_7 \rightarrow Sc_6Co_7Ga_{16}$, $Ce_2Sc_3Ge_4 \rightarrow V_3Sc_2Ge_4$, $ScCo_3C \rightarrow SnSc_3B$.

$Ho_{11}Ge_{10}$ is the binary prototype of differently ordered or partially ordered ternary structures (superstructures) $Sc_7Cr_{4+x}Si_{10-x}$ (Kotur et al. 1985a), $Sc_7Re_{4-x}Si_{10+x}$ (Zhao et al. 1988) and $Sc_{11}Al_2Ge_8$ (Zhao and Parthé 1991) and $Sc_6Yb_5Ge_{10}$ (Kotur et al. 1996b). A detailed analysis of these structures has been reported in the latter paper. The stoichiometries of these phases vary in wide limits as the result of substitution of different R and X atomic sites by d elements (Cr, Mn), and by statistical mixtures of d and p elements (Re, Si). Other ternary substitution variants of the $Ho_{11}Ge_{10}$ binary prototype are also possible. It can be expected that in the near future the $Ho_{11}Ge_{10}$ structure type may belong to the group of most frequently occurring structure types of intermetallic compounds.

The structures of many binary and ternary scandium borides and carbides may be deducted from other structure types by a multiple substitution of larger atoms by B–B or C–C pairs or by the inclusion of B or C atoms into the cavities of the parent structure types. The same is valid for the structures of scandium intermetallics with the 6B elements. The Ti_7S_{12}, NiAs, $ErAgSe_2$ and Al_2MgO_4 structure types can be obtained by an inclusion of cations of metals into the octahedral and tetrahedral cavities of different packings (usually close ones) of 6B anions. Frequently the inclusion of atoms causes a distortion of the parent close-packed structure.

A large group of scandium intermetallics contain fragments of simpler structure types connected in different manners. Some of these hybrid structures contain fragments of two, three or even more structure types. Usually the initial fragments are distorted during their connection in the hybrid structure. Such distortions are minimal in linear hybrid structures. The dimensions of initial fragments, their number and the manner of mutual connection determine the dimensions and the symmetry of the resulting hybrid structure. Often fragments of the following structure types: αPo (empty cube), αFe (body-centered cube), AlB_2 (body-centered trigonal prism) and $BaAl_4$ (body-centered tetragonal antiprism), are observed as the initial fragments for hybrid structures. Besides these, atomic groups (clusters) such as octahedron- and icosahedron-shaped are found as the structure fragments. The initial fragments can be eliminated from the parent structures along the axes of the unit cells or eliminated randomly in comparison to these axes. Substitutions of atomic positions of the same structure fragments by different atoms with different sizes cause distortions of the same fragments in different structures. In the following discussion possible distortions of structure fragments will not be taken into consideration and we will use the names of ideal clusters.

While analysing the compositions of scandium intermetallic compounds we hinted at the regularity of occurrence of large numbers of compounds on some characteristic cross sections of phase diagrams (see figs. 93 and 94). The crystal structures of these compounds which are in two-phase equilibrium with each other are related and contain one or more mutual fragments, but in different ratios. For example, on the cross-section Sc:X = 1:1 of the ternary systems Sc–M–X (M = Fe, Co, Ni; X = Si, Ge) the following ternary compounds occur: ScMX (ST TiNiSi), $Sc_3M_2X_3$ (ST $Hf_3Ni_2Si_3$), Sc_2MX_2 (ST Sc_2CoSi_2), Sc_3MX_3 (ST Sc_3NiSi_3), and ScX (ST CrB). These compounds form an interesting series of structures ScMX → $Sc_3M_2X_3$ → Sc_2MX_2 → Sc_3MX_3 → ScX (Gladyshevsky and Kotur 1978, Kotur and Gladyshevsky 1983). As can be seen from fig. 96 three intermediate members of this series contain fragments of the outer two, ScMX and ScX. In this series the Sc:X ratio remains the same, 1:1, however, the decrease of the number of the M atoms cause the decrease and finally the disappearing of the TiNiSi-type fragments. The number of CrB-type fragments increases from the $Sc_3M_2X_3$ structure towards ScX. Thus, TiNiSi and CrB are the parent structure types of the homological series of structures with three known members. It is possible to predict the existence of other members in this series and construct their hypothetical structures. In particular, if we add one unit cell of ScSi along the *c* direction in the Sc_3NiSi_3 (I) structure, we obtain a structure of the same symmetry (SG *C*2/*m*) represented by the formula Sc_4NiSi_4 (II). The monoclinic unit cell of this hypothetical structure will have the following dimensions: $a(\mathrm{II}) \approx a(\mathrm{I}) \approx 10$ Å, $b(\mathrm{II}) \approx b(\mathrm{I}) \approx 4$ Å, $c(\mathrm{II}) \approx c(\mathrm{I}) + c(\mathrm{ScSi}) \approx 16.5$ Å, $\beta \approx 95$–$98°$ (Kotur and Gladyshevsky 1983). Taking into account that the CrB-type structure is the linear hybrid structure of AlB_2 and αFe types, the structures of above discussed homological series are thus two-dimensional hybrids of three structure types, namely αFe, AlB_2 and TiNiSi.

The germanide $Sc_9Ni_5Ge_8$ occurs very close to the Sc:X = 1:1 cross-section. Its structure has been determined by Andrusyak et al. (1989), and appeared to be a more

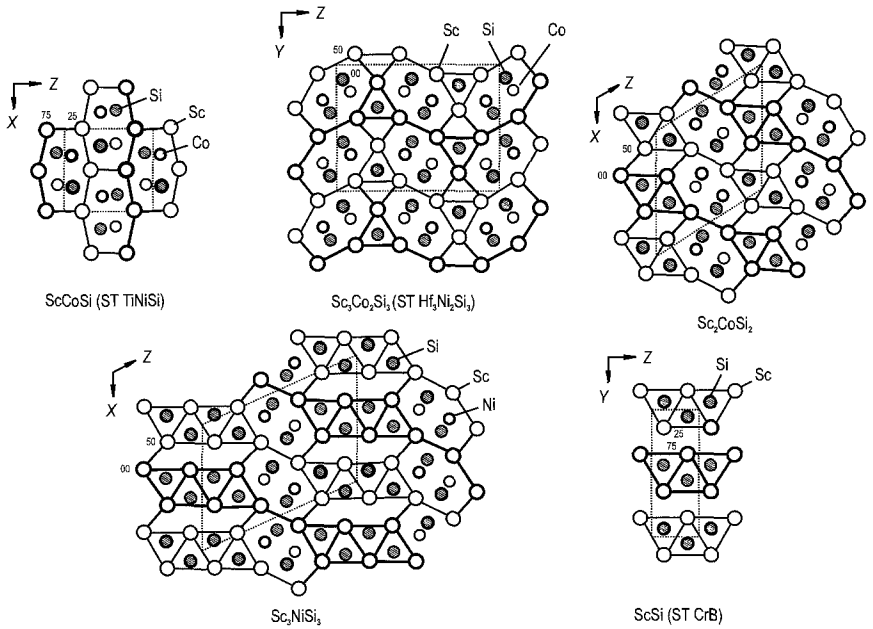

Fig. 96. Relations between the structure types TiNiSi (ScCoSi), $Hf_3Ni_2Si_3$ ($Sc_3Co_2Si_3$), Sc_2CoSi_2, Sc_3NiSi_3 and CrB (ScSi). The structures are presented in the projections along 010 or 100. Unit cells and structure fragments are indicated by dashed and solid lines respectively.

complicated two-dimensional hybrid of four structure types, namely αFe, AlB_2, TiNiSi and Mo_2NiB_2 (fig. 97).

The structure of ScNiSi of the TiNiSi type can be presented as consisting of infinite zig-zag walls of trigonal prisms $[XM_4X_2]$ (see Kotur and Sikirica 1982b). Also the structure of $Sc_3Ni_4Si_4$ (ST $Gd_6Cu_8Ge_8$) contains trigonal prisms and is in equilibrium with ScNiSi. In the Sc–Cu–Si ternary system the compound $Sc_3Cu_4Si_4$ (ST $Gd_6Cu_8Ge_8$) is in equilibria with ScCuSi (r) (ST TiNiSi) and ScCuSi (h) (ST ZrNiAl). The structure of the latter compound is also built of trigonal prisms. As is seen from the stoichiometries of the ternary compounds presented, they occur on the cross-sections M : X = 1 : 1 and therefore their crystal structures are related and contain mutual fragments.

In the numerous ternary R–M–X systems on the cross-sections R : M = 1 : 1 there are ternary compounds of the compositions RMX_2 and RMX_3, which belong to the structure types of $CeNiSi_2$ and $ScNiSi_3$ (Gladyshevsky and Bodak 1982). As follows from fig. 98, the structures of these compounds are related and contain mutual fragments of AlB_2 and $CeGa_2Al_2$ (superstructure to $BaAl_4$) types. Although there are no data to date for any scandium compound of $CeNiSi_2$ type, the silicide $ScNiSi_3$ contains its fragments in its structure. There are relations between the structures of compounds occurring on other cross-sections, e.g. Sc : M = 1 : 2. The compounds $ScNi_2Si_3$ (ST $ScNi_2Si_3$) and $ScNi_2Si_2$ (ST $CeGa_2Al_2$) are in equilibrium with each other and contain a mutual structure fragment

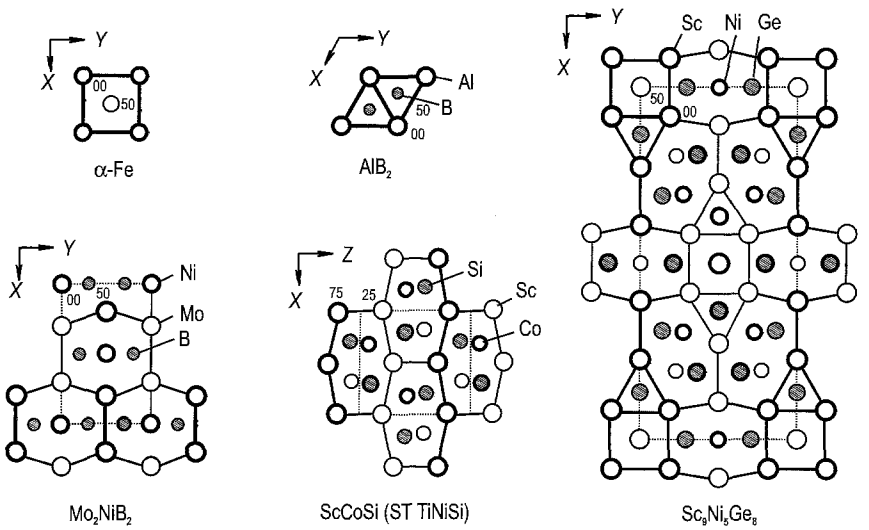

Fig. 97. Connection of fragments (indicated by solid lines) of α-Fe, AlB_2, Mo_2NiB_2 and TiNiSi structure types in the structure of $Sc_9Ni_5Ge_8$. Unit cells are indicated by dashed lines. The structures are presented in the projections along 001 or 010.

(fig. 98). The structures $ScNiSi_3$, $ScNi_2Si_3$ and $CeNiSi_2$ presented in fig. 98 are linear hybrid structures.

The linear hybrids of two structure types, $CeGa_2Al_2$ and αFe, are ternary carbides Sc_3CoC_4 and $ScCoC_2$, which are in equilibrium with each other and occur on the isoconcentrate of 50 at.% C in the Sc–Co–C system.

The examples, discussed above, show that ternary compounds which are in equilibrium with each other are related with respect to their crystal structure. These compounds contain at least one mutual fragment or atomic cluster. Sometimes they form homologous series of structures. This fact can be used for the investigation of compounds with unknown crystal structure. However, to date there are a number of powerful program packages available for the determination of crystal structures by direct methods. However, the application of direct methods for structure determination using powder X-ray data is sometimes not successful, especially for complex structures. In such cases the knowledge of structure relations between compounds which are in equilibria becomes very useful if the structures of some of them are known.

We used such an approach for determination of the crystal structure of $ScFe_6Ge_5$ (Kotur 1995). In the ternary systems Sc–Mn–Ge and Sc–Fe–Ge on the cross-sections Sc : Mn(Fe) = 1 : 6 the compounds ScM_6Ge_6 (M = Mn, Fe), $ScFe_6Ge_5$ and ScM_6Ge_4 (M = Mn, Fe) exist. The germanides ScM_6Ge_6 and ScM_6Ge_4 belong to the structure types $HfFe_6Ge_6$ (Olenych et al. 1981) and $ZrFe_6Ge_4$ (Olenych 1989), respectively. The structure of the $HfFe_6Ge_6$ type can be deducted from the $CaCu_5$ type by a multiple substitution of the pair of X–X atoms for the M atoms in every second layer (fig. 99). The structure of

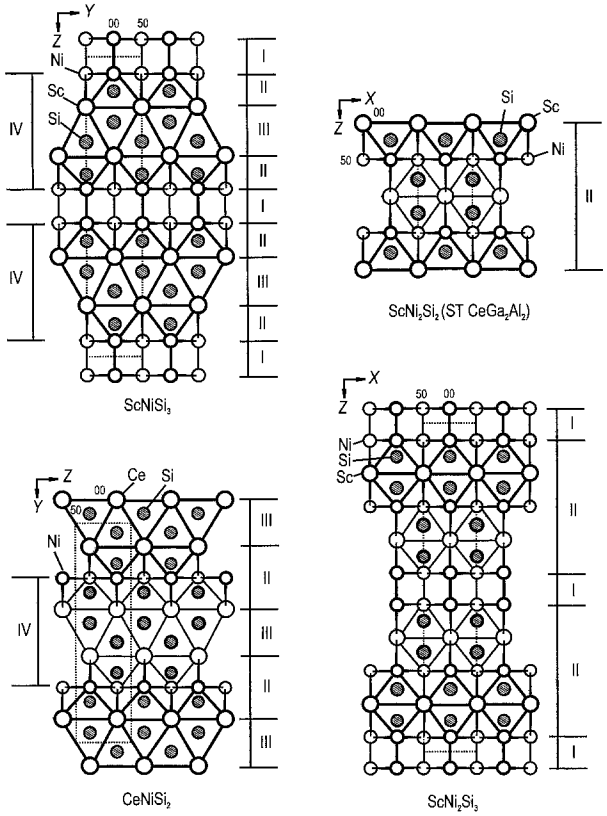

Fig. 98. Relations between structures $ScNiSi_3$, $CeNiSi_2$ occurring on the cross-sections R:M = 1:1 and $ScNi_2Si_3$, $ScNi_2Si_2$ (ST $CeGa_2Al_2$) occurring on the cross-sections R:M = 1:2. The structures are presented in the projections along 100 or 010. Unit cells are indicated by dashed lines. Fragments of the structures: (I) αPo, (II) $CeGa_2Al_2$, (III) AlB_2, (IV) $CeNiSi_2$.

$HfFe_6Ge_6$ (IV) is also a linear hybrid of the $CaCu_5$ (I) and the Zr_4Al_3 (II) types (fig. 99), whereas the structure of the $ZrFe_6Ge_4$ (V) type is a linear hybrid of the $CaCu_5$ (I) and Fe_3Sn_2 (III) types (fig. 99). The $ZrFe_6Ge_4$ type structure can also be treated as resulting from an inclusion of R(Sc) atoms into the Fe_3Sn_2 structure (fig. 99).

Expecting genetic relations between the structures of $ScFe_6Ge_5$ and $ScFe_6Ge_6$ (IV) and $ScFe_6Ge_4$ (V), with which the first one are in equilibria, Kotur (1995) deducted a theoretical model for the crystal structure of $ScFe_6Ge_5$ as a linear hybrid of the fragments IV and V. This model, containing 72 atoms in the unit cell, is presented in fig. 99. The dimensions of the fragments IV and V, their quantities, 3 + 3, and symmetry allowed one to determine roughly the unit cell dimensions and the symmetry: SG $R\bar{3}m$, $a \approx 5$ Å, $c \approx 44$ Å. This theoretically predicted structure has been confirmed experimentally by X-ray powder diffraction data; the refined lattice parameters are: $a = 5.063(1)$ Å, $c = 44.11(1)$ Å (Kotur 1995).

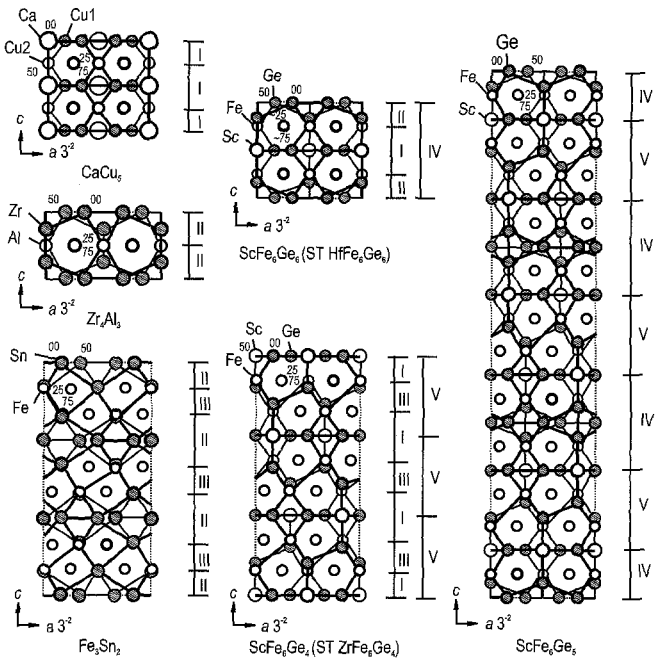

Fig. 99. Relations of the structures $CaCu_5$, $ScFe_6Ge_6$ (ST $HfFe_6Ge_6$), Zr_4Al_3, Fe_3Sn_2, $ScFe_6Ge_4$ (ST $ZrFe_6Ge_4$) and $ScFe_6Ge_5$. The structures are presented in the projections on the plane of the large diagonal of the hexagonal basis. Unit cells are indicated by dashed lines. Fragments of the structures: (I) $CaCu_5$, (II) Zr_4Al_3, (III) Fe_3Sn_2, (IV) $ScFe_6Ge_6$, (V) $ScFe_6Ge_4$.

The change of compositions of compounds is connected with the changes of coordination surroundings of atoms. Kotur (1995) performed a crystal structure analysis of all known structure types of scandium intermetallics based on the classification presented by Kripyakevich (1977). The structure types have been classified on the basis of the CN and the shape of the CP of the smallest atoms in the structure. In some cases the X atoms are the smallest in the structure but sometimes the M atoms are the smallest, especially if M is a d element. It was found that the compounds with a high M content (>50 at.%) and a low X content (<30 at.%) frequently have the CN 12 and the CP of icosahedra and cubooctahedra for the smallest atoms. The compounds of the central part of ternary systems with Sc content 15 up to 30 at.% and the X content between 30 and 50 at.% have CN 8 (+1 or 2) and a CP of tetragonal antiprism for the smallest atoms. For high X (>50 at.%) and Sc (>30 at.%) content the compounds are characterised by a trigonal prismatic coordination of the smallest atoms [CN 6 (+1, 2 or 3)]. At high Sc content binary compounds have icosahedral coordination of the smallest atoms. These regularities are invalid in the systems of X elements (B, C, As), with a pronounced nonmetal character. Scandium intermetallics with these elements have, as usual, trigonal prismatic, octahedral (CN 6) and tetrahedral (CN 4) coordination of the X atoms.

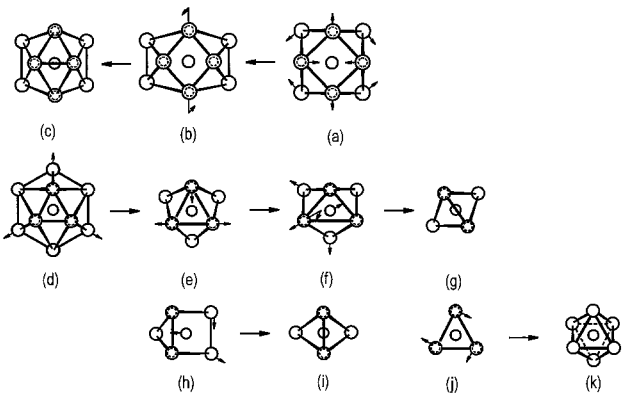

Fig. 100. Coordination polyhedra of atoms: (a) cubooctahedron; (b) icosahedron with two tetrangular planes; (c, d) normal icosahedron in two projections; (e) trigonal prism with three additional atoms; (f) tetragonal antiprism with one additional atom; (g, i, k) octahedron in different projections; (h) trigonal prism with one additional atom. The arrows near atoms show the approximate direction of their shifts, which cause the transformation of this CP into the neighbouring one, indicated by a long arrow (for additional explanation see text).

Figure 100 represents the transformations of the CP of atoms observed in the structures: cubooctahedron (CN 12) → icosahedron with two quadrangular planes (CN 12) → normal icosahedron (CN 12) → trigonal prism with additional atoms [CN 6 (+3)] → tetragonal antiprism with additional atom [CN 8 (+1)] → octahedron (CN 6) and also the transformation of trigonal prism with additional atom [CN 6 (+1)] → octahedron (CN 6). Numerous examples of these CP can be found in the original papers for the structures of intermetallics. Namely, CP (a) from fig. 100 is observed for the atoms of the $AuCu_3$ ST, $[AuCu_{12}]$ and $[CuAu_4Cu_8]$ (Kripyakevich 1977). Slightly distorted cubooctahedrons $[ScRh_6Ge_6]$ exist in the $Sc_4Rh_7Ge_6$ structure (ST $U_4Re_7Si_6$, Engel et al. 1984). CP (b) and (c) have Cu atoms in the $CaCu_5$ type structure (Kripyakevich 1977). Upon formation of the superstructure of the $CeCo_3B_2$ type to this prototype the c/a ratio (=0.600) decreases remarkably in comparison to the binary RM_5 structures (c/a=0.774–0.822). This is caused by the substitution of two boron atoms for two cobalt atoms in the unit cell. The CP of boron atoms changes from icosahedra to trigonal prism with three additional atoms (Kuz'ma 1983). This example shows the mechanism of the transformation of the (d)-type CP into the (e)-type CP. A classical representative of the (e)-type CP is the AlB_2-type structure (Kripyakevich 1977). A CP of the (f) type is found in the $BaAl_4$ or the $CeGa_2Al_2$ ST (Kripyakevich 1977) or the $Sc_4Rh_7Ge_6$ (ST $U_4Re_7Si_6$, Engel et al. 1984) type structure. An intermediate position between the CP of the (d) and (e) types is occupied by Co atoms in the structure of $Sc_5Co_4Si_{10}$ (Braun et al. 1980). This structure is a two-dimensional hybrid of the following four types: AlB_2 (trigonal prisms $[SiSc_6]$), CsCl (empty tetrahedra $(Sc_2Si_2]$), $AuCu_3$ (cubooctahedra $[ScSi_{12}]$) and $CeGa_2Al_2$ (tetragonal antiprisms $[CoSc_4Si_4]$) (fig. 101). A CP intermediate between (f) and (g) and between (h) and (i) [or (i) and (k)] contains the structure of

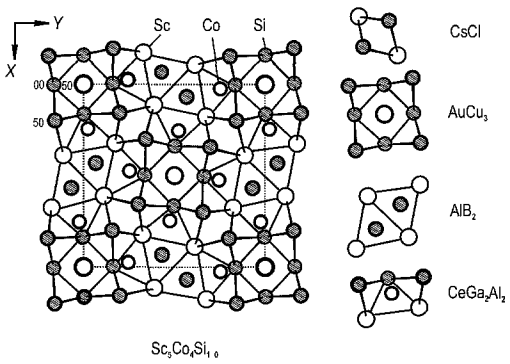

Fig. 101. Connections of fragments of AlB_2, CsCl, $AuCu_3$ and $CeGa_2Al_2$ types in the structure of $Sc_5Co_4Si_{10}$. The structure is presented in the projection along 001.

V_3As_2-type (Berger 1977). Transformation of CP of atoms can also occur in the opposite direction, from CP 6 to CP 12. It is caused by a change of the dimensions of different atoms and their content in the structures. Other types of coordination surroundings of the smallest atoms in the structures of intermetallics are observed rarely.

Figure 102 represents generalised relations between the majority of the structure types of scandium intermetallics. Some of these relations have been established by Gladyshevsky and Bodak (1982). Relations between other structure types, published after 1980, have been established by Kotur (1995). Analysis of the structure types of intermetallic compounds leads to an enrichment and a broadening of our knowledge about relationships between structure types. These investigations are basic for the illumination of the nature of intermetallics and the functional relations between the compositions and structures of compounds and the factors which govern these changes.

6. Physical properties of scandium based intermetallics

Among scandium compounds and in compounds where scandium replaces other rare-earth elements, magnetic and nonmagnetic intermetallics exist, however, there are also scandium compounds showing superconductivity, although the scandium metal is neither magnetic nor shows superconductivity at atmospheric pressure. An extensive part of this section deals with interesting magnetic phenomena observed in the ScM_2 (M = Mn, Fe, Co, Ni) Laves phases. In the Mn- and Co-containing Laves phases the influence of spin fluctuations on the various physical properties is demonstrated.

Since scandium is one of the nonmagnetic elements among the rare-earth series one might expect that the physical properties of compounds with scandium and the other nonmagnetic rare-earth elements (Y, La or Lu) are the same or at least very similar. This supposition is true in principle, however because of the much smaller atomic size of scandium compared with yttrium and also lutetium a deviating physical behaviour of the corresponding scandium compounds is frequently observable.

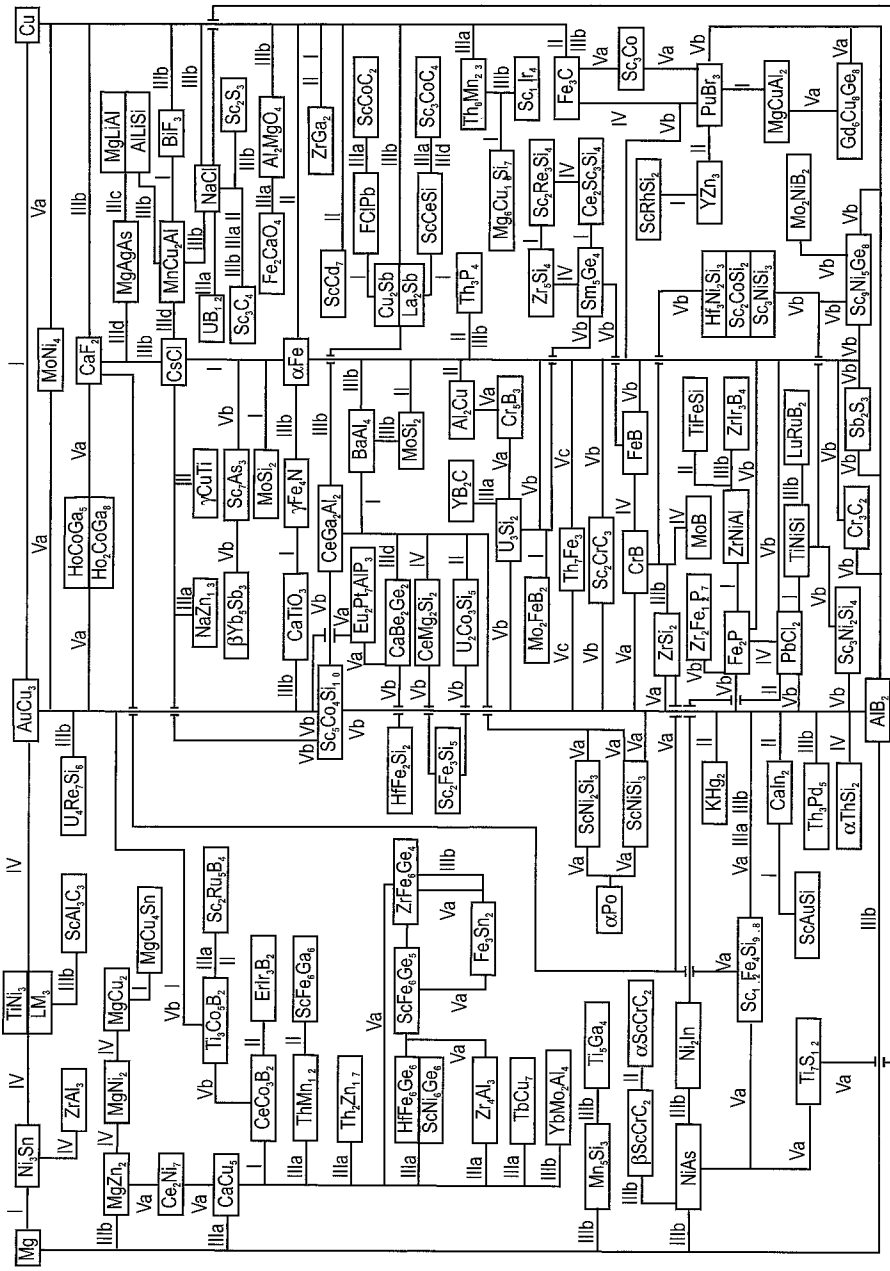

Fig. 102. Relations between structure types of Sc intermetallic compounds as derived from two close-packed structures Mg and Cu. Roman numerals I–V indicate the ways of transformation used in table 33.

6.1. *Compounds with non-magnetic and non-superconducting ground state*

6.1.1. *RAuGe (R = Sc, Y and Lu)*

The ternary RAuGe series of compounds exhibits interesting physical properties, as shown by Rossi et al. (1992) and Pöttgen et al. (1996). Details of the crystal structure, the magnetic susceptibility, the electrical resistivity, the specific heat and the electronic band structure of the four isostructural nonmagnetic RAuGe compounds (R = Sc, Y, La, Lu) have been studied recently by Schnelle et al. (1997). These four compounds are weak diamagnets. The Sc-based compound has been included in this investigation because of the small atomic size of scandium. As will be shown, the variation of the rare-earth ionic radius among this series improves our general understanding of the physical properties in this family of rare-earth intermetallics.

The structures of these compounds are derived from the $CaIn_2$-type structure by an ordered arrangement of the gold and germanium atoms on the indium position. The gold and germanium atoms form two-dimensional Au–Ge polyanions. However a three-dimensional network of elongated tetrahedra is present in ScAuGe (Pöttgen et al. 1996).

The degree of puckering of the Au–Ge hexagons is strongly dependent on the size of the rare-earth atoms. While the layers are almost flat in the La compound, strong puckering is observed in the other germanides. In LaAuGe and YAuGe the interlayer Au–Ge distance is 3.858 Å and 3.106 Å, respectively; the Au–Ge polyanions are two-dimensional and separated from each other. In LuAuGe the interlayer Au–Ge distance amounts to 2.927 Å, indicating a weak coupling between the layers. The transition from Au–Ge layers to a three-dimensional network of elongated tetrahedra occurs for ScAuGe. The structure of LaAuGe and YAuGe may therefore be described as being of the NdPtSb type, whereas the structures of ScAuGe and LuAuGe (with the smaller rare-earth ionic sizes) are closer to that of LiGaGe (Pöttgen et al. 1996).

The use of rare-earth atoms with different radii among this series reveals a remarkable variation of the c/a ratio (ScAuGe: $c/a = 1.589$, LaAuGe: $c/a = 1.830$) which leads to a flattening of the three-dimensional Au–Ge network of elongated tetrahedra (in ScAuGe) towards LaAuGe accompanied by an increasing of the coupling between the Au–Ge layers in the c-direction. The electronic band structure and the density of states deduced from this calculation is in general similar for the compounds with Sc, Y and Lu. Only LaAuGe shows some small but important differences. In fig. 103 the calculated densities of states of the four compounds are shown and can be compared. The Ge s bands are around 11 eV below ε_F, except for LaAuGe where the Ge s bands are about 1 eV higher in energy. The Au d bands are situated at around −6 eV and again these bands are 1 eV higher in LaAuGe. For LuAuGe the Lu f bands coincide with the d bands. The lowest unoccupied bands are the Sc,Y, La or Lu d bands. The densities of states at the Fermi level N_F are: ScAuGe, 1.4, YAuGe, 0.6, LaAuGe, 2.1, LuAuGe, 0.4 in units of eV^{-1} for two spins and one RAuGe formula unit. The higher density of states of the LaAuGe compound explains its exceptional behaviour among the four compounds in this series. This will be seen from the discussion of other physical properties. The magnetic susceptibility (χ) of the RAuGe compounds in a field of 4 T is shown in fig. 104. An attempt to fit their

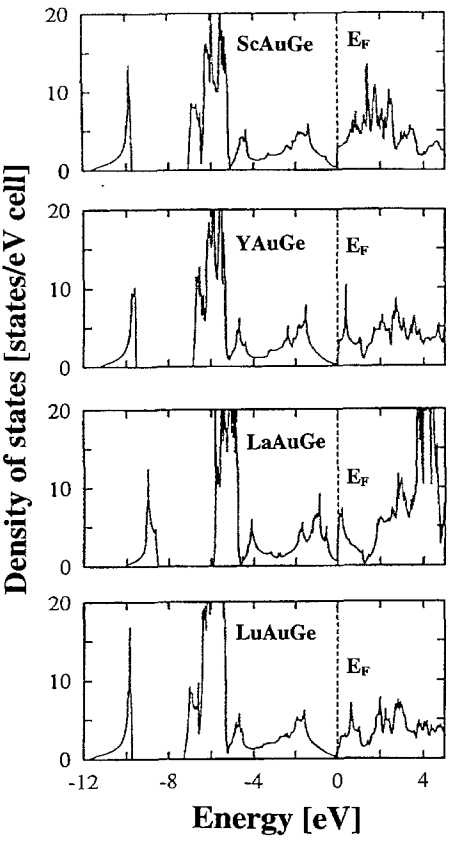

Fig. 103. The density of states of ScAuGe, YAuGe, LaAuGe and LuAuGe. The dashed line (at $E=0$) is the Fermi level (Schnelle et al. 1997).

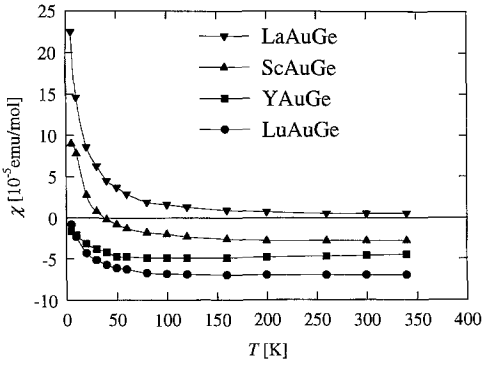

Fig. 104. Magnetic susceptibility of the RAuGe compounds at a field of 4 T (Schnelle et al. 1997).

$\chi(T)$ behaviour has been undertaken using the following formula: $\chi(T)=C/T+\chi_0+aT$. The upturn in the region below 50 K described by the Curie-term (C/T) is thought to be due to magnetic impurities. The temperature-independent part χ_0 is the sum of the diamagnetic susceptibility of the closed shell and conduction-electron contributions. The linear decrease in case of ScAuGe, LaAuGe and LuAuGe towards room temperature is taken into account by the aT term and has been attributed to a temperature dependence of the conduction-electron susceptibility.

The specific heat data have been analysed in a c_P/T vs. T^2 representation. From the respective intercepts and the slopes of the straight lines fitted to the data the electronic specific heat coefficient γ and the Debye temperature Θ_D at lowest temperature are obtained. While the ScAuGe, YAuGe, and LuAuGe compound exhibit γ values below 1 mJ mol^{-1} K^{-2}, LaAuGe has a markedly larger electronic specific term of 2.5 mJ mol^{-1} K^{-2}. The so-called Wilson ratio χ_P/γ (where χ_P denotes the Pauli susceptibility of the conduction electrons) is similar for YAuGe, LaAuGe, and LuAuGe, however the values are enhanced over the value of unity expected for a Fermi–Sommerfeld

free electron gas. Values between 3.6 and 3.8 are found for the Y, La and Lu compound, while for ScAuGe 6.4 has been obtained (the possible reasons for this high value have been discussed by Schnelle et al. 1997).

LaAuGe exhibits the highest values of γ and χ_P among the four compounds. This correlates well with the larger density of states obtained in the band-structure calculations. Similar observations have been made in other series, namely $LaAl_2$, YAl_2 and $LuAl_2$ (Hungsberg and Gschneidner 1972, Bauer et al. 1985), and LaAg, YAg and LuAg (Bauer et al. 1986) for the corresponding La compounds. In this latter cases the La compounds show superconductivity below 4.2 K. Thus it might be that also in LaAuGe a superconducting transition exists at temperatures below 4.2 K. The much stronger curvature of the $\rho(T)$ curves of LaAuGe (shown in figure 7 of Schnelle et al. 1997) is obviously a further indication for the possibility of superconductivity in this compound.

6.1.2. *Crystal field parameters of lanthanides diluted in $ScAl_2$, YAl_2 and $LuAl_2$*

An example where a Sc compound is included in a systematic investigation (because of its small lattice parameter) is described as follows. A systematic inelastic neutron scattering experiment has been performed by Frick and Loewenhaupt (1985) on diluted lanthanide elements in the nonmagnetic matrix of $ScAl_2$, YAl_2 and $LaAl_2$. The aim was to obtain information about the origin of the crystal field (CF) in metals in general and especially to determine a set of CF parameters for the lanthanides when diluted in different nonmagnetic matrices of cubic Laves phases.

The concentration of the lanthanide elements in the hosts $ScAl_2$, YAl_2 and $LaAl_2$ was chosen to be between 0.3 and 3 at%. The time-of-flight experiment was performed at an elevated temperature where the neutrons can gain energy from the system. The intensity caused by magnetic scattering was limited to the energy range below 10 meV, and it is well separated from the phonon intensity which is typically in the range of about 10 to 30 meV. The scattering data was then fitted to a theoretical model given in Becker et al. (1977) yielding the temperature-independent CF parameters x and W in the Lea–Leask–Wolf notation (Lea et al. 1962). From x and W the parameters $A_4\langle r^4\rangle$ and $A_6\langle r^6\rangle$ and finally A_4 and A_6 were calculated using $\langle r^n\rangle$ from Freeman and Desclaux (1979). The resultant crystal field parameters A_4 and A_6 in the hosts ($ScAl_2$, YAl_2 and $LaAl_2$) are plotted as a function of the atomic number of the lanthanide element in fig. 105. (There are no data for the CF levels of the elements Pm, Sm, Eu and Gd because Pm does not exist naturally, the CF of Sm, Eu show the influence of higher multiplets, and the CF influence is zero in Gd). As can be seen the A_4 values are all positive whereas all the A_6 values are negative. The values of A_4 and A_6 increase from $ScAl_2$ to YAl_2 to $LaAl_2$. The variation of A_4 and A_6 with the atomic number shows a similar behaviour for the three matrices. A calculation of the electronic potential of the point charges surrounding the 4f ions leads to negative A_4 and A_6 values, assuming positive charges of the same order for Sc, Y, La and Al. Taking into account the difference in the lattice constant of $ScAl_2$, YAl_2 and $LaAl_2$ and the difference in the electronegativity of Sc, Y and La, the relative distance between the A_4 and A_6 levels from in experiment and those calculated

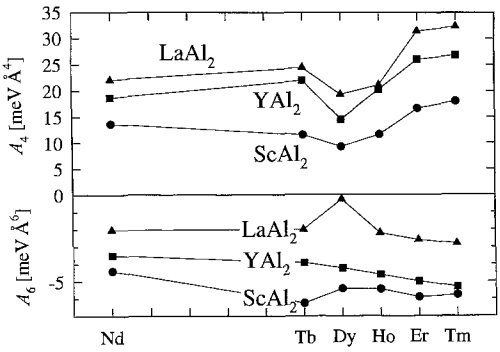

Fig. 105. The experimentally determined crystal field parameters A_4 and A_6 in the hosts $ScAl_2$, YAl_2 and $LaAl_2$ as a function of the rare-earth atom [the elements Pm, Sm, Eu and Gd do not exist naturally (Pm), show the influence of higher CF level (Sm, Eu), or the CF influence is zero (Gd)] (Frick and Loewenhaupt 1985).

are in agreement. However the more surprising observation was the positive sign of the A_4 CF parameters which should be negative as are the A_6 values according to the simple point-charge calculation. In the paper of Frick and Loewenhaupt (1985) it is argued that not well-screened effective point charges on the neighbouring atoms of the 4f ions and the nonspherical conduction electrons are responsible for the shape of the CF potential in RAl_2 and especially for the deviation of the experiment from the calculation based on a simple point-charge model.

6.1.3. *Spin fluctuations in RCo_2 compounds (R = Sc, Y, Lu)*

$ScCo_2$ crystallises in the cubic Laves phase type structure. It belongs to the family of the rare-earth–transition metal compounds with 1:2 stoichiometry where the magnetic state of the Co sublattice is strongly influenced by the magnetic partner elements. In compounds with magnetic rare-earth atoms as partner elements, induced moments appear on the Co sites in the magnetically ordered state. These induced 3d moments exist only in the presence of a magnetic surroundings and range from $1.05\mu_B$ in $GdCo_2$ down to $0\mu_B$ in $ScCo_2$, YCo_2 and $LuCo_2$. Due to the variability of the Co moments in combination with the stable permanent moments on the lanthanide atoms in the magnetically ordered RCo_2 compounds Bloch and Lemaire (1970) used the concept of the exchange-enhanced paramagnetism for the Co sublattice and developed a phenomenological model to decribe the exchange-induced moment on Co. From this model it was deduced that the R–Co interaction is about twice as strong as the Co–Co interaction, which is in agreement with investigations of the magnetoelastic properties first performed by Lee and Pourarian (1976). The magnetic fields available nowadays in some laboratories are high enough to exit the critical field for induced Co moments in YCo_2 which is about 70 T (Goto et al. 1990). These three Co-based Laves phases to which $ScCo_2$ belongs are enhanced paramagnets. The temperature variation of the susceptibility shows maxima at elevated temperatures (YCo_2: 260 K, $LuCo_2$: 370 K, $ScCo_2$: 550 K, see fig. 106) whereas in the low-temperature region an increase of $\chi(T)$ proportional to T^2 has been found (Burzo et al. 1993). The χ-values at 0 K as given by Ikeda et al. (1991) are: $\chi(YCo_2) = 6.0$, $\chi(LuCo_2) = 3.96$, $\chi(ScCo_2) = 3.67$ in units of 10^{-4} emu/(g-atom). The values for YCo_2 and $LuCo_2$ are not in complete agreement with the data shown in fig. 106 at the lowest

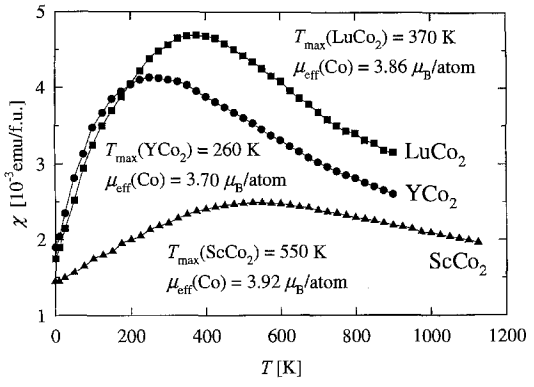

Fig. 106. The high-field dc magnetic susceptibility of the three spin fluctuation systems $ScCo_2$, YCo_2 and $LuCo_2$ (Burzo et al. 1993).

temperatures. This is however not surprising, since the χ-values are strongly influenced by the quality of the sample material (Steiner and Ortbauer 1974 found that grinding of the sample material can cause a rise in susceptibility by a factor of three).

There is also an enhancement of the electronic specific heat coefficients γ ($\gamma(YCo_2)=33.1$, $\gamma(LuCo_2)=26.6$, and $\gamma(ScCo_2)=18.4$ in units of mJ (mol–Co)$^{-1}$ K^{-2}) (Ikeda et al. 1991), which in the case of $ScCo_2$ is larger by a factor of three than that of $ScNi_2$.

The concept of spin fluctuations (details are given in the book by Moriya 1985) has been successfully used to describe the enhanced γ-value and the temperature variation of the susceptibility. The influence of spin fluctuations on the transport phenomena in these RCo_2 compounds (R = Sc, Y, Lu) has been investigated recently by Gratz (1997).

Spin fluctuations contribute to the transport phenomena since they scatter conduction electrons through the exchange interaction. This problem has been treated using a two-band model where the electrons in the conduction band carry charge or heat while those in the narrow d band contribute to the spin fluctuations which scatter the conduction electrons through the s–d exchange interaction. The first publications dealing with this problem date back to the late 1960s (Mills and Lederer 1966, Schindler and Rice 1967, Mathon 1968). These calculations were later continued by Coqblin et al. (1978).

The results can be summarised as follows:

Electrical resistivity: $\rho \propto T^2$, with the tendency to saturate at elevated temperatures;

Thermal resistivity: $W \propto T$ at low temperatures, followed by a maximum.

Magnetoresistance: $(\Delta\rho/\rho)$ is negative and proportional to the square of the applied field.

The temperature dependence of the electrical resistivity ρ of $ScCo_2$, YCo_2 and $LuCo_2$ is shown in fig. 107. To illustrate the influence of the spin fluctuation scattering in these Co-based compounds, the $\rho(T)$ dependence of the two isostructural non-spin-fluctuation compounds YAl_2 and $LuNi_2$ is given in this figure too. Both phonon scattering and spin-fluctuation scattering cause a change of ρ with temperature. For the spin-fluctuation contribution to $\rho(T)$ the curvature at elevated temperatures and the T^2 increase at low temperatures is confirmed by the experiment. A quantitative analysis of $\rho(T)-\rho_0$ versus T^2 is depicted in the inset of fig. 107. The low-temperature resistivity is dominated by the quadratic increase due to the spin-fluctuation scattering giving rise to the enhanced

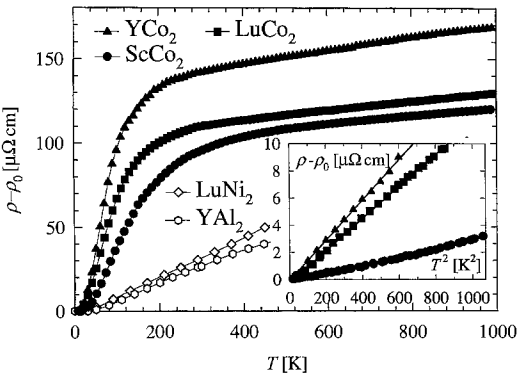

Fig. 107. The electrical resistivity of $ScCo_2$, YCo_2 and $LuCo_2$ from 4 K to 1000 K, where $\rho_0(RCo_2) = 18$, 24 and 17 μΩcm, respectively. The increase of $\rho(T)$ in the non-spin-fluctuation systems YAl_2 and $LuNi_2$ ($\rho_0 = 5.6$ and 4.2 μΩcm, respectively) is shown for comparison. Inset: low-temperature T^2 dependence of the spin fluctuation systems (Gratz 1997).

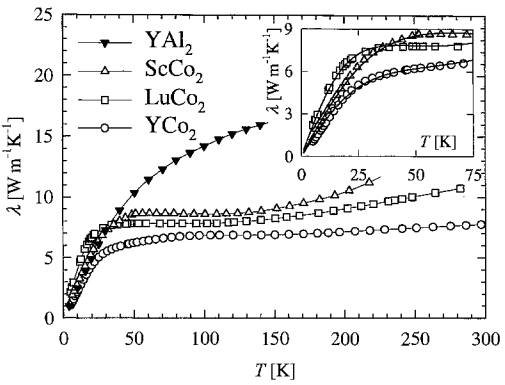

Fig. 108. The thermal conductivity of $ScCo_2$, YCo_2, $LuCo_2$ and YAl_2 from 4 K to 300 K. Inset: the fit of $\lambda(T) = (aT^{-1} + bT^2 + cT)^{-1} + dT^2$ to the experimental data is given by the solid lines (Gratz 1997).

factor A. According to the theory of spin fluctuations (Coqblin et al. 1978) the factor A is related to the corresponding spin-fluctuation temperatures by the relation $A \propto T_{sf}^{-2}$. This factor has the following values: $A(YCo_2) = 16$, $A(LuCo_2) = 12$ and $A(ScCo_2) = 4.3$ in units of $n\Omega\,cm\,K^{-2}$. The thermal conductivity λ of these spin-fluctuation systems is shown in fig. 108 (again the $\lambda(T)$ curve for YAl_2 is included). In the spin-fluctuation compounds one observes a pronounced curvature in $\lambda(T)$ in the region $20\,K \leqslant T \leqslant 60\,K$ which is not observable in YAl_2. For temperatures higher than about 50 K $\lambda(T)$ is nearly constant and decreases from $ScCo_2$ towards YCo_2. Since the analysis of thermal conductivity data is not frequently shown in the literature it should be outlined here in more detail. Using the theoretically obtained $\lambda(T)$ dependencies for the different scattering processes (see also Ziman 1960), one can account for the variation of $\lambda(T)$ at low temperatures:

$$\lambda(T) = \lambda_e + \lambda_l = \frac{1}{W_{e,0} + W_{e,ph} + W_{e,sf}} + \lambda_l,$$

where λ_e and λ_l denote the electronic and the lattice thermal conductivity, respectively, and $W_{e,0}$, $W_{e,ph}$ and $W_{e,sf}$ are the thermal resistivities due to impurity-, phonon- and spin-

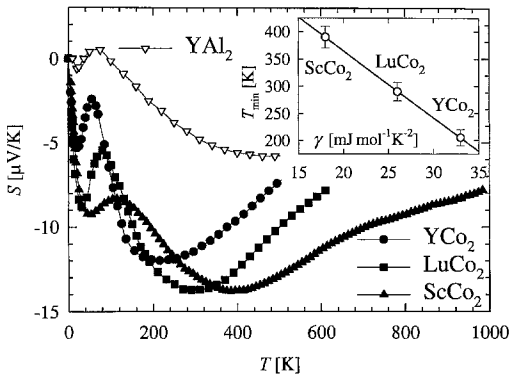

Fig. 109. The thermopower of $ScCo_2$, YCo_2, $LuCo_2$ and YAl_2 from 4 K to 1000 K. Inset: correlation between the position of the high-temperature minima T_{min} and the γ value of the specific heat in $ScCo_2$, YCo_2 and $LuCo_2$ (Gratz 1997).

fluctuation-scattering processes, respectively). With $W_{e,0} \propto 1/T$, $W_{e,ph} \propto T^2$, $W_{e,sf} \propto T$ and $\lambda_l \propto T^2$ we finally obtain

$$\lambda(T) = \frac{1}{a(1/T) + bT^2 + cT} + dT^2.$$

Using the Wiedemann–Franz law, the coefficient a can be determined from the residual electrical resistivity ρ_0. Least-squares fits to the experimental data up to 75 K are given by the solid lines in the inset of fig. 108. Interestingly the fit procedure shows that the $W_{e,ph}$ term is much smaller compared to $W_{e,sf}$ in these RCo_2 series. The linear $W_{e,sf}$ term is dominating and responsible for the pronounced curvature in λ vs. T between 20 K and 60 K. The c-values ($W_{e,sf} = cT$) are related to the spin-fluctuation temperatures $c \propto T_{sf}^{-1}$ (Coqblin et al. 1978). The c-values are: $c(YCo_2) = 23 \times 10^{-5}$, $c(LuCo_2) = 21 \times 10^{-5}$, and $c(ScCo_2) = 11 \times 10^{-5}$ in units of cm/mW. Note that, from the tendency of the c-values as well as from the A coefficients in $\rho_{sf}(T) = AT^2$, it follows that $T_{sf}(YCo_2) < T_{sf}(LuCo_2) < T_{sf}(ScCo_2)$.

In fig. 109 the temperature dependence of the thermopower S of the RCo_2 compounds is depicted and compared with YAl_2. Note that in the Co compounds the minima in S vs. T at low temperature are much more pronounced than in the non-spin-fluctuation system YAl_2. The tiny minimum at low temperature, existing also in YAl_2, has been referred to as 'phonon drag' effect (Gratz and Nowotny 1985). In general such a 'drag effect' is thought to be caused by the situation that, in addition to the conduction electron system, other subsystems (phonons or magnons) are thermally in non-equilibrium and may cause an additional contribution to the total thermopower. This is usually taken into account by putting $S_{tot} = S_{diff} + S_{drag}$, where S_{diff} and S_{drag} are the diffusion and drag terms (Ziman 1960). Although no theoretical confirmation for such a '*paramagnon drag effect*' yet exists, experimentally minima (or sometimes maxima, depending on the slope of the density-of-states function at ε_F) have been observed in many paramagnetic spin fluctuation systems near their spin fluctuation temperatures, e.g. in UAl_2 (Coqblin et al. 1978). The broad minima at elevated temperatures are intimately correlated to changes of $dN(\varepsilon)/d\varepsilon$ at ε_F with temperature (Gratz et al. 1995). Density-of-states properties at the Fermi level

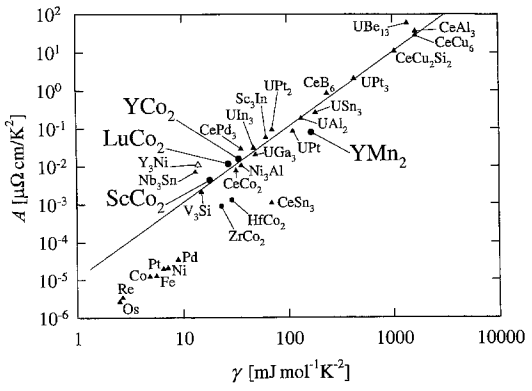

Fig. 110. The locations of the three RCo_2 (R = Sc, Y, Lu) spin fluctuation systems in the Kadowaki–Woods plot.

[$N(\varepsilon_F)$ and $dN(\varepsilon)/d\varepsilon$ at ε_F] are much more important for the diffusion thermopower at high temperature than for any of the other transport phenomena (Ziman 1960, Gratz et al. 1995). A correlation between the position of the high-temperature minima T_{min} in $S(T)$ and the γ-value of the specific heat has been found by Gratz et al. (1995) and is shown in the inset of fig. 109. As has been shown by Kadowaki and Woods (1986) there exists an important relation between A (the prefactor in $\rho = AT^2$) and the coefficient of the electronic specific heat γ for all strongly correlated electron systems. As such a Kadowaki–Woods plot (fig. 110) shows, the positions of the three RCo_2 spin-fluctuation systems fall in the range where many of the other known spin-fluctuation systems, such as Sc_3In, YMn_2 (under pressure in the paramagnetic state) UPt_2 or UAl_2, lie.

It follows from these data that spin fluctuations significantly influence transport phenomena. The question of whether these kinds of excitations (such as spin fluctuations) can be observed in an experiment depends on their characteristic time scale and the time window of the experiment used. An estimation of the characteristic time window of the transport phenomena gives about 10^{-14} s, which is of the same order of magnitude as the time scale of spin fluctuations in the d-electron subsystem.

6.2. *Compounds with magnetic ground state*

6.2.1. *Sc_3In*

Sc_3In crystallises in the Ni_3Sn-type structure (SG: $P6_3/mmc$) and has been classified as a weak ferromagnetic material. The onset of long-range ferromagnetic order as reported in the literature is between 5.5 K and 6 K depending on the stoichiometry of the sample (see Ikeda and Gschneidner 1981). The itinerant character of a ferromagnetic compound can best be seen from a so-called Rhodes–Wohlfarth plot (Rhodes and Wohlfarth 1963, Wohlfarth 1978) where p_s is the saturation moment per magnetic atom and p_c the effective moment per magnetic atom deduced from the Curie constant. Figure 111 shows the location of Sc_3In within a Rhodes–Wohlfarth plot. The p_c/p_s ratio for Sc_3In is 6.1 (Matthias et al. 1961), which is remarkably beyond the local moment limit of $p_c/p_s = 1$ for a strongly localised magnetically ordered material such as, e.g., Gd. In the local

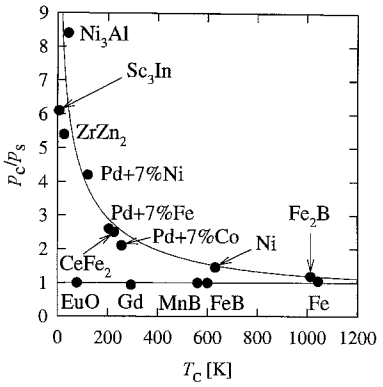

Fig. 111. p_C/p_S vs. T_C, a Rhodes–Wohlfarth plot; p_S is the saturation moment per magnetic atom and p_C is the corresponding effective moment deduced from the Curie constant (Wohlfarth 1978).

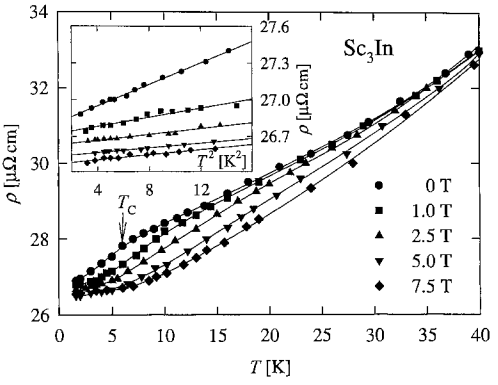

Fig. 112. The temperature dependence of the electrical resistivity of Sc_3In in different external magnetic fields. Inset: the T^2 dependence of the resistivity under the influence of the magnetic fields (Ikeda et al. 1984).

moment limit $p_c/p_s = 1$, and in the opposite weakly ferromagnetic limit theory predicts the divergence of this ratio as $p_s \rightarrow 0$ or $T_C \rightarrow 0$, since the Curie constant in this case is independent of p_s or T_C.

The effect of spin fluctuations in ferromagnetic and nearly ferromagnetic metals has been the subject of considerable interest for a long time. First Moriya and Kawabata (1973a,b) have developed a theory which considers the effect of spin fluctuations in a self-consistent way, thus taking account of the interaction among the spin-fluctuation modes. For the description of the magnetic properties of Sc_3In the concept of spin fluctuations is used. Ikeda and Gschneidner (1981) performed measurements of the specific heat and resistivity (Ikeda et al. 1984) in external fields with the aim to show that in materials with large spin-fluctuation enhancement, it is possible that a field of 10 T is sufficient to produce a measurable change in the magnetic specific heat and the low-temperature resistivity behaviour. Some of these results are given in the following figures. Figure 112 shows the temperature dependence of the electrical resistivity in different magnetic fields. The zero-field measurement clearly shows a kink in $\rho(T)$ indicating the Curie temperature at about 6 K. The inset shows a T^2 plot of the electrical resistivity at 0 T, 1 T, 2.5 T, 5 T and 7.5 T. As can be seen there is a T^2 dependence up to about 4 K. The prefactor A in the $\rho = AT^2$ relation strongly decreases with increasing field and becomes constant roughly above 5 T. The strong decrease of A with the magnetic field has been referred to as quenching of spin fluctuations. It should be noted however, that one always observes a negative magnetoresistance $\Delta\rho/\rho_0 \equiv [\rho(B) - \rho(B = 0)]/\rho(B = 0)$ in ferromagnets around T_C with a minimum in $\Delta\rho/\rho_0$ vs. T at T_C (Fournier and Gratz 1993). **The minimum at T_C in $\Delta\rho/\rho_0$ vs. T is more pronounced the lower the ferromagnetic transition takes place.** If this is taken into account the question arises whether this experiment can be considered as a test for the suppression of spin fluctuations in Sc_3In.

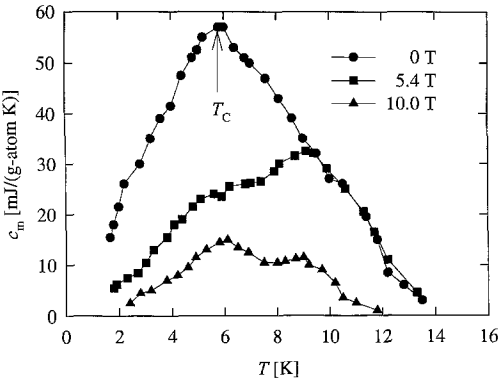

Fig. 113. The temperature dependence of the magnetic contribution to the specific heat c_m, in different magnetic fields (Ikeda and Gschneidner 1981).

Specific-heat experiments in magnetic fields performed by Ikeda and Gschneidner (1981) are presented in fig. 113, showing the magnetic contribution to the specific heat determined from the analysis of the experimental data by $c_m = c - \gamma T - \beta T^3$. As can be seen from this figure, c_m becomes smaller with increasing magnetic field, and in fields of about 10 T the height of its peak around T_C is only about $\frac{1}{4}$ of the zero-field value. Moreover, another peak around 8–9 K is found to be more pronounced at 5.4 T than in the highest field of 10 T. This new peak is thought to be due to the induced magnetisation of Sc_3In by the magnetic field.

6.2.2. *$ScFe_2$ and related compounds*

Among the RFe_2 series only $ScFe_2$ crystallises in a hexagonal Laves phase ($MgZn_2$ type structure) whereas all the remaining compounds have the cubic Laves phase ($MgCu_2$ type structure). All these RFe_2 Laves phases ($ScFe_2$ included) form ferromagnets with the nonmagnetic lanthanides and co-linear ferromagnets with the light lanthanides, or a ferrimagnetic structure with the heavy lanthanides with comparatively high Curie temperatures (>500 K). The high T_C values are primarily caused by the strong Fe–Fe exchange interaction. The ferromagnetic transition temperature of a $ScFe_2$ sample with the exact 1:2 stoichiometry is close to 540 K (see below). The magnetic moments per Fe atom vary roughly from $1.4\mu_B$ in case of Sc, Y and Lu to $1.8\mu_B$ for the compounds with the magnetic lanthanides as partner elements, thus proving that the Fe sublattice does not reach the saturated state in $ScFe_2$, YFe_2 and $LuFe_2$ (Rhyne 1987, Franse and Radwanski 1993). Band-structure calculations in the paramagnetic state of $ScFe_2$ by Ishida and Asano (1985) revealed that there is a peak in the density of states (DOS) due to the 3d bands of iron at the Fermi level on both Fe sites (2a and 6h). However, there is a small difference found in the DOS between Fe(2a) and Fe(6h) revealing different magnetic moments of $1.4\mu_B$/Fe(2a) and $1.46\mu_B$/Fe(6h). This bandstructure calculation also reveals an induced magnetic moment on the Sc sites of $0.27\mu_B$/Sc with the direction opposite to the moments on the Fe sites. However, these induced Sc–moments have not yet been observed experimentally. The calculated value of the

magnetic moments per formula unit is within the range of experimental values obtained by magnetic measurements; $2.9\mu_B/ScFe_2$ (Sankar and Wallace 1976), $2.23\mu_B/ScFe_{1.96}$ and $2.75\mu_B/ScFe_{2.05}$ (Grössinger et al. 1980). All these experimental values were obtained neglecting the existence of an induced Sc–moment as predicted by the theory. The slightly different values for the magnetic moments on the Fe(2a) and Fe(6h) sites are confirmed by differences in the hyperfine field observed in the Mössbauer effect which are 170 kOe for Fe(2a) sites and 176 kOe for Fe(6h) (Grössinger et al. (1980)). These authors investigated the influence of the stoichiometry on the bulk magnetisation and the hyperfine interaction by studying a second sample with a different Fe content: $ScFe_{2.05}$. They showed that the magnetocrystalline anisotropy differs considerably in magnitude depending on the composition. The average hyperfine field at 4.2 K increases from 176 kOe for the sample $ScFe_{1.96}$ up to 201 kOe in the sample $ScFe_{2.05}$. The conclusion drawn by Grössinger et al. (1980) is that the magnetic behavior of $ScFe_2$ is obviously very sensitive to the average d_{Fe-Fe} value. These arguments are further supported by the study of a hydrogenised $ScFe_2$ sample ($ScFe_2H_2$) (Smit and Buschow 1980) where the lattice constants are $a = 5.279$ Å, $c = 8.507$ Å (to be compared with $a = 4.977$ Å, $c = 8.146$ Å for $ScFe_2$). By means of magnetic measurements an increase of the moment per Fe from $1.4\mu_B$ in $ScFe_2$ to $2.2\mu_B$ in $ScFe_2H_2$ has been found. Using ^{57}Fe Mössbauer spectroscopy an increase of the hyperfine splitting by about 60% was observed, whereas, on the other hand, only a rather small change in the isomer shift was observed in $ScFe_2H_2$. Arguments are given in Smit and Buschow (1980) that it is difficult to explain the moment change in terms of a single 3d band picture and charge-transfer effect.

The dependence of the Curie temperature on the composition in $ScFe_2$ has been studied by the authors (Kotur et al. 1998). This investigation showed that a sample with the composition 1 : 1.92 exhibits an increase of the Curie temperature by about 100 K compared to the sample with the 1 : 2 stoichiometry with $T_C = 540$ K. This sensitivity of the magnetic properties to the composition has been suggested to be due to the chemical pressure the Fe atoms experience in this Sc-based hexagonal Laves phase. As noted above the $ScFe_2$ compound does not crystallize in the cubic $MgCu_2$-type structure, which is obviously due to the much smaller atomic radius of Sc. Furthermore, a change in the structural surroundings also influences the magnetic properties. Xia et al. (1996) have shown that a partial chemical disorder produced by ball milling leads to an increase of the Fe moment. Finally, amorphisation due to a long-lasting ball milling reduces the Curie temperature from 540 K down to 250 K (Xia et al. 1996).

For purpose of comparison the magnetic susceptibilities (or the magnetisations) of $ScNi_2$, $ScCo_2$ and $ScFe_2$, respectively, are shown in fig. 114. This picture clearly shows that among the ScM_2 (M = Ni, Co, Fe) there is one weak paramagnet ($ScNi_2$), one enhanced paramagnet ($ScCo_2$, see also sect. 6.1.3) and the ferromagnetic compound $ScFe_2$, with a long-range ferromagnetic order, caused by the 3d exchange interaction.

Another comparison has been made in fig. 115, where the temperature dependence of the electrical resistivity of these three compounds is depicted. It is interesting to note that although $ScCo_2$ does not show a long-range magnetic order, there is a huge magnetic contribution to the total resistivity, $\rho_{mag}(T) = \rho_{ges} - \rho_0 - \rho_{ph}$, which is of the same

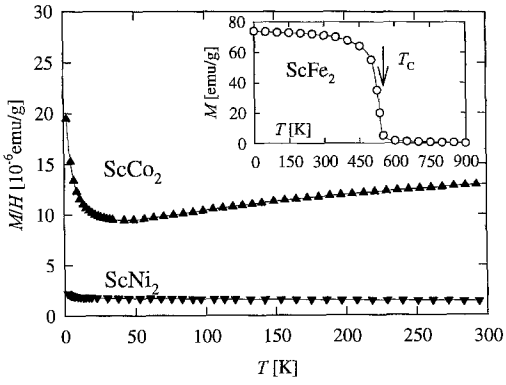

Fig. 114. The temperature dependence of the dc susceptibility of $ScNi_2$ and $ScCo_2$ (Kotur et al. 1998), and the magnetization of $ScFe_2$ (in a field of 4.5 T) (Sankar and Wallace 1976).

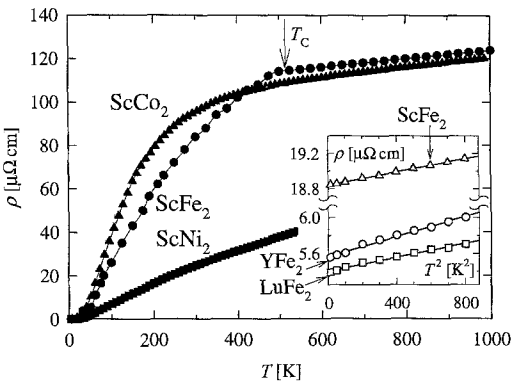

Fig. 115. A comparison of the electrical resistivity of $ScFe_2$, $ScNi_2$ (Kotur et al. 1998) and $ScCo_2$ (Gratz 1997). Inset: the low-temperature T^2 dependence of the three Fe-based ferromagnetic Laves phases (Kotur et al. 1998).

order of magnitude (about 100 μΩ cm) as in the ferromagnetic $ScFe_2$ compound, with a paramagnetic moment of the order of $1.4\mu_B$/Fe (see above). (The phonon resistivity ρ_{ph} for all three compounds is roughly given by the $\rho(T)$ data of $ScNi_2$, the residual resistivity ρ_0 has been subtracted from the data in this presentation). This picture underlines the statement in sect. 6.1.3 that the electrical resistivity (transport phenomena in general) is very sensitive to scattering processes of the conduction electrons with spin fluctuations. In sect. 6.1.3 it has been shown that there is a T^2 dependence of $\rho_{mag}(T)$ at low temperatures due to the spin-fluctuation scattering of the conduction electrons. Note that there is also a $\rho(T) = AT^2$ dependence in $ScFe_2$, caused by the spin-wave (magnon) scattering of the conduction electrons (Gratz et al. 1989). However A for $ScFe_2$ is roughly one order of magnitude smaller than the A-values found in the RCo_2 spin-fluctuation systems. The inset in fig. 115 shows the T^2 dependence of the resistivity for the three ferromagnetic RFe_2 (R = Sc, Y, Lu) compounds.

6.2.2.1. *$Sc(M_{1-x}Si_x)_2$ (M = Fe, Co, Ni).* As discussed in sect. 3.6, the substitution of Fe by Si in $ScFe_2$ reveals a change of the structure from the hexagonal $MgZn_2$-type structure ($ScFe_2$) to the cubic $MgCu_2$ type structure, if about 6 at% of Fe are substituted

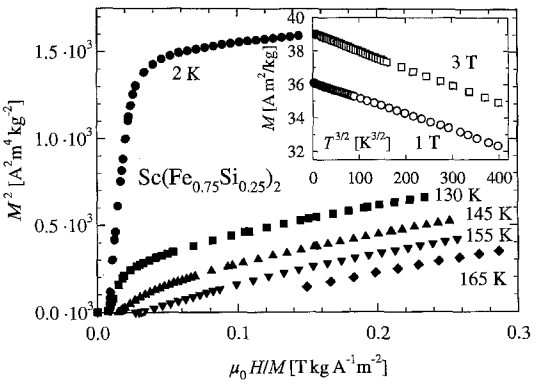

Fig. 116. Arrott plots of the $Sc(Fe_{0.75}Si_{0.25})_2$ compound. Inset: the low-temperature magnetisation in an M vs. $T^{3/2}$ representation. The spin wave stiffness thus obtained is 66 meV Å (Kotur et al. 1998).

by Si. The $MgZn_2$-type structure reappears around a substitution of 16 at% Fe by Si (Gladyshevsky et al. 1977). The influence of the Si substitution on the physical properties in the series of the $Sc(Fe_{1-x}Si_x)_2$ has been investigated by Kotur et al. (1998). In this investigation the Co- and Ni-based $Sc(M_{1-x}Si_x)_2$ compounds are included. Starting with $ScFe_2$, two other samples, $Sc(Fe_{0.94}Si_{0.06})_2$ with the $MgCu_2$-type structure and $Sc(Fe_{0.75}Si_{0.25})_2$ with the $MgZn_2$-type structure have been investigated in order to study the change of the magnetic properties due to the Fe substitution. For this study a number of measuring methods, namely magnetisation, specific heat, thermal expansion, resistivity and Mössbauer spectroscopy have been utilized by Kotur et al. (1998). The cubic sample $Sc(Fe_{0.94}Si_{0.06})_2$ shows a small decrease of T_C whereas all the other physical properties are similar to those of $ScFe_2$. These investigations however revealed that there is a dramatic lowering of the onset of the magnetic order in the sample $Sc(Fe_{0.75}Si_{0.25})_2$ ($T_C = 145$ K) in combination with a decrease of the averaged Fe moment ($0.67\mu_B$/Fe). The M^2 vs. B/M plot (Arrott plot) of the sample $Sc(Fe_{0.75}Si_{0.25})_2$ is given in fig. 116. The curvature of the M^2 vs. B/M curves in the ordered state was thought to be due to the local character of the Fe moments in these compound. The inset in fig. 116 shows the low-temperature magnetisation in a M vs. $T^{3/2}$ representation. From this an estimation of the spin-wave stiffness constant has been obtained. The value for $Sc(Fe_{0.75}Si_{0.25})_2$ is 66 meV Å^3, which is distinctly reduced when compared to $ScFe_2$ (465 meV Å^3).

The resistivity behaviour for the sample with $Sc(Fe_{0.75}Si_{0.25})_2$ is remarkable, since there is a negative slope in the temperature range from 4 K up to room temperature. The normalised resistivity curves $(\rho(T)/\rho(295\,K)$ vs. $T)$ for the $Sc(Fe_{0.75}Si_{0.25})_2$ sample, together with the resistivity of the isostructural Co- and Ni-based compounds $Sc(Co_{0.75}Si_{0.25})_2$, and $Sc(Ni_{0.75}Si_{0.25})_2$ are given in fig. 117. The residual resistivity for these compounds is of the order of 300–400 μΩ cm. This has been interpreted as a sign for a charge transfer from the silicon p bands to the 3d band of Fe, Co or Ni and the begin of a gap-opening.

There is an increase of the electronic specific heat coefficient γ from $\gamma(ScFe_2) = 10$ mJ mol^{-1} K^{-2} to $\gamma(Sc(Fe_{0.75}Si_{0.25})_2) = 38$ mJ mol^{-1} K^{-2}. $Sc(Fe_{0.75}Si_{0.25})_2$ has a small thermal expansion coefficient ($\alpha = 12\times10^{-6}$ K^{-1}) without any anomaly at $T_C = 145$ K.

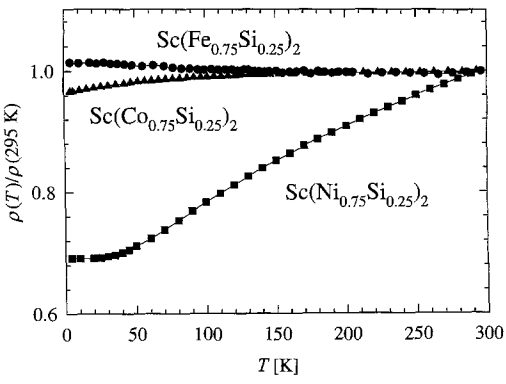

Fig. 117. The normalised resistivity $\rho(T)/\rho(295\,K)$ for $Sc(Fe_{0.75}Si_{0.25})_2$, $Sc(Co_{0.75}Si_{0.25})_2$, and $Sc(Ni_{0.75}Si_{0.25})_2$ (Kotur et al. 1998).

These investigations also revealed that an annealing procedure as well as a change of the 1:2 stoichiometry within the corresponding homogeneity range changes the physical properties considerably.

6.2.2.2. *$(Sc_{1-x}Ti_x)Fe_2$.* $ScFe_2$ is a ferromagnet (as shown above) whereas $TiFe_2$ shows antiferromagnetism with $T_N \approx 270\,K$ (Nakamichi 1968). Both compounds crystallise in the hexagonal $MgZn_2$ Laves phase structure. Thus in the pseudobinary system $(Sc_{1-x}Ti_x)Fe_2$ the magnetic properties change from ferromagnetism to antiferromagnetism as the Sc:Ti ratio changes. The system shows the $MgZn_2$ type structure over the whole concentration range. Along this pseudobinary the Curie temperature on the Sc-rich side (up to $x = 0.2$) is nearly constant with a saturation magnetisation for $ScFe_{1.95}$ of about 81 emu/g (Nishihara and Yamaguchi 1986). However, with increasing Ti concentration the saturation magnetisation increases up to about 94 emu/g for $x = 0.65$ and a decreasing saturation field. This tendency however changes abruptly at about $x = 0.7$, the saturation magnetisation for this sample is about half (48 emu/g) of that for the sample with $x = 0.65$. A small discontinuity at 150 K in the temperature dependence of the magnetisation for $x = 0.7$ has been interpreted as the onset of antiferromagnetism in the low-temperature region causing the decrease of the saturation magnetisation (Nishihara and Yamaguchi 1985, 1986). Interestingly, in the temperature dependence of the magnetisation for $x = 0.65$ to $x = 0.4$ there is a step-like increase of the ferromagnetic magnetisation at the corresponding transition temperature (for $x = 0.65$ at 80 K) due to a temperature-induced increase of the ferromagnetic Fe moments. The saturation magnetisation at 0 K is $1.3\mu_B$/Fe and about $0.9\mu_B$/Fe just above the transition temperature for the sample $x = 0.65$. This difference in the saturation moment between both ferromagnetic states become smaller as the Ti content is further decreased. No such a transition has been found for $0 \leqslant x \leqslant 0.2$.

Investigations of the paramagnetic susceptibility exhibit that for all the samples the Curie–Weiss law is fulfilled however the Curie constants are larger for the sample with $x > 0.75$ than for that with $x < 0.5$. Interestingly the χ^{-1} vs. T plots for $0.5 \leqslant x \leqslant 0.75$ show kinks at temperatures about 100 K higher than the corresponding Curie temperatures. The

change in the effective moment, deduced from the Curie constant, is $2.5\mu_B$/Fe above the kink in χ^{-1} vs. T and about $1.6\mu_B$/Fe below the kink.

It seems that this finding is a confirmation that the change in the chemical pressure the Fe atoms experience within this pseudobinary caused by the small atomic diameter (of both Sc and Ti) destabilises the magnetic moments of the Fe atoms. This is, for example, quite in contrast to YFe_2 with stable moments on the iron sites.

6.2.3. *Sc substitution in YMn_2*

Rare-earth Laves phases with 3d transition metals as a partner element are interesting mainly because of the great variety of magnetic phenomena observed in this family of intermetallics. The intercorrelation between the two types of Laves phases C15 (cubic) and C14 (hexagonal) is similar to that between the fcc and hcp, i.e., a different order of packing of atomic layers. Therefore, the coordination number is the same for both structures. One of the characteristics of this structure is that the nearest neighbour of a transition-metal atom is also a transition-metal atom. The atomic distances between the transition metals in RM_2 is similar to that in the pure 3d metals. Comparing the density of states of the elementary "heavy" 3d elements (Mn, Fe, Co, Ni) shows that the 3d density of states is similar to that of the Laves phases RMn_2, RFe_2, RCo_2 and RNi_2. However within one such a series the position of the Fermi level can be shifted by selecting RE elements with different atomic diameter. This is why Sc with its small atomic size is frequently used as an alloying element.

In the following a well-known example, $Y(Sc)Mn_2$, will be discussed. In a number of investigations it has been shown that the magnetic state of Mn in these Laves phases depends sensitively on the Mn–Mn distance (d_{Mn-Mn}) (Shiga 1988). Above a critical value of $d_{Mn-Mn} = 2.7$ Å there exist spontaneous Mn moments which in general are antiferromagnetically ordered at low enough temperatures. Below this critical d_{Mn-Mn} value the spontaneous Mn moments are zero, however, induced Mn moments can appear in RMn_2 compounds with magnetic rare-earth elements as partner elements (for a review see Hauser et al. 1994). The sensitivity of the magnetic ground state to d_{Mn-Mn} is why in YMn_2 a relatively small pressure of about 3 kbar is enough to suppress the antiferromagnetic order (Oomi et al. 1987). However, what is interesting for the subject under consideration, is that a substitution of a small amount of Sc in YMn_2 causes also a nonmagnetic ground state, due to the negative chemical pressure. In the χ vs. T curves of the pseudobinary $(Y_{1-x}Sc_x)Mn_2$ system the discontinuity at T_N shifts below 4.2 K for $x > 0.02$, indicating the collapse of the antiferromagnetic state (Nakamura et al. 1988). Another indication for the suppression of the antiferromagnetic state within this pseudobinary system is the vanishing zero-field NMR spectrum with increasing Sc concentration (Yoshimura et al. 1987). However the collapse of the antiferromagnetic order in $(Y_{1-x}Sc_x)Mn_2$ can most clearly be seen in the temperature dependence of the lattice parameter within this pseudobinary system. These measurements are given in fig. 118 (Shiga 1988). The sharp decrease of the lattice constant at T_N is due to the partial collapse of the Mn moments from $2.7\mu_B$/Mn (estimated from neutron diffraction

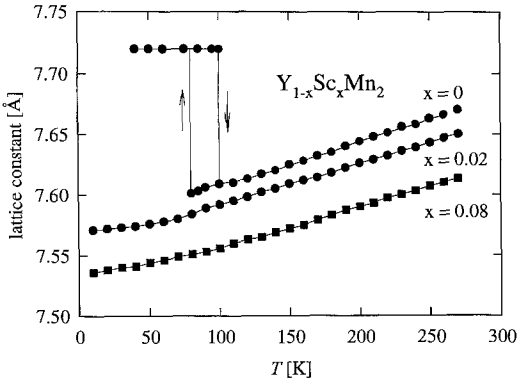

Fig. 118. The temperature dependence of the cubic lattice parameters of $(Y_{1-x}Sc_x)Mn_2$. The step-like increase of $a(T)$ indicates the onset of long-range antiferromagnetic order in YMn_2. This transition is of first-order type with a huge hysteresis (the arrows indicate the measurements on heating and cooling) (Shiga 1988).

experiments, Nakamura et al. 1989) to about $1.7\mu_B$/Mn just above T_N. The huge hysteresis is an indication that the magnetic transition is of first-order type. Interestingly the very large thermal expansion coefficient α measured in pure YMn_2 in the paramagnetic temperature range ($\alpha = 50\times10^{-6}\,K^{-1}$) is still observable in the compounds with the Sc substitution. This large α-value has been attributed to the existence of strong spin fluctuations in YMn_2 by Shiga (1988). Recently it has been proposed that the large coefficient α observed in nearly all the Mn intermetallics in their paramagnetic state (e.g. in YMn_2, YMn_{12}, Y_6Mn_{23} and also in the Mn metal) might be due to different valence states of the Mn atoms. The assumption is made that this multi-valence state changes as a function of temperature, pressure or composition (Gratz et al. 1997).

6.3. *Compounds with superconducting ground state*

6.3.1. *$Sc_{1-x}M_x$ alloys (M = Co, Rh, Ir, Pd, Pt)*

The appearance of superconductivity in Sc-based binary alloys with Co, Rh, Ir, Pd and Pt has been investigated by Geballe et al. (1965). Superconductivity with transition temperatures above 0.35 K (the lowest available temperature of the experiments in this investigation) has been found in the Sc_xCo_{1-x} system in the range $x = 0.28$–0.32. It was however reported by Geballe et al. (1965) that it was not possible to isolate the superconducting phase. Indications for superconductivity occur at 0.8 K in a Sc–Rh alloy in the Sc-rich concentration region, however as it was expressed there, only about $\frac{1}{4}$ of the sample was superconducting as deduced from the smaller signal obtained for a powder. In the Sc–Ir system only one superconducting phase has been identified, namely that with the $MgCu_2$-type structure $ScIr_2$ which has a transition temperature of 2.07 K according to Geballe et al. (1965). The maximum transition temperature for the C15-type alloys is 2.46 K which occurs in $ScIr_{2.5}$, however after powdering the sample two transitions exist, one at 2.13 K (which is that of the C15 type) and one that begins at 0.42 K. The lower temperature has been ascribed to the transition of a nonstoichiometric $ScIr_2$ alloy. According to Geballe et al. (1965) there is no superconducting phase in the Sc–Pd and

Sc–Pt system. This has been ascribed to the lack of favourable intermediate phases in these systems.

Alloys of Y and Lu with Co, Rh, Ir, Pd and Pt have been studied and compared. This comparison shows that in the alloys with Sc the smallest number of superconducting compounds exist. Interestingly, in none of these series based on Sc, Y or Lu superconductivity has been observed in compounds with Pd.

6.3.2. *$Sc_5M_4Si_{10}$ (M = Co, Rh, Ir) and $R_2Fe_3Si_5$ (R = Sc, Y, Lu)*

Among the Sc-containing superconductors the most interesting are the superconducting ternary iron and cobalt silicides. The discovery of $Sc_5Co_4Si_{10}$ with a superconducting transition temperature of $T_S = 4.9$ K demonstrated that relatively high transition temperatures may be found among compounds containing 3d transition elements as intrinsic constituents (Braun and Segre 1980). In this paper a class of ternary compounds with the general formula $R_5M_4X_{10}$, (where R = Sc or Y, M = Co, Rh, Ir, and X = Si or Ge) has been described the first time. These $R_5M_4X_{10}$ compounds crystallise in a primitive tetragonal lattice with SG *P4/mbm*. The superconducting transition temperatures of the Sc-containing samples are: 4.9 K for $Sc_5Co_4Si_{10}$, 8.5 K for $Sc_5Rh_4Si_{10}$, and 8.4 K for $Sc_5Ir_4Si_{10}$. The occurrence of superconductivity at temperatures up to 8.4 K in the $Sc_5M_4Si_{10}$ phases is remarkable since elements like Sc and Si become superconducting only under pressure. Ir is superconducting below 0.66 K and Rh and Co are not superconducting at all. The comparatively high T_S of $Sc_5Co_4Si_{10}$ indicates that the magnetic character of the Co atoms is either lost in these phases or does not interfere significantly with the BCS pairing. This behaviour is intriguing in view of the existence of "isolated" transition-metal atoms in these compounds.

Later it has been shown that there are other ternary superconducting compounds containing iron as the transition metal (Vining et al. 1983). The ternary iron silicides $R_2Fe_3Si_5$ (R = Lu, Sc, Y) were first reported to become superconducting by Braun (1980). The crystal structure of $Sc_2Fe_3Si_5$ which belongs to the SG *P4/mnc* has been solved by Bodak et al. (1977). The superconducting transition temperatures for the three compounds are not very sharp and are given by Braun (1980) as: $T_S = 4.52$–4.25 K for $Sc_2Fe_3Si_5$, $T_S = 2.4$–2.0 K for $Y_2Fe_3Si_5$, and $T_S = 6.1$–5.8 K for $Lu_2Fe_3Si_5$. ^{57}Fe Mössbauer effect measurements of these Fe-based series in magnetic fields show quadrupole-splitted spectra with small positive values of the isomer shift, indicating the absence of magnetic moments at the iron sites (Braun et al. 1981). An estimation of the upper limit of the magnetic moments on the two iron sites at 4.2 K with a magnetic field (5.6 T) and without a magnetic field has been given in Cashion et al. (1980, 1981). These measurements revealed $\mu_{Fe} \leqslant 0.03\mu_B$. To explain the nonmagnetic ground state of Fe in these compounds two models have been discussed earlier in the literature. One model is based on the assumption that a charge transfer from Si to Fe takes place in these compounds. The other concept assumes an influence of the crystal field on the 3d orbital. The charge transfer model requires a rather unrealistic large charge transfer from the d^6 configuration of Fe into a d^{10} configuration. However, the very small Fe–Si interatomic distances

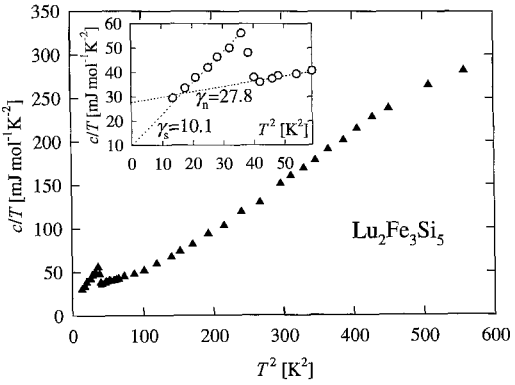

Fig. 119. The temperature variation of the specific heat of $Lu_2Fe_3Si_5$ in a c/T vs. T^2 presentation. Inset: the coefficient of the linear term in the heat capacity for the normal state (γ_n) and the superconducting state (γ_s) in mJ mol^{-1} K^{-2} (Vining et al. 1983).

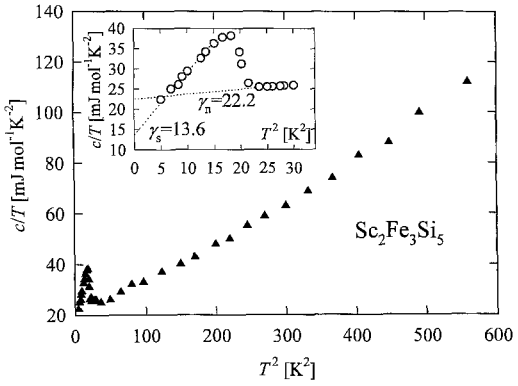

Fig. 120. The temperature variation of the specific heat of $Sc_2Fe_3Si_5$ in a c/T vs. T^2 presentation. Inset: the coefficient of the linear term in the heat capacity for the normal state (γ_n) and the superconducting state (γ_s) in mJ mol^{-1} K^{-2} (Vining et al. 1983).

in this compound (see table 2 in Braun 1981) might support this explanation. The assumption that the crystal field in a transition metal compound is strong enough to cause a zero Fe moment seems questionably too. We feel that as yet the question of why Fe is nonmagnetic in such systems is unsolved. The low-temperature heat capacity measurements performed on the three $R_2Fe_3Si_5$ (R = Lu, Sc, Y) compounds by Vining et al. (1983) revealed several anomalous properties in their superconducting state. Most remarkable in these heat-capacity results are the large linear term in the superconducting state and a reduced normalised jump in the specific heat at T_S. These measurements are shown in figs. 119, 120 and 121 in c/T vs. T^2 representations. The respective c/T vs. T^2 plots around T_S are shown in the insets. The superconducting transition temperatures as obtained from these specific-heat measurements are 6.3 K, 4.4 K and 1.7 K for $Lu_2Fe_3Si_5$, $Sc_2Fe_3Si_5$ and $Y_2Fe_3Si_5$, respectively. Deviations from linearity above T_S especially in $Lu_2Fe_3Si_5$ are apparent. A fit of these data in the temperature range from above T_S to about 18 K with $c = \gamma_n T + \beta_n T^3 + \alpha_n T^5$ (the subscript n denotes the non-superconducting state) with a root mean square deviation of about 1% revealed that in each case the lattice contribution $\beta_n T^3 + \alpha_n T^5$ to the total specific heat represents less than 20% of the total heat capacity at T_S. The prefactor α_n is smallest in the Sc compound. The jump at T_S is

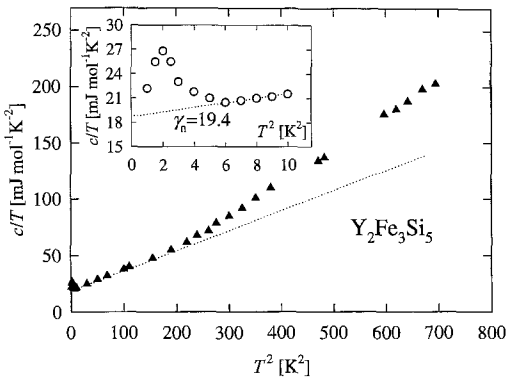

Fig. 121. The temperature variation of the specific heat of $Y_2Fe_3Si_5$ in a c/T vs. T^2 presentation. Inset: the coefficient of the linear term in the heat capacity for the normal state (γ_n) in mJ mol^{-1} K^{-2} (Vining et al. 1983).

sharp for $Lu_2Fe_3Si_5$ and $Sc_2Fe_3Si_5$ whereas it is broad in $Y_2Fe_3Si_5$; this is ascribed to a somewhat lower quality of the latter sample. The normalised jump $\Delta c/(\gamma_n T_S)$ in the heat capacity at T_S in $Sc_2Fe_3Si_5$ and $Y_2Fe_3Si_5$ is less than 60% of the BCS value of 1.43. Below T_S the heat capacity of $Lu_2Fe_3Si_5$ and $Sc_2Fe_3Si_5$ has been fitted to the expression $c = \gamma_s T + \beta_s T^3$ (the subscript s denotes the superconducting state). The measured $Y_2Fe_3Si_5$ data do not permit an estimation of γ_s. An extrapolation towards lowest temperatures reveals $\gamma_s = 13.6$ mJ mol^{-1} K^{-2} for $Sc_2Fe_3Si_5$ and 10.1 mJ mol^{-1} K^{-2} for $Lu_2Fe_3Si_5$. The reduced normalised jump at T_S and the large linear γ_s values have been explained by Vining et al. (1983) assuming a two-band model in which one band remains in the normal state. These can be understood in terms of a topological complex Fermi surface in which pockets of electrons remain.

6.3.3. *RRu_4B_4*

Within the RRu_4B_4 series of compounds the body-centred tetragonal (bct) structure occurs for all members except for La, the largest of the rare-earth elements (Johnston 1977). Similarly, within the set of primitive tetragonal RRh_4B_4 compounds $NdRh_4B_4$, which contains the largest rare-earth ion which forms this structure, has been found to be metastable (Johnston 1977). A structural instability of the various RM_4B_4 structure classes also occurs with decreasing size of the rare-earth ions; the smallest rare-earth atom which has been reported to form any of these phases is Lu. Ku et al. (1979) reported that Sc, with a much smaller ionic radius, does form $ScRu_4B_4$, however it was found that this compound is metastable. Surprisingly however, $ScRu_4B_4$ becomes superconducting at a temperature of about 7.2 K, much higher than the T_S of the other two superconducting members of the body-centred tetragonal RRu_4B_4 series, namely 1.8 K for $LuRu_4B_4$ and 1.4 K for YRu_4B_4. Since the $ScRu_4B_4$ sample, where the superconductivity has been found, was a multi-phase sample, a comprehensive investigation around the $ScRu_4B_4$ composition in the Sc–Ru–B ternary phase diagram has been undertaken. However, no single-phase $ScRu_4B_4$ sample could be obtained. The effect of annealing was that the superconductivity disappeared in these ternary body-centred tetragonal phases.

6.3.4. *$ScNi_2B_2C$*

Superconductivity with relatively high transition temperatures up to 23 K has been reported in R–M–B–C systems (R = Y and M = Ni, Pd or Pt) (see e.g. Ku et al. 1994). In the Ni-based system superconductivity was first observed in the compound with R = Lu with the tetragonal $LuNi_2B_2C$-type structure (SG *I4/mmm*). Among the RNi_2B_2C the highest T_S (16.6 K) has been reported for $LuNi_2B_2C$ followed by YNi_2B_2C with 15.6 K (Nagarajan et al. 1994, Cava et al. 1994, Siegrist et al. 1994). For magnetic rare-earth compounds lower superconducting transition temperatures (due to the pair-breaking effect) have been observed. Superconductivity has been observed in $ScNi_2B_2C$ by Ku et al. (1994), however, only in an as-cast multi-phase sample. As in the other RNi_2B_2C systems the superconducting phase in $ScNi_2B_2C$ is found only in those phases with the tetragonal $LuNi_2B_2C$-type structure. Obviously because of the much smaller ionic radius of Sc^{3+} this superconducting phase is metastable in $ScNi_2B_2C$ and vanishes (together with the superconductivity) after the sample has been annealed at 1050°C for 24 h. The superconducting transition temperature for this metastable $ScNi_2B_2C$ compound is between 15 and 16 K, thus only slightly lower than 16.7 K for the $LuNi_2B_2C$ compound and almost equal to 15.6 K for YNi_2B_2C, which indicates that the superconducting properties of these systems are essentially independent of the relative size of the nonmagnetic R^{3+} ions (R = Sc, Y or Lu).

Acknowledgement

We acknowledge with gratitude the help of Andreas Kottar in the preparation of part of the manuscript.

Appendix 1. Structure types of intermetallic compounds of scandium

Table 36 collects the structure types of intermetallic compounds of scandium.

Table 36
Structure types of intermetallic compounds of scandium

Structure type	Pearson's symbol	Space group	Number of compounds	Including		Including in ternary systems Sc–M–... Sc–...											Binary prototype	Composition of ternary compound(s)
				binary	ternary	B	Al	Ga	In	C	Si	Ge	Sn	5b-	6b-	X–X′	M–M′	
$MgZn_2$	hP12	$P6_3/mmc$	20	6	14	–	6	3	–	–	3	1	–	–	–	–	1		$ScM_{2-x}X_x$; $ScM_{1.5}X_{0.5}$
TiNiSi	oP12	*Pnma*	19	0	19	–	–	2	–	–	8	4	4	1	–	–	–	anti-$PbCl_2$	ScMX
$MnCu_2Al$	cF16	*Fm3m*	18	0	18	–	5	3	6	–	–	–	4	–	–	–	–	BiF_3	ScM_2X
CsCl	cP2	*Pm3m*	16	16	0	–	–	–	–	–	–	–	–	–	–	–	–		
$Mg_6Cu_{16}Si_7$	cF116	*Fm3m*	15	0	15	–	7	5	–	–	2	1	–	–	–	–	–	Th_6Mn_{23}	$Sc_6M_{16}X_7$; $Sc_6M_7X_{16}$
$CaTiO_3$	cP5	*Pm3m*	14	0	14	2	–	–	–	3	–	–	–	–	–	9	–	$\gamma'Fe_4N$	ScM_3C; Sc_3XX'
ZrNiAl	hP9	$P\bar{6}2m$	14	0	14	–	–	–	–	–	3	8	2	1	–	–	–	Fe_2P	ScMX
$Ce_2Sc_3Si_4$	oP36	*Pnma*	12	0	12	–	–	–	–	–	5	7	–	–	–	–	–	Sm_5Ge_4	$Sc_2M_3X_4$; $Sc_3M_{2-x}X_4$
ScCeSi	tI12	*I4/mmm*	11	0	11	–	–	–	–	–	5	6	–	–	–	–	–	La_2Sb	ScMX
Sm_5Ge_4	oP36	*Pnma*	10	1	9	–	–	–	–	–	2	7	–	–	–	–	–		$Sc_{2-4}M_{3-1}X_4$
$ZrCrSi_2$	oP48	*Pbam*	10	0	10	–	–	–	–	–	2	8	–	–	–	–	–		$ScMX_2$
$MgCu_2$	cF24	*Fd3m*	9	5	4	–	1	1	–	–	1	1	–	–	–	–	–		$ScM_{2-x}X_x$
AlB_2	hP3	*P6/mmm*	8	3	5	–	–	–	–	–	4	–	–	–	–	1	–		$Sc_{1-x}M_xSi_{2-x}$; $ScAl_{2-x}Ga_x$
Mn_5Si_3	hP16	$P6_3/mcm$	8	6	2	–	–	–	–	–	2	–	–	–	–	–	–		$Sc_2V_3Si_3$; $Sc_{0.35}Fe_{4.65}Si_3$
$AuCu_3$	cP4	*Pm3m*	7	7	0	–	–	–	–	–	–	–	–	–	–	–	–		
$CaIn_2$	hP6	$P6_3/mmc$	7	0	7	–	–	5	–	–	–	–	1	–	–	–	1		$ScM_{2-x}Ga_x$; ScCuSn; ScCuZn
Mo_2FeB_2	tP10	*P4/mbm*	7	0	7	–	–	–	–	–	5	–	1	–	–	1	–	U_3Si_2	ScM_2Si_2; Sc_2Ni_2Sn; Sc_2AlSi_2
MgAgAs	cF12	$F\bar{4}3m$	7	0	7	–	–	–	–	–	–	1	2	4	–	–	–	CaF_2	ScMX
$ThMn_{12}$	tI26	*I4/mmm*	7	1	6	–	2	3	–	–	1	–	–	–	–	–	–		$ScM_{4+x}X_{8-x}$; $ScFe_{10}Si_2$
$HfFe_6Ge_6$	hP13	*P6/mmm*	6	0	6	–	–	–	–	–	–	4	2	–	–	–	–		ScM_6X_6
$U_4Re_7Si_6$	cI34	*Im3m*	6	0	6	–	–	–	–	–	1	5	–	–	–	–	–		$Sc_4M_7X_6$
$Ho_{11}Ge_{10}$	tI84	*I4/mmm*	6	2	4	–	–	3	–	–	–	1	–	–	–	–	–		$Sc_{9.4-x}M_{1.6+x}Ga_{10}$; $Sc_6Yb_5Ge_{10}$
CrB	oS8	*Cmcm*	5	4	1	–	–	–	–	–	1	–	–	–	–	–	–		$Sc_{0.2-0.4}Sm_{0.8-0.6}Si$

continued on next page

Table 36, *continued*

Structure type	Pearson's symbol	Space group	Number of compounds	Including		Including in ternary systems Sc–M–... Sc–...												Binary prototype	Composition of ternary compound(s)
				binary	ternary	B	Al	Ga	In	C	Si	Ge	Sn	5b-	6b-	X–X′	M–M′		
$ZrSi_2$	oS12	*Cmcm*	5	1	4	–	–	–	–	–	4	–	–	–	–	–	–		$ScM_{0.25}Si_{1.75}$
$YCrB_4$	oP24	*Pbam*	5	0	5	5	–	–	–	–	–	–	–	–	–	–	–		$ScMB_4$
$Zr_4Co_4Ge_7$	tI34	*I4/mmm*	5	0	5	–	–	–	–	–	2	3	–	–	–	–	–		$Sc_4M_4Si_7$; $Sc_4M_4Ge_{7-x}$
Ti_2Ni	cF96	*Fd3m*	5	3	2	–	–	–	–	–	2	–	–	–	–	–	–		$Sc_2M_{1-x}Si_x$ (M = Co, Cu)
$Zr_2Fe_{12}P_7$	hP21	$P\bar{6}$	4	0	4	–	–	–	–	–	–	–	–	4	–	–	–		$Sc_2M_{12}P_7$
$Gd_6Cu_8Ge_8$	oI22	*Immm*	4	0	4	–	–	–	–	–	2	2	–	–	–	–	–		$Sc_3M_4X_4$ (M = Ni, Cu)
$MgCu_4Sn$	cF24	$F\bar{4}3m$	4	0	4	–	–	–	1	–	–	–	2	–	–	–	1	$MgCu_2$	ScM_4X; $ScNi_4Au$
$Hf_3Ni_2Si_3$	oS32	*Cmcm*	4	0	4	–	–	–	–	–	3	1	–	–	–	–	–		$Sc_3M_2X_3$
Ti_6Ge_5	oI44	*Ibam*	4	2	2	–	–	–	–	–	1	1	–	–	–	–	–		ScV_5Si_5; $Sc_{1-1.8}V_{5-4.2}Ge_5$
$Sc_7Cr_{4+x}Si_{10-x}$	tI84	*I4/mmm*	4	0	4	–	–	–	–	–	2	2	–	–	–	–	–	$Ho_{11}Ge_{10}$	$Sc_7M_{4+x}X_{10-x}$
$Sc_{57}Rh_{13}$	cP140	$Pm\bar{3}$	4	4	0	–	–	–	–	–	–	–	–	–	–	–	–		
$MoSi_2$	tI6	*I4/mmm*	3	3	0	–	–	–	–	–	–	–	–	–	–	–	–		
Ni_2In	hP6	$P6_3/mmc$	3	3	0	–	–	–	–	–	–	–	–	–	–	–	–		
$HoCoGa_5$	tP7	*P4/mmm*	3	0	3	–	–	3	–	–	–	–	–	–	–	–	–		$ScMGa_5$ (M = Co, Ni)
$ScCoC_2$	tP8	*P4/nmm*	3	0	3	–	–	–	–	3	–	–	–	–	–	–	–		$ScMC_2$ (M = Fe, Co, Ni)
Ni_3Sn	hP8	$P6_3/mmc$	3	3	0	–	–	–	–	–	–	–	–	–	–	–	–		
$CeGa_2Al_2$	tI10	*I4/mmm*	3	0	3	–	–	–	–	–	3	–	–	–	–	–	–	$BaAl_4$	ScM_2Si_2 (M = Co, Ni, Cu)
KHg_2	oI12	*Imma*	3	1	2	–	–	2	–	–	–	–	–	–	–	–	–		$ScM_{2-x}Ga_x$ (M = Co, Cu)
$ZrFe_4Si_2$	tP14	$P4_2/mnm$	3	0	3	–	–	–	–	1	–	–	–	2	–	–	–		ScM_4X_2
Sc_3CoC_4	oI16	*Immm*	3	0	3	–	–	–	–	3	–	–	–	–	–	–	–		Sc_3MC_4 (M = Fe, Co, Ni)
Sc_2CoSi_2	mS20	*B2/m*	3	0	3	–	–	–	–	–	2	1	–	–	–	–	–		Sc_2MX_2
$Sc_2Re_3Si_4$	tP36	$P4_12_12$	3	0	3	–	–	–	–	–	3	–	–	–	–	–	–	Zr_5Si_4	$Sc_2M_3Si_4$ (M = V, Cr, Re)

continued on next page

Table 36, *continued*

Structure type	Pearson's symbol	Space group	Number of compounds	Including		Including in ternary systems Sc–M–... Sc–...												Binary prototype	Composition of ternary compound(s)
				binary	ternary	B	Al	Ga	In	C	Si	Ge	Sn	5b-	6b-	X–X′	M–M′		
$Sc_5Co_4Si_{10}$	tP38	*P4/mbm*	3	0	3	–	–	–	–	–	3	–	–	–	–	–	–		$Sc_5M_4Si_{10}$ (M = Co, Rh, Ir)
Al_2MgO_4	cF56	*Fd3m*	3	0	3	–	–	–	–	–	–	–	–	–	3	–	–		Sc_2MSe_4 (M = Mg, Mn, Cd)
$Sc_{11}Ir_4$	cF120	*Fm3m*	3	3	0	–	–	–	–	–	–	–	–	–	–	–	–		
Ru_3Be_{17}	cI160	*Im*$\bar{3}$	3	1	2	–	–	2	–	–	–	–	–	–	–	–	–		$ScCu_{3.7}Ga_{2.3}$; $ScNi_{2.36}Ga_{3.64}$
NiAs	hP4	$P6_3/mmc$	2	2	0	–	–	–	–	–	–	–	–	–	–	–	–		
$CaCu_5$	hP6	*P6/mmm*	2	2	0	–	–	–	–	–	–	–	–	–	–	–	–		
$MoNi_4$	tI10	*I4/m*	2	2	0	–	–	–	–	–	–	–	–	–	–	–	–		
Ho_2CoGa_8	tP11	*P4/mmm*	2	0	2	–	–	2	–	–	–	–	–	–	–	–	–		Sc_2MGa_8 (M = Co, Ni)
$\alpha ThSi_2$	tI16	$I4_1/amd$	2	0	2	–	–	–	–	–	2	–	–	–	–	–	–		$Sc_{0.3}M_{0.7}Si_2$ (M = Sm, Dy)
AlLiSi	cF12	*F*$\bar{4}$*3m*	2	0	2	–	–	–	–	–	–	–	2	–	–	–	–		ScMSn (M = Pt, Au)
$YbMo_2Al_4$	tI14	*I4/mmm*	2	0	2	–	–	2	–	–	–	–	–	–	–	–	–		ScM_2Ga_4 (M = Ti, V)
$TiNi_3$	hP16	$P6_3/mmc$	2	0	2	–	2	–	–	–	–	–	–	–	–	–	–		$Sc_{1-x}M_xAl_3$ (M = Y, Tb)
Cr_3C_2	oP20	*Pnma*	2	2	0	–	–	–	–	–	–	–	–	–	–	–	–		
Sb_2S_3	oP20	*Pnma*	2	2	0	–	–	–	–	–	–	–	–	–	–	–	–		
$Sc_2Ru_5B_4$	mP22	*P2/m*	2	0	2	2	–	–	–	–	–	–	–	–	–	–	–		$Sc_2M_5B_4$ (M = Ru, Os)
$MgNi_2$	hP24	$P6_3/mmc$	2	1	1	–	1	–	–	–	–	–	–	–	–	–	–		$ScCu_{0.6}Al_{1.4}$
$Sc_5Ni_{1-x}Ga_{1-x}$	hP28	$P6_3/mmc$	2	0	2	–	–	2	–	–	–	–	–	–	–	–	–		$Sc_5M_{1-x}Ga_{1-x}$ (M = Co, Ni)
βYb_5Sb_3	oP32	*Pnma*	2	2	0	–	–	–	–	–	–	–	–	–	–	–	–		
$ZrFe_6Ge_4$	hR33	*R*$\bar{3}$*m*	2	0	2	–	–	–	–	–	–	2	–	–	–	–	–		ScM_6Ge_4 (M = Mn, Fe)
YCo_5P_3	oP36	*Pnma*	2	0	2	–	–	–	–	–	–	–	–	2	–	–	–		ScM_5P_3 (M = Fe, Co)
TiFeSi	oI36	*Ima2*	2	0	2	–	–	2	–	–	–	–	–	–	–	–	–		$ScM_{0.35}Ga_{1.65}$ (M = Co, Ni)

continued on next page

Table 36, *continued*

Structure type	Pearson's symbol	Space group	Number of compounds	Including		Including in ternary systems Sc–M–... Sc–...												Binary prototype	Composition of ternary compound(s)
				binary	ternary	B	Al	Ga	In	C	Si	Ge	Sn	5b-	6b-	X–X′	M–M′		
$Sc_3Ni_{11}Si_4$	hP36	$P6_3/mmc$	2	0	2	–	–	–	–	–	1	1	–	–	–	–	–		$Sc_3Ni_{11}X_4$ (X = Si, Ge)
$Sc_3Mn_2Ga_6$	oP44	$Pnma$	2	0	2	–	–	2	–	–	–	–	–	–	–	–	–		$Sc_3M_2Ga_6$ (M = Mn, Fe)
$Nb_2Cr_4Si_5$	oI44	$Ibam$	2	0	2	–	–	–	–	–	1	1	–	–	–	–	–	Ti_6Ge_5	$Sc_2Cr_4X_5$ (X = Si, Ge)
$Y_2Co_3Ga_9$	oS56	$Cmcm$	2	0	2	–	1	1	–	–	–	–	–	–	–	–	–		$Sc_2Co_3X_9$ (X = Al, Ga)
αMn	cI58	$I\bar{4}3m$	2	2	0	–	–	–	–	–	–	–	–	–	–	–	–		
$ScRh_3Si_7$	hR66	$R\bar{3}c$	2	0	2	–	–	–	–	–	2	–	–	–	–	–	–		ScM_3Si_7 (M = Rh, Ir)
$ScCo_{1.2}Ga_{1.8}$	tP80	$P4mm$	2	0	2	–	–	2	–	–	–	–	–	–	–	–	–		$ScM_{1.2}Ga_{1.8}$ (M = Co, Ni)
$W_2Cr_{21}C_6$	cF116	$Fm3m$	2	0	2	2	–	–	–	–	–	–	–	–	–	–	–	$Cr_{23}C_6$	$Sc_2Co_{21}B_6$; $Sc_{3-4}Ni_{21-19}B_6$
$Sc_6Ni_{18}Si_{11}$	oI140	$Immm$	2	0	2	–	–	–	–	–	1	1	–	–	–	–	–		$Sc_6Ni_{18}X_{11}$ (X = Si, Ge)
$Sc_{8.5}Mn_{1.2}Ga$	oI142	$Immm$	2	0	2	–	–	2	–	–	–	–	–	–	–	–	–		$Sc_{8.5}M_{1.2}Ga$ (M = Mn, Fe)
$Mg_{44}Rh_7$	cF408	$F\bar{4}3m$	2	2	0	–	–	–	–	–	–	–	–	–	–	–	–		
AuCu	tP4	$P4/mmm$	1	1	0	–	–	–	–	–	–	–	–	–	–	–	–		
γCuTi	tP4	$P4/nmm$	1	0	1	–	–	–	–	–	–	–	–	–	–	–	1		$ScHf_4Ir_5$
$ErCuS_2$	hP5	$P\bar{3}$	1	0	1	–	–	–	–	–	–	–	–	–	1	–	–		$Sc_{1-0.67}Cu_{1-2}Se_2$
Cu_2Sb	tP6	$P4/nmm$	1	1	0	–	–	–	–	–	–	–	–	–	–	–	–		
ScAuSi	hP6	$P\bar{6}m2$	1	0	1	–	–	–	–	–	1	–	–	–	–	–	–	$CaIn_2$	ScAuSi
$CeCo_3B_2$	hP6	$P6/mmm$	1	0	1	1	–	–	–	–	–	–	–	–	–	–	–	$CaCu_5$	$ScCo_3B_2$
YCo_6Ge_6	hP7	$P6/mmm$	1	0	1	–	–	–	–	–	–	–	1	–	–	–	–		$ScCo_6Sn_6$
$TbCu_7$	hP8	$P6/mmm$	1	0	1	–	–	1	–	–	–	–	–	–	–	–	–		$ScCo_{4.5}Ga_{4.1}$
$ScCrC_2$ (β)	hP8	$P6_3/mmc$	1	0	1	–	–	–	–	1	–	–	–	–	–	–	–		$ScCrC_2$ (β)
Sc_2BC_2	tI10	$I4/mmm$	1	0	1	–	–	–	–	–	–	–	–	–	–	1	–		Sc_2BC_2
$ErIr_3B_2$	mS12	$C2/m$	1	0	1	1	–	–	–	–	–	–	–	–	–	–	–	$CaCu_5$	$ScIr_3B_2$
Co_2Si	oP12	$Pnma$	1	1	0	–	–	–	–	–	–	–	–	–	–	–	–		

continued on next page

Table 36, *continued*

Structure type	Pearson's symbol	Space group	Number of compounds	Including		Including in ternary systems Sc–M–... Sc–...												Binary prototype	Composition of ternary compound(s)
				binary	ternary	B	Al	Ga	In	C	Si	Ge	Sn	5b-	6b-	X–X′	M–M′		
$ZrGa_2$	oS12	*Cmmm*	1	1	0	–	–	–	–	–	–	–	–	–	–	–	–		
Al_2Cu	tI12	*I4/mcm*	1	1	0	–	–	–	–	–	–	–	–	–	–	–	–		
$ScAl_3C_3$	hP14	*P6$_3$/mmc*	1	0	1	–	–	–	–	–	–	–	–	–	–	1	–		$ScAl_3C_3$
$Sc_{1.2}Fe_4Si_{9.8}$	hP15	*P6$_3$/mmc*	1	0	1	–	–	–	–	–	1	–	–	–	–	–	–		$Sc_{1.2}Fe_4Si_{9.8}$
DyAl	oP16	*Pbcm*	1	0	1	–	–	–	–	–	–	–	–	–	–	1	–		$ScGa_{0.4}Al_{0.6}$
Fe_3C	oP16	*Pnma*	1	1	0	–	–	–	–	–	–	–	–	–	–	–	–		
$LuRuB_2$	oP16	*Pnma*	1	0	1	1	–	–	–	–	–	–	–	–	–	–	–	FeB	$ScOsB_2$
$ScCrC_2$ (α)	oP16	*Pmmn*	1	0	1	–	–	–	–	1	–	–	–	–	–	–	–		$ScCrC_2$ (α)
$ScRhSi_2$	oP16	*Pnma*	1	0	1	–	–	–	–	–	1	–	–	–	–	–	–	YZn_3	$ScRhSi_2$
$ErAgSe_2$	oP16	*P2$_1$2$_1$2$_1$*	1	0	1	–	–	–	–	–	–	–	–	–	1	–	–		$ScAgSe_2$
$MgCuAl_2$	oS16	*Cmcm*	1	0	1	–	–	1	–	–	–	–	–	–	–	–	–	Re_3B	$ScNiGa_2$
MoB	tI16	*I4$_1$/amd*	1	0	1	–	–	1	–	–	–	–	–	–	–	–	–		$Sc_{0.2-0.9}Hf_{0.8-0.1}Ga$
$ZrAl_3$	tI16	*I4/mmm*	1	0	1	–	–	1	–	–	–	–	–	–	–	–	–		$Sc_{0.2}Hf_{0.8}Ga_3$
$ZrIr_3B_4$	hP16	*P6$_3$/m*	1	0	1	1	–	–	–	–	–	–	–	–	–	–	–		$ScIr_3B_4$
$CeCo_4B_4$	tP18	*P4$_2$/nmc*	1	0	1	1	–	–	–	–	–	–	–	–	–	–	–		$ScCo_4B_4$
Ti_5Ga_4	hP18	*P6$_3$/mcm*	1	1	0	–	–	–	–	–	–	–	–	–	–	–	–		
$HfFe_2Si_2$	oP20	*Pbcm*	1	0	1	–	–	–	–	–	1	–	–	–	–	–	–		$ScFe_2Si_2$
ScB_2C_2	oP20	*Pbam*	1	0	1	–	–	–	–	–	–	–	–	–	–	1	–		ScB_2C_2
$ScNiSi_3$	oS20	*Amm2*	1	0	1	–	–	–	–	–	1	–	–	–	–	–	–		$ScNiSi_3$
V_3As_2	tP20	*P4/m*	1	1	0	–	–	–	–	–	–	–	–	–	–	–	–		
Th_7Fe_3	hP20	*P6$_3$mc*	1	1	0	–	–	–	–	–	–	–	–	–	–	–	–		
Sc_2CrC_3	oP24	*Pbam*	1	0	1	–	–	–	–	1	–	–	–	–	–	–	–		Sc_2CrC_3
$ScNi_2Si_3$	tI24	*I4/mmm*	1	0	1	–	–	–	–	–	1	–	–	–	–	–	–		$ScNi_2Si_3$
$ScSn_2$	tI24	*I4$_1$/amd*	1	1	0	–	–	–	–	–	–	–	–	–	–	–	–		
Ti_7S_{12}	hR24	*R$\bar{3}$m*	1	1	0	–	–	–	–	–	–	–	–	–	–	–	–		
$ScFe_6Ga_6$	oI26	*Immm*	1	0	1	–	–	1	–	–	–	–	–	–	–	–	–	$ThMn_{12}$	$ScFe_6Ga_6$

continued on next page

Table 36, *continued*

Structure type	Pearson's symbol	Space group	Number of compounds	Including		Including in ternary systems Sc–M–... Sc–...												Binary prototype	Composition of ternary compound(s)
				binary	ternary	B	Al	Ga	In	C	Si	Ge	Sn	5b-	6b-	X–X′	M–M′		
$Eu_2Pt_7AlP_3$	tI26	*I4/mmm*	1	0	0	–	–	–	–	–	–	–	–	–	–	–	–		$ScCa_2Pt_7P_3$
Sc_3NiSi_3	mS28	*C2/m*	1	0	1	–	–	–	–	–	1	–	–	–	–	–	–		Sc_3NiSi_3
Fe_2CaO_4	oP28	*Pnma*	1	0	1	–	–	–	–	–	–	–	–	–	1	–	–		Sc_2EuSe_4
$Sc_5Re_2C_7$	oS28	*Cmmm*	1	0	1	–	–	–	–	1	–	–	–	–	–	–	–		$Sc_5Re_2C_7$
Th_3P_4	cI28	$I\bar{4}3d$	1	1	0	–	–	–	–	–	–	–	–	–	–	–	–		
Sc_3Co	oP32	*Pnma*	1	1	0	–	–	–	–	–	–	–	–	–	–	–	–		
Tm_3Ga_5	oP32	*Pnma*	1	1	0	–	–	–	–	–	–	–	–	–	–	–	–		
Pu_3Pd_5	oS32	*Cmcm*	1	1	0	–	–	–	–	–	–	–	–	–	–	–	–		
$ScCd_7$	oS32	*Cmcm*	1	1	0	–	–	–	–	–	–	–	–	–	–	–	–		
YB_2C	tP32	$P4_2/mbc$	1	0	1	–	–	–	–	–	–	–	–	–	–	1	–		ScB_2C
W_5Si_3	tI32	*I4/mcm*	1	0	1	–	–	–	–	–	1	–	–	–	–	–	–		$Sc_{0.4}Nb_{4.6}Si_3$
YCo_5P_3	oP36	*Pnma*	1	0	1	–	–	–	–	–	–	–	–	1	–	–	–		$ScCo_5P_3$
Y_2ReB_6	oP36	*Pbam*	1	0	1	1	–	–	–	–	–	–	–	–	–	–	–		Sc_2ReB_6
$Sc_3Ni_2Si_4$	oP36	*Pnma*	1	0	1	–	–	–	–	–	1	–	–	–	–	–	–		$Sc_3Ni_2Si_4$
Ce_2Ni_7	hP36	$P6_3/mmc$	1	1	0	–	–	–	–	–	–	–	–	–	–	–	–		
$Sc_5Co_{19}P_{12}$	hP36	$P\bar{6}2m$	1	0	1	–	–	–	–	–	–	–	–	1	–	–	–		$Sc_5Co_{19}P_{12}$
Mg_2Zn_{11}	cP39	$Pm\bar{3}$	1	0	1	–	–	1	–	–	–	–	–	–	–	–	–		$Sc_2Co_7Ga_4$
$U_2Co_3Si_5$	oI40	*Ibam*	1	0	1	–	–	–	–	–	1	–	–	–	–	–	–		$Sc_2Co_3Si_5$
$Sc_2Fe_3Si_5$	tP40	*P4/mnc*	1	0	1	–	–	–	–	–	1	–	–	–	–	–	–		$Sc_2Fe_3Si_5$
$Sc_9Ni_5Ge_8$	oI44	*Immm*	1	0	1	–	–	–	–	–	–	1	–	–	–	–	–		$Sc_9Ni_5Ge_8$
$ScNi_6Ge_6$	hP52	*P6/mmm*	1	0	1	–	–	–	–	–	–	1	–	–	–	–	–		$ScNi_6Ge_6$
UB_{12}	cF52	*Fm3m*	1	1	0	–	–	–	–	–	–	–	–	–	–	–	–		
$Sc_6Co_{30}Si_{19}$	hP55	$P6_3/m$	1	0	1	–	–	–	–	–	1	–	–	–	–	–	–		$Sc_6Co_{30}Si_{19}$
Th_2Zn_{17}	hR57	$R\bar{3}m$	1	0	1	–	–	1	–	–	–	–	–	–	–	–	–		$Sc_2Fe_{8.83}Ga_{8.17}$
$Gd_{14}Ag_{51}$	hP65	*P6/m*	1	0	1	–	–	1	–	–	–	–	–	–	–	–	–		$Sc_{14}Cu_{37}Ga_{14}$
Sc_3C_4	tP70	*P4/mnc*	1	1	0	–	–	–	–	–	–	–	–	–	–	–	–		

continued on next page

Table 36, *continued*

Structure type	Pearson's symbol	Space group	Number of compounds	Including		Including in ternary systems Sc–M–... Sc–...												Binary prototype	Composition of ternary compound(s)
				binary	ternary	B	Al	Ga	In	C	Si	Ge	Sn	5b-	6b-	X–X′	M–M′		
$Sc_3Re_2Si_4$	mS72	*C2/c*	1	0	1	–	–	–	–	–	1	–	–	–	–	–	–		$Sc_3Re_2Si_4$
$LuRu_4B_4$	tI72	$I4_1/acd$	1	0	1	1	–	–	–	–	–	–	–	–	–	–	–		$ScRu_4B_4$
$ScFe_6Ge_5$	hR72	$R\bar{3}m$	1	0	1	–	–	–	–	–	–	1	–	–	–	–	–		$ScFe_6Ge_5$
Se_2S_3	oF80	*Fddd*	1	1	0	–	–	–	–	–	–	–	–	–	–	–	–		
Gd_3Ga_2	tI80	*I4/mcm*	1	1	0	–	–	–	–	–	–	–	–	–	–	–	–		
Sc_7As_3	tI80	*I4/mcm*	1	1	0	–	–	–	–	–	–	–	–	–	–	–	–		
$Sc_{11}Al_2Ge_8$	tI84	*I4/mmm*	1	0	1	–	–	–	–	–	–	–	–	–	–	1	–	$Ho_{11}Ge_{10}$	$Sc_{11}Al_2Ge_8$
$Sc_4Ni_{29}B_{10}$	tI86	$I4_1/amd$	1	0	1	1	–	–	–	–	–	–	–	–	–	–	–		$Sc_4Ni_{29}B_{10}$
$ScFeSi_2$	oS96	*Cmca*	1	0	1	–	–	–	–	–	1	–	–	–	–	–	–		$ScFeSi_2$
$Sc_5Re_8Si_{12}$	oS100	*Amm2*	1	0	1	–	–	–	–	–	1	–	–	–	–	–	–		$Sc_5Re_8Si_{12}$
$NaZn_{13}$	cF112	$Fm\bar{3}c$	1	1	0	–	–	–	–	–	–	–	–	–	–	–	–		
$Sc_{29}Fe_6$	cP140	$Pm\bar{3}$	1	1	0	–	–	–	–	–	–	–	–	–	–	–	–		
$Gd_{13}Cd_{58}$	hP142	$P6_3/mmc$	1	1	0	–	–	–	–	–	–	–	–	–	–	–	–		
$Hf_2Ni_{6.5}Ga_{4.5}$	hP169	*P6/mmm*	1	0	1	–	–	1	–	–	–	–	–	–	–	–	–		$Sc_2Ni_{7.0-5.5}Ga_{4.0-5.5}$
$Se_{12.3}Ni_{40.7}Ge_{31}$	hP169	*P6/mmm*	1	0	1	–	–	–	–	–	–	1	–	–	–	–	–		$Sc_{12.3}Ni_{40.7}Ge_{31}$

References

Aldred, A.T., 1962, Trans. Met. Soc. AIME **224**, 1082.

Altynbaev, R.A., S.H. Hairidinov and A.V. Vahobov, 1987, Izv. Akad. Nauk SSSR, Met. (4), 193.

Altynbaev, R.A., S.H. Hairidinov and A.V. Vahobov, 1988, Izv. Akad. Nauk SSSR, Met. (1), 203.

Altynbaev, R.A., F.U. Obidov, A.V. Vahobov and S.H. Hairidinov, 1990, Izv. Akad. Nauk Tadzh. SSR, Otdel Fiz.-Mat., Khim. Geol. Nauk (1), 31.

Andrusyak, R.I., 1986, Vestn. Lvov Univ., Ser. Khim. (27), 24.

Andrusyak, R.I., 1988, Kristallografiya **33**, 1012 [Sov. Phys.-Crystallogr. **33**, 599].

Andrusyak, R.I., and B.Ya. Kotur, 1987, Kristallografiya **32**, 1018 [Sov. Phys.-Crystallogr. **32**, 598].

Andrusyak, R.I., and B.Ya. Kotur, 1989, Kristallografiya **34**, 740 [Sov. Phys.-Crystallogr. **34**, 440].

Andrusyak, R.I., and B.Ya. Kotur, 1991, Izv. Akad. Nauk SSSR, Met. (4), 198.

Andrusyak, R.I., B.Ya. Kotur and V.E. Zavodnik, 1989, Kristallografiya **34**, 996 [Sov. Phys.-Crystallogr. **34**, 600].

Arbuckle, J., and E. Parthé, 1962, Acta Crystallogr. **15**, 1205.

Arskaya, E.P., M.A. Tylkina and E.M. Savitskii, 1970, in: Renij v Novoj Tehnike, eds E.M. Savitskii and M.A. Tylkina (Nauka, Moscow) **2**, 50.

Artyukh, L.V., O.V. Gordijchuk and T.Ya. Velikanova, 1989, in: Pyataya Vsesoyuznaya Konf. po Kristalokhimii Intermetallicheskikh Soyedinenij, Lvov 17–19 October, Abstracts, p. 59.

Artyukh, L.V., T.Ya. Velikanova, S.M. Ilyenko and V.M. Petyukh, 1997, Poroshkovaya Metallurgiya (3/4), 18.

Auer-Welsbach, H., and H. Nowotny, 1961, Monatsh. Chem. **92**, 198.

Badaeva, T.A., and R.I. Kuznetsova, 1969, Izv. Akad. Nauk SSSR, Met. (5), 156 [Russ. Met. (5), 101].

Ballagny, A., R. Boucher and C. Carrard, 1970, Nucl. Met. **17**, 699.

Banakh, O.E., and B.Ya. Kotur, 1997, Sixth Sci. Conf. "Lvivs'ki Khimichni Chytannia-97", Lviv, 29–30 May, 1997, Abstracts, p. 23.

Banakh, O.E., and B.Ya. Kotur, 1998, J. Alloys & Compounds **268**, L3.

Bauer, E., E. Gratz, H. Kirchmayr, N. Pillmayr and H. Nowotny, 1985, J. Less-Common Met. **111**, 369.

Bauer, E., E. Gratz and H. Nowotny, 1986, Z Phys. B **64**, 151.

Bauer, J., 1982, J. Less-Common Met. **87**, 45.

Beaudry, B.J., and A.H. Daane, 1962, Trans. Met. Soc. AIME **224**, 770.

Beaudry, B.J., and A.H. Daane, 1963, Trans. Met. Soc. AIME **227**, 865.

Beaudry, B.J., and A.H. Daane, 1964, J. Less-Common Met. **6**, 322.

Beaudry, B.J., and A.H. Daane, 1969, J. Less-Common Met. **18**, 305.

Beaudry, B.J., M. Michel, A.H. Daane and F.H. Spedding, 1965, in: Proc. Fourth Conf. on Rare Earth Research, April 22–25, 1964, ed. L. Eyring (Gordon and Breach, New York) p. 247.

Becker, K.W., P. Fulde and J. Keller, 1977, Z. Phys. B **28**, 9.

Belyavina, N.M., 1983, Ph.D. Thesis (Kiev State University, Kiev).

Belyavina, N.M., and V.Ya. Markiv, 1980a, Dopov. Akad. Nauk Ukr. RSR, Ser. A (4), 87.

Belyavina, N.M., and V.Ya. Markiv, 1980b, Vestn. Kiev. Univ., Phys. (21), 15.

Belyavina, N.M., and V.Ya. Markiv, 1982a, Dokl. Akad. Nauk Ukr. RSR, Ser. B (12), 31.

Belyavina, N.M., and V.Ya. Markiv, 1982b, Dopov. Akad. Nauk Ukr. RSR, Ser. B (5), 39.

Belyavina, N.M., and V.Ya. Markiv, 1989, Dokl. Akad. Nauk Ukr. RSR, Ser. A (9), 78.

Belyavina, N.M., and V.Ya. Markiv, 1992, Dopov. Akad. Nauk Ukr. RSR (11), 126.

Belyavina, N.M., A.I. Skripka and V.Ya. Markiv, 1981, in: Fazovye Ravnovesiya v Metallicheskikh Splavakh, ed. M.E. Drits (Nauka, Moscow) p. 154.

Berezina, A.L., V.A. Volkov, B.P. Domashnikov, L.N. Trofimova and K.V. Chuistov, 1986, Metallofizika **8** (3), 116.

Berger, R., 1977, Acta Chem. Scand. A **31**, 514.

Berger, R., 1980a, Acta Chem. Scand. A **34**, 231.

Berger, R., 1980b, Acta Chem. Scand. A **34**, 463.

Berger, R., 1981, Acta Chem. Scand. A **35**, 635.

Berger, R., B.I. Noland and L.E. Tergenius, 1981, Acta Chem. Scand. A **35**, 679.

Bloch, D., and R. Lemaire, 1970, Phys. Rev. B **2**, 2648.

Block, H., T. Wolpl and W. Jeitschko, 1990, in: Fifteenth Congr. Int. Union Crystallogr. Coll., 19–28 July, Bordeaux, Abstracts, p. 290.

Bodak, O.I., and E.I. Gladyshevsky, 1985, Ternary Systems Containing Rare Earth Metals (Vyshcha Shkola Publ., Lvov). In Russian.

Bodak, O.I., and Z.M. Kokhan, 1983, Izv. Akad. Nauk SSSR, Neorg. Mater. **19**, 1094 [Inorg. Mater. **19**, 987].

Bodak, O.I., B.Ya. Kotur and E.I. Gladyshevsky, 1976, Dopov. Akad. Nauk Ukr. RSR, Ser. A (7), 655.

Bodak, O.I., B.Ya. Kotur, V.I. Yarovets and E.I. Gladyshevsky, 1977, Kristallografiya **22**, 385 [Sov. Phys.-Crystallogr. **22**, 217].

Bodak, O.I., B.Ya. Kotur, I.S. Gavrilenko, V.Ya. Markiv and V.G. Ivanchenko, 1978, Dopov. Akad. Nauk Ukr. RSR, Ser. A (4), 365.

Bodak, O.I., V.K. Pecharsky, Ya.M. Kalychak, O.I. Kharchenko, I.R. Mokra, L.A. Muratova, D.A. Bereziuk and M.M. Shevchuk, 1981, in: Fazovye Ravnovesiya v Metallicheskikh Splavakh, ed. M.E. Drits (Nauka, Moscow) p. 57.

Bodak, O.I., V.V. Pavlyuk, R.I. Andrusyak, B.Ya. Kotur, V.K. Pecharsky and V.A. Bruskov, 1990, Kristallografiya **35**, 312 [Sov. Phys.-Crystallogr. **35**, 173].

Bodak, O.I., J. Stępień-Damm, H. Drulis, B.Ya. Kotur, W. Suski, F.G. Vagizov, K. Wochowski and T. Mydlarz, 1995, Physica B **210**, 183.

Bodak, O.I., Z.M. Shpyrka and I.R. Mokra, 1997, J. Alloys & Compounds **247**, 217.

Braslavskaya, G.S., and S.B. Maslenkov, 1987, Izv. Akad. Nauk SSSR, Met. (1), 112 [Russ. Met. (1), 107].

Braun, H.F., 1980, Phys. Lett. **75A**, 386.

Braun, H.F., 1981, in: Ternary Superconductors, eds G.K. Shenoy, B.D. Dunlop and F.Y. Fradin (North-Holland, Amsterdam) p. 226.

Braun, H.F., and C.U. Segre, 1980, Solid State Commun. **35**, 735.

Braun, H.F., G. Burri and L. Rinderer, 1979, J. Less-Common Met. **68**, 1.

Braun, H.F., K. Yvon and R.M. Braun, 1980, Acta Crystallogr. B **36**, 2397.

Braun, H.F., C.U. Segre, F. Acker, H. Rosenberg, S. Dey and P. Deppe, 1981, J. Magn. Magn. Mater. **25**, 117.

Brewer, L., and R.H. Lamoreaux, 1980, Atomic Energy Rev. Special Issue (7), 317.

Brixner, L.H., 1960, J. Inorg. Nucl. Chem. **15**, 199.

Bronger, W., 1967, J. Less-Common Met. **12**, 63.

Brozek, V., J. Flahaut, M. Guittard, M. Julien-Pouzol and M.-P. Pardo, 1974, Bull. Soc. Chim. Fr. (9/10), 1740.

Bruskov, V.A., L.V. Zavalii and Yu.B. Kuz'ma, 1988, Izv. Akad. Nauk SSSR, Neorg. Mater. **24**, 506 [Inorg. Mater. **24**, 420].

Buchholz, W., and H.-U. Schuster, 1981, Z. Anorg. Allg. Chem. **482**, 40.

Burnashova, V.V., A.V. Ivanov, V.A. Yartys' and K.N. Semenenko, 1981, Izv. Akad. Nauk SSSR, Neorg. Mater. 17, 980 [Inorg. Mater. **17**, 704].

Burzo, E., E. Gratz and V. Pop, 1993, J. Magn. Magn. Mater. **123**, 159.

Callmer, B., 1978, J. Solid State Chem. **23**, 391.

Cashion, J.D., G.K. Shenoy, D. Niarchos, P.J. Viccaro and C.M. Falco, 1980, Phys. Lett. **79A**, 454.

Cashion, J.D., G.K. Shenoy, D. Niarchos, P.J. Viccaro, A.T. Aldred and C.M. Falco, 1981, J. Appl. Phys. **52**, 2180.

Cava, R.J., H. Takagi, B. Batlogg, H.W. Zandbergen, J.J. Krajewski, W.F. Peck Jr, R.B. van Dover, R.J. Felder, T. Siegrist, K. Mizuhashi, H. Eisaki, S.A. Carter and U. Uchida, 1994, Nature **367**, 146.

Cavin, O.B., R.M. Steele, L.A. Harris and H.L. Yakel, 1967, Oak Ridge National Laboratory Report ORNL-4170 (November) (Oak Ridge, TN).

Cenzual, K., B. Chabot and E. Parthé, 1985, Acta Crystallogr. C **41**, 313.

Chabot, B., and E. Parthé, 1978, Acta Crystallogr. B **34**, 3173.

Chabot, B., and E. Parthé, 1979, Acta Crystallogr. B **35**, 1745.

Chabot, B., and E. Parthé, 1985, Acta Crystallogr. B **41**, 213.

Chabot, B., and E. Parthé, 1987, Acta Crystallogr. C **43**, 1665.

Chabot, B., K. Cenzual and E. Parthé, 1980a, Acta Crystallogr. B **36**, 7.

Chabot, B., K. Cenzual and E. Parthé, 1980b, Acta Crystallogr. B **36**, 2202.

Chabot, B., H.F. Braun, K. Yvon and E. Parthé, 1981a, Acta Crystallogr. B **37**, 668.

Chabot, B., N. Engel and E. Parthé, 1981b, Acta Crystallogr. B **37**, 671.

Chabot, B., N. Engel and E. Parthé, 1984, J. Less-Common Met. **96**, 331.

Cheldieva, G.M., E.M. Sokolovskaya and E.F. Kazakova, 1989, in: Piataya Vsesoyuznaya Konf. po kristallokhimii Intermetallich. Soyedinenij, Lvov, 17–19 Oct. 1989, Abstracts, p. 121.

Chen, S.K., and J.G. Duh, 1988, J. Appl. Phys. **64**, 5546.

Colinet, C., and A. Pasturel, 1994, in: Handbook on the Physics and Chemistry of Rare Earths, Vol. 19, eds K.A. Gschneidner Jr, L. Eyring, G.H. Lander and G.R. Choppin (Elsevier, Amsterdam) p. 479.

Compton, V.B., and B.T. Matthias, 1959, Acta Crystallogr. **12**, 651.

Compton, V.B., and B.T. Matthias, 1962, Acta Crystallogr. **15**, 94.

Cooper, A.S., 1980, Mater. Res. Bull. **15**, 799.

Coqblin, B., J.R. Iglesias-Sicardi and R. Jullien, 1978, Contemp. Phys. **19**, 327.

Darby Jr, J.B., D.J. Lam, L.J. Norton and J.W. Downey, 1962, J. Less-Common Met. **4**, 558.

de Boer, F.R., W.H. Dijkman, W.C.M. Mattens and A.R. Miedema, 1979, J. Less-Common Met. **64**, 241.

Dennison, D.H., M.J. Tschetter and K.A. Gschneidner Jr, 1966a, J. Less-Common Met. **10**, 108.

Dennison, D.H., M.J. Tschetter and K.A. Gschneidner Jr, 1966b, J. Less-Common Met. **11**, 423.

Derkach, V.A., and B.Ya. Kotur, 1994, Izv. RAN, Neorg. Mater. **30**, 1001.

Derkach, V.A., and B.Ya. Kotur, 1996, Visn. Lviv Univ., Ser. Khim. (36), 44.

Dhar, S.K., K. Ghosh and S. Ramakrishnan, 1996, Physica B **223&224**, 215.

Dismukes, J.P., and J.G. White, 1965, Inorg. Chem. **4**, 970.

Drits, M.E., Z.S. Sviderskaya and N.I. Nikitina, 1971, Izv. Akad. Nauk SSSR, Met. (6), 194 [Russ. Met. (6), 138].

Drits, M.E., E.S. Kadaner, T.V. Dobatkina and N.I. Turkina, 1973, Izv. Akad. Nauk SSSR, Met. (4), 213 [Russ. Met. (4), 152].

Drits, M.E., Z.S. Sviderskaya, L.L. Rokhlin and N.I. Nikitina, 1977, in: Tehnologiya Legkikh Splavov. Nauchno-Tehnich. Bull. VILSa (6), 73.

Drits, M.E., L.S. Toropova and F.L. Gushchina, 1984, Izv. Akad. Nauk SSSR, Met. (4), 221.

Dwight, A.E., 1961a, Trans. ASM **53**, 479.

Dwight, A.E., 1961b, U.S. Atomic Energy Comm. Report ANL-6516, p. 257.

Dwight, A.E., 1968, in: Proc. 7th Rare Earth Research Conf., 28–30 October, Coronado, CA, p. 273.

Dwight, A.E., 1974, in: Proc. 11th Rare Earth Research Conf., 7–10 October, Traverse City, MI, Vol. 2, p. 642.

Dwight, A.E., 1975, J. Less-Common Met. **43**, 117.

Dwight, A.E., 1976, in: Proc. 12th Rare Earth Research Conf., Coronado, CA, Vol. 1, p. 480.

Dwight, A.E., 1977, Acta Crystallogr. B **33**, 1579.

Dwight, A.E., and C.W. Kimball, 1987, J. Less-Common Met. **127**, 179.

Dwight, A.E., J.W. Downey and R.A. Conner Jr, 1961, Acta Crystallogr. **14**, 75.

Dwight, A.E., R.A. Conner Jr and J.W. Downey, 1963a, Nature **197**, 587.

Dwight, A.E., J.B. Darby Jr, D.J. Lam and M.V. Nevitt, 1963b, U.S. Atomic Energy Comm. Report ANL-6868, p. 303.

Dwight, A.E., R.A. Conner Jr and J.W. Downey, 1965, Acta Crystallogr. **18**, 835.

Dwight, A.E., J.W. Downey and R.A. Conner Jr, 1966, Trans. Met. Soc. AIME **236**, 1509.

Dwight, A.E., J.W. Downey and R.A. Conner Jr, 1967, Acta Crystallogr. **22**, 745.

Dwight, A.E., W.C. Harper and C.W. Kimball, 1973, J. Less-Common Met. **30**, 1.

Dwight, A.E., C.W. Kimball, R.S. Preston, S.P. Taneja and L. Weber, 1975, J. Less-Common Met. **40**, 285.

Dzuraev, T.D., and R.A. Altynbaev, 1986, Dokl. Akad. Nauk Tadzh. SSR **29**, 472.

Eberz, U., W. Seelentag and H.-U. Schuster, 1980, Z. Naturforsch. **35B**, 1341.

Ellinger, F.H., W.N. Miner, D.R. O'Boyle and F.W. Shonfeld, 1968, U.S. Atomic Energy Commission Report LA-3870, p. 98.

Ellinger, F.H., K.A. Johnson and C.C. Land, 1972, U.S. Atomic Energy Commission Report LA-5055.

Engel, N., B. Chabot and E. Parthé, 1984, J. Less-Common Met. **96**, 291.

Erdmann, B., and C. Keller, 1973, J. Solid State Chem. **7**, 40.

Eremenko, V.N., I.M. Obushenko, Yu.I. Buyanov and K.A. Meleshevich, 1981, Dopov. Akad. Nauk Ukr. RSR, Ser. A (4), 80.

Eremenko, V.N., K.A. Meleshevich, Yu.I. Buyanov and P.S. Martsenyuk, 1988, Poroshk. Metallurg. (12), 52 [Sov. Powder Metall. Met. Ceram. **27** (12), 967].

Eremenko, V.N., T.Ya. Velikanova, A.M. Khar'kova and A.A. Bondar, 1989a, Poroshk. Metallurg. (10), 62.

Eremenko, V.N., T.Ya. Velikanova and A.A. Bondar, 1989b, Poroshk. Metallurg. (1), 46.

Eremenko, V.N., M.V. Bulanova and P.S. Martsenyuk, 1990, in: Fazovye Ravnovesiya, Struktura I Svojstva Splavov, ed. V.N. Eremenko (Naukova Dumka, Kiev) p. 70.

Eremenko, V.N., V.G. Khorujaya and P.S. Martsenyuk, 1994, J. Alloys & Compounds **204**, 83.

Eremenko, V.N., V.G. Khorujaya, K.Ye. Korniyenko and T.Ya. Velikanova, 1996, Poroshk. Metallurg. (7/8), 141.

Espinosa, G.P., A.S. Cooper and H. Barz, 1982, Mater. Res. Bull. **17**(8), 963.

Eymond, S., and E. Parthé, 1969, J. Less-Common Met. **19**, 441.

Fornasini, M.L., A. Iandelli and M. Pani, 1992, J. Alloys & Compounds **187**, 243.

Fournier, J.M., and E. Gratz, 1993, in: Handbook on the Physics and Chemistry of Rare Earths, Vol. 17, eds K.A. Gschneidner Jr, L. Eyring, G.H. Lander and G.R. Choppin (Elsevier, Amsterdam) ch. 115.

Franse, J.J.M., and R.J. Radwanski, 1993, in: Handbook of Magnetic Materials, Vol. 7, ed. K.H.J. Buschow (North-Holland, Amsterdam) p. 307..

Freeman, A.J., and J.P. Desclaux, 1979, J. Magn. Magn. Mater. **52**, 11.

Frick, B., and M. Loewenhaupt, 1985, Physica **130B**, 372.

Gajewski, D.A., P. Allenspach, C.L. Seaman and M.B. Maple, 1994, Physica B **199&200**, 419.

Gangleberger, E., H. Nowotny and F. Benesovsky, 1966, Monatsh. Chem. **97**, 101.

Gardner, W.E., T.F. Smith, B.W. Howlett, C.W. Chu and A. Sweedler, 1968, Phys. Rev. **166**, 577.

Gavrilenko, I.S., 1982, Ph.D. Thesis (Kiev State University, Kiev).

Gavrilenko, I.S., and V.Ya. Markiv, 1978a, Vestn. Kiev. Univ., Ser. Phys. (19), 18.

Gavrilenko, I.S., and V.Ya. Markiv, 1978b, Dokl. Akad. Nauk Ukr. RSR, Ser. A (3), 272.

Gavrilenko, I.S., and V.Ya. Markiv, 1979, Metallofizika (75), 103.

Geballe, T.H., B.T. Matthias, V.B. Compton, E. Corenzwit, G.W. Hull Jr and L.D. Longinotti, 1965, Phys. Rev. **137**, A119.

Ghetta, V.P., P. Chaudouet, B. Lambert-Andron, M.-N. Deschizeaux-Cherny, R. Madar and J.-P. Senateur, 1986, C.R. Acad. Sci. Paris, Ser. II **303**, 357.

Gladyshevsky, E.I., 1971, Kristallokhimiya Silicidov i Germanidov (Metallurgiya, Moscow).

Gladyshevsky, E.I., and O.I. Bodak, 1982, Kristallokhimiya Intermetallicheskikh Soyedinenij Redkozemelnykh Metallov (Vyshcha Shkola, Lvov).

Gladyshevsky, E.I., and E.I. Emes-Misenko, 1963, Zh. Strukt. Khim. **4**, 861 [Russ. J. Struct. Chem. **4**, 793].

Gladyshevsky, E.I., and B.Ya. Kotur, 1978, Kristallografiya **23**, 946 [Sov. Phys.-Crystallogr. **23**, 533].

Gladyshevsky, E.I., V.Ya. Markiv and Yu.B. Kuz'ma, 1962, Dopov. Akad. Nauk Ukr. RSR, Ser. A (5), 481.

Gladyshevsky, E.I., P.I. Kripyakevich, Yu.B. Kuz'ma and V.S. Protasov, 1964, in: Voprosy Teorii i Primeneniya Redkozemelnykh Metallov, eds E.M. Savitskii and V.F. Terekhova (Nauka, Moscow) p. 153.

Gladyshevsky, E.I., B.Ya. Kotur, O.I. Bodak and V.P. Skvorchuk, 1977, Dopov. Akad. Nauk Ukr. RSR, Ser. A (8), 751.

Gladyshevsky, E.I., O.I. Bodak and V.K. Pecharsky, 1990, In: Handbook on the Physics and Chemistry of Rare Earths, Vol. 13, eds K.A. Gschneidner Jr and L. Eyring (Elsevier, Amsterdam) ch. 88, pp. 1–190.

Gladyshevsky, E.I., Z.M. Shpyrka and M.B. Konyk, 1992, in: VI Soveshchaniye po Kristallokhimii Neorganicheskikh I Koordinatsionnykh Soyedinenij, Lvov, 21–25 September 1992, Abstracts, p. 170.

Goebel, S., and S. Rosen, 1968, J. Less-Common Met. **16**, 441.

Gordijchuk, O.V., 1987, Ph.D. Thesis (Kiev Institute of Problems of Materials Science, Kiev).

Gordijchuk, O.V., T.Ya. Velikanova and V.N. Eremenko, 1981, in: Diagrammy Sostoyaniya Karbid – I Nitridsoderzhashchikh Sistem (Naukova Dumka, Kiev) p. 104.

Goto, T., T. Sakakibara, K. Murata, H. Komatsu and F. Fukamichi, 1990, J. Magn. Magn. Mater. **90–91**, 700.

Gratz, E., 1997, Physica B **237–238**, 470.

Gratz, E., and H. Nowotny, 1985, Physica B **30**, 75.

Gratz, E., E. Bauer, H. Nowotny, A.T. Burkov and M.V. Vedernikov, 1989, Solid State Commun. **69**, 1007.

Gratz, E., R. Resel, A.T. Burkov, E. Bauer, A.S. Markosyan and A. Galatanu, 1995, J. Phys.: Condens. Matter **7**, 6687.

Gratz, E., D. Gurjazkas, H. Müller, A. Kottar, I.S. Dubenko, S.A. Granovsky and A.S. Markosyan, 1997, Physica B **237–238**, 474.

Grin', Yu.N., I.S. Gavrilenko, V.Ya. Markiv and Ya.P. Yarmolyuk, 1980, Dokl. Akad. Nauk Ukr. RSR, Ser. A (8), 75.

Grössinger, R., R. Haferl, G. Hilscher, G. Wiesinger, K.H.J. Buschow and P.H. Smit, 1980, in: Physics of Transition Metals, Int. Phys. Conf. Ser. **5**(ch. 4), 295.

Grund, I., 1985, Diss. Dokt. Naturwiss. (Univ. Köln).

Gschneidner Jr, K.A., 1961, Rare-Earth Alloys (van Nostrand, Princeton, NJ).

Gschneidner Jr, K.A., 1975, in: Scandium. Its Occurrence, Chemistry, Physics, Metallurgy, Biology and Technology, ed. C.T. Horovitz (Academic Press, London) pp. 152–322.

Gschneidner Jr, K.A., and F.W. Calderwood, 1982a, Bull. Alloy Phase Diagrams **3**, 93.
Gschneidner Jr, K.A., and F.W. Calderwood, 1982b, Bull. Alloy Phase Diagrams **3**, 189.
Gschneidner Jr, K.A., and F.W. Calderwood, 1982c, Bull. Alloy Phase Diagrams **3**, 356.
Gschneidner Jr, K.A., and F.W. Calderwood, 1983a, Bull. Alloy Phase Diagrams **4**, 75.
Gschneidner Jr, K.A., and F.W. Calderwood, 1983b, Bull. Alloy Phase Diagrams **4**, 79.
Gschneidner Jr, K.A., and F.W. Calderwood, 1983c, Bull. Alloy Phase Diagrams **4**, 163.
Gschneidner Jr, K.A., and F.W. Calderwood, 1983d, Bull. Alloy Phase Diagrams **4**, 170.
Gschneidner Jr, K.A., and F.W. Calderwood, 1983e, Bull. Alloy Phase Diagrams **4**, 171.
Gschneidner Jr, K.A., and F.W. Calderwood, 1986a, in: Handbook on the Physics and Chemistry of Rare Earths, Vol. 8, eds K.A. Gschneidner Jr and L. Eyring (North-Holland, Amsterdam) pp. 1–161.
Gschneidner Jr, K.A., and F.W. Calderwood, 1986b, Bull. Alloy Phase Diagrams 7, 348.
Gschneidner Jr, K.A., and F.W. Calderwood, 1986c, Bull. Alloy Phase Diagrams 7, 559.
Gschneidner Jr, K.A., and F.W. Calderwood, 1987, in: Phase Diagrams of Binary Beryllium Alloys, p. 184. [Also in: Massalski et al. (1990).]
Gschneidner Jr, K.A., and F.W. Calderwood, 1989a, Bull. Alloy Phase Diagrams **10**, 34.
Gschneidner Jr, K.A., and F.W. Calderwood, 1989b, Bull. Alloy Phase Diagrams **10**, 450.
Gschneidner Jr, K.A., O.D. McMasters, D.G. Alexander and R.F. Venteicher, 1970, Metall. Trans. **1**, 961.
Guittard, M., O. Souleau and H. Farsam, 1964, C.R. Acad. Sci. **259**, 2847.
Halet, J.F., J.Y. Saillard and J. Bauer, 1990, J. Less-Common Met. **158**, 239.
Hanel, G., and H. Nowotny, 1970, Monatsh. Chem. **101**, 463.
Hauser, R., E. Bauer, E. Gratz, Th. Häufler, G. Hilscher and G. Wiesinger, 1994, Phys. Rev. B **50**, 18, 13493.
Hellawell, A., 1962, J. Less-Common Met. **4**, 101.
Hines, W.A., and I.R. Harris, 1971, J. Phys. F **1**, 93.
Hodeau, J.L., and M. Marezio, 1984, Acta Crystallogr. B **40**, 26.
Holleck, H., 1977, J. Less-Common Met. **52**, 167.
Hovestreydt, E., N. Engel, K. Klepp, B. Chabot and E. Parthé, 1982, J. Less-Common Met. **85**, 247.
Hulliger, F., and G.W. Hull Jr, 1970, Solid State Commun. **8**, 1379.
Hulliger, F., and O. Vogt, 1966, Phys. Lett. **21**, 138.
Hungsberg, R.E., and K.A. Gschneidner Jr, 1972, J. Phys. Chem. Solids **33**, 401.
Iandelli, A., 1985, J. Less-Common Met. **113**, L25.
Iandelli, A., and G.L. Olcese, 1985, J. Less-Common Met. **111**, 145.
Ikeda, K., and K.A. Gschneidner Jr, 1981, J. Magn. Magn. Mater. **22**, 207.
Ikeda, K., K.A. Gschneidner Jr, N. Kobayashi and K. Noto, 1984, J. Magn. Magn. Mater. **42**, 1.
Ikeda, K., S.K. Dhar, M. Yoshizawa and K.A. Gschneidner Jr, 1991, J. Magn. Magn. Mater. **100**, 292.
Ilyenko, S.M., T.Ya. Velikanova, V.M. Danilenko and L.V. Artyukh, 1996, in: Fifth Int. School "Phase Diagrams in Materials Science", Katsyveli, Crimea, Ukraine, September 23–29, Abstracts, p. 54.
Ishida, S., and S. Asano, 1985, J. Phys. Soc. Japan **54**, 4688.
Ito, T., K. Mizuno, K. Ito and B.J. Beaudry, 1988, J. Phys. Colloq. C8 **49** (N12, Suppl.), C8-343.
Jansen, K., and G. Sperlich, 1975, Solid State Commun. **17**, 1179.
Jedlichka, H., H. Nowotny and F. Benesovsky, 1971, Monatsh. Chem. **102**, 389.
Jeitschko, W., and E. Parthé, 1965, Acta Crystallogr. **19**, 275.
Jeitschko, W., and E.J. Reinbold, 1985, Z. Naturforsch. **40B**, 900.
Jeitschko, W., L.J. Terbuchte, E.J. Reinbold, P.G. Pollmeier and T. Vomhof, 1990, J. Less-Common Met. **161**, 125.
Jeitschko, W., P.G. Pollmeier and U. Meisen, 1993, J. Alloys & Compounds **196**, 105.
Johnson, M.J., and R.N. Shelton, 1984, Solid State Commun. **52**, 839.
Johnston, D.C., 1977, Solid State Commun. **24**, 699.
Julien-Pouzol, M., and M. Guittard, 1969, C.R. Acad. Sci. **269C**, 316.
Julien-Pouzol, M., M. Guittard and J. Flahaut, 1968, Bull. Soc. Chim. France (2), 533.
Kadowaki, K., and S.B. Woods, 1986, Solid State Commun. **58**, 507.
Karatygina, E.P., V.V. Burnashova, M.V. Raevskaya and E.M. Sokolovskaya, 1974a, Metallofizika (52), 105.
Karatygina, E.P., V.V. Burnashova, M.V. Raevskaya and E.M. Sokolovskaya, 1974b, Paper deponated in VINITI. N 3021-74-Dep.

Kharakterova, M.L., 1991, Izv. Akad. Nauk SSSR, Met. (4), 191.

Khorujaya, V.G., and K.Ye. Korniyenko, 1996, J. Alloys & Compounds **243**, 156.

Khorujaya, V.G., and K.Ye. Korniyenko, 1997, Poroshk. Metall. (1/2), 31.

Khorujaya, V.G., K.Ye. Korniyenko and P.S. Martsenyuk, 1995, J. Alloys & Compounds **229**, 283.

Komissarova, L.N., A.A. Men'kov and L.M. Vasil'eva, 1965, Izv. Akad. Nauk SSSR, Neorg. Mater. **1**, 1493 [Inorg. Mater. **1**, 1361].

Kondrashov, A.I., 1978, in: Poluchenie I Issledovanie Svojstv Novykh Materialov (Naukova Dumka, Kiev) p. 48.

Koshel', O.S., R.I. Rebko and Ya.O. Golubets, 1984, Vestn. Lvov Univ., Ser. Khim. (25), 24.

Kotroczo, V., and I.J. McColm, 1987, J. Less-Common Met. **132**, 1.

Kotroczo, V., and I.J. McColm, 1994, J. Alloys & Compounds **203**, 259.

Kotur, B.Ya., 1977a, Ph.D. Thesis (I. Franko Lviv State University, Lviv).

Kotur, B.Ya., 1977b, Dokl. Akad. Nauk Ukr. RSR, Ser. A (2), 165.

Kotur, B.Ya., 1983, unpublished data.

Kotur, B.Ya., 1984, Vestn. Lvov Univ., Ser. Khim. (25), 20.

Kotur, B.Ya., 1986, Dopov. Akad. Nauk Ukr. RSR, Ser. A (1), 79.

Kotur, B.Ya., 1987, Izv. Akad. Nauk SSSR, Neorg. Mater. **23**, 558 [Inorg. Mater. **23**, 493].

Kotur, B.Ya., 1989, unpublished data.

Kotur, B.Ya., 1991, Izv. Akad. Nauk SSSR, Met. (3), 213.

Kotur, B.Ya., 1995, D.Sc. Thesis (I. Franko Lviv State University, Lviv).

Kotur, B.Ya., and R.I. Andrusyak, 1984a, Dokl. Akad. Nauk Ukr. RSR, Ser. B (12), 41.

Kotur, B.Ya., and R.I. Andrusyak, 1984b, Vestn. Lvov Univ., Ser. Khim. (25), 35.

Kotur, B.Ya., and R.I. Andrusyak, 1991, Izv. Akad. Nauk SSSR, Neorg. Mater. **27**, 1433.

Kotur, B.Ya., and O.I. Bodak, 1977, Kristallografiya **22**, 1209 [Sov. Phys.-Crystallogr. **22**, 687].

Kotur, B.Ya., and O.I. Bodak, 1980, Izv. Akad. Nauk SSSR, Neorg. Mater. **16**, 459.

Kotur, B.Ya., and O.I. Bodak, 1981, Izv. Akad. Nauk SSSR, Neorg. Mater. **17**, 265.

Kotur, B.Ya., and O.I. Bodak, 1987, Ukr. Khim. Zh. **53**, 151 [Sov. Progr. Chem. **53**, 43].

Kotur, B.Ya., and O.I. Bodak, 1988, Izv. Akad. Nauk SSSR, Met. (4), 189 [Russ. Metall. (4), 193].

Kotur, B.Ya., and O.I. Bodak, 1990, Izv. Akad. Nauk SSSR, Met. (6), 200.

Kotur, B.Ya., and L.A. Boichuk, 1988, Vestn. Lvov Univ., Ser. Khim. (29), 51.

Kotur, B.Ya., and M. Bruvo, 1991, Kristallografiya **36**, 1391 [Sov. Phys.-Crystallogr. **36**, 787].

Kotur, B.Ya., and V.O. Derkach, 1994, Visn. Lviv Univ., Ser. Khim. (33), 38.

Kotur, B.Ya., and E.I. Gladyshevsky, 1983, Kristallografiya **28**, 461 [Sov. Phys.-Crystallogr. **28**, 271].

Kotur, B.Ya., and I.P. Klyuchka, 1989, Izv. Akad. Nauk SSSR, Neorg. Mater. **25**, 597 [Inorg. Mater. **25**, 518].

Kotur, B.Ya., and I.R. Mokra, 1994, Izv. RAN, Neorg. Mater. **30**, 783.

Kotur, B.Ya., and I.R. Mokra, 1995, unpublished data.

Kotur, B.Ya., and O.V. Parasiuk, 1994, Izv. RAN, Metal. (6), 157.

Kotur, B.Ya., and G.M. Ratush, 1991, Izv. Akad. Nauk SSSR, Neorg. Mater. **27**, 513.

Kotur, B.Ya., and M. Sikirica, 1982a, J. Less-Common Met. **83**, L29.

Kotur, B.Ya., and M. Sikirica, 1982b, Acta Crystallogr. B **38**, 917.

Kotur, B.Ya., and M. Sikirica, 1983, Kristallografiya **28**, 798 [Sov. Phys.-Crystallogr. **28**, 472].

Kotur, B.Ya., and M. Sikirica, 1991, Kristallografiya **36**, 1179 [Sov. Phys.-Crystallogr. **36**, 666].

Kotur, B.Ya., O.I. Bodak and E.I. Gladyshevsky, 1977a, Dopov. Akad. Nauk Ukr. RSR, Ser. A (7), 664.

Kotur, B.Ya., O.I. Bodak and O.Ya. Kotur, 1977b, in: IX Ukrain. Respublik. Nauchn. Konfer. po Neorgan. Khimii, Lvov 28–30 September 1977, Abstracts, p. 191.

Kotur, B.Ya., O.I. Bodak, M.G. Mys'kiv and E.I. Gladyshevsky, 1977c, Kristallografiya **22**, 267 [Sov. Phys.-Crystallogr. **22**, 151].

Kotur, B.Ya., O.I. Bodak and E.I. Gladyshevsky, 1978, Kristallografiya **23**, 189 [Sov. Phys.-Crystallogr. **23**, 101].

Kotur, B.Ya., O.I. Bodak and O.Ya. Kotur, 1980, Dokl. Akad. Nauk Ukr. RSR, Ser. A (8), 82.

Kotur, B.Ya., E.I. Gladyshevsky and M. Sikirica, 1981, J. Less-Common Met. **81**, 71.

Kotur, B.Ya., O.I. Bodak, M. Sikirica and M. Bruvo, 1983a, Dokl. Akad. Nauk Ukr. RSR, Ser. B (10), 47.

Kotur, B.Ya., M. Sikirica, O.I. Bodak and E.I. Gladyshevsky, 1983b, Kristallografiya **28**, 658 [Sov. Phys.-Crystallogr. **28**, 387].

Kotur, B.Ya., O.I. Bodak and V.E. Zavodnik, 1985a, Kristallografiya **30**, 899 [Sov. Phys.-Crystallogr. **30**, 521].

Kotur, B.Ya., N.Z. Litvinko and O.I. Bodak, 1985b, Dopov. Akad. Nauk Ukr. RSR, Ser. B (1), 34.

Kotur, B.Ya., O.I. Bodak, R.I. Andrusyak, V.E. Zavodnik and V.K. Belsky, 1986a, Dokl. Akad. Nauk Ukr. RSR, Ser. B (11), 29.

Kotur, B.Ya., O.I. Bodak and V.E. Zavodnik, 1986b, Kristallografiya **31**, 793 [Sov. Phys.-Crystallogr. **31**, 469].

Kotur, B.Ya., O.I. Bodak and V.E. Zavodnik, 1986c, Kristallografiya **31**, 868 [Sov. Phys.-Crystallogr. **31**, 513].

Kotur, B.Ya., E.I. Gladyshevsky and M. Sikirica, 1986d, Kristallografiya **31**, 796 [Sov. Phys.-Crystallogr. **31**, 470].

Kotur, B.Ya., R.I. Andrusyak and V.E. Zavodnik, 1988a, Kristallografiya **33**, 240 [Sov. Phys.-Crystallogr. **33**, 141].

Kotur, B.Ya., A.B. Kravs and R.I. Andrusyak, 1988b, Izv. Akad. Nauk SSSR, Met. (6), 198.

Kotur, B.Ya., O.M. Vozniak and O.I. Bodak, 1989a, Izv. Akad. Nauk SSSR, Neorg. Mater. **25**, 399 [Inorg. Mater. **25**, 345].

Kotur, B.Ya., V.V. Kinzhibalo, A.T. Tyvanchuk and A.N. Kamardinkin, 1989b, in: V Vsesoyuznoye Soveshchaniye "Diagrammy Sostoyaniya Metallicheskikh Sistem", Abstracts (Nauka, Moscow) p. 117.

Kotur, B.Ya., L.O. Dobrianskaya and I.D. Shcherba, 1989c, in: Pyataya Vsesoyuz. Konfer. po Kristallokhimii Intermetallich. Soyedinenij, Lvov, 17–19 October 1989, Abstracts, p. 161.

Kotur, B.Ya., R.I. Andrusyak and V.E. Zavodnik, 1989d, Kristallografiya **34**, 1298 [Sov. Phys.-Crystallogr. **34**, 783].

Kotur, B.Ya., I.R. Mokra and A.Ya. Toporinskii, 1991, Izv. Akad. Nauk SSSR, Met. (5), 204.

Kotur, B.Ya., O.E. Semenyshyn and M. Sikirica, 1992, in: IV Soveshchaniye po Kristallokhimii Neorganicheskikh I Koordinatsionnykh Soyedinenij, Lvov, 21–25 September 1992, Abstracts, p. 191.

Kotur, B.Ya., V.O. Derkach, I.S. Dutsyak and A.Z. Pavlyshyn, 1996a, J. Alloys & Compounds **238**, 81.

Kotur, B.Ya., R. Cerny, I.R. Mokra and K. Yvon, 1996b, J. Alloys & Compounds **245**, L21.

Kotur, B.Ya., O.E. Banakh, R. Cerny and J.V. Pacheco Espejel, 1997a, J. Alloys & Compounds **260**, 157.

Kotur, B.Ya., R. Cerny, J.V. Pacheco Espejel and K. Yvon, 1997b, Z. Kristallogr. **212**, 289.

Kotur, B.Ya., E. Gratz, E. Bauer, G. Hilscher, A. Kottar, H. Michor, Ch. Reichl, G. Wiesinger and A.S. Markosyan, 1998, J. Alloys & Compounds **278**, 49.

Kresse, G., and J. Furthmueller, 1996a, Comput. Mat. Sci. **6**, 15.

Kresse, G., and J. Furthmueller, 1996b, Phys. Rev. B **55**, 11961.

Kresse, G., and J. Hafner, 1993, Phys. Rev. B **48**, 13115.

Kresse, G., and J. Hafner, 1994a, Phys. Rev. B **49**, 14251.

Kresse, G., and J. Hafner, 1994b, J. Phys.: Condens. Matter **6**, 8245.

Krikorian, N.H., A.L. Bowman, M.C. Krupka and G.P. Arnold, 1969a, High Temp. Sci. **1**, 360.

Krikorian, N.H., A.L. Giorgi, E.G. Szklarz, M.C. Krupka and B.T. Matthias, 1969b, J. Less-Common Met. **19**, 253.

Kripyakevich, P.I., 1977, Structure Types of Intermetallic Compounds (Nauka, Moscow). In Russian.

Kripyakevich, P.I., V.S. Protasov and Yu.B. Kuz'ma, 1964, Dopov. Akad. Nauk Ukr. RSR (3), 212.

Kripyakevich, P.I., V.S. Protasov and Yu.B. Kuz'ma, 1965, Visn. Lviv Univ., Ser. Khim. (8), 80.

Kripyakevich, P.I., V.S. Protasov and Yu.B. Kuz'ma, 1966, Izv. Akad. Nauk SSSR, Neorg. Mater. **2**, 1571 [Inorg. Mater. **2**, 1351].

Krupka, M.C., A.L. Giorgi and E.G. Szklarz, 1973, J. Less-Common Met. **30**, 217.

Ku, H.C., and G.P. Meissner, 1981, J. Less-Common Met. **78**, 99.

Ku, H.C., D.C. Johnston, B.T. Matthias, H. Barz, G. Burri and L. Rinderer, 1979, Mater. Res. Bull. **14**, 1591.

Ku, H.C., C.C. Lai, Y.B. You, J.H. Shieh and W.Y. Guan, 1994, Phys. Rev. B **50**, 351.

Kubashewski, O., 1982, Iron Binary Phase Diagrams (Springer, Berlin).

Kutaitsev, V.I., N.T. Chebotarev, I.G. Lebedev, M.A. Andrianov, V.N. Konev and T.S. Menshikova, 1967, in: Plutonium, 1965, eds A.E. Kay and M.B. Waldon (Chapman and Hall, London) p. 420.

Kuz'ma, Yu.B., 1983, Kristallokhimiya Boridov (Vyshcha Shkola, Lvov).

Kuz'ma, Yu.B., and Yu.V. Voroshilov, 1967, Kristallografiya **12**, 353.

Kuz'ma, Yu.B., P.I. Kripyakevich and N.S. Bilonizhko, 1969, Dopov. Akad. Nauk Ukr. RSR, Ser. A (10), 939.

Kuz'ma, Yu.B., O.M. Dub, V.A. Bruskov, N.F. Chaban and L.V. Zavalii, 1988, Kristallografiya **33**, 841.

Kuzmenko, P.P., V.Ya. Markiv and N.M. Belyavina, 1983, Vestn. Kiev. Univ., Fizika (24), 3.

Kyrchiv, G.I., 1983, in: Chetviortaya Vsesoyuznaya Konfer. po Kristallokhimii Intermetallich. Soyedinenij, Lvov, 18–20 October 1983, Abstracts, p. 36.

Laube, E., and H. Nowotny, 1962, Monatsh. Chem. **93**, 681.

Laube, E., and H. Nowotny, 1963a, Monatsh. Chem. **94**, 162.

Laube, E., and H. Nowotny, 1963b, Monatsh. Chem. **94**, 851.

Lea, K.R., M.J.M. Leask and W.P. Wolf, 1962, J. Phys. Chem. Solids **23**, 1381.

Lee, E.W., and F. Pourarian, 1976, Phys. Status Solidi **33a**, 483.

Lelievre-Berna, E., B. Ouladdiaf, R.M. Galera, J. Deportes and R. Ballou, 1993, J. Magn. Magn. Mater. **123**, L249.

Lukashenko, G.M., V.R. Sidorko and Yu.I. Buyanov, 1990a, Poroshk. Metall. (7) 66.

Lukashenko, G.M., V.R. Sidorko and K.A. Meleshevich, 1990b, Dokl. Akad. Nauk Ukr. RSR, Ser. A (5), 86.

Lukashenko, G.M., V.R. Sidorko and Yu.I. Buyanov, 1991, Dopov. Akad. Nauk Ukr. RSR (4), 73.

Lux, C., G. Wenski and A. Mewis, 1991, Z. Naturforsch. **46b**, 1035.

Malaman, B., G. Venturini and B. Roques, 1988, Mater. Res. Bull. **23**, 1629.

Malik, S.K., A.M. Umarji and G.K. Shenoy, 1985, Phys. Rev. B **31**, 6971.

Maple, M.B., D.A. Gajewski, R. Chau, P. Dai, H.A. Mook, R. Movshovich and C.L. Seaman, 1996, Physica B **223&224**, 447.

Markiv, V.Ya., and N.M. Belyavina, 1981, Izv. Akad. Nauk SSSR, Met. (3), 213.

Markiv, V.Ya., and N.M. Belyavina, 1983, Dopov. Akad. Nauk Ukr. RSR, Ser. B (12), 30.

Markiv, V.Ya., and N.M. Belyavina, 1987a, Vestn. Kiev. Univ., Fizika (28), 17.

Markiv, V.Ya., and N.M. Belyavina, 1987b, Dopov. Akad. Nauk Ukr. RSR, Ser. B (7), 54.

Markiv, V.Ya., and N.M. Belyavina, 1989a, Dopov. Akad. Nauk Ukr. RSR, Ser. A (8), 75.

Markiv, V.Ya., and N.M. Belyavina, 1989b, Dopov. Akad. Nauk Ukr. RSR, Ser. A (1), 75.

Markiv, V.Ya., and N.M. Belyavina, 1990a, Vestn. Kiev. Univ., Fizika (31), 55.

Markiv, V.Ya., and N.M. Belyavina, 1990b, Vestn. Kiev. Univ., Fizika (31), 58.

Markiv, V.Ya., and N.M. Belyavina, 1992, Dokl. Akad. Nauk Ukr. SSR (10), 142.

Markiv, V.Ya., and V.V. Burnashova, 1969, Dopov. Akad. Nauk Ukr. RSR, Ser. A (5), 463.

Markiv, V.Ya., and A.I. Storozhenko, 1973, Dopov. Akad. Nauk Ukr. RSR, Ser. A (10), 941.

Markiv, V.Ya., I.S. Gavrilenko, V.V. Petkov and N.M. Belyavina, 1977, Dokl. Akad. Nauk Ukr. RSR, Ser. A (2), 167.

Markiv, V.Ya., I.S. Gavrilenko, V.V. Petkov and N.M. Belyavina, 1978, Metallofizika (73), 39.

Markiv, V.Ya., A.I. Skripka and L.S. Golubiak, 1979, Dokl. Akad. Nauk Ukr. RSR, Ser. A (12), 1054.

Markiv, V.Ya., T.G. Zhunkivska and N.M. Belyavina, 1981, Dopov. Akad. Nauk Ukr. RSR, Ser. A (3), 84.

Markiv, V.Ya., N.M. Belyavina and I.S. Gavrilenko, 1984, Izv. Akad. Nauk SSSR, Met. (5), 216.

Markiv, V.Ya., N.M. Belyavina and V.P. Shestakov, 1987, Dokl. Akad. Nauk Ukr. RSR, Ser. A, (3), 80.

Markiv, V.Ya., N.M. Belyavina and A.S. Kazachkova, 1989, Izv. Akad. Nauk SSSR, Met. (3), 200.

Marusin, E.P., O.I. Bodak, A.O. Tsokol' and M.G. Baivel'man, 1985, Kristallografiya **30**, 541 [Sov. Phys.-Crystallogr. 30, 340].

Maslenkov, S.B., and G.S. Braslavskaya, 1984, Izv. Akad. Nauk SSSR, Met. (1), 203 [Russ. Met. (1), 203].

Maslenkov, S.B., and G.S. Braslavskaya, 1986a, Izv. Akad. Nauk SSSR, Met. (2), 193 [Russ. Met. (2), 198].

Maslenkov, S.B., and G.S. Braslavskaya, 1986b, Izv. Akad. Nauk SSSR, Met. (5), 213 [Russ. Met. (5), 210].

Massalski, T.B., 1990, Binary Alloy Phase Diagrams, Vols. 1–3, 2nd Ed., eds T.B. Massalski, H. Okamoto, P.R. Subramanian and L. Kacprzak (ASM International, Metals Park, OH).

Mathon, J., 1968, Proc. R. Soc. A **306**, 355.

Matkovich, M.V., J. Economy, R.F. Giese Jr and R. Barrett, 1965, Acta Crystallogr. **19**, 1056.

Matthias, B.T., A.M. Clogston, H.J. Williams, E. Corenzwit and R.C. Sherwood, 1961, Phys. Rev. Lett. 7, 7.

Matthias, B.T., C.K.N. Patel, H. Barz, E. Corenzwit and J.M. Vandenberg, 1978, Phys. Lett. **68A**, 119.

McColm, I.J., and V. Kotroczo, 1987, J. Less-Common Met. **131**, 191.

McMasters, O.D., K.A. Gschneidner Jr and R.F. Venteicher, 1970, Acta Crystallogr. B **26**, 1224.

Men'kov, A.A., L.N. Komissarova, Yu.P. Simanov and V.I. Spitsyn, 1959, Dokl. Akad. Nauk SSSR **128**, 92.

Men'kov, A.A., L.N. Komissarova, Yu.P. Simanov and V.I. Spitsyn, 1961, Dokl. Akad. Nauk SSSR **141**, 364 [Dokl. Chem. **141**, 1137].

Meyer, M., G. Venturini, B. Malaman, J. Steinmetz and B. Roques, 1983, Mater. Res. Bull. **18**, 1529.

Miedema, A.R., 1976, J. Less-Common Met. **46**, 167.

Mikhalenko, S.I., L.V. Zavalii, Yu.B. Kuz'ma and L.I. Boiko, 1991, Poroshk. Metall. (8), 67.

Mills, D.L., and P. Lederer, 1966, J. Phys. Chem. Solids **27**, 1805.

Mokra, I.R., 1979, Ph.D. Thesis (I. Franko Lviv State University, Lviv).

Mokra, I.R., and O.I. Bodak, 1979, Dokl. Akad. Nauk Ukr. RSR, Ser. A (4), 312.

Mokra, I.R., O.I. Bodak and E.I. Gladyshevsky, 1979, Kristallografiya 24, 1274.

Moriya, T., 1985, in: Spin Fluctuations in Itinerant Electron Magnetism, (Springer, Berlin).

Moriya, T., and A. Kawabata, 1973a, J. Phys. Soc. Japan **34**, 639.

Moriya, T., and A. Kawabata, 1973b, J. Phys. Soc. Japan **35**, 699.

Muratova, L.A., 1978, in: Tretya Vsesoyuznaya Konfer. po Kristallokhimii Intermetallich. Soyedinenij, Lvov, 4–6 October 1978, Abstracts, p. 98.

Murray, J.L., 1987, in: Phase Diagrams of Binary Titanium Alloys, p. 284. [Also in: Massalski et al. (1990).]

Nagarajan, R., Z. Mazumdar, Z. Hossain, S.K. Dhar, K.V. Gopaalakrishnan, L.C. Gupta, C. Godart, B.D. Padalia and R. Vijayaraghavan, 1994, Phys. Rev. Lett. **72**, 274.

Nakamichi, T., 1968, J. Phys. Soc. Japan **25**,1189.

Nakamura, H., H. Wada, K. Yoshimura, M. Shiga, Y. Nakamura, J. Sakurai and Y. Komura, 1988, J. Phys. F **18**, 91.

Nakamura, Y., M. Shiga and S. Kawano, 1989, Physica B **120**, 427.

Nakonechna, N.Z., and Z.M. Shpyrka, 1996, Visn. Lviv. Univ., Ser. Khim. (36), 29.

Naumkin, O.P., V.F. Terekhova and E.M. Savitskii, 1964, Zh. Neorg. Khim. **9**, 2497 [Russ. J. Inorg. Chem. **9**, 1347].

Naumkin, O.P., V.F. Terekhova and E.M. Savitskii, 1965, Izv. Akad. Nauk SSSR, Met. (4), 176 [Russ. Met. (4), 128].

Naumkin, O.P., V.F. Terekhova and E.M. Savitskii, 1967, Izv. Akad. Nauk SSSR, Neorg. Mater. **3**, 711 [Inorg. Mater. **3**, 628].

Naumkin, O.P., V.F. Terekhova and E.M. Savitskii, 1969, Izv. Akad. Nauk SSSR, Met. (3), 161 [Russ. Met. (3), 125].

Naumkin, O.P., V.F. Terekhova and E.M. Savitskii, 1970, Izv. Akad. Nauk SSSR, Met. (4), 137 [Russ. Met. (4), 99].

Naumkin, O.P., V.F. Terekhova and E.M. Savitskii, 1971, in: Redkozemelnye Metally I Splavy, eds E.M. Savitskii and V.F. Terekhova (Nauka, Moscow) p. 28.

Nayeb-Hashemi, A.A., and J.B. Clark, 1986, Bull. Alloy Phase Diagrams **7**, 574.

Nishihara, Y., and Y. Yamaguchi, 1985, J. Phys. Soc. Japan **54**, 1122.

Nishihara, Y., and Y. Yamaguchi, 1986, J. Phys. Soc. Japan **55**, 920.

Norman, M., and I.R. Harris, 1969, J. Less-Common Met. **18**, 333.

Nowotny, H., and H. Auer-Welsbach, 1961, Monatsh. Chem. **92**, 789.

Odinaev, H.O., I.N. Ganiev, V.V. Kinzhibalo and B.Ya. Kotur, 1989, Dokl. Akad. Nauk Tadzh. SSR **32** (1), 37.

Odinaev, H.O., I.N. Ganiev and A.V. Vahobov, 1991, Izv. Akad. Nauk SSSR, Met. (4), 195.

Okamoto, H., 1992, J. Phase Equilibria **13**, 679.

Okamoto, H., 1993, J. Phase Equilibria **14**, 655.

Olenych, R.R., 1989, Ph.D. Thesis (I. Franko Lviv State University, Lviv).

Olenych, R.R., L.G. Akselrud and Ya.P. Yarmolyuk, 1981, Dopov. Akad. Nauk Ukr. RSR, Ser. A (2), 84.

Oomi, G., T. Terada, M. Shiga and Y. Nakamura, 1987, J. Magn. Magn. Mater. **70**, 137.

Palenzona, A., and S. Cirafici, 1993, J. Phase Equilibria **12**, 53.

Palenzona, A., and P. Manfrinetti, 1995, J. Alloys & Compounds **220**, 157.

Palenzona, A., and P. Manfrinetti, 1996, J. Alloys & Compounds **237**, 121.

Palenzona, A., and P. Manfrinetti, 1997, J. Alloys & Compounds **247**, 195.

Palenzona, A., P. Manfrinetti and R. Palenzona, 1996, J. Alloys & Compounds **243**, 182.

Pandian, S., S.V. Nagender Naidu and P. Rama Rao, 1988, J. Alloy Phase Diagrams **4**, 74.

Pani, M., P. Manfrinetti and M.L. Fornasini, 1995, Z. Kristallogr. **210**, 975.

Parthé, E., and B. Chabot, 1984, in: Handbook on the Physics and Chemistry of Rare Earths, Vol. 6, eds K.A. Gschneidner Jr and L. Eyring (North-Holland, Amsterdam) p. 113.

Parthé, E., and Edda Parthé, 1963, Acta Crystallogr. **16**, 71.

Parthé, E., D. Hohnke, W. Jeitschko and O. Schob, 1965, Naturwissenschaften 7, 155.

Pawlak, L., K. Falkowski and S. Pokrzywnicki, 1981, J. Solid State Chem. **37**, 228.

Pecharskaya, A.O., 1989, Ph.D. Thesis (I. Franko Lviv State University, Lviv).

Pecharskaya, A.O., E.P. Marusin, O.I. Bodak and M.D. Mazus, 1990, Kristallografiya **35**, 47.

Pecharsky, V.K., 1979, Ph.D. Thesis (I. Franko Lviv State University, Lviv).

Pecharsky, V.K., O.I. Bodak and E.I. Gladyshevsky, 1978, Dopov. Akad. Nauk Ukr. RSR, Ser. A (8), 755.

Pecharsky, V.K., O.I. Bodak and E.I. Gladyshevsky, 1979, Kristallografiya **24**, 757 [Sov. Phys.-Crystallogr. **24**, 433].

Pecharsky, V.K., Yu.V. Pankevich and O.I. Bodak, 1983, Kristallografiya **28**, 173.

Peshev, P., J. Etourneau and R. Naslain, 1970, Mater. Res. Bull. **5**, 319.

Pöttgen, R., and R. Dronskowski, 1996, Z. Anorg. Allg. Chem. **622**, 355.

Pöttgen, R., and W. Jeitschko, 1991, Inorg. Chem. **30**, 427.

Pöttgen, R., and W. Jeitschko, 1992, Z. Naturforsch. B **47**, 358.

Pöttgen, R., A.M. Witte, W. Jeitschko and T. Ebel, 1995, J. Solid State Chem. **119**, 324.

Pöttgen, R., H. Borrmann, C. Felser, O. Jepsen, R. Henn, R.K. Kremer and A. Simon, 1996, J. Alloys & Compounds **235**, 170.

Prevarskii, A.P., O.S. Zarechnyuk, E.E. Cherkashin and V.I. Polikha, 1976, Visn. Lviv. Univ., Ser. Khim. (18), 14.

Prokin, E.S., Z.V. Ershova and E.E. Ermolaev, 1977, Radiokhimiya **19**, 845.

Protasov, V.S., and E.I. Gladyshevsky, 1964, Kristallografiya **9**, 267.

Przybylska, M., A.H. Reddoch and G.J. Ritter, 1963, J. Am. Chem. Soc. **85**, 407.

Raevskaya, M.B., and E.M. Sokolovskaya, 1979, Fizikokhimiya Ruteniya I Ego Splavov (MGU Publishers, Moscow) p. 105.

Ramakrishnan, S., K. Ghosh and G. Chandra, 1992, Phys. Rev. B **46**, 2958.

Rechkin, V.N., V.F. Terekhova and E.M. Savitskii, 1965, Izv. Akad. Nauk SSSR, Met. (4), 176.

Reinbold, E.J., and W. Jeitschko, 1987, Z. Kristallogr. **178**, 188.

Reule, H., S. Steeb and C. Donolato, 1971, J. Less-Common Met. **24**, 108.

Rhodes, P., and E.P. Wohlfarth, 1963, Proc. R. Soc. A **273**, 247.

Rhyne, J.J., 1987, J. Magn. Magn. Mater. **70**, 963.

Rider, P.E., K.A. Gschneidner Jr and O.D. McMasters, 1965, Trans. Met. Soc. AIME **233**, 1488.

Rogl, P., 1984a, J. Solid State Chem. **55**, 262.

Rogl, P., 1984b, in: Handbook on the Physics and Chemistry of Rare Earths, Vol. 7, eds K.A. Gschneidner Jr and L. Eyring (North-Holland, Amsterdam) ch. 51, pp. 1–190.

Rogl, P., and H. Nowotny, 1979, J. Less-Common Met. **76**, 41.

Rosen, S., and P.G. Sprang, 1965, Adv. X-Ray Anal. **8**, 91.

Rossi, D., R. Marazza and R. Ferro, 1992, J. Alloys & Compounds **187**, 267.

Sabirzyanov, N.A., 1988, Ph.D. Thesis (Sverdlovsk).

Sabirzyanov, N.A., 1989, in: V Vsesoyuznoye Soveshchaniye "Diagrammy Sostoyaniya Metallicheskih Sistem", Abstracts (Nauka, Moscow) p. 144.

Samsonov, G.V., A.I. Kondrashov, L.N. Okhremchuk, A.I. Podchernyaeva, N.I. Siman and V.S. Fomenko, 1979, J. Less-Common Met. **67**, 415.

Sankar, S.G., and W.E. Wallace, 1976, AIP Conf. Proc. **29**, 334.

Savitskii, E.M., and G.S. Burkhanov, 1961, Zh. Neorg. Khim. **6**, 1253 [Russ. J. Inorg. Chem. **6**, 642].

Savitskii, E.M., and Yu.V. Efimov, 1972, Monatsh. Chem. **103**, 270.

Savitskii, E.M., M.A. Tylkina and O.Kh. Khamidov, 1966, Izv. Akad. Nauk SSSR, Met. (4), 116 [Russ. Met. (4), 52].

Savitskii, E.M., V.F. Terekhova, R.S. Torchiniva, I.A. Markova, O.P. Naumkin, V.E. Kolesnichenko and V.F. Stroganova, 1970, in: Les Elements des Terres Rares, Vol. 1 (CNRS, Paris) p. 47.

Savitskii, E.M., O.P. Naumkin and Yu.V. Efimov, 1971a, Izv. Akad. Nauk SSSR, Met. (2), 178 [Russ. Met. (2), 119].

Savitskii, E.M., V.P. Polyakova and N.B. Gorina, 1971b, Izv. Akad. Nauk SSSR, Met. (6), 161 [Russ. Met. (6), 117].

Savitskii, E.M., V.P. Polyakova, B.P. Krivdin, A.A. Kozlov and E.M. Khorlin, 1971c, in: Diagrammy Sostoyaniya Metallicheskih Sistem (Nauka, Moscow) p. 200.

Savitskii, E.M., V.P. Polyakova, N.B. Gorina and N.R. Roshan, 1971d, in: Redkozemelnye Metally I Splavy, eds E.M. Savitskii and V.F. Terekhova (Nauka, Moscow) p. 63.

Savitskii, E.M., M.A. Tylkina and E.P. Arskaya, 1972, in: Splavy Tsvetnykh Metallov (Nauka, Moscow) p. 220.

Savitskii, E.M., Yu.V. Efimov and O.I. Zvolinskii, 1975, in: Redkiye Metally v Tsvetnykh Splavah, ed. E.M. Savitskii (Nauka, Moscow) p. 26.

Savitskii, E.M., V.P. Polyakova, N.B. Gorina and N.R. Roshan, 1978a, Physical Metallurgy of Platinum Metals (Mir Publishers, Moscow) p. 257.

Savitskii, E.M., Yu.V. Efimov, V.Ya. Markiv, I.S. Gavrilenko, O.I. Zvolinskii and T.M. Frolova, 1978b, Izv. Akad. Nauk SSSR, Met. (1), 211.

Savitskii, E.M., Yu.V. Efimov, V.Ya. Markiv, I.S. Gavrilenko and T.M. Frolova, 1980a, Dokl. Akad. Nauk Ukr. RSR, Ser. A (3), 81.

Savitskii, E.M., V.P. Polyakova and V.P. Urvachev, 1980b, Izv. Akad. Nauk SSSR, Met. (4), 226.

Schablaske, R.V., B.S. Tani and M.G. Chasanov, 1964, Trans. Met. Soc. AIME **230**, 248.

Schindler, A.L., and M.J. Rice, 1967, Phys. Rev. **164**, 759.

Schnelle, W., R. Pöttgen, R.K. Kremer, E. Gmelin and O. Jepsen, 1997, J. Phys.: Condens. Matter **9**, 1435.

Schob, O., and E. Parthé, 1964a, Acta Crystallogr. **17**, 1335.

Schob, O., and E. Parthé, 1964b, Monatsh. Chem. **95**, 1466.

Schob, O., and E. Parthé, 1965, Acta Crystallogr. **19**, 214.

Schuster, J.C., and J. Bauer, 1985, J. Less-Common Met. **109**, 345.

Semenova, O.L., N.Yu. Rusetskaya and V.M. Petyukh, 1996a, Poroshk. Metall. (11/12), 37.

Semenova, O.L., N.Yu. Rusetskaya, T.Ya. Velikanova and V.M. Vereshchak, 1996b, Poroshk. Metall. (7/8), 134.

Shamrai, V.F., Yu.V. Efimov, E.A. Miasnikova, L.A. Riabtsev and A.P. Brovko, 1988, Izv. Vuzov, Tsvet. Metallurg. (4), 83.

Shelton, R.N., and H.C. Ku, 1980, Mater. Res. Bull. **15**, 1445.

Shiga, M., 1988, Physica B **149**, 293.

Shpyrka, Z.M., 1990, Ph.D. Thesis (I. Franko Lviv State University, Lviv).

Shpyrka, Z.M., and I.R. Mokra, 1991, Visn. Lviv Univ., Ser. Khim. (31), 36.

Siegrist, T., H.W. Zandbergen, R.J. Cava, J.J. Krajewski and W.F. Pech Jr, 1994, Nature **367**, 254.

Smit, P.H., and K.H.J. Buschow, 1980, Phys. Rev. B **21**, 3839.

Smith, G., Q. Johnson and P. Nordine, 1965, Acta Crystallogr. **19**, 668.

Smith, J.F., and K.J. Lee, 1989, in: Phase Diagrams of Binary Vanadium Alloys. [Also in: Massalski et al. (1990).]

Sokolovskaya, E.M., E.F. Kazakova and E.I. Poddiakonova, 1989, Metallovedeniye I Termich. Obrabotka Met. (11), 29.

Spear, K.E., 1976, in: Phase Diagrams, Vol. IV, ed. A.M. Alper (Academic Press, New York) pp. 91–159.

Spear, K.E., 1977, in: Boron and Refractory Borides (Springer, Berlin) pp. 439–457.

Spear, K.E., and P.K. Liao, 1990, Bull. Alloy Phase Diagrams **11**, 321.

Stapf, I., G. Kiessler and E. Gebhardt, 1975, J. Less-Common Met. **39**, 219.

Steiner, W., and H. Ortbauer, 1974, Phys. Status Solidi **26a**, 451.

Stepanchikova, G.F., 1979, Visn. Lviv. Politekhn. Inst. (130), 58.

Stepanchikova, G.F., and Yu.B. Kuz'ma, 1981, Vestn. Lvov. Univ., Ser. Khim. (23) 48.

Subramanian, P.R., D.E. Laughlin and D.J. Chakrabarti, 1988, Bull. Alloy Phase Diagrams **9**, 378.

Svechnikov, V.M., G.F. Kobzenko and V.G. Ivanchenko, 1972, Dopov. Akad. Nauk Ukr. RSR, Ser. A (3), 266.

Sviderskaya, Z.A., and N.I. Nikitina, 1972, in: Metallovedeniye Tsvetnykh Metallov i Splavov, ed. M.E. Drits (Nauka, Moscow) p. 61.

Taylor, A., W.M. Hickman and N.J. Doyle, 1965, J. Less-Common Met. **9**, 214.

Terekhov, G.I., and S.U. Sinyakova, 1990, Izv. Akad. Nauk SSSR, Met. (3), 215.

Terekhov, G.I., and S.U. Sinyakova, 1992, Izv. RAN, Met. (3), 200 [Russ. Met. (3), 187].

Teslyuk, M.Yu., and V.S. Protasov, 1965a, Dopov. Akad. Nauk Ukr. RSR (5), 599.

Teslyuk, M.Yu., and V.S. Protasov, 1965b, Kristallografiya **10**, 561.

Thirion, F., J. Steinmetz and B. Malaman, 1983, Mater. Res. Bull. **18**, 1537.

Toropova, L.S., T.V. Dobatkina and M.L. Kharakterova, 1985, in: Metallovedeniye Legkikh Splavov, ed. A.F. Belov (VILS Publishers, Moscow) p. 54.

Toropova, L.S., M.L. Kharakterova and B.Ya. Kotur, 1989, in: V Vsesoyuznoye Soveshchaniye "Diagrammy Sostoyaniya Metallicheskikh Sistem", Abstracts (Nauka, Moscow) p. 124.

Toropova, L.S., A.N. Kamardinkin, V.V. Kinzhibalo and A.T. Tyvanchuk, 1990, Fiz. Met. Metalloved. (12), 108.

Trubniakova, E.D., and I.N. Ganiev, 1989, in: V Vsesoyuznoye Soveshchaniye "Diagrammy Sostoyaniya Metallicheskikh Sistem", Abstracts (Nauka, Moscow) p. 128.

Trubniakova, E.D., O.I. Bodak, I.N. Ganiev and A.V. Vahobov, 1987, Izv. Akad. Nauk SSSR, Met. (3), 221.

Tsokol', A.O., O.I. Bodak and E.P. Marusin, 1986a, Kristallografiya **31**, 788 [Sov. Phys.-Crystallogr. **31**, 466].

Tsokol', A.O., O.I. Bodak, E.P. Marusin and M.G. Baivel'man, 1986b, Kristallografiya **31**, 791 [Sov. Phys.-Crystallogr. **31**, 467].

Tsolovski, L.A., and P.D. Peshev, 1972, C.R. Bulgar. Acad. Sci. **25**, 209.

Turkina, A.I., and V.I. Kuzmina, 1976, Izv. Akad. Nauk SSSR, Met. (4), 208.

Tyvanchuk, A.T., T.I. Yanson, B.Ya. Kotur, O.S. Zarechnyuk and M.L. Kharakterova, 1988, Izv. Akad. Nauk SSSR, Met. (4), 187 [Russ. Met. (4), 190].

Urvachev, V.P., V.P. Polyakova and E.M. Savitskii, 1983, in: Splavy Redkikh Metallov s Osobymi Fizicheskimi Svojstvami: Redkozemelnye I Blagorodnye Metally, ed. E.M. Savitskii (Nauka, Moscow) p. 141.

Vandenberg, J.M., and B.T. Matthias, 1977, Proc. Acad. Sci. U.S.A. **74**, 1336.

Vanderbilt, D., 1990, Phys. Rev. B **41**, 7892.

Velikanova, T.Ya., V.N. Eremenko, L.V. Artyukh, A.A. Bondar and O.V. Gordijchuk, 1989, Poroshk. Metall. (9), 49 [Sov. Powder Metall. Ceram. **28**, 711].

Venkatraman, M., and J.P. Neumann, 1985, Bull. Alloy Phase Diagrams **6**, 422.

Venturini, G., M. Méot-Meyer and B. Roques, 1985, J. Less-Common Met. **107**, L5.

Venturini, G., B. Malaman and B. Roques, 1989, J. Less-Common Met. **152**, 185.

Villars, P., 1995, in: Intermetallic Compounds, Vol. 1, eds J.H. Westbrook and R.L. Fleischer (Wiley, Chichester) p. 227.

Villars, P., and L.D. Calvert, eds, 1991, Pearson's Handbook of Crystallographic Data for Intermetallic Phases, Vols. 1–4 (ASM International, Metals Park, OH).

Vining, C.B., R.N. Shelton, H.F. Braun and M. Pelizzone, 1983, Phys. Rev. B **27**(5), 2800.

Voroshilov, Yu.V., V.Ya. Markiv and E.I. Gladyshevsky, 1967, Izv. Akad. Nauk SSSR, Neorg. Mater. **3**, 1404 [Inorg. Mater. **3**, 1224].

White, J.G., and J.P. Dismukes, 1965, Inorg. Chem. **4**, 1760.

Wohlfarth, E.P., 1978, J. Magn Magn. Mater. 7, 113.

Xia, S.R., E. Baggio-Saitovich, V.A. Rodrigues, E. Passamani, A.Y. Takeuchi, M. Ghfari, R.R. Avillez and F.C. Rizzo-Assuncao, 1996, J. Alloys & Compounds **242**, 85.

Yarmolyuk, Ya.P., B.Ya. Kotur and Yu.N. Grin', 1980, Dopov. Akad. Nauk Ukr. RSR, Ser. B (11), 68.

Yatsenko, S.P., A.A. Semyannikov, B.G. Semenov and K.A. Chuntonov, 1979, J. Less-Common Met. **64**, 185.

Yatsenko, S.P., A.A. Semyannikov, H.O. Shakarov and E.G. Fedorova, 1983, J. Less-Common Met. **90**, 95.

Yim, W.M., E.J. Stofko and R.T. Smith, 1972, J. Appl. Phys. **43**, 254.

Yoshimura, K., H. Nakamura, H. Takigawa, H. Yasuoka, M. Shiga and Y. Nakamura, 1987, J. Magn. Magn. Mater. **70**, 142.

Zalutska, O.I., V.R. Riabov and I.I. Zalutskii, 1969, Dopov. Akad. Nauk Ukr. RSR, Ser. A (3), 255.

Zalutska, O.I., V.G. Kontsevii, M.I. Karamishev, V.R. Riabov and I.I. Zalutskii, 1970, Dopov. Akad. Nauk Ukr. RSR, Ser. A (8), 751.

Zalutska, O.I., E.E. Cherkashin and I.I. Zalutskii, 1974, in: Struktura Faz, Fazovye Prevrashcheniya I Diagrammy Sostoyaniya Metallicheskikh Sistem (Nauka, Moscow) p. 186.

Zalutskii, I.I., and P.I. Kripyakevich, 1967, Kristallografiya **12**, 394 [Sov. Phys.-Crystallogr. **12**, 341].

Zarechnyuk, O.S., and R.M. Rykhal, 1977, Vestn. Lvov. Univ., Ser. Khim. (19), 51.

Zarechnyuk, O.S., O.I. Vivchar and V.R. Riabov, 1970, Dopov. Akad. Nauk Ukr. RSR, Ser. A (10), 943.

Zaremba, V.I., V.M. Baranyak and Ya.M. Kalychak, 1984, Vestn. Lvov Univ., Ser. Khim. (25), 18.

Zavalii, L.V., and S.I. Mikhalenko, 1989, in: V Vsesoyuznoye Soveshchaniye "Diagrammy Sostoyaniya Metallicheskikh Sistem", Abstracts (Nauka, Moscow) p. 151.

Zavalii, L.V., Yu.B. Kuz'ma and S.I. Mikhalenko, 1988, Izv. Akad. Nauk SSSR, Neorg. Mater. **24**, 1814.

Zhao, J.T., and E. Parthé, 1989a, J. Less-Common Met. **154**, 31.

Zhao, J.T., and E. Parthé, 1989b, in: Twelfth European Crystallogr. Meeting, Moscow, 20–29 August 1989 (Moscow) Coll. Abstracts, Vol. 2, p. 182.

Zhao, J.T., and E. Parthé, 1991, Acta Crystallogr. C **47**, 4.

Zhao, J.T., B. Chabot and E. Parthé, 1988, Acta Crystallogr. C **44**, 397.

Zhuravlev, N.N., and E.M. Smirnova, 1962, Kristallografiya **7**, 312 [Sov. Phys.-Crystallogr. **7**, 243].

Zhuravlev, N.N., and A.A. Stepanova, 1958, Sov. Phys.-Crystallogr. **3**, 76.

Ziman, J.M., 1960, Electrons and Phonons (Oxford University Press, Oxford).

AUTHOR INDEX

SUBJECT INDEX